

Seongwoo Woo

Reliability Design of Mechanical Systems

A Guide for Mechanical and Civil
Engineers

Second Edition

Reliability Design of Mechanical Systems

Seongwoo Woo

Reliability Design of Mechanical Systems

A Guide for Mechanical and Civil Engineers

Second Edition



Springer

@Seismicisolation

Seongwoo Woo
Reliability Association of Korea
Seoul, Korea (Republic of)

ISBN 978-981-13-7235-3 ISBN 978-981-13-7236-0 (eBook)
<https://doi.org/10.1007/978-981-13-7236-0>

1st edition: © Springer International Publishing AG 2017

2nd edition: © Springer Nature Singapore Pte Ltd. 2020

This work is subject to copyright. All rights are reserved by the Publisher, whether the whole or part of the material is concerned, specifically the rights of translation, reprinting, reuse of illustrations, recitation, broadcasting, reproduction on microfilms or in any other physical way, and transmission or information storage and retrieval, electronic adaptation, computer software, or by similar or dissimilar methodology now known or hereafter developed.

The use of general descriptive names, registered names, trademarks, service marks, etc. in this publication does not imply, even in the absence of a specific statement, that such names are exempt from the relevant protective laws and regulations and therefore free for general use.

The publisher, the authors and the editors are safe to assume that the advice and information in this book are believed to be true and accurate at the date of publication. Neither the publisher nor the authors or the editors give a warranty, expressed or implied, with respect to the material contained herein or for any errors or omissions that may have been made. The publisher remains neutral with regard to jurisdictional claims in published maps and institutional affiliations.

This Springer imprint is published by the registered company Springer Nature Singapore Pte Ltd.
The registered company address is: 152 Beach Road, #21-01/04 Gateway East, Singapore 189721,
Singapore

Preface to the First Edition

In the beginning of the twentieth century, new sophisticated mechanical systems such as bridges, rockets, automobiles, airplanes, and space shuttles were designed and built for people to live comfortable lives through the engineering design processes. Typical design process can be broadly summarized as (1) define the problems, (2) develop the product—prototype, design and testing, (3) production. Due to the frequent occurrence of disasters for new products, product reliability has become one of increasingly important factors (to consider) because of cost, competition, public demand, and adaptation of new technology. The most effective way to protect the reliability disaster is to develop the reliability-embedded design process including its methodology in parallel with the established design process.

As products with multiple modules require higher performance and material cost reduction, the reliability design of product has become more complex and increases the risk of product failure. The studies of reliability engineering have been deepened to prevent the reliability disasters of the past century. Even though there are a large number of concepts, theory, and texts on reliability, an up-to-date book for emphasizing the new methodology of reliability design is still required to prevent the reliability disasters of the mechanical/civil system.

From the standpoint of economics, company will decrease the operation profit for a failure in its expected product lifetime because of Product Liability Law in the global market. All products from tires to electric components are fabricated from the structure (or materials) that will tend to degrade or break down abruptly by random loads. The mechanical system can eventually fracture due to fatigue which can result from cyclical stresses (or loads). When products are subjected to random loads, they start the void in material (or design defects), propagate, and rupture it. If failure for a new product happens, the product may no longer meet the established specifications for proper product functionality. To avoid product failure in lifetime, product should be designed to robustly withstand a variety of loads.

The main objectives of writing this book are focused on explaining the development necessity of the reliability-embedded design process and its methodology. As reliability methodology, we will suggest the new parametric accelerated life testing (ALT) that meets those market requirements—higher performance, material

cost reduction, and higher reliability in field. The reliability-embedded design process consists of parametric ALT plan, failure mechanism and design, acceleration factor, sample size equation, and the parametric ALT. It produces the reliability quantitative test specifications (RQ) in accordance with the reliability target. A parametric ALT method therefore will assess the reliability of product subjected to repetitive stresses.

Based on the market data, parametric ALT plan will set up the reliability target of product and its modules. Mechanical system in field subjected to loads arise how to design product for the failure mechanisms—fatigue and fracture. The accumulated damage in system like palmer miner rule can be represented at the time-to-failure model. The acceleration factor with a new effort concept (or loads) was derived from a generalized life-stress failure model. So the new sample size equation with the acceleration factor enabled the parametric ALT to quickly evaluate the expected lifetime of product. This parametric ALT should help an engineer to uncover the missing design parameters affecting reliability during the design process of new product.

Consequently, if applied in the established design process, new parametric ALT helps companies to improve new product reliability and avoid the recalls of product failures in field. As the improper design parameters in the design phase are identified by this reliability design method, the product will improve the reliability that will be measured by the increase in lifetime, L_B , and the reduction in failure rate, λ . Product will meet the reliability target in industry. This book will help to prevent the reliability disaster through the parametric ALT. We also provide a lot of parametric ALT examples that are effective to be understood in the mechanical/civil field.

This book is composed of nine chapters. Chapter 1 presents the present aspect and need of reliability engineering in the advance of modern technology. Chapter 2 reviews the historical reliability disasters and their root cause within the past century. It will explain the significance of reliability assessment, and its methodology need to prevent reliability disasters in the design process. Chapter 3 will explain the most important fundamental definitions of statistics and probability theory, the mathematical essentials of reliability engineering, and the most significant aspects of reliability engineering developed within the past century. It will help one to understand the basic concepts of reliability methodologies that will be discussed in Chap. 8. Chapter 4 through Chap. 6 present load analysis, stress concept, and a brief overview of the typical reliability failure mechanism of product—fatigues and fractures. Chapter 7 will present the fundamental concepts of the parametric ALT in product that will be the core of this book. Chapter 8 will also present case studies that are useful in a variety of engineering areas. Chapter 9 will cover the future aspects of parametric ALT in mechanical product that will be developed as system engineering.

This book is intended to introduce the prerequisite concepts of the parametric ALT for senior level undergraduate and graduate students, professional engineers, college and university level lecturers, researchers, and design managers of the engineering system. We hope this noble methodology explained in this book will

help to prevent the reliability disasters of new product in field. The authors would also like to thank Springer for the publishing of this work, especially Mayra Castro, Springer DE. With their help, this book has been published.

Seoul, Korea (Republic of)

Seongwoo Woo

Preface to the Second Edition

In the last century, new sophisticated mechanical systems such as automobiles and airplanes were designed and built to make human lives comfortable. Mechanical systems are required with higher performance and material cost reduction. As a result, the design of product has become more complex and increases the risk of product failure. As seen in modern mechanical products from tires to electric components, they assembled in one structure (or platforms). They will tend to degrade by a variety of loads and eventually fracture. If closely looked, they would start the design defects in structure, propagate, and rupture it. If failure for new product happens, the product may no longer meet the company established specifications for proper product functionality and reject in marketplace immediately.

Due to the frequent recalls for new products, product reliability has become one of the critical factors of product design as well as with cost and quality. The studies of mechanical engineering also have been deepened to reflect the design concepts in the past century. To avoid product failure in lifetime, product should be designed to robustly withstand a variety of loads. Many engineers had to wonder why the product recalls often happen. They thought such possibility could be assessed: (1) mathematical modeling like Newtonian method, (2) the time response of system simulation for (random) dynamic loads, (3) the rainflow-counting method, and (4) Miner's rule that the system damage could be estimated. However, because there are a lot of assumptions, this analytic methodology is exact but complex to reproduce the product failures due to the design flaws in product operation.

Consequently, new parametric accelerated life testing method can be an alternative to make better the reliability design of mechanical system. Based on the market data, parametric ALT plan will set up the reliability target of product and its modules. The acceleration factor with a new effort concept (or loads) was derived from a generalized life-stress failure model. So the new sample size equation with the acceleration factor enabled the parametric ALT to quickly evaluate the expected lifetime of product. This parametric ALT should help an engineer to uncover the missing design parameters affecting reliability and assess whether the target of the product reliability is achieved during the design process of new product. As a result, it produces the reliability quantitative (RQ) test specifications in accordance with

the reliability target. A parametric ALT method will assess the reliability of product (or module) subjected to repetitive stresses.

The primary purpose of writing this book in the first edition was to figure out the design problems of mechanical system and prevent them by parametric ALT. The first edition book focused on the exact description of parametric ALT. Several core concepts in each chapter seem to be missing that it is not easy for mechanical engineer to read this book. For example, there is vibration (or noise) in mechanical system that can be often claimed by customer. The dynamic analysis of mechanical system is modeled as mass in the form of the body, spring in the form of suspension, and damper in the form of shock absorbers. But we did not mention it in the first edition. Some topics in the second edition are modified and rewritten, many new topics are added, and several new features have been introduced.

1. The abstracts of each chapter will be restated at the beginning. Each topic in reliability design of mechanical systems is self-contained, with all concepts fully explained and the derivations presented in complete detail.
2. The presentation of some of the topics in each chapter is modified for expanded coverage and better clarity. New topics in Chaps. 1, 4, 5, and 6 are presented.
3. All new topics related to product development process will be added in Chap. 1. To better understand the failure mechanics, design and reliability testing, reliability block diagram, and reliability testing will be included in Chap. 4. Fluid analysis and vibration will be added in Chap. 5. Chapter 6 will be included in the strength of product materials, failure analysis with modified example, and corrosion problem of product. Examples of reliability block diagram in mechanical product like automobile will be introduced in Chap. 7. Chapter 8 will be re-explained in detail with illustrative examples.

This book serves as an introduction to the subject of the reliability design of the mechanical system. It also will have some unique points:

- Widely used for senior-level undergraduate and graduate students, professional engineers, college- and university-level lecturers, researchers, and design managers in the field of mechanical and civil engineering.
- Unique in the noble reliability methodology explained in this book to prevent it from the product recalls of new mechanical product in the fields like automobile and airplane.
- Supplied with detailed case studies based on methodology of parametric ALT that will be obtained in the process of product developing and helpful to the mechanical/civil engineer.

Seoul, Korea (Republic of)

Seongwoo Woo

Contents

1	Introduction to Reliability Design of Mechanical/Civil System	1
1.1	Introduction	1
1.2	Development of Mechanical Product	6
1.2.1	Introduction	6
1.2.2	Mechanical Engineering Design Process	7
Reference		17
2	Product Recalls and Its Assessment Significance	19
2.1	Introduction	20
2.2	Product Recalls	22
2.2.1	Versailles Rail Accident in 1842	28
2.2.2	Tacoma Narrows Bridge in 1940	30
2.2.3	De Havilland DH 106 Comet in 1953	31
2.2.4	G Company and M Company Rotary Compressor Recall in 1981	32
2.2.5	Firestone and Ford Tire in 2000	34
2.2.6	Toshiba Satellite Notebook and Battery Overheating Problem in 2007	35
2.2.7	Toyota Motor Recalls in 2009	35
2.3	Development of Reliability Methodologies in History	36
2.3.1	In the Early of 20s Century—Starting Reliability Studies	36
2.3.2	In the World War II—New Electronics Failure in Military	41
2.3.3	In the End of World War II and 1950s—Starting the Reliability Engineering	43
2.3.4	In the 1960s and Present: Mature of Reliability Methodology—Physics of Failure (PoF)	47
References		52

3 Modern Definitions in Reliability Engineering	53
3.1 Introduction	53
3.2 Reliability and Bathtub Curve	54
3.2.1 Reliability Function and Failure Rate	54
3.2.2 Bathtub Curve	55
3.3 Reliability Lifetime Metrics	57
3.3.1 Mean Time to Failure (MTTF)	57
3.3.2 Mean Time Between Failure (MTBF)	59
3.3.3 Mean Time to Repair (MTTR)	59
3.3.4 BX% Life	60
3.3.5 The Inadequacy of the MTTF (or MTBF) and the Alternative Metric BX Life	61
3.4 Fundamentals in Statistics and Probability Theory	62
3.4.1 Statistics	62
3.4.2 Probability	64
3.5 Probability Distributions	67
3.5.1 Introduction	67
3.5.2 Binomial Distribution	67
3.5.3 Poisson Distributions	68
3.5.4 Normal Distribution	70
3.5.5 Exponential Distributions	72
3.6 Weibull Distributions and Its Applications	74
3.6.1 Weibull Parameter Estimation	74
3.6.2 Weibull Parameter Estimation	76
3.6.3 Confidence Interval	81
3.7 Sample Distributions	84
3.7.1 Introduction	84
3.7.2 The Distribution of Sample Mean	85
3.7.3 The Distribution of Sample Variation	87
3.8 Relationship Between Reliability and Cumulative Distribution Function	89
3.9 Design of Experiment (DOE)	93
3.9.1 Terminologies	93
3.9.2 Analysis	95
Reference	99
4 Failure Mechanics, Design and Reliability Testing	101
4.1 Introduction	101
4.2 Failure Mechanics and Designs	104
4.2.1 Introductions	104
4.2.2 Product Design—Intended Functions	106
4.2.3 Specified Design Lifetime, B_x	108

4.2.4	Dimensional Differences Between Quality Defects and Failures	110
4.2.5	Classification of Failures	112
4.3	Reliability Block Diagram	113
4.3.1	Introduction	113
4.3.2	Comparison Between Reliability Block Diagram and Fault Tree	117
4.4	Failure Mode and Effect Analysis (FMEA)	119
4.4.1	Introduction	119
4.4.2	Types of FMEA	121
4.4.3	System-Level FMEA	121
4.4.4	Design-Level FMEA	122
4.4.5	Process-Level FMEA	122
4.4.6	Steps for Performing FMEA	123
4.5	Fault Tree Analysis (FTA)	129
4.5.1	Introduction	129
4.5.2	Reliability Evaluation of Standard Configuration	134
4.6	Robust Design (or Taguchi Methods)	137
4.6.1	A Specific Loss Function	138
4.6.2	Robust Design Process	140
4.6.3	Parameter (Measure) Design	141
4.6.4	Tolerance Design	142
4.6.5	A Parameter Diagram (P-Diagram)	142
4.6.6	Taguchi's Design of Experiment (DOE)	144
4.6.7	Inefficiencies of Taguchi's Designs	145
4.7	Reliability Testing	146
4.7.1	Introduction	146
4.7.2	Lifetime Estimation—Maximum Likelihood Estimation (MLE)	148
4.7.3	Time-to-Failure Models	151
4.7.4	Data Analysis	156
5	Structures (or Mechanisms) and Load Analysis	163
5.1	Introduction	163
5.2	Mechanical Structures (and Its Mechanisms)	164
5.3	Modeling of Mechanical System	172
5.3.1	Introduction	172
5.3.2	Newton's Mechanics	174
5.3.3	D'Alembert's Modeling for Automobile	175
5.4	Bond Graph Modeling	177
5.4.1	Introduction	177
5.4.2	Basic Elements, Energy Relations, and Causality of Bond Graph	178

5.4.3	Case Study: Hydrostatic Transmission (HST) in Sea-Borne Winch	183
5.4.4	Case Study: Failure Analysis and Redesign of a Helix Upper Dispenser	189
5.5	Load Spectrum and Rain-Flow Counting	192
5.5.1	Introduction	192
5.5.2	Rain-Flow Counting for Load Spectrum	194
5.5.3	Goodman Relation	196
5.5.4	Palmgren-Miner's Law for Cumulative Damage	199
5.5.5	Inefficiency of Load Spectrum and Rain-Flow Counting	204
	References	204
6	Fluid Motion and Mechanical Vibration	205
6.1	Introduction	205
6.1.1	Fluid Motion	205
6.1.2	Buckingham Pi Theorem	207
6.1.3	Forces Acting on the Air Vehicle—Thrust, Drag, Weight and Lift	208
6.1.4	Basic Concept of Lift	209
6.2	Fluid Modeling	210
6.2.1	Introduction	210
6.2.2	Conservation Laws for Mass and Momentum	216
6.2.3	Bernoulli's Equation	221
6.3	Viscous Flow and Boundary Layers	222
6.3.1	Introduction	222
6.3.2	The Boundary-Layer Characteristics	224
6.3.3	The Boundary-Layer Equations	228
6.3.4	Blasius Solution for Laminar Boundary Layer	232
6.3.5	Velocity Boundary Layer for Turbulent Flow	237
6.4	Parametric Accelerated Life Testing of Fluid Systems	237
6.5	Mechanical Vibrations	238
6.5.1	Introduction	238
6.5.2	Mechanical Systems and Their Modeling	239
6.5.3	Reduction of the Vibratory Motion Due to the Mass	242
6.5.4	Vibration Design of Mechanical Product	245
7	Mechanical System Failures	249
7.1	Introduction	249
7.2	Strength of Mechanical Product	252
7.2.1	Introduction	252
7.2.2	Classical Beam Theory—Euler–Bernoulli Beam Theory	255

7.3	Mechanism of Slip	261
7.4	Fatigue Failure	263
7.4.1	Introduction	263
7.4.2	Fluctuating Load	263
7.4.3	Stress Concentration at Crack Tip	267
7.4.4	Crack Propagation and Fracture Toughness	269
7.4.5	Crack Growth Rates	272
7.4.6	Fatigue Analysis	274
7.5	Fracture Failure	283
7.5.1	Introduction	283
7.5.2	Ductile-Brittle Transition Temperature (DBTT)	285
7.6	Stress-Strength Analysis	287
7.7	Failure Analysis	289
7.7.1	Introduction	289
7.7.2	Procedure of Failure Analysis	290
7.7.3	Case Study: Fracture Faces of Product Subjected to Loads	294
7.8	Corrosion Materials	298
7.8.1	Introduction	298
7.8.2	Pourbaix Diagrams	299
7.8.3	Major Modes of Corrosion	301
	References	306
8	Parametric Accelerated Life Testing in Mechanical/Civil System	307
8.1	Introduction	307
8.2	Mechanical Product Breakdown	309
8.2.1	Introduction	309
8.2.2	Reliability Block Diagram	309
8.2.3	Product Configurations in RBD—Serial or Parallel	310
8.2.4	Automobile	311
8.2.5	Airplane	313
8.2.6	Domestic Appliance	313
8.2.7	Machine Tools	315
8.2.8	Agricultural Machinery and Heavy Construction Equipment	316
8.3	Reliability Design in Mechanical System	317
8.3.1	Introduction	317
8.3.2	Parametric ALT Plan for Mechanical System	318
8.4	Reliability Targeting of Mechanical Product	320
8.4.1	Introduction	320
8.4.2	Criteria and Method of Reliability Allocation	321
8.5	Failure Mechanics and Design	322

8.6	Parametric Accelerated Life Testing	324
8.6.1	Introduction	324
8.6.2	Acceleration Factor (AF)	326
8.6.3	Derivation of General Sample Size Equation	331
8.6.4	Derivation of Approximate Sample Size Equation	334
8.7	The Reliability Design of Mechanical System and Its Verification	337
8.7.1	Introduction	337
8.7.2	Reliability Quantitative (RQ) Specifications	339
8.7.3	Conceptual Framework of Specifications for Quality Assurance	343
8.8	Testing Equipments for Quality and Reliability	345
8.8.1	Introduction	345
8.8.2	Procedure of Testing Equipment Development (Example: Solenoid Valve Tester)	349
	References	359
9	Parametric ALT and Its Case Studies	361
9.1	Failure Analysis and Redesign of Ice-Maker	361
9.2	Residential Sized Refrigerators During Transportation	370
9.3	Water Dispenser Lever in a Refrigerator	375
9.4	Refrigerator Compressor Subjected to Repetitive Loads	385
9.5	Hinge Kit System (HKS) in a Kimchi Refrigerator	395
9.6	Refrigerator Drawer System	403
9.7	Compressor Suction Reed Valve	414
9.8	Failure Analysis and Redesign of the Evaporator Tubing	420
9.9	Improving the Noise of Mechanical Compressor	432
9.10	French Refrigerator Drawer System	440
9.11	Improving Reliability of the Hinge Kit System (HKS) in Refrigerator	448
10	Parametric ALT: A Powerful Tool for Future Engineering Development	461
10.1	Introduction	461
	Reference	464

Chapter 1

Introduction to Reliability Design of Mechanical/Civil System



Abstracts This chapter will be discussed with the necessities of new reliability methodology such as parametric accelerated life testing (ALT) in the established product developing process. By adopting new technologies of product in compliance with customer needs from marketplace, mechanical engineer tries to design new structure and mechanism embodied with the sophisticated features. By doing so, the modern mechanical products might survive in global competition. They are often required to have higher performance and reliability for the necessary intended functions, although the product cost and developing time reduce gradually. Mechanical products therefore have faulty designs in the structure configuration. Repeated loads or overloading in the product cause structural damage and finally reduce its lifetime. A failure of products with rare possibility might suddenly arise in field. Because new product has faulty designs in the speedy development time, there is the presence of risks on product recalls at all times. The design process of company requires new assessment methodology of reliability in lifetime. It includes discovering the design defects, correcting them, and checking if the lifetime target of product is achieved.

Keywords Design problems · Reliability assessment methodology · Parametric accelerated life testing · Customer requirements · Performance · Cost-down

1.1 Introduction

As customer requires living more comfortable, a myriad of technology innovations are constantly emerging and disappearing in market. Owing to state-of-the-art technical renovations, people broaden their lives and widen their boundaries. Competitive companies in high technology only can prosper in markets whose customers satisfy extreme needs, such as safety-critical mechanisms (aircraft) or high technology military armaments.

As the frequent recalls for new product occur globally, the term of product reliability seems to friendly be used to everyday life. The product reliability is to

design a product that can properly work the required intended functions under all environmental and operational conditions in lifetime of product. The product quality and reliability seem to become important requisites to ensure the continued success. If the company doesn't satisfy the product quality, it will be expelled in the current global competitive marketplace. Thus, it is important for the product design team to understand customer expectations or voices.

The product development in the mechanical/civil engineering system is continually confronting to be satisfied with the end user requirements—high control performance, high response, energy efficiency, low noise, high reliability, long life time, the latest hardware design, contamination resistance, low price, compact and highly-portable weight, and precision control for wide frequency range. As a result, the company should manufacture the high-performance products that meet the customer expectations or their specifications to survive the competitive global environments (Fig. 1.1).

Engineers, however, wonders if product development satisfies the requirement of these attributes in reality. To get those attributes in the product design such as automotive and cell phones, the product development periods are continually decreasing in response to the customer demands. On the other hands, product reliability in marketplace is highly required due to the recall costs. Thus, new product is hard to match the market requirements of product—cost reduction, the shortening developing time, higher performance and reliability. From the standpoint of system engineering, companies are asked to establish the design process of satisfying the product requirements in the short development time. For example,

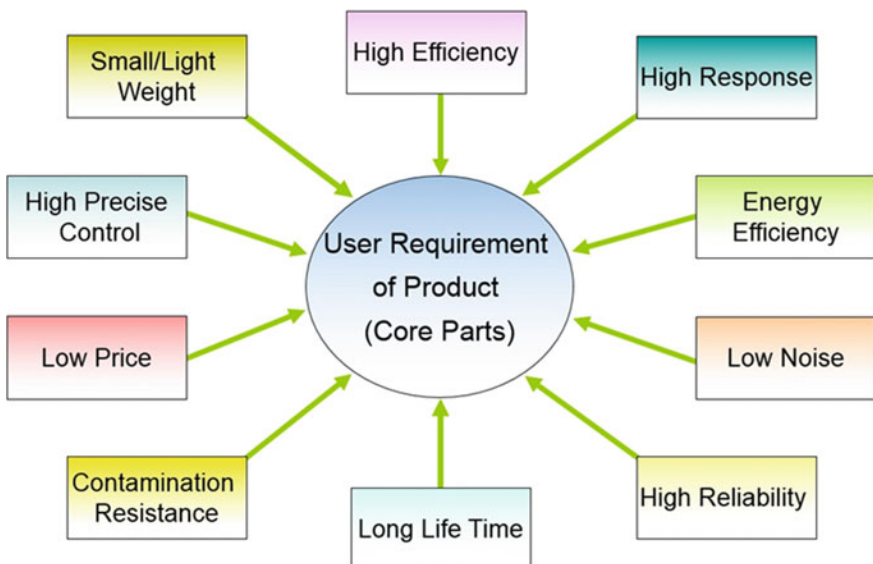


Fig. 1.1 Customer requirements of product (or core parts)

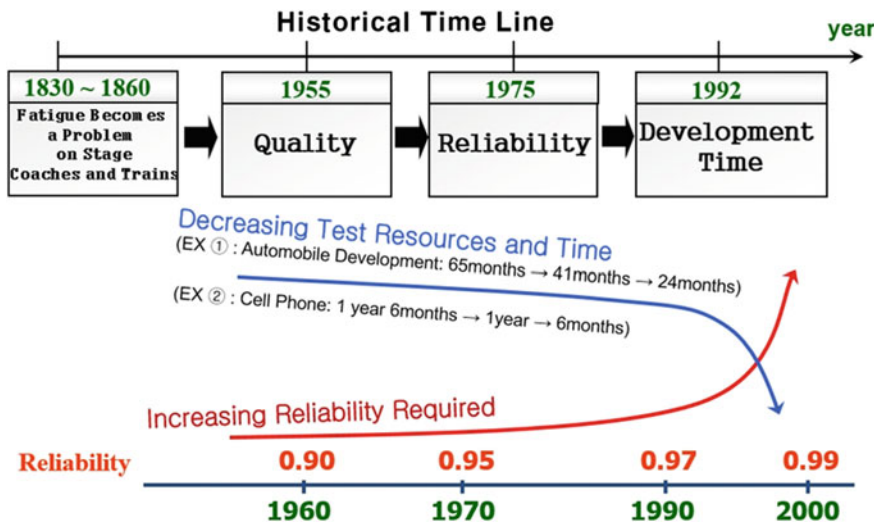


Fig. 1.2 Historical time line for product quality

while product development time of automobile continued to shorten from 65 to 24 months, the required reliability increases from 0.9 to 0.99. These declines mean that the global companies are required to have reliability methodology tools closely tied to the development process because it is not easy to meet two standards—developing time and reliability (Fig. 1.2).

In the relationship between failure costs and product life cycles, we know that the earlier reliability in the design process is applied, the greater the profit is obtained. Total cost of a product is determined by its design and its value is approximately known to have 70%. For example, if cost \$1 is required to rectify a design defect in the prior design stage, the cost would increase to \$10 after final engineering stage, \$100 at the initial production, and \$1000 at the mass product stage (Fig. 1.3).

Manufacturers experience frequent malfunctions as new product has been released in the marketplace. Customers ask to replace the problematic product with new one. To find out the faulty designs of product, most global companies have developed a variety of techniques in the product developing process. The product development in company can be largely classified as Research & Development (R&D) and Quality Assurance (QA).

R&D is a core part of the modern company because major design decisions are made to reveal the product features based on its technical level. As companies define the design requirements from customer needs or past experiences, they start to develop new product that satisfies those specifications. R&D activities also are conducted by departments with person specialized in technique. They design architectural structures, proper materials, and robust systems while considering the limitations—practicality, regulation, safety, and cost. A professional engineer can

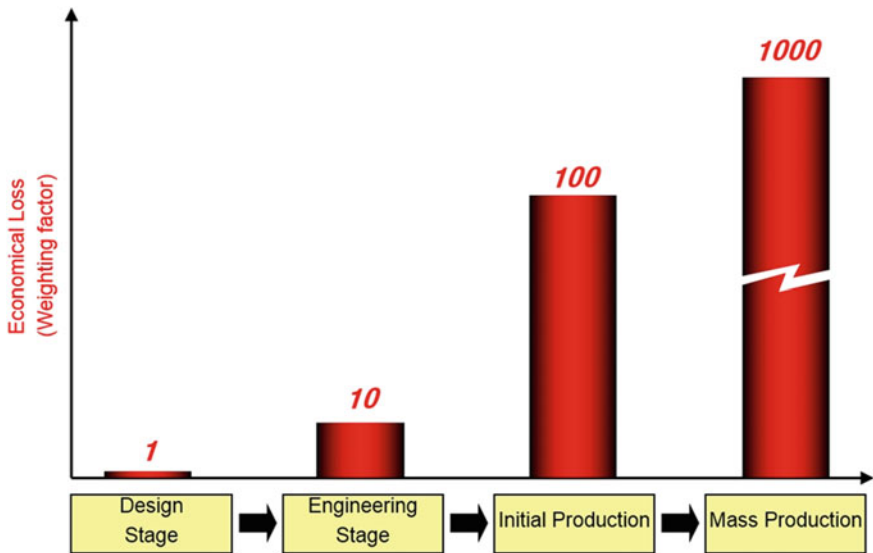


Fig. 1.3 Relationship between failure costs and product life cycles

apply the scientific methods to solve out engineering problems in the design process. They also use advanced manufacturing processes, expensive safety certifications, specialized embedded software, computer-aided design software, electronic designs and mechanical subsystems. The design process of product embedded in reliability concept can be briefly defined as qualitative design process and quantitative design process. It will briefly flow down the product planning, concept design, basic design, prototype, detail design, and production (Fig. 1.4).

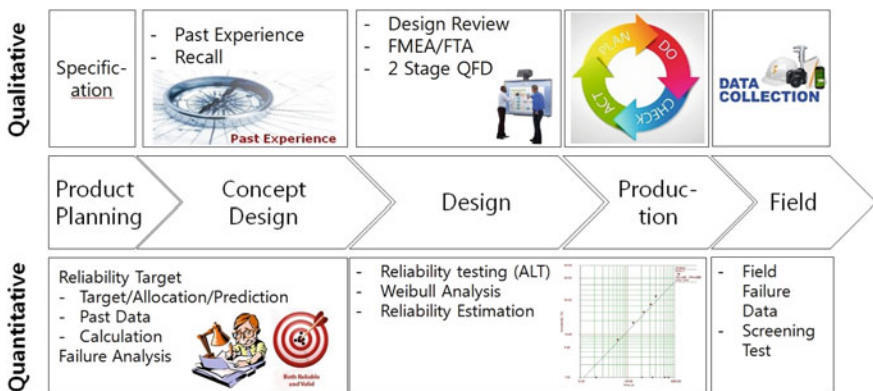


Fig. 1.4 New reliability-embedded design process

QA will determine if the detailed design of product is satisfactory to each company specifications. In other words the quality of product may be defined as the product specifications that are summarized in perception of the degree or the end-user's expectations. Quality verifications in these forms were initially established by National Aeronautics and Space Administration (NASA), the military and nuclear industries in the 1960s. The specification-oriented development process was designed to develop better products that have no design modifications or technical innovations at that time. And it was focused on manufacturing, testing and quality control, rather than design. At that time the typical design tools—design review, FMEA and FTA are to qualitatively accomplish the specifications of product quality. They focus on finding the causes of functional and physical failure, rather than statistic mathematic methods. But from a standpoint of quantitative quality, there is no design process whether product achieves the reliability targets for final design.

The traditional methodology in the design process cannot find the chronic problems for design issues of new technologies. Products always have inherent design problems in marketplace that might unceasingly give rise to massive recalls. For instance, the Boeing 787 Dreamliner experienced some problems due to new design elements—the fuselage of carbon-fiber-reinforced plastic (CFRP) and the electrical system incorporating lithium-ion batteries, which ultimately resulted in grounding.

From a standpoint of reliability engineering, why do the historical product recalls such as the explosion of challenger happen continually? They might come from the components that have the faulty designs not found in the established design process. The suspected components mounted in product determine the lifetime of product when they are subjected to the wear out stress or overstress under the end user operating or environmental conditions.

Mechanical products are continually required to find out the problematic parts mounted in product. New reliability-embedded developing process with new reliability methodology might be included: (1) product reliability target/allocation/prediction, (2) reliability testing and Weibull analysis, (3) finding the design problem of the suspected parts and modifying it, (4) checking if the final design meets the reliability requirements, and (5) proving the effectiveness through the analysis of the field failure data.

Before releasing the product to the marketplace, the quality activities are to discover the faulty designs of final product that have not been found in the design process. As a result, new quantitative reliability methodologies—parametric ALT in the reliability-embedded developing process would reveal the problematic components and prevent product recalls in the design phase that traditional R&D developing process can't solve. When failures in field happen for new product, Failure Analysis (FA) also will closely look up the returned samples to find out the design problems. Engineer in the early stage of reliability-embedded process generates reliability quantitative specifications to determine whether product achieves the reliability target. They can fit to a newly developed product and increase the lifetime of product by correcting the faulty designs.

Traditionally, fatigue testing (or fatigue analysis) without accelerated life testing can assess fatigue failure due to design defects. Fatigue testing is critical, but it has many limitations—(1) requires many physical prototypes (sample size), (2) difficult to achieve realistic tests because the failure concepts in field are not specified clearly, (3) slow and expensive difficult to conduct early in the design process, (4) requires many tests and statistical interpretation. However, the product still has the inherent design errors that will reveal to use in field soon or late.

Companies therefore are required to develop new reliability methodology like parametric ALT that finds the weak points in the design process. It consists of parametric ALT plan, parametric ALTs with acceleration factor and sample size equation, and design modifications with action plans. As a quantitative method, the parameter ALT will be helpful to assess whether product achieves the reliability target of product by establishing the verification specifications.

This book will describe the reliability design of mechanical system. First, after product recalls are reviewed in Chap. 2, reliability assessment tools developed in history will explain its strengths and weaknesses. To achieve the reliability requirements in field, numerous concepts—bathtub, MTBF and failure rate have been established through studies in the last century. They also require the fundamental knowledge of the other fields—probability and statistics. We will look over the basic notions such as failure mechanism, design and reliability testing in the consequent chapters. Chapter 7 will suggest the fundamental concepts of new reliability methodology—parametric ALT. A variety of parametric ALT case studies in Chap. 8 will also be proposed to clearly understand the methodology of the parametric ALTs.

1.2 Development of Mechanical Product

1.2.1 *Introduction*

To lead a comfortable life, engineers will design the mechanical systems—automobile, airplane, washing machine, air-conditioner, and the others. A mechanical system manages power to accomplish a task that involves forces and movement. Mechanical is derived from the Latin word *machina*, which can be defined as relating to machinery or tools. A mechanical system typically consists of (1) a power source and actuators that generate forces and movement, (2) a system of mechanisms that shape the actuator input to achieve a specific application of output forces and movement, and (3) a controller with sensors that compares the output to a performance goal and then directs the actuator input.

To better understand the design concept of mechanical system, we can see Boulton and Watt steam engine. The power is provided by steam expanding to drive the piston. The walking beam, coupler and crank transform the linear movement of the piston into rotation of the output pulley. Finally, the pulley

rotation drives the flyball governor which controls the valve for the steam input to the piston cylinder. The Boulton and Watt steam engine can schematically be described as slider-crank mechanism for changing reciprocating motion to rotary motion (Fig. 1.5).

Development of modern sophisticated mechanical system also requires the system engineering. It is an interdisciplinary field of engineering and engineering management that focuses on how to design and manage complex systems over their life cycles. At its core systems engineering utilizes systems thinking principles to organize this body of knowledge. Systems engineering [1] uses a host of tools that include modeling and simulation, requirements analysis and scheduling to manage complexity (Fig. 1.6).

Therefore, mechanical engineers design and build all types of products that are important in our everyday lives. The engineering design process will enable engineers to solve problems. Engineer also requires the inventive thoughts to settle the limited conditions. The engineering design process also is a multi-step process including the research, conceptualization, feasibility assessment, establishing design requirements, preliminary design, detailed design, production planning and tool design, and finally production. The basic patterns remain the same, though design process may depends on product type (Figs. 1.7 and 1.9).

1.2.2 *Mechanical Engineering Design Process*

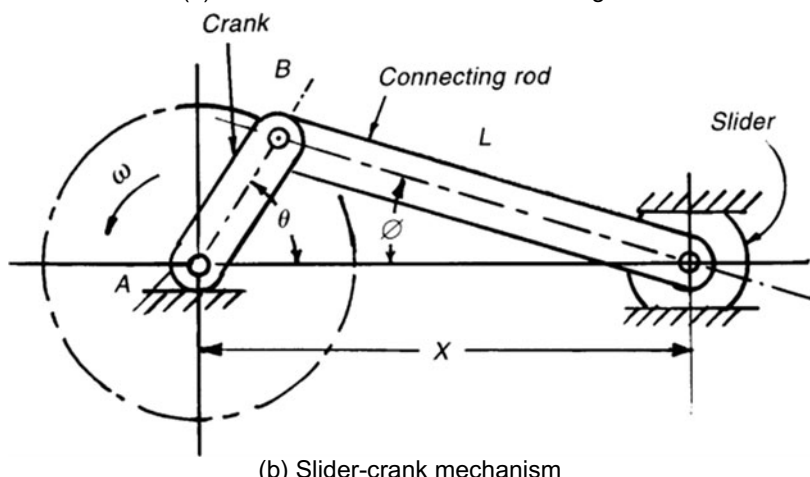
Design process of mechanical system is a formulation of plan to assist a mechanical engineer in creating a new product. The basic mechanical engineering concepts in mechanical engineering are applied to convert resources optimally to meet a stated objective. Most of mechanical product development covers a complete process: (1) generates the user requirement from market, (2) makes conceptual and physical design, (3) constructs prototype, (4) demonstrates the product, and (5) evaluates the final product (Fig. 1.8).

It therefore can transform a technical market opportunity into a product available for sale. The main variables that drive end user needs are cost, time and quality. Aiming at these three variables, companies have to develop new mechanical product that better satisfy customer requirements and increase their own market share. There are many technical uncertainties in market which companies must face throughout the process (Fig. 1.9).

The design of mechanical system process begins with understanding the customers and their needs. Ideas for new products can come from a variety of sources both within and outside the firm. Internal sources include employees, research and development, market research sales force and reverse engineering. The external sources include customers, legislation, environment, technology and strategic position of the organization. Competitors are the source of ideas for new products or services. Perceptual maps, bench marking and reverse engineering can help companies learn from their competitors.



(a) James Watt's Industrial Steam Engine



(b) Slider-crank mechanism

Fig. 1.5 James Watt's Industrial Steam Engine, Boulton & Watt, Soho, 1788

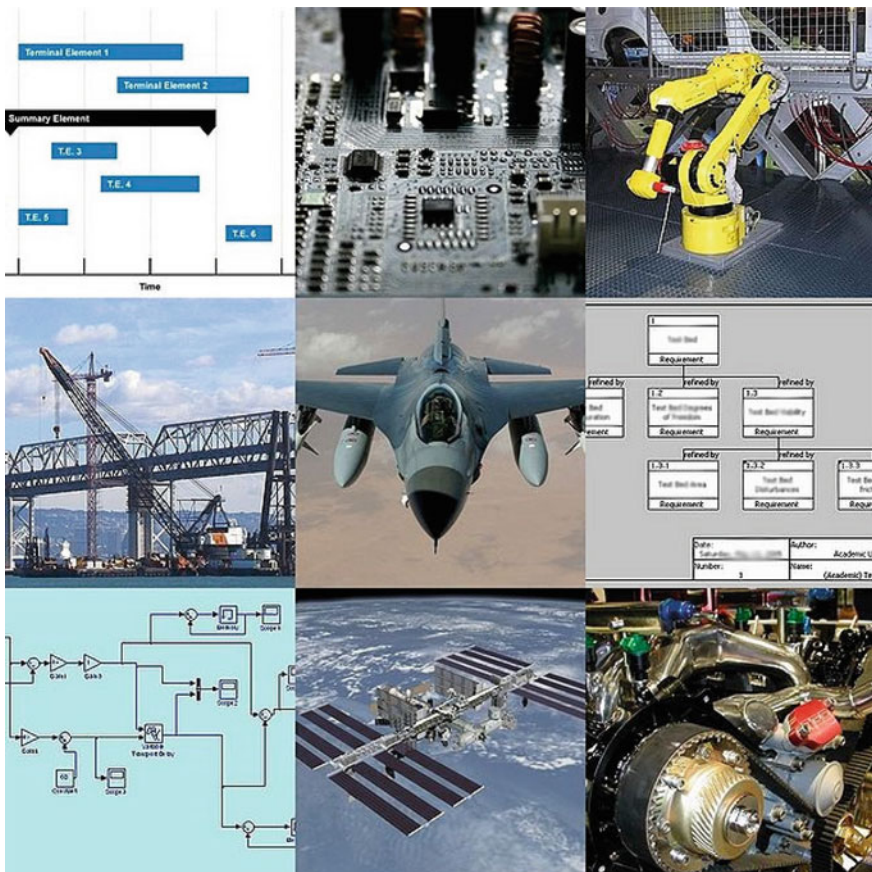


Fig. 1.6 Development of mechanical product from Wikipedia

Perceptual maps helps to compare the customer perceptions of a company's products with competitor's products. It is a visual method of comparing customer perceptions of different product or services. Bench marking refers to finding the best in class product or process, measuring the performance of your product or process against it and making recommendations for improvement based on the results. Reverse engineering refers to carefully dismantling and inspecting competitor's products to look for design features that can be incorporated to improve one's own products.

Each of these sources gives a different emphasis on the requirements and importance of idea generation for new product. They become the concept requirements in the product planning before advancing the feasibility assessment for new product.

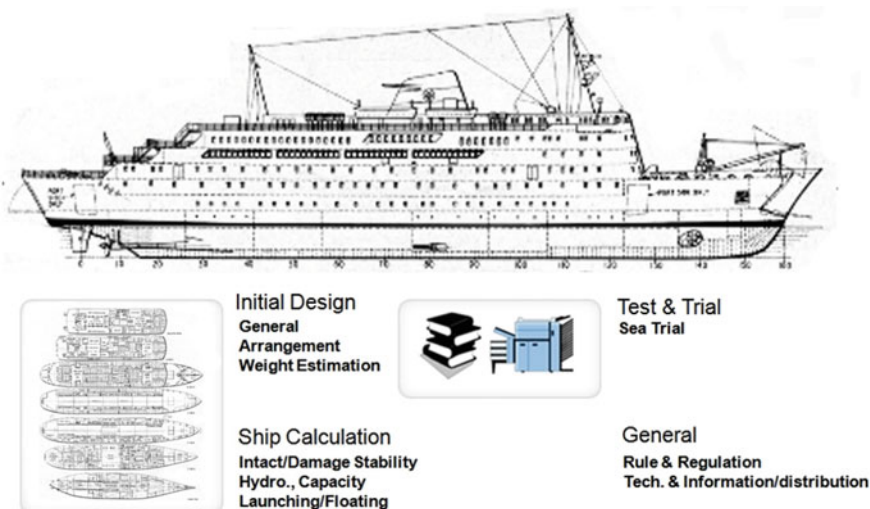


Fig. 1.7 Development process of ship

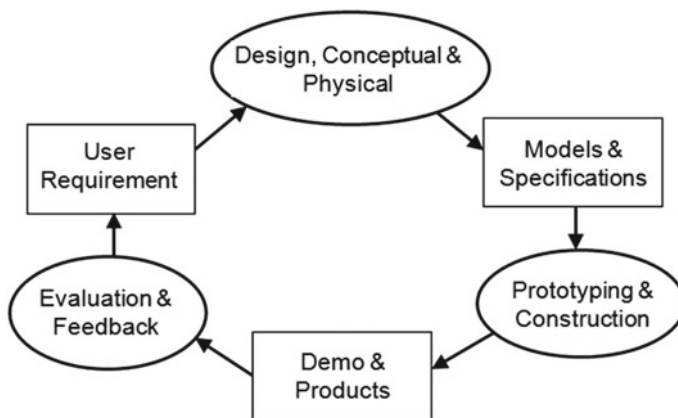


Fig. 1.8 Iterative design overview of mechanical product

1.2.2.1 Feasibility Assessment

The purpose of a feasibility assessment is to determine whether the engineer's project can proceed into the design phase. Engineer will question whether this project is based on two criteria: (1) achievable engineer idea and (2) cost constraints. The feasibility study is a critical process to have an engineer with experience and good judgment because they know whether the engineer's project is possible or not. The following questions also may be useful:

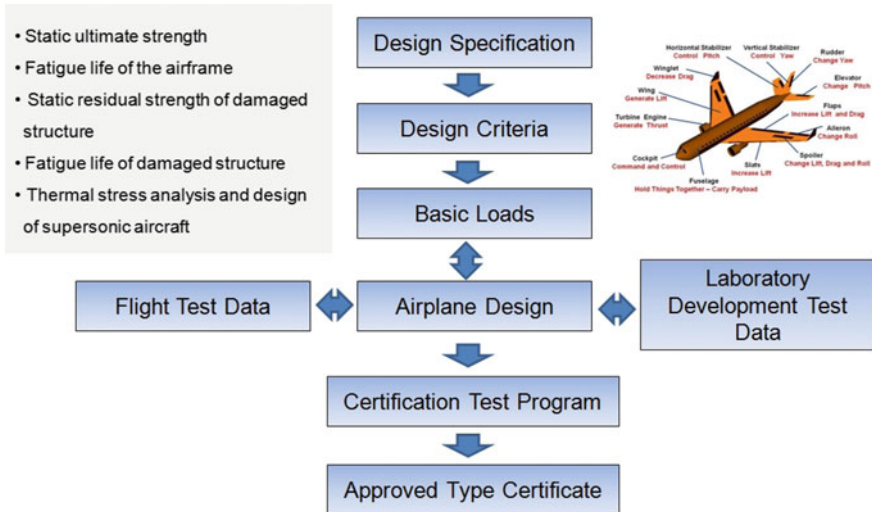


Fig. 1.9 Development process of airplane

- Are the proposed technologies commercially available?
- Does product use any proprietary technologies?
- Are the components needed to build the system commercially available?
- Can the know-how on product be obtained on the market?
- Are there any product features that are not suited to the project requirements?

To answer the above questions in the engineering design process, designers jump back and forth between steps. This way of working is called iteration.

1.2.2.2 Establishing the Design Requirements

Establishing design requirement analysis is one of the most important elements in the design process. A design requirement is a statement about an intended function that specifies what it should do or how it should perform. There are two types of requirements: (1) functional requirements, i.e., what the system should do? (2) Non-functional requirements, i.e., what constraints there are on the system and its development—data, environment, user, and usability (Fig. 1.10).

1.2.2.3 Preliminary Design

In the preliminary design, mechanical engineers create a design from the specifications. They make an engineering model and have design before creating engineering drawings and documents. The preliminary design bridges the gap between

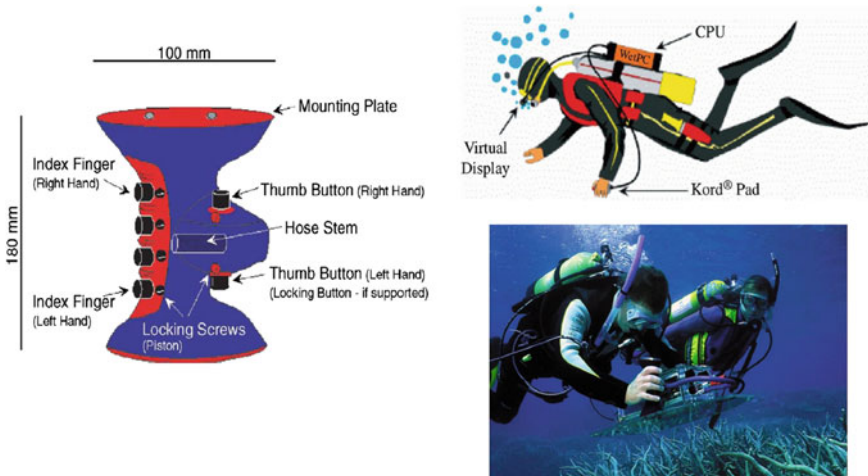


Fig. 1.10 Establishing the design requirements (an extreme example)

the design concept and the detailed design phase. If the overall system configuration in this task is defined, it will provide schematics, diagrams, and layouts as the project early project configuration. In the preliminary design engineer focuses on making the general framework of product.

It is difficult to find and apply an algorithm of the solution finding process in mechanical engineering. In most cases new solutions come from past experience, observations and common sense. The engineering solution at this stage must be free hand sketched or by using simple drawing conventions. And from the standpoint of kinematics it must be viable when the configuration is implemented. For ship, preliminary design includes determination of the main hull characteristics that is dimensions, form coefficients, lightship weights, basic hydrostatics and rough-order-of-magnitude cost estimate (Fig. 1.11).

Which the solution of preliminary design is the best? A set of criteria should be established for decision. The selected idea has to be refined in order to meet the assumed specifications. This procedure consists in the selection of an arrangement of the component in product module, link lengths, angles etc., and it is done either analytically, or—my recommendation—by a scaled drawing. We can use drawing instruments like CAD at this stage.

At the end of this phase the engineer works and their report are summarized and delivered to the customer. They should be clear to all parties what the final product will look like and what its features will be. If, after the review, parts of the design need to be modified, this will be incorporated into the next phase.

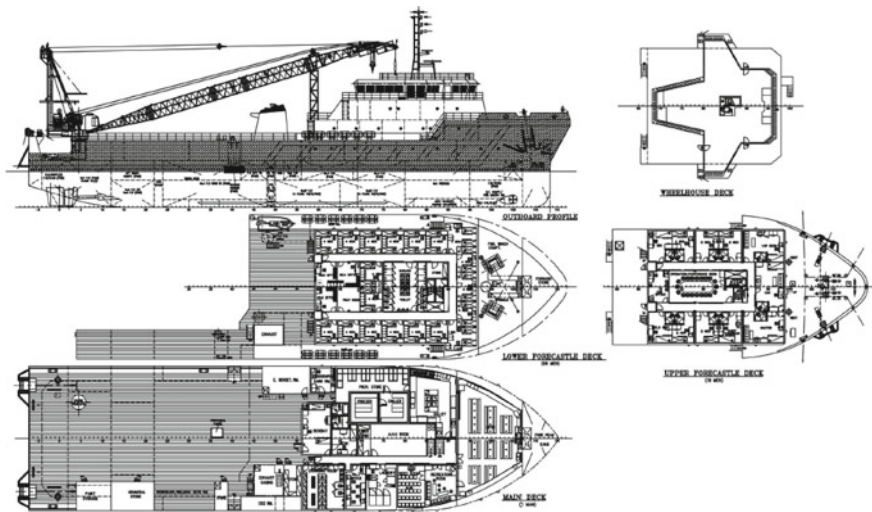


Fig. 1.11 Preliminary design for ship

1.2.2.4 Conceptual Design

Conceptual design is often a phase of project planning to describe how a new product will work and meet the design requirements. It includes producing ideas and taking into account the pros and cons of implementing those ideas. Engineers in this phase have to identify the problems—the external load, limitations in terms of geometry, manufacturing methods, etc. The project is to minimize the probability of error, manage costs, assess risks, and evaluate the potential success of the intended project. If an engineering issue or problem is defined, potential solutions must be identified. These solutions can be found by the mental process such as inventive ideas (Fig. 1.12).

To expand the conceptual model into detailed design, the following questions have:

- What functions will the product perform?
- How are the functions related to each other?
 - Temporal (sequential or parallel)
 - Categorization
- What information needs to be available?

What are you seeing?



By shifting perspective you might see an old woman or young woman

Fig. 1.12 Shift perspective for inventive thoughts (example)

Form design refers to the physical appearance of a product, its shape, size, color, styling etc. Aesthetics aspects such as image, market appeal, special identification, finish etc. will also form a part of the form design.

1.2.2.5 Detailed Design

As a core in the engineering design process, the detailed design consists in the selection of geometry (shape and dimensions), materials and of some dynamic properties for the selected solution.

- (1) Selection of shape: The shape should be best suited to the load transferred. There is no problem with the power screw and pins. These are standardized. The problem is with the links. What shape is good for a compressed member (buckling)? A channel (roll-formed), a double flat bar arrangement will do.
- (2) Selection of material: The power screw must be flexible yet tough. Medium carbon plain or alloy steel might be a good choice. Links: as buckling depends on the section modulus only, low carbon steel is the best choice. Finally pins (resistance to wear): high carbon steel.
- (3) Selection of dimensions: There is a distinct difference in the way problems are solved in the Strength of Materials and (Optimal) Design courses. In the strength course all dimensions are usually given, and controlled are actual stresses in an element. For a simple round bar with a cross-section A subjected to a tensile load F we have: $= F/A \leq k_r$; where $k_r = R_e/FS$ (R_e = the yield strength; FS = the factor of safety).

In the design approach, assumed are limiting stresses and calculated are dimensions, here: $d \geq \sqrt{4F/(k_r)}$. Unfortunately, this approach is not always possible. If all the necessary data (tensile/compressive load, torque) are given, we use a complex stress formula. In the design approach, we usually know only the tensile load. The diameter is calculated based upon a simple formula for tensile stress, but

using a very high value of the factor of safety or a correction factor to make up for additional load.

As computer-aided design advances, the detailed design enables the engineer to completely describe a product through solid modeling and drawings. This is because a CAD program can provide optimization, where it can reduce volume without hindering the part's quality. Using the finite element method, engineer can also calculate stress and displacement to determine stresses throughout the part. It is the engineer's responsibility to determine whether these stresses and displacements are allowable, so the part is safe (Figs. 1.13 and 1.14).

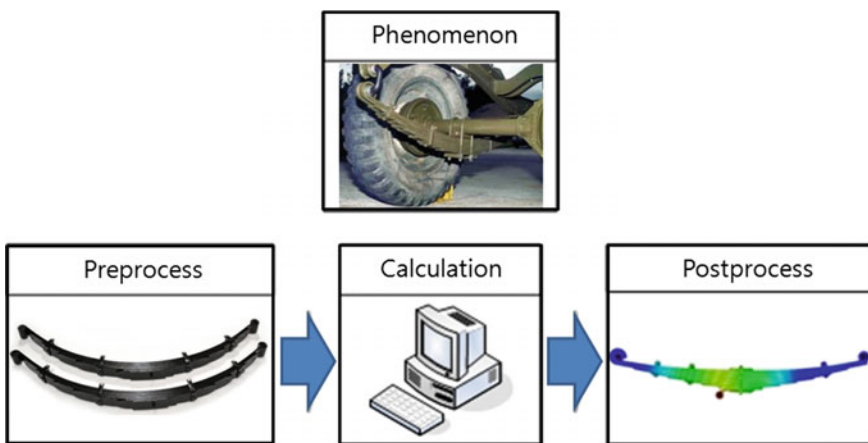


Fig. 1.13 Detailed design by finite element analysis (FEA)

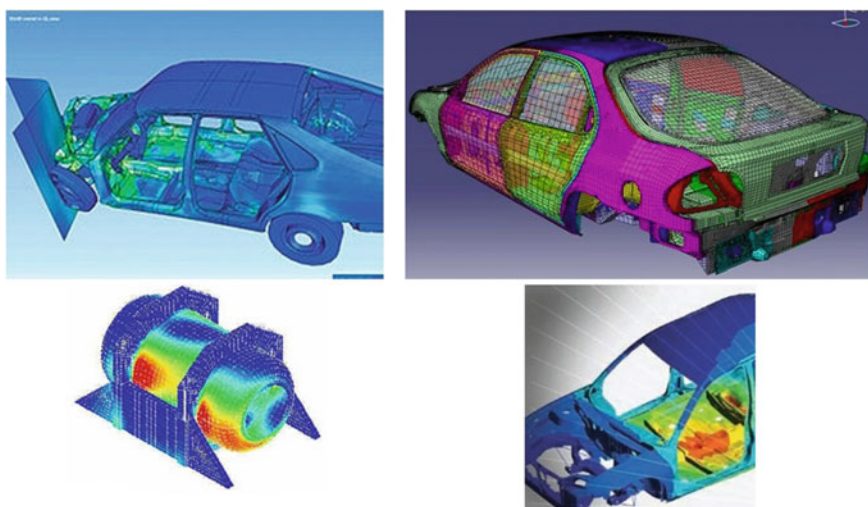


Fig. 1.14 Typical results of finite element analysis (FEA)

The final design consists of detailed drawings and specifications for the new product. The accompanying process plans are workable instructions for manufacture including necessary equipment's and tooling, component sources job descriptions, work instructions and programs for computer-assisted machines.

1.2.2.6 Production Planning and Tool Design

The production planning and tool design is planning how to mass produce the project and which tools should be used in the manufacturing of the part. Tasks to complete in this step include selecting the material, selection of the production processes, determination of the sequence of operations, and selection of tools, such as jigs, fixtures, and tooling. This task also involves testing a working prototype to ensure the created part meets qualification standards.

Production design is concerned with how the product will be made. Design is difficult to make result in poor quality products. During the design stage itself the manufacturing aspects should be considered. The production design includes simplification, standardization and modularity.

Design simplification attempts to reduce the number of parts, subassemblies and options into a product. Standardization refers to use of commonly available and interchangeable parts and subassemblies. Modular design consists of combining standardized building blocks or modules in a variety of ways to create a unique finished product.

1.2.2.7 Production

Launching a new product or service involves ramp up production. The process has been refined and debugged, but it has yet to operate at a sustained level of production. In ramp up, production starts at a relatively low level of volume as the organization develops confidence in its abilities to execute production consistently and marketing's abilities to sell the product, the volume increases. Launching the new product or service involves co-coordinating the supply chain and rolling out marketing plans. Marketing and production will work in a co-coordinated way during this phase (Fig. 1.15).

1.2.2.8 Limitations of the Established Design Process

The established developing process of product often focuses on implementing the customer requirements, and company produces their architecture (or structure) confirmed by Research & Development (R&D) and Quality Assurance (QA). As previously studied in Sect. 1.2, the engineering design process consists of establishing design requirements, preliminary design, detailed design, production planning and tool design, and finally production.

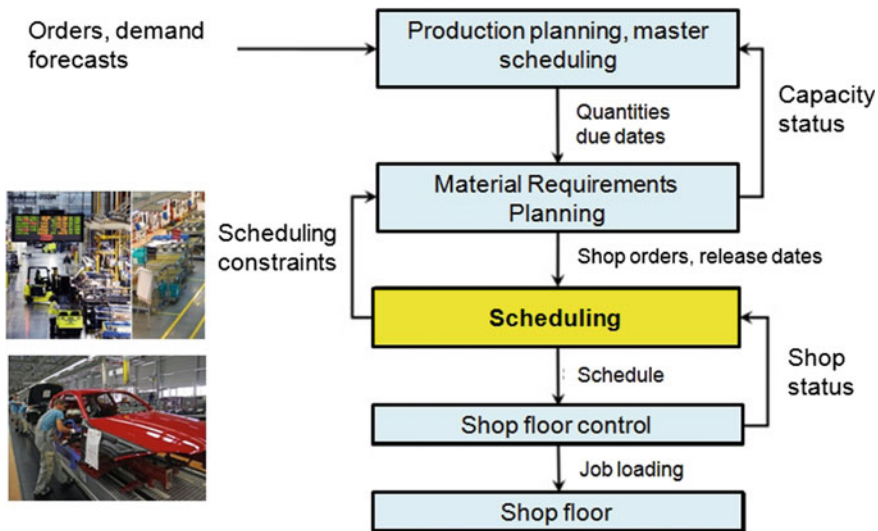


Fig. 1.15 Automobile production (example)

Therefore, mechanical engineers make a design and build new product architecture. However, there is no design process to confirm if new architecture of mechanical product has a good quality—enough strength and stiffness. As a result, company often recalls new product. Based on the reliability concept, company requires new reliability-embedded developing process with reliability methodology that will be discussed in Chaps. 8 and 9. It consists of (1) product reliability target/allocation/prediction, (2) parametric Accelerated Life Testing with accelerated factor and sample size equation, (3) finding the design problems of the suspected parts and modifying it, and (4) proving the effectiveness through the analysis of the field failure data.

Reference

1. Defense of Department (2001) Systems engineering fundamentals. Defense Acquisition University Press, Fort Belvoir, VA, p 31

Chapter 2

Product Recalls and Its Assessment Significance



Abstract This chapter will review the historical product recalls including natural hazard and the methodology of its reliability assessment that were developed in the last century. Based on product specifications, engineer would develop new mechanism and its structure. In marketplace product recalls frequently happen. They come from the inheritance design defects in the problematic parts and are determined by the lifetime of product. If product is subjected to repeated loads or overloading and there is faulty design, product failure suddenly arises in its lifetime. To prevent it, engineers in the previous century have developed new reliability concepts such as the bathtub curve, Weibull analysis, data analysis, and the others. For instance, the frequent derail accidents of railroad in the early of nineteen century started the research for its root cause and made the S-N Curve. The chronic failed vacuum tube in the WWII created the bathtub curve. As NASA developed for the space shuttle program in the mid-sixties, FMEA, FTA and Weibull analysis for reliability testing today have been widely used in company. Now since Integrated Circuit (IC), transistor radio and TV in the late of 1960s are introduced, Physics Of Failure (POF) become more important tools to analyze the failure mechanics in product. However, in the field of mechanical/civil system, representative POFs were still fracture and fatigue. As improperly choosing shape and material in the design process, product has faulty design—enough strength and stiffness in the final structure of product. As a solution mechanical engineer should find the problematic parts by reliability testing method and modify them before product launches in market.

Keywords Product recalls • Reliability concepts • Bathtub curve • Physics of failure (POF)

2.1 Introduction

A disaster—oil spill, nuclear plant accident and the others is a deep-felt functional failure of the product accompanying catastrophic human, economic or environmental impacts, which has no predicting ability of the community or society to manage its own resources. Thus, peoples often have been learning the lessons because they can be prevented if its root causes were known previously. For instance, the RMS Titanic in 1912 had approximately 2200 people on board. When the crews sighted the iceberg, Titanic was unable to quickly turn and collided the floating ice in right side. It took two hours and forty minutes to sink and drowned to deaths of more than 1500 people. There was no rescue plan, though the ship was sinking fast in few hours.

From standpoint of engineering the sinking of the titanic was caused primarily by the brittleness of the steel used to construct the hull of the ship for the icy water of the North Atlantic Ocean. Even a small impact between ice burger and ship, it could have caused a large amount of damage. As a result, the bolts that were holding the steel plates together fracture, and finally break down the hull (Fig. 2.1).

After the disasters of RMS titanic, every ship has to have an evacuation plan in danger. When disasters have been studied for more than 40 years, disasters might have been seen as the result of inappropriately risk management or mutual



Fig. 2.1 Sinking picture of the RMS Titanic Illustration for “Die Gartenlaube” magazine by Willy Stöwer, 1912

combination of hazards and vulnerability. If properly controlled, it can be prevented from developing into a disaster.

Another interesting story for product recall is the development of V-1 missile by Germany engineering group during World War II. In spite of attempts to provide high-quality parts and careful attention, the first ten V-1 missiles ended in a total fiasco. All the first missiles either exploded on the launching pad or landed “too soon”. Robert Lusser, a mathematician, analyzed the missile system. He derived the product probability law of series components—systems functioning only if all the components are functioning. That is, system reliability is equal to the product of the reliabilities of the individual components.

If the system comprises a large number of components, the system reliability would be low. In the United States, the quality of the individual components attempts to improve low system reliability. As better raw materials and better designs for the products were selected, high system reliability was achieved. However, there was no extensive systematic analysis of the problem and the experimental methodology like reliability testing—parametric accelerated life testing that can find the problematic parts and improve them.

After World War II, the product globally continued to develop in market required a multiple function of products, composed of many components like automobile, airplane, television sets, electronic computers, etc. Furthermore, as complicated control and safety systems also became steadily more requiring, the probability for product recall increased in market. Because the lifetime of mechanical product was determined by the faulty design of problematic parts, it was important to find out it in the design process before launching product.

In addition, a natural hazard will briefly be explained before going into the product recalls. Developing countries—the Philippines, Nepal and the others are suffering from natural hazards that are caused into more than 95% of all deaths, and they are 20 times greater than that of industrialized countries. They are all natural hazards that kill thousands of people and destroy billions of dollars of habitat and property each year. Because there is no single root cause from natural hazards, they are more common in developing countries than those countries have no emergency systems. Typical examples are flood, transport accidents, nuclear explosions/radiation, and an earthquake that causes a tsunami, resulting in coastal flooding. Recorded in magnitude 9.2, the 1964 Alaskan earthquake occurred in March 27 and resulted in 139 deaths. Anchorage experienced great destruction or damage to many houses, buildings, and infrastructures like roads, particularly in the several landslide zones along Knik Arm.

Recently the population growth in the world and its environmental effects has increased the severity of natural hazards due to the global warming, depletion of the ozone layer, and the Central Pacific El Nino phenomenon. The well-known several reasons—the tropical climate and unstable land forms, coupled with the deforestation of the Amazon, unplanned growth proliferation, non-engineered barbaric constructions—in the worldwide make the natural hazard areas more vulnerable (see Fig. 2.2).

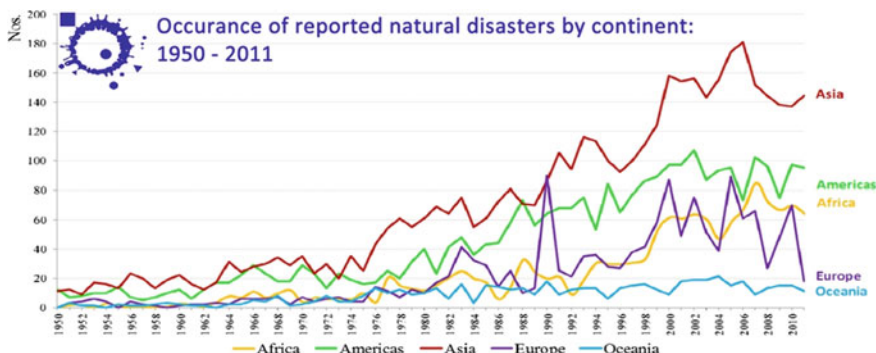


Fig. 2.2 Occurrence of reported natural disasters by continent (1950–2011). *Sources* Reported natural disasters 1950–2011 from CRED

Typical counter measures against natural hazards can be classified into (1) research into the scientific aspects of disaster prevention, (2) the reinforcement of the disaster prevention system, its facilities and equipment, and other preventive measures, (3) construction projects—dam and meteorological [weather] observations—designed to enhance the country's ability to defend against disasters, (4) and emergency measures and recovery operations. Developing countries suffer chronically from natural hazards, though several preventions for natural hazard.

For instance, after the Kobe earthquake in 1981 claimed some 5100 lives, Japan updated its building guidelines, added fresh fuel to another round of research on earthquake safety and disaster management. In 2000, the country's building codes with specific requirements and mandatory checks were revised. From 1979 to 2009, Shizuoka prefecture poured more than \$4 billion into improving the safety of hospitals, schools and social welfare facilities. Though Japanese cities often shake, they rarely topple. Because Japan is located in the Pacific Rim, one of the Earth's most violent earthquake and volcano zones, they are still vulnerable.

2.2 Product Recalls

Product recalls are the consequence of technological risks due to product design failures or human-induced damages. It comes from the problematic parts that are determined by product lifetime. Typical examples include transport accidents, industrial accidents, oil spills and nuclear explosions/radiation. Deliberate terrorism, like the September 11 attacks, may also be put in this category. When the root causes of product recalls are considered, there might have been product complexity as demanded by customers and the faulty designs of its parts.

For example, today a typical Boeing 747 jumbo jet airplane is made of approximately 4.5 million parts including fasteners, multiple modules, and

subsystems. An automobile is made of more than 25,000 parts, multiple modules, and subsystems. In 1935 a farm tractor was made of 1200 critical parts and in 1990 the number increased to around 2900. Even for relatively simpler products such as bike, there has been a significant increase in complexity with respect to parts. Consequently, the product design like automobile depends on these parts (Fig. 2.3).

Together with product complexity, there are possibilities for the inherent design problems of the parts as new product structure due to the product performance and cost-down is adapted. A study performed by the U.S. Navy concerning parts failure causes attributed 43% of the failures to design, 30% to operation and maintenance, 20% to manufacturing, and 7% to miscellaneous factors. While the design cost occupies only 5% in actual cost, the cost influence holds 70% (Fig. 2.4).

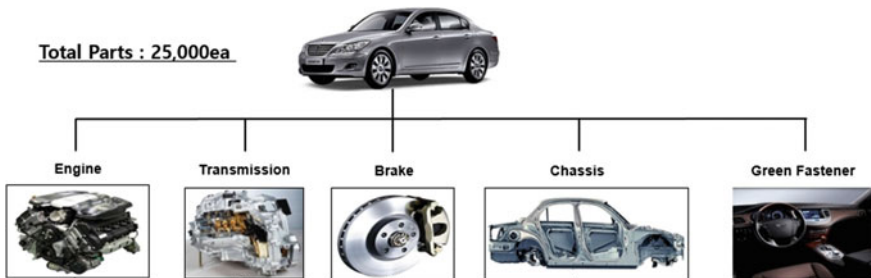


Fig. 2.3 Breakdown of passenger automobile with multi-modules

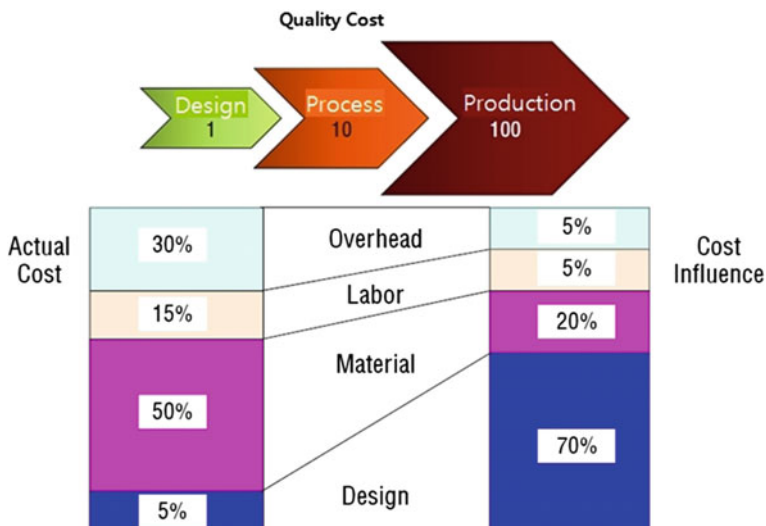


Fig. 2.4 Leverage in product design: total cost of product is determined by its design (approximately 70%)

Thus we will have suggested typical examples for product recalls—space shuttle challenger, Chernobyl nuclear reactor, Point Pleasant Bridge, hull and deck cracks in Liberty ships, leaked gas in McKee Refinery, and the others. They also might have been prevented if reliability in product design had been known and considered seriously. It also will help to understand why the reliability concept of modern product is critical.

- Space Shuttle Challenger: This debacle occurred in 1986, in which all crew members lost their lives. Sadly, many Americans are suffering from low self-esteem because of failure. The main reason for this disaster was design defects of rubber o-rings under cold winter in Texas (Table 2.1).
- Chernobyl Nuclear Reactor Explosion: This disaster occurred in 1986, in the former Soviet Union, in which 31 lives were lost and still contaminated by radioactivity in this area. The debacle was the result of design defects such as faulty switch in reactor design (Table 2.2).

Table 2.1 Summary of space shuttle challenger disaster

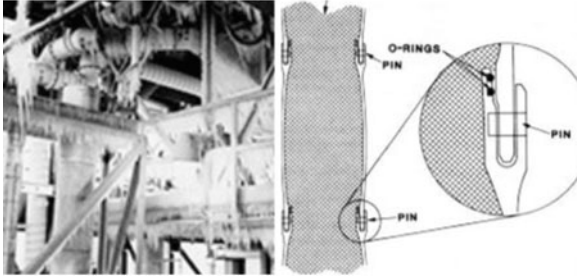
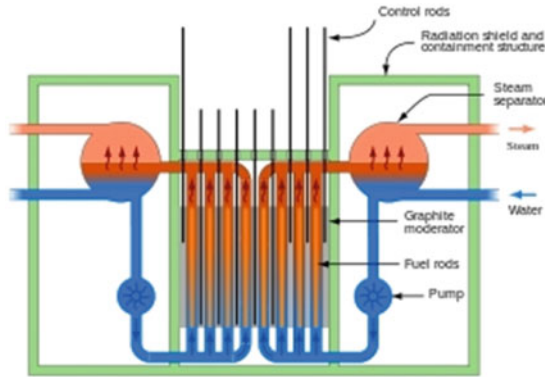
	Product recall
Phenomenon	
Structure	
Root Cause	<p>Failure of two rubber O-rings (Environment conditions: A Cold Launch Day)</p>

Table 2.2 Summary of chernobyl nuclear reactor explosion

	Product recall
Phenomenon	
Structure	
Root Cause	Reactor explosion due to faulty components (Reactor is jumped to around 30,000 MW thermal)

- Point Pleasant Bridge Disaster: Bridge located on the West Virginia/Ohio border collapsed in 1967. The disaster resulted in the loss of 46 lives and its basic cause was the metal fatigue of a critical eye bar in suspension bridge (Table 2.3).

And in the following sections we can suggest the numerous other cases for product recalls that will help to understand their root causes of modern products.

- Early Liberty ships suffered hull and deck cracks: During World War II, there were nearly 1500 instances of significant brittle fractures. Twelve ships, including three of the 2710 Liberties built, broke in half without warning,

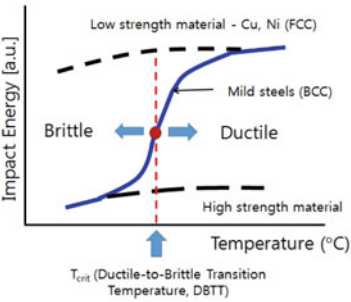
Table 2.3 Summary of point pleasant bridge disaster

	Product recall
Phenomenon	
Structure	
Root Cause	Metal fatigue of a critical eye bar

including the SS John P. Gaines which sank on 24 November 1943 with the loss of 10 lives (Table 2.4).

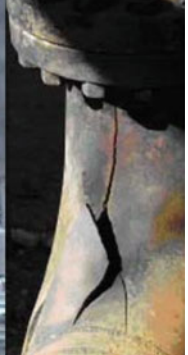
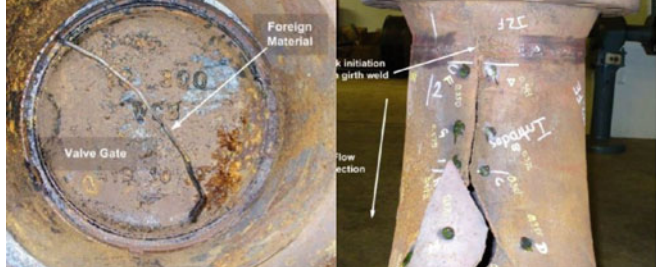
- A Day at McKee Refinery, 2007: Propane gas leaked from the McKee Refinery's Propane Deasphalting Unit in Sunray, Texas. Three workers suffered serious burns and the refinery was shut down for two months. Gas prices increased 9 cents per gallon in the west (Table 2.5).

Table 2.4 Summary of early liberty ships disaster

	Product recall
Phenomenon	
Structure	
Root Cause	Low temperature embrittlement of the steel (short timescale from design to construction)

- Seongsu Bridge Collapse: This disaster occurred in October 21, 1994. Because of the improper welding of the steel trusses, the bridge collapsed. 32 people died and 17 were injured in the accident. Afterwards, the bridge was supposed to be repaired, but, it had to be completely redesigned and rebuilt. The new design was finished on 15 August 1997, and is similar to the original design (Table 2.6).

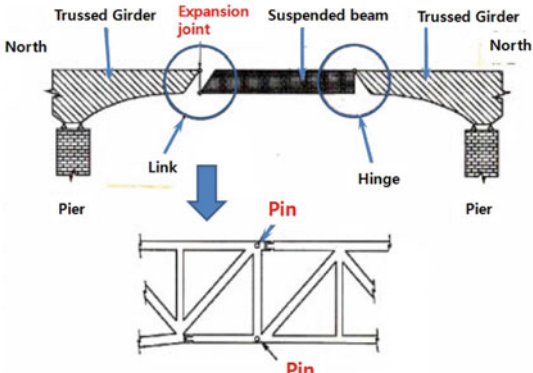
Table 2.5 Summary of McKee refinery disaster

	Product recall
Phenomenon	 
Structure	
Root Cause	Freezing water cracked a pipe that had been unused for fifteen years

2.2.1 Versailles Rail Accident in 1842

The Versailles rail accident in 1842 occurred on the railway between Versailles and Paris. Following King Louis Philippe I's celebrations at the Palace of Versailles, a train returning to Paris derailed at Meudon. After the leading locomotive broke an axle, the carriages behind piled into it and caught fire. With approximately 200 deaths including that of the explorer Jules Dumont d'Urville, the first French

Table 2.6 Summary of Seongsu bridge collapse

	Product recall
Phenomenon	
Structure	
Root Cause	Improper welding of the steel trusses of the suspension structure beneath the concrete slab roadway.

railway accident and the deadliest in the world recorded. Because most of passengers wearing the seat belt were died, the accident led to abandon the practice of locking passengers in their carriages. It started the study of metal fatigue subjected to repetitive loads like S-N curve (see Fig. 2.5).

- Root Cause: Metal fatigue of rail was poorly understood at the time and the accident is linked to the beginnings of systematic research into the failure problem.



Fig. 2.5 Versailles rail accident (1842) from Wikipedia

2.2.2 *Tacoma Narrows Bridge in 1940*

The Tacoma Narrows Bridge is a pair of twin suspension bridges that connect the city of Tacoma to the Kitsap Peninsula. It went past State Route 16 over the strait and was collapsed by a wind-induced natural frequency on November 7, 1940. The collapse of the bridge had no loss of human life. As recorded on film, it has still been well-known to engineering, architecture, and physics students as a cautionary tale (see Fig. 2.6).

Whenever the natural frequency of vibration of mechanical structure coincides with the frequency of the external excitation like winds, resonance occurs. Due to excessive deflections and the subsequent system failure brought, vibration testing has become a standard procedure in the design and development of most mechanical systems.

- Root Cause: without any definitive conclusions, three possible failure causes are assumed.
 - (1) Aerodynamic instability by self-induced vibrations in the bridge structure
 - (2) Periodic eddy formations in bridge
 - (3) Random turbulence effects—the random fluctuations by wind velocity of the bridge.



Fig. 2.6 Tacoma narrows bridge (1940) from Wikipedia

2.2.3 *De Havilland DH 106 Comet in 1953*

The de Havilland DH 106 Comet was the first commercial jet engine airplane that replaced the propeller plane and enable people to have a transatlantic flight. The Comet prototype first had an aerodynamically design with four turbojet engines in two wings, an aerodynamic fuselage, and large square windows. It first flew on 27 July, 1949. For the 1952 appearance, it offered a quiet and comfortable passenger cabin.

One year later the Comets began to suffer the design problems that three airplanes were breaking up in flight. Due to airframe metal fatigue, the Comet eventually discovers the design flaw sat the corners of the square windows subjected to repetitive stresses. As a result, the Comet was redesigned with oval windows, structural reinforcement, and other changes (Figs. 2.7 and 2.8).

- Root Cause: fine cracks near the fixed nails of large square windows → repeated pressurization and decompression in airplane → spreading cracks → limit crack → blast in air by the broken window of airplane.



Fig. 2.7 De Havilland DH 106 Comet (1954) from Wikipedia

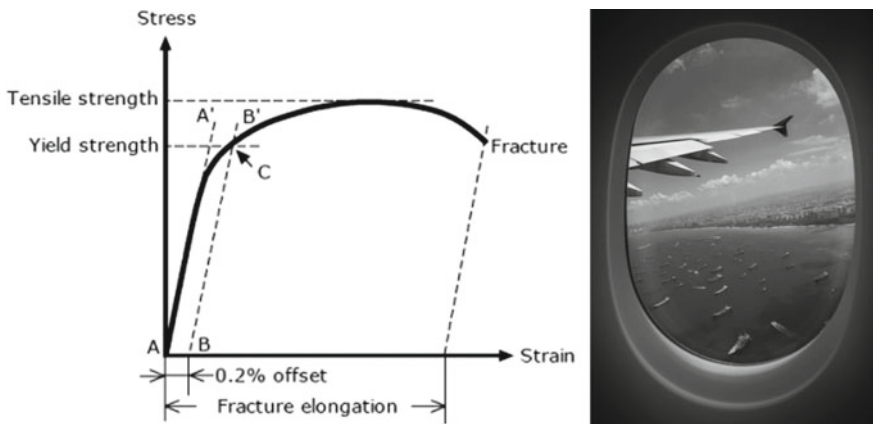


Fig. 2.8 Stress-strain curve and the modified oval window in airplane

2.2.4 G Company and M Company Rotary Compressor Recall in 1981

In 1981, market share and profits in G company appliance division were falling. For example, making refrigerator compressor required 65 min work of labor in comparison to 25 min for competitors in Japan and Italy. Moreover, labor costs of G

Company were higher than that of Japan companies. The alternatives were to purchase compressors from a better design model of Japan or Italy. By 1983, G Company was decided to build a new rotary compressor in-house along with a commitment for a new \$120 million factory. G Company and a rival M company had invented the rotary compressor technology that had been using it in air-conditioners for many years.

A rotary compressor had the less weighted part because of one third fewer and was more energy efficient than the conventional reciprocating compressors. The rotary compressors took up less space, thus providing more room inside the refrigerator and better meeting customer requirements. The rotary compressor for refrigerator was nearly identical to that used in air conditioners.

However, in a refrigerator, the coolant flows only one-tenth as fast and the unit runs about four times longer in one year than an air conditioner. Two small parts inside the compressor were made out of powdered metal rather than the hardened steel and cast iron used in air conditioners because this material could be much closer tolerances and reduce the machining costs. The design engineers did not consider the critical failure in rotary compressor until the noise claims of domestic house in 1987.

When a rotary compressor was abnormally locking in 1987, G Company and M Company experienced massive recalls of the rotary compressor. As the oil sludge in the refrigeration system blocked the capillary tube, the cooling capacity of the refrigerator decreased. In the compressor development process, reproducing this failure mode and preventing the blocking of this tube were very important to the reliability of the refrigerator. However, reliability testing methods such as the parametric ALT was not used at that time (Table 2.7).

- Root Cause: Abnormal wear out at sintered iron under severe operating conditions.

Table 2.7 G company and M company rotary compressor recall summary

	G company	M company
Product	Household refrigerator	
Unit	Rotary comp (sealed refrigerant compressor)	
Production date	1986.3	1985.1
Issued date	1987.7	1991.10
Failed cost	450 million \$	560 million \$
Failed amount	1.1 million	1 million
Failure mechanism	Abnormal wear out (sintered iron)	Wear out (lubrication at high temp)
	Oil reaction/sludge imbedding	Oil reaction/sludge imbedding
User environment	Worst case	Worst case
After disaster	Withdraw comp BIZ	Lock out factory

2.2.5 Firestone and Ford Tire in 2000

In the early of 2000 the Firestone and Ford tire experienced an unusually tire failures on the Ford Explorer equipped with Firestone tires. The Ford Motor Company had a historically good relationship with Firestone. As Firestone became a subsidiary of Japanese tire manufacturer Bridgestone in 1988, they drifted apart. The U.S. National Highway Traffic Safety Administration (NHTSA) contacted Ford in May 2000 and asked about the high incidence of Firestone tire failure on Ford Explorers model. Immediately Ford found that it had very high failure rates from 15-inch Firestone tires models (see Fig. 2.9).

Firestone recalled the millions of tires including 2.8 million Firestone Wilderness AT tires. A large number of lawsuits have been filed against both Ford and Firestone that there had been over 240 deaths and 3000 catastrophic injuries. The actual accidents come from separating a kind of tire tread when cornering on cloverleaf interchange in high speed.

- Root Cause: Remove air from the tires (Minor design change) → Tire heat up → Damage the tire → Interaction of steel and rubber tire → Tread separation.



(a) Ford Explorer and Firestone Tires



(b) Firestone fallout

Fig. 2.9 Firestone and Ford tire controversy from Wikipedia



Fig. 2.10 Toshiba Satellite T130 notebook and battery overheating problem

2.2.6 *Toshiba Satellite Notebook and Battery Overheating Problem in 2007*

As approximately 41,000 Toshiba laptops were reported for more than 100 cases of melting laptop and minor injuries, Toshiba had to fall massive recalls in 2007. The basic cause might overheat and expose a burning to consumers. Heat will generate when processors and batteries run. Laptops are designed to provide adequate airflow for the fan and eliminate the overheating from the case. However, due to the requirements of slim, less weight and compact design, notebooks will push heat-generating components into a smaller space (Fig. 2.10).

- Root Cause: pushing so much processing power and battery into such a small space (design problem).

2.2.7 *Toyota Motor Recalls in 2009*

The recalls of automobiles by Toyota Motor Corporation occurred in 2009 for approximately 5.2 million vehicles—the pedal entrapment/floor mat problem, and for 2.3 million vehicles—the accelerator pedal problem. As Toyota widened the recalls to include 1.8 million vehicles in Europe and 75,000 in China, total recall number of cars in the world were considerable 9 million. The U.S. National Highway Traffic Safety Administration (NHTSA) reached to conclusion that pedal misapplication was found responsible for most of the incidents (see Fig. 2.11).

- Root Cause: the pedal entrapment/floor mat problem.

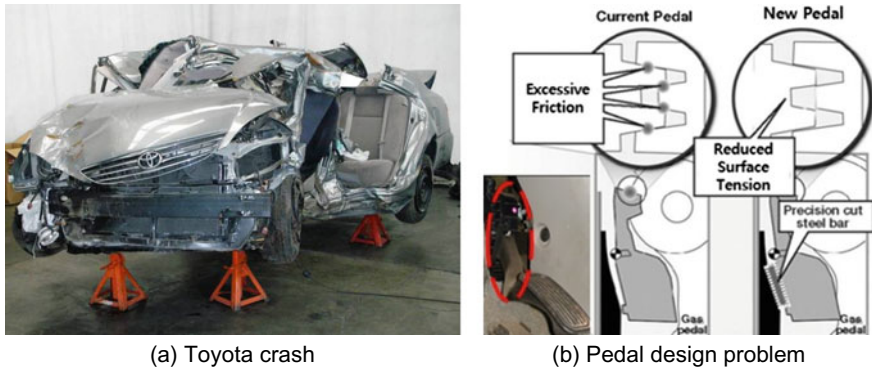


Fig. 2.11 Recalls of automobiles by Toyota Motor Corporation

2.3 Development of Reliability Methodologies in History

2.3.1 In the Early of 20s Century—Starting Reliability Studies

Reliability, as a human attribute, has been praised for a very long time. The modern concept for reliability was beginning in 1816. The word “reliability” was first coined by poet Samuel Taylor Coleridge [1]. At that time reliability in statistics was defined as the consistency of a set of measurements to express a test. A test is reliable if the same result is repeated. For instance, if a test is designed to measure special marks, the results should be approximately nearly identical to the one. Reliability was a common concept that had been perceived as an attribute of a product. For technical systems, however, the reliability concept has not been applied in the previous centuries (Table 2.8).

In the early times, product recalls were the rail accident that France Versailles frequently occurred in 1842. August Wöhler investigated the causes of fracture in railroad axles and started the first systematic studies of S-N Curve (or Wöhler Curve) [2, 3]. To prevent the railroad disasters, S-N curve of materials can be used to minimize the fatigue problem by lowering the stress at critical points in a component. Griffith during World War I developed fracture mechanics to explain the failure of brittle materials. He suggested that the low fracture strength observed in experiments was due to the presence of microscopic flaws in the bulk material that can be still useful (Fig. 2.12) [4].

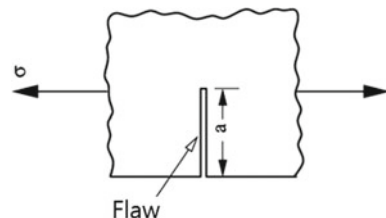
$$\sigma_f \sqrt{a} \approx C \quad (2.1)$$

where σ_f is the failure stress.

Failure occurs when the free energy attains a peak value at a critical crack length.

Table 2.8 History summary of reliability technology

~ 1950	-	Wilhelm Albert publishes the first article on fatigue (1837) A. Wöhler summarized fatigue test results on rail-road axles (1870) O. H. Basquin proposes a log-log relationship for S-N curves (1901) John Ambrose Fleming invented vacuum tubes in 1904 Griffith's theory of fracture (1921) A. M. Miner introduces a linear damage hypothesis (1945)
WW II	Germany	V-I, V-II rocket development (R. Lusser's Law)
WW II	US	Reliability of the electron power tube (aircraft electronic devices failure in the WW II)
1954	Japan	Surveys and studies on the electron power tube reliability in the vacuum committee of the institute of electrical engineers
1952–1957	US	US DOD formed the advisory group on the reliability of electronic equipment (AGREE) AGREE suggest vacuum tube follows the bathtub curve
1954	US	First national symposium on reliability and quality control, New York
1950s	US	Several conferences began to focus on various reliability topics (e.g., 1955 Holm conference on electrical contacts)
1961	Italy	The Rome Air Development Center (RADC) introduced a PoF program
1962	US	Launched the Apollo program (FMEA & FTA), first reliability and maintainability conference
1962	US	First symposium on physics of failure in electronics, Chicago
1965	IEC	Reliability and maintainability technical committee, TC 56, Tokyo
1968	-	Tatsuo endo introduces the rain-flow cycle count algorithm
1971	Japan	First reliability and maintainability symposium

Fig. 2.12 An edge crack (flaw) of length a in a material

$$C = \sqrt{\frac{2E\gamma}{\pi}} \quad (2.2)$$

where E is the Young's modulus of the material and γ is the surface energy density of the material.

Invented in 1904 by John Ambrose Fleming, vacuum tubes were a basic component for electronics—the diffusion of radio, television, radar, sound reinforcement, sound recording and reproduction, large telephone networks, analog and digital computers, and industrial process control. The invention of the vacuum tube

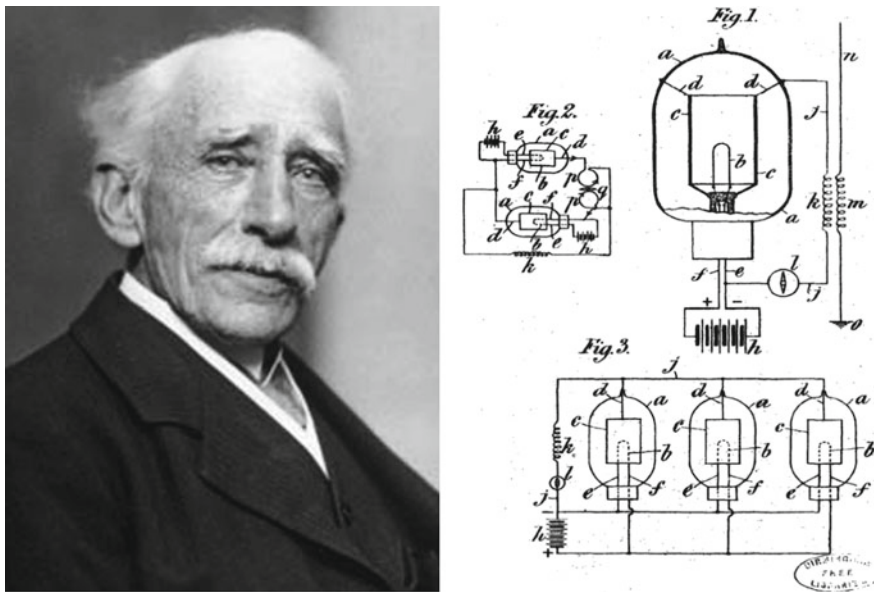


Fig. 2.13 British engineer John Ambrose Fleming and his vacuum tubes patents [5]

made modern technologies of product applicable. By 1916, radio with vacuum tubes was used to begin in the public (Fig. 2.13). The concept of reliability by the problematic vacuum tubes began in earnest to develop.

Karl Pearson first mentioned “negative exponential distribution” in 1895. His exponential distribution had a number of interesting properties that were available in the 1950s and 60s. That is, one property of serial system is the ability to add failure rates of different components in product. Simply adding it was rather easily applicable at the time when using mechanical and later electric systems.

$$R(t) = R_1(t) \cdot R_2(t) \dots R_n(t) \quad (2.3)$$

$$R(t) = e^{-\lambda_1 t} \cdot e^{-\lambda_2 t} \dots e^{-\lambda_n t} \quad (2.4)$$

$$R(t) = e^{-(\lambda_1 + \lambda_2 + \dots + \lambda_n)t} \quad (2.5)$$

where R is reliability function, λ is the failure rate, and t is the use time.

As automobiles came into more common use in the early 1920s, product improvement by the statistical quality control was introduced by Walter A. Shewhart at Bell Laboratories. He developed the control chart in 1924 and the concept of statistical control. Statistics as a measurement tool would become connected with the development of reliability concepts. While designers were

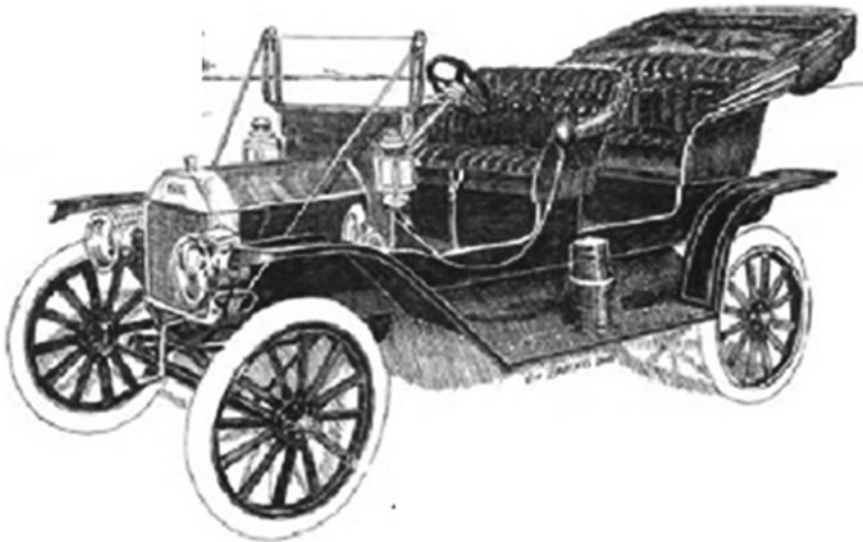


Fig. 2.14 A popular automobile in the early 1920s [6]

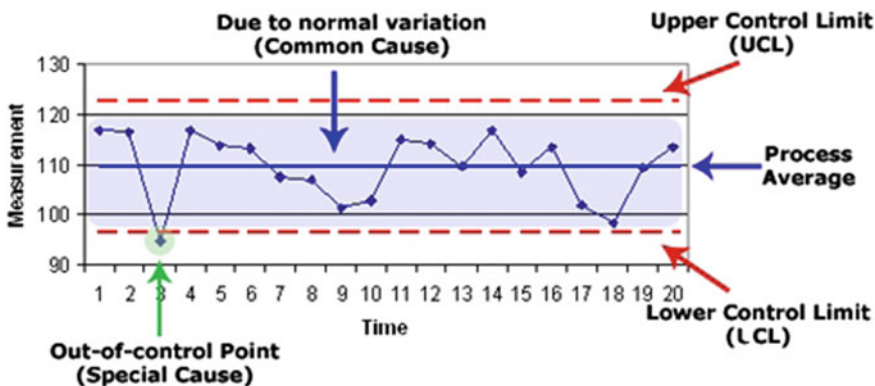


Fig. 2.15 Typical control chart [7]

responsible for product quality and reliability, technician took care of the failures. In the 1930s Quality and process measures in automobile were still growing (Figs. 2.14 and 2.15).

In the 1940s W. Edwards Deming stressed management responsibility for quality in the military short lecture. He expressed that most of quality problems are actually due to system design errors, not worker error [8]. For instance, an initial reliability concept was applied to the spark transmitters telegraph because of the uncomplicated design. It was a battery powered system with simple transmitters by

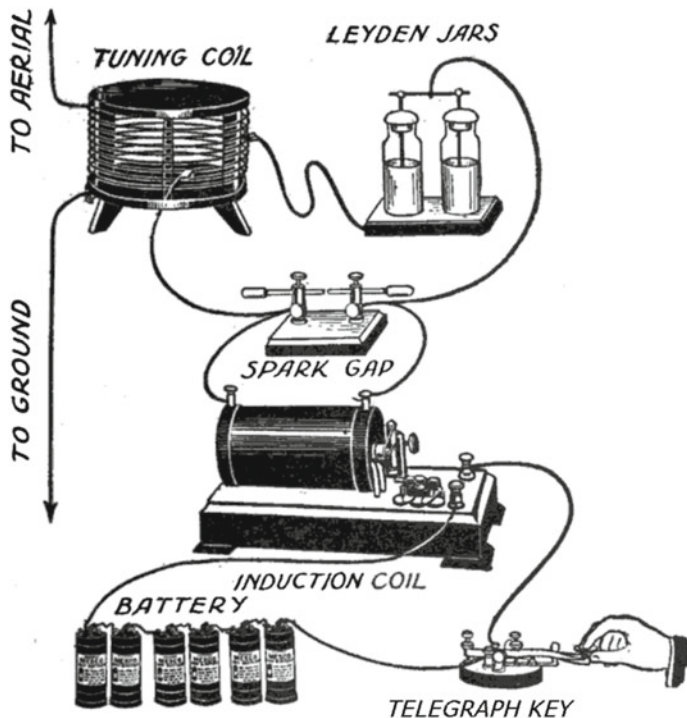


Fig. 2.16 A simple spark-gap transmitter with HV capacitor and output tuning coil

wire. The main failure mode was a broken wire or insufficient voltage. After WWI, this system was replaced with greatly improved transmitters based on vacuum tubes (Fig. 2.16).

It emerged with a technological meaning just and was then used in connection with comparing operational safety of one-, two-, and four-engine airplanes. The reliability was measured as the number of accidents per hour of flight time. At the beginning of the 1930s, Walter Shewhart, Harold F. Dodge, and Harry G. Romig laid down the theoretical basis for utilizing statistical methods in quality control of industrial products. Such methods were, however, not brought into use to any great extent until the beginning of World War II. Products like airplane and tanks were composed of a large number of parts but often did not function, despite the fact that they were made up of individual high-quality components. Because of that, the study for reliability started with World War II.

2.3.2 In the World War II—New Electronics Failure in Military

Before World War II, many concepts in reliability engineering still did not exist. However, many new electronic products such as electronic switches, vacuum tube portable radios, radar and electronic detonators are introduced into the military during the WWII (Fig. 2.17).

As the war began, it was discovered that half of the airborne electronics equipment in storage was down in lifetime and unable to meet the military requirements (the Air Core and Navy). Reliability work for this period had to do with new metal materials testing. Study for failure mechanism was only its fatigue or fracture. For instance, M. A. Miner published the seminal paper titled

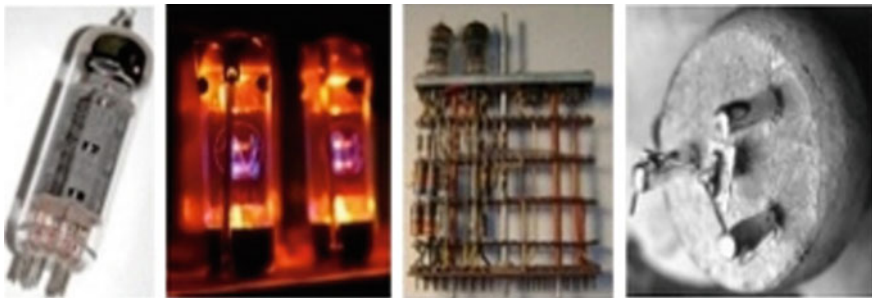


Fig. 2.17 Reliability metric tailored to the leading electronic technology of the world war II and 1950s—vacuum tube and its assembly, discreet transistor and diodes

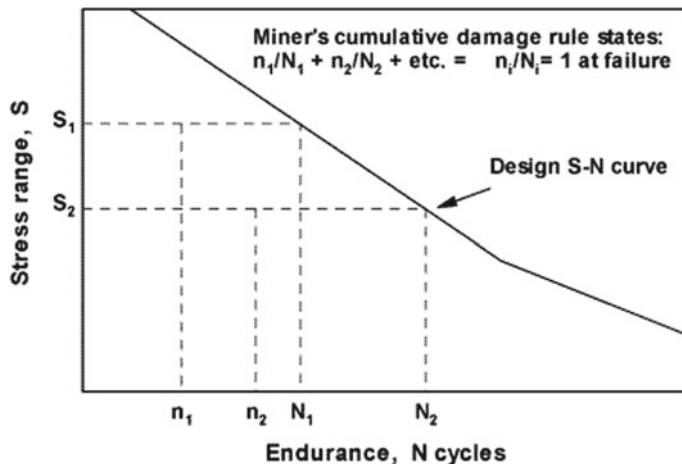


Fig. 2.18 Palmgren-Miner linear damage hypothesis

“Cumulative Damage in Fatigue” in 1945 in an ASME Journal. B [9]. Epstein published “Statistical Aspects of Fracture Problems” in the Journal of Applied Physics in February 1948 [10] (Fig. 2.18).

During World War II a group in Germany was working under Wernher von Braun developing the V-1 missile. After the war, it was reported that first V-1 missiles were totally failure. In spite of attempts to provide high-quality parts and careful attention to details, all first missiles either exploded on the launching pad or landed “too soon”. They had to find solutions and develop the reliability theory.

For some more interesting facts, Germany during World War II applied the basic reliability concepts to improve reliability of their V1 and V2 rockets that consist of multi-modules (Fig. 2.19). To complete the mission of V1 and V2 rockets, Germany engineer had to improve their reliability. Robert Lusser, a mathematician, was called in as a consultant. His task was to analyze the missile system, and he quickly derived the product probability law of series components. This theorem concerns systems functioning only if all the components are functioning and is valid under special assumptions. It says that the reliability of a series system is equal to the product of the reliability of its component subsystems. It means that a series system is “weaker than its weakest link”, as the product reliability of a series of components can be less than the lowest-value component. If the system comprises a large number of components, the system reliability may therefore be rather low, even though the individual components have high reliabilities. The product lifetime therefore is determined by the weakest link (or module) and extended from its design improvement.

After World War II, the United States Department of Defense seriously recognized the necessity for reliability improvement of its military equipment. This law became theoretical basis of MIL-HDBK-217 and MIL-STD-756. But the reliability engineering was yet full-blown because of the limited knowledge on the failure mechanism, design and reliability testing.



Lusser's Law

Lusser's law (multiplication principle) is a prediction of reliability named after Robert Lusser. It states that the reliability of a series system is equal to the product of the reliability of its component subsystems, if their failure modes are known to be statistically independent. This method is similar to the

$$R = R_1 \times R_2 \times R_3 \times R_4 \times R_5 \times \dots \times R_X$$

Deterioration makes reliability go down.



Fig. 2.19 V-1 and V-2 missiles and Lusser's law

2.3.3 *In the End of World War II and 1950s—Starting the Reliability Engineering*

In the start of the 1950s the main military applications for reliability were the vacuum tube in radar systems or other electronics because these systems proved problematic and costly during the World War II (see Fig. 2.20). The vacuum tube computers that had a 1024 bit memory were invented to fill a large room and consume kilowatts of power, though grossly inefficient in modern.

During the war numerous airplanes were crashed during a bombing. The vacuum tubes mounted in these airplanes had been proved as the problematic parts, though the component price was cheap. After the war, half of the electronic equipment for shipboard was failed in lifetime. The root cause of failure also came from the vacuum tubes. Failure modes of vacuum tubes in sockets were intermittent working problems. The action plans for a failed electronic system were to exploding the system, removing the tubes and re-installing them at proper time.

In the renovation process, because the military had to consider the cost issues, the operation and logistics costs for the vacuum tubes would become huge. To solve the problem of vacuum tube, Institute of Electrical and Electronic Engineers (IEEE) in 1948 formed the Reliability Society. Z. W. Birnbaum in 1948 had founded the Laboratory of Statistical Research at the University of Washington, which served to use the concept of statistics. In 1951, to study reliability problems with the Air Force Rome, Air Development Center (RADC) was established in Rome and New York.

In 1950 a study group in military was initiated, which was thereafter called the Advisory Group on the Reliability of Electronic Equipment (AGREE). By 1959, reports of this group suggested the following three recommendations for the reliable systems such as vacuum tube: (1) there was a need to develop reliable components for supplier, (2) the military should establish quality and reliability requirements (or specifications) for component suppliers, and (3) actual field data should be collected on components to search out the root causes of problems.

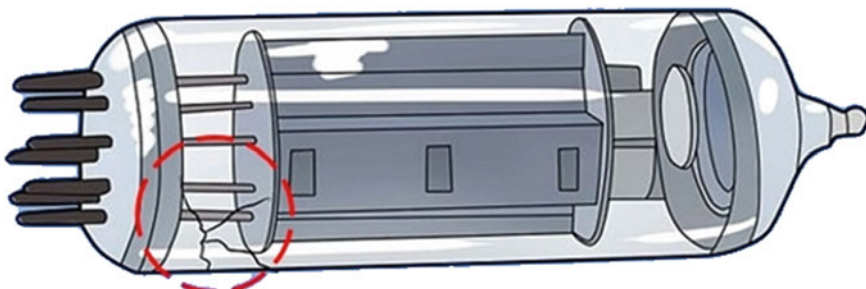


Fig. 2.20 Typical vacuum tube failure—air leakage into the tube due to the crack tube

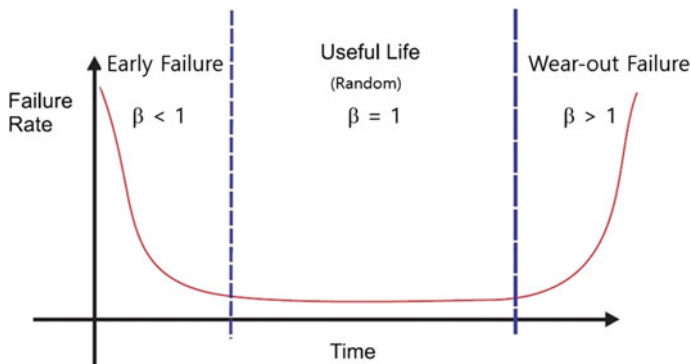


Fig. 2.21 Bathtub curve for vacuum tube radio systems

A definition of product lifetime originally came from 1957 AGREE Commission Report. Task Group 1 in AGREE has developed minimum-acceptable measures for the reliability of various types of military electronic equipment, expressed in terms of Mean Time Between Failures (MTBF), though defining lifetime for electronic components were currently inadequate. The final report of AGREE committee suggested the reliability of product such as most vacuum tube followed the bathtub curve. Consequently, reliability of components is often defined as “the bathtub curve” that has early failure, useful life, and wear-out failure (Fig. 2.21). Now the cumulative distribution function corresponding to a bathtub curve is replaced with a Weibull chart in reliability engineering.

AGREE committee also recommended to formally testing products with statistical confidence. And it would carry out the environmental tests that have ultimate temperature and vibration conditions, which became Military Standard 781. The AGREE report originally stated that the definition for reliability is “the probability of a product performing without failure a specified function under given conditions for a specified period of time”.

In the early of 1950s, a conference on electrical contacts and connectors was initiated to study the reliability physics—failure mechanisms and reliability topics. In 1955, RADC issued “Reliability Factors for Ground Electronic Equipment.” by Naresky [11]. The conference was publishing proceedings, entitled as “Transaction on Reliability and Quality Control in Electronics”, merged with an IEEE Reliability conference and became the Reliability and Maintainability Symposium.

As television in the 1950s was introduced, more vacuum tubes were utilized in America house. Repair problems were often due to the failure of one or more vacuum tubes. Vacuum tube was a critical switching device that controls electric current through a vacuum in a sealed container—cathode ray tube. Typical reliability problems of the tubes with oxide cathodes evolved as (1) reduce its ability to emit electrons, (2) a stress-related fracture of the tungsten wire, (3) air leakage into the tube, and (4) glowing plate—a sign of an overloaded tube. Most vacuum tube in radio systems followed a bathtub-type curve was easy to develop replaceable

electronic modules—Standard Electronic Modules (SEM), and then restore a failed system.

Robert Lusser, Redstone Arsenal, pointed out that 60% of the failures of one Army missile system were due to components that reported on “Predicting Reliability” in 1957. He also stressed that current quality methods for electronic components were inadequate and that new concepts for electric components was implemented. ARINC set up an improvement process with vacuum tube suppliers and reduced infant mortality removals by a factor of four. This decade ended with Radio Corporation of America (RCA) publishing information in TR1100 on the failure rates of some military components. RADC used these concepts, which became the basis for Military Handbook 217. Over the next several decades, Birnbaum made suggestions on Chebychev’s inequalities, non-parametric statistics, reliability of complex systems, cumulative damage models, competing risk, survival distributions and mortality rates.

Walodie Weibull was working in Sweden and investigated the fatigue of materials. He created a Weibull distribution. In 1939 Weibull suggested a simple mathematical distribution, which could represent a wide range of failure characteristics by changing two parameters. The Weibull failure distribution does not apply to every failure mechanism but it is useful tool to analyze many of the reliability problems. In 1951 he presented his most famous papers to the American Society of Mechanical Engineers (ASME) on Weibull distribution with seven case studies. Between 1955 and 1963, he investigated the fatigue and creep mechanisms of materials. He derived the Weibull distribution on the basis of the weakest link model of failures in materials. By 1959, he produced “Statistical Evaluation of Data from Fatigue and Creep Rupture Tests: Fundamental Concepts and General Methods” as a Wright Air Development Center Report 59-400 for the US military [12].

In 1961, Weibull published a book on materials and fatigue testing while working as a consultant for the US Air Force Materials Laboratory [13]. The American Society of Mechanical Engineers awarded Weibull their gold medal in 1972. The Great Gold Medal from the Royal Swedish Academy of Engineering Sciences was personally presented to him by King Carl XVI Gustaf of Sweden in 1978 (Fig. 2.22).

As Weibull analysis methods and applications were propagating, a number of people began to use the Weibull chart. Dorian Shainin wrote an early booklet on Weibull in the late of 1950s, while Leonard Johnson at General Motors helped improve the plotting methods by suggesting median ranks and beta Binomial confidence bounds in 1964. Dr. Robert Abernethy developed a number of applications, analysis methods and corrections for the Weibull function. Professor Gumbel demonstrated that the Weibull distribution is a Type III Smallest Extreme Value distribution such as Eqs. (2.6) and (2.7) [14]. Dr. Robert Abernethy developed a number of applications, analysis methods and corrections for the Weibull function

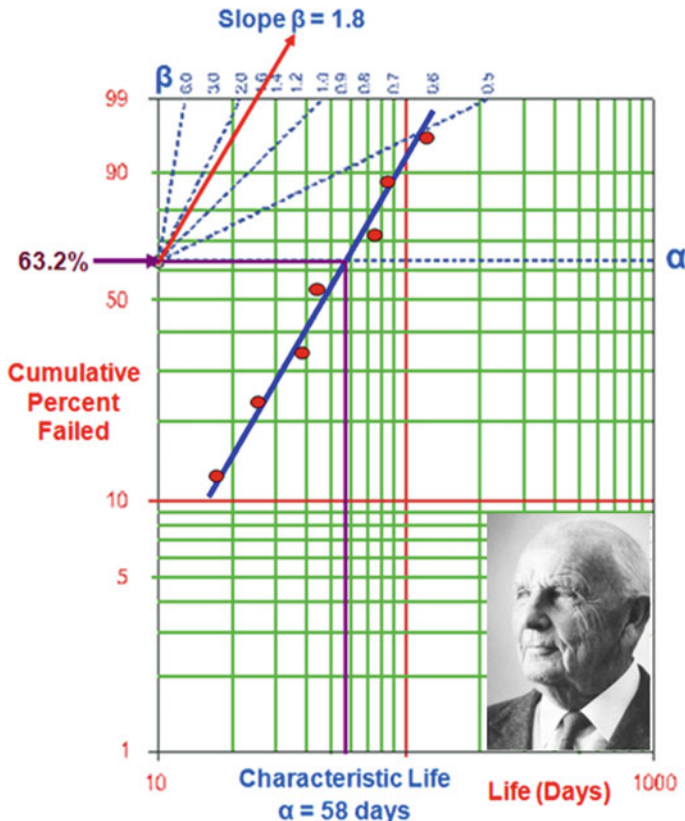


Fig. 2.22 Sweden engineer Waloddi Weibull and his Weibull distribution

$$F(x) = \exp\left(-\left(\frac{x}{\alpha}\right)^{\beta}\right) \quad (2.6)$$

where $x \leq a$, $b > 0$, $c > 0$.

$$K = A \exp\left(-\frac{E_a}{RT}\right) \quad (2.7)$$

where k is the rate constant of a chemical reaction, T is the absolute temperature, A is the pre-factor, E_a is the activation energy, and R is the universal gas constant.

In 1963, Weibull was a visiting professor at Columbia and there worked with professors Gumbel and Freudenthal in the Institute for the Study of Fatigue and Reliability. While he was a consultant for the US Air Force Materials Laboratory, he published a book on materials and fatigue testing and the related reports till 1970.

The United States between the end of the 1950s and the beginning of the 1960s was interested in intercontinental ballistic missiles and space research—the Mercury and Gemini programs. To firstly put men on the moon in the race with the Russians, it was critical that the launching of a manned spacecraft should succeed. An association for engineers working with reliability questions was soon established. IEEE Transactions on reliability came out in 1963, and the related textbooks on the subject were published in the 1960s.

Aeronautical Radio, Incorporated (ARINC) set up an improvement process with vacuum tube suppliers to reduce its infant mortality removals. As publishing information in TR1100 on the failure rates of some military components, it became the basis for Military Handbook 217—“Reliability Prediction of Electronic Equipment”. “Navy Military” published Handbook 217 in 1962. Papers for electronic components were being published at conferences: “Reliability Handbook for Design Engineers” published in Electronic Engineers, in 1958 by F. E. Dreste and “A Systems Approach to Electronic Reliability” by W. F. Leubbert in the Proceedings of the IRE (1956) [15]. C. M. Ryerson produced a history of reliability to 1959 in the proceedings of the IRE entitled as Proceedings of the IEEE [16].

Therefore, attempts in the United States were made to compensate low system reliability by improving the quality of the individual components. Better raw materials and better designs for the products were demanded. Higher system reliability was obtained, but extensive systematic analysis of the problem was probably not carried out at that time.

2.3.4 In the 1960s and Present: Mature of Reliability Methodology—Physics of Failure (PoF)

After World War II, the development continued throughout the world as increasingly more complicated products were produced, composed of an ever-increasing number of components (television sets, electronic computers, etc.). With automation, the need for complicated control and safety systems also became steadily more pressing.

Physics of Failure (PoF) for electronic components in 1960s started with several significant events—invention of the transistor in 1947 and transistor radio in 1954, which became the most popular electronic communication device during the 1960s and 1970s. People with pocket size listened to music everywhere (Fig. 2.23). These devices had some problems—electromechanical faults, transistor failure, and capacitor problems. PoF is a kind of systematic approach to the design and development of reliable product to prevent failure. Based on the knowledge for the root cause of failure mechanisms, system can improve its performance.

RADC worked in earnest the Physics of Failure in Electronics Conference sponsored by Illinois Institute of Technology (IIT). In the 1960s America strong commitment to space exploration would turn into National Aeronautics and Space

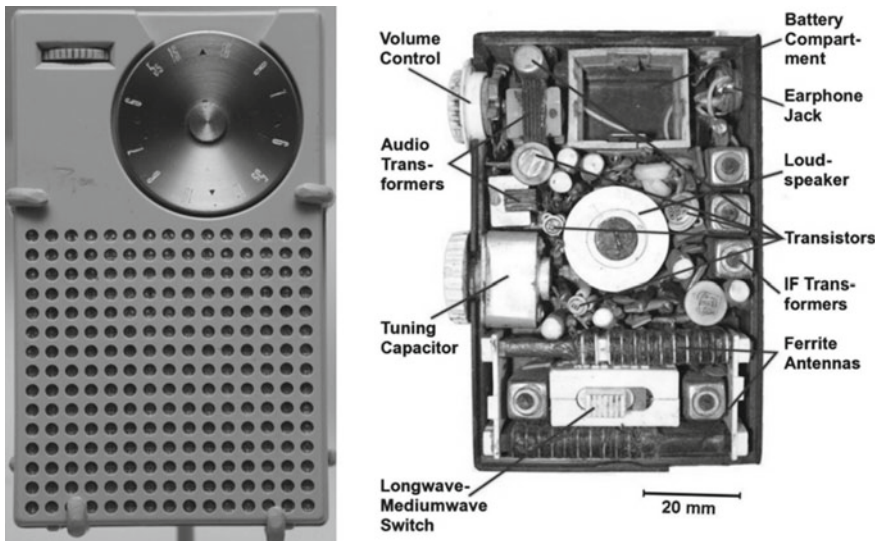


Fig. 2.23 A transistor radio with multiple parts from Wikipedia

Administration (NASA), a key efforts to improve the reliability of components and systems that could work properly to complete the space missions. RADC produced the document “Quality and Reliability Assurance Procedures for Monolithic Microcircuits.” Semiconductors were a popular use in small portable transistor radios. Next, low cost germanium and silicon diodes were able to meet the requirements. Dr. Frank M. Gryna published a Reliability Training Text through the Institute of Radio Engineers (IRE).

In this period the nuclear power industry and the military—missiles, airplanes, helicopters and submarine applications enabled the reliability problems of a variety of technologies to initiate POF. The study of Electro-Magnetic Compatibility (EMC) system effects was initiated at RADC in the 1960s (Fig. 2.24).

One of the milestones in the Proceedings of the 7th National Symposium of Reliability and Quality Control was the proof of the effectiveness of the Arrhenius model for semiconductors in 1962. G. A. Dodson and B. T. Howard of Bell Labs published the papers, entitled as “High Stress Aging to Failure of Semiconductor Devices” [17]. This conference also issued lots of other papers. It could look at the technical improvement of at the technical improvement of other electronic components, and renamed as the Reliability Physics Symposium (RPS) in 1967. Shurtliff and Workman in the late of sixty issued the original paper on step stress testing that establishes limits when applied to Integrated Circuits.

Electro-migration in electronic system is one of failure mechanism which applied to the transport of mass in metals when the metals are stressed at high current densities. J. R. Black published his work on the physics of electro-migration in 1967. Since the number of free charge carriers increases with temperature, silicon in

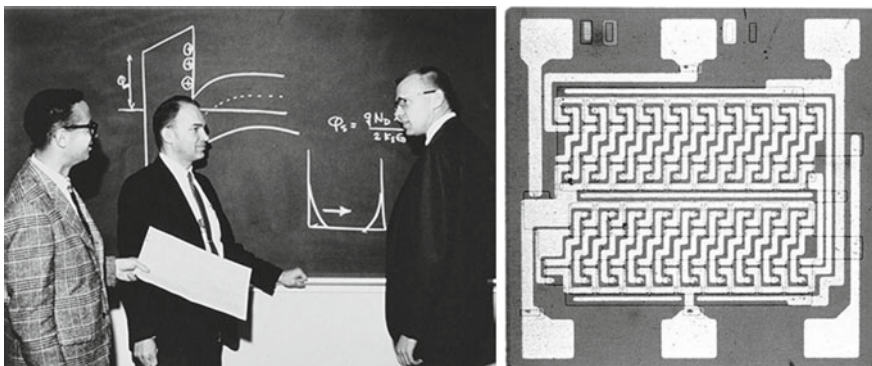


Fig. 2.24 Andy Grove, Bruce Deal, and Ed Snow at the Fairchild Palo Alto R & D laboratory and first commercial metal oxide semiconductor (MOS) IC in 1964 from Wikipedia

semiconductor began to dominate reliability activities for a variety of industries. The U.S. Army Material Command issued a Reliability Handbook (AMCP 702-3) in 1968. On the other hands Shooman's Probabilistic Reliability also was issued to explain statistical methods.

To investigate the failure mode of electronic components, automotive industry was published a FMEA handbook for technical improvement of suppliers, not yet published as a Military standard. As a series of commercial satellites were launched, the reliability study for communications was strengthened by International Telecommunications Satellite Organization (INTELSAT) that was providing international broadcast services between the U.S. and Europe in 1965. Professionals around the world took part in reliability conferences. As Apollo was landing a moon, people recognized how far reliability had progressed in the recent decade.

$$f(t) = \frac{1}{2\mu^2\gamma^2\sqrt{\pi}} \left(\frac{t^2 - \mu^2}{\sqrt{\frac{t}{\mu}} - \sqrt{\frac{\mu}{t}}} \right) \exp \left[-\frac{1}{\gamma^2} \left(\frac{t}{\mu} + \frac{\mu}{t} - 2 \right) \right] \quad (2.8)$$

where γ is a shape parameter, μ is a scale parameter.

As seen in Eq. (2.8), in 1969, Birnbaum and Saunders suggested a life distribution model that could be derived from a physical fatigue process where crack growth causes failure. Since one of the best ways to choose a life distribution model is to derive it from a physical/statistical argument that is consistent with the failure mechanism, the Birnbaum-Saunders fatigue life distribution is worth considering.

As the microcomputer had been invented in the 1970s, RAM memory size was growing at a rapid rate. Vacuum tube was replaced with Integrated Circuit (IC). The variety of ICs—Bipolar, NMOS and CMOS increased very rapidly. In the middle of the 1970s, Electrostatic discharge (ESD) and Electrical Over Stress (EOS) were discussed by some papers and eventually became the hot issues of a conference in the decade end.

In the same manner, studies for passive components—resistor, inductor, and capacitor in International Reliability Physics Symposium (IRPS) moved to a Capacitor and Resistor Technology Symposium (CARTS). The progressive papers on gold aluminum inter-metallics, accelerated testing, and the use of Scanning Electron Microscopes (SEM) were in a few highlights of the decade.

In middle of 1970s, Hakim and Reich published a paper on the evaluation of plastic encapsulated transistors and ICs on field data. And two most memorable reliability papers were one on soft-errors from alpha particles first reported by Woods and May and on accelerated testing of ICs with activation energies calculated for a variety of failure mechanisms by D. S. Peck. In the end of the decade, Bellcore collected commercial field data and became the basis of the Bellcore reliability prediction methodology used widely with MIL-STD-217F.

Toward the end of the 1950s and the beginning of the 1960s, interest in the United States was concentrated on intercontinental ballistic missiles and space research, especially connected to the Mercury and Gemini programs. In the race with the Russians to be the first nation to put men on the moon, it was very important that the launching of a manned spacecraft be a success. During the Apollo space program, the spacecraft and its components worked reliably all the way to the moon and back. In coming to the Navy, all contracts should contain specifications for reliability and maintainability instead of just performance requirements. Military Standard 1629 on FMEA was issued in 1974, NASA made great strides at designing and developing spacecraft such as the space shuttle. Their emphasis was on risk management through the use of statistics, reliability, maintainability, system safety, quality assurance, human factors and software assurance. Reliability had expanded into a number of new areas as technology rapidly advanced.

Emphasizing temperature cycling and random vibration became ESS testing, eventually issued as a Navy document P-9492 in 1979 and make a book on Random Vibration with Tustin in 1984. The older quality procedures were replaced with the Navy Best Manufacturing Practice program. An association for engineers working with reliability questions was soon established. The first journal on the subject, IEEE Transactions on reliability came out in 1963, and a number of textbooks on the subject were published in the 1960s.

In the 1970s interests on risk and safety aspects of the building and operation of nuclear power plants increased in the United States as well as in the other areas of the world. In the United States, a large research commission funded by the multimillion dollar project, so-called Rasmussen report, was set up to analyze the problem. Despite its weaknesses, this report represents the first safety analysis of so complicated a system as a nuclear power plant.

Similar work in the industries of Europe and Asia has also been carried out the analysis of risk and reliability problems. Especially, the same is true in the offshore oil industry of Norway. As the offshore oil and gas development in the North Sea is progressing into deeper and more hostile waters, an increasing number of remotely operated subsea production systems are operated. In many respects parallel to the

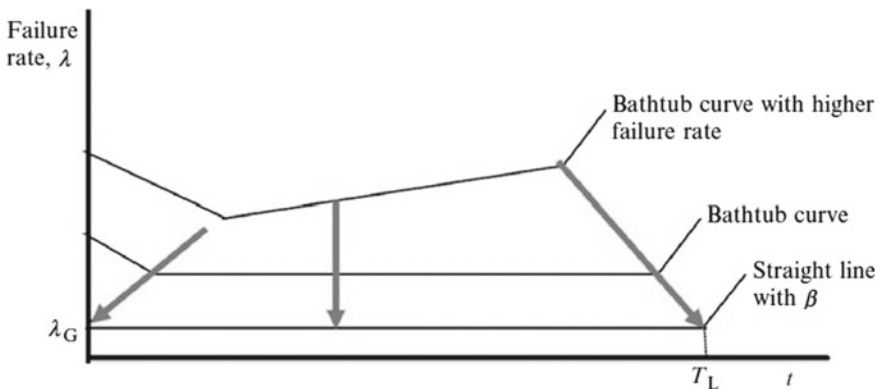


Fig. 2.25 Bathtub curve and straight line with slope β

reliability of space crafts the reliability of subsea systems is important because a low reliability cannot be compensated by extensive maintenance.

In the 1980s, televisions had become product that used all semiconductors. Automobiles rapidly increased their use of semiconductors with a variety of microcomputers. Large air conditioning systems, microwave ovens, and a variety of other appliances developed one chip electronic controllers. Communications systems began to adopt electronics to replace older mechanical switching systems. Bellcore issued the first consumer prediction methodology for telecommunications and SAE developed a similar document SAE870050 for automotive applications.

During this decade, as the failure rate of many electronic components including mechanical components were dropped by a factor of 10, engineer questioned on the bathtub curve. For such a situation, the traditional failure rate typified by the bathtub curve can be reduced to resemble the failure rate represented by a flat, straight line with the shape parameter β (Fig. 2.25).

Software became important to the systems improvement by advancing with work at RADC. Software reliability developed models such as Musa Basic to predict the number of missed software faults that might remain in code. The Naval Surface Warfare Center issued Statistical Modeling and Estimation of Reliability Functions for Software in 1983. Contributions by William Meeker, Gerald Hahn, Richard Barlow and Frank Proschan developed models for wear, degradation and system reliability.

The PC came into dominance as a tool for measurement & control and enhanced the possibility of canned programs for evaluating reliability. In the end of the decade, FMEAs, FTAs, reliability predictions, block diagrams and Weibull Analysis programs were performed in the commercial use. The challenger disaster caused people to recognize the assessment significance of system reliability. Many of the military specifications—Military Handbook 217 became obsolete and best commercial practices were often adopted.

Most industries developed their own reliability standards like the JEDEC Standards for semiconductors and the Automotive Standard Q100 and Q101. Afterward the last century the rise of the internet created a variety of new challenges—micro-electro mechanical systems (MEMS), hand-held GPS, and handheld devices—for reliability. Consumers have become more aware of product recalls. In many ways, reliability became part of everyday life and consumer expectations. The developed methodology in reliability engineering has widely been developing until now.

However, new methodology for reliability is still required to find the problematic parts that are the main cause of recall before production. Later, it will deal with new reliability methodology—parametric ALT in Chaps. 8 and 9.

References

1. Saleh JH, Marais K (2006) Highlights from the early (and pre-) history of reliability. *Eng Reliab Eng Syst Saf* 91(2):249–256
2. Wöhler A (1855) Theorie rechteckiger eiserner Brückengelenke mit Gitterwänden und mit Blechwänden. *Zeitschrift für Bauwesen* 5:121–166
3. Wöhler A (1870) Über die Festigkeitsversuche mit Eisen und Stahl. *Zeitschrift für Bauwesen* 20:73–106
4. Griffith AA (1921) The phenomena of rupture and flow in solids. *Philos Trans R Soc Lond A* 221:163–198
5. Fleming JA, U.S. Patent 803,684, 17 Nov. 1815
6. Ford (1929) 1930 model brochure—beauty of line—mechanical excellence. Retrieved 24 May 2012
7. Shewhart WA (1931) Economic control of quality of manufactured product. D. Van Nostr and Company, New York
8. Deming WE, Stephan F (1940) On a least squares adjustment of a sampled frequency table when the expected marginal totals are known. *Ann Math Stat* 11(4):427–444
9. Miner MA (1945) Cumulative damage in fatigue. *J Appl Mech* 12(3):59–64
10. Epstein B (1948) Statistical aspects of fracture problems. *J Appl Phys* 19
11. Naresky JJ (1962) Foreword. In: Proceedings of first annual symposium on the physics of failure in electronics, September 26–27
12. Weibull W (1959) Statistical evaluation of data from fatigue and creep rupture tests, part I: fundamental concepts and general methods. Wright Air Development Center Technical Report 59-400, Sweden, September
13. Weibull W (1961) Fatigue testing and analysis of results. Pergamon Press, London
14. Abernethy R (2002) The new weibull handbook, 4th edn. Self published ISBN 0-9653062-1-6
15. Lloyd D, Lipow M (1962) Reliability: management, methods and mathematics. Prentice Hall, Englewood Cliffs
16. Knight R (1991) Four decades of reliability progress. In: Proceedings of annual RAMS, pp 156–160
17. George E (1998) Reliability physics in electronics: a historical view. *IEEE Trans Reliab* 47 (3):379–389

Chapter 3

Modern Definitions in Reliability Engineering



Abstract To better understand the parametric ALT that is a core of this book, this chapter will briefly review the basic definitions of reliability engineering that can be used widely for reliability testing. It consists of bathtub, reliability index, fundamentals in statistics and probability theory, statistical distributions like Weibull, and experimental design. When product is designed, engineer knows if final design has problems and is satisfied with the reliability target. Engineer should fully recognize the basic concepts that reliability testing is required. From customer's standpoint, reliability depends on the product design and can be explained as two separate concepts—product of lifetime and failure rate. Engineer for reliability theory may feel complex because it requires an extensive concepts of probability and statistics. To conduct the reliability testing of mechanical product and obtain the reasonable test data, mechanical engineer should understand the modern definitions that can be used. When product is subjected to repetitive stresses (sole factor) and there is design faulty in it, product will fail. However, there is no current methodology because product failures rarely happen in its lifetime. As an alternative, we might suggest parametric ALT in Chap. 8.

Keywords Reliability concepts · Reliability testing · Probability theory · Statistics · Reliability testing · Robust design

3.1 Introduction

The ability of an item is to perform a required function under given environmental and operational conditions for a stated period of time (ISO8402). Reliability theory developed apart from the mainstream of probability and statistics, which was used primarily as a tool to help nineteenth century maritime and life insurance companies compute profitable rates to charge their customers. The modern concepts in reliability engineering started from bathtub, which was found in the reliability study of vacuum tube—problematic parts in the WW2. Invented in 1904 by John Ambrose Fleming, vacuum tubes were a basic component for electronics throughout the first half of the twentieth century.

The reliability concepts except the quality control in product manufacture can focus on the study of quality itself in design. When mechanical system is subjected to random stress (or loads), mechanical structures are designed to withstand the loads with proper stiffness and strength. Requirements on stiffness, being the resistance against reversible deformation, may depend on their applications. Strength, the resistance against irreversible deformation, is always required to be high, because this deformation may lead to loss of functionality and even failure. Modern definitions in reliability engineering will be required to develop the methodology of reliability testing—parametric Accelerated Life Testing in Chaps. 8 and 9. It will uncover the faulty designs of product and modify them. Finally, it confirms whether the reliability of final designs is achieved.

3.2 Reliability and Bathtub Curve

3.2.1 Reliability Function and Failure Rate

Reliability is the probability that a mechanical product will properly operate for a design life under the environmental or operating conditions. If T is a random variable denoting the time to failure, the reliability function at time t can be expressed as

$$R(t) = P(T > t) \quad (3.1)$$

The cumulative distribution function (CDF) as the complement of $R(t)$ can also be expressed as:

$$F(t) = 1 - R(t) \quad (3.2)$$

If the time to failure, T , has a probability density function $f(t)$, Eqs. (3.1) and (3.2) can be rewritten as

$$R(t) = 1 - F(t) = 1 - \int_0^t f(\xi)d\xi \quad (3.3)$$

The failure rate in a time interval $[t_1, t_2]$ can be defined as the probability that a failure rate unit time occurs in the interval given that no failure has occurred prior to t_1 , the beginning of the interval. Thus, the failure rate is expressed as:

$$\frac{R(t_1) - R(t_2)}{(t_2 - t_1)R(t_1)} \quad (3.4)$$

If we replace t_1 by t and t_2 by $t + \Delta t$, we rewrite Eq. (3.4) as

$$\frac{R(t) - R(t + \Delta t)}{\Delta t R(t)} \quad (3.5)$$

As Δt approaches zero, the instantaneous failure rate can be redefined as:

$$\lambda(t) = \lim_{\Delta t \rightarrow 0} \frac{R(t) - R(t + \Delta t)}{\Delta t R(t)} = \frac{1}{R(t)} \left[-\frac{d}{dt} R(t) \right] = \frac{f(t)}{R(t)} \quad (3.6)$$

3.2.2 Bathtub Curve

The bathtub curve for the faulty product such as vacuum tube was created by mapping the rate of early “infant mortality” failures, the rate of random failures with constant failure rate during its “useful life”, and finally the rate of “wear out” failures. As defective products are removed, the failure rate in the early life of a product is high but rapidly decreasing. Early sources of potential failure such as storage, handling and installation error are dominated and aging test can remove them immediately. In the mid-life of a product the failure rate is constant. In this period product may experience the random failure like the usage of end-users or overstress. However, if design problems in product exist, the failure of product will increase catastrophically. Engineer should be removed by proper testing methods such as parametric ALT. For bathtub there are three types of reliability testing in accordance with the failure rate (Figs. 3.1 and 3.2).

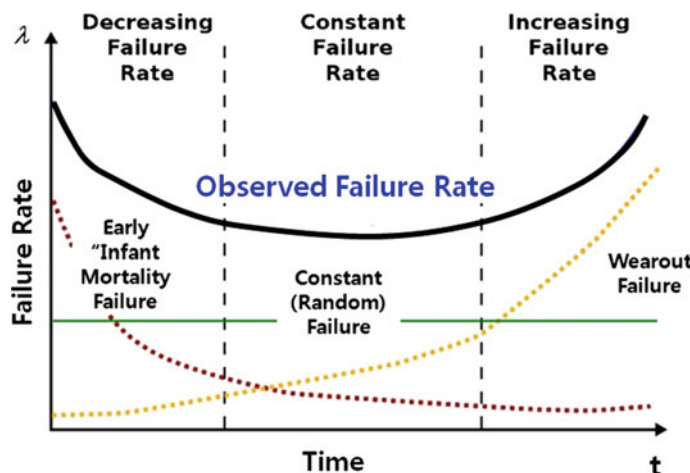


Fig. 3.1 Bathtub curve

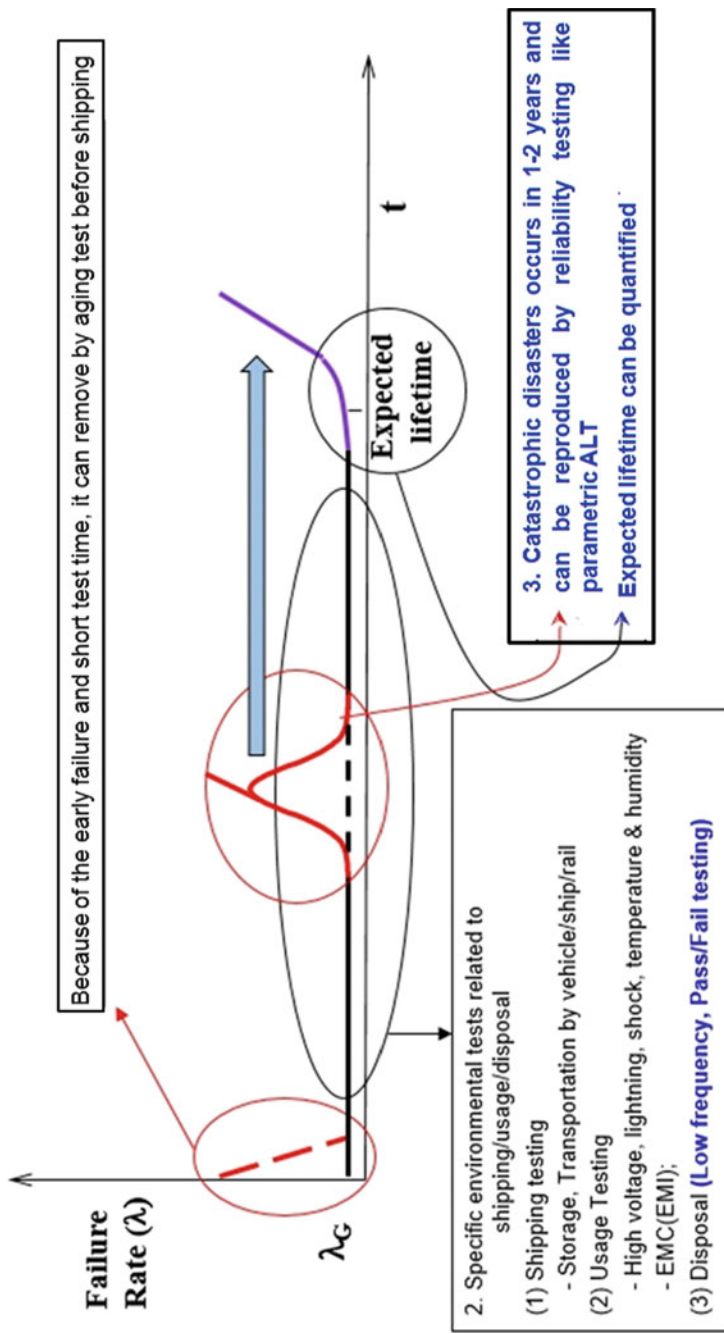


Fig. 3.2 Three types of reliability tests in accordance with the failure rate

- Early failures: Because it requires the short test time, it easily improve by aging test prior to shipment
- Random failures: Specific environmental tests related to shipping/usage/disposal
 - Shipping testing: storage, transportation by vehicle/ship/rail
 - Usage Testing: High voltage, lightning, shock, temperature and humidity, EMC (EMI);
 - Disposal (Low frequency, Pass/Fail testing)
- Catastrophic disasters: It often happens in 1–2 years after production, which comes from the design failure. If it is reproduced and corrected by reliability testing like parametric Accelerated Life Testing described in Chaps. 8 and 9, it can be eliminated.

3.3 Reliability Lifetime Metrics

An important goal for reliability designers is to assess lifetime from product failures or testing data. Reliability lifetime metrics are used to quantify a failure rate and the resulting time of expected performance. MTTF, MTBF, MTTR, FIT and BX% life are reliability lifetime metrics as follows:

- MTTF (Mean Time To Failure),
- MTBF (Mean Time Between Failure),
- MTTR (Mean Time To Repair),
- BX% life.

3.3.1 Mean Time to Failure (MTTF)

A non-repairable system is one for which individual items that fail are removed permanently from the population. MTTF is a basic lifetime metric of reliability to specify the lifetime of non-repairable systems—“one-shot” devices like light bulbs. It is the mean time until a piece of equipment fails at first statistically. MTTF is the mean over a long period of time with a large unit (Fig. 3.3).

$$MTTF = \frac{t_1 + t_2 + \dots + t_n}{n} \quad (3.7)$$

Because we know that MTTF in Fig. 3.3 is 23,000 km, the MTTF can be described with other mathematical terms:

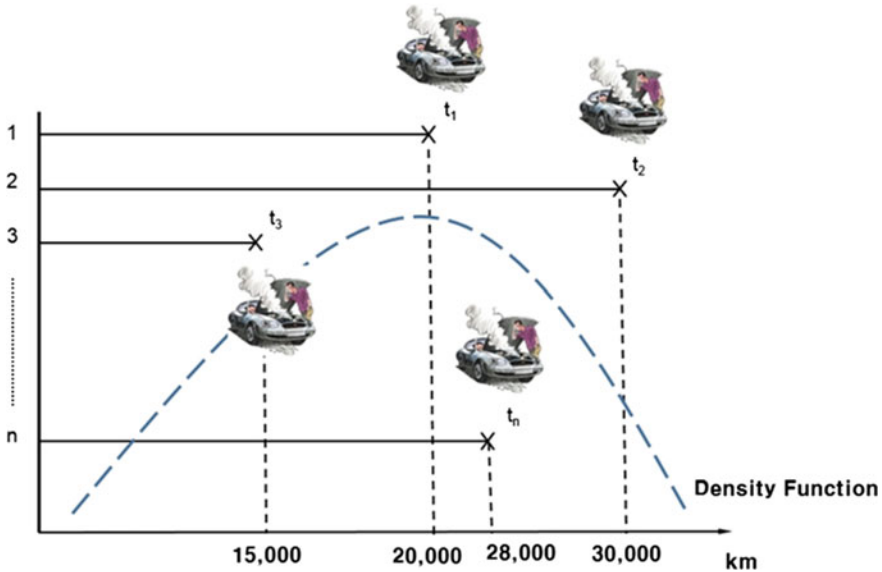


Fig. 3.3 Concept of Mean Time To Failure

$$MTTF = E(T) = \int_0^{\infty} t \cdot f(t) dt = - \int_0^{\infty} t \frac{dR(t)}{dt} dt = \int_0^{\infty} R(t) dt \quad (3.8)$$

where $f(t) = \frac{d}{dt}F(t) = -\frac{d}{dt}R(t)$.

Example 3.1 Consider a system with reliability function

$$R(t) = \frac{1}{(0.2t + 1)^2}, \quad \text{for } t > 0$$

Find the probability density function, failure rate, and MTTF.

$$\text{Probability density } f(t) = -\frac{d}{dt}R(t) = \frac{0.4}{(0.2t + 1)^3}$$

$$\text{Failure rate } \lambda(t) = \frac{f(t)}{R(t)} = \frac{0.4}{(0.2t + 1)}$$

$$\text{Mean time to failure } MTTF = \int_0^{\infty} R(t) dt = 5 \text{ months}$$

3.3.2 Mean Time Between Failure (MTBF)

A repairable system is one which can be restored to satisfactory operation by any action, including parts replacements or changes to adjustable settings. Mean Time Between Failure (MTBF) is a reliability metric used to describe the mean lifetime of repairable components—automobiles, refrigerator, and airplanes. MTBF remains a basic measure of a systems' reliability for most products, though it still is debated and changed. MTBF still is more important for industries and integrators than for consumers (Fig. 3.4).

$$MTBF = \frac{T}{n} \quad (3.9)$$

MTBF value is equivalent to the expected number of operating hours (service life) before a product fails. There are several variables that can impact failures. Aside from component failures, customer use/installation can also result in failure. MTBF is often calculated based on an algorithm that factors in all of a product's components to reach the sum life cycle in hours. MTBF is considered a system failure. It is still regarded as a useful tool when considering the purchase and installation of a product. For repairable complex systems, failures are considered to be those out of design conditions which place the system out of service and into a state for repair. Technically, MTBF is used only in reference to a repairable item, while MTTF is used for non-repairable items like electric components.

3.3.3 Mean Time to Repair (MTTR)

Mean Time To Repair (MTTR) is the average lifetime needed to fix a problem. In an operational system, repair generally means replacing a failed hardware part. Thus, hardware MTTR could be viewed as mean time to replace a failed

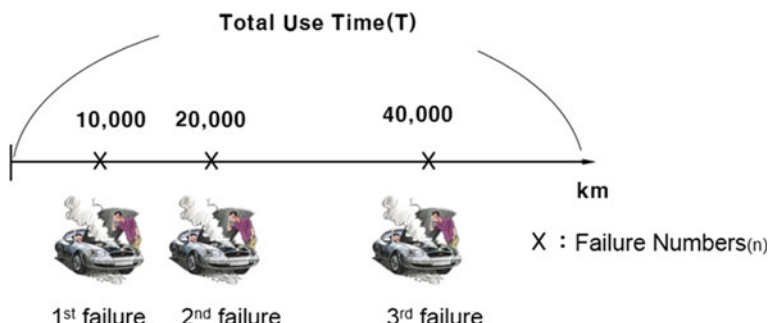


Fig. 3.4 Concept of Mean Time Between Failure

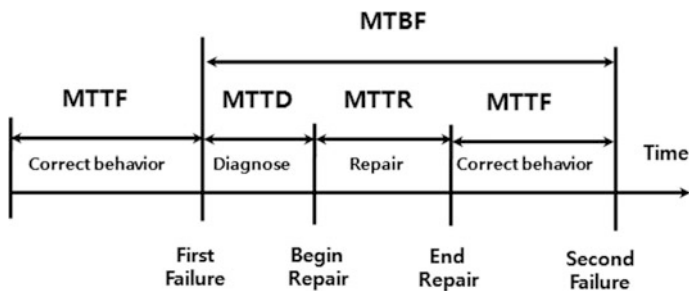


Fig. 3.5 A schematic diagram of MTTF, MTTR, and MTBF

hardware module. Taking too long to repair a product drives up the cost of the installation in the long run, due to down time until the new part arrives and the possible window of time required scheduling the installation. To avoid MTTR, many companies purchase spare products so that a replacement can be installed quickly. Generally, however, customers will inquire about the turn-around time of repairing a product, and indirectly, that can fall into the MTTR category. And relationship among MTTF, MTBF and MTTR can be described in Fig. 3.5.

3.3.4 BX% Life

The BX life metric originated in the ball and roller bearing industry, but has become a product lifetime metric used across a variety of industries today. It's particularly useful in establishing warranty periods for a product. The BX% life is the lifetime metric which takes to fail X% of the units in a population. For example, if an item has a B10 life of 1000 km, then 10% of the population will have failed by 1000 km of operation.

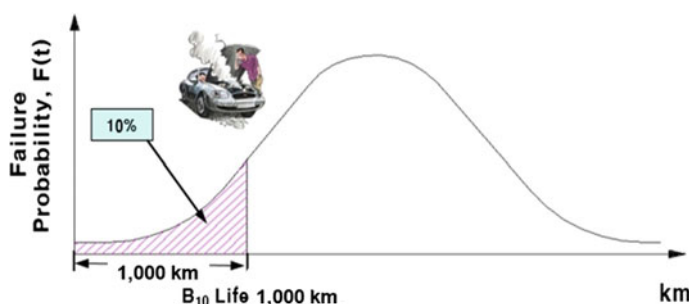


Fig. 3.6 Concept of BX% life

Alternatively, the B10% life has the 90% reliability of a population at a specific point in product lifetime. The “BX” or “Bearing Life” nomenclature refers to the time at which X% of items in a population will fail. The B10 life metric became popular among product industries due to the industry’s strict requirement. Now B1, B10 and B50 lifetime values serve as a measurement for the reliability of a product (Fig. 3.6).

3.3.5 The Inadequacy of the MTTF (or MTBF) and the Alternative Metric BX Life

Two representative metrics of reliability may describe product lifetime and the failure rate. The failure rate is adequate for understanding situations that include unit periods, such as the annual failure rate. But the lifetime is frequently indexed using the mean time to failure.

The MTTF are misinterpreted. For instance, assume that the MTTF of a printed circuit assembly for television is 40,000 h. Annual usage reaches 40,000 divided by 2000 and become 20 years, which is regarded as the lifetime of the unit. The average lifetime of the television PCA is assumed to be 20 years. But because actual customer experience is that the lifetime of a television is a 10 years, this can lead to misjudgments or overdesign that wastes material.

MTTF is often assumed to be the same as lifetime because customers understand the MTTF as, literally, the average lifetime because customers understand the average lifetime of their appliances, so they suppose products will operate well until they reach the MTTF. In reality, this does not happen. By definition, the MTTF is an arithmetic mean; specifically, it equals the period from the start of usage to the time that the 63rd item fails among 100 sets of one production lot when arranged in the sequence of failure times.

Under this definition, the number of failed televisions before the MTTF is reached would be so high that customers would never accept the MTTF as a lifetime index in the current competitive market. The products of first-class companies have fewer failures in a lifetime than would occur at the MTTF. In the case of home appliances, customers expect no failure for the 10 years. The failure of the TV is accepted from the customer’s perspective in the later time. Customers would expect the failure of all televisions once the expected use time is exceeded—12 years in the case of a television set—but they will not accept major problems within the first 10 years,

The MTTF is inappropriate as a lifetime index of product design. Alternatively, it is reasonable to define the lifetime as the point in time when the accumulated failure rate has reached X%. This is called the BX life. The value X may vary from product to product, but for home appliance, the time to achieve a 10–30% cumulative failure rate failure rate, B20–30 life, exceeds 10 years. Thus, an average annual failure rate equals to 1–3%.

Table 3.1 Results of 1987 Army SINCGARS study^a

Vendor	<i>MIL—HDBK-217</i> MTBF (h)	<i>Actual Test</i> MTBF (h)
A	2840	1160
B	1269	74
C	2000	624
D	1845	2174
E	2000	51
F	2304	6903
G	3080	3612
H	811	98
I	2450	472

^aThe transition from statistical field failure based models to physics-of-failure based models for reliability assessment of electronic packages, EEP-Vol. 10-2, 619–625, Advances in Electronic Packaging ASME 1995,—T. J. Stadterman et al.

Now let's calculate the B10 life from the MTTF of 40,000 h. Since the annual usage is 2000 h, the B10 life is 2 years, which means that the yearly failure rate would be 5%. The reliability level of this television, then, would not be acceptable in light of the current annual failure rate of 1–3%. The misinterpretation of reliability using an MTTF of 20 years would lead to higher service expenses if the product were released into the market without further improvement. The lifetime of a television is 12–14 years, not 20 years. Since random failure cannot account for the sharply increasing failure rate, the MTTF based on random failure or on an exponential distribution is obviously not the same as the design lifetime of product (Table 3.1).

3.4 Fundamentals in Statistics and Probability Theory

When new product is launched, engineer obtains the failure data of products in marketplace. Company analyzes the failure behavior of product and its components through the statistics and probability theory. We can find the MTTF, MTBF, and BX life from these random events in field. For example, if thousand aircraft engine controllers are operating in service, collect all the times to failure data and analyze them. Finally, engineer estimates the lifetime of product from failure data.

3.4.1 Statistics

As seen in Fig. 3.7, statistics in engineering is a kind of the methodology for collecting, analyzing, interpreting and drawing conclusions from field information (or testing data). In other words, it is the methodology which engineering principles

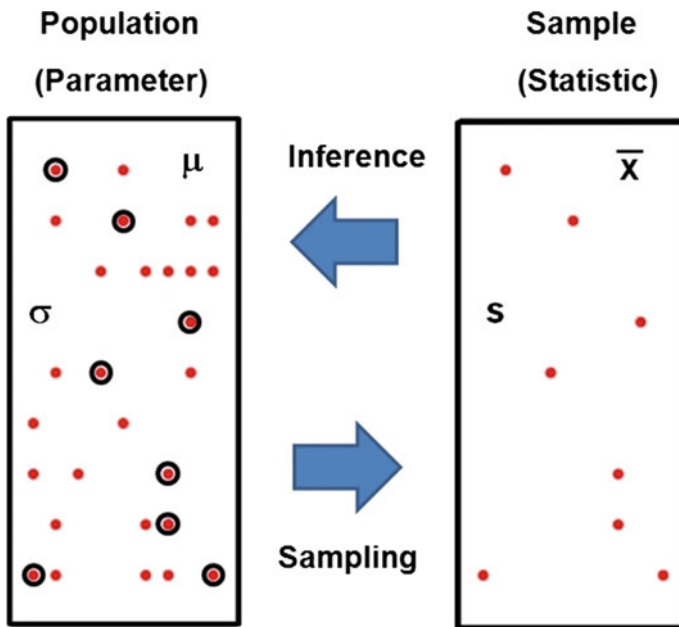


Fig. 3.7 Statistics concepts

and statistical knowledge have been combined for interpreting and drawing conclusions from collected data. Everything that deals with the collection, processing, interpretation and presentation of field data belongs to the domain of statistics in designing new products. And it will be a basis of decision-making for new design.

There are descriptive statistics and inferential statistics in statistics. Descriptive statistics is a kind of methods for organizing and summarizing information. It includes the construction of graphs, charts, and tables, and the calculation of various descriptive measures such as averages, measures of variation, and percentiles. On the other hands, inferential statistics is concerned with using sample data to make an inference about a population of data. It includes methods like point estimation, interval estimation and hypothesis testing which are all based on probability theory.

To improve the product designs from test data, statistics in engineering is more than just the tabulation of numbers and its graphical presentation. Major factor in experimental design can find the fundamental principle of mechanical engineering—load analysis in Chap. 5. The statistical methods therefore are used to provide the solutions for (1) experimental design, (2) description: summarizing and exploring data, (3) inference: confirming whether product meets the reliability targets—10 years of B1 life that will be the accumulated failure rate 1% (Chap. 8).

3.4.2 Probability

Lots of similar phenomena in our modern life happen frequently or repeatedly with chance, not certainly (Fig. 3.8). The probability was originally established by gamblers who were interested in high stakes. To answer the basic question “how probable”, a game of gambling occurs. An early mathematician, Laplace and Pascal, invented the probability. That is, when N is the number of times that X occurs in the n repeated experiments, the probability of occurrence of event X , $P(X)$, can be defined as:

$$P(X) = \lim_{n \rightarrow \infty} \left(\frac{\text{number of cases favorable to } X}{\text{number of all possible cases}} \right) = \lim_{n \rightarrow \infty} (N/n) \quad (3.10)$$

where X is a random variable.

For example, if trials n approaches ∞ , the probability of rolling a 1 with a die is:

$$P(X = 1) = \frac{1}{6} = 0.167 \quad (3.11)$$

In modern theory, axiomatic probability has the assumptions:

- Each random variable X has $0 \leq P(X) \leq 1$.
- The area under the curve is equal to 1: $\int P(X)dX = 1$, where $0 \leq X \leq \infty$.
- If X_1, X_2, X_3, \dots are random variables, then $P(X_1 \cup X_2 \cup \dots) = P(X_1) + P(X_2) + \dots$

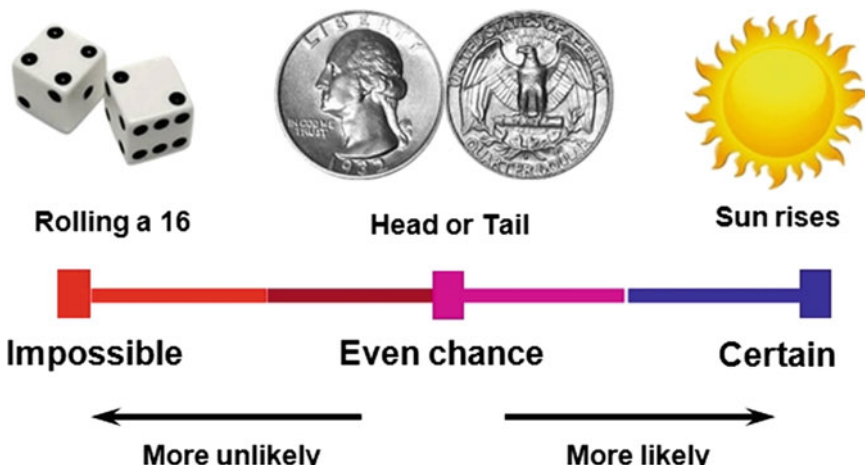


Fig. 3.8 Probability line

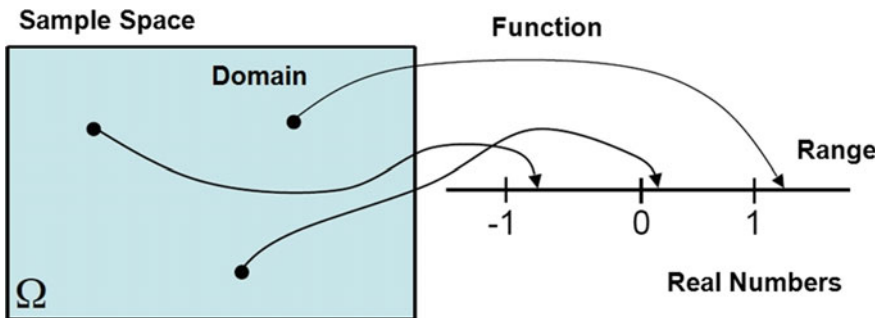


Fig. 3.9 Random variable

A random variable, usually written X , is a variable whose possible values are numerical outcomes of a random phenomenon from statistical experiment. A random variable is a function from a sample space S into the real numbers (Fig. 3.9).

There are two types of random variables—discrete and continuous. A discrete random variable is one which may take on only a countable number of distinct values such as 0, 1, 2, 3, 4. Examples of discrete random variables are wrong typing per page, defective product per lot in manufacturing, the number of children in a family, the number of defective light bulbs in a box of ten. On the other hands, a continuous random variable is one which takes an infinite number of possible values in real interval. Examples include height, weight, departing time of airplane, the time required to run a mile.

For a data set, mean refers to one measure of the central tendency either of a probability distribution or of the random variable characterized by that distribution. If we have a data set containing the failure times t_1, t_2, \dots, t_n , the mean is defined by the formula:

$$t_m = \frac{t_1 + t_2 + t_3 + \dots + t_n}{n} = \frac{\sum_{i=1}^n t_i}{n} \quad (3.12)$$

The mean describes the parameter where the middle of the failure times approximately locates. The mathematical mean is affected to the lowest or highest failure times.

Median is the number separating the higher half of a data sample. In reliability testing, the median is the time in the middle of failure data. The median may be determined by the cumulative distribution function $F(t)$.

$$F(t_{median}) = 0.5 \quad (3.13)$$

The mathematical median is not affected to the lowest or highest failure times.

The mode is the value that appears most often in a set of data. In reliability testing, the mode is the most frequent failure time. The mode is the maximum value of the density function $f(t)$. It can be expressed as:

$$f'(t_{\text{mode}}) = 0 \quad (3.14)$$

The mathematical median is not affected to the lowest or highest failure times.

In statistics, the standard deviation (SD) is used to quantify the variation amount of a set of data values. In reliability testing, the standard deviation is the square root of the variance. This is expressed by

$$\sigma = \left[\frac{\sum_{i=1}^n (t_i - t_m)^2}{n} \right]^{1/2} \quad (3.15)$$

The standard deviation has the same dimension as the failure times t_i .

In probability theory, the expected value of a random variable is the average value of the experiment repetitively. For example, the expected value in rolling a six-sided die is 3.5. Let X be a continuous random variable with range $[a, b]$ and probability density function $f(x)$. The expected value of X is defined as:

$$E(X) = \int_a^b xf(x)dx \quad (3.16)$$

As before, the expected value is also called the mean or average. In general, this is adequate for gambling. In technical reality, the failure probabilities happen to vary amounts in time. Because not all data is normally distributed, other distributions—Weibull is especially suited to analysis of product failures.

If select the failure data and draw histogram, we can find the skewed right (or left) histogram. We know that the probability concepts—mean, median and mode depend on the histogram of data (Fig. 3.10).

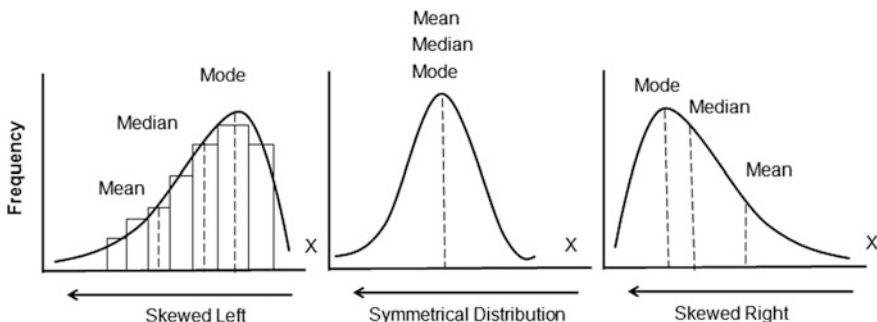


Fig. 3.10 Mean, median and mode for skewed left/right, and symmetric distribution

3.5 Probability Distributions

3.5.1 Introduction

A probability distribution is a mathematical function that provides the probabilities of occurrence of different possible outcomes in an experiment. Probability distributions are generally divided into two classes. A discrete probability distribution can be applicable to the scenarios where the set of possible outcomes is discrete. For example, there are binomial distribution and Poisson distribution. On the other hand, a continuous probability distribution can be applicable to the scenarios where the set of possible outcomes can take on values in a continuous range, such as the temperature on a given day. The normal distribution is a commonly encountered continuous probability distribution. And there are typical lifetime distribution models that can model failure times arising from a wide range of products, such as exponential distribution and Weibull distribution.

3.5.2 Binomial Distribution

Binomial distribution happens in everyday life. Typical occasions are in the following: (1) the number of heads/tails in a sequence of coin flips, (2) vote counts for two different candidates in an election, (3) the number of male/female employees in a company, (4) the number of successful sales calls, and (5) the number of defective products in manufacturing line.

There are several assumptions which accounts for a binomial distribution: (1) n fixed statistical experiments are conducted, (2) each trial is one of two outcomes—a success or a failure (Bernoulli trial), (3) the probability of “success” p is the same for each outcome, (4) the outcomes of different trials are independent, (5) we are interested in the total number of successes in these n trials.

Under the above assumptions, let random variable X be the total number of successes, the probability distribution of X is called the binomial distribution. Probability is expressed as:

$$P(X = x) = \binom{n}{x} p^x (1-p)^{n-x} = \frac{n!}{x!(n-x)!} p^x (1-p)^{n-x} \quad \text{for } x = 0, 1, 2, \dots, n. \quad (3.17)$$

And binomial Mean and Variance can be shown as:

$$\mu = E(X) = np, \quad \text{Var}(X) = np(1-p) \quad (3.18)$$

where the values of n and p are called the parameters of the binomial distribution.

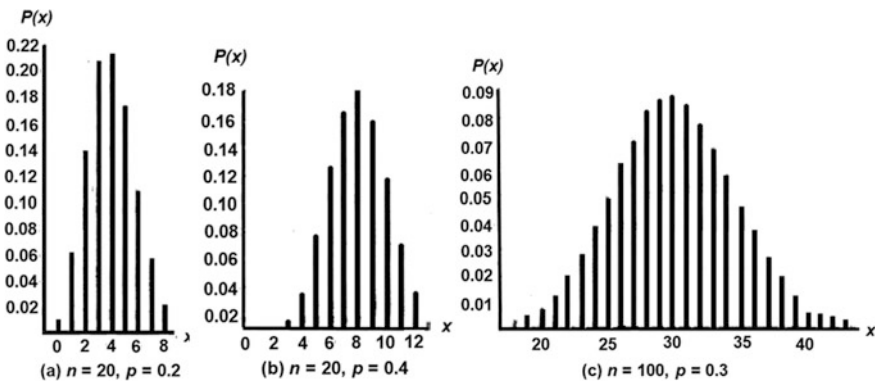


Fig. 3.11 Shape of the binomial distribution according to n and p

When $p = 0.5$, the binomial distribution is symmetrical—the mean and median are equal. Even when $p < 0.5$ (or $p > 0.5$), the shape of the distribution becomes more and more symmetrical the larger the value of N . Because the binomial distribution can quickly become unwieldy, there are approximations to the binomial that can be much easier to use when N is large (Fig. 3.11).

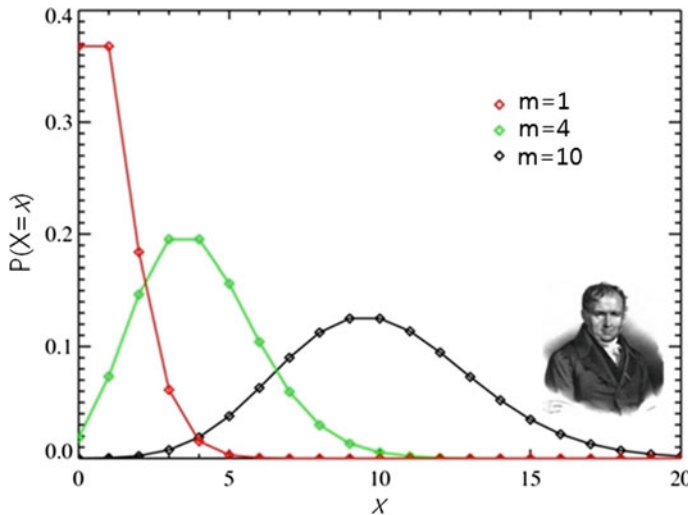
3.5.3 Poisson Distributions

The Poisson distribution is named after Simeon Poisson (1781–1840), a French mathematician, and used in situations where big declines in a time period occurs with a specific average rate, regardless of the time that has elapsed. More specifically, this distribution is used when the number of possible events is large, but the occurrence probability over a specified time period is small (Fig. 3.12).

Two examples of such a situation are as follows:

- A store that rents books has an average rental of 200 books every Saturday night. Using this data, you can predict the probability that more books will sell (perhaps 300 or 400) on the following Saturday nights.
- Another example is the number of diners in a certain restaurant every day. If the average number of diners for seven days is 500, you can predict the probability of a certain day having more customers.

A Poisson distribution has the following properties: (1) The experiment results in outcomes that can be classified as successes or failures. (2) The average number of successes (μ) that occurs in a specified region is known. (3) The probability that a success will occur is proportional to the size of the region. (4) The probability that a success will occur in an extremely small region is virtually zero.

**Fig. 3.12** Poisson Distributions

This distribution also has applications in many reliability areas when one is interested in the occurrence of a number of events that are of the same type. Each event's occurrence is denoted as a time scale and each event represents a failure.

If probability p is very small and trial is far enough, Poisson probability function from Eq. (3.17) can be approximated. That is,

$$\begin{aligned} {}_n C_x p^x (1-p)^{n-x} &= \frac{n(n-1) \cdots (n-x+1)}{x!} \left(\frac{m}{n}\right)^x \left(1 - \frac{m}{n}\right)^{n-x} / \left(1 - \frac{m}{n}\right)^x \\ &= \frac{m^x}{x!} \underbrace{1 \left(1 - \frac{1}{n}\right) \left(1 - \frac{2}{n}\right) \cdots \left(1 - \frac{x-1}{n}\right)}_A \underbrace{\left(1 - \frac{m}{n}\right)^n}_B / \underbrace{\left(1 - \frac{m}{n}\right)^x}_C \end{aligned} \quad (3.19)$$

As n increases, $A-C$ can be rearranged.

$$A = 1 \left(1 - \frac{1}{n}\right) \left(1 - \frac{2}{n}\right) \cdots \left(1 - \frac{x-1}{n}\right) \xrightarrow{n \rightarrow \infty} 1 \quad (3.20a)$$

$$B = \left(1 - \frac{m}{n}\right)^n \xrightarrow{n \rightarrow \infty} e^{-m} \quad (3.20b)$$

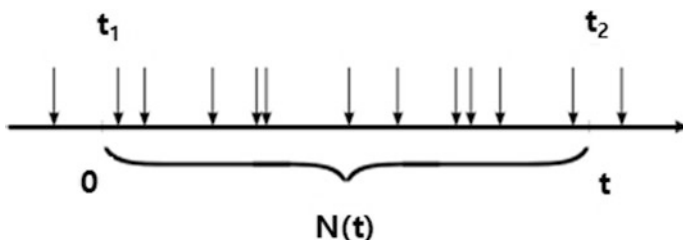
$$C = \left(1 - \frac{\lambda}{n}\right)^x \xrightarrow{n \rightarrow \infty} 1 \quad (3.20c)$$

Therefore, we can summarize as following:

$$P(X = x) = \frac{(m)^x e^{-m}}{x!} \quad (3.21)$$

Poisson process: The Poisson process is one of the most important random processes in probability theory. It is widely used to model random “points” in time and space. Several important probability distributions arise naturally from the Poisson process such as the exponential distribution. That is, the constant failure rate in bathtub can be described by a Poisson process.

In the following it is instructive to think that the Poisson process we consider represents discrete failure time.



Mathematically the process is described by the so called counter process N , or $N(t)$. The counter tells the number of failure that have occurred in the interval $(0, t)$ or, more generally, in the interval (t_1, t_2) .

$N(t)$ = number of failure in the interval $(0, t)$ (the stochastic process)

$N(t_1, t_2)$ = number of arrival in the interval (t_1, t_2) (the increment process $N(t_2) - N(t_1)$)

A counting process $\{N(t), t \geq 0\}$ is a Poisson process with rate λ if all the following conditions hold:

- (i) $N(0) = 0$,
- (ii) $N(t)$ has independent increments,
- (iii) $N(t) - N(s) \sim \text{Poisson } (\lambda(t-s))$ for $s < t$.

3.5.4 Normal Distribution

Normal distribution was first introduced by French mathematician Abraham de Moivre (1667–1754). After that, German mathematician and physicist Johann Carl Friedrich Gauss (1777–1855) made significant contributions to many fields—physics and astronomy. The normal distribution function or Gaussian distribution function is given by:

$$f(x) = \frac{1}{\sqrt{2\pi}\sigma} \exp\left\{-\frac{1}{2}\left(\frac{x-\mu}{\sigma}\right)^2\right\} \quad \text{for } -\infty < x < \infty \quad (3.22)$$

Thus, the curve has two parameters—mean μ and standard deviation σ , which has bell shaped and is symmetric around the mean μ . If a random variable X is normally distributed with mean μ and variance σ^2 , the notation will be represented by $X \sim N(\mu, \sigma^2)$. The characteristics of such normal distribution can be summarized as:

- Bell shaped and continuous for all values of X between $-\infty$ and ∞ .
- Symmetric around the mean μ . Probability for the left and right of mean is 0.5 separately.
- Depends on parameters— μ and σ , there are infinite normal distributions.
- Probability for interval $[\mu - \sigma \leq X \leq \mu + \sigma]$ is 0.6826. Probability for interval $[\mu - 2\sigma \leq X \leq \mu + 2\sigma]$ is 0.9544. And probability for interval $[\mu - 3\sigma \leq X \leq \mu + 3\sigma]$ is 0.997. That is, most of data in normal distribution locate around mean and there is very little data at more than three times of standard deviation.

The normal distribution is the most important distribution in statistics, since it arises naturally in numerous applications. The key reason is that large sums of (small) random variables often turn out to be normally distributed. When random variable X follows $N(\mu, \sigma^2)$, probability for interval $[a, b]$ will be the area of $f(x)$ that is enclosed by a and b on x axis. The mathematical area is given by:

$$P(a \leq X \leq b) = \int_a^b \frac{1}{\sqrt{2\pi}\sigma} \exp\left\{-\frac{1}{2}\left(\frac{x-\mu}{\sigma}\right)^2\right\} dx \quad (3.23)$$

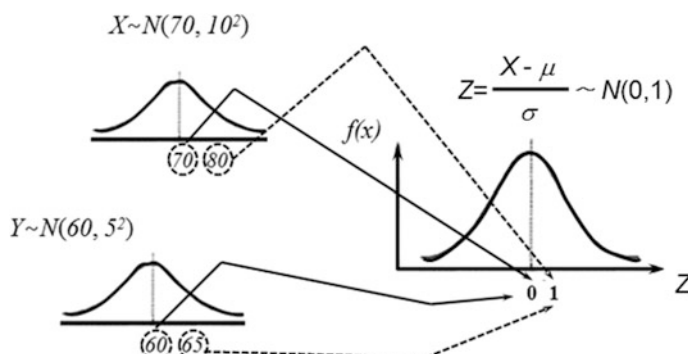


Fig. 3.13 Standardization normal distribution

However, this integral is very difficult. Fortunately, in case of a normal random variable X with arbitrary parameters μ and σ , we can transform it into a standardized normal random variable Z with parameters 0 and 1 (Fig. 3.13).

$$Z = \frac{X - \mu}{\sigma} \quad (3.24)$$

3.5.5 Exponential Distributions

The exponential distribution, with only one unknown parameter, is the simplest of all life distribution models in reliability engineering. Many engineering modules exhibit constant failure rate during the product lifetime if they follows the exponential distribution. Also, it is relatively easy to handle in performing reliability analysis. The key equations for the exponential are shown below:

From Poisson distribution Eq. (3.21), let $N(t)$ be a Poisson process with rate λ . Let X_1 be the time of the first failure.

$$R(t) = P(X_1 > t) = P(\text{no failure in } (0, t]) = \frac{(m)^0 e^{-m}}{0!} = e^{-m} = e^{-\lambda t} \quad (3.25)$$

So the cumulative distribution function also is obtained as:

$$F(t) = 1 - e^{-\lambda t} \quad (3.26)$$

If the cumulative distribution function is differentiated, the probability density function is obtained as:

$$f(t) = \lambda e^{-\lambda t} \quad t \geq 0, \lambda > 0 \quad (3.27)$$

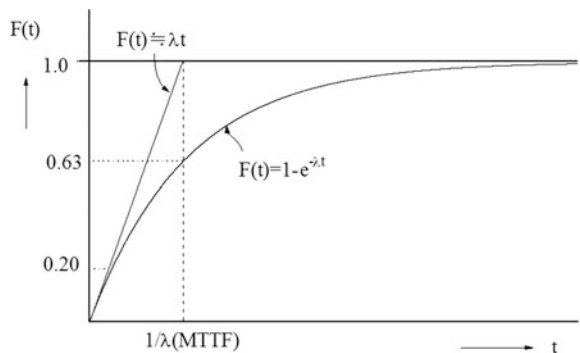
Failure rate $\lambda(t)$ is defined by:

$$\lambda(t) = f(t)/R(t) = \lambda e^{-\lambda t} / e^{-\lambda t} = \lambda \quad (3.28)$$

Note that the failure rate reduces to the constant λ for any time. The exponential distribution is the only distribution to have a constant failure rate. Also, another name for the exponential mean is the Mean Time To Fail or MTTF and we have $MTTF = 1/\lambda$. In general, if product follows the exponential distribution, mean time to failure (MTTF) is 0.63 at $1/\lambda$. Exponential distribution model is useful as following:

- Because of its constant failure rate property, the exponential distribution is an excellent model for the long flat “useful life” portion of the Bathtub Curve.

Fig. 3.14 Cumulative distribution function $F(t)$ of exponential distribution



Since most mechanical systems spend most of their lifetimes in this portion of the Bathtub Curve, this justifies frequent use of the exponential distribution.

2. Just as it is often useful to approximate a curve by piecewise straight line segments, we can approximate any failure rate curve by week-by-week or month-by-month constant rates that are the average of the actual changing rate during the respective time durations.
3. Some natural phenomena have a constant failure rate (or occurrence rate) property. The exponential model works well for inter arrival times while the Poisson distribution describes the total number of events in a given period (Fig. 3.14).

Example 3.2 In a certain region, the number of traffic accidents averages one per two days happens. Find the probability that $x = 0, 1, 2$ accidents will occur in a given day.

So the number of traffic accidents averages one per two days, $m = \lambda t = 0.5$,

$$X = 0, \quad f(0) = \frac{(0.5)^0 e^{-0.5}}{0!} = 0.606,$$

$$\text{Accident days} = 365 \text{ day} \times 0.606 = 221 \text{ day}$$

$$X = 1, \quad f(1) = \frac{(0.5)^1 e^{-0.5}}{1!} = 0.303,$$

$$\text{Accident days} = 365 \text{ day} \times 0.303 = 110 \text{ day}$$

$$X = 2, \quad f(2) = \frac{(0.5)^2 e^{-0.5}}{2!} = 0.076,$$

$$\text{Accident days} = 365 \text{ day} \times 0.076 = 27 \text{ day}$$

Example 3.3 TV is selling in a certain area and average failure rate is 1%/2000 h. If 100 TV units are sampling and testing for 2000 h, find the probability that no accidents, $x = 0$, will occur.

$$m = n \cdot \lambda \cdot t = 100 \times 0.01/2000 \times 2000 = 1$$

Because no accident, the probability is

$$X = 0, \quad f(0) = \frac{(1)^0 e^{-1}}{0!} = 0.36$$

We can estimate the confidence level is 63% for 100 TV units. If no accidents, $x = 0$, the confidence level would like to increase to 90%, how many TV units will it requires?

$$X = 0, \quad f(0) = \frac{(m)^0 e^{-m}}{0!} = 0.1$$

So if $m = 2.3$, the required sample size $n = 230$ will be obtained as

$$m = n \cdot \lambda \cdot t = n \times 0.01/2000 \times 2000 = 2.3$$

3.6 Weibull Distributions and Its Applications

3.6.1 Weibull Parameter Estimation

The main challenge of fitting distributions to reliability data is to find the type of distribution and the values of the parameters that give the highest probability of producing the observed data. One of the most common probability density functions used in industry is the Weibull Distribution. It was invented by W. Weibull in 1937, who found it to be so flexible that it effectively worked on a very wide range of problems. Many other extensions of the Weibull distribution have been proposed to enhance its capability to fit diverse lifetime data since 1970s.

This is mainly due to its weakest link properties, but other reasons have its increasing failure rate with component age and the variety of distribution shapes. The increasing failure rate accounts to some extent for fatigue failures. The density function depend upon the shape parameter β . For low β values ($\beta < 1$), the failure behavior can be similar to the exponential distribution. For $\beta > 1$, the density function always begins at $f(t) = 0$, reaches a maximum with increasing lifetime and decreasing slowly again. Two-parameter fit is more common in reliability testing and more efficient with the same sample size. If the shape parameter is assumed to be known, it can reduce fit to one parameter (Fig. 3.15).

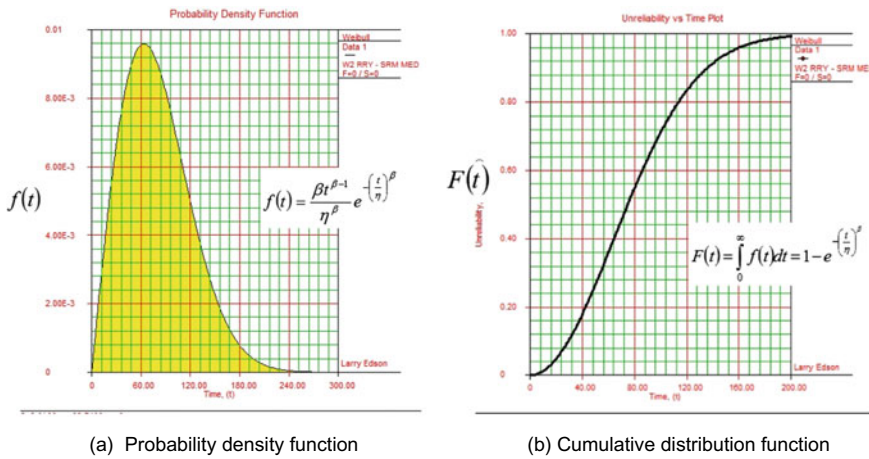


Fig. 3.15 Probability density and cumulative distribution function on the Weibull distributions

Because the Weibull is a very flexible life distribution model with two parameters, the probability density function is defined as:

$$f(t) = \frac{\beta t^{\beta-1}}{\eta^\beta} e^{-(\frac{t}{\eta})^\beta}, \quad t \geq 0, \eta > 0, \beta > 0 \quad (3.29)$$

where η and β are characteristic life and shape parameters, respectively.

When Eq. (3.29) is integrated, the cumulative distribution function is obtained as:

$$F(t) = \int_0^\infty f(t) dt = 1 - e^{-(\frac{t}{\eta})^\beta}, \quad t > 0 \quad (3.30)$$

Reliability function $R(t)$ is defined as:

$$R(t) = 1 - F(t) = e^{-(\frac{t}{\eta})^\beta}, \quad t > 0 \quad (3.31)$$

Hazard (or failure) rate function $\lambda(t)$ can be described by:

$$\lambda(t) = \frac{f(t)}{R(t)} = \frac{\beta}{\eta} \left(\frac{t}{\eta} \right)^\beta, \quad t > 0 \quad (3.32)$$

For $\beta = 1$ and 2 , the exponential and Rayleigh distributions are especially called in Weibull distribution, respectively.

Abernathy (1996) recommended Weibayes as best practice for all small samples, 20 failures or less, if a reasonable point estimate of β is available. Using Weibayes

method, $\hat{\beta}$ can be assumed from some historical data or prior knowledge, leaving $\hat{\eta}$ as the single parameter, which can be estimated using maximum likelihood as:

$$\hat{\eta} = \left[\sum_{i=1}^N \left(\frac{t_i^\beta}{r} \right)^{\frac{1}{\beta}} \right] \quad (3.33)$$

where t is testing time, r is the number of failed sample, N is the total number of failures.

The various failure rates of the Weibull distribution specified in bathtub curve can be divided into three regions.

- $\beta < 1.0$: Failure rates decrease with increasing lifetime (early failure)
- $\beta = 1.0$: Failure rates are constant
- $\beta > 1.0$: Failure rates increase with increasing lifetime.

The characteristic lifetime η is assigned to the cumulative distribution function $F(t) = 63.2\%$ for exponential distribution.

A shape parameter estimated from the data affects the shape of a Weibull distribution, but does not affect the location or scale of its distribution. The spread of the shape parameters represents the confidence intervals and a dependency of the stress level. A summary of the determined shape parameters is approximately described as:

- High temperature, high pressure, high stress: $2.5 < \beta < 10$
 - Low cycle fatigue: depend on cycle times
e.g., disk, shaft, turbine
- Low temperature, low pressure, low stress: $0.7 < \beta < 2$
 - Degradation: depend on use time
e.g., electrical appliance, pump, fuel control value

Shape parameter β of a certain component would be invariable, but its characteristic life η varies according to use condition and material status. Thus, shape parameter (β) would be estimable and then will be confirmed after test. The density function and hazard rate function for the Weibull distribution range from shape parameters $\beta \approx 1.0\text{--}5.0$.

3.6.2 Weibull Parameter Estimation

There are two widely used general methods that can estimate life distribution parameters from a particular data set: (1) Graphical estimation in Weibull plotting, (2) Maximum Likelihood Estimation (MLE) and median rank regression (MRR). Weibull plotting is a graphical method for informally checking on the assumption

of Weibull distribution model and also for estimating the two Weibull parameters—shape parameter and characteristic life.

For a Weibull probability plot draw a horizontal line from the y-axis to the fitted line at the 62.3 percentile point. That estimation line intersects the line through the points at a time that is the estimate of the characteristic life parameter η . In order to estimate the slope of the fitted line (or the shape parameter β), choose any two points on the fitted line and divide the change in the y variable by the change in x variable.

There are several different methods of estimating Weibull parameters such as Maximum Likelihood and median rank regression (MRR). Olteanu and Freeman [1] have investigated the performance of MLE and MRR methods and concluded that the median rank regression method is the best combination of accuracy and ease of interpretation when the sample size and number of suspensions are small. This method is popular in industry because fitting can be easily visualized.

The Median Ranks method is used to obtain an estimate of the unreliability for each failure.

First, we will examine the fitting of two-parameter Weibull using median rank regression method. Median rank regression determines the best-fit straight line by least squares regression curve fitting. This method proceeds as follows:

- (1) Obtain failure data.
- (2) The cumulative distribution function $F(t)$ has an S-like shaped curve (Fig. 3.16a). With a Weibull Probability Paper, If plotted the function $F(t)$ in Weibull Probability Paper, it is useful to evaluate the lifetime of mechanical system in reliability testing.

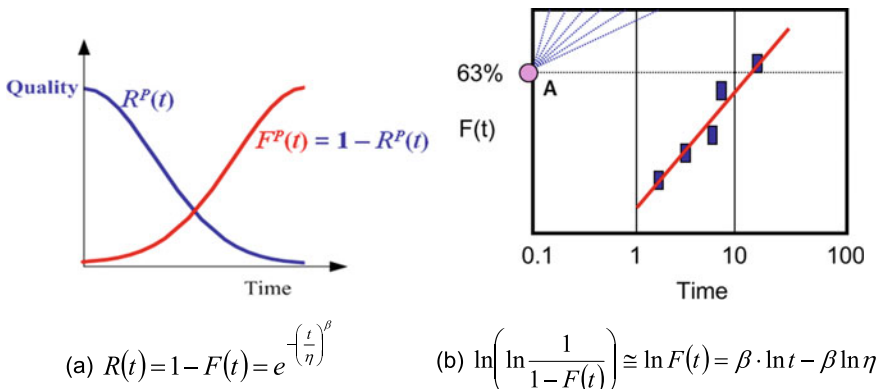


Fig. 3.16 A plotting of Weibull probability paper

After taking inverse number and logarithmic transformation from reliability Eq. (3.31), it can be expressed as:

$$\ln(1 - F(t))^{-1} = \left(\frac{t}{\eta}\right)^\beta \quad (3.34)$$

After taking logarithmic transformation one more time, it can be expressed as:

$$\ln\left(\ln\frac{1}{1 - F(t)}\right) = \beta \cdot \ln t - \beta \ln \eta \quad (3.35)$$

If F is sufficiently small, then Eq. (3.35) can be modified as:

$$\ln\left(\ln\frac{1}{1 - F(t)}\right) \cong \ln F(t) = \beta \cdot \ln t - \beta \ln \eta \quad (3.36)$$

Equation (3.36) corresponds to a linear equation in the form. That is,

$$y = ax + b \quad (3.37)$$

with the variables

$$a = \beta \quad (\text{slope}) \quad (3.38a)$$

$$b = -\beta \ln \eta \quad (\text{axis intersection}) \quad (3.38b)$$

$$x = \ln t \quad (\text{abscissa scaling}) \quad (3.38c)$$

$$y = \ln(-\ln(1 - F(t))) \quad (\text{ordinate scaling}) \quad (3.38d)$$

That is, two parametric Weibull distribution can be expressed as a straight line on the Weibull Probability Paper. The slope of its straight line becomes the shape parameter β (see Fig. 3.16b).

- (3) Calculate median ranks: Rank failure times in ascending order. Mean ranks are less accurate for the skewed Weibull distribution, therefore median ranks are preferable. Median ranks can be calculated as follows:

$$\sum_{k=i}^N \binom{N}{k} (MR)^k (1 - MR)^{N-k} = 0.5 = 50\% \quad (3.39)$$

Bernard used an approximation of it as follows:

$$F(t_i) \approx \frac{i - 0.3}{n + 0.4} \times 100 \quad (3.40)$$

where i is failure order number, N is total sample size.

Step 1: Rank the times-to-failure in according to ascending order $t_1 < t_2 \dots < t_n$

i	1	2	3	...	r - 1	r
t_i	t_1	t_2	t_3		t_{r-1}	t_r

By ordering the failure times, an overview is won over the timely progression of the failure times. In addition, the ordered failure times are required in the next analysis step and are referred to as order statistics. Their index corresponds to their rank.

Step 2: Determine the failure probability $F(t_i)$ of the individual order statistics from Eq. (3.51).

Step 3: Enter the coordinate $(t_i, F(t_i))$ in the Weibull probability paper.

Step 4: Approximate sketch the best fit straight line through the entered points and determine the Weibull parameters $\hat{\beta}$. At the $F(t) = 63.2\%$ ordinate point, draw a straight horizontal line until this line intersects the fitted straight line. Draw a vertical line through this intersection until it crosses the abscissa. The value at the intersection of the abscissa is the estimate of $\hat{\eta}$ (Fig. 3.17).

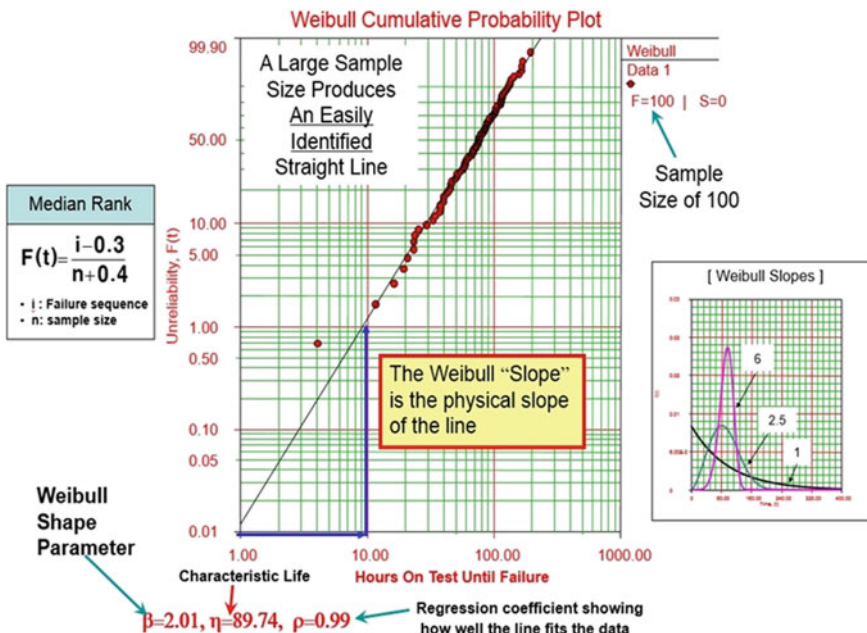


Fig. 3.17 A typical characteristics of Weibull plot with a large sample size

The best fit line in least squares is defined as the one that minimizes the sum of squared differences between the true and estimated values. Suppose we have a set of points $(x_1, y_1), (x_2, y_2), \dots, (x_n, y_n)$, obtained by linearization of life data. We can use the ordinary least squares to estimate the slope \hat{b} and the intercept \hat{a} of the straight line defined by the equation $\bar{y} = \hat{a} + \hat{b}\bar{x}$ as follows:

$$\hat{b} = \frac{\sum_{i=1}^n x_i y_i - \frac{\sum_{i=1}^n x_i}{N} \sum_{i=1}^n y_i}{\sum_{i=1}^n x_i^2 - \frac{(\sum_{i=1}^n x_i)^2}{N}} \quad (3.41)$$

$$\hat{a} = \frac{\sum_{i=1}^n y_i}{N} - \hat{b} \frac{\sum_{i=1}^n x_i}{N} = \bar{y} - \hat{b}\bar{x} \quad (3.42)$$

Example 3.4 Assume that six automobile units are tested. All of these units fail during the test after operating the following number of hours t_i : 93, 34, 16, 120, 53 and 75. Estimate the values of the parameters for a two-parameter Weibull distribution and determine the reliability of the units at a time of 15 h.

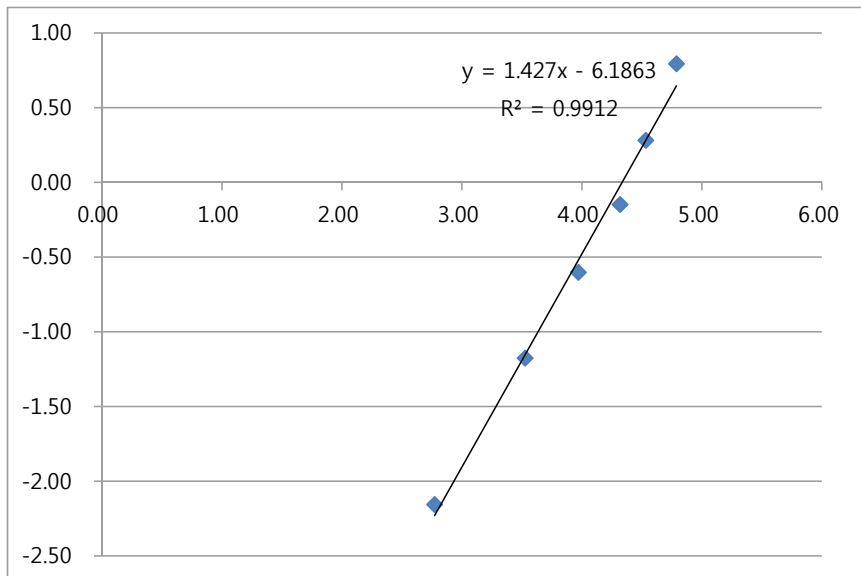
First, rank the times-to-failure in ascending order as shown next.

Failure order (i)	Time-to-failure, hours (t_i)	$F(t_i) \%$
1	16	10.94
2	34	26.56
3	53	42.19
4	75	57.81
5	93	73.44
6	120	89.06

Second, by using Excel, approximate sketch the best fit straight line through the entered points $(\ln(t_i), \ln[-\ln(1 - F(t))])$.

Failure order (i)	$\ln(t_i)$	$\ln[-\ln(1 - F(t))]$
1	2.77	-2.16
2	3.53	-1.18
3	3.97	-0.60
4	4.32	-0.15
5	4.53	0.28
6	4.79	0.79

We can obtain the estimated shape parameter $\hat{\beta} = \text{slope} = 1.427$, estimated characteristic life $\hat{\eta}(Q(t))$ is 63.2% ordinate point) = $e^{\frac{6.187}{1.427}} = 76.3226$ h.
where $\ln[-\ln(1 - 0.63)] = -0.00576$, $-0.00576 = 1.427x - 6.186$.



A Weibull distribution with the shape parameter $\beta = 1.427$ and $\eta = 76.32$ h is drawn on the Weibull Probability Paper. The cumulative distribution function is described as

$$F(t) = 1 - e^{-\left(\frac{t}{76.32}\right)^{1.43}}$$

In result a straight line is sketched with slope $\beta = 1.4$ on the Weibull Probability Paper. The characteristic lifetime is 76.0 h when the cumulative distribution function, i $F(t)$ is 63% (Fig. 3.18).

3.6.3 Confidence Interval

In statistics the purpose of taking a random sample from population is to approximate the mean of the population. Because life data analysis results are estimates based on the observed lifetimes of a sampling of units, there is uncertainty in the results due to the limited sample sizes. How well the sample statistic estimates the underlying population value is always an issue. A confidence interval addresses this issue because it provides a range of values which is likely to contain the population parameter of interest (Fig. 3.19).

A confidence interval (CI) is characterized as the probability that a random value lies within a certain range. CI is represented by a percentage. For example, a 90% confidence interval implies that in 90 out of 100 cases, the observed value falls within this certain interval. After any particular sample is taken, the population

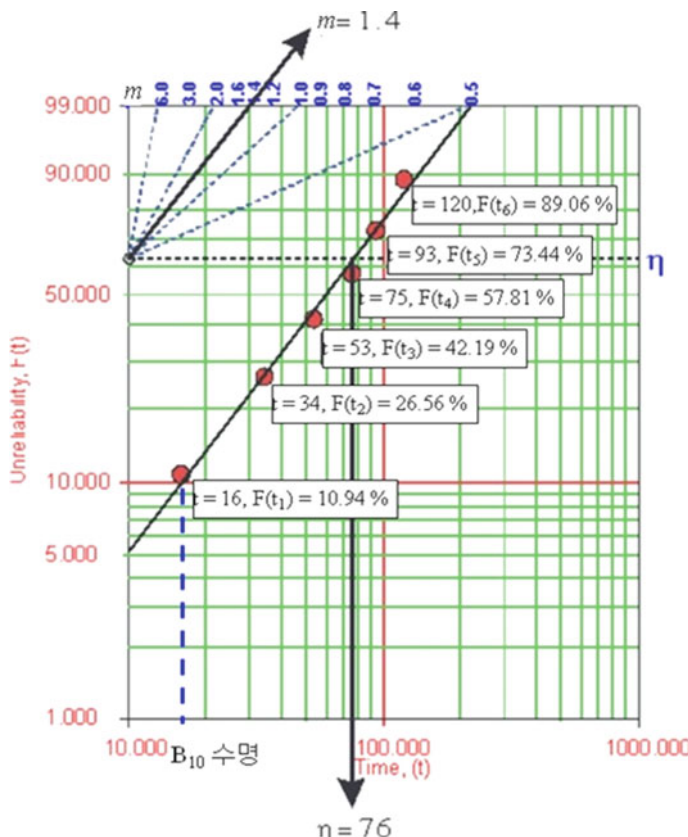


Fig. 3.18 How to use Weibull CDF

parameter is either in the interval realized or not. The desired level of confidence is set by the researcher. A 90% confidence interval reflects a significance level of $\alpha = 0.1$. The confidence level also depends on the product field.

The average of failure times can often deviate within a certain range. The Weibull line may describe experimental results. If the median is used to determine $F(t_i)$, 50% of the experimental results lie below the Weibull line. To know the truth of the Weibull line, it is necessary to determine its confidence interval.

Over an observation of several test samples, the Weibull line drawn in Fig. 3.20 is the most probable in the middle—median values and its confidence intervals. The line in the middle represents the population mean—observed over several test specimens—thus 50% of the cases lie above and 50% lie below this line.

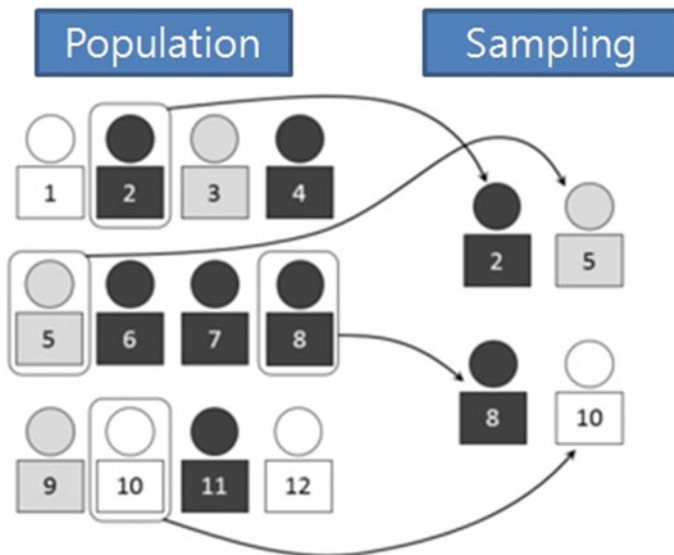


Fig. 3.19 Concept of confidence interval

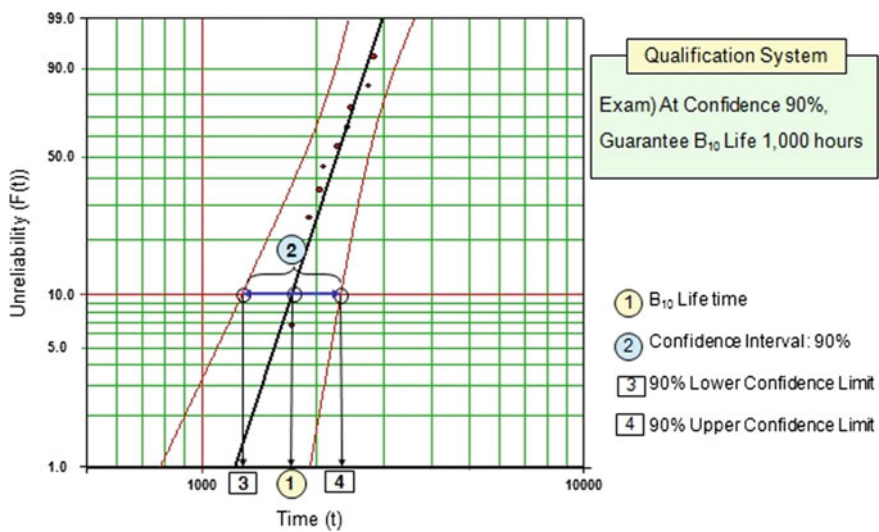


Fig. 3.20 Weibull plot of five failures with 90% confidence interval

3.7 Sample Distributions

3.7.1 Introduction

Until now, we have studied to analyze the sample on the premise the characteristics of population are known. However, in real life or academic study, we have frequently confronted the situations we have to search out its characteristics in case populations are unknown.

If we want to know mean capacity of battery produced in a company, we have to investigate its whole products. To complete this case, it is impossible because a lot of time and cost are required. After we choose a proper sample, we will compute its statistics. Based on that, we will figure out parameters of populations—mean and standard deviations. In the same manner, selecting sample from population and leading the estimation or conclusion on population, we call it statistical inference.

These statistics vary for each different random sample we select. That is, they are random variables. If the sampling is done randomly, the value of a statistic will be random. Since statistics are random variables, they have the sampling distribution. It provides the following information: (1) What values of the statistic can occur, (2) What is the probability of each value to occur (Fig. 3.21).

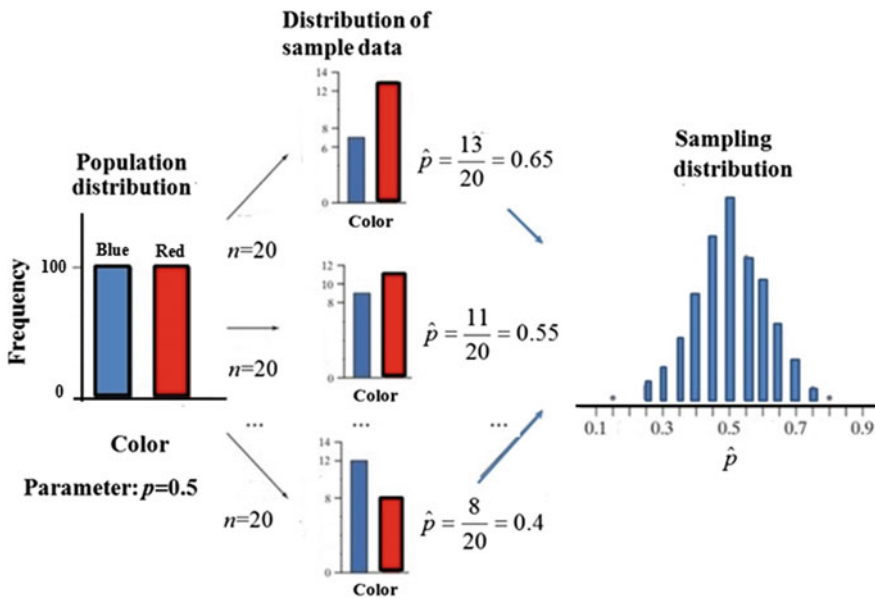


Fig. 3.21 Sample distributions in case of the known population

3.7.2 The Distribution of Sample Mean

Sample mean \bar{x} that is computed from a large sample tends to be closer to μ than does \bar{x} based on a small n . Suppose X_1, \dots, X_n are random variables with the same distribution with mean μ and population standard deviation σ . Now look at the random variable \bar{X} .

$$\bar{X} = \frac{1}{n}(X_1 + X_2 + \dots + X_n) \quad (3.43)$$

$$E(\bar{X}) = \frac{1}{n}(E(X_1) + E(X_2) + \dots + E(X_n)) = \frac{1}{n} \cdot n\mu = \mu \quad (3.44)$$

$$V(\bar{X}) = \frac{1}{n^2}(V(X_1) + V(X_2) + \dots + V(X_n)) = \frac{1}{n^2} \cdot n\sigma^2 = \frac{\sigma^2}{n} \quad (3.45)$$

The expectation value is $E(\bar{X}) = \mu$ and variation is $V(\bar{X}) = \sigma^2/n$. That is,

1. The population mean of \bar{X} , denoted $\mu_{\bar{X}}$, is equal to μ .
2. The population standard deviation of \bar{X} , denoted $\sigma_{\bar{X}}$, is equal to

$$\sigma_{\bar{X}} = \frac{\sigma}{\sqrt{n}} \quad (3.46)$$

This means that the sampling distribution of \bar{x} is always centered at μ and the second statement gives the rate the spread of the sampling distribution (sampling variability) decreases as n increases. The standard deviation of a statistic is called the standard error of the statistic. The standard error gives the precision of statistic for estimating a population parameter. The smaller the standard error, the higher the precision.

The standard error of the mean \bar{X} is

$$SE(\bar{X}) = \sigma / \sqrt{n} \quad (3.47)$$

Now that we learned about the mean and the standard deviation of the sampling distribution of the sample mean, we might ask, if there is anything we can tell about the shape of the density curve of this distribution.

If population is infinite and sample size n is large enough, we know the distribution of sample mean is approximately normal distributed regardless the population characteristics. Namely, the Central Limit Theorem states that under rather general conditions, means of random samples drawn from one population tend to have an approximately normal distribution. We find that it does not matter which kind of distribution we find in the population. It even can be discrete or extremely skewed (Fig. 3.22).

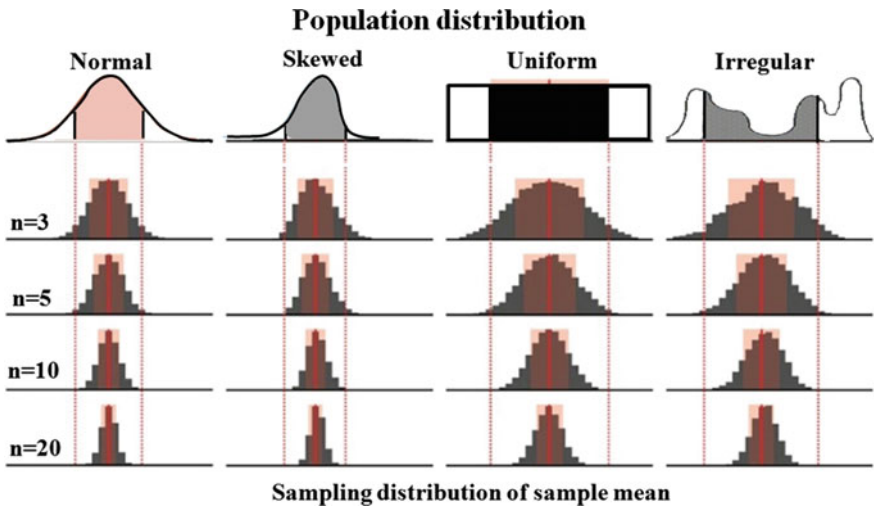


Fig. 3.22 Central Limit Theorem

Central Limit Theorem: From any population with finite mean μ and standard deviation σ , when n is large, if random samples of n observations are chosen, the sampling distribution of the mean \bar{X} is approximately normal distributed, with mean μ and standard deviation σ/\sqrt{n} . That is,

$$\bar{X} \sim N\left(\mu, \frac{\sigma^2}{n}\right) \quad (3.48)$$

The Central Limit Theorem becomes very substantial one in modern statistics. Now look at a binomial distributed random variable X . With probability p (Bernoulli trial), we can carry out the experiment of n trials. Using Central Limit Theorem, as n increase infinitely, the random variable X will be distributed normally.

The random variable X is binomial distributed $B(n, p)$ with mean pn and standard deviation equals $\sqrt{p(1-p)}$. Since \hat{p} is simply the value of X expressed as a proportion, the sampling distribution of \hat{p} is identical to the probability distribution of X . Then is $\hat{p} = \sum X_i/n = \bar{X}$. Using the Central Limit Theorem, as n increase infinitely, it will be normally distributed $N(np, np(1-p))$, which mean is np and variation is $np(1-p)$. That is, as n increases infinitely, the random variable X is normally distributed:

$$\frac{X - np}{\sqrt{np(1-p)}} \sim N(0, 1) \quad (3.49)$$

3.7.3 The Distribution of Sample Variation

If relationship between population variation and sample variation is known, it will be helpful to estimate the unknown population variation. We would figure out the distribution of sample variance with Example 3.4.

Example 3.4 There are five salesmen in a company. The working periods are 6, 2, 4, 8, and 10.

- (1) Select a random sample of size 2 with replacement and observe the working period. And find each sample variation and compare the mean and variation of total sample variation with population variation.
- (2) Write down the frequency distribution table and draw the bar graph.

Solution: (1) The mean of this population is $\mu = 6$ and its variation is $\sigma^2 = 8$. The variation of all possible samples with replacement can be summarized in Table 3.2. We know that some match that of population variation and the other have gaps like 0 or 32. The mean of all sample variation can be found as:

$$E(s^2) = \frac{0 \times 5 + 2 \times 8 + 8 \times 6 + 18 \times 4 + 32 \times 2}{25} = 8,$$

That is, we can see that the mean of all possible sample variation is equal to variation of population. We can call the sample variation the *unbiased estimator* of population variation.

(2) Figure 3.23 is its bar graph. We call them the distribution of sample variation. What we see from the above figure and table is that the small sample variation is large and the large sample variation is small. That is, it is distributed asymmetrically. The mean of all possible sample variation ($E(s^2)$) is equal to variation of population (σ^2). The sample variation is the *unbiased estimator* of population variation.

As seen in Example 3.4, the sample variation is asymmetrically distributed. That is, the frequency at small sample variation is large. On the other hands, the frequency at large sample variation is small. Supposed that population is normally distributed and population variation is σ^2 , sample variation follows chi-squared

Table 3.2 The variation of all possible samples with $n = 2$ that can be chosen from the population $N = 5$

Sample	s^2								
2, 2	0	4, 2	2	6, 2	8	8, 2	18	10, 2	32
2, 4	2	4, 4	0	6, 4	2	8, 4	8	10, 4	18
2, 6	8	4, 6	2	6, 6	0	8, 6	2	10, 6	8
2, 8	18	4, 8	8	6, 8	2	8, 8	0	10, 8	2
2, 10	32	4, 10	10	6, 10	8	8, 10	2	10, 10	0

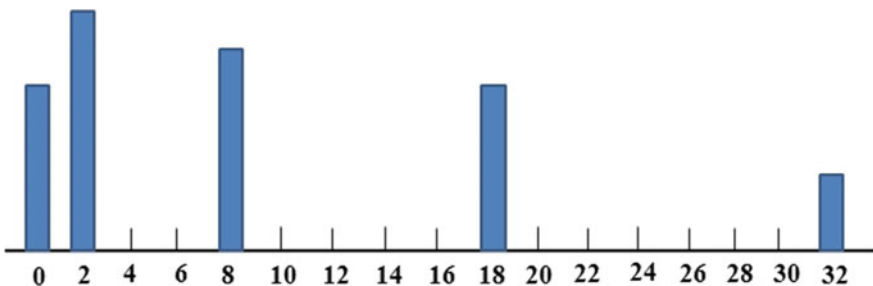


Fig. 3.23 Bar graph of the distribution of sample variation

distribution with k degrees of freedom. Depending on integer k (or degrees of freedom), Chi-squared distribution is a kind of family, written as $\chi^2(1)$ with one degree of freedom, $\chi^2(2)$ with two degree of freedom, ..., and $\chi^2(27)$ with twenty seven degree of freedom. As seen in Fig. 3.24, according to k degrees of freedom, Chi-squared distribution is asymmetrically distributed.

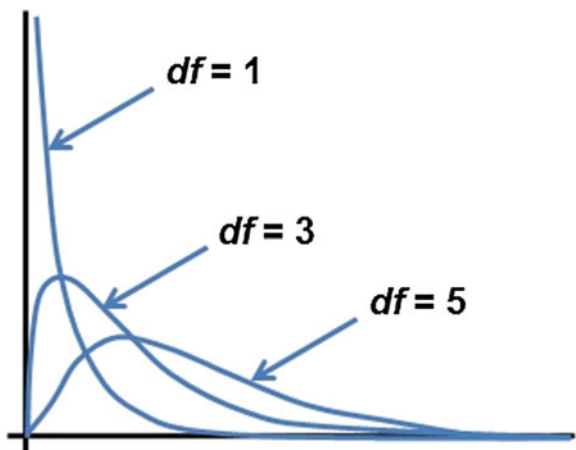
Distribution of sample variation: Supposed that population with variation σ^2 is normally distributed, if n sample is chosen randomly, $(n - 1)S^2/\sigma^2$ follows Chi-squared distribution with $(n - 1)$ degrees of freedom. That is,

$$(n - 1)S^2/\sigma^2 \sim \chi^2(n - 1) \quad (3.50)$$

where

$$S^2 = \frac{\sum_{i=1}^n (X_i - \bar{X})^2}{n - 1} \quad (3.51)$$

Fig. 3.24 Chi-squared distribution according to k degrees of freedom



3.8 Relationship Between Reliability and Cumulative Distribution Function

To define the reliability function from the standpoint of load-strength interference, the strength of a product is modeled as a random variable S . The product is exposed to a load L that is also modeled as a random variable. The distributions of the strength and the load at a specific time t are illustrated in Fig. 3.25. A failure will occur as soon as the load is higher than the strength. The reliability R of the item is defined as the probability that the strength is greater than the load,

$$R(t) = P(S > L) \quad (3.52)$$

where $\Pr(A)$ denotes the probability of event A.

The load will usually vary with time and may be modeled as a time-dependent variable $L(t)$. The product will deteriorate with time, due to failure mechanisms like fatigue, fracture, and corrosion. The strength of the product will therefore also be a function of time, $S(t)$. The time to failure T of the product is the (shortest) time until $S(t) < L(t)$,

$$T = \min\{t : S(t) < L(t)\} \quad (3.53)$$

and the reliability $R(t)$ of the item may be expressed as:

$$R(t) = P(T > t) = 1 - F(t) = \int_t^{\infty} f(x)dx \quad (3.54)$$

$R(t)$ is the probability that the item will not fail in the interval $(0, t]$. $R(t)$ is the probability that it will survive at least until time t —it is sometimes called the survival function (Fig. 3.26).

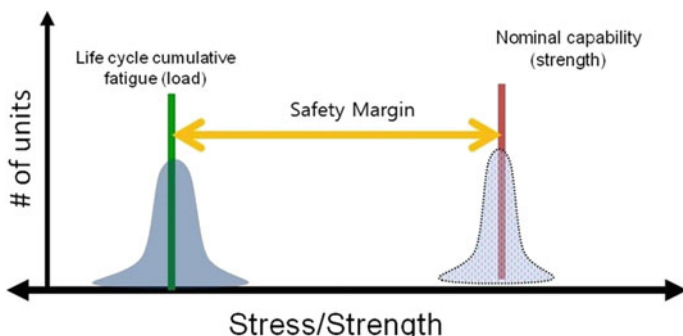
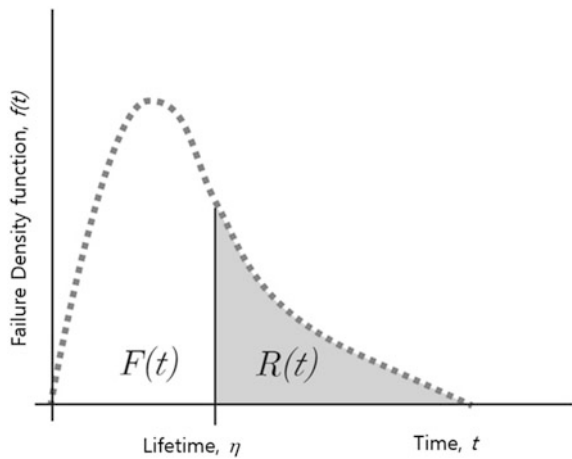


Fig. 3.25 Load and the strength distributions

Fig. 3.26 Cumulative distribution function $F(t)$ and reliability function $R(t)$



The cumulative distribution function (CDF) is the probability that the variable t takes a value less than or equal to T . CDF associated with the time to failure T is expressed as:

$$F(t) = P(T \leq t) \quad (3.55)$$

which is the probability that the system fails within the time interval $(0; t]$. If T is a continuous random variable, the probability function is related to its probability density function $f(t)$ by

$$F(t) = \int_0^t f(x)dx \quad (3.56)$$

In probability theory, a probability density function (PDF) is a function that describes the relative likelihood for this random variable to take on a given value. In reliability testing, density function $f(t)$ is defined by:

$$\frac{dF(t)}{dt} = \frac{d \int_0^t f(x)dx}{dt} = f(t) \quad (3.57)$$

Failure rate (or Hazard rate function) is the frequency with which an engineered system or component fails. Consider the conditional probability:

$$P(t < T < t + \Delta t | T > t) = \frac{P(t < T \leq t + \Delta t)}{R(t)} = \frac{F(t + \Delta t) - F(t)}{R(t)} \quad (3.58)$$

In reliability engineering, failure rate (or hazard rate function) $\lambda(t)$ is defined by:

$$\lambda(t) = \lim_{\Delta t \rightarrow 0} \frac{P(t < T < t + \Delta t | T > t)}{\Delta t} = \frac{f(t)}{R(t)} \quad (3.59)$$

$\lambda(t) dt$ is the probability that the system will fail during the period $(t; t + dt]$, given that it has survived until time t .

A survival and hazard function is to analyze the expected duration of time until one or more events happen, such as failure in mechanical systems. Cumulative hazard rate function $\Lambda(t)$ is defined by:

$$\Lambda(t) = \int_0^t \lambda(x) dx \quad (3.60)$$

Suppose the failure rate $\lambda(t)$ is known. Then it is possible to obtain $f(t)$, $F(t)$, and $R(t)$.

$$f(t) = \frac{dF(t)}{dt} = -\frac{dR(t)}{dt} \Rightarrow \lambda(t) = -\frac{dR/dt}{R} \quad (3.61)$$

If Eq. (3.61) is integrated, then reliability function becomes

$$R(t) = \exp \left[- \int_0^t \lambda(\tau) d\tau \right] \quad (3.62)$$

So the density function and cumulative distribution function are defined as:

$$f(t) = \lambda(t) \exp \left[- \int_0^t \lambda(\tau) d\tau \right] \quad (3.63)$$

$$F(t) = 1 - \exp \left[- \int_0^t \lambda(\tau) d\tau \right] \quad (3.64)$$

Relationship between reliability function $R(t)$ and cumulative distribution function $F(t)$ can be summarized in Fig. 3.27.

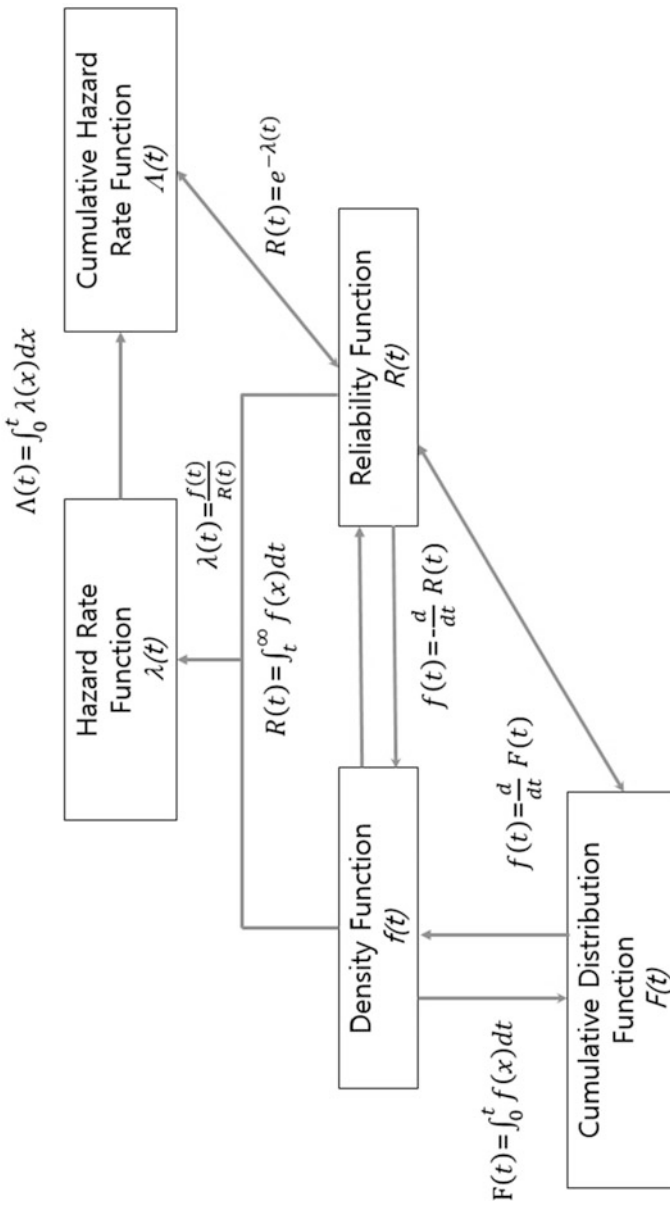


Fig. 3.27 Relationship between reliability function $R(t)$ and cumulative distribution function $F(t)$

3.9 Design of Experiment (DOE)

Engineering discoveries often come from performing experiments. To verify them, we use the statistical methodology. Engineering learning is an iterative process, as represented in Fig. 3.28.

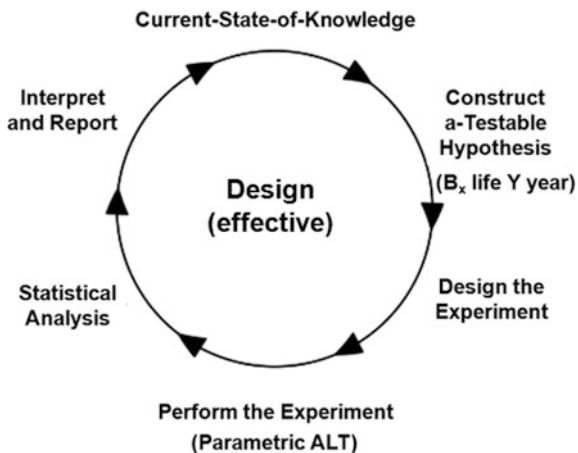
If we start at current knowledge, the next step is choosing a new knowledge and constructing a testable hypothesis. Statistical theory focuses on “null hypothesis” which often represents the exact opposite of what an experimenter expects. On the other hands, “alternative hypothesis” that is contrary to the null hypothesis is suggested. The next step in the cycle is to “Design an Experiment” and “Perform the Experiment.” Finally, we perform statistical analyses and interpret it, which leads to possible modification of the “Current State of Knowledge.”

Design of experiment (DOE) is a systematic method to determine the relationship between factors affecting a process and its output. The designing of experiment and the analysis like ANOVA from obtained data are inseparable. If the experiment is properly designed, the data can carry out the statistical inferences. It is important to understand first the basic terminologies used in the experimental design. For mechanical system the factor that product lifetime influences is stress due to the repetitive loads. If product is to estimate its lifetime, we have to carry out parametric ALT. Accelerated loads reveals the faulty designs at each ALT stage. If the mission cycle is achieved, we can evaluate the product lifetime.

3.9.1 Terminologies

Experimental unit: For conducting an experiment, the experimental material is divided into smaller parts and each part is referred to as experimental unit. The

Fig. 3.28 Engineering learning is an iterative process



experimental unit is randomly assigned to a treatment is the experimental unit. The phrase “randomly assigned” is very important in this definition.

Experiment: A way of getting an answer to a question which the experimenter wants to know.

Treatment: Different objects or procedures compared in an experiment are called treatments.

Factor: A factor is a variable defining a categorization. A factor can be fixed or random in nature. A factor is termed as fixed factor if all the levels of interest are included in the experiment. A factor is termed as random factor if all the levels of interest are not included in the experiment.

Replication: It is the repetition of the experimental situation by replicating the experimental unit.

Experimental error: The unexplained random part of variation in any experiment is termed as experimental error. An estimate of experimental error can be obtained by replication.

Treatment design: A treatment design is the manner in which the levels of treatments are arranged in an experiment.

Design of experiment: One of the main objectives of designing an experiment is how to verify the hypothesis in an efficient and economical way. In the contest of the null hypothesis of equality of several means of normal populations having same variances, the analysis of variance technique can be used. Note that such techniques are based on certain statistical assumptions. If these assumptions are violated, the outcome of the test of hypothesis then may also be faulty and the analysis of data may be meaningless. So the main question is how to obtain the data such that the assumptions are met and the data is readily available for the application of tools like analysis of variance. The designing of such mechanism to obtain such data is achieved by the design of experiment. After obtaining the sufficient experimental unit, the treatments are allocated to the experimental units in a random fashion. Design of experiment provides a method by which the treatments are placed at random on the experimental units in such a way that the responses are estimated with the utmost precision possible.

Principles of experimental design: There are three basic principles of design—
(1) Randomization, (2) Replication, and (3) Local control (error control).

Completely randomized design (CRD): For completely randomized designs, the levels of the primary factor are randomly assigned to the experimental units. By randomization, the run sequence of the experimental units is determined randomly. Following steps are needed to design a CRD:

- Divide the entire experimental material or area into a number of experimental units, say n .
- Fix the number of replications for different treatments in advance (for given total number of available experimental units).
- No local control measure is provided as such except that the error variance can be reduced by choosing a homogeneous set of experimental units.

3.9.2 Analysis

There is only one factor which is affecting the outcome—treatment effect. So the setup of one way analysis of variance (ANOVA) is to be used.

y_{ij} : Individual measurement of j th experimental units for i th treatment $i = 1, 2, \dots, v, j = 1, 2, \dots, n_i$

Independently distributed following with $N(\mu + \alpha_i, \sigma^2)$ with $\sum_{i=1}^v n_i \alpha_i = 0$.

μ : overall mean

α_i : i th treatment effect

H_0 : $\alpha_1 = \alpha_2 = \dots = \alpha_v = 0$

H_1 : All α_i 's are not equal.

The data set is arranged as follows (Table 3.3):

where $T_i = \sum_{j=1}^n y_{ij}$ is the treatment total due to i th effect, $G = \sum_{i=1}^v T_i = \sum_{i=1}^v \sum_{j=1}^n y_{ij}$ is the grand total of all the observations.

In order to derive the test for H_0 , we can use either the likelihood ratio test or the principle of least squares. Since the likelihood ratio test has already been derived earlier, so we choose to demonstrate the use of least squares principle.

The linear model under consideration is

$$y_{ij} = \mu + \alpha_i + \varepsilon_{ij}, \quad i = 1, 2, \dots, v \quad (3.65)$$

where ε_{ij} 's are identically and independently distributed random errors with mean 0 and variance σ^2 .

The normality assumption of ε 's is not needed for the estimation of parameters but will be needed for deriving the distribution of various involved statistics and in deriving the test statistics. ε 's is not needed for the estimation of parameters but will be needed for deriving the distribution of various involved statistics and in deriving the test statistics.

Table 3.3 Data set with one factor which is affecting the outcome—treatment effect

Treatments			
1	2	...	v
y_{11}	y_{21}		y_{v1}
y_{12}	y_{22}		y_{v2}
...
y_{1n}	y_{2n}		y_{vn}
T_1	T_2		T_v

Let

$$S = \sum_{i=1}^v \sum_{j=1}^n \varepsilon_{ij}^2 = \sum_{i=1}^v \sum_{j=1}^n (y_{ij} - \mu - \alpha_i)^2 \quad (3.66)$$

Minimizing S with respect to μ and α_i , the normal equations are obtained as

$$\frac{\partial S}{\partial \mu} = 0 \Rightarrow n\mu + \sum_{i=1}^v n_i \alpha_i = 0 \quad (3.67a)$$

$$\frac{\partial S}{\partial \alpha_i} = 0 \Rightarrow n_i \mu + n_i \alpha_i = \sum_{j=1}^n y_{ij}, \quad i = 1, 2, \dots, v. \quad (3.67b)$$

Solving them using $\sum_{i=1}^v n_i \alpha_i = 0$, we get

$$\hat{\mu} = \bar{y}_{oo} \quad (3.67c)$$

$$\hat{\alpha}_i = \bar{y}_{io} - \bar{y}_{oo} \quad (3.67d)$$

where $\bar{y}_{io} = \frac{1}{n_i} \sum_{j=1}^n \bar{y}_{ij}$ is the mean of observation receiving the i th treatment and $\bar{y}_{oo} = \frac{1}{n} \sum_{i=1}^v \sum_{j=1}^n \bar{y}_{ij}$ is the mean of all the observations.

The fitted model is obtained after substituting the estimate $\hat{\mu}$ and $\hat{\alpha}_i$ in the linear model, we get

$$y_{ij} = \hat{\mu} + \hat{\alpha}_i + \hat{\varepsilon}_{ij} \quad (3.68)$$

Squaring both sides and summing over all the observation, we have

$$\sum_{i=1}^v \sum_{j=1}^n (y_{ij} - \bar{y}_{oo})^2 = \sum_{i=1}^v n_i (\bar{y}_{io} - \bar{y}_{oo})^2 + \sum_{i=1}^v \sum_{j=1}^n (y_{ij} - \bar{y}_{io})^2 \quad (3.69)$$

$$\begin{aligned} \text{Total sum of squares} &= \text{Sum of squares due to treatment effects} \\ &\quad + \text{Sum of squares due to error} \end{aligned}$$

Since $\sum_{i=1}^v \sum_{j=1}^n (y_{ij} - \bar{y}_{oo})^2 = 0$, so TSS is based on the sum of $(n - 1)$ squared quantities. The TSS carries only $(n - 1)$ degrees of freedom.

Since $\sum_{i=1}^v n_i (\bar{y}_{io} - \bar{y}_{oo})^2 = 0$, so SST is based on the sum of $(v - 1)$ squared quantities. The TSS carries only $(v - 1)$ degrees of freedom. Since $\sum_{i=1}^v n_i (\bar{y}_{ij} - \bar{y}_{io})^2 = 0$ for all $i = 1, 2, \dots, v$, so SSE is based on the sum of squaring n quantities like $(\bar{y}_{ij} - \bar{y}_{io})$ with v constraints $\sum_{j=1}^n (\bar{y}_{ij} - \bar{y}_{io}) = 0$.

So SSE carries $(n - v)$ degrees of freedom. $TSS = SST + SSE$ with degrees of freedom partitioned as $(n - 1) = (v - 1) + (n - v)$. Moreover, the equality in

$TSS = SSTR + SSE$ has to hold exactly. In order to ensure that the equality holds exactly, we find one of the sum of squares through subtraction. Generally, it is recommended to find SSE by subtraction as:

$$TSS = \sum_{i=1}^v \sum_{j=1}^n (y_{ij} - \bar{y}_{io})^2 = \sum_{i=1}^v \sum_{j=1}^n y_{ij}^2 - \frac{G^2}{n} \quad (3.70)$$

where $G = \sum_{i=1}^v \sum_{j=1}^n y_{ij}$.

$$SSTR = \sum_{i=1}^v n_i (\bar{y}_{io} - \bar{y}_{oo})^2 = \sum_{i=1}^v \left(\frac{T_i^2}{n} \right) - \frac{G^2}{n} \quad (3.71)$$

where $T_i = \sum_{j=1}^n y_{ij}$, $\frac{G^2}{n}$: correction factor.

Under $H_0: \alpha_1 = \alpha_2 = \dots = \alpha_v = 0$, the model become

$$Y_{ij} = \mu + \varepsilon_{ij} \quad (3.71)$$

and minimizing $S = \sum_{i=1}^v \sum_{j=1}^n \varepsilon_{ij}^2$ with respect to μ gives

$$\frac{\partial S}{\partial \mu} = 0 \Rightarrow \hat{\mu} = \frac{G}{n} = \bar{y}_{oo} \quad (3.72)$$

The SSE under H_0 becomes

$$SSE = \sum_{i=1}^v \sum_{j=1}^n (y_{ij} - \bar{y}_{oo})^2 \quad (3.73)$$

and thus $TSS = SSE$.

This TSS under H_0 contains the variation only due to the random error whereas the earlier $TSS = SSTR + SSE$ contains the variation due to treatments and errors both. The difference between the two will provides the effect of treatments in terms of sum of squares as

$$SSTR = \sum_{i=1}^v n (\bar{y}_i - \bar{y}_{oo})^2 \quad (3.74)$$

The expectations are given as:

$$\begin{aligned}
 E(SSE) &= \sum_{i=1}^v \sum_{j=1}^n E(y_{ij} - \bar{y}_{io})^2 \\
 &= \sum_{i=1}^v \sum_{j=1}^n (\varepsilon_{ij} - \bar{\varepsilon}_{io})^2 = \sum_{i=1}^v \sum_{j=1}^n E(\varepsilon_{ij}^2) - \sum_{i=1}^v n_i E(\bar{\varepsilon}_{io}^2) \\
 &= n\sigma^2 - \sum_{i=1}^v n_i \frac{\sigma^2}{n_i} = (n - v)\sigma^2
 \end{aligned} \tag{3.75}$$

$$E(MSE) = E\left(\frac{SSE}{n - v}\right) = \sigma^2 \tag{3.76}$$

$$\begin{aligned}
 E(SSTr) &= \sum_{i=1}^v nE(\bar{y}_{io} - \bar{y}_{oo})^2 = \sum_{i=1}^v nE(\alpha_i + \bar{\varepsilon}_{io} - \bar{\varepsilon}_{oo})^2 \\
 &= \sum_{i=1}^v n_i \alpha_i^2 + \left[\sum_{i=1}^v n_i \frac{\sigma^2}{n_i} - n \frac{\sigma^2}{n} \right] = \sum_{i=1}^v n_i \alpha_i^2 + (v - 1)\sigma^2
 \end{aligned} \tag{3.77}$$

$$E(MStr) = E\left(\frac{SSTr}{v - 1}\right) = \frac{1}{v - 1} \sum_{i=1}^v n_i \alpha_i^2 + \sigma^2 \tag{3.78}$$

In general $E(MStr) \neq \sigma^2$ but under H_0 , all $\alpha_i = 0$ and so

$$E(MStr) = \sigma^2 \tag{3.79}$$

Using the normal distribution property of ε_{ij} 's we find that y_{ij} 's are also normal as they are the linear combination of ε_{ij} 's

$$-\frac{SSTr}{\sigma^2} \sim \chi^2(v - 1) \text{ under } H_0 \tag{3.80}$$

$$-\frac{SSE}{\sigma^2} \sim \chi^2(n - v) \text{ under } H_0 \tag{3.81}$$

Table 3.4 Analysis of variance (ANOVA) table

Source of variation	Degrees of freedom	Sum of squares	Mean sum of squares	F
Between treatments	$v - 1$	$SSTr$	$MStr$	$\frac{MStr}{MSE}$
Errors	$n - v$	SSE	MSE	
Total	$n - 1$	TSS		

$SSTr$ and SSE are independently distributed

$$-\frac{MStr}{MSE} \sim F(v - 1, n - v) \text{ under } H_0 \quad (3.82)$$

Reject H_0 at α^* level of significance if $F > F_{\alpha; v-1, n-v}$.

The analysis of variance table is as follows (Table 3.4).

Reference

1. Olteanu DA, Freeman LJ (2010) The evaluation of median rank regression and maximum likelihood estimation techniques for a two-parameter Weibull distribution. Qual Eng 22: 256–272

Chapter 4

Failure Mechanics, Design and Reliability Testing



Abstract This chapter will deal with concepts of failure mechanism, design and reliability testing. Important design aspects of mechanical structures that implement the intended function and have its mechanism in the design process have a good quality—stiffness and strength for its own loading. Product requirements on stiffness, being the resistance against reversible deformation, may depend on their application. Strength, the resistance against irreversible deformation, is always required to be high through the design of product shape. If there is faulty design in the structure where the loads as an uncontrollable noise factor are applied, product will suddenly collapse in its lifetime. The failure mechanics of mechanical product is fracture and fatigue—main Physics Of Failure (POF), which can be characterized by the stress (or loads) and materials on the structure. As modifying the shape and material in the structure, engineer would improve the faulty designs and increase its lifetime. These activities are called design. To improve the quality (or design) of product, (qualitative) method like FMEA, FEA, and Taguchi method will be established in the last century. On the other hand, quantitative method using reliability testing is still developing. The final goal of reliability testing is to discover the design problems and reveal if the reliability target for product is achieved.

Keywords Failure mechanics • Design • Reliability testing • Physics Of Failure (POF) • Fracture

4.1 Introduction

In today's technological world people want to continue the functioning of mechanical systems—cars, airplane, construction machine, computers, appliances, televisions, etc.—during lifetime. When they fail, the results can be catastrophic: injury, loss of life and/or costly lawsuits. More often, repeated failure leads to annoyance, inconvenience, and lasting customer dissatisfaction that can change the company's marketplace position. It takes a long time for company to build up a

product reputation for good quality, and only a short time to be branded as “unreliable” in marketplace (Fig. 4.1).

The most critical failures are no longer satisfied with the customer requirements (or specifications) due to unidentified factors before the product releases. When field failure occurs, we also determine whether the company specifications are inappropriate or whether verifiers are incorrectly conforming to the specifications instantaneously. If engineer looks into the problematic product, they will find the failure mechanism due to faulty design. Therefore, we should know what product failure is.

The definition of a failure may not precise if a gradual, suddenly, or intermittent loss of performance over time is observed. For example, seals experience a degradation of material properties and no longer satisfy the specifications. In this case we can adequately replace old part with new one. So we have to introduce the concept of Physics Of Failure (POF)—Fatigue and Fracture.

Specifically, if product subjected to repetitive loads no longer works in lifetime, we can also say it is failure. A disaster due to product design failure is always an undesirable event for several reasons: putting human lives in jeopardy, causing economic losses and interfering with the availability of products and services. The failure causes come from improper materials selection, inadequate design of the parts and its misuse. So it is the engineer responsibility to be prepared when failure is expected to occur.

To perform the required intended functions, the mechanical products like automobile comprise a number of subsystems (or module) and its parts that are closely interconnected in the mechanism. Each module in the mechanical system



Fig. 4.1 Train wreck or train crash from Wikipedia

can be typically specified as functional block that is represented as reliability. A failure of a component in module is often described as the termination of functional block. It is therefore necessary for mechanical engineer to identify all relevant functions and the performance criteria related to each intended function (Fig. 4.2).

To define failures, failure modes, and failure effects in product, reliability analysis methods are required for functional block of components. The representative methodologies developed in the last century are classified as following:

- Reliability block diagrams: A reliability block diagram is a success-oriented network illustrating how the functioning of the various functional blocks may secure that the system function is fulfilled. The structure of the reliability block diagram is described mathematically by structure functions. The structure functions will be used in the following chapters to calculate system reliability indices.
 - Failure modes, effects, and criticality analysis (FMEA/FMECA): This method is used to identify the potential failure modes of each of the functional blocks of a system and to study the effects these failures might have on the system. FMEA/FMECA is primarily a tool for designers but is frequently used as a basis for more detailed reliability analyses and for maintenance planning.
 - Fault tree analysis (FTA): The fault tree illustrates all possible combinations of potential failures and events that may cause a specified system failure. Fault tree construction is a deductive approach where we start with the specified system failure and then consider what caused this failure. Failures and events are combined through logic gates in a binary approach. The fault tree may be

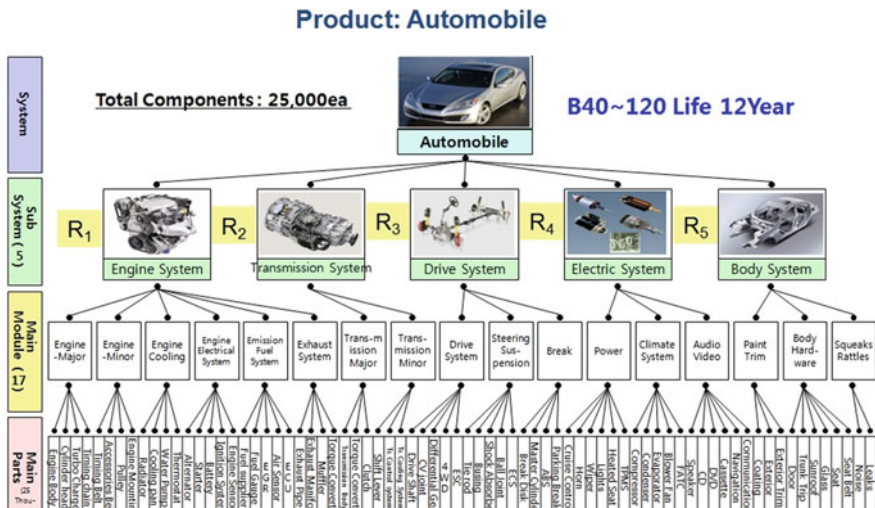


Fig. 4.2 Breakdown of automobile with multi-modules

evaluated quantitatively if we have access to probability estimates for the basic events.

- 3 Cause and effect diagrams: Cause and effect diagrams are frequently used within quality engineering to identify and illustrate possible causes of quality problems. The same approach may also be used in reliability engineering to find the potential causes for system failures. Cause and effect diagrams are qualitative and cannot be used as a basis for quantitative analyses.
- Parameter ALT: It can improve the reliability of mechanical systems subjected to repetitive stresses. A generalized life-stress failure model with effort concepts, acceleration factor, and sample size equation are utilized. Parametric ALT can quickly discover the missing design parameters in the mechanical system and determined if its reliability target is achieved. This new parametric ALT will help engineer to confirm the final design in the mechanical system and assess it.

There are two closely related problems of the reliability testing in the mechanical system—(1) censoring (when the observation period ends, not all units have failed—some are survivors) and (2) lack of failures (if there is too much censoring, even though a large number of units may be under observation, the information in the data is limited due to the lack of actual failures). To properly carry out the reliability testing, engineer knows the concepts of failure mechanics, designs, and accelerating testing in mechanical product.

Mechanical design is a developing process to determine whether product has a good quality—suitable strength and stiffness for structure that intended functions are implemented. If mechanical products are improperly designed, they will fail because the intended function of product or modules in lifetime does not fulfill specifications. Engineer needs to assess its cause and take action appropriate preventive measures against future incidents. One of solutions is the parametric ALT discussed in Chaps. 8 and 9. It also is carried out as reliability verification specifications if sample size equation is used.

4.2 Failure Mechanics and Designs

4.2.1 *Introductions*

In design critical aspects of mechanical structures subjected to a variety of loads have a good quality—enough stiffness and strength. Requirements on stiffness, being the resistance against reversible deformation, may vary over a wide range. Strength, the resistance against irreversible deformation, is always required to be high through the design of product shape, because this deformation may lead to crack, fracture, and finally loss of product intended functions.

If there is faulty design in the structure where the loads as uncontrollable noise factor are applied, the product will fracture in its lifetime due to improper strength and stiffness for load. The engineer would improve the faulty design of product

subjected to repetitive loads. Consequently, mechanical structure might be reshaped to have a better design in product lifetime.

The failure mechanics of components that might no longer be functioned can be characterized by two factors: (1) the stress (or loads) on the structure, (2) The type of materials and their shape used in the structure. To prevent the failure due to repetitive loads, mechanical engineer should design product by choosing proper product shape and material that products have proper strength and stiffness. Product requirements on stiffness, being the resistance against reversible deformation, may depend on their application. Strength, the resistance against irreversible deformation, is always required to be high through the design of product shape. Therefore, mechanical system can endure the loads (or stress) in its lifetime. If not, product will suddenly break up in its lifetime (Fig. 4.3).

Product failure in mechanical system is a physical problem that might arise when stress due to repetitive loads causes a fracture. Failure mechanics seeks to understand the process how product materials subjected to stress induce the failure. The applied loads cause stresses on the module structure. Consequently, the failure site of the product (or module) structure might be observable when the failed products are taken apart in the field or could be from the results of reliability testing—parametric ALT.

As a design result, if the product structure is ideally designed to have enough strength and stiffness for stresses, there should be no problems with the failure of the module in product lifetime. Though the mechanical design is developed with an optimal design process—Finite Element Analysis (FEA), it may have design flaws that will unexpectedly show up in the field. To withstand the repetitive stresses due to loads over the product lifetime, the product structure experimentally verifies if it has a good quality—enough strength and stiffness that is established through the design process.

As mentioned before, most products with mechanical or electrical components are composed of multi-module structures. Although the product is optimally

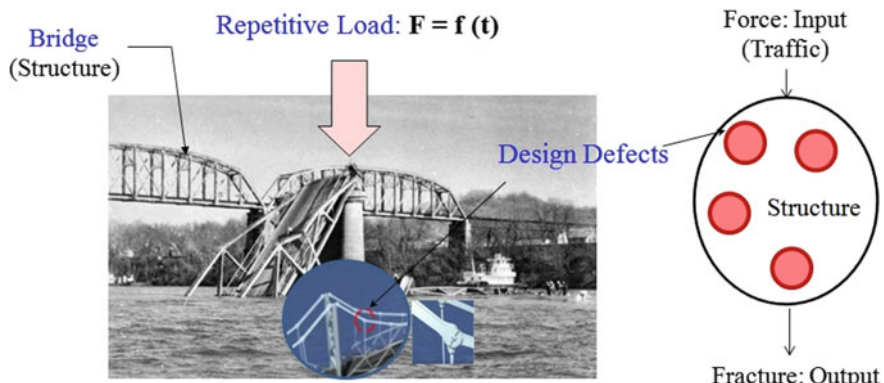


Fig. 4.3 Failure mechanics created by a load on a component made from a specific material

designed, one of product modules has an improper design. The problematic module subjected to repetitive loads will reveal in the near future from the field and determine the lifetime of the product. By experiments such as reliability testing, the design problems of the module might be corrected before products launch. Because testing is carried out in Quality Assurance, the product design should be effectively cooperated with Design Engineering and Test Engineering in the design process. Design engineer tries to build the structure of intended functions based on the customer requirements. On the other hands, test engineer will confirm final designs whether the reliability target of modules in product is achieved.

4.2.2 Product Design—Intended Functions

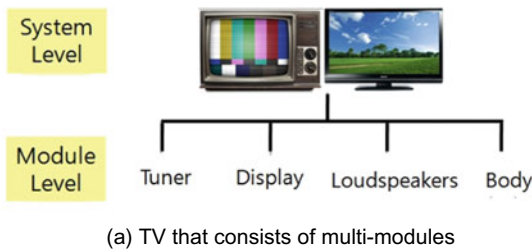
Engineer understands the intended functions that shall implement the customer's needs in product. For television, the intended function is to watch the program that consists of moving images for a very short period of time. TV also is required as the fundamental advantage like the superiority of picture and sound. To take dominance in marketplace, companies in rivalry develop product that has a good quality. A product like TV consists of multiple modules that can be put together as a subassembly. When product has an input as power source, it has output as response (picture and sound—intended functions) that want to be implemented. Intended functions are embodied in the product structure. Their performance of final design will be measured by specifications.

On the other hand, to expresses the robust design of the intended function of product, Taguchi uses parametric diagram that consists of input, system (TV), response (intended function). And there are noise factor and design factor that product design influences. Because noise factors like customer usage or environmental conditions don't know, engineer should be designed to adjusts control factors that can robustly withstand the noise factors (Fig. 4.4).

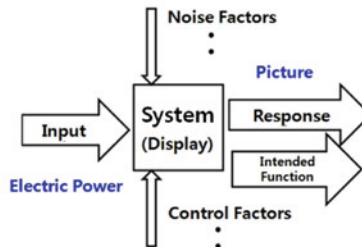
Intended functions of a product are the functionalities that product is to perform the voices of the customer and explain the company specifications. They must be recognized in the design to ensure whether critical customer requirements (or specifications) work properly in product. Thus, the fulfillment of each intended function should be understood by product specifications from a standpoint of the customer's expectations. As time goes by, product fails to perform its intended functions. Therefore, reliability of a product will assess whether or not a product meets its intended function as time function.

In the current global competitive marketplace, product quality of intended functions for its lifetime is an important requisite to ensure continued success in the marketplace. On the other hand, the failure of product quality expels from the customer satisfaction and loyalty. Thus, it is important for engineer to understand the difference between the performance and reliability, which comprises two faces of product quality. When engineer develops product, they have to keep in minds.

Fig. 4.4 Intended function and its example—TV



(a) TV that consists of multi-modules



(b) Intended function of TV display in parameter diagram

Design idea that improves intended functions of product comes from research results. They shall be implemented in the product developing process as Chap. 1 was discussed. Designers might refer to the past failure experiences, which are documented as company specifications. There are possibilities for solving design problems and choosing the best solution that product features could be embodied in the product. Product development refines and improves a solution in the design phase before a product launches to customers. Basically, the engineering design process starts to define the problems to be implemented: (1) What is the problem? (2) How have engineers approached it? (3) What are the design constraints?

A prototype is a first operating version of a solution (or intended function) that satisfies the customer requirements. The product design process involves multiple iterations like redesigns of your solution using prototype before settling on a final design. Final product can define the performance criteria in evaluating the specifications of product quality—(a) intended functions (or fundamental advantage), (b) specified product life, and (c) the failure rate of product under operating and environmental conditions. After completing final design, performances for the key features of intended function in product will be evaluated by a variety of company specifications.

The engineering design team may often neglect the potential customer usage pattern, although customer properly uses. Sometimes the failure of a returned product in field may be perceived to be customer abuses of product, generally not failure. From a standpoint of robust design, the intended functions might be designed to withstand the customer misusages (or overloads) for customer's proper uses. For this case the robust concept in the Taguchi's method is effective. To

robustly keep the intended functions, product withstands noise factors like customer usage (or loads) as optimally designed.

Engineer for reliability identifies the failure mode through reliability testing over lifetime. Modules in product are required to assign a reliability target in the early design phase. They determine if product achieves reliability target from final design. The methodology for reliability testing will be discussed in Chap. 8. In manufacturing product engineer will decide if it conforms to manufacture specifications. After production, current product design will be confirmed by the feedback of customer in field (Fig. 4.5).

4.2.3 Specified Design Lifetime, B_X

When product is initially selling to customer, it is designed to have safe margin between environmental stress and product strength. As customer uses product, failure initially appears in the weakest part of product and increase like the curve of bathtub. Based on information coming from the customer and competitive benchmarks, design lifetime has maximum failure rate at acceptance criteria of design quality. Generally, design lifetime is 2–3 times greater than qualification lifetime. Engineers often define a design lifetime to represent an engineer's specifications of product usage under which the reliability must be verified. It is important that careful thought go into the synthesis of this specification to ensure that product quality do not result in customer's dissatisfaction due to the end of the useful life (Fig. 4.6).

Product qualification refers to the tests that are done on prototypes or the final product to be sure that it will properly operate across all external conditions and will conform to all government regulations. As qualification index, specified design

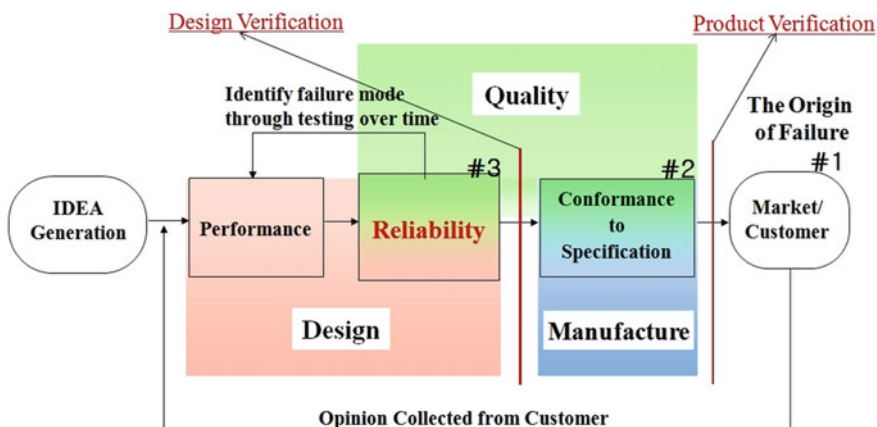


Fig. 4.5 Implementing intended functions in the design process

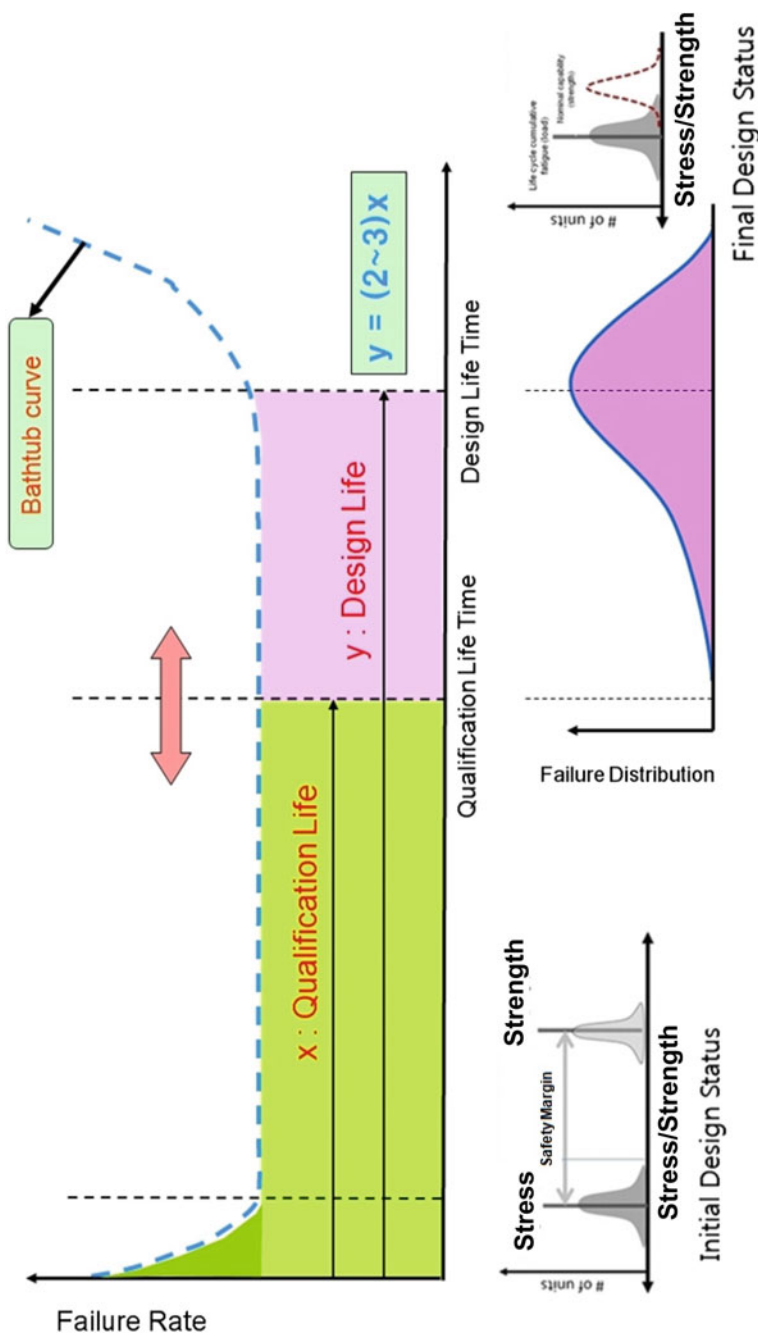


Fig. 4.6 Qualification life and design life

lifetime, MTTF, MTBF, and BX, is often used. The design life of product is the time period which the product works properly within the life expectancy. The design life of products, BX, might differ from the reliability lifetime metrics—MTTF or MTBF.

For example, if the MTTF of product may be 100,000 h, B10 life will be 10,000 h. It means that one failure occur every 100,000 population operating hours. Because product cannot reach 100,000 operating hours, most of these units will be replaced by a new unit. Aluminum electrolytic capacitors, fans, and batteries will fail due to wear-out before they could achieve the operating time—MTBF. As a metric of design lifetime, BX life mentioned in Chap. 3 can be useful. It means the life time at which X% of the units in a population will have failed. For example, if unit has a B10 life of 10,000 h, 10% of the population will have failed by 10,000 h of operation.

The specified design lifetime provides a usage or time frame for reliability analysis or testing. Some organization might simply choose to design a product to be reliable over the stated warranty (qualification) period. Because it is commensurate with how long the product is expected to be used in the field, an enlightened organization might choose a design life. Depending on the designer's perspective, the life specification might be based on any of the design life time—BX life.

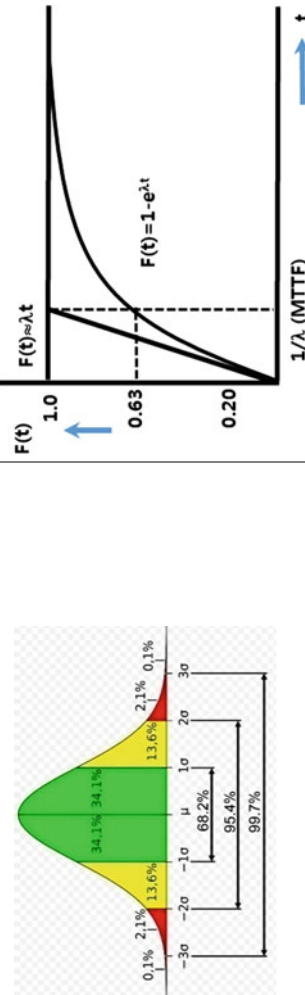
4.2.4 Dimensional Differences Between Quality Defects and Failures

The everyday usage term “quality of a product” is loosely taken to mean its inherent degree of excellence. In industry, this is made more precise by defining quality to be “conformance to requirements at the start of use”. Assuming the product specifications adequately capture customer requirements, the quality level can now be precisely measured by the fraction of units shipped that meet specifications.

But we have a basic question: how many of these units still meet specifications at the end of a one year warranty period? That is where “reliability” comes in. The terms “reliability” and “quality” have different meanings: reliability is concerned with the performance of a product through some desired period (product lifetime), whereas quality is concerned with the performance of a product at a particular point in time. Therefore, reliability testing that finds failure due to faulty design requires usually more complex procedures than quality testing (Table 4.1).

Quality defects appear for one of three reasons: (1) Incompleteness of design specification, (2) Nonconformance to specifications during manufacture, (3) Customer misuse of the product. The established specifications in company can perceive them whether product quality meet. For some aspect of the product, quality defect is out of tolerance in manufacturing. If something can be found to be out of specifications, it is considered to have a quality defect that follows the normal distribution.

Table 4.1 Quality defects and failures

Concept	Quality defects	Failure
Index	Out of established specifications	Physical trouble
Unit	Defect rate, ppm	Failure rate, lifetime
Area	Percent, ppm	Percent/year, year
Probability	Normal distribution $f(x) = \frac{1}{\sigma\sqrt{2\pi}} e^{-\frac{(x-\mu)^2}{2\sigma^2}}$	 <p>The figure consists of two graphs. The top graph shows the cumulative distribution function $F(t) = 1 - R(t) = 1 - e^{-\lambda t}$ plotted against time t. It features two curves: an exponential decay curve labeled $F(t) \approx \lambda t$ and a Weibull-like curve labeled $F(t)$. A vertical dashed line at $t = 1/\lambda$ corresponds to a failure probability of 0.63. The bottom graph shows a normal distribution curve with a mean μ and standard deviation σ. It highlights the 68.2% central region between $\mu \pm \sigma$ and the 99.7% region between $\mu \pm 3\sigma$. The tails of the distribution are divided into segments: 0.13%, 2.1%, 13.6%, 34.1%, 34.1%, 13.6%, 2.1%, 0.1%, and 0.1%.</p>

On the other hands, failure clearly indicates a physical performance disorder related to the product as time goes on. The number of failure per year for a given production lot results in the annual failure rate. Any mistakes or omissions of design will induce results in failure. The quality level might be described by a single fraction defective. To describe reliability fallout, a probability model that describes the fraction fallout over time is needed. This is known as the life distribution model—the exponential or Weibull distributions. It also requires the data analysis to analyze the product lifetime from testing results.

4.2.5 Classification of Failures

The definition of failure is obvious when there is a total loss of product (intended) functions that can be differentially perceived from the viewpoints of the customers or by specifications. If something breaks during product usage unintentionally, it may fail. However, if only a partial loss of (intended) function is involved, it will be complicated to define the product failure. In such instances the definition of the failure may not be precise when one observes a gradual or intermittent loss of performance over time. Although the activity is completed successfully, a person may still feel dissatisfied if the underlying process is perceived to be below expected standard (or specification). To figure out failure type, we also need to understand the Physics Of Failure (POF)—Fatigue and Fracture. For example, a variety of automobile failures might be classified as (Fig. 4.7).

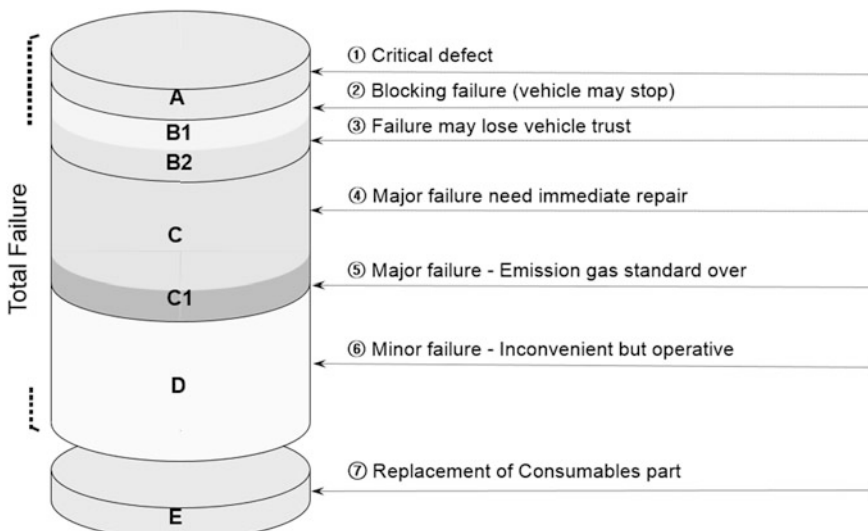


Fig. 4.7 Definition for failure class (example: automobile)

A Class is said that failure will damage the body of passenger or the loss of car control, failure of brake equipment, and fire risk. Examples are too many to be expected: (1) Accident due to loss of acceleration control, (2) Differential gear fixation, (3) Air exposure of pump, (4) Overheat or disconnection of cable, (5) Damaged flywheel, (6) Malfunctioned clutch, and (7) Malfunctioned injection pump.

B1 Class is said that failure will stop car. Examples are too many to be expected: (1) Engine stop or no starting from computing engine, injection, pump, common rail, ignition coil, car starting, engine control, engine fixation, distribution chain, (2) Transmission stop, and (3) Stop of gear box, no reverse operation.

B2 Class is said that failure may stop car. There are a lot of examples: (1) Abnormal noise of engine or gear box, (2) Overheat Engine, and (3) Vibration of engine or gearbox.

C Class is said that car can be drivable, but it requires the high cost to recover it. Examples also are too many to be expected: (1) It make car inoperative, (2) It affects visual, hearing, and smell, (3) Critical motor surges and power loss, (4) Abnormal noise, oil spill, cooling water spill, smell, over oil leakage, (5) abnormal smell, and (6) Clutch malfunction, inoperative gear transmission. C1 Class also is inconsistent to the standard of discharge gas. Example is not to meet for standard of emission gas.

D Class is said that using car is no effect but minor operational failure. Examples are too many to be expected: (1) Driving car is inconvenient, (2) Affect visual and hearing, (3) Over fuel consumption, (4) Slowly acceleration, (5) Idle speed is instable, (6) Engine is not starting, (7) Vibration, and (8) A few of noise (discharge noise, cracking noise, vibration noise, cooling pump noise, starting noise, noise in gear transmission, erosion of engine part).

E Class is wearable parts such as filter, spark plug, and timing belt need to be replaced periodically. In a result, we can say failure is defined as A, B, C, and D class.

4.3 Reliability Block Diagram

4.3.1 Introduction

A Reliability Block Diagram (RBD) is a graphical representation of reliability relationship between the system and its module (or components). The diagram represents the reliability of the system (or module) in terms of the functioning states of its components. RBD also is a success-oriented network that the logical connections of (functioning) components in product will fulfill an intended function. If the product has more than one function, each function can establish a separate reliability block diagram. RBD are suitable for systems which the failure order does not matter. For instance, consider automobile. As engine generates power, it transfers transmission, drive, and wheel. Each block represents critical module like transmission. The product reliability can be calculated from failure rate and lifetime (Fig. 4.8).

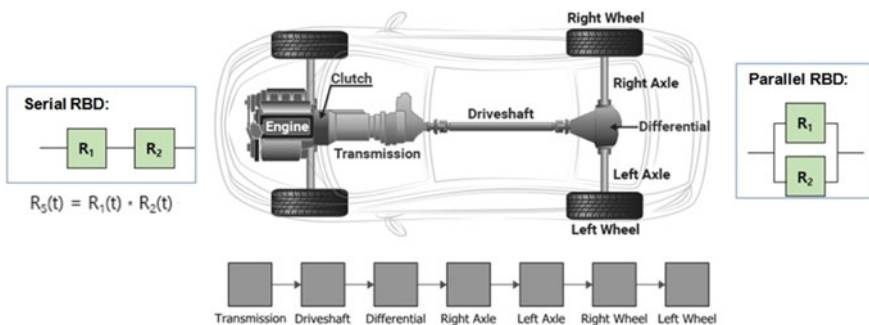


Fig. 4.8 Automobile and its module for reliability block diagram

For any life data analysis, mechanical engineer chooses one module in product at which no more detailed information about the object of analysis is known to be considered. At that module, engineer treats the object of analysis as a “black box or block diagram.” The objective of reliability data analysis is to obtain a life distribution that describes the times-to-failure of a product (or module) and estimate the parameters in Weibull. It is based on time-to-failure data of the product (or module) in block diagram that consists of serial-connected or parallel connected parts.

Consider a system that the n components are described by a block. If there is connection between the end points a and b , component i in product is functioning. It means that the specified function of component product is achieved. It is also possible to put more information into the block that briefly describes the required function of the component (Fig. 4.9).

Basic configurations in RBD consist of serial configuration, parallel configuration, and the combinations. As mentioned, the reliability of the components in product can be calculated by the failure rate λ and product lifetime L_B . In reliability analysis, a “system” model is constructed from these module models. For example, a series configuration indicates that all of the modules must operate for the system operation. A parallel configuration indicates that at least one of the modules must operate—redundancy. Therefore, RBD provides a framework for understanding system configuration (Fig. 4.10).

A system that is functioning if and only if all of its n components (or modules) are functioning is called a series structure. Product has connection between the end points a and b (the system is functioning) if and only if it has connection through all the n blocks representing the components (or module). For serial structure, if product consists of n modules with each modules reliability $R_1, R_2, R_3, \dots, R_n$, the system reliability can be expressed as:

$$R = R_1 \cdot R_2 \cdot R_3 \cdots R_n = \prod_{i=1}^n R_i \quad (4.1)$$

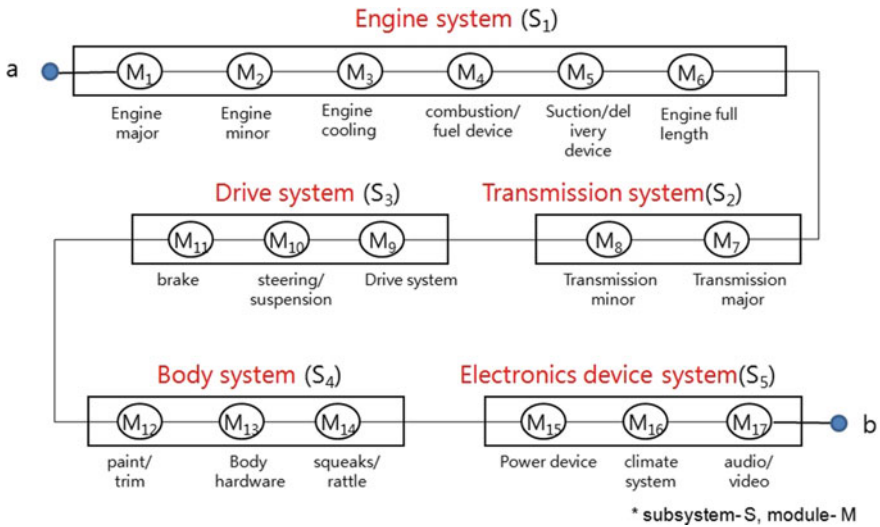


Fig. 4.9 Reliability block diagram for automobile (example)

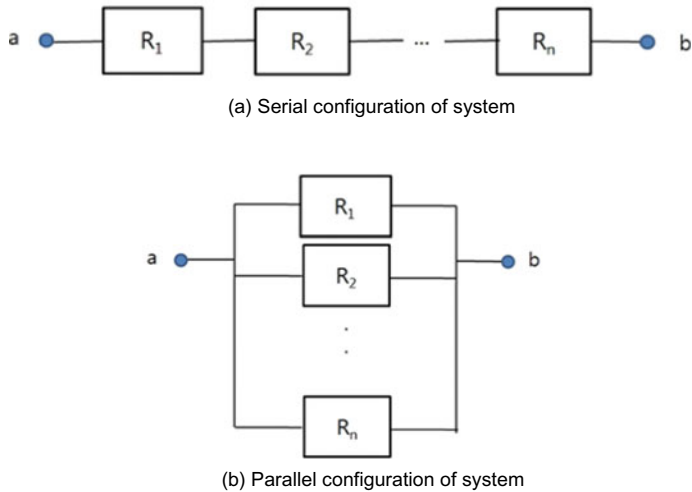


Fig. 4.10 Serial or parallel configuration of system (or module)

A system that is functioning if at least one of its n components (or modules) is functioning is called a parallel structure. Product has connection between the end points a and b (the system is functioning) if and only if it has connection through all the n blocks representing the components (or module). For parallel structure, if

system consists of n modules with each part reliability $R_1, R_2, R_3, \dots, R_n$, the system reliability can be expressed as:

$$R = 1 - (1 - R_1) \cdot (1 - R_2) \cdots (1 - R_n) = 1 - \prod_{i=1}^n (1 - R_i) \quad (4.2)$$

Each block in RBD represents the module of interest. At the very least, a reliability block must include information as to how this item fails (i.e., the reliability model of the block). Once the blocks' properties have been defined, the blocks can then be connected to create a reliability block diagram for the system. The RBD represents the functioning state (i.e. success or failure) of the module that consists of its components. In other words, this diagram demonstrates the effect of the success or failure of a component on the success or failure of the system. For example, if all modules in a system must succeed in order for the system to succeed, the modules will be arranged reliability-wise in series. If one of two modules must succeed in order for the system to succeed, those two modules will be arranged in parallel.

Because RBD provides a success oriented view of the system, it facilitates the computation of system reliability from module reliabilities. A RBD is defined as follows: A reliability block diagram is a graph whose edges are the system modules. The way the n components are interconnected to fulfill a specified intended function may be illustrated by a reliability block diagram like the truck differential gear equipment like automobile. If there is a path between the terminal nodes which contains only edges with functional modules, the entire system is functional. Otherwise it is not functional (Fig. 4.11).

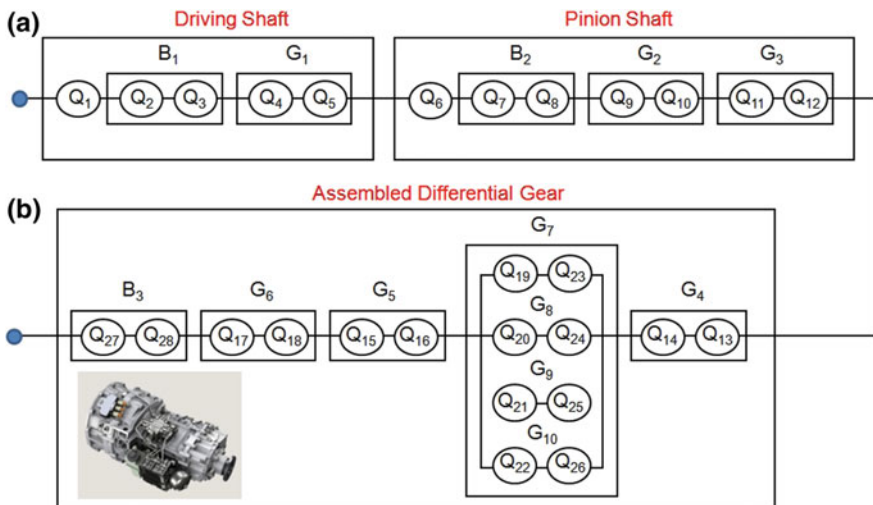


Fig. 4.11 RBD for the transmission system of automobile (example)

4.3.2 Comparison Between Reliability Block Diagram and Fault Tree

In some practical applications, engineer may determine whether the product is modeled by choosing structure by a reliability block diagram or by a fault tree. Because the fault tree is limited to only OR-gates and AND-gates, the fault tree can be converted to a reliability block diagram (or vice versa).

As a matter of fact, RBDs and fault trees may provide the same information. In a reliability block diagram, block connections signifies that the component (or modules) in product is functioning. The fault tree takes a failure perspective, while the reliability block diagram takes a success perspective in terms of the reliability. A series structure is equivalent to a fault tree where all the basic events are connected through an OR-gate. The TOP event occurs if either component 1 or component 2 or component 3 or ... component n fails. Therefore, serial configuration in fault tree is identical to parallel configuration in RBD.

On the other hands, a parallel structure may be represented as a fault tree where all the basic events are connected through an AND-gate. The TOP event occurs if component 1 and component 2 and component 3 and ... component n fail. Parallel configuration in fault tree is identical to serial configuration in RBD. The following examples demonstrate how the same analysis scenario using either RBDs or fault trees is modeled.

Example 4.1 If product that consists of three parts can be drawn in RBD as the following Fig. 4.12, find the equivalent fault tree.

Since part 1 and part 2 in RBD are connected in parallel, the equivalent fault tree can be represented as AND gate. Because the part3 and equivalent of part1 and part2 in RBD are connected in serial, the total product can be represented in OR gate. If summarized in process, the equivalent fault tree can be drawn as following Fig. 4.13.

Example 4.2 Assume that the probability of occurrence of five fault events is 0.1, equally. Calculate the probability of occurrence of the top event in the following fault tree (Fig. 4.14).

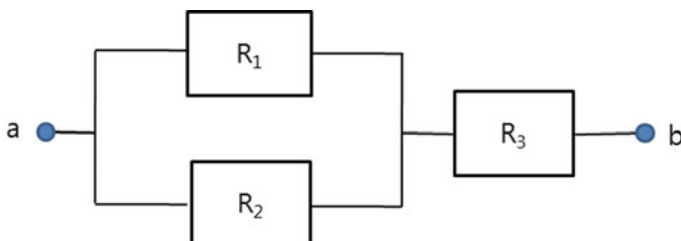


Fig. 4.12 RBD for product that consists of three parts

Fig. 4.13 Equivalent fault tree analysis for RBD of Fig. 4.11

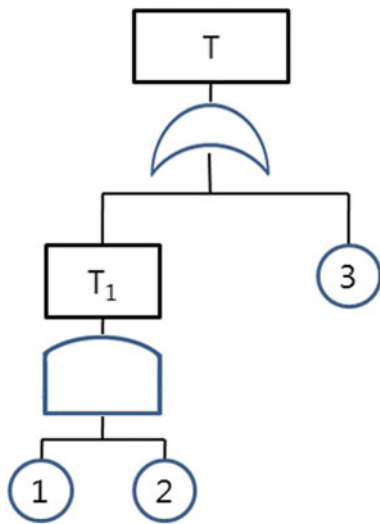
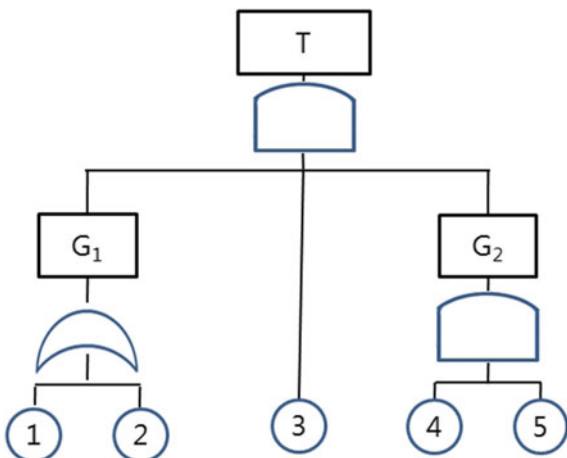


Fig. 4.14 Example for fault tree analysis



Because the probability of occurrence of G1 is connected in OR gate, it can be calculated as:

$$G_1 = 1 - (1 - 0.1) \times (1 - 0.1) = 0.19 \quad (4.2)$$

Because the probability of occurrence of G2 is connected in AND gate, the probability of occurrence of G2 can be calculated as:

$$G_1 = 0.1 \times 0.1 = 0.01 \quad (4.3)$$

Thus, the probability of occurrence of the top event can be obtained as:

$$T = G_1 \times 3 \times G_2 = 0.19 \times 0.1 \times 0.01 = 0.00019 \quad (4.4)$$

4.4 Failure Mode and Effect Analysis (FMEA)

4.4.1 Introduction

Failure mode and effect analysis (FMEA), one of qualitative method in the product development, is a widely used method to study product problems. The history of FMEA goes back to the early 1950s with the development of flight control systems when the U.S. Navy's Bureau of Aeronautics developed a requirement called "Failure Analysis". In the mid-sixties FMEA was set to work in earnest by NASA for the Apollo project. In the 1970s, the U.S. Department of Defense developed military standards entitled "Procedures for Performing a Failure Mode, Effect, and Criticality Analysis". For use in aerospace, defense, and nuclear power generation, FMEA/FMECA methods are widely used to conduct analysis of system safety. The Ford Company integrated this method into its quality assurance concept.

- In the early of 1950s: Propeller airplane → Reliability design of Jet airplane with flight control systems
- In the middle of 1960s: Apollo program used in real earnest
- In the 1970s: US NAVY (MIL-STD-1629) was adopted
- In the late of 1970s: widely used in the industry due to the introduction of product liability law.

In the first step of a system reliability study, FMEA involves reviewing the design of many components, assemblies, and subsystems to identify failure modes, and their causes and effects. To determine whether an optimum criterion of reliability assessment is achieved, FMEA is to analyze and modify many components in system. FMEA uses the risk priority number (RPN). A qualitative analysis is mainly used in the light of FMEA team experience.

It may be described as an approach used to perform analysis of each potential failure mode in the systems under consideration to examine the effects of such failure modes on that system. When FMEA is extended to classify each potential failure effect according to its severity, the method is known as failure mode effects and criticality (FMECA).

As seen in Fig. 4.15, the FMEA is carried out in interdisciplinary groups—members in the planning, R&D and QA. It is reasonable to execute an FMEA in teams, since it is only then possible to incorporate all operational areas affected by the analysis. In practice it is beneficial to execute an FMEA under the direction of an FMEA moderator, who is familiar with the methodical procedure. In this way, time consuming discussions concerning the method can be avoided.

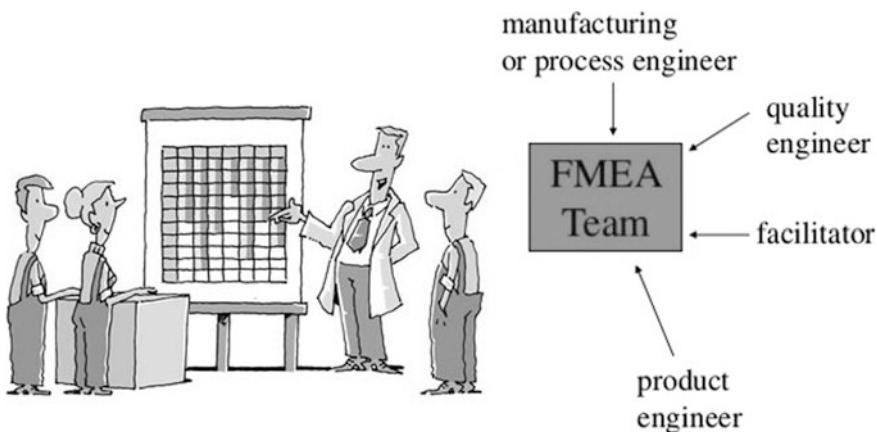


Fig. 4.15 Members of FMEA team

In general, the FMEA team consists of a moderator, who offers methodical knowledge. They can offer technical knowledge concerning the product or process to be analyzed. The moderator, who also may possess a marginal know-how concerning the product or process, certifies that the team members acquire a basic knowledge of the FMEA methodology. A brief training at the beginning of an FMEA assignment is useful.

FMEA is a systematical method that the fundamental idea is the determination of all possible failure modes for arbitrary systems or modules and the possible failure effects and failure causes are presented. The aim of the method is to recognize the risks and weak points of product design as early as possible in order to enable execution improvements in timely manner. There are many terms used in performing FMEA/FMECA and some of them are as follows:

- **Failure cause.** The factors such as design defects, quality defects, physical or chemical processes, or part misapplications are the primary reason for failure or they start the physical process which deterioration progresses to failure.
- **Failure mode.** The notion or manner through which a failure is perceived.
- **Failure effect.** The consequence a failure mode has on item's function, operation, or status.
- **Single failure point.** An item's malfunction that would lead to system failure and is not compensated through redundancy or through other operational mechanisms.
- **Criticality.** A relative measure of a failure mode's consequences and its occurrence frequency.
- **Severity.** A failure mode's consequences, taking into consideration the worst case scenario of a failure, determined by factors such as damage to property, the degree of injury, or ultimate system damage.

- **Criticality analysis.** An approach through which each possible failure mode is ranked with respect to the combined influence of occurrence probability and severity.
- **Undetectable failure.** A postulated failure mode in the FMEA for which no failure detection approach is available through which the concerned operator can be alerted of the failure.
- **Local effect.** The consequences a failure mode has on the function, operation, or status of the item currently being analyzed.

4.4.2 Types of FMEA

The types of FMEA are classified as (1) System-level FMEA, (2) Design-level FMEA, and (3) Process-level FMEA (Fig. 4.16).

4.4.3 System-Level FMEA

Failure functions as well as failure modes for product are analyzed in the system-level FMEA. The analysis is carried out in various hierarchical system

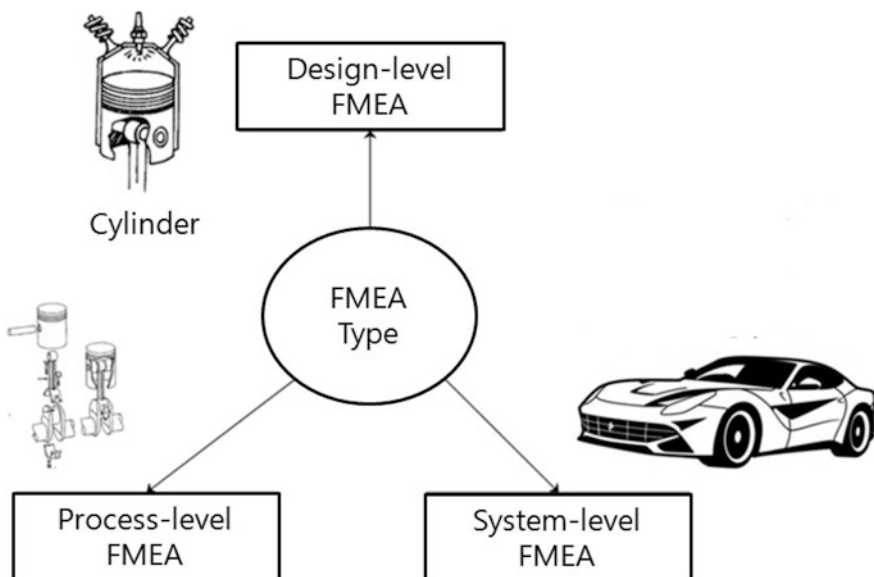


Fig. 4.16 Types of failure mode and effect analysis (FMEA)

levels all the way to the failure on the module level. This is the highest-level FMEA that can be performed and its purpose is to identify and prevent failures related to system/subsystems during the early conceptual design. System-level FMEA is carried out to validate that the system design specifications reduce the risk of functional failure to the lowest level during the operational period.

Some benefits of the system-level FMEA are identification of potential systemic failure modes due to system interaction with other systems and/or by subsystem interactions, selection of the optimum system design alternative, identification of potential system design parameters that may incorporate deficiencies prior to releasing hardware/software to production, a systematic approach to identify all potential effects of subsystem/assembly part failure mode for incorporation into design-level FMEA, and a useful data bank of historical records of the thought processes as well as of action taken during product development efforts.

4.4.4 Design-Level FMEA

The purpose of performing design-level FMEA is to help identify and stop product failures related to design. This type of FMEA can be carried out upon component-level/subsystem-level design proposal and its intention is to validate the design chosen for a specified functional performance requirement. The advantages of performing design-level FMEA include identification of potential design-related failure modes at system/subsystem/component level, identification of important characteristics of a given design, documentation of the rationale for design changes to guide the development of future product design, help in the design requirement objective evaluation of design alternatives, systematic approach to reduce criticality and risk, accumulated data serve as a useful historical record of the thought processes and the actions taken during the product development effort, and useful tool to establish priority for design improvement actions.

4.4.5 Process-Level FMEA

This identifies and prevents failures related to the manufacturing/assembly process for a certain product. The benefits of the process-level FMEA include identification of important characteristics associated with the process, identification of potential process shortcomings early in the process planning cycle, development of priorities for process improvement actions, and documentation of rationale for process changes to help guide the establishment of potential manufacturing processes.

4.4.6 Steps for Performing FMEA

The distinction between technical knowledge in various fields and the methodology of an FMEA execution offers the advantage that the experts from the respective fields only offer their technical knowledge free of any methodical considerations. Thus, merely a basic knowledge of FMEA is adequate of the team of experts. The team size ranges ideally between 4 and 6 members—supervisors, moderator, and a small product team.

The fundamental step of an FMEA searches for all conceivable failure modes. Thus, this step should be executed most carefully. Each failure mode not found can lead to dangerous failure effects. Options available to discover failure modes are damage statistics, experience of the FMEA participants, checklists, brainstorming, and systematic analysis over failure functions. An imperative principle is the observation of former arisen failures in similar cases. All further failure modes can be derived with the help of the experience of the FMEA participants.

The first sections of the FMEA form sheet are reserved for the description of the system, product or process and their function. The next section of the form sheet deals with the risk analysis. This is followed by a risk assessment in order to rank the numerous failure causes. The last step is a concept optimization derived from the analysis of the risk assessment (see Fig. 4.17).

The completed form sheet represents a tree structure. A certain component has one or more functions and normally several failure modes. Each failure mode has again various failure effects and different failure causes (see Fig. 4.18).

FMEA can be performed in the following six steps.

4.4.6.1 Defines System and Its Associated Requirements (Step1)

This is a first step of FMEA. Define the system under consideration how complex the system is. The analyst must develop the system definition using documents such as reports, drawings, development plans (or specifications). The system structure arbitrarily orders the individual system elements into various hierarchical levels.

- The definition of design (or process) interfaces
- Dividing the system into its individual system elements—module and components
- Arranging system elements hierarchically in product structure.

4.4.6.2 Describe the System and Its Associated Functional Blocks (Step2)

- The arrangement of the system structure is the basis for determining the preparation of the description of the system under consideration. Such description may be grouped into two parts.

Fig. 4.17 FMEA form sheet that consists of four sections

Fig. 4.18 FMEA example for mechanical/civil parts with tree structure

- **Narrative functional statement (Top down).** The functions are created by preparing for each module and component as well as for the total system. It provides narrative description of each item's operation for each mode/mission phase. The degree of the description detail depends on factors such as an item's application and the uniqueness of the functions performed.
- **System block diagram.** The purpose of this block diagram is to determine the success/failure relationships among all the system components.

4.4.6.3 Identify Failure Modes and Their Associated Effects (Failure Analysis, Step3)

A failure analysis performs the analysis and determination of the failure modes and their effects. The failure leads to the dissatisfaction of a module. Compensating provisions and Criticality classification are described below.

- **Compensating provisions.** Design provisions or operator actions that is circumventing or mitigating the failure effect.
- **Criticality classification.** This is concerned with the categorization of potential effect of failure.
 - People may lose their lives due to failure
 - Failure may cause mission loss
 - Failure may cause delay in activation
 - Failure has no effect.

4.4.6.4 Risk Assessment (Step4)

The objective of the risk assessment is to prioritize the failure modes discovered during the system analysis on the basis of their effects and occurrence likelihood. Thus, for making an assessment of the severity of an item failure, two commonly used methods are Risk Priority Number (RPN) Technique that is widely used in the automotive industrial (Tables 4.2, 4.3 and 4.4).

4.4.6.5 RPN (Risk Priority Number)

This method calculates the risk priority number for apart failure mode using three factors: (1) failure severity ranking (SR), (2) failure mode occurrence ranking (OR), and (3) failure detection probability (DR). For example, if people are put into danger, the severity is evaluated higher, whereas a minimum limitation of comfort

Table 4.2 Failure detection ranking

Item no.	Likelihood of detection	Rank meaning	Rank
1	Very high	Potential design weakness almost certainly detected	1, 2
2	High	There is a good chance of detecting	3, 4
3	Moderate	There is a possibility of detecting potential design weakness	5, 6
4	Low	Potential design weakness is unlikely to be detected	7, 8
5	Very low	Potential design weakness probably will not be detected	9
6	Delectability absolutely uncertain	Potential design weakness cannot be detected	10

Table 4.3 Failure mode occurrence probability

Item no.	Ranking term	Rank meaning	Occurrence probability	Rank
1	Remote	Occurrence of failure is quite unlikely	<1 in 10^6	1
2	Low	Relatively few failures are expected	1 in 20,000	2
			1 in 4000	3
3	Moderate	Occasional failures are expected	1 in 1000	4
			1 in 400	5
			1 in 80	6
4	High	Repeated failures will occur	1 in 40	7
			1 in 20	8
5	Very high	Occurrence of failure is almost inevitable	1 in 8	9
			1 in 2	10

would receive a respectively lower value. With assessment value DR it is determined how successful the detection of the failure cause is before delivery to the customer. More specifically, the risk priority number is computed by multiplying the ranking (i.e., 1–10) assigned to each of these three factors. Thus, the risk priority is expressed by

$$\text{Risk Priority Number (RPN)} = (\text{Severity}) (\text{Occurrence}) (\text{Severity}) \quad (4.1)$$

With the RPN a ranking of the identified failure causes and their failure connection to the failure effect can be done.

Since the above three factors are assigned rankings from 1 to 10, the value of the RPN will vary from 1 to 1000. The average RPN is normally 125 ($5*5*5$). Failure modes with a high RPN are considered to be more critical; thus, they are given a higher priority in comparison to the ones with lower RPN. Nonetheless, ranking

Table 4.4 Severity of the failure-mode effect

Item no.	Failure effect severity category	Severity category description	Rank
1	Minor	No real effect on system performance and the customer	1
2	Low	may not even notice the failure	2, 3
3	Moderate	The occurrence of failure will only cause a slight customer	4, 5, 6
4	High	Annoyance	7, 8
5	Very high	Some customer dissatisfaction will be caused by failure High degree of customer dissatisfaction will be caused by failure but the failure itself does not involve safety or noncompliance with government rules and regulations The failure affects safe item operation, involves noncompliance with government rules and regulations	9, 10

and their interpretation may vary from one organization to another. Table 4.2 through 4.4 present rankings for failure detection, failure mode occurrence probability, and failure effect severity used in one.

4.4.6.6 Optimization (Step5)

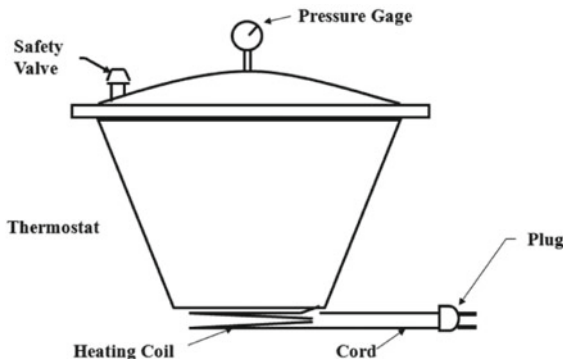
The last phase of the FMEA is the optimization phase. First, the calculated RPN are ordered according to their values. According to the Pareto principle, 20–30% of the RPN has been optimized.

- Ranking of failure causes according to their RPN value
- Concept optimization beginning with the failure causes with the highest RPN (Pareto principle)
- Failure causes with OR > 8, DR > 8, DR > 8 separately.

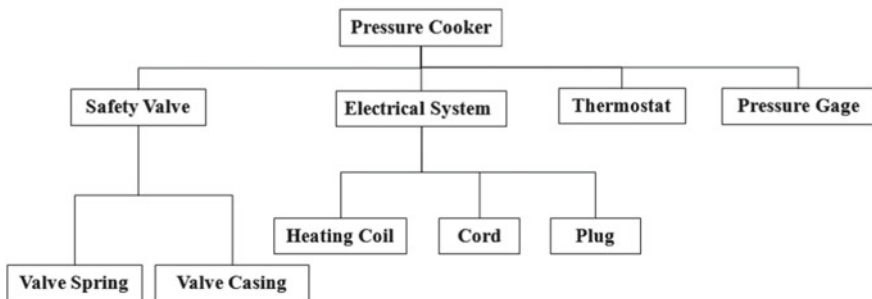
The new optimization actions are entered on the right side of the form sheet for the optimized failure causes and the responsibility is recorded. An improved RPN is calculated for the improved state the new assessment values assigned to RPN (Tables 4.2, 4.3 and 4.4).

Example 4.3 Develop a FMEA for pressure cooker like Fig. 4.19. The safety features of pressure cooker have as following:

- (1) Safety valve relieves pressure before it reaches dangerous levels.
- (2) Thermostat opens circuit through heating coil when the temperature rises above 250 °C.
- (3) Pressure gauge is divided into green and red sections. That is, “Danger” is indicated when the pointer is in the red section.



(a).A schematic diagram of pressure cooker



(b).System block diagram of pressure cooker

Fig. 4.19 FMEA for pressure cooker

First of all, problem should define scope:

- (1) Resolution: The analysis will be restricted to the four major subsystems (electrical system, safety valve, thermostat, and pressure gauge)
- (2) Focus—Safety.

Based on a focus of safety of pressure cooker, perform Failure Modes, Effects and (Criticality) Analysis for a Pressure Cooker with (Table 4.5).

4.5 Fault Tree Analysis (FTA)

4.5.1 Introduction

As seen in Fig. 4.20, Fault tree analysis (FTA) is one of the most widely used methods in the industrial area to identify the internal (or external) causes of failures.

Table 4.5 Failure modes, effects and (criticality) analysis for a pressure cooker

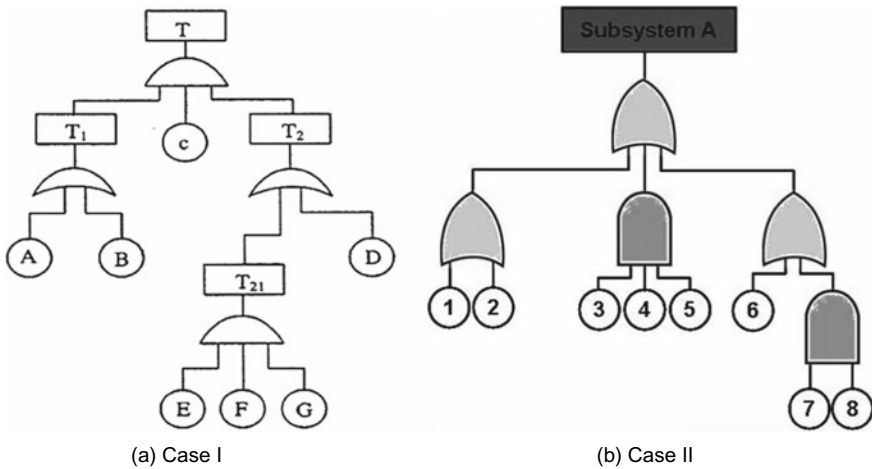
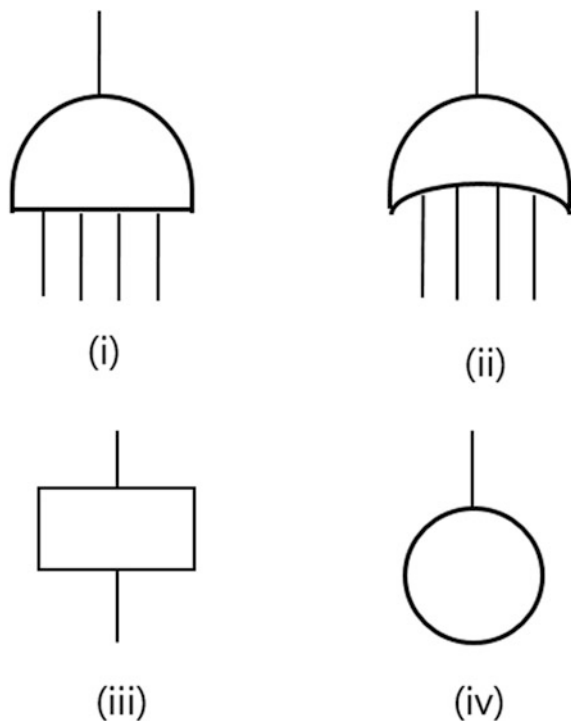
Item	Failure mode	Failure causes	Failure effects	S	O	C	Control measures/remarks
Electrical system	No current	Defective cord Defective plug Defective heating coil	Cooking interruption (mission failure)	1	2	2	Use high-quality components Periodically inspect cord and plug
	Current flows to ground by an alternate route	Faulty Insulation	Shock Cooking interruption	2	1	2	Use a grounded (3-prong) plug Only plug into outlets controlled by ground-fault circuit interrupters
Safety valve	Open	Broken valve spring	Steam could burn operator Increased cooking time	2	2	4	Design spring to handle the fatigue and corrosion that it will be subjected to
	Closed	Corrosion Faulty manufacture	Potential over pressurization	1	2	2	Use corrosion-resistant materials Test the safety valve
Thermostat	Open	Defective thermostat	Cooking interruption	1	2	2	Use a high-quality thermostat
	Closed	Defective thermostat	Over pressurization eventually opens valve	1	2	2	Use a high-quality thermostat

Thus, the FTA defines the system behavior in regard to fault. FTA was developed in the early 1950s at Bell Telephone Laboratories and started to use the FTA for the development of commercial aircrafts (1966). In the 1970s this method was used in the area of nuclear power. Now it is spread in many different areas—automobile, communication, and robotics.

FTA is used to show the system functions and their reliability. In the early design stage it may be applied as a diagnosis and development tool. The potential system faults can be identified and the design action plans can be setup. One of the major advantages of FTA is that the method provides both qualitative and quantitative results. FTA also with Boolean algebra and probability theory is beneficial to the preventative quality assurance (Fig. 4.21).

Although many symbols are used in performing FTA, the four commonly used symbols are described as:

- **AND gate.** This denotes that an output fault event occurs only if all of the input fault events occur

**Fig. 4.20** A typical example of fault tree analysis**Fig. 4.21** Commonly used fault tree symbols: (i) AND gate, (ii) OR gate, (iii) rectangular, (iv) OR gate

- **Or gate.** This denotes that an output fault event occurs only if one or more of the input fault events occur
- **Rectangle.** This denotes a fault event that results from the logical combination of fault events through the input of a logic gate
- **Circle.** This represents a basic fault event or the failure of an elementary component. The event's probability of occurrence, failure, and repair rates are normally obtained from field failure data.

The objectives of FTA are (1) systematic identification of all possible failures and their causes, (2) illustration of critical failures, (3) evaluation of system concepts, and (4) documentation of the failure mechanism and their functional relations. It begins by identifying an undesirable system event (Top Event). Top event are generated and connected by logic gates such as OR and AND. The fault tree constructions are repeated successively until the lowest events are developed.

Example 4.4 Assume that electric circuit system contains motor system, two switches, and electric power source. Develop a fault tree for the top event “no operating motor”, if the interruption of motor power can only be caused either by current failure or motor failure (Fig. 4.22).

By using the Fig. 4.21 symbols, a fault tree for motor system can be developed as following:

Each fault event in the figure is labeled as $X_0, X_1, X_2, X_3, X_4, X_5, X_6, X_7$, and X_8 . For independent fault events, the probability of occurrence of top events of fault trees can easily be evaluated by applying the basic rules of probability to the output fault events of logic gates. For example, we have

$$P(x_{4\backslash}) = P(x_7) + P(x_8) - P(x_7)P(x_8) \quad (4.5)$$

$$P(x_{1\backslash}) = P(x_3) + P(x_4) - P(x_3)P(x_4) \quad (4.6)$$

$$P(x_2) = P(x_5) + P(x_6) - P(x_5)P(x_6) \quad (4.7)$$

$$P(x_0) = 1 - [1 - P(x_1)][1 - P(x_2)] \quad (4.8)$$

where $P(X_i)$ is the probability of occurrence of fault event X_i , for $i = 1, 2, 3, \dots, 8$.

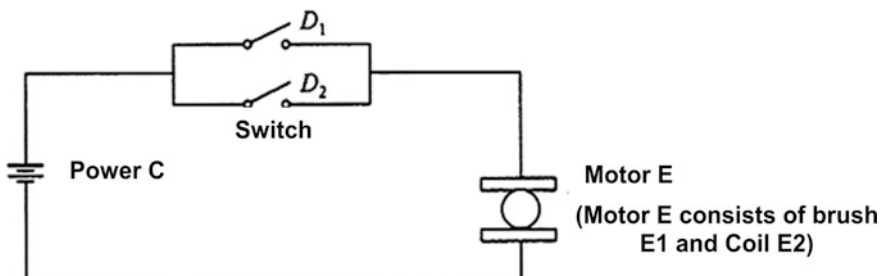


Fig. 4.22 A circuit diagram for Example 4.2

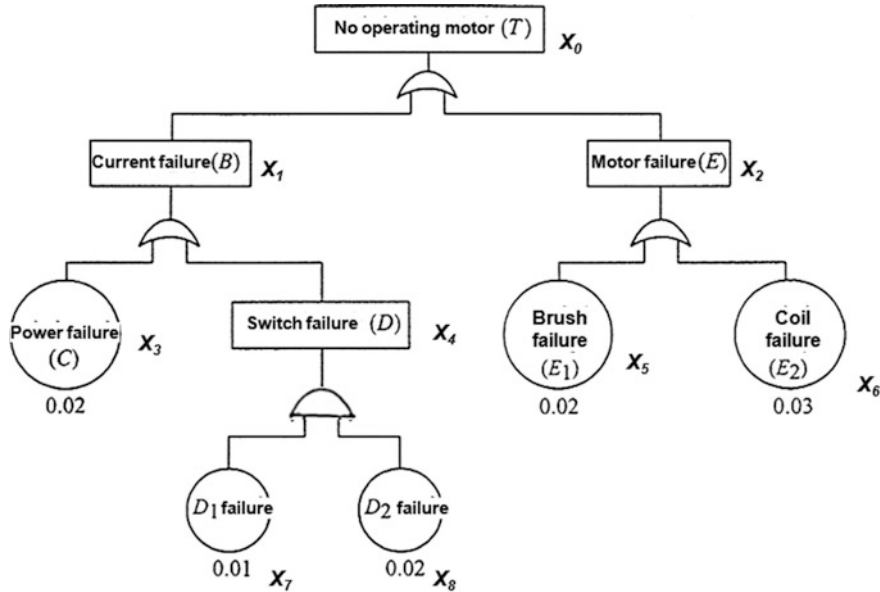


Fig. 4.23 A fault tree for Example 4.1

Example 4.5 In Fig. 4.23, assume that the probability of occurrence of fault events X_3 , X_5 , X_6 , X_7 , and X_8 are 0.02, 0.02, 0.03, 0.01, and 0.02, respectively. Calculate the probability of occurrence of the top event “no operating motor” by using Eqs. (4.5)–(4.8).

Thus, by substituting the given data values into Eqs. (4.5)–(4.8), we can get

$$P(x_4) = P(x_7)P(x_8) = (0.01)(0.02) = 0.0002 \quad (4.9)$$

$$\begin{aligned} P(x_{1\setminus}) &= P(x_3) + P(x_4) - P(x_3)P(x_4) = (0.02) + (0.0002) - (0.02)(0.0002) \\ &= 0.020196 \end{aligned} \quad (4.10)$$

$$P(x_2) = P(x_5) + P(x_6) - P(x_5)P(x_6) = (0.02) + (0.03) - (0.02)(0.03) = 0.0494 \quad (4.11)$$

$$P(x_0) = 1 - [1 - P(x_1)][1 - P(x_2)] = 1 - (1 - 0.020196)(1 - 0.0494) = 0.0686 \quad (4.12)$$

Thus, the probability of occurrence of the top event “no operating motor” is 0.0686. The approximate reliability of this electric circuit system is 0.9314.

4.5.2 Reliability Evaluation of Standard Configuration

Engineering systems can form various types of configurations in performing reliability analysis. A system is said to be a serial system if failure of one or more components within system results in failure of the entire system. On the other hands, parallel system is that the failure of all components within the system results in the failure of the entire system. For example, the lighting system that consists of four bulbs in a room is a parallel system, because room blackout happens only when all four bulbs break. The reliabilities of the serial or parallel systems are summarized in Table 4.6.

Example 4.6 Assume that an aircraft has four independent and identical engines and all must work normally for the aircraft to fly successfully. Calculate the reliability of the aircraft flying successfully, if each engine's reliability is 0.99.

By substituting the given data values of equation system reliability in Table 4.6, we can get

$$R_s = (0.99)^4 = 0.9606 \quad (4.13)$$

Thus, the reliability of the aircraft flying successfully is 0.9606.

Example 4.7 A system is composed of two independent and identical active units and at least one unit must operate normally for the system success. Each unit's constant failure rate is 0.0008 failures per hour. Calculate the system mean time to failure and reliability for a 150-h mission.

Substituting the given data values of parallel system MTTF Eq. in Table 4.6 yields

$$MTTF_{ps} = \int_0^{\infty} \left[1 - (1 - e^{-\lambda t})^m \right] dt = \frac{1}{\lambda} \sum_{i=1}^m \frac{1}{i} = \frac{1}{(0.0008)} \left(1 + \frac{1}{2} \right) = 1875 \text{ h} \quad (4.14)$$

Using the specified data values of parallel system reliability equation in Table 4.6 yields

$$R_{ps}(150) = \left[1 - \left\{ 1 - e^{-(0.0008)(150)} \right\}^2 \right] = 0.9872 \quad (4.15)$$

Thus, the system mean time to failure and reliability are 1875 h and 0.9872, respectively.

Table 4.6 Standard configuration with m units

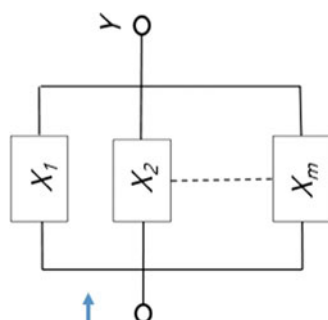
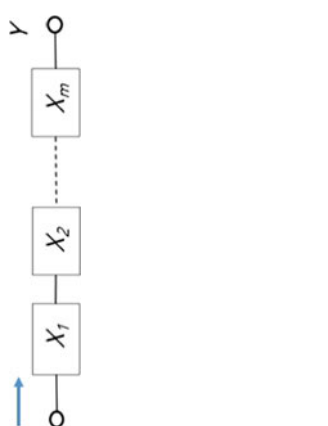
System structure	Serial systems	Parallel systems	(continued)
Block diagram			
			

Table 4.6 (continued)

System structure	Serial systems	Parallel systems
System reliability	$R_s(t) = \prod_{i=1}^m R_i(t)$	$R_s(t) = 1 - \prod_{i=1}^m (1 - R_i(t))$
ith unit constant failure rate	$R_i(t) = e^{-\int \lambda_i dt} = e^{-\lambda_i t}$	$R_{ps} = 1 - \prod_{i=1}^m (1 - e^{\lambda_i t})$
MTTF	$\int_0^\infty R_i(t)dt = 1 / \sum_{i=1}^n \lambda_i$	$\int_0^\infty R_i(t)dt = \frac{1}{\lambda} \sum_{i=1}^n \frac{1}{\lambda_i}$

4.6 Robust Design (or Taguchi Methods)

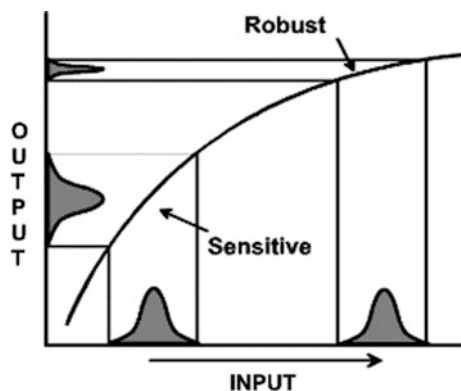
The success of modules in product can be expressed as robust design. Robust design first developed by Taguchi is a powerful technique for improving reliability at low cost in a short time. Robust design is a statistical engineering methodology for optimizing product conditions so that product performance is minimally sensitive to various noise sources of variation (see Fig. 4.24). Since 1980s, it has been applied extensively to improve the quality of countless products and processes.

Robustness is defined as the ability of a product to perform its intended function consistently at the presence of noise factors such as environmental loads. Here, the noise factors are the variables that have adverse effects on the intended function and are impractical to control. Environmental stresses (or loads) are the typical noise factors. This definition is widely applied in the field of quality engineering to address initial robustness when the product service time is zero. If customer satisfaction over time is concerned, the effect of time should be taken into account.

Reliability of mechanical/civil system can be perceived as robustness over time or environmental conditions. A reliable product has a high robustness value under different use conditions. To achieve high robustness, Taguchi methods recommend the optimal design parameters insensitive to noise parameters.

Taguchi methods are originally a kind of method to improve the product quality and recently applied to engineering as robust design method. Professional statisticians have welcomed the goals and improvements brought about by Taguchi methods, particularly by Taguchi's development of designs for studying variation, but have criticized the inefficiency of some of Taguchi's proposals. As alternative methods, parametric Accelerated Life Testing in Chaps. 8 and 9 will be studied.

Fig. 4.24 Robust design—
inputs that make the outputs
less sensitive



4.6.1 A Specific Loss Function

To estimate these hidden quality costs, Taguchi's quality loss function (QLF) has been proposed. Taguchi's approach is different than the traditional approach of quality costs. In the traditional approach, if you have two products that one is within the specified limits and the other is just outside of the specified limits, the difference is small. Although the difference is small, the product within the limits is considered a good product. On the other hands, the outside one is considered a bad product. Taguchi disagrees with this approach. Taguchi believes that when a product moves from its target value, that move causes a loss. It doesn't matter if the move falls inside or outside the specified limits. For this reason, Taguchi developed the QLF to measure the loss that is associated with hidden quality costs. This loss happens when a variation causes the product to move away from its target value.

As seen in Fig. 4.25, QLF is a "U" shaped parabola. The horizontal axis is tangent with the parabola at the target value. This is a quadratic loss function because it assumes that when a product is at its target value (T), the loss is zero.

Quality characteristics can be categorized into three situations: (1) On-target, minimum-variation, (2) Smaller the better, and (3) Larger the better.

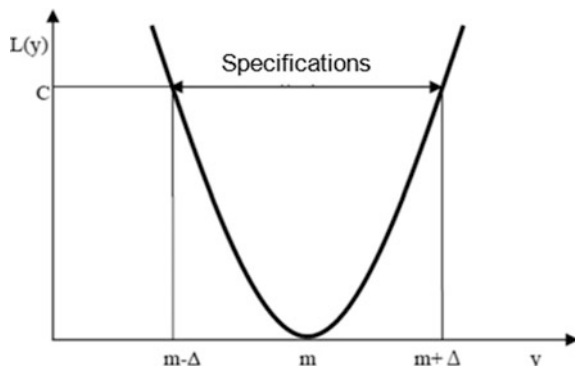
4.6.1.1 On-Target, Minimum-Variation (For Example, a Mating Part in an Assembly)

In engineering design we frequently encounter the on-target characteristics. Due to production process variation, the characteristics are allowed to vary within a range, say $\pm\Delta$, where Δ is called the tolerance. Equation (4.16) describes the quality loss of this type of characteristics.

The unit loss is determined by the formula:

$$L(t) = k(y - T)^2 \quad (4.16)$$

Fig. 4.25 Taguchi quality loss function for a nominal-the-best (on-target) characteristics



where k = a proportionality constant dependent upon the organization's failure cost structure, y = actual value of quality characteristic, T = target value of quality characteristic.

The value of k must first be determined before the loss can be estimated. To determine the value of k :

$$k = c/\Delta^2 \quad (4.17)$$

where c = loss associated with the specification limit, and Δ = deviation of the specification from the target value.

The target function is described as

$$f(y) = 1/(y - t)^2. \quad (4.18)$$

4.6.1.2 Smaller the Better—Variance (For Example, Carbon Dioxide Emissions)

If y is a smaller-the-better characteristic, its range can be written as $[0, d]$, where 0 is the target value and d is the upper specification limit. The quality loss function is obtained by substituting $T = 0$ into Eq. (4.18) and can be written as

$$L(t) = ky^2 \quad (4.19)$$

The target function is described as

$$f(y) = 1/y^2 \quad (4.20)$$

4.6.1.3 Larger the Better—Performance (for Example, Agricultural Yield)

If y is a larger-the-better characteristic, its range is $[d, \infty]$, where d is the lower limit. Because the reciprocal of a larger-the-better characteristic has the same quantitative behavior as a smaller-the-better one, the quality loss function can be obtained by substituting $1/y$ for y in Eq. (4.19). Then we have

$$L(t) = k \left(\frac{1}{y} \right)^2 \quad (4.21)$$

The target function is described as

$$f(y) = y^2 \quad (4.22)$$

Example 4.8 A product with on-target and minimum-variation has 100 (target value). The unit loss is determined by the formula:

$$L(t) = 40(y - 100)^2 \quad (4.23)$$

Find out the expectation of quality loss function of process line1 and line2.
So expectation of quality loss function can be expressed as:

$$E[L] = E[k(y - m)^2] = kVar[y] + k(E[y] - m)^2 \quad (4.24)$$

If process line1 has mean 96 and standard deviation 3, the expectation of quality loss function of process line1 is

$$E[L] = 40(3)^2 + 40(96 - 100)^2 = 1000 \$ \quad (4.25)$$

If process line 2 has mean 98 and standard deviation 5, the expectation of quality loss function of process line2 is

$$E[L] = 40(5)^2 + 40(98 - 100)^2 = 1160 \$ \quad (4.26)$$

If the standard variation of process line 2 decreases from 5 to 3, the cost reduction is

$$\Delta E[L] = 40(5)^2 - 40(3)^2 = 640 \$ \quad (4.27)$$

4.6.2 Robust Design Process

As seen in Fig. 4.26, robust design is a statistical engineering methodology for minimizing the performance variation of a product by choosing the optimal design conditions of the product to make the performance insensitive to noise factors. Taguchi realized that the best opportunity to eliminate variation is during the design of a product and its manufacturing process. Consequently, he developed a strategy for quality engineering that the process consists of three stages—system design, parameter design, and tolerance design.

4.6.2.1 System Design

System design involves selection of technology and components for use, design of system architecture, development of a prototype that meets customer requirement,

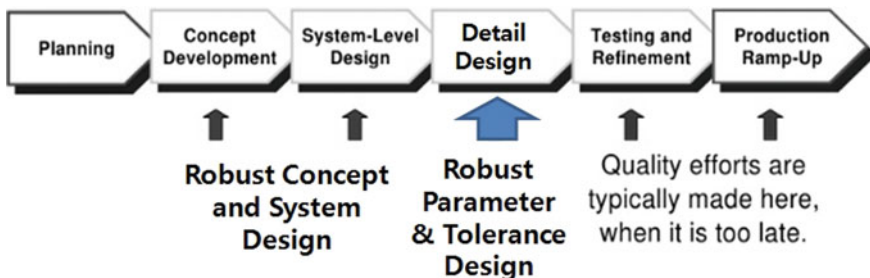


Fig. 4.26 Steps of robust design

and determination of manufacturing process. System design has significant impacts on cost, yield, reliability, maintainability, and many other performances of a product. It also plays a critical role in reducing product sensitivity to noise factors. If a system design is defective, the subsequent parameter design and tolerance design aimed at robustness improvement are ineffective. In recent years, some system design methodologies have emerged and shown effective, such as TRIZ (a problem-solving, analysis and forecasting tool derived from the study of patterns of invention in the global patent literature).

This step is indeed the conceptual design level, involving creativity and innovation.

- Getting into the ‘design space’
- Creating a feasible design
- Involves innovation.

4.6.3 *Parameter (Measure) Design*

Parameter design aims at minimizing the sensitivity of the product performance to noise factors by setting its design parameters at the optimal levels. In this step, designed experiments are usually conducted to investigate the relationships between the design parameters and performance characteristics of the product. Using such relationships, one can determine the optimal setting of the design parameters.

Once the concept is established, the nominal values of the various dimensions and design parameters in the product need to be set, the detail design phase of conventional engineering. In many circumstances, this allows the parameters to be chosen so as to minimize the effects on performance arising from variation in environmental noise—loads. Strictly speaking, parameter design might signify the robust design.

- Optimizing within the ‘design space’ (not changing anything fundamentally)
- Settings for the factors identified in systems design.

4.6.4 Tolerance Design

With a successfully completed parameter design, tolerance design is to choose the tolerance of important parts to reduce the performance sensitivity to noise factors under cost constraints. Tolerance design may be conducted after the parameter design is completed. If the parameter design cannot achieve sufficient robustness, tolerance design is completed. In this step, the important parts whose variability has the largest effects on the product sensitivity are identified through experimentation. Then the tolerance of these parts is tightened by using higher-grade parts based on the trade-off between the increased cost and the reduction in performance variability.

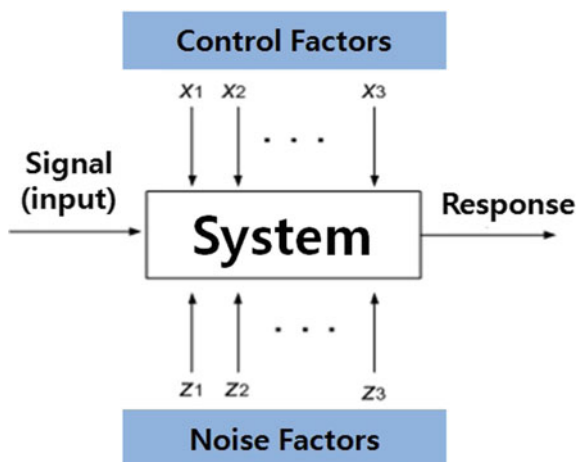
- Tightening tolerances on important factors
- Better materials/new equipment may be needed
- Has significant cost implications.

4.6.5 A Parameter Diagram (P-Diagram)

A P-diagram in the mechanical/civil system illustrates the input (signals), outputs (intended functions or responses), control factors, and noise factors. Figure 4.27 shows a generic P-diagram.

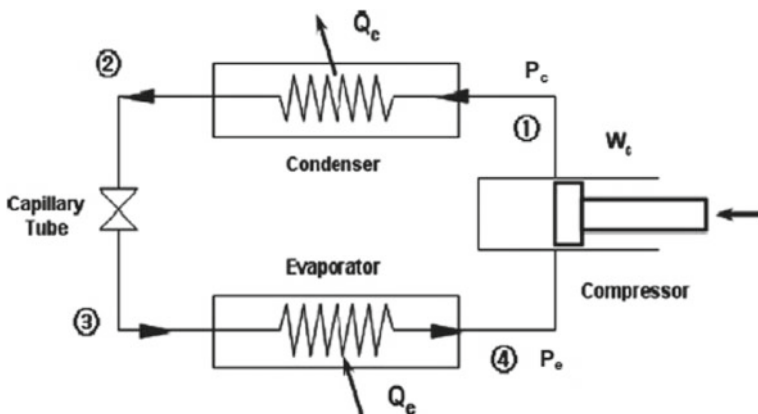
Signals are inputs from subsystems or modules to the system. The system transforms the signals into functional responses. Signals are essential to fulfilling the function of a system. Noise factors are variables that have adverse effects on robustness. Typical examples in the mechanical/civil system are a variety of random loads.

Fig. 4.27 Generic parameter diagram

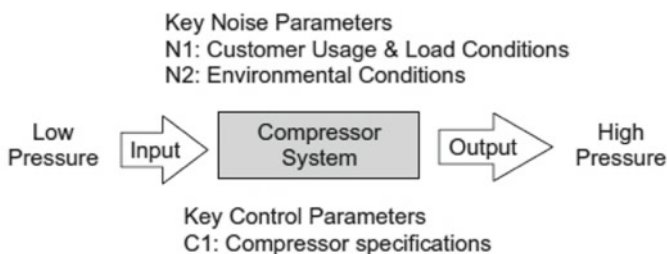


Control factors are the design parameters whose levels are specified by designers. The purpose of a robust design is to choose optimal levels of the parameters. In practice, mechanical/civil systems have a large of design parameters, which are not important in terms of the robustness. Thus, the key design parameters are included in a robust design. These key design parameters are identified by using engineering judgment, analytical study, a preliminary test, or field data.

For example, compressor increases from the evaporator pressure to the condensing pressure. It needed to be designed robustly to operate under a wide range of consumer usage conditions. Because customer usage and load conditions are unknown, engineer should design the compressor optimally by using engineering skill, analytical simulation, and reliability testing (Fig. 4.28).



(a) Compressor system in a vapor-compression refrigeration cycle



(b) Parameter diagram of compressor system

Fig. 4.28 Schematic diagram for mechanical system (Example: compressor system)

4.6.6 Taguchi's Design of Experiment (DOE)

Design of Experiment is a statistical technique for studying the effects of multiple factors on the experimental response. The factors are laid out in a structured array in which each row combination are conducted and response data are collected. Through experimental data analysis, we can choose the optimal levels of controls factors that minimize the sensitivity of the response to noise factors.

4.6.6.1 Orthogonal Arrays

An orthogonal array is a balanced fractional matrix in which each row represents the levels of factors of each run and each column represents the levels of specific factor that can be changed from each run. In a balanced matrix,

- All possible combinations of any two columns of the matrix occurs an equal number of times within the two columns. The two columns are also said to be orthogonal.
- Each level of specific factor within a column has an equal number of occurrences within the column.

Example 4.9 If product on-target and minimum-variation have the following experimental data, find out the optimal factor combinations (Table 4.7).

First of all, make the simplified analysis for level 1 and 2 per A, B, C, D like Table 4.8.

Draw the Pareto chart and find the factors that consists of 80–90%, based on the accumulated total sum (Fig. 4.29).

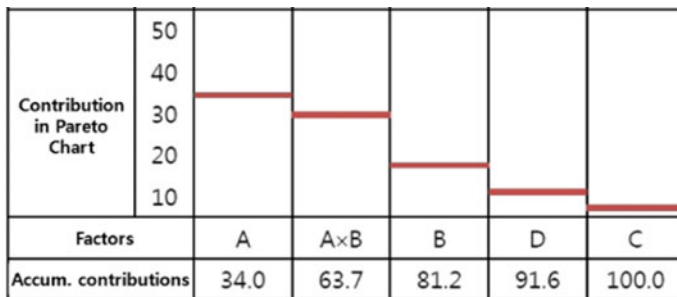
Then we know that A, B, and A × B occupy approximately 80% from Pareto charts. Find out the proper levels of A, B factors by Table 4.9.

Table 4.7 Experimental data

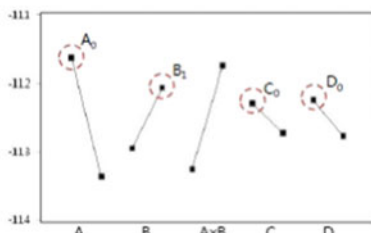
	A	B	AB	C	D	E	E	Experiment					S/N _i
	1	2	3	4	5	6	7	1	2	3	4	5	
1	0	0	0	0	0	0	0	34	22	29	14	25	-28.20
2	0	0	0	1	1	1	1	32	24	26	16	28	-28.22
3	0	1	1	0	0	1	1	24	18	25	27	22	-27.38
4	0	1	1	1	1	0	0	27	22	26	23	25	-27.84
5	0	0	1	0	1	0	1	30	25	27	29	20	-28.44
6	0	0	1	1	0	1	0	19	16	33	34	19	-28.04
7	0	1	0	0	1	1	0	25	33	24	25	21	-28.27
8	0	1	0	1	0	0	1	26	27	27	28	26	-28.57

Table 4.8 Simplified analysis for experimental data

Factor	A	B	AB	C	D	Total
S/N ratio	Level 1	-111.64	-112.95	-113.26	-112.29	-112.24
	Level 2	-113.37	-112.06	-113.26	-112.29	-112.24
Level range	1.73	0.89	1.51	0.43	0.53	5.09
Contribution (%)	34.0	17.5	29.7	8.4	10.4	100.0



(a) Pareto Charts



(b) Interaction effects between A, B, C, D factors

Fig. 4.29 Simplified analysis for A, B, C, D factors**Table 4.9** Simplified analysis for A, B factors

	A ₀	A ₁
B ₀	S/N ₀₀ = -56.42	S/N ₁₀ = -56.53
B ₁	S/N₀₁ = -55.22	S/N ₁₁ = -56.84

Consequently, we know that S/N ratio for A₀ and B₁ is the smallest among the levels of A, B, and A×B.

4.6.7 Inefficiencies of Taguchi's Designs

Taguchi's robust design method uses parameter design to place the design in a position where random "noise" does not cause failure and to determine the proper design parameters and their levels. However, for a simple mechanical structure, a

lot of design parameters should be considered in the Taguchi method's robust design process. Those mechanical/civil products with the missing or improper minor design parameters may result in recalls and loss of brand name value.

Interactions also are part of the real world. In Taguchi's arrays, interactions are confounded and difficult to resolve. Response surface methodology (RSM) is a "follow-up design" that resolves only the confounded interactions. RSM design may be used to explore possible high-order univariate effects of the remaining variables and have great statistical efficiency. The sequential designs of response surface methodology decreases experimental runs than would a sequence of Taguchi's designs. But Taguchi's designs still require a lot of experimental runs.

4.7 Reliability Testing

4.7.1 Introduction

Many manufactures use reliability testing to determine whether final designs meet customer demand for high quality and reliable products. In reliability test there are the following basic questions: (1) How long should you test? (2) How many units have to be put on test? (3) If acceleration modeling is part of the experimental plan, (4) What combination of stresses and how many experimental cells? (5) How many units go in each cell? The answers to these questions depend on: (1) What models are you assuming? (2) What decisions or conclusions do you want to make after running the test and analyzing the data? (3) What risks are you willing to take of making wrong decisions or conclusions?

Defined by the Advisory Group on Reliability of Electronic Equipment (AGREE), reliability is the "probability of performing without failure a specified function under given conditions for a specified period of time." This definition can be specifically analyzed as:

- Perform means that the item does not fail.
- The given conditions include the customer usage conditions and total physical environmental conditions, i.e., shipping, regional climate, mechanical, electrical, and thermal conditions.
- The stated time interval means the product lifetime and can be very long (twenty years, for telecommunication equipment), long (a few years) or short (a few hours or weeks, for space research equipment). The time also can be replaced by other parameters, such as: the mileage (of an automobile) or the number of cycles (i.e., for a capacity or a relay unit).

Reliability testing involves simulation of conditions under which the item will be used during its lifespan. Reliability does not compare the product to some predefined specifications, such as the case with quality assurance, but rather investigates the performance over a predefined period of time.

To reduce the cost of reliability testing, manufacturers employ sampling schemes to select sample that represent all product. As in any sampling, it is assumed that we can make appropriate inference about the true population characteristics based on appropriately selected samples.

For example, sampling can be typically formulated as the following statistical hypothesis:

H_0 : μ (mean life) is greater or equal to 20 h

H_1 : μ is less than 20 h.

It has producer's risks and consumer's risks that are similar to Type I and Type II errors. Producer's Risks is the probability of failing satisfactory items—the probability of rejecting H_0 when it holds. It is associated with the level of reliability which has a high probability of acceptance, and, therefore, low fraction of non-conforming units. On the other hands, Consumer's Risk is the probability of passing flawed items—the probability of accepting H_0 when it is false.

If product failures use concepts of load and strength under severe test conditions, reliability testing will be used to determine whether the product is adequate to meet the requirements of reliability under accelerated testing. If the accelerated factor and sample size are developed, product also can estimate lifetime under proper lifetime specification. Reliability testing during design and development therefore is mandatory to prove whether the lifetime of product is sufficient for customer requirements.

For reliability testing, engineer also determines that reliability test criteria can be specified in units of time (Type I censoring) or failure number (Type II censoring). In Type I censoring the items will be tested for a certain amount of time, whereas in Type II censoring the items will be tested until a certain number of failures. Because it is not uncommon in time-terminated tests to have many survived units when the test is finished, engineer will use failure number (Type II censoring).

To predict the product lifetime, maximum-likelihood estimation (MLE) is a popular method based on the observed data of reliability testing. MLE is the statistical method of estimating the parameters of a statistical model—some unknown mean and variance that are given to a dataset. It selects the set of values of the model parameters that maximizes the likelihood function.

For example, engineer may be interested in the lifetime of product (or module), but be unable to measure the lifetime of every single product in a population due to cost or time constraints. Assuming that the lifetime are normally distributed with some unknown mean and variance, the mean and variance can be estimated with MLE while only knowing the lifetime of some sample of the overall population. MLE would accomplish this by taking the mean and variance as parameters and finding particular parametric values that make the observed results the most probable given the model.

4.7.2 Lifetime Estimation—Maximum Likelihood Estimation (MLE)

The popular method for Weibull parameter estimation in data analysis is Maximum Likelihood Estimation (MLE). MLE method produces best estimates with large sample sizes. MLE estimates tend to be optimistic with small samples.

For a fixed set of data and underlying statistical model, the method of maximum likelihood estimates the set of values of the model parameters that maximizes the likelihood function. Intuitively, this maximizes the “agreement” of the selected model with the observed data, and for discrete random variables it indeed maximizes the probability of the observed data under the resulting distribution. MLE would give a unified approach to estimation, if the case of the normal distribution or many other problems is well-defined.

One very good statistical method for the determination of unknown parameters of a distribution is the Maximum Likelihood Method. It assumes that the histogram of the failure frequency depicts the number of failure per interval. For larger test sample sizes n it is possible to derive function out of the histogram and thus to exchange the frequencies to the probabilities.

In this way it is possible to state, for example that during the first interval probably 3% of all failures will occur. In the second interval it is most likely that 45% of the failures occur, etc. According to theory, the probability L of test sample can be obtained by the product of the probability of the individual intervals.

Suppose there is a sample t_1, t_2, \dots, t_n of n independent and identically distributed failure times, coming from a distribution with an unknown probability density function $f_0(\cdot)$. On the other hands, supposed that the function f_0 belongs to a certain family of distributions $\{f(\cdot|\theta), \theta \in \Theta\}$ (where θ is a vector of parameters), called the parametric model, so that $f_0 = f(\cdot|\theta_0)$. The unknown value θ_0 is expected to as the true value of the parameter vector. An estimator $\hat{\theta}$ would be fairly close to the true value θ_0 . The observed variables t_i and the parameter θ are vector components.

$$L(\Theta; t_1, t_2, \dots, t_n) = f(t_1, t_2, \dots, t_n | \Theta) = \prod_{i=1}^n f(t_i | \Theta) \quad (4.28)$$

This function is called the likelihood. The idea of this procedure is to find a function f , for which the product L is maximized. Here, the function must possess high values of the density function f in the corresponding region with several failure times t_i . At the same time only low value of f in regions with few failures are found. Thus, the actual failure behavior is accurately represented. If determined in this way, the function f gives the best probability to describe the test samples.

It is often more effective to use the log-likelihood function. Thus, the product equation becomes an addition equation, which greatly simplifies the differentiation. Since the natural log is a monotonic function, this step is mathematically logical.

$$\ln L(\Theta; t_1, t_2, \dots, t_n) = \sum_{i=1}^n \ln f(t_i | \Theta) \quad (4.29)$$

By differentiate Eq. (4.29), the maximum of the log-likelihood function and thus the statistically optimal parameters Θ_l can be obtained as:

$$\frac{\partial \ln(L)}{\partial \theta_l} = \sum_{i=1}^n \frac{1}{f(t_i; \Theta)} \cdot \frac{\partial f(t_i; \Theta)}{\partial \theta_l} = 0 \quad (4.30)$$

These equations can be nonlinear in the parameters; therefore it is often useful to apply approximate numerical procedures. By the Likelihood function value the opportunity is given to estimate the quality of the adaptation of a distribution to the failure data. The greater the likelihood function value is, the better the conclusive distribution function represents the actual failure behavior. However, based on MLE, the characteristic life η_{MLE} from the reliability testing (or lifetime testing) can be estimated on the Weibull chart (Refer to Sect. 3.4).

Example 4.10 Normal distribution—Maximum Likelihood Estimation.

This example deals with maximum likelihood estimation of the parameters of the normal distribution. It will be the basics of maximum likelihood estimation.

Assumptions

Testing samples are following the normal distribution having mean and variance. The probability density function of a generic term of the sample sequence is

$$f_{\mu, \sigma}(x_i) = \frac{1}{\sqrt{2\pi}\sigma} \exp\left(\frac{-(x_i - \mu)^2}{2\sigma^2}\right) \quad (4.31)$$

where random variables $x_i = x_1, x_2, \dots, x_3$.

The likelihood function can be expressed as

$$L(\Theta) = \prod_i f_{\mu, \sigma}(x_i) = \prod_i \frac{1}{\sqrt{2\pi}\sigma} \exp\left(\frac{-(x_i - \mu)^2}{2\sigma^2}\right) \quad (4.32)$$

If differentiated for mean μ and the variance σ^2 , find the maximum value

$$\frac{\partial}{\partial \theta_l} L^*(\Theta) = \frac{1}{\sigma^2} \sum_i (x_i - \mu) = \frac{1}{\sigma^2} \left(\sum_i x_i - n\mu \right) = 0 \quad (4.33)$$

$$\frac{\partial}{\partial \mu} L^*(\Theta) = -\frac{n}{\sigma} + \frac{1}{\sigma^2} \sum_i (x_i - \mu)^2 = 0 \quad (4.34)$$

Finally, maximum likelihood estimation for normal distribution can be found at

$$\mu = \left(\sum_i x_i \right) / n \quad (4.35)$$

$$\sigma^2 = \sum_i (x_i - \mu)^2 / n \quad (4.36)$$

Example 4.11 Weibull distribution—Maximum Likelihood Estimation Joint density function can be expressed as:

$$\prod_{i=1}^n \left(\frac{\beta}{\eta} \right) \left(\frac{t_i}{\eta} \right)^{\beta-1} \exp \left(-\frac{t_i}{\eta} \right) \quad (4.37)$$

It would describe the likelihood function for n failed items. To account for the k suspended items, a factor $(1 - F(t))$ should be multiplied. So the complete likelihood function in Weibull distribution becomes:

$$L(\Theta) = \prod_{i=1}^n \left(\frac{\beta}{\eta} \right) \left(\frac{t_i}{\eta} \right)^{\beta-1} \exp \left(-\frac{t_i}{\eta} \right) \prod_{j=1}^k \exp \left(-\frac{t_j}{\eta} \right) \quad (4.38)$$

To find the maximum of this function with respect to β and η , we should differentiate logarithm of the likelihood with the corresponding parameter. In the complete sample case, the maximum likelihood estimate of β , can be obtained as

$$\frac{\sum_{i=1}^n t_i^\beta \ln x_i}{\sum_{i=1}^n t_i^\beta} - \frac{1}{n} \sum_{i=1}^n \ln t_i - \frac{1}{\beta} = 0 \quad (4.39)$$

Given the failure times t_1, t_2, \dots, t_n , the maximum likelihood estimate of β is found using iterative procedures.

The maximum likelihood estimate of η is:

$$\eta^\beta = \left(\frac{\sum_{i=1}^n t_i^\beta}{r} \right) \quad (4.40)$$

where r is number of failed number.

Example 4.12 Find the shape parameter and characteristic life by using the maximum likelihood method and the censored data listed below.

Cycles	Status	Cycles	Status
1500	Failure	4300	Failure
1750	Suspension	5000	Suspension
2250	Failure	7000	Failure
4000	Failure		

Estimate the shape parameter and characteristic life. From Eq. (4.40), the maximum likelihood estimate, β , is the root of the equation

$$\frac{\sum_{i=1}^7 t_i^\beta \ln x_i}{\sum_{i=1}^7 t_i^\beta} - \frac{1}{5} \sum_{i=1}^5 \ln t_i - \frac{1}{\beta} = 0 \quad (4.41)$$

The Weibull plot estimate, 1.8, was used as the initial value of β . The estimates of β are listed below with the corresponding value of $G(\beta)$. If using a modified Newton-Raphson procedure, find the value of β giving $G(\beta) = 0$.

- 1.800 -0.1754 (1st iteration)
- 1.802 -0.1746 (2nd iteration)
- 2.179 -0.0255 (3rd iteration)
- 2.182 -0.0248 (4th iteration)
- 2.253 -0.0007 (5th iteration)
- 2.256 -0.0005 (6th iteration)
- 2.257 -0.0000 (Maximum likelihood estimate of Beta).

The maximum likelihood estimate of η is

$$\hat{\eta} = \left(\frac{\sum_{i=1}^7 t_i^{2.257}}{5} \right)^{1/2.257} = 4900.1$$

4.7.3 Time-to-Failure Models

Since time is a common measure of life, life data points are often called “times-to-failure.” The failure time T of a product is a random variable. Time can take on different meanings depending on operational time, distance driven by a vehicle, and number of cycles for a periodically operated system. Time-to-Failure model usually provides all the tools for reliability testing, especially data analysis of accelerated life testing. It is designed for use with complete (time-to-failure), right censored (suspended), interval or left censored data. Data can be entered individually or in groups.

Time-to-Failure model generally has the following types:

- Arrhenius: a single stress model typically used when temperature is the accelerated stress.
- Inverse Power Law (IPL): a single stress model typically used with a non-thermal stress, such as vibration, voltage or temperature cycling.
- Eyring: a single stress model typically used when temperature or humidity is the accelerated stress.
- Temperature-Humidity: a double-Arrhenius model that is typically used when temperature and humidity are the acceleration variables.
- Temperature-Nonthermal: a combination of the Arrhenius and IPL relationships that is typically used when one stress is temperature and the other is non-thermal (e.g., voltage).

4.7.3.1 Arrhenius Equation

The Arrhenius equation proposed by Arrhenius in 1889 is a formula for the temperature dependence of reaction rates. As seen in Fig. 4.30, reactivity modeling consists of computing the energy of the products, the reactants, and the transition state (TS) connecting them. These three points are the critical features on a reaction pathway. The difference between the energies of the transition state and reactants ($\Delta E_a = E_{TS} - E_r$) is the activation energy ΔE_a . The activation energy is important in understanding the rate of chemical reactions as expressed in the Arrhenius Equation which relates the rate constant K of a chemical reaction to its activation energy.

One of the earliest and most successful acceleration models predicts how time-to-fail varies with temperature. The Arrhenius equation empirically based model is known as:

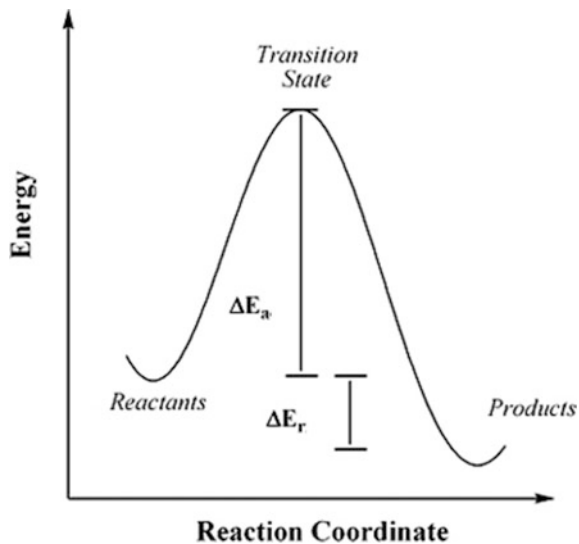
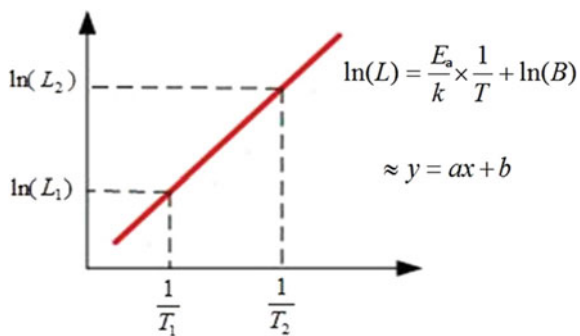
$$TF(\text{or } L) = A \exp\left(\frac{E_a}{kT}\right) \quad (4.42)$$

where T denoting temperature measured in degrees Kelvin at the point when the failure process takes place, k is Boltzmann's constant (8.617×10^{-5} in eV/K), and constant A is a scaling factor that drops out when calculating acceleration factors, with E_a denoting the activation energy, which is the critical parameter in the model.

If Eq. (4.42) takes logarithm, the simple straight line can be obtained. That is,

$$\ln(L) = \ln(A) + \frac{E_a}{k} \times \frac{1}{T} \quad (4.43)$$

So we can estimate the product lifetime (Fig. 4.31 and Example 4.13).

Fig. 4.30 Arrhenius equation**Fig. 4.31** Arrhenius model

The acceleration factor between a higher temperature T_2 and a lower temperature T_1 is given by

$$AF = \exp\left(\frac{E_a}{k}\left(\frac{1}{T_1} - \frac{1}{T_2}\right)\right) \quad (4.44)$$

The value of E_a depends on the failure mechanism and the materials involved. It typically ranges from 0.3 or 0.4 up to 1.5, or even higher.

The Arrhenius model has been used successfully for failure mechanisms that depend on chemical reactions, diffusion processes or migration processes. This covers many of the non-mechanical (or non-material fatigue) failure modes that cause electronic equipment failure.

Example 4.12 The acceleration factor between 25 and 125 °C is 133 if $E_a = 0.5$ and 17,597 if $E_a = 1.0$ from Eq. (4.44).

4.7.3.2 Inverse Power Law

In statistics, a power law is a functional relationship between two quantities, where a relative change in one quantity results in a proportional relative change in the other quantity, independent of the initial size of those quantities: one quantity varies as a power of another.

For example, the “life” of a product will go down as stress goes up. While this is not a hard and fast rule, very few systems do not behave in this intuitive fashion. This allows for shorter test times at higher levels of stress. With solid knowledge of the life-stress relationship, effective predictions of life at normal or usage conditions can be made.

The most important and widely used model for mechanical systems is the inverse power law (IPL). It has forms:

$$TF = AS^{-n} \quad (4.45)$$

$$K = BS^n \quad (4.46)$$

The most critical factor is n , the life-stressor slope with s being stress applied to the system. A is a constant; in reality it relates the basic mechanical strength of the design to resist the stress applied to it. If Eq. (4.44) takes logarithm, the simple straight line can be obtained (Fig. 4.32).

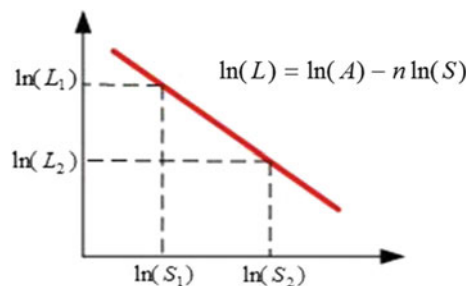
For instance, this model, used for capacitors, has only voltage dependency and takes the form:

$$TF = AV^{-n} \quad (4.47)$$

4.7.3.3 Eyring Equation

For chemical reaction rate theory, Eyring acceleration model has led to a very general and powerful one. This model has several key features:

Fig. 4.32 Inverse power law



- It has a theoretical basis from chemistry and quantum mechanics.
- If a chemical process (chemical reaction, diffusion, corrosion, migration, etc.) is causing degradation leading to failure, the Eyring model describes how the rate of degradation varies with stress or, equivalently, how time to failure varies with stress.
- The model includes temperature and can be expanded to include other relevant stresses.
- The temperature term by itself is very similar to the Arrhenius empirical model, explaining why that model has been so successful in establishing the connection between the ΔE parameter and the quantum theory concept of “activation energy needed to cross an energy barrier and initiate a reaction”.

The model for temperature and one additional stress takes the generic form:

$$TF = BS^{-n} \exp\left(\frac{E_a}{kT}\right) \quad (4.48)$$

where k is the Boltzmann constant, T is the thermodynamic temperature, and E_a is the activation energy.

4.7.3.4 Acceleration Factor

Acceleration means that operating a unit at high stress (i.e., higher temperature or voltage, etc.) produces the same failures that would occur at typical-use stresses, except that they happen much quicker. Mechanical failure may be due to fatigue, corrosion, etc. These are the same causes of failure under normal stress, though the time scale is simply different.

Acceleration factors show how time-to-fail at a particular operating stress level (for one failure mode or mechanism) can be used to predict the equivalent time to fail at a different operating stress level. For instance, if time-to-failure of test data follows Eyring acceleration model, the acceleration factor between a higher temperature T_2 and a lower temperature T_1 is given by

$$AF = \left(\frac{S_2}{S_1}\right)^n \exp\left(\frac{E_a}{k} \left(\frac{1}{T_1} - \frac{1}{T_2}\right)\right) \quad (4.49)$$

We know that the acceleration factor in Eyring equation Eq. (4.49) is similar to Eq. (7.18) that is derived from the generalized stress model Eq. (7.17).

When there is true acceleration, changing stress is equivalent to transforming the time scale used to record when failures occur. The transformations commonly used

are linear, which means that time-to-fail at high stress just has to be multiplied by a constant (the acceleration factor) to obtain the equivalent time-to-fail at use stress. Then, an acceleration factor AF between accelerated stress and normal stress means the following relationships hold:

$$h = AF \times h_a \quad (4.50)$$

A model that predicts time-to-fail as a function of operating stresses is known as an acceleration model. Acceleration models are usually based on the physics or chemistry underlying a particular failure mechanism. Successful empirical models often turn out to be approximations of complicated physics or kinetics models. A variety of typical models are Arrhenius, Eyring, and the generalized stress model that will be studied in Chaps. 8 and 9.

4.7.4 Data Analysis

4.7.4.1 Introduction

In life data analysis, engineers can predict the product lifetime by fitting a statistical distribution to testing data from a representative sample of units. Life data analysis requires (1) Gather life data for the product, (2) Select a lifetime distribution that will fit the data and model the life of the product, (3) Estimate the parameters that will fit the distribution to the data, (4) Generate plots and results that estimate the life characteristics of the product.

After product reliability data have been obtained, how do you fit Weibull distribution and estimate its parameters? Reliability data analysis like Weibull distribution and its application answers these kinds of questions.

Reliability data that come from environment conditions include values reported as “below detection limit” along with the stated detection limit. A sample contains censored observations if only information about some of the observations is that they are below or above a specified value. In the environmental literature, such values are often called “non-detects”. Although this result has some loss of information, we can still do graphical and statistical analyses of data with non-detects.

A reliability data set may have a single or multiple detection limits. Type I, left, censored, and single are specific choices of four characteristics of data—(1) observed, truncated, or censored, (2) left, right, or interval censored, (3) Type I, Type II, or randomly censored, and (4) single or multiple censoring values.

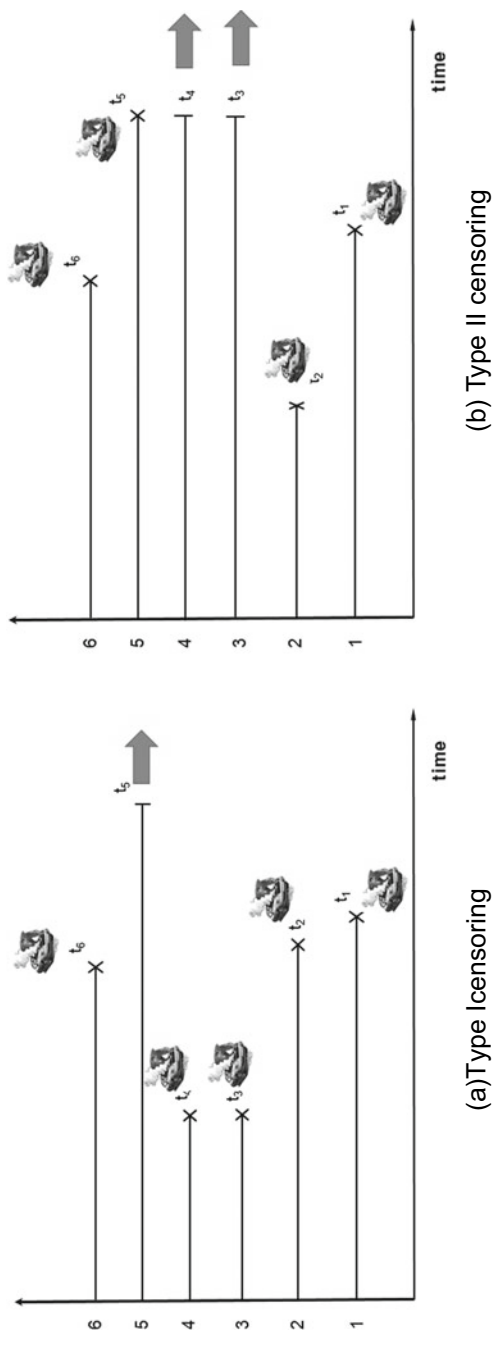


Fig. 4.33 Schematic of type I (a) and type II censoring (b)

4.7.4.2 Type I or Type II Censoring

A sample is Type I censored when the censoring levels are known in advance. The number of censored observations is a random outcome, even if the total sample size, N , is fixed. Environmental data are almost always type I censored (Fig. 4.33a).

A sample is Type II censored if the sample size N and number of censored observations are fixed in advance. The censoring level(s) are random outcomes. Type II censored samples most commonly arise in time-to-event studies that are planned to end after a specified number of failures, and Type II censored samples are sometimes called failure-censored samples (Fig. 4.33b).

The time and effort in testing can be significantly reduced by censored tests, and they can estimate the product lifetime. If a test trial is interrupted before all n test units have failed, a censored test may produce. If the interruption occurs after a given time, one is dealing with censoring of type I.

On the other hands, if a trial is interrupted after a given amount of test units r has failed, one is dealing with censoring of type II. The trials stop after 4 failures. The point in time at which the failure r occurs is a random variable. Thus, leaving the entire trial time length opens until the end of the trial.

The fact that $n - r$ test units have not failed is taken into account by substituting r for n in the denominator of the approximation equation. With type I or II censoring it is necessary to estimate the characteristic lifetime η in the Weibull chart by extrapolating the best fit line beyond the last failure time. This is generally problematic as long as further failure mechanisms cannot be neglected. A statistical statement concerning the failure behavior can be obtained on the observed lifetime. The procedures and methods for the assessment of complete data or censored data can be found in Table 4.10.

Table 4.10 Overview of procedures for the assessment of censored data

Data type	Type of censor	Description	Procedure
Complete data $r = n$	No censoring	All samples have failed	Median procedure $F(t_i) \approx \frac{i-0.3}{n+0.4}$ For $j = 1, 2, \dots, n$
Censored data $r < n$	Censoring Type I or Type II	Lifetime characteristics of all intact units are larger than the lifetime characteristics of the units r which failed last	Median procedure $F(t_i) \approx \frac{i-0.3}{n+0.4}$ For $i = 1, 2, \dots, r$

4.7.4.3 Estimating Distribution Parameters

In Chap. 3 we discussed the Weibull distribution and its distribution parameters. Maximum likelihood (MLE) also can estimate them. These procedures can easily be extended to account for Type I or Type II censored observations. MLE's assume that the data are a sample from a specific probability distribution like Weibull.

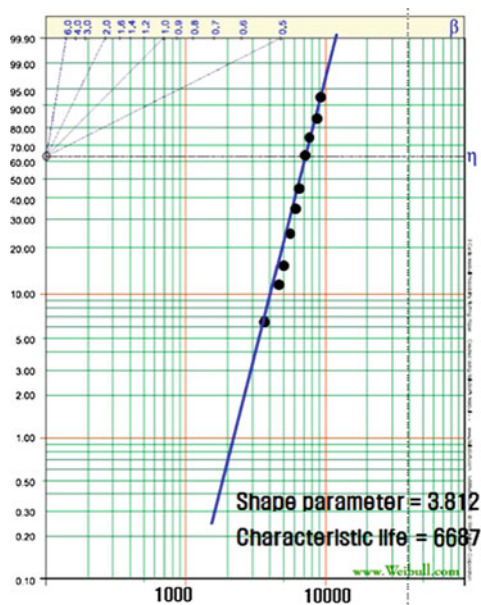
Probability Weibull plots are simple visual ways of summarizing reliability data by plotting CDF estimates versus time using a log-log scale. The x axis is labeled “Time” and the y axis is labeled “cumulative percent”. When the points are plotted, the analyst fits a straight line to the data with the aid of a least squares fitting program in Excel. Every straight line on a Weibull probability plot uniquely corresponds to a particular Weibull life distribution model. If the points follow the line reasonably well, the model is consistent with the data. There is a simple way to find the parameter estimates that correspond to the fitted straight line.

Example 4.13 Select the ten samples from a Integrated Circuit chip manufactured in August, 2016 and perform the reliability testing at 120, 135, and 150 °C. Under 30 °C normal conditions, search B10 life for 30 °C on Weibull or excel program.

	Temperature (°C)		
	120	130	150
1	3450	3300	2650
2	4340	3720	3100
3	4760	4180	3400
4	5320	4560	3800
5	5740	4920	4100
6	6160	5280	4400
7	6580	5640	4700
8	7140	6230	5100
9	8100	6840	5700
10	8960	7380	6400

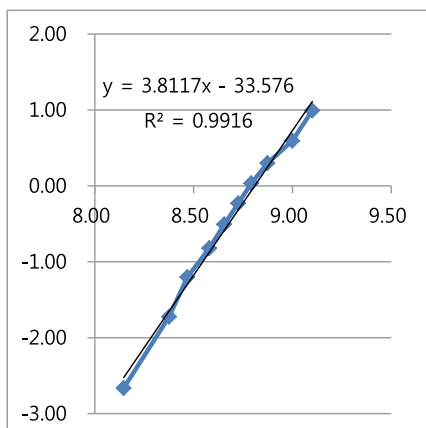
Case (I) for 120 °C, because temperature data have complete with no censoring, plot them on Weibull chart. We can approximate sketch the best fit straight line through the entered points and determine the Weibull parameters $\hat{\beta} = 3.812$. At the $Q(t) = 63.2\%$ ordinate point, draw a straight horizontal line until this line intersects the fitted straight line. Draw a vertical line through this intersection until it crosses the abscissa. The value at the intersection of the abscissa is the estimate of $\hat{\eta} = 6692$.

i	120°C	$F(t) \times 100$
1	3450	6.73077
2	4340	16.3462
3	4760	25.9615
4	5320	35.5769
5	5740	45.1923
6	6160	54.8077
7	6580	64.4231
8	7140	74.0385
9	8100	83.6538
10	8960	93.2692

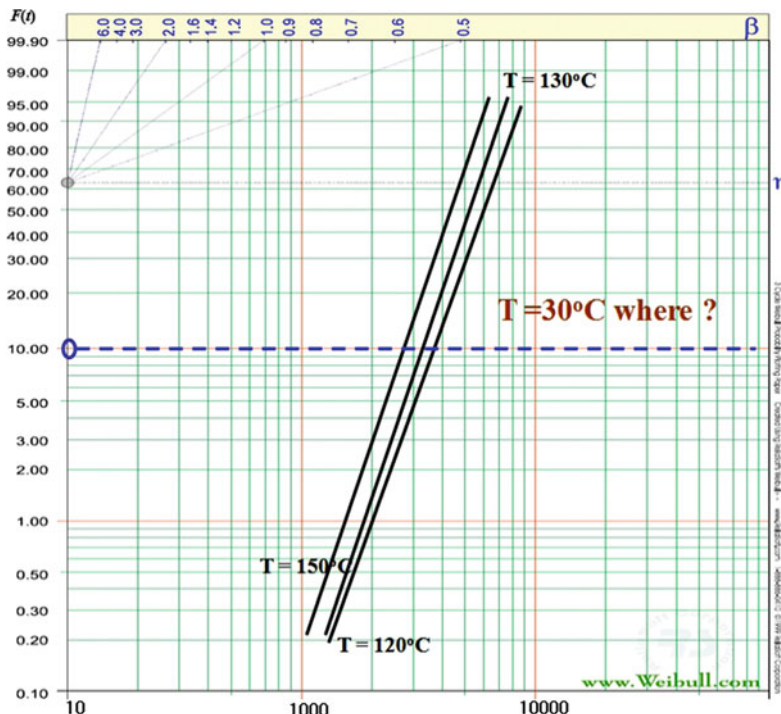


Case (II) Using Excel program, for 120 °C, we obtain the estimated shape parameter $\hat{\beta} = \text{slope} = 3.812$, estimated characteristic life $\hat{\eta}(F(t))$ is 63.2% ordinate point) = $e^{\frac{33.576}{3.812}} = 6692$ h
where $\ln[-\ln(1 - 0.63)] = -0.00576$, $-0.00576 = 3.811x - 33.57$.

X: LN(t)	Y: LN(LN(1/(1-F(t))))
8.15	-2.66384
8.38	-1.72326
8.47	-1.20202
8.58	-0.82167
8.66	-0.50860
8.73	-0.23037
8.79	0.03293
8.87	0.29903
9.00	0.59398
9.10	0.99269



In same way, we can obtain the analysis result of data for 130 and 150 °C. Plot them on the Weibull chart.



B10 life for 120, 130 and 150 °C can be obtained from $L_{BX}^{\beta} = \left(\ln \frac{1}{1-x}\right) \cdot \eta^{\beta}$.

Temp, °C	B10 Life
120	3706
130	3355
150	2728



1/T	Ln(B10)
0.002544	8.217708
0.00248	8.118207
0.002363	7.911324

Because accelerated life testing is carried out for temperature, Arrhenius equation in Eq. (4.43) can be used to fit data in 30 °C. That is,

$$\ln(L) = \ln(A) + \frac{E_a}{k} \times \frac{1}{T} \quad \leftrightarrow \quad y = 3.8782 + 1707.4x \quad (\text{Fitting cue in Excel})$$

$$\ln(A) = 3.878204, \frac{E}{k} = 1707.392$$

$A = \exp(a) = 48.3373, E = 1707.392 \times (8.617 \times 10^{-5}) = 0.147126 \text{ eV}$.
So the estimated life-stress model from Eq. (4.42) is

$$TF = A \exp\left(\frac{E_a}{kT}\right) = 48.3373 \exp\left(\frac{1707.392}{T}\right)$$

So B10 life for 30 °C is obtained from

$$TF = 48.3373 \exp\left(\frac{1707.392}{30 + 273.16}\right) = 13,506.$$

Chapter 5

Structures (or Mechanisms) and Load Analysis



Abstract After mechanical products are designed, we can find the structure and their mechanism. In operation the mechanical/civil systems will work interactively and is subjected to (random) loads. This chapter will discuss how to analyze the loading characteristics of that is the root cause and dominant factor of the product failure. Product has their own particular structural loads in field. Mechanical engineer is designed to have the proper shape and material of mechanical structure with enough strength and stiffness. It therefore can withstand the effects—deformation, vibration, etc.—of system loads in its lifetime. If not, a typical pattern of repeated load or overloading may cause a small portion of structural failures suddenly in its lifetime. Rare possibility such as product failure should be assessed through parametric Accelerated Life Testing in the design phase whether final design of product is properly designed. As first step, there is a modeling of the dynamics systems that can be implemented by traditional method like Newtonian or bond-graph. The time response of mechanical system for (random) dynamic loads represents from its modeling. If simplified and counted as a sinusoidal input for mechanical (or civil) structure, the rain-flow counting method and miner's rule can enable engineer to assess the system damages—fracture and vibration—for dynamic loading. However, because there are a lot of assumptions for this analytic methodology, it is exact but complex to reproduce the product recalls due to the design failures. So we should develop the final solutions—experimental method like parametric ALT that will be discussed in Chaps. 8 and 9. Load analysis also will be helpful to figure out why the failure of problematic parts in mechanical engineering is revealed.

Keywords Structures • Mechanisms • Load analysis • Mathematical modeling • Bond-graph • Miner's rule • Rain-flow counting

5.1 Introduction

Static or dynamic loads in the product structures cause stresses, vibration, deformations, and displacements. As a result, repeated load or overloading may cause structural failure in mechanical system. Engineer assesses their effects by the structural modeling and its analysis using finite element for design.

There are two generic types of mechanical static or dynamic loading. Static loads—tension, twist or compression can exhibit motion or permanent change like dislocation if repeated in product lifetime. Eventually, they will be a permanent deformation, void, and the permanent failures. To withstand it, the mechanical structure is designed to have enough strength in product lifetime for static load. The examples of static loading are as following:

- Structural load and deflection versus material stress and strain
- Tension and compression loads
- Torsion and bending loads

A dynamic load, sometimes also referred to as probabilistic (or random) loads, is a force exerted by a moving body on a resisting member, usually in a relatively short period of time. Because such loads are usually unstable, we can say the dynamic load. Dynamic loads lead to motion like vibration, fatigue damage, cumulative damage, or fracture. Therefore, to withstand it, structure also is designed to have enough stiffness in product lifetime for dynamic loads. The examples of dynamic loading are as following:

- Impact, vibration and shock loads
- Unbalanced inertia loads

An impact load is one whose time of application on a material is less than one-third of the natural period of vibration of that material. Before we discuss the structure loading, we have to understand the basic structure in mechanical system.

5.2 Mechanical Structures (and Its Mechanisms)

As seen in Fig. 5.1, modern structures like building, bridge, and vehicle are a central part of life and depend on various mechanisms in mechanical products. They can be defined as an arrangement of parts joined together in a manner which provides strength in order to facilitate the carrying of loads. They come from thousand shapes and sizes in nature, with their own function. Therefore, these structures have inherent strength for loading. Mechanical products from internal combustion engines to helicopters and machine tools include a variety of mechanisms. Machines transform energy to do work. But only some mechanisms are capable of performing work. Many tools such as screwdrivers, wrenches, jacks, and hammers also contain mechanisms. Besides, the hands and feet, arms, legs, and jaws play an important role (mechanisms) in humans as do the paws and legs, flippers, wings, and tails of animals.

A mechanism is a system of moving parts that performs some function. In other words we can simplify learning about these various machines by realizing that every machine is made up of a variety of working parts. These working parts are called mechanisms. As seen in Fig. 5.2, we know that the bicycle is driven by a large driver gear wheel with pedals attached. As the back wheel turns, the bicycle



Fig. 5.1 Golden gate bridge (Wikipedia)

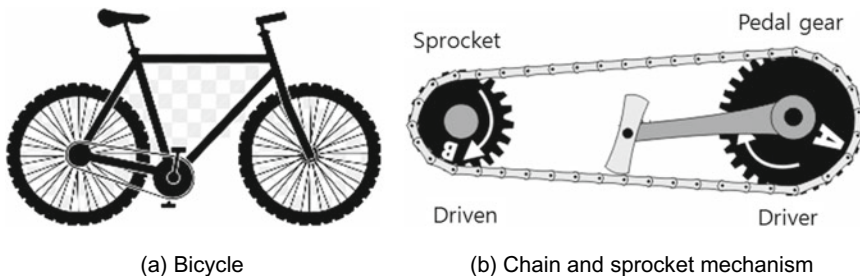


Fig. 5.2 Bicycle and its chain and sprocket mechanism

moves forwards. It is clearly constructed around a frame structure and mechanisms like the chain and sprocket. Gears driven by chains are used in machinery, motorcycles, in car engines and have many more applications (Fig. 5.2).

Structural Arches in Buildings

In everyday applications the arch is a central and defining feature of many famous building, such as the Colosseum in Rome. Arches also can be seen in fields and over rivers all over the countryside in the form of bridges. Builders use stone to form these arch shapes. These bridges have their origins in Ancient Rome and are, therefore, sometimes known as The Roman Arch Bridge. The main feature of this style of bridge structure is a keystone, as shown in Fig. 5.3.

Shell Structures in Design

As seen in Fig. 5.4, ‘Shell’ is a word used to give an account of the hard surface of eggs, tortoises, crustaceans, etc. Though having lightweight, a shell would protect and provide shelter from danger because of its hardness in a curved form. Shell structures of product are widely used in engineering. That is, masonry or stone

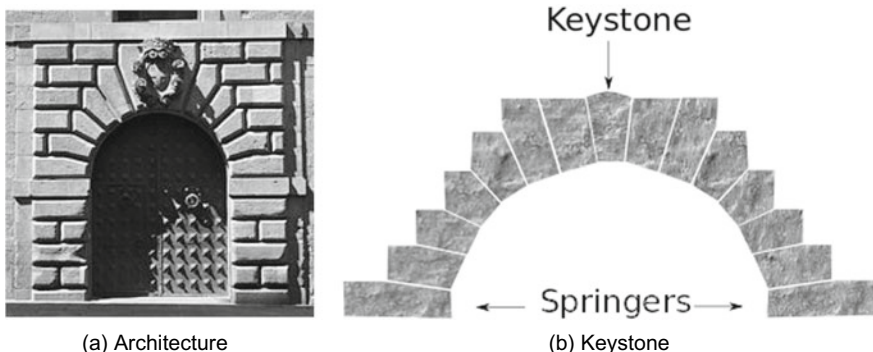


Fig. 5.3 Keystone in architecture (Wikipedia)

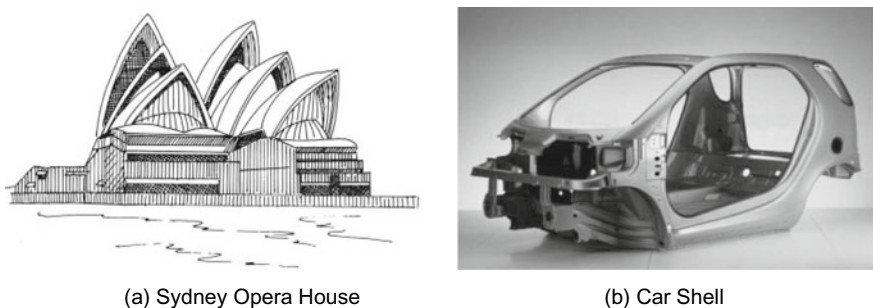


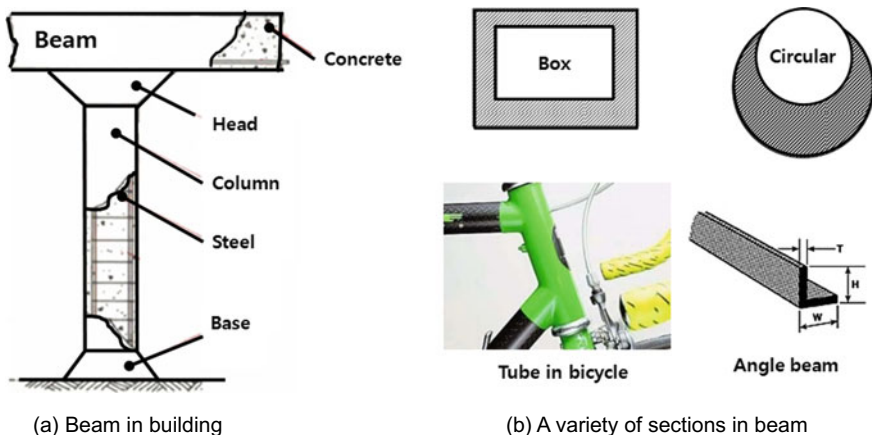
Fig. 5.4 Shell structures in design

domes or vaults in the middle Ages or modern have facilitated the construction of more spacious buildings.

Shell structures might be regarded as a set of beams, arches and catenaries because of carrying large point loads. Rather than the materials, the shape of a shell is the key to structure strength. For example, we can suggest the Sydney Opera House. Shell structures play a very important part in mechanical design.

Beams

As seen in Fig. 5.5, a beam in structure is a material section that can be used to span a distance and support a load. As used in conjunction with posts or columns, it can be used to reinforce structure strength and compose the upright element of the structure. A beam on both top and bottom constantly supports the forces of tension and compression. Because beams don't happen along the neutral axis, they are designed to be strongest along the top and bottom of beams. In saving material, some beams can be constructed in hollow sections. For example, to be lightweight and make cycling it easier, a bicycle reduces the amount of material used. Therefore a bicycle is often constructed using a circular section and makes it more appealing to the consumer. These circular or box sections are sometimes referred to as 'tube'.

**Fig. 5.5** Beams

Beams can be manufactured in many different shapes and sizes, and when fixed together, they can lend enormous strength to a structure (Fig. 5.5).

Frames

As used as the basis for the construction of many different artifacts, frames are structures made from sections of materials. They enclose spaces without filling them with solid material. To be rigid in frames, there is a member in a part of a complex structure. The point which the members meet or join is called a joint. Joints can be either fixed or pivoted. Pivoted joints are not very stable because the frame may lose its shape if a large force is applied to a corner. A fixed joint is much stronger and can resist larger forces than a pivot joint.

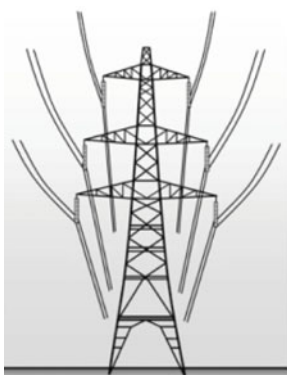
If adding a strut to create triangular shape, the triangle structure does not distort and becomes more stable and rigid structures. The term triangulation is used to describe the arrangement of triangles together in the formation of a frame. Square, rectangular and other frames can be made more rigid by bracing. In other words, bracing involves placing a diagonal piece or strut to create a triangle (Fig. 5.6).

Mechanical Advantage

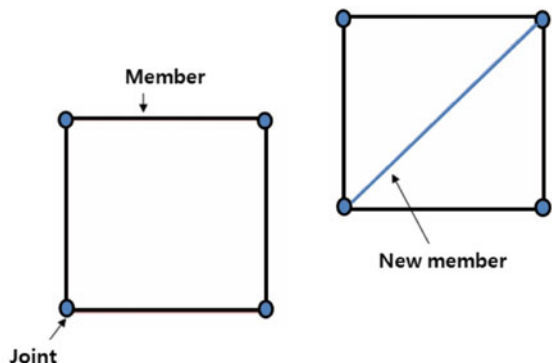
The image 5.7 shows a man using a stake to lift a rock. This is an example of a mechanism. As the man exerts a small amount of effort to the end of the lever, the rock is moved. This gain in effort is known as Mechanical Advantage (Fig. 5.7).

Linkages

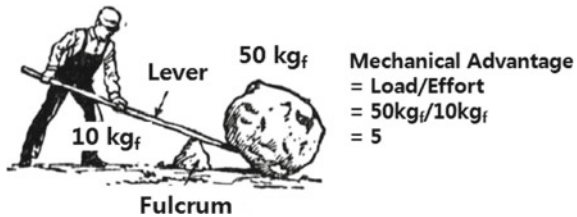
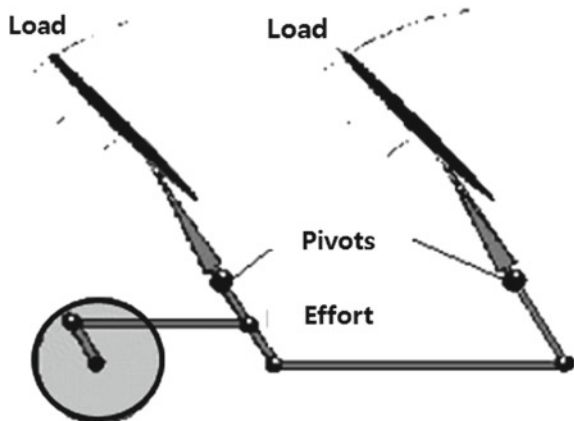
As seen in Fig. 5.8, a mechanical linkage is a mechanism made by connecting two or more levers together and is used to manage forces and movement. It makes two or more things move at the same time. A link body is moved using geometry so the link is considered to be rigid. Therefore, the joints between links might be providing pure rotation or sliding.



(a) Frame in a transmission tower



(b) A variety of sections in beam

Fig. 5.6 Frame and triangulation**Fig. 5.7** Man lifting a stone with a lever**Fig. 5.8** Windscreens wiper linkage (example)

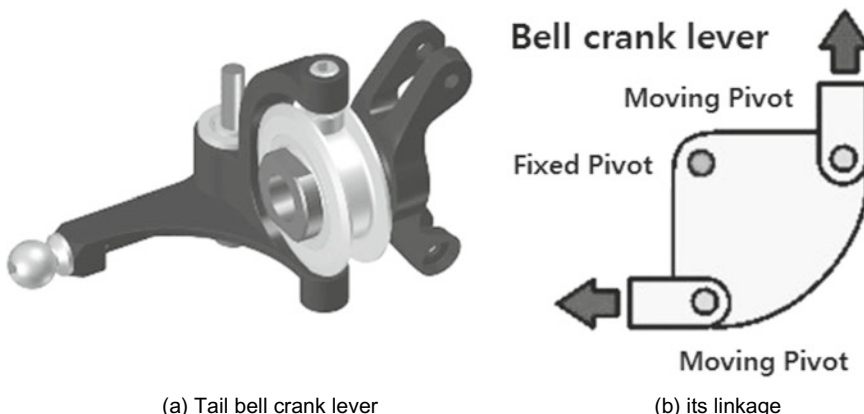


Fig. 5.9 Tail bell crank lever and its linkage

Bell Crank Levers

Bell Crank Levers are used when it is necessary to change the direction of movement or force through 90° . If the fulcrum is at an equal distance from the input and output, the movement of the output will be equal to the movement of the input. Otherwise, the movement will be different and the system will have Mechanical Advantage (Fig. 5.9).

Pulleys

A pulley wheel is a mechanism which helps lift objects. Like most wheels, pulley wheels spin or rotate on an axis. The centre of a pulley wheel has a groove that is nested in a rope, belt or cable. According to the number of pulley wheels and their positioning, there are three basic types of pulley: (1) a fixed pulley, (2) moveable pulley, (3) a block and tackle pulley (Fig. 5.10).

A fixed pulley does not rise or fall with the load being moved and changes the direction of the applied effort. On the other hands, a moveable pulley rises and falls with the load being moved. A block and tackle pulley consists of two or more pulleys (fixed and moveable). The block and tackle is capable both of changing the direction and creating a Mechanical Advantage.

The pulley is really a wheel and axle with a rope or chain attached. A pulley makes work seem easier because it changes the direction of motion to work with gravity. If a heavy load, like a bale of hay, needs to be lifted up to the second floor of a barn, you could tie a rope to the bale of hay, stand on the second floor, and pull it straight up. Or you could put a pulley at the second floor, stand at the first floor, and lift the bale of hay by pulling straight down. It would be the same amount of work in either case, but the action of pulling down feels easier because you're working with the force of gravity.

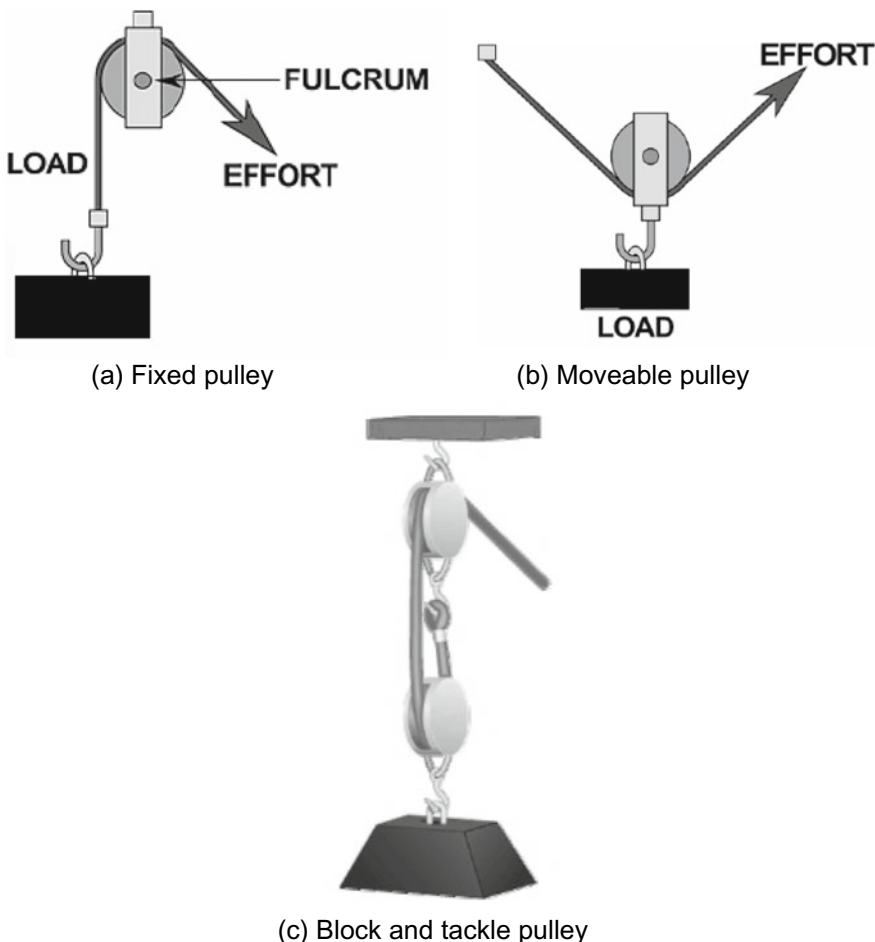


Fig. 5.10 Pulley and its linkage

Cam and Follower

The Cam and Follower is a device which can convert rotary motion (circular motion) into linear motion. A cam is a specially shaped piece of material, made of metal or hard-wearing plastic, which is fixed to a rotating shaft. There are several different types of cam, but most of these can be placed into two groups, namely rotary or linear. Many machines use cams. A car engine uses cams to open and close valves (Fig. 5.11).

Gears

The rotating force produced by an engine, windmill or other device, needs to be transferred or changed in order to do something useful. That's why gear is required in mechanical mechanism. As two meshed gears—driver gear and driven gear always rotate in opposite directions, the output force is yielded. A gear is a wheel

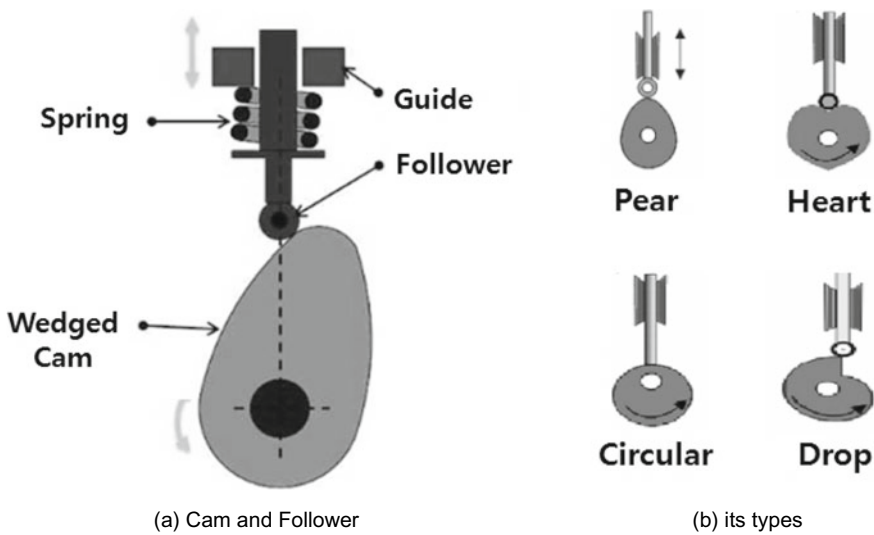


Fig. 5.11 Cam and Follower

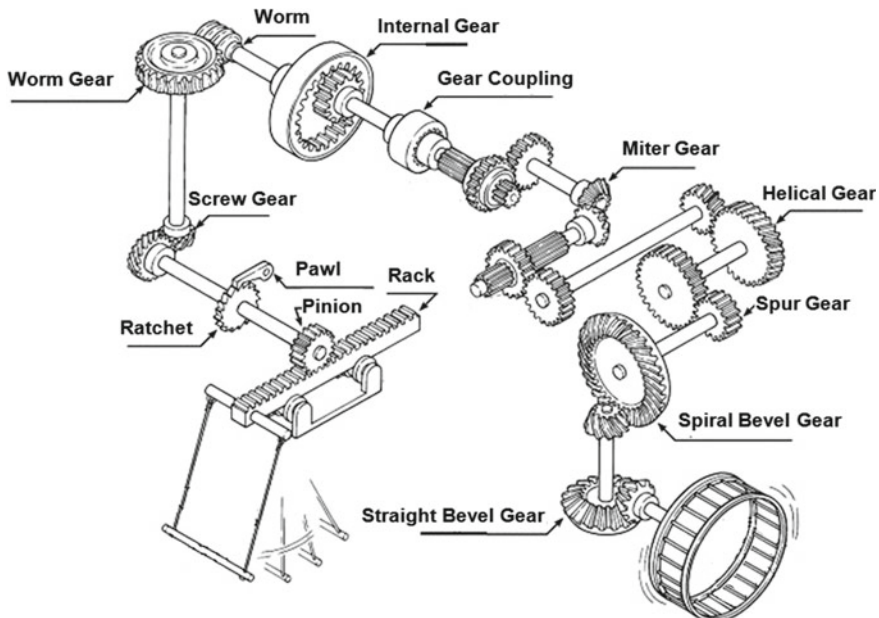


Fig. 5.12 Gear systems

with teeth on its outer edge. As gears rotate on a central axis, they transmit turning force to other gears. The teeth of one gear engage with the teeth of another. Gears can also change the amount of force, speed and direction of rotation (Fig. 5.12).

5.3 Modeling of Mechanical System

5.3.1 Introduction

A modeling of mechanical product is a mathematical representation of the dynamics structural systems to figure out their characteristics under the action of forces. Typical modeling methods commonly used in dynamic system are Newton, Lagrange, Hamiltonian mechanics, and D'Alembert's Law. As an output, models might describe the system behavior that can be represented in random variables (or state space). The state space is expressed as vectors (displacement, velocity, and acceleration). It also provides a convenient and compact way to analyze systems with multiple inputs and outputs.

When observed in most mechanical/civil components, field loads follows a random curve that load amplitudes change in time. For example, automobiles possess completely random stochastic load curves due to the street roughness, car speed, and environmental conditions. And for airplane, a mean load change like drag due to wind repetitively occurs on the wing of a transportation airplane when it takes off or lands. On the other hands, the load of the gas turbine blade in an airplane is to a large extent deterministic that there is no randomness in the system states, though the load sequence is still variable (Fig. 5.13).

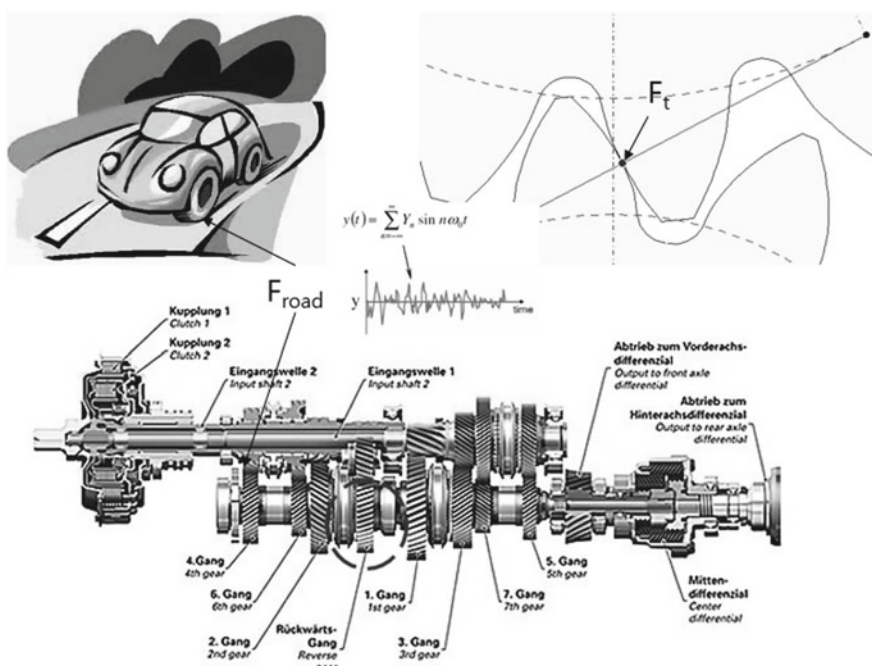
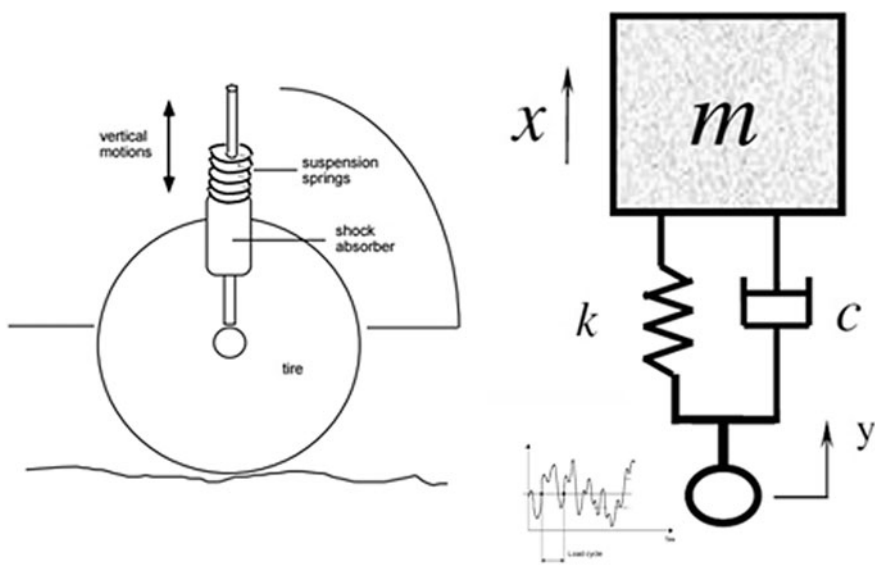
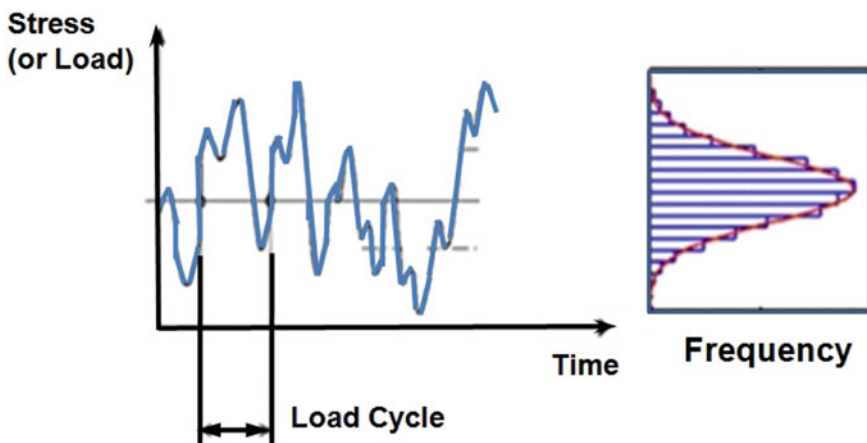


Fig. 5.13 Operational loads of mechanical parts subjected to the random vibration on off/on road

With simple algorithms and fast processors an on-line load measurement for parts can be directly measured during operation. However, a measurement during operation is quite time-consuming and actually impossible to understand the whole transmitted loads in product lifetime. To efficiently figure out the load history of product in time, the engineer depends on the mathematical modeling and its response analysis such as the Newtonian model that was developed for long time ago (Fig. 5.14).



(b) A simplified modeling of the automobiles

Fig. 5.14 Random loads and modeling of the automobiles by Newtonian modeling

5.3.2 Newton's Mechanics

Mechanics is a physical science which deals with the state of rest or motion of bodies under the action of forces. No one subject plays a greater role in engineering analysis than does mechanics. Therefore, the beginnings of engineering started from the study of mechanics. Modern research and development in the field of product reliability may be dependent upon the basic principles of mechanics including probability and statistical methods.

Mechanics is the oldest of the physical sciences. The earliest study was those of Archimedes (287–212 B.C.) which concerns the principle of the lever and the principle of buoyancy. The first investigation of a dynamic problem was credited to Galileo (1564–1642) in connection with his experiments with falling stones. The accurate formation of the laws of motion, as well as the law of gravitation, was made by Newton (1642–1727). Fundamental contributions to the development of mechanics were also made by D'Alembert, Lagrange, Laplace, and others.

The principles of mechanics as a science depend on the rigorous mathematics. On the other hand, the purpose of engineering mechanics is the application of its principles to the product design. The basic principle of mechanics are relatively few in number, but they have wide applications—vibrations, stability and strength of structures and machines, rocket and spacecraft design, automatic control, engine performance, and fluid flow.

Using just a few equations, scientists can describe the motion of a projectile flying through the air and the pull of a magnet, and forecast eclipses of the moon (see Fig. 5.15). The mathematical study of the motion is called Newtonian

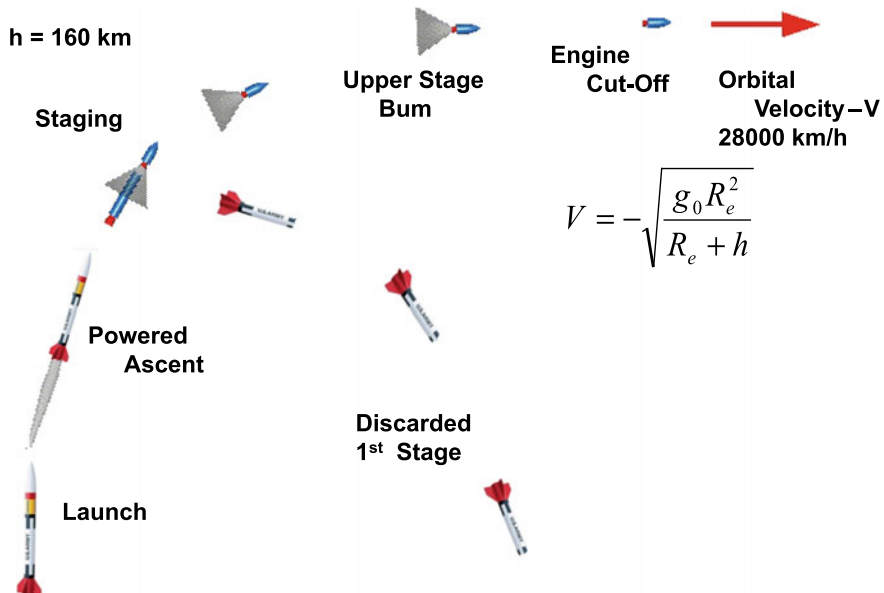


Fig. 5.15 Flight to orbit in projectile

mechanics because nearly the entire study builds on the work of Isaac Newton. Some mathematical laws and principles at the core of Newtonian mechanics include the following:

- Newton's First Law of Motion: In an inertial reference frame, an object either remains at rest or continues to move at a constant velocity, unless acted upon by a force.
- Newton's Second Law of Motion: The net force acting on an object is equal to the mass of that object times its acceleration.

$$F = \frac{dp}{dt} = \frac{d(mv)}{dt} \quad (5.1)$$

- Newton's Third Law of Motion: For every action, there is an equal and opposite reaction. That is, when one body exerts a force on a second body, the second body simultaneously exerts a force equal in magnitude and opposite in direction on the first body.

5.3.3 D'Alembert's Modeling for Automobile

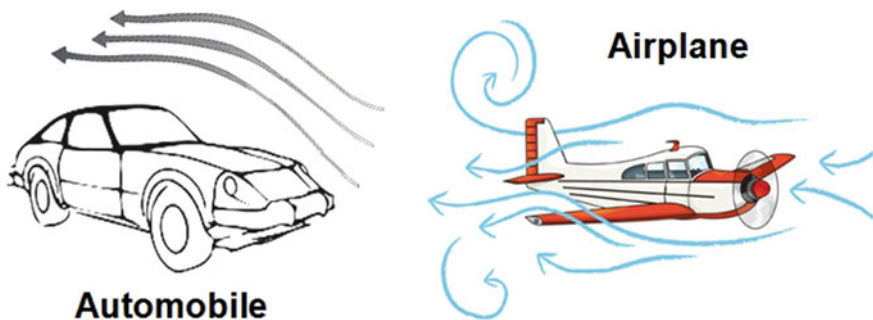
Engineer uses D'Alembert's principle and free body diagram to model mechanical system. If there is an automobile in transportation, we can model a simple system with a mass that is separated from a wall by a spring and a dashpot. The mass could represent an automobile, with the spring and dashpot representing the automobile's bumper. If only horizontal motion and forces like wind are considered, it is represented in Fig. 5.16.

The free body diagram is a drawing method showing all external forces acting on a body. There is only one position in this system defined by the variable "x" that is positive to the right. It is assumed that $x = 0$ when the spring is in its relaxed state. As seen in Fig. 5.17, there are four forces to develop a model from the free body diagram: (1) An external force (F_e) such as friction force and air resistance force, (2) A spring force that will be a force from the spring, $k \cdot x$, to the left, (3) A dashpot force that will be a force from the dashpot, $b \cdot v$, to the left, (4) Finally, there is the inertial force which is defined to be opposed to the defined direction of motion. This is represented by $m \cdot a$ to the left.

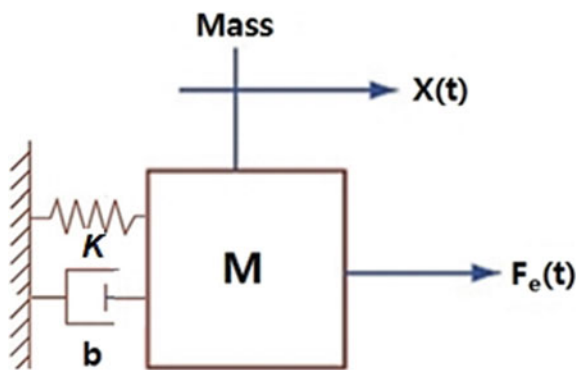
Newton's second law states that an object accelerates in the direction of an applied force, and that this acceleration is inversely proportional to the force, or

$$\sum_{\text{all external}} F = m \cdot a \quad (5.2)$$

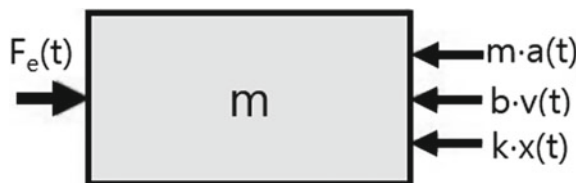
Subtracting the right-hand side results in D'Alembert's principle,



(a) Typical automobile and airplane subjected to wind flow



(b) Mass-spring-dashpot system

Fig. 5.16 Typical mechanical automobile modeling**Fig. 5.17** Completed free body diagram for automobile modeling

$$\sum_{\text{all } \text{external}} F - m \cdot a = 0 \quad (5.3)$$

If we consider the $m \cdot a$ term to be inertia force (or D'Alembert's force), D'Alembert's law will be left

$$\sum_{all} F \cdot \delta r = 0 \quad (5.4)$$

To visualize this consider pushing against a mass (in the absence of friction) with your hand in the positive direction. Your hand experiences a force in the direction opposite to that of the direction of the force (this is the $-m \cdot a$ term). The inertial force is always in a direction opposite to the defined positive direction. We sum all of these forces to zero and get

$$F_e(t) - ma(t) - bv(t) - k \cdot x(t) = 0 \quad (5.5)$$

In other words, we can change

$$m \frac{d^2x}{dt^2} + b \frac{dx}{dt} + kx(t) = F_e(t) \quad (5.6)$$

5.4 Bond Graph Modeling

5.4.1 Introduction

Bond Graph is an explicit graphical tool for modeling multidisciplinary dynamic systems including components from different engineering areas—the mechanical/civil, the electrical, the thermal, and the hydraulic system. When designing a new dynamic system, it is a good method to utilize a graphical representation for communicating other engineers to express the dynamic modeling. In engineering disciplines, linear graphs have long traditions among several graphical representation means.

In 1959 Bond Graph method was developed by Professor Henry Payner and his former students at MIT, who gave the revolutionary idea of portraying systems in terms of power bonds, connecting the elements of the physical system to the so called junction structures which were manifestations of the constraints. This power exchange portray of a system is called bond graph.

In 1961 the Paynter's books were published as entitled "Analysis and Simulation of Simulation of Multiport Systems." In 2006, the three authors have published the fourth edition entitled as "System Dynamics—Modeling and Simulation of Mechatronic Systems". Now several disciplines of Bond Graph have been widely accepted in the world as a modeling methodology. There are many literatures about Bond Graph method and its applications to analyze dynamic systems. In a result this method will give a brief description for analyzing loads applied to structure and understanding its work (Figs. 5.18 and 5.19).

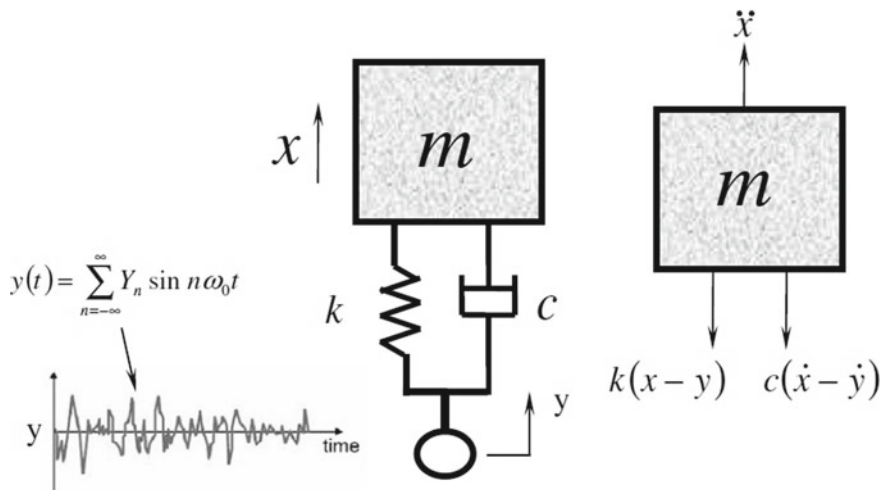


Fig. 5.18 Typical modeling of the automobiles subjected to repetitive random vibrations

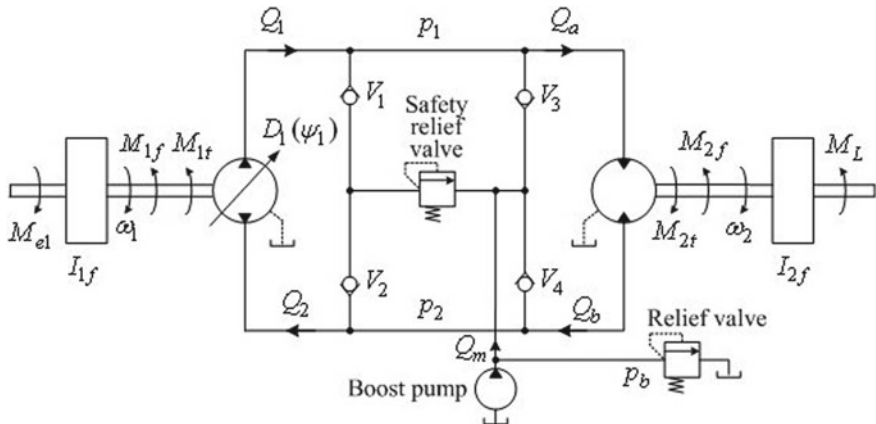


Fig. 5.19 Typical hydrostatic transmission modeling

5.4.2 Basic Elements, Energy Relations, and Causality of Bond Graph

A Bond Graph is a graphical representation of a physical dynamic system. It is similar to the better known block diagram and signal-flow graph. While the symbols in Bond Graph represent bi-directional exchange of physical energy, those in block diagrams and signal-flow graphs represent uni-directional flow of information. Bond Graph also can be applicable in multi-energy domain—mechanical/civil, electrical, and hydraulic system.

The dynamic systems analysis is relatively simple when the steady state behavior or the few degrees of freedom has. In most of the cases, the main concern of engineers is to establish the mathematical model that represents the dynamic behavior of the system and how the different parameters influence the system behavior, because the system dynamic equations are usually partial differential equations, whose solutions require deep mathematical knowledge.

As the fundamental bases of the Bond Graph theory, energy flow is a basic element in a system. It flows in from one or more sources, is temporarily stored in system components or partially dissipated in resistances as heat, and finally arrives at “loads” where it produces some desired effects. Power is the rate of energy flow without direction.

Bond Graph represents this power flow between two systems. This flow is symbolized through an arrow (Bond) as Fig. 5.20 illustrated. Each bond represents the instantaneous energy flow or power. The flow in each bond is denoted by a pair of variables called ‘power variables’ whose product is the instantaneous power of the bond. Because power is not easy to measure directly, engineers can be represented as two temporary variables—flow and effort. Every domain has a pair of effort and flow variable. For example in mechanical system, flow represents the “velocity” and effort the “force”, in electrical system, flow represents the “current” and effort the “voltage”. The product of both temporary variables—power is represented as:

$$P = e(t) \cdot f(t) \quad (5.7)$$

The method makes possible the simulation of multiple physical domains, such as mechanical, electrical, thermal, hydraulic, etc. Flows and efforts should be identified with a particular variable for each specific physical domain which is working. Table 5.1 also shows the physical meanings of the variables in different domains.

The Bond Graph is composed of the “bonds” which link together “1-port”, “2-port” and “3-port” elements. Whether power in bond graph is continuous or not, every element is represented by a multi-port. Ports are connected by bonds. The basic blocs of standard bond graph theory are listed in Table 5.2.

For 1-ports there are effort sources, flow sources, C-type elements, I-type elements, and R-type elements that can connect power discontinuously. For 2-ports, there are Transformer and Gyrator that can connect power continuously. For 3-ports, there are 0-junction and 1-junction that can make up the network.

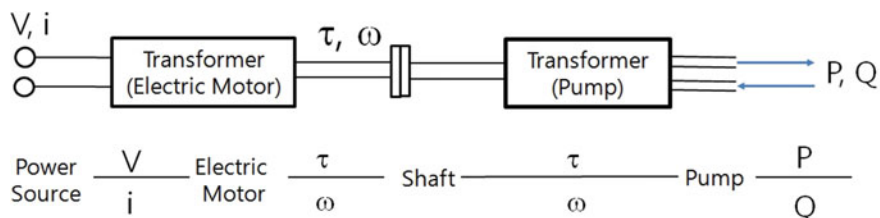


Fig. 5.20 Power flow in Bond Graph for electric-hydraulic system

Table 5.1 Energy flow in the multi-port physical system

Modules	Effort, $e(t)$	Flow, $f(t)$
Mechanical translation	Force, $F(t)$	Velocity, $V(t)$
Mechanical rotation	Torque, $\tau(t)$	Angular velocity, $\omega(t)$
Compressor, pump	Pressure difference, $\Delta P(t)$	Volume flow rate, $Q(t)$
Electric	Voltage, $V(t)$	Current, $i(t)$
Thermal	Temperature, T	Entropy change rate, ds/dt
Chemical	Chemical potential, μ	Mole flow rate, dN/dt
Magnetic	Magneto-motive force, e_m	Magnetic flux, φ

Table 5.2 Basic elements of Bond Graph

Elements	Symbol	Relation equations
1-port elements (sources)	S_e ———	$S_e = e(t)$
	S_f ———	$S_f = f(t)$
1-port elements	C-type elements	$\frac{de(t)}{dt} = \frac{1}{C}f(t)$
	I-type elements	$\frac{df(t)}{dt} = \frac{1}{I}e(t)$
	R-type elements	$e(t) = R \cdot f(t)$
2-port elements	Transformer	$\begin{array}{ c c c } \hline 1 & \text{TF} & 2 \\ \hline \end{array}$ $e_2(t) = TF \cdot e_1(t)$ $f_2(t) = \frac{1}{TF} \cdot f_1(t)$
	Gyrator	$\begin{array}{ c c c } \hline 1 & \text{GY} & 2 \\ \hline \end{array}$ $e_2(t) = GY \cdot f_1(t)$ $f_2(t) = \frac{1}{GY} \cdot e_1(t)$
3-port junction elements	0-junction	$\begin{array}{ c c c } \hline 1 & 0 & 2 \\ \hline \end{array}$ $e_2(t) = e_1(t)$
	1-junction	$\begin{array}{ c c c } \hline 1 & 1 & 2 \\ \hline \end{array}$ $f_2(t) = f_1(t)$

Power bonds may join at one of two kinds of junctions: a “0” junction and a “1” junction. In a “0” junction, the flow and the efforts satisfy Eqs. (5.8–5.9):

$$\sum \text{flow}_{\text{input}} = \sum \text{flow}_{\text{output}} \quad (5.8)$$

$$\text{effort}_1 = \text{effort}_2 = \dots = \text{effort}_n \quad (5.9)$$

This corresponds to a node in an electrical circuit (where Kirchhoff’s current law applies). In a “1” junction, the flow and the efforts satisfy Eqs. (5.10–5.11):

$$\sum \text{effort}_{\text{input}} = \sum \text{effort}_{\text{output}} \quad (5.10)$$

$$\text{flow}_1 = \text{flow}_2 = \dots = \text{flow}_n \quad (5.11)$$

This corresponds to force balance at a mass in a system. An example of a “1” junction is a resistor in series. In junction, the premise of energy conservation is assumed, no lost is allowed. There are two additional variables, important in the description of dynamic systems.

For any element with a bond with power variables—*effort* and *flow*, the energy variation from t_0 to t can be expressed by:

$$H(t) - H(t_0) = \int_{t_0}^t e(\tau)f(\tau)d\tau \quad (5.12)$$

For C-type elements, e (effort) is a function of q (displacement). If displacement is differentiated, flow is obtained as

$$q(t) = \int f(t)dt \Rightarrow \frac{dq}{dt} = f(t) \quad (5.13)$$

If Eq. (5.13) is changing variables from t to q , the linear case can be expressed as:

$$H(q) - H(q_0) = \frac{1}{2C}(q^2 - q_0^2) \quad (5.14)$$

For I-type elements, f (flow) is a function of p (momentum). If momentum is differentiated, effort is obtained as

$$p(t) = \int e(t)dt \Rightarrow \frac{dp}{dt} = e(t) \quad (5.15)$$

If Eq. (5.12) is changing variables from t to p , the linear case can be expressed as:

$$H(p) - H(p_0) = \frac{1}{2I}(p^2 - p_0^2) \quad (5.16)$$

Resistor elements represent situations where energy dissipates—electrical resistor, mechanical damper, and coulomb frictions. In these sorts of elements there is a relationship between flow and effort as Eq. (5.16) shows. The value of “ R ” can be constant or function of any system parameter including time.

$$e(t) = R \cdot f(t) \quad (5.17)$$

Compliance elements represent the situations where energy stores—electrical capacitors, mechanical springs, etc. In these sorts of elements there is a relationship between effort and displacement variable as Eq. (5.17) shows. The value of “ K ” can be constant or function of any system parameter including time.

$$e(t) = K \cdot q(t) \quad (5.18)$$

Inertia elements represent the relationship between the “flow” and Momentum (electrical coil, mass, moment of inertia, etc.) as Eq. (5.19) shows. The value of “I” tends to be constant

$$p(t) = I \cdot f(t) \quad (5.19)$$

A transformer adds no power but transforms it, such as an electrical transformer or a lever. Transformers represent those physical phenomena that are variation of the values of output flow and effort on the values of input flow and effort. If the transformation ratio is given by the “TF” value, then the relationship between input and output is shown in Eqs. (5.20–5.21).

$$e_{output}(t) = TF \cdot e_{input}(t) \quad (5.20)$$

$$f_{output}(t) = \frac{1}{TF} \cdot f_{input}(t) \quad (5.21)$$

One is the “half-arrow” sign convention. This defines the assumed direction of positive energy flow. As with electrical circuit diagrams and free-body diagrams, the choice of positive direction is arbitrary, with the caveat that the analyst must be consistent throughout with the chosen definition. The other feature is the “causal stroke”. This is a vertical bar placed on only one end of the bond. It is not arbitrary (Fig. 5.21).

On each Bond, one of the variables must be the cause and the other one the effect. This can be deduced by the relationship indicated by the arrow direction. Effort and flow causalities always act in opposite directions in a Bond. The causality assignment procedure chooses who sets what for each bond. Causality assignment is necessary to transform the bond graph into computable code.

Any port (single, double or multi) attached to the bond shall specify either “effort” or “flow” by its causal stroke, but not both. The port attached to the end of the bond with the “causal stroke” specifies the “flow” of the bond. And the bond imposes “effort” upon that port. Equivalently, the port on the end without the “causal stroke” imposes “effort” to the bond, while the bond imposes “flow” to that port.

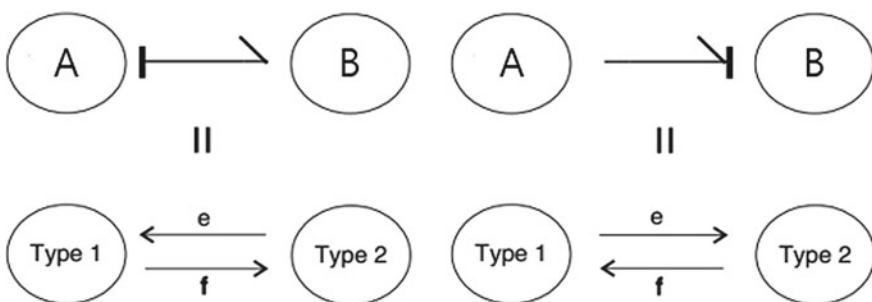


Fig. 5.21 “Half-arrow” sign convention and meaning of the causal stroke

Once the system is represented in the form of bond-graph, the state equations that govern its behavior can be obtained directly as a first order differential equations in terms of generalized variables defined above, using simple and standardized procedures, regardless of the physical domain to which it belongs, even when interrelated across domains.

5.4.3 Case Study: Hydrostatic Transmission (HST) in Sea-Borne Winch

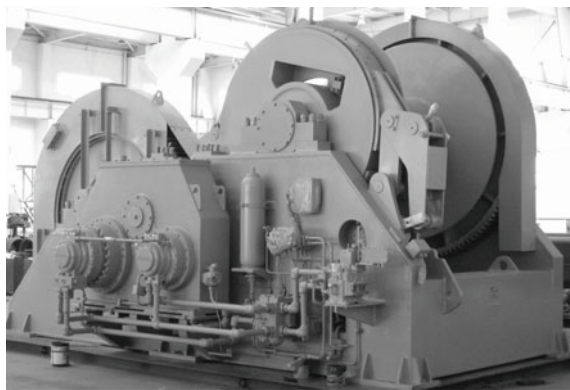
The winch structure is designed for launching, owing, and handling the cable and array in ship. The operation conditions of sea-borne winch can be varied such as operation conditions—sea state, ship speed, and towing cable length. Because its operation requires high tension, sea-borne winch is commonly used by the hydrostatic transmission (HST). It consists of electric motor, pump, piping, hydraulic motor, and loads. Tension and the response characteristics under the states of launching, towing, and hauling should be known before the design of HST. Tension data can be obtained from tension experiment. However, as an experiment, obtained the exact time response characteristics has many difficulties. And many previous design methods for HST involve extensive calculations because energy type of HST changes from mechanical to hydraulic, and then mechanical system. Bond Graph can easily model HST system and the dynamic response (Fig. 5.22).

HST as shown in Fig. 5.23 is commonly divided into electric motor, hydraulic pump, piping system, safety switches, and hydraulic motor. A rotating electric motor operates a hydraulic pump, which supplies oil to pipe system.

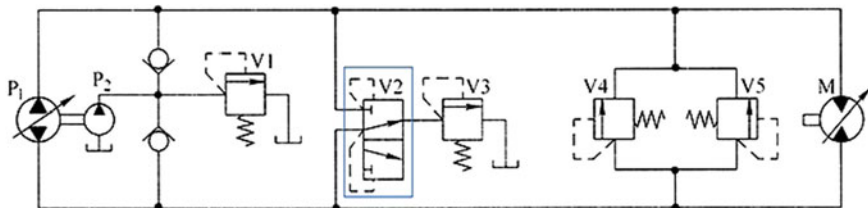
As cylinders in a hydraulic motor are filled with oil, shat rotates load. Therefore, HST is a kind of the closed-loop power transmission. The effort and flow in the rotating mechanical/civil system are torque and angular velocity, respectively. If two elements are integrated, they became momentum and volume. No matter what systems in HST may be, power does not change.

Bond Graph of electric motor and hydraulic pump is shown in Fig. 5.24. Source flow SF_{11} indicates an electric motor with constant angular velocity. It is assumed that a 10% among total torque perishes out by resistance element R_{12} . Transducer element MTF_{11} represents the capacity of a variable piston pump which can control capacity with swivel angle α_o .

A bulk modulus B with implies oil compressibility chooses 10,000 bar among 6000–12,000 bar. Fluid condensers $C_{23} = C_{21}$ are described as V/B. Fluid inertia I_{24} represents oil mass. Using the least square method, resistance R_{22} and R_{26} are calculated from the pump and motor leakage. Because pipe flow is laminar, fluid resistance R_{25} can be calculated. Motor capacity TF_{3128} is determined from the number of filling cylinders. Moment of inertia of drum and flange I_{33} can be calculated. It is assumed that torque loss of flange R32 is about 10%. When Bond Graph is drawn from top and bottom—starting with the electric motor and ending with the load, a total Bond Graph and derivation of the state equations of a HST is represented as:



(a) Winch system driven by hydraulic circuits



(b) Hydrostatic transmission

Fig. 5.22 Hydraulic-driven winch system in ship-borne

To obtain non-dimensional state equations, non-dimensional variables are introduced as

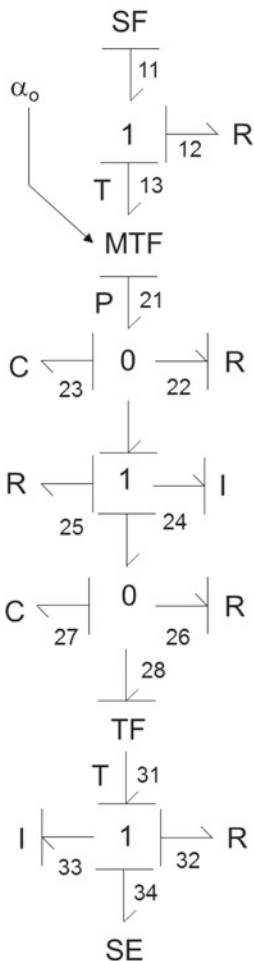
$$\tilde{p} = \frac{P}{I\bar{Q} \text{ or } \omega}, \quad \tilde{q} = \frac{Q}{C\bar{P}}, \quad \tilde{t} = \frac{t}{\omega_n^{-1}} = \frac{1}{\sqrt{IC}} \quad (5.22)$$

$$\frac{dQ}{dt} = \frac{d(C\bar{P}\tilde{q})}{dt} = \frac{d(C\bar{P}\tilde{q})}{d\tilde{t}} \frac{d\tilde{t}}{dt} = C\bar{P}\omega_n \dot{\tilde{q}} \quad (5.23)$$

$$\frac{dP}{dt} = \frac{d(I\bar{Q}\tilde{p})}{dt} = \frac{d(I\bar{Q}\tilde{p})}{d\tilde{t}} \frac{d\tilde{t}}{dt} = I\bar{Q}\omega_n \dot{\tilde{p}} \quad (5.24)$$

where P , Q and t are dimensional integral of pressure, volume and time \tilde{p} , \tilde{q} and \tilde{t} are non-dimensional integral of pressure, volume and time, respectively. Therefore, non-dimensional state equations are derived as:

$$\frac{C_{23}\omega_n \bar{P}}{SF_{11}MTF_{2113}} \dot{\tilde{q}}_{23} + \frac{\bar{P}}{R_{23}SF_{11}MTF_{2113}} \tilde{q}_{23} + \frac{\bar{Q}}{SF_{11}MTF_{2113}} \tilde{p}_{24} = 1 \quad (5.25)$$



$F_{11} = SF_{11}$	$E_{34} = SE_{34}$
$E_{11} = E_{12} + E_{13}$	$F_{12} = F_{11}$
$F_{13} = F_{11}$	$E_{13} = E_{21} * MTF_{1321}$
$F_{21} = F_{13} * MTF_{1321}$	$F_{23} = F_{21} - F_{22} - F_{24}$
$E_{22} = E_{23}$	$E_{21} = E_{23}$
$E_{24} = E_{23} - E_{25} - E_{27}$	$F_{25} = F_{24}$
$E_{26} = E_{27}$	$F_{27} = F_{24} - F_{26} - F_{25}$
$E_{28} = E_{27}$	$E_{31} = E_{28} * TF_{3128}$
$F_{28} = F_{31} * TF_{3128}$	$F_{33} = F_{31} - F_{32} - F_{34}$
$F_{31} = F_{33}$	$F_{32} = F_{33}$
$F_{34} = F_{33}$	$E_{12} = F_{12} * R_{12}$
$\frac{dQ_{23}}{dt} = F_{23}$	$E_{23} = Q_{23}/C_{23}$
$F_{22} = E_{22}/R_{22}$	$E_{25} = F_{25} * R_{25}$
$\frac{dP_{24}}{dt} = E_{24}$	$F_{24} = P_{24}/I_{24}$
$\frac{dQ_{27}}{dt} = F_{27}$	$E_{27} = Q_{27}/C_{27}$
$\frac{dP_{33}}{dt} = E_{33}$	$F_{26} = E_{26}/R_{26}$
$E_{32} = F_{32} * R_{22}$	$F_{33} = P_{33}/I_{33}$

Fig. 5.23 Bond Graph and derivation of the state equations of the hydrostatic transmission in sea-borne winch

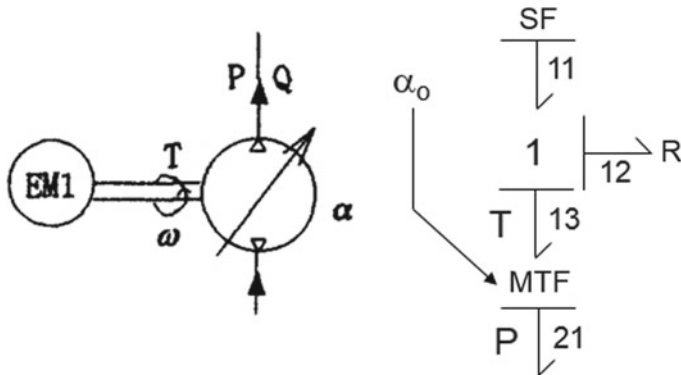


Fig. 5.24 Electric motor and hydraulic pump modeling

$$\frac{I_{24}\omega_n}{R_{25}}\dot{\tilde{p}}_{24} - \frac{\bar{P}}{R_{25}\bar{Q}}\tilde{q}_{23} + \tilde{p}_{24} + \frac{\bar{P}}{R_{25}\bar{Q}}\tilde{q}_{27} = 0 \quad (5.26)$$

$$C_{27}\omega_n R_{26}\dot{\tilde{q}}_{27} - \frac{\bar{Q}R_{26}}{\bar{P}}\tilde{p}_{24} + \tilde{q}_{27} + \frac{\omega T F_{3128} R_{26}}{\bar{P}}\tilde{p}_{33} = 0 \quad (5.27)$$

$$\frac{I_{33}\omega\omega_n}{SE_{34}}\dot{\tilde{p}}_{33} - \frac{\bar{P}TF_{3128}}{SE_{34}}\tilde{q}_{27} + \frac{R_{32}\omega}{SE_{34}}\tilde{p}_{33} = 0 \quad (5.28)$$

To investigate the dynamic stability of the system, simple asymptotic approach can be used and perturbations around stable points are expressed as:

$$\tilde{q}_{23} = \tilde{q}_{230} + \varepsilon^1 \tilde{q}_{231} + O(\varepsilon^2) \quad (5.29)$$

$$\tilde{p}_{24} = \tilde{p}_{240} + \varepsilon^1 \tilde{p}_{241} + O(\varepsilon^2) \quad (5.30)$$

$$\tilde{q}_{27} = \tilde{q}_{270} + \varepsilon^1 \tilde{q}_{271} + O(\varepsilon^2) \quad (5.31)$$

$$\tilde{p}_{33} = \tilde{p}_{330} + \varepsilon^1 \tilde{p}_{331} + O(\varepsilon^2) \quad (5.32)$$

where ε^1 is very small value.

Substitute Eqs. (5.25–5.28) into (5.29–5.32), then the terms of ε^0 is yield

$$\frac{\bar{P}}{R_{22}SF_{11}MTF_{2113}}(\tilde{q}_{230}) + \frac{\bar{Q}}{SF_{11}MTF_{2113}}\tilde{p}_{240} = 1 \quad (5.33)$$

$$-\frac{\bar{P}}{R_{25}\bar{Q}}\tilde{q}_{230} + \tilde{p}_{240} + \frac{\bar{P}}{R_{25}\bar{Q}}\tilde{q}_{270} = 0 \quad (5.34)$$

$$-\frac{\bar{Q}R_{26}}{\bar{P}}\tilde{p}_{240} + \tilde{q}_{270} + \frac{\omega TF_{3128}R_{26}}{\bar{P}}\tilde{p}_{330} = 0 \quad (5.35)$$

$$-\frac{\bar{P}TF_{3128}}{SE_{34}}\tilde{q}_{270} + \frac{R_{32}\omega}{SE_{34}}\tilde{p}_{330} = -1 \quad (5.36)$$

And then the terms of ε^1 is yield

$$\frac{C_{23}\omega_n\bar{P}}{SF_{11}MTF_{2113}}\dot{\tilde{q}}_{231} + \frac{\bar{P}}{R_{23}SF_{11}MTF_{2113}}\tilde{q}_{231} + \frac{\bar{Q}}{SF_{11}MTF_{2113}}\tilde{p}_{241} = 0 \quad (5.37)$$

$$\frac{I_{24}\omega_n}{R_{25}}\dot{\tilde{p}}_{241} - \frac{\bar{P}}{R_{25}\bar{Q}}\tilde{q}_{231} + \tilde{p}_{241} + \frac{\bar{P}}{R_{25}\bar{Q}}\tilde{q}_{271} = 0 \quad (5.38)$$

$$C_{27}\omega_nR_{26}\dot{\tilde{q}}_{271} - \frac{\bar{Q}R_{26}}{\bar{P}}\tilde{p}_{241} + \tilde{q}_{271} + \frac{\omega TF_{3128}R_{26}}{\bar{P}}\tilde{p}_{331} = 0 \quad (5.39)$$

$$\frac{I_{33}\omega\omega_n}{SE_{34}}\dot{\tilde{p}}_{331} - \frac{\bar{P}TF_{3128}}{SE_{34}}\tilde{q}_{271} + \frac{R_{32}\omega}{SE_{34}}\tilde{p}_{331} = 0 \quad (5.40)$$

If the perturbed Eqs. (5.37–5.40) are expressed as state space form $[dx/dt] = [A][X]$, then

$$\begin{bmatrix} \dot{\tilde{q}}_{231} \\ \dot{\tilde{p}}_{241} \\ \dot{\tilde{q}}_{271} \\ \dot{\tilde{p}}_{331} \end{bmatrix} = \begin{bmatrix} -\frac{1}{R_{22}C_{23}\omega_n} & -\frac{\bar{Q}}{C_{23}\omega_n\bar{P}} & 0 & 0 \\ \frac{-\bar{P}}{\bar{Q}I_{24}\omega_n} & -\frac{R_{25}}{I_{24}\omega_n} & -\frac{\bar{P}}{\bar{Q}\omega_n I_{24}} & 0 \\ 0 & \frac{1}{\bar{P}C_{27}\omega_n} & -\frac{1}{C_{27}\omega_n R_{26}} & -\frac{\omega TF_{3128}}{\bar{P}C_{27}\omega_n} \\ 0 & 0 & \frac{-\bar{P}TF_{3128}}{I_{33}\omega\omega_n} & -\frac{R_{32}}{I_{33}\omega\omega_n} \end{bmatrix} \begin{bmatrix} \tilde{q}_{231} \\ \tilde{p}_{241} \\ \tilde{q}_{271} \\ \tilde{p}_{331} \end{bmatrix} \quad (5.41)$$

To investigate the dynamic stability of the non-dimensional state Eq. (5.41), eigen-value of the Bond Graph can be represented as a state equation form $|A - \lambda I||X| = 0$. The system is unstable if eigen-value is $\lambda > 0$ and the system is stable $\lambda < 0$. When the state equations are represented as state space form of

$$\begin{bmatrix} \frac{dQ_{23}}{dt} \\ \frac{dP_{24}}{dt} \\ \frac{dQ_{27}}{dt} \\ \frac{dP_{33}}{dt} \end{bmatrix} = \begin{bmatrix} -\frac{1}{C_{23}R_{22}} & -\frac{1}{I_{24}} & 0 & 0 \\ \frac{1}{C_{23}} & -\frac{R_{25}}{I_{24}} & -\frac{1}{C_{27}} & 0 \\ 0 & \frac{1}{I_{24}} & -\frac{1}{C_{27}R_{26}} & -\frac{TF_{3128}}{I_{33}} \\ 0 & 0 & \frac{TF_{3128}}{C_{27}} & -\frac{R_{32}}{I_{33}} \end{bmatrix} \begin{bmatrix} Q_{23} \\ P_{24} \\ Q_{27} \\ P_{33} \end{bmatrix} + \begin{bmatrix} MTF_{2113} \\ 0 \\ 0 \\ 0 \end{bmatrix} [SF_{11}] + \begin{bmatrix} 0 \\ 0 \\ 0 \\ -1 \end{bmatrix} [SE_{34}] \quad (5.42)$$

When Eq. (5.42) is integrated, the pump pressure and motor pressure are obtained as

$$\begin{bmatrix} \bar{P}_{\text{pump}} \\ \bar{P}_{\text{motor}} \end{bmatrix} = \begin{bmatrix} 1/C_{23} & 0 \\ 0 & 1/C_{27} \end{bmatrix} \begin{bmatrix} Q_{23} \\ Q_{27} \end{bmatrix} \quad (5.43)$$

HST simulations are classified as models of low speed, high, and maximum tension. The tension values might be obtained by the drag force analysis of cable. A steady solution of ε^0 equation and eigen-values from high speed, low speed, and maximum tension are calculated as stable. The values of (a) perturbed state Q_{23} (b) perturbed state P_{24} (c) perturbed state Q_{27} (d) perturbed state P_{33} from high speed mode are shown in Fig. 5.25. State variables are converged after they perturbed around steady state value ε^0 . It can figure out that simulations results with a big overshoot reach a steady state value (Fig. 5.26).

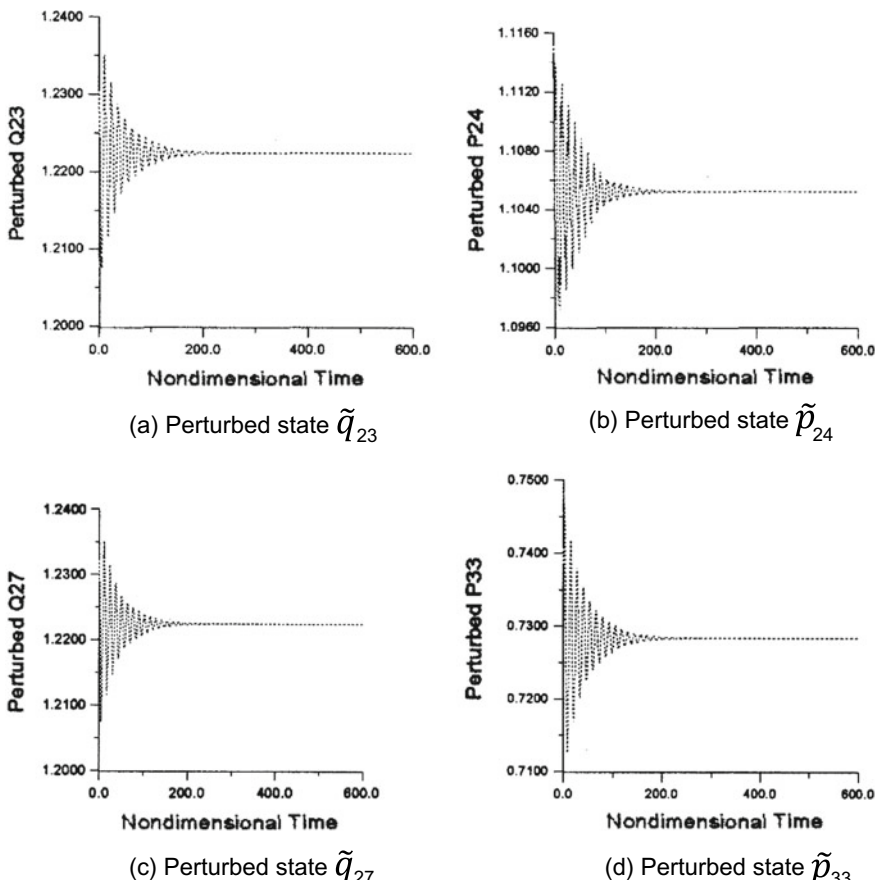


Fig. 5.25 Perturbed state $\tilde{q}_{23}, \tilde{p}_{24}, \tilde{q}_{27}$ and \tilde{p}_{33}

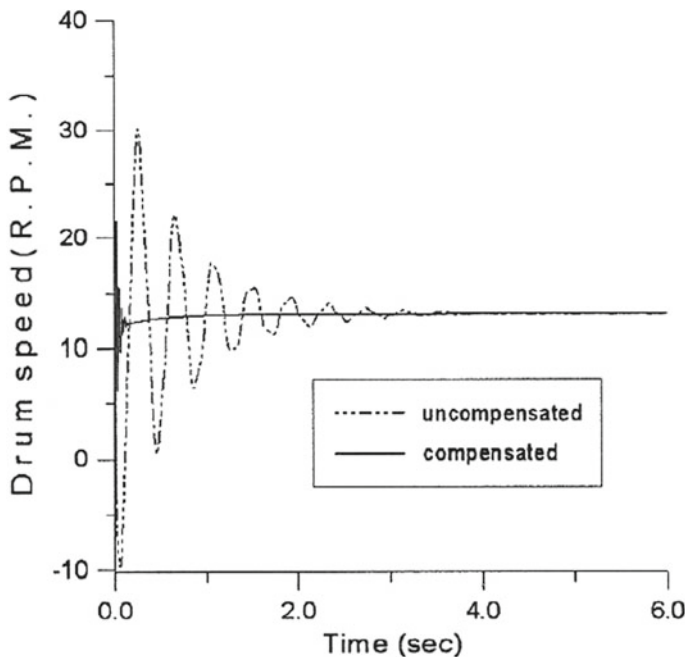


Fig. 5.26 Simulation results for hydrostatic transmission

5.4.4 Case Study: Failure Analysis and Redesign of a Helix Upper Dispenser

The mechanical icemaker system in a side-by-side (SBS) refrigerator with a dispenser system consists of many structural parts. Depending on the customer usage conditions, these parts receive a variety of mechanical loads in the ice making process. Ice making involves several mechanical processes: (1) the filtered water is pumped through a tap line supplying the tray; (2) the cold air in the heat exchanger chills the water tray; and (3) after ice is made, the cubes are harvested, stocking the bucket until it is full. When the customer pushes the lever by force, cubed or crushed ice is dispensed. In the United States, the customer typically requires an SBS refrigerator to produce 10 cubes per use and up to 200 cubes a day. Ice production may be influenced by uncontrollable customer usage conditions such as water pressure, ice consumption, refrigerator notch settings, and the number of times the door is opened. When the refrigerator is plugged in, the cubed ice mode is automatically selected. A crusher breaks the cubed ice in the crushed mode. Normally, the mechanical load of the icemaker is low because it is operated without fused or webbed ice.

However, for Asian customers, fused or webbed ice will frequently form in the tray because they dispense ice in cubed mode infrequently. When ice is dispensed

under these conditions, a serious mechanical overload occurs in the ice crusher. However, in the United States or Europe, the icemaker system operates continuously as it is repetitively used in both cubed and crushed ice modes. This can produce a mechanical/civil overload.

Figure 5.27 overviews the schematic of the ice maker. Figures 5.28 and 5.29 show a schematic diagram of the mechanical/civil load transfer in the ice bucket assembly and its bond-graphs. An AC auger motor generates enough torque to crush the ice. Motor power is transferred through the gear system to the ice bucket assembly—that is, to the helix upper dispenser, the blade dispenser and the ice crusher.

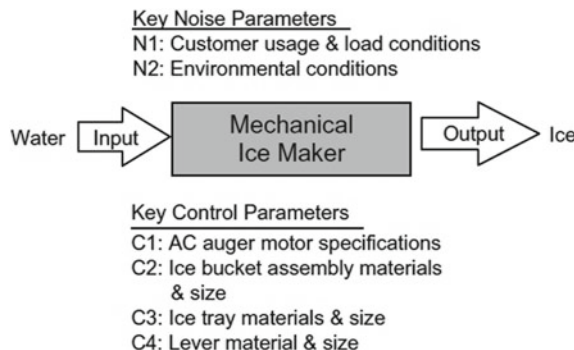


Fig. 5.27 Robust design schematic of ice-maker

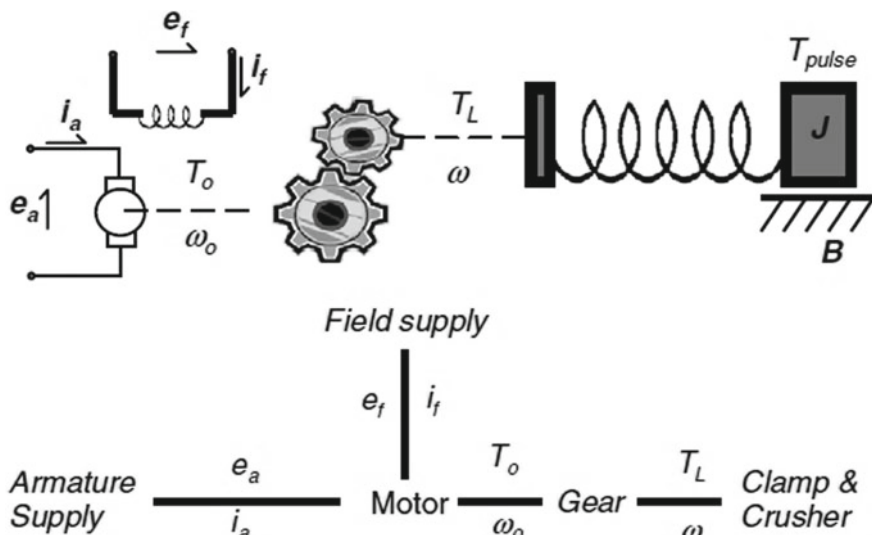


Fig. 5.28 Schematic diagram for mechanical ice bucket assembly

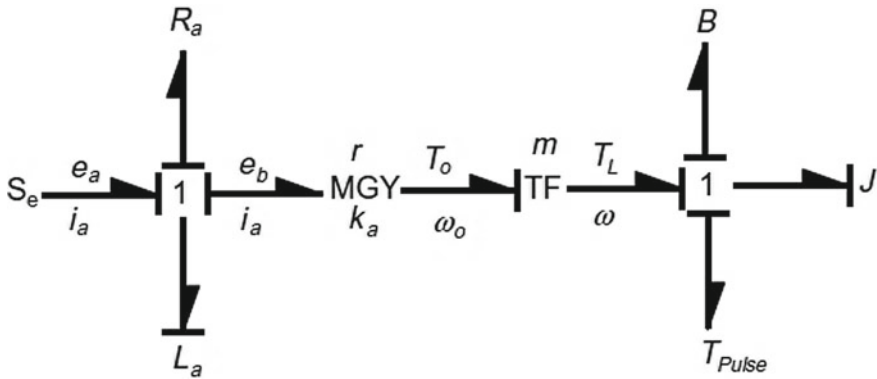


Fig. 5.29 Bond graph of ice bucket assembly

The Bond graph can be represented as a state equation form, that is,

$$dE_2/dt = 1/L_a \times eE_2 \quad (5.44)$$

$$dM_2/dt = 1/J \times eM_2 \quad (5.45)$$

The junction from Eq. (5.44)

$$eE_2 = e_a - eE_3 \quad (5.46a)$$

$$eE_3 = R_a \times fE_3 \quad (5.46b)$$

The junction from Eq. (5.45)

$$eM_2 = eM_1 - eM_3 \quad (5.47a)$$

$$eM_1 = (K_a \times i) - T_{pulse} \quad (5.47b)$$

$$eM_3 = B \times fM_3 \quad (5.47c)$$

Because $fM_1 = fM_2 = fM_3 = \omega$ and $i = fE_1 = fE_2 = fE_3 = i_a$.
From Eq. (5.46)

$$eE_2 = e_a - R_a \times fE_3 \quad (5.48)$$

$$fE_2 = fE_3 = i_a \quad (5.49)$$

If substituting Eqs. (5.48) and (5.49) into (5.44), then

$$di_a/dt = 1/L_a \times (e_a - R_a \times i_a) \quad (5.50)$$

And from Eq. (5.47) we can obtain

$$eM_2 = [(K_a \times i) - T_{Pulse}] - B \times fM_3 \quad (5.51a)$$

$$i = i_a \quad (5.51b)$$

$$fM_3 = fM_2 = \omega \quad (5.51c)$$

If substituting Eq. (5.51) into (5.45), then

$$d\omega/dt = 1/J \times [(K_a \times i) - T_{Pulse}] - B \times \omega \quad (5.52)$$

So the state equation can be obtained from Eq. (5.50) and (5.52) as following

$$\begin{bmatrix} di_a/dt \\ d\omega/dt \end{bmatrix} = \begin{bmatrix} -R_a/L_a & 0 \\ mk_a & -B/J \end{bmatrix} \begin{bmatrix} i_a \\ \omega \end{bmatrix} + \begin{bmatrix} 1/L_a \\ 0 \end{bmatrix} e_a + \begin{bmatrix} 1 \\ -1/J \end{bmatrix} T_{Pulse} \quad (5.53)$$

When Eq. (5.53) is integrated, the angular velocity of the ice bucket mechanical assembly is obtained as

$$y_p = [0 \quad 1] \begin{bmatrix} i_a \\ \omega \end{bmatrix} \quad (5.54)$$

5.5 Load Spectrum and Rain-Flow Counting

5.5.1 Introduction

As seen in previous sections, we know that product subjected to a variety of loads can be simulated through dynamics modeling like bond-graph and its analysis. As a result, the time response can be obtained to describe the load history of product. The load history on a product structure in time may be generally referred to as the load spectrum on the frequency domain. There are a variety of characteristic occurrences in the whole load history—the maximum and minimum loads, P_{max} and P_{min} . At these load levels, the reversals of cyclic slip occur in the crack tip plastic zone. They are critical for fatigue damage in a structure (Fig. 5.30).

To experimentally measure the load over time, strain gage type transducers are attached to the critical areas of the component. The acquired data from the transducers are usually recorded and stored by a computer or by other devices. After the recorded data is filtered to isolate the primary loads from noise, the recorded data converted from the strain values to torque are counted by rain-flow counting methods. After simplifying the fatigue damage computations, we can apply the Miner's rule and assess whether product design can endure the damage (Fig. 5.31).

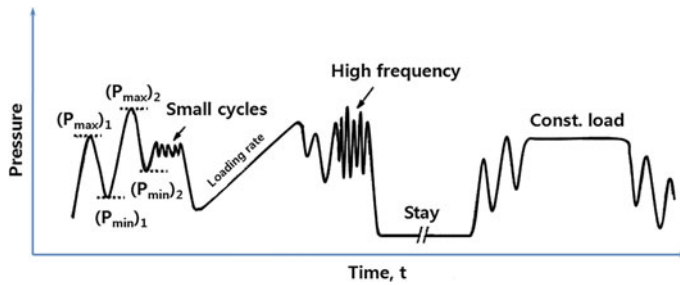


Fig. 5.30 A load history $P(t)$ in accordance with time

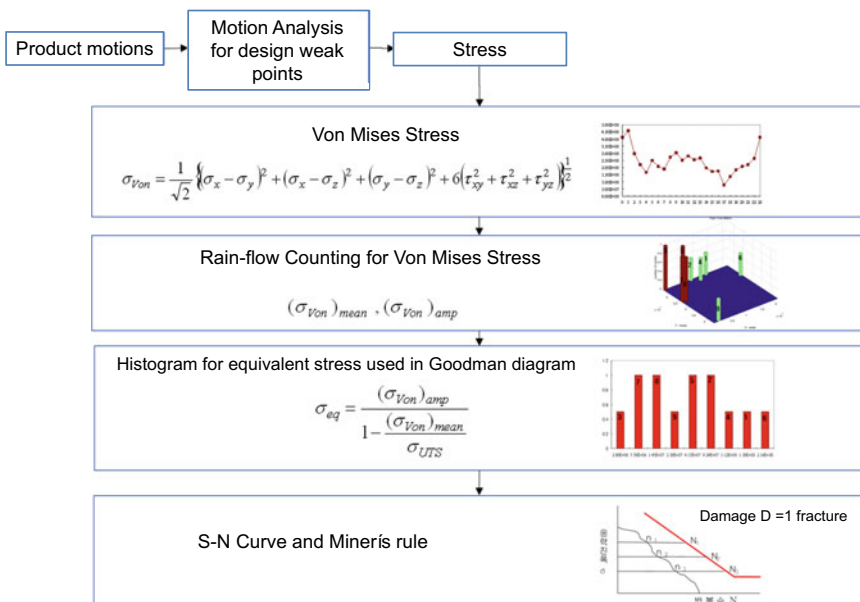


Fig. 5.31 Classification and counting of the dynamic load (assessment process)

With the measurement data (or analysis) over time, we can make the load spectrum. Information on the anticipated load spectrum will enable engineer to analyze the strength of a structure. This load spectrum is very important during the design phase because it can evaluate the field failure like fatigue or fracture. The information from the load spectrum can be used with reliability testing. Next, by using load counting technique, known as rain-flow counting, we can count each load cycles in the measured data. So the output of this calculation is called the torque count statistics. Using the rain-flow data, it is then possible to calculate the histogram. Finally, with this histogram we can assess the product failure if the modified miner's law is used.

5.5.2 Rain-Flow Counting for Load Spectrum

Realistic representation of loads is a key ingredient to the mechanical design for successful fatigue analysis. It will accurately measure the applied loads on an existing product and predict the load effects of a component or structure. As a first step of the analysis for product damage, complex load histories are often replaced by more simplified loadings. Using the rain-flow cycle counting, we can calculate fatigue cycles from a time history. Because the fatigue cycles are stress-reversals, the rain-flow method enables them to apply Miner's rule and assess the fatigue life of a structure subject to complex loading. As a result, we know the cumulative damage or the fatigue effects of loading events. The term "spectrum" in fatigue often means a series of fatigue loading events other than uniformly repeated cycles. Sometimes spectrum means a listing, ordered by size, of components of irregular sequences. Maximum and minimum loads in spectrum are also used to define the classifications in which the counts of cycles are listed.

The basic concepts of rain-flow counting are that with the load-time, stress-time, or strain-time history, rain flowing down a roof can be represented by the history of peaks and valleys. Rain-flow counting is a concept developed in Japan by Tatsuo Endo and M. Matsuishi in 1968 [1] and in the USA for the segmentation of any arbitrary stress curve into complete oscillation cycles. Rain-flow counting counts closed hysteresis loops in a load-time-function, which are decisive for the damage of metal materials.

The following assumptions are valid for rain flow counting

- Cyclic stable material behavior, that means that the cyclic stress-strain curve remains constant, thus no hardening or softening of the material takes place.
- Validity of the masing hypothesis, which means that the form of the hysteresis loop branches correspond to the double of the initial load curve.
- Memory behavior of the material which means that after a closed hysteresis loop, a previously not yet completely closed hysteresis loop follows the same σ , ϵ path.

As seen in Fig. 5.32, the tips of the largest hysteresis loop are at the largest tensile and compressive loads in the load history (points 1 and 4). The notch strain-time history (Fig. 5.21c) is quite different from the corresponding notch stress-time history (Fig. 5.21e). During each segment of the loading the material remembers its prior deformation called material memory. The damage from each counted cycle can be computed from the strain amplitude and mean stress for that cycle as soon as it has been identified in the counting procedure. The corresponding reversal points can then be discarded.

If sequence clearly has 10 cycles of amplitude 10 MPa, a structure's life can be estimated from a simple application of the relevant S-N curve. However, in real, as seen in Fig. 5.33, it is very complex and cannot be assessed in terms of simply-described stress reversals. An advantage of rain-flow counting is when it is used with notch strain analysis. The rain-flow counting results in closed hysteresis

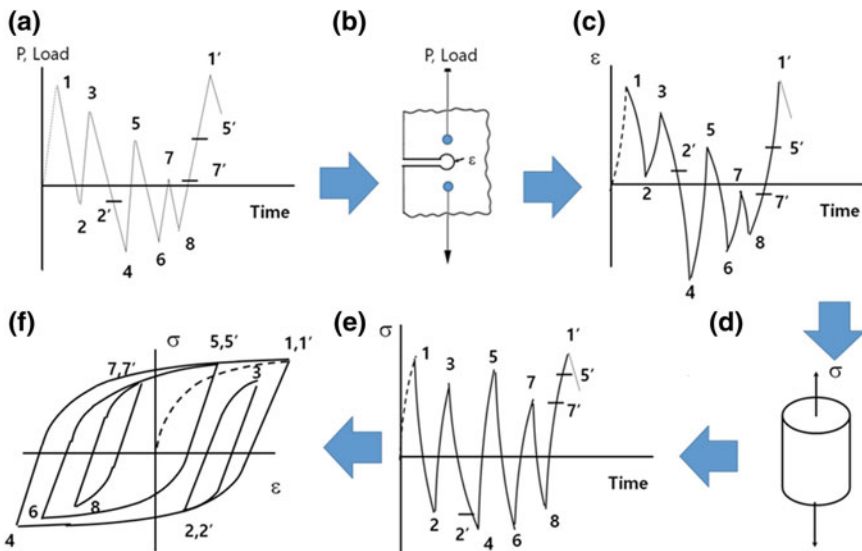
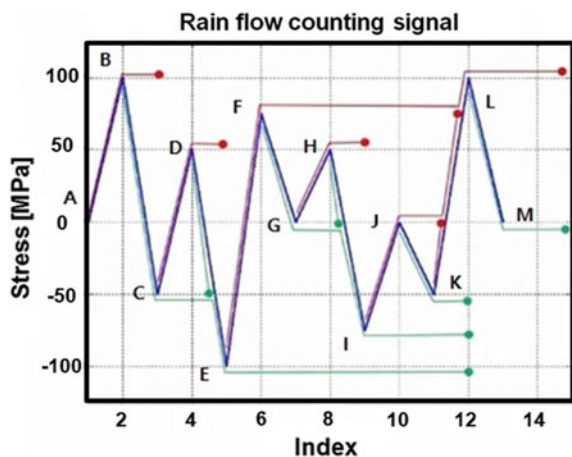


Fig. 5.32 Rain-flow counting method

Fig. 5.33 Acquisition of the dynamic load-time behavior with rain-flow counting algorithm



loops, which representing a counted cycle. Therefore, the closed hysteresis loops can also be used to obtain the cycle counting.

If the dynamic load-time behaviors are acquired in Fig. 5.33, they can be summarized by rain-flow counting as Table 5.3.

- Half-cycle starts at (A) and terminates opposite a greater tensile stress, peak (B); its range is 100 MPa.
- Half-cycle starts at tensile peak (B), flow through (C), and terminates a greater tensile stress, peak (E); its range is 200 MPa.

Table 5.3 Summary of the dynamic loads by using rain-flow counting

Path	From (MPa)	To (MPa)	Range (MPa)	Cycles
A–B	0	100	100	0.5
B–E	100	-100	200	0.5
C–D	-50	50	100	0.5
D–C	50	-50	100	0.5
E–F	-100	100	200	0.5
F–I	75	-75	150	0.5
G–H	0	50	50	0.5
H–G	50	0	50	0.5
K–J	-50	0	50	0.5
J–K	0	50	50	0.5
I–F	-75	75	150	0.5
L–M	100	0	100	0.5

Consequently, as seen in Table 5.3, we can count two cycles for 50 MPa range, two cycles for 100 MPa range, one cycle for 150 MPa range, and one cycle for 200 MPa range. Since calculated lifetime estimations are afflicted with large uncertainties, it is desired to reconstruct the stochastic load-time functions out of the load spectrums, in order to carry out experimental lifetime proofs with servo-hydraulic facilities.

However, the reconstruction of a representative load-time function is not possible with the load spectra alone. Two parametric rain-flow counting method is the most suitable method for the acquisition of the local stress-strain hysteresis curves and influences the result of lifetime estimation.

5.5.3 Goodman Relation

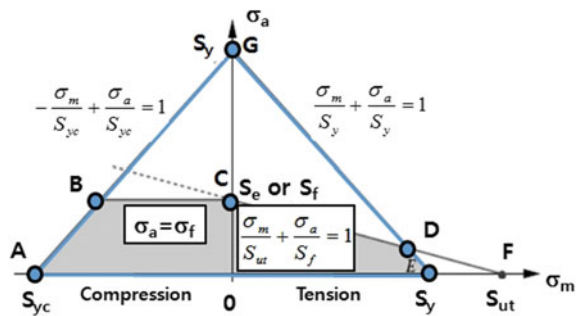
In the presence of a steady stress superimposed on the cyclic loading, the Goodman relation [2] can be used to estimate a failure condition. It plots stress amplitude against mean stress with the fatigue limit and the ultimate tensile strength of the material as the two extremes.

$$\sigma_a = \sigma'_e \times \left(1 - \frac{\sigma_m}{\sigma'_u} \right) \quad (5.55)$$

where σ'_e effective alternating stress at failure for a lifetime of N_f cycles, σ'_u is ultimate stress.

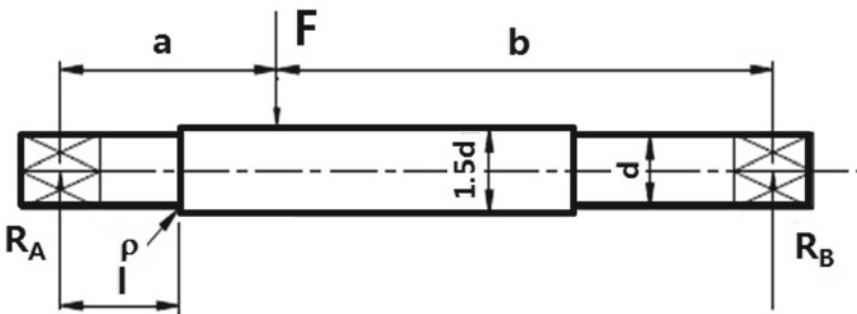
A very substantial amount of testing is required to obtain as *S-N* curve for the simple case of fully reversed loading, and it will usually be impractical to determine whole families of curves for every combination of mean and alternating stress. There are a number of stratagems for finessing this difficulty, one common one being the “Augmented” Modified-Goodman diagram, shown in Fig. 5.34.

Fig. 5.34 “Augmented” Modified-Goodman diagram



Here a graph is constructed with mean stress as the abscissa and alternating stress as the ordinate, and a straight “lifeline” is drawn from σ_e on the σ_a axis to the ultimate tensile stress σ_f on the σ_m axis. Then, for any given stress, the endurance limit (or fatigue limit)—the value of alternating stress at which fatigue failure never occurs—can be read directly as the ordinate of the lifeline at line is drawn from the origin with a slope equal to that ratio. Its intersection with the lifeline then gives the effective endurance limit for that combination of σ_f and σ_m .

Example 5.1 The beam shown has a circular cross-section and supports a load of $F = 15$ kN that is repeated (zero maximum). The beam is machined from AISI 1020 (20) steel, as rolled. Determine the diameter d if $\rho = 0.2d$, the shoulder height is $0.25d$ [$R/r = 1.5$] and $FS = 2$. Draw to scale Soderberg’s diagram for this problem. Data: $a = 200$ mm; $b = 400$ mm; $l = 150$ mm; $R_e = 360$ MPa; $R_m = 450$ MPa; $Z_{go} = 228$ MPa.



Reactions: $R_A = 10$ kN; $R_B = 5$ kN

Bending moment in section I-I: $M = R_A l = 10 \times 10^3 \times 150 = 1500 \times 10^3$ N mm
Theoretical stress concentration factor: $\alpha_k = 1.5$ ($R/r = 1.5$; $\rho/r = 0.4$)

Notch sensitivity factor: $\eta = 0.65$

Stress concentration factor: $\beta_k = 1 + \eta(\alpha_k - 1) = 1 + 0.68(1.5 - 1) = 1.34$

Surface finish factor: $\beta_p = 1.15$. See that the abscissa (R_m) is still in obsolete units (kG/mm²; multiply by 10 to get MPa). Material is considered as rolled but after rough turning.)

Resultant stress concentration factor: $\beta = \beta_k + \beta_p - 1 = 1.34 + 1.15 - 1 = 1.45$

As the problem is of design nature, the size factor shall be omitted, i.e. we assume $\gamma = 1$.

Amplitude stress (as a function of the beam diameter):

$$\sigma_a = \sigma_m = \frac{\sigma_{\max}}{2} = \frac{M}{2Z_{xx}} = \frac{1500 \times 10^3 \cdot 32}{2 \cdot \pi \cdot d^3} = \frac{7,639,437}{d^3}$$

Inclination of the Soderberg line:

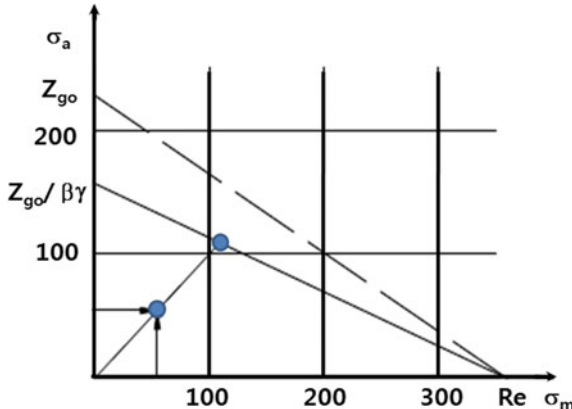
$$\tan \Psi = \frac{Z_{go}}{\beta \gamma R_e} = \frac{228}{1.45 \cdot 1 \cdot 360} = 0.437$$

From the formula for FS we isolate d :

$$d = \sqrt[3]{\frac{7,639,437 \cdot \beta \gamma \cdot FS(1 + \tan \Psi)}{Z_{go}}} = \sqrt[3]{\frac{7,639,437 \cdot 1.45 \cdot 1 \cdot 2(1 + 0.437)}{228}} \\ = 51.7 \text{ mm}$$

Actual value of the amplitude (mean) stress (assumed $d = 52 \text{ mm}$):

$$\sigma_a = \sigma_m = \frac{7,639,437}{d^3} = \frac{7,639,437}{52^3} = 54.3 \frac{\text{N}}{\text{mm}^2}$$



Example 5.2 An automobile engine part rotates, and in each rotation stress varies from $S_{\max} = 140 \text{ MPa}$ to $S_{\min} = 10 \text{ MPa}$. The material has $S_u = 550 \text{ MPa}$,

$S_{yp} = 410 \text{ MPa}$, $S_e = 200 \text{ MPa}$. Assume $K = K_f = 1$. Find N_{fs} , with (1) Soderberg's, (2) Goodman's and (3) modified Goodman's equations.

$$\text{Steady stress} = S_{avg} = \frac{S_{max} + S_{min}}{2} = \frac{140 + 10}{2} = 75 \text{ MPa}$$

$$\text{Reversing stress} = S_r = \frac{S_{max} - S_{min}}{2} = \frac{140 - 10}{2} = 65 \text{ MPa}$$

$$\text{Soderberg's Equation: } N_{fs} = \frac{S_{yp}}{S_{avg} + S_r K_f \left(\frac{S_{yp}}{S_e} \right)} = \frac{410}{75 + 65 \times 1 \times \left(\frac{410}{200} \right)} = 1.97$$

$$\text{Goodman's Equation: } N_{fs} = \frac{S_u}{S_{avg} + S_r K_f \left(\frac{S_u}{S_e} \right)} = \frac{550}{75 + 65 \times 1 \times \left(\frac{550}{200} \right)} = 2.17$$

Modified Goodman's Equation:

$$N_{fs1} = \frac{S_u}{S_{avg} + S_r K_f \left(\frac{S_u}{S_e} \right)} = \frac{550}{75 + 65 \times 1 \times \left(\frac{550}{200} \right)} = 2.17$$

$$N_{fs1} = \frac{S_{yp}}{S_{avg} + S_r K_f \left(\frac{S_u}{S_e} \right)} = \frac{410}{75 + 65 \times 1} = 2.93$$

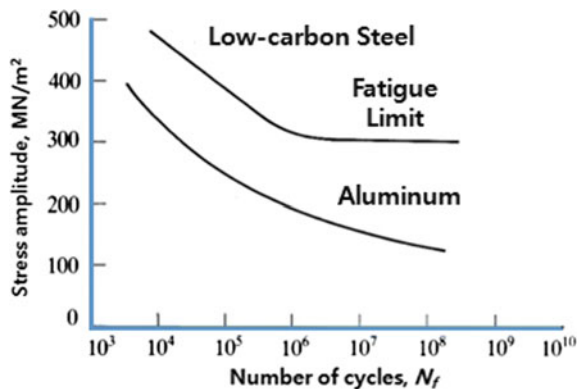
$$N_{fs1} = 2.17 \text{ (Smaller one)}$$

5.5.4 Palmgren-Miner's Law for Cumulative Damage

Miner's rule is one of the most widely used cumulative damage models for fatigue failures. Fatigue properties of a material ($S-N$ curves) can be evaluated in rotating-bending tests with fatigue testing apparatus. The $S-N$ curve is required as a description of the material behavior for the calculation of fatigue strength and operational fatigue strength. Well before a micro-structural understanding of fatigue processes was developed, engineers had developed empirical means of quantifying the fatigue process and designing against it. Perhaps the most important concept is the $S-N$ diagram, such as those shown in Fig. 5.35, in which a constant cyclic stress amplitude S is applied to a specimen and the number of loading cycles N until the specimen fails. Millions of cycles might be required to cause failure at lower loading levels, so the abscissa is usually plotted logarithmically.

There are three zones to distinguish between in the double logarithmic representation of $S-N$ curve

Fig. 5.35 *S-N* diagram for aluminum and low-carbon steel



- Low cycle fatigue: high loads, plastic and elastic deformation, $N = 10^3$ cycles (1 stage)
- High cycle fatigue: fatigue strength, the zone of the sloped lines, until the corner load cycles to failure $N_D = 10^6\text{--}10^7$ (2 stage)
- Fatigue limit (endurance limit), zone of the horizontal lines starting from $N > N_D$. However, several materials such as austenite steels do not possess a distinct endurance strength (3 stage).

In this case, the *S-N* curve becomes horizontal at large N . The fatigue limit is maximum stress amplitude below which the material never fails, no matter how large the number of cycles is. In most alloys, S decreases continuously with N . In this case the fatigue properties are described by fatigue strength at which fracture occurs after a specified number of cycles (e.g. 10^7). Fatigue life is number of cycles to fail at a specified stress level.

Fatigue failure has three stages: (1) crack initiation in the areas of stress concentration or near stress raisers, (2) incremental crack propagation, and (3) final rapid crack propagation after crack reaches critical size. The total number of cycles to failure is the sum of cycles at the first and the second stages. That:

$$N_f = N_i + N_p \quad (5.56)$$

where N_f number of cycles to failure, N_i number of cycles for crack initiation, N_p number of cycles for crack propagation.

In the fatigue strength zone, the *S-N* curve can be described by the following equation if represented in the double logarithmic form.

$$N = N_D \cdot \left(\frac{\sigma_a}{\sigma_D} \right)^{-k} \quad (5.57)$$

If possible, the determination of the *S-N* curve for operational fatigue strength calculation should be carried out on real parts. Often, however, due to cost and time limitations, the calculations are only carried out on special test samples.

The resulting load cycles to failure are random variables, which mean that they lie scattered around the mean value. Today, the transformation of results won from a tension/compression trial onto a real component is difficult. Thus, the exact determination of a notch over the entire load cycle zone is still not possible today. Therefore, one is forced to rely on tests and trials.

In some materials, notably ferrous alloys, the S - N curve flattens out eventually, so that below a certain fatigue limit σ_e failure does not occur no matter how long the loads are cycled. Obviously, the designer will size the structure to keep the stresses below σ_e by a suitable safety factor if cyclic loads are to be withstood. For some other materials such as aluminum, no fatigue limit exists and the designer will size the structure to keep the stresses below σ_e by a suitable safety factor if cyclic loads are to be withstood. For some other materials such as aluminum, no fatigue limit exists and the designer must arrange for the planned lifetime of the structure to be less than the fatigue point on the S - N diagram.

Statistical variability is troublesome in fatigue testing; it is necessary to measure the lifetimes of perhaps twenty specimens at each of ten or so load levels to define the S - N diagram with statistical confidence. It is generally impossible to cycle the specimen at more than approximately 10 Hz and at that speed it takes 11.6 days to reach 10^7 cycles of loading. Obtaining a full S - N curve is obviously a tedious and expensive procedure.

At first glance, the scatter in measured lifetimes seems enormous, especially given the logarithmic scale of the abscissa. If the coefficient of variability in conventional tensile testing is usually only a few percent, why do the fatigue lifetimes vary over orders of magnitude? It must be remembered that in tensile testing, we are measuring the variability in cycles at a given number of cycles, while in fatigue we are measuring the variability in cycles at a given stress. State differently, in tensile testing we are generating vertical scatters bars, but in fatigue they are horizontal. Note that we must expect more variability in the lifetimes as the S - N curve becomes flatter, so that materials that are less prone to fatigue damage require more specimens to provide a given confidence limit on lifetime.

Numerous different researchers have occupied themselves with the damage accumulation hypothesis in fatigue failure, so that currently several variations exist. In general, the variations only distinguish themselves by the fundamental S - N curve used: either fictitiously extrapolated or the real curve itself.

Oscillating loads cause an effect in materials, this is often referred to as “Damage” as soon as this load surpasses a certain limit. It is assumed that this damage accumulates from the individual load cycles and leads to a material fatigue. For an exact calculation this damage must be collected and recorded quantitatively. This, however, has not yet been achieved with success.

Despite this fact, in order to gather information concerning the lifetime L out of the results of Wöhler trials with irregular load cycle effects, around the year 1920, Palmgren [3] developed the fundamental idea of linear accumulation, specific for roll bearing calculation. In 1945, Miner published the same idea in a general form.

Miner assumes that a part absorbs work during the fatigue process subjected to the load spectrum (Fig. 5.36). The ratio of already absorbed work to the maximal

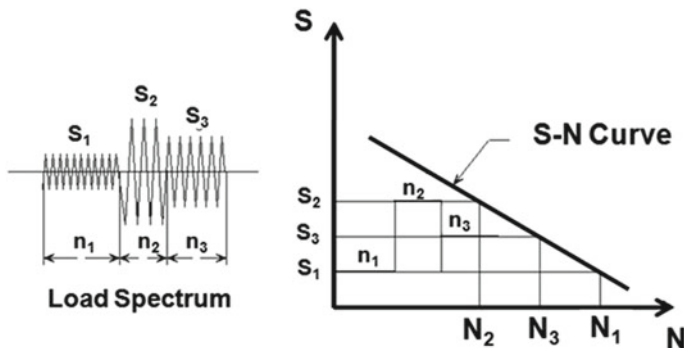


Fig. 5.36 Miner's cumulative damage summation for load spectrum and its counting

work which can be absorbed is a measurement for the current damage. Thus, the ratio of the load cycle number n to the load cycles to failure N , which is determined in the single-stage zone with the corresponding amplitude, is equal to the ratio of absorbed work w to absorbed work W . This is denoted as the damage portion

$$\frac{w}{W} = \frac{n}{N} \quad (5.58)$$

When the cycle load level varies during the fatigue process, a cumulative damage model is often hypothesized. By definition of the S - N curve, take the lifetime to N_1 cycles at stress level S_1 and N_2 at S_2 . If damage is assumed to accumulate at a constant rate during fatigue and a number of cycles n_1 is applied at stress S_1 , where $n_1 < N_1$, then the fraction of lifetime consumed will be n_1/N_1 .

The Palmgren-Miner hypothesis asserts that the damage fraction at any level S_i is linearly proportional to the ratio of number of cycles of operation to the total number of cycles that would produce failure at that stress level; that is

$$D_i = \frac{n_j}{N_j} \quad (5.59)$$

The limiting condition of strength happens when the absorbed work and absorbable work are the same. That is, the prerequisite that the absorbed fracture work W is the same for all occurring load sizes, allows the addition of the individual damage portions for load cycles of different sizes

$$\frac{w_1 + w_2 + \cdots + w_m}{W} = 1 \quad (5.60)$$

So failure is predicted as follows,

$$D_1 + D_2 + \dots + D_i = \frac{w_1}{W} + \frac{w_2}{W} + \dots + \frac{w_m}{W} = \frac{n_1}{N_1} + \frac{n_2}{N_2} + \dots + \frac{n_m}{N_m} = 1 \quad (5.61)$$

The generalization of this approach is called Palmgren-Miner's Law, and can be written

$$\sum \frac{n_j}{N_j} \leq 1 \quad (5.62)$$

where n_j is the number of cycles applied at a load corresponding to a lifetime of N_j .

Miner confined the applicability of this equation by the following conditions.

- Sinus formed load curve
- No hardening or softening appearances in the material
- The begin of a crack is considered as an incipient damage
- Some loads lie above the endurance strength

Miner's law should be viewed like many other material laws that might be accurate enough to use in design. But damage accumulation in fatigue is usually a complicated mixture of several different mechanisms, and the assumption of linear damage accumulation inherent in Miner's law should be viewed skeptically. If portions of the material's microstructure become unable to bear load as fatigue progresses, the stress must be carried by the surviving micro-structural elements. The rate of damage accumulation could drop during some part of the material's lifetime. Miner's law ignores such effects, and often fails to capture the essential physics of the fatigue process.

With knowledge of the load spectrum and the tolerable material load in the form of the $S-N$ curve, a lifetime prediction can be made for a mechanical/civil system with the help of a damage accumulation hypothesis. Here it should be considered, that this prediction can only be made with a certain probability, since among other things the load spectrum as well as the load capacity expressed in the form of $S-N$ curve are random variables. Likewise, the damage accumulation hypotheses known today have only been proven empirically in material science. Therefore, a practical lifetime prediction requires balance field tests, test stand trials, calculation and a careful assessment and evaluation of the data, if the prediction should be able to serve as an effective tool for the designer.

Example 5.3 Stress σ_1 has lifetime $N_1 = 10^4$ cycles, and a more rigorous stress σ_2 has lifetime $N_2 = 10^3$ cycles. If 700 cycles at stress σ_2 is operated, when will it stop to operate at stress σ_1 ?

From Palmgren-Miner's Law Equation (5.62), we can calculate the cycles to fail.

$$\frac{700}{1000} + \frac{x}{10,000} = 1$$

So the expected failure cycle is $x = 3000$ cycles.

Example 5.4 A part is subjected to a fatigue environment where 10% of its life is spent at an alternating stress level, σ_1 , 30% is spent at a level σ_2 , and 60% at a level σ_3 . How many cycles, n , can the part undergo before failure?

If, from the S-N diagram for this material the number of cycles to failure at σ_i ($i = 1, 2, 3$), then from the Palmgren-Miner rule failure occurs when:

$$\frac{0.1 n}{N_1} + \frac{0.3 n}{N_2} + \frac{0.6 n}{N_3} = 1$$

so solving for n gives

$$n = \frac{1}{\frac{0.1}{N_1} + \frac{0.3}{N_2} + \frac{0.6}{N_3}}$$

If N_1, N_2, N_3 are $10^3, 10^4$, and 10^5 , the time to failure n will be 7353 cycles.

5.5.5 Inefficiency of Load Spectrum and Rain-Flow Counting

Fracture (or fatigue) means to represent that the material get tired due to repeated loading, and eventually disintegrated. A typical pattern of repeated load or overloading may cause structural failure over a product's lifetime. Many engineers think such possibility can be assessed: (1) mathematical modeling like Newtonian method, (2) the time response of system simulation for (random) dynamic loads, (3) the rain-flow counting method, and (4) miner's rule that the system damage can be estimated.

However, there are many assumptions in this methodology. For example, to assess the product damage, engineer should select the critical locations (stress concentration points) in the mechanical structure, and can calculate the elastic local stress, σ_{peak} , at the critical point (usually the notch tip). In the complex product assembly it is very hard to choose which components and their shapes are weak. This analytic methodology like load spectrum and rain-flow counting is exact but complex to assess the product failures due to the design flaws in product operation. Consequently, the parametric accelerated life testing that will be discussed in Chaps. 8 and 9 may be a alternative to reproduce the product failure and assess its reliability.

References

1. Matsuishi M, Endo T (1968) Fatigue of metals subjected to varying stress. Jpn Soc Mech Eng
2. Mott, Robert L (2004) Machine elements in mechanical design, 4th edn. Pearson Prentice Hall, Upper Saddle River NJ, pp 190–192
3. Palmgren AG (1924) Die Lebensdauer von Kugellagern. Z Ver Dtsch Ing 68(14):339–341

Chapter 6

Fluid Motion and Mechanical Vibration



Abstract This chapter will demonstrate the fluid motion and mechanical vibration of product. When airplane is in taxi, take-off or landing, a variety of functions such as airframe, wings, fuselage, engine, control, etc. are required. Especially, fluid mechanics is the critical area that studies the effect of forces on fluid motion. Due to fluid motion, they might be repetitively subjected to (random) loads and make problems—fracture or vibration. To withstand their own loads in airplane, mechanical structures like wing are designed to have proper stiffness and strength. If not, airplane will abruptly cause some problems in flight. To experimentally assess the structural effects of fluid force, engineers should understand the basic concepts of fluid mechanics—viscosity, boundary layer, etc. And we also will discuss the mechanical vibration which happens when system is applied by undesired force—imbalances in the rotating parts or the movement of a tire on a gravel road. Unless isolated by proper stiffness design, system will create unwanted sound or waste energy. Ultimately mechanical system will fracture. To prevent it, engineers might find and correct the design faults of mechanical products. Therefore, parametric ALT might be a kind of engineering solutions.

Keywords Fluid mechanics · Viscosity · Boundary layer · Vibration · Fatigue · Design · Failure analysis

6.1 Introduction

6.1.1 Fluid Motion

Aerodynamics is the study of the motion of air, particularly its interaction with a solid object such as an airplane wing that provides the lift necessary for flight. In the eighteenth century the study of modern aerodynamics began. As Wilbur and Orville Wright in 1903 were successful for first flight, aerodynamics was directed toward achieving heavier-than-air powered aircraft. After many trials and errors, the use of aerodynamics through mathematical analysis, empirical approximations, wind

tunnel experimentation, and computer simulations has formed a rational basis for the development of heavier-than-air flight. Recently aerodynamics has focused on issues related to compressible flow, turbulence and boundary layers. As the finite element analysis advances, computational fluid dynamics has become more important.

First of all, fluids are conventionally classified as either incompressible fluid (liquids) or compressible fluid (gases). The most important difference between two types of fluid is compressibility. To be more exact, gases can be compressed much more easily than liquids. Consequently, for gas, any motion that involves significant pressure variations is generally accompanied by much larger density changes than that of a liquid.

We will begin the mathematical models of fluid dynamic including aerodynamics used to describe the chronic failure due to the repetitive fluid stress (or loads) in the airplane wing or engine. A fluid material possesses no rigidity at all. In other words, because a small fluid element is unable to withstand an applied shear stress, it would change its shape. However, any resistance must be incapable of preventing the change in shape from eventually occurring, which implies that the force of resistance vanishes with the rate of deformation. The shear stress obviously must be zero everywhere inside a fluid that is in mechanical equilibrium.

A fluid macroscopically consists of an amount of molecules. However, most of fluid mechanics have behavior on length scales that are much longer than the common intermolecular spacing. Under definition of continuum mechanics, the bulk properties of a given fluid like viscosity have same property as if it were completely continuous in fluid structure. Suppose infinitesimal volume elements are, they have constant bulk fluid properties such as mass density, pressure, and velocity, though they contain a very great number of molecules. The continuum hypothesis also requires infinitesimal volume elements to be much longer than the molecular mean-free-path between collisions. In addition to the continuum hypothesis, the general study of fluid mechanics is premised on three major assumptions:

1. Fluids are isotropic media that there is no preferred direction in a fluid.
2. Fluids are Newtonian. In other words, there is a linear relationship between the local shear stress and the local rate of strain. It is also assumed that there is a linear relationship between the local heat flux density and the local temperature gradient.
3. The motion of ordinary fluids macroscopically can be described by Newtonian dynamics, and both quantum and relativistic effects can be ignored.

6.1.2 Buckingham Pi Theorem

Let $q_1, q_2, q_3 \dots q_n$ be n dimensional variables that are physically relevant in a given problem and that are inter-related by an unknown dimensionally homogeneous set of equations. These can be expressed via a functional relationship of the form

$$F(q_1, q_2, \dots, q_n) = 0 \quad \text{or equivalently} \quad q_1 = f(q_2, \dots, q_n) \quad (6.1)$$

If k is the number of fundamental dimensions required to describe the n variables, there will be k primary variables and the remaining variables can be expressed as $(n - k)$ dimensionless and independent quantities or ‘Pi groups’, $\Pi_1, \Pi_2, \dots, \Pi_{n-k}$. The functional relationship can thus be reduced to the much more compact form:

$$\Phi(\Pi_1, \Pi_2, \dots, \Pi_n) = 0 \quad \text{or equivalently} \quad \Pi_1 = \Phi(\Pi_2, \dots, \Pi_{n-k}) = 0 \quad (6.2)$$

Example 6.1 Find the relationship of the effect on pressure drop (ΔP) of the variables d, L, p, μ and v

$$f(\Delta P, d, L, p, \mu, v) = 0$$

Number of variables: $n = 6$ (That is: $\Delta P, d, L, p, \mu, v$).

Number of fundamental dimensions: $m = 3$ (That is, [M], [L], [T]).

By Buckingham’s theorem, number of dimensionless groups: $n - m = 6 - 3 = 3$. The recurring set must contain three variables that cannot themselves be formed into a dimensionless group. In this case there are two restrictions: (1) Both L and d cannot be chosen as they can be formed into a dimensionless group, (L/d) . (2) Since $(\Delta P/pv^2) = 0$ is dimensionless, $\Delta P, p$, and v cannot be used.

The variables d, v and p are chosen as the recurring set.

The dimensions of these variables are $d = [L], v = [LT^{-1}], p = [ML^{-3}]$

Rewriting the dimensions in terms of the variables chosen:

$$[L] = d, [M] = pd^3, [T] = dv^{-1}.$$

The dimensionless groups are formed by taking each of the remaining variables $\Delta P, L$ and μ in turn:

ΔP has dimensions of $[ML^{-1}T^{-2}]$. Therefore, $\Delta P M^{-1}L T^2$ is dimensionless

Substituting the dimensions in terms of variables

$$\Pi_1 = \Delta P (pd^3)^{-1} (d) (dv^{-1})^2 = \Delta P / pv^2$$

L has dimensions of $[L]$. $L[L]^{-1}$ is therefore dimensionless

$$\Pi_2 = L/d$$

μ has dimensions of $[ML^{-1}L^{-1}]$. $\mu[M^{-1}LT]$ is therefore dimensionless

$$\Pi_3 = \mu(pd^3)^{-1}(d)(dv^{-1})^2 = \mu/dvp$$

Thus, we can summarize the relationship of the effect on pressure drop (ΔP) as following:

$$f(\Delta P/pv^2, L/d, \mu/vpd),$$

$$\Delta P/pv^2 = f(L/d, \mu/vpd)$$

6.1.3 Forces Acting on the Air Vehicle—Thrust, Drag, Weight and Lift

The basic principles of why and how airplanes fly are the same from the Wright Brothers' first machine Wright Flyer to a modern Stealth Bomber. Once an airplane leaves the ground, it is acted upon by four aerodynamic forces; thrust, drag, lift and weight. Understanding how these forces work and knowing how to control them with the use of power and flight controls are essential to flight.

Thrust is the forward force produced by the power plant/propeller or rotor. It overcomes the force of drag. As a general rule, it acts parallel to the longitudinal axis. Drag is a rearward, retarding force caused by disruption of airflow by the wing, rotor, fuselage, and other protruding objects. Drag opposes thrust and acts rearward parallel to the relative wind. Weight is the combined load of the aircraft itself, the crew, the fuel, and the cargo or baggage. Weight pulls the aircraft downward because of the force of gravity.

It opposes lift and acts vertically downward through the aircraft's center of gravity (CG). Lift opposes the downward force of weight and produced by the dynamic effect of the air acting on the airfoil, and acts perpendicular to the flight path through the center of lift. Lift is generated when an object changes the direction of flow of a fluid or when the fluid is forced to move by the object passing through it.

When the object and fluid move relative to each other and the object turns the fluid flow in a direction perpendicular to that flow, the force required to do this work creates an equal and opposite force that is lift. The object may be moving through a stationary fluid, or the fluid may be flowing past a stationary object—these two are effectively identical as, in principle, it is only the frame of reference of the viewer which differs. The lift generated by an airfoil depends on such factors: (1) Speed of the airflow, (2) Density of the air, (3) Total area of the segment or airfoil, and (4) Angle of attack (AOA) between the air and the airfoil (Fig. 6.1).

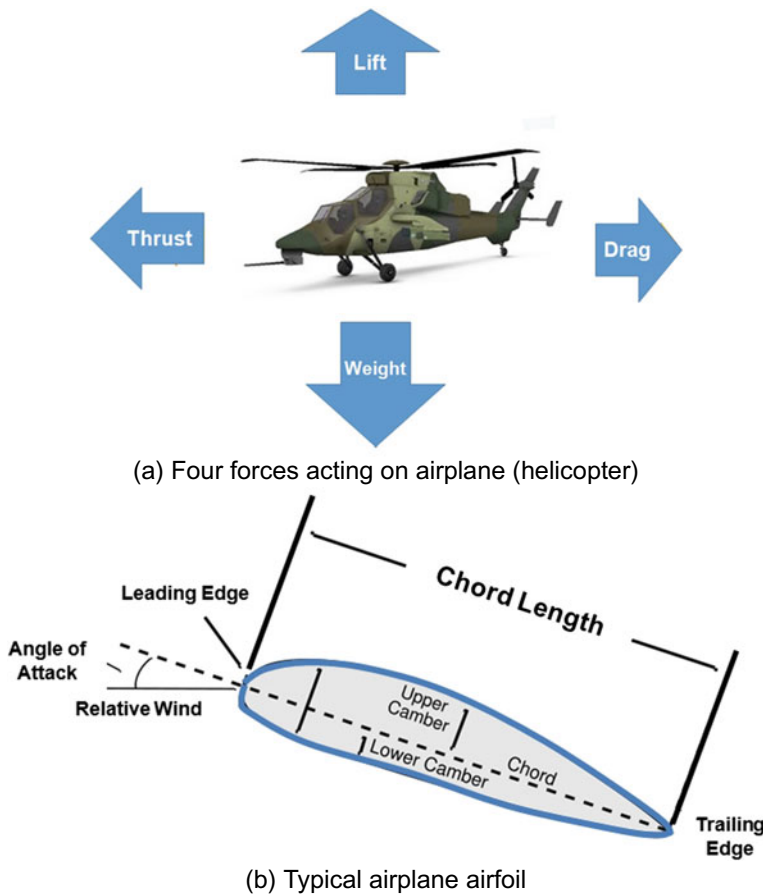


Fig. 6.1 Four forces acting on airplane (helicopter) in forward flight and airfoil

6.1.4 Basic Concept of Lift

The AOA is the angle at which the airfoil meets the oncoming airflow (or vice versa). In the case of a helicopter, the object is the rotor blade (airfoil) and the fluid is the air. Lift is produced when a mass of air is deflected, and it always acts perpendicular to the resultant relative wind. A symmetric airfoil must have a positive AOA to generate positive lift. At a zero AOA, no lift is generated. At a negative AOA, negative lift is generated. A cambered or non-symmetrical airfoil may produce positive lift at zero, or even small negative AOA (Fig. 6.2).

The basic concept of lift is simple. However, the details of how the relative movement of air and airfoil interact to produce the turning action that generates lift are complex. In any case causing lift, an angled flat plate, revolving cylinder, airfoil, etc., the flow meeting the leading edge of the object is forced to split over and under

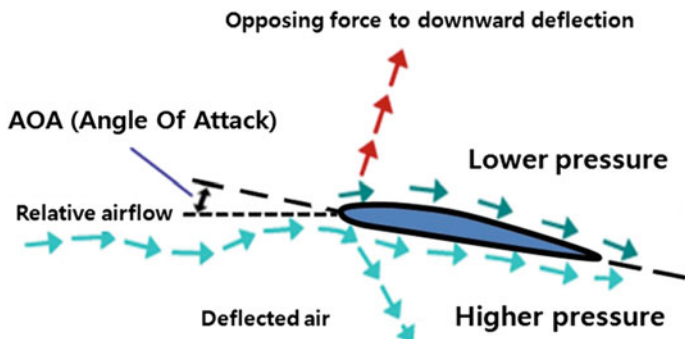


Fig. 6.2 General movement of air over an airfoil

the object. The sudden change in direction over the object causes an area of low pressure to form behind the leading edge on the upper surface of the object. In turn, due to this pressure gradient and the viscosity of the fluid, the flow over the object is accelerated down along the upper surface of the object. At the same time, the flow forced under the object is rapidly slowed or stagnated causing an area of high pressure. This also causes the flow to accelerate along the upper surface of the object. The two sections of the fluid each leave the trailing edge of the object with a downward component of momentum, producing lift.

6.2 Fluid Modeling

6.2.1 Introduction

As seen in Fig. 6.3, fluids on infinite control volume are experienced by two distinct types of force—a body (volume) force and a surface force. As increasing distance between interacting elements, Volume force like gravity decreases slowly and is capable of perfectly penetrating into the interior of a fluid. One consequence of the relatively slow variation of volume forces with position is that they act equally on fluid in a sufficiently small volume. The net force acting on the element becomes directly proportional to its control volume.

Suppose there is a fluid contained in a small volume element dV , total volume force acting at time t on it is expressed as $F(r, t)dV$. Surface forces are modeled as momentum transport within the fluid. Such transport comes from a combination of the mutual forces exerted by contiguous molecules, and momentum fluxes caused by relative molecular motion. The net surface force exerted by the fluid on the planar surface element, dS_j , can be expressed as:

$$\sigma_{ij}dS_j \quad (6.3)$$

where σ_{ij} are the local stress tensor and dS_j are the components of an arbitrary first-order tensor as surface elements.

The i -component of the total force acting on infinitesimal surface element is a combination of body force and surface force. That is, it is written by,

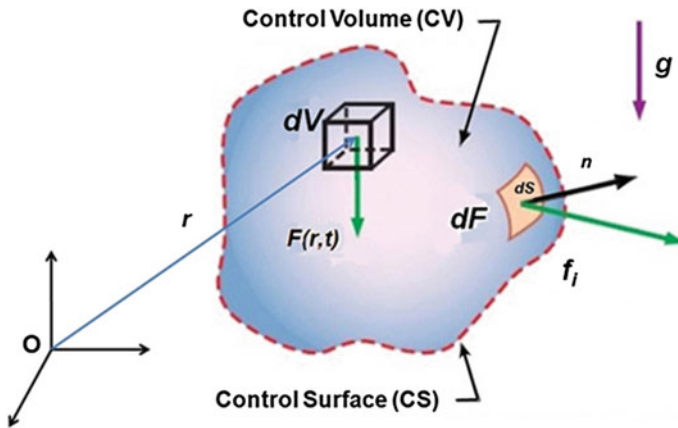


Fig. 6.3 Fluid Forces of a surface element on infinite control volume (or control surface)

$$f_i = f_V + f_S = \iiint_V F_i dV + \iint_S \sigma_{ij} dS_j \quad (6.4)$$

Here f_i is the force per volume, separated into those forces arising from volume force (f_V , long range) and from surface force (f_S , short range) with infinitesimal contribution dF .

If the tensor divergence theorem is used, Eq. (6.4) becomes

$$f_i = \iiint_V F_i dV + \iiint_V \frac{\partial \sigma_{ij}}{\partial x_j} dV \quad (6.5)$$

As we can take the limit where $V \rightarrow 0$, F_i and $\frac{\partial \sigma_{ij}}{\partial x_j}$ approach constant across the element. Both contributions on the right-hand side in Eq. (6.5) are $O(V)$. According to Newtonian dynamics, the i -component of the net force acting on the volume element is equal to the i -component of the rate of change of its linear momentum. However, if volume approaches infinitely smaller, the linear acceleration and mass density of the fluid are both approximately constant across the element. Therefore, the rate of change of the element's linear momentum also is $O(V)$. We know that the linear equation of motion on an infinitesimal fluid element places no particular restrictions on the stress tensor.

Suppose there is a fluid element enclosed by a surface S in a fixed volume V , the i -component of the total torque in the origin O of the coordinate system is expressed as:

$$\tau_i = \iiint_V \xi_{ijk} x_j F_k dV + \iint_S \xi_{ijk} x_j \sigma_{kl} dS_l \quad (6.6)$$

where the first and second terms on the right-hand side are due to volume and surface forces.

If the tensor divergence theorem is used, Eq. (6.6) becomes

$$\tau_i = \iiint_V \xi_{ijk} x_j F_k dV + \iiint_V \xi_{ijk} \frac{\partial(x_j \sigma_{kj})}{\partial x_j} dV \quad (6.7)$$

It can be modified as

$$\tau_i = \iiint_V \xi_{ijk} x_j F_k dV + \iiint_V \xi_{ijk} \sigma_{kj} dV + \iiint_V \xi_{ijk} x_j \frac{\partial \sigma_{kj}}{\partial x_j} dV \quad (6.8)$$

As the fluid particle is reduced to a point where $V \rightarrow 0$, we can assume that F_i , σ_{ij} and $\frac{\partial \sigma_{ij}}{\partial x_j}$ are all approximately constant across the element. Because $x \approx V^{1/3}$, the first, second, and third terms on the right-hand side of Eq. (6.8) is $O(V^{4/3})$, $O(V)$, and $O(V^{4/3})$, respectively.

According to Newtonian mechanics, the i -component of the total torque acting on the fluid element is equal to the i -component of the rate of change of its net angular momentum about O. Assuming that the linear acceleration and density of the fluid are approximately constant across the element, we deduce that the rate of change of its angular momentum is $O(V^{4/3})$.

We know that the rotational equation of motion of a fluid element depends on the second term on the right-hand side of Eq. (6.8). If not, the second term is zero. So it is applicable if

$$\xi_{ijk} \sigma_{kj} = 0 \quad (6.9)$$

From Eq. (6.9) we know that the stress tensor must be symmetric,

$$\sigma_{ji} = \sigma_{ij} \quad (6.10)$$

These six stress tensor (i.e., σ_{11} , σ_{22} , σ_{33} , σ_{12} , σ_{13} , and σ_{23}) are the independent components of a quantity. With reference to the principal axes, the diagonal components of the stress tensor σ_{ij} become principal stresses— σ'_{11} , σ'_{22} , and σ'_{33} .

In general, the orientation of the principal axes varies with position. The normal stress σ_{11}' acting across a surface element perpendicular to the first principal axis corresponds to a tension in the direction of that axis. It is same for σ'_{22} and σ'_{33} . Thus, the general state of the fluid can be regarded as a superposition of tensions or compressions at a particular point in space. Independent of the orientation of the principle axes, because the trace of the stress tensor, $\sigma_{ii} = \sigma_{11} + \sigma_{22} + \sigma_{33}$, is a scalar, the trace of the stress tensor at a given point is equal to the sum of the principal stresses,

$$\sigma_{ii} = \sigma'_{11} + \sigma'_{22} + \sigma'_{33} \quad (6.11)$$

Suppose that there is the surface forces exerted on the infinitesimal cubic volume element of a static fluid. The components of the stress tensor are approximately constant across the element. The sides of the cube are aligned parallel to the principal axes of the local stress tensor. This tensor, which has zero non-diagonal components, is the sum of two tensors,

$$\begin{pmatrix} \frac{1}{3}\sigma_{ii} & 0 & 0 \\ 0 & \frac{1}{3}\sigma_{ii} & 0 \\ 0 & 0 & \frac{1}{3}\sigma_{ii} \end{pmatrix} \quad (6.12)$$

And

$$\begin{pmatrix} \sigma'_{11} - \frac{1}{3}\sigma_{ii} & 0 & 0 \\ 0 & \sigma'_{22} - \frac{1}{3}\sigma_{ii} & 0 \\ 0 & 0 & \sigma'_{33} - \frac{1}{3}\sigma_{ii} \end{pmatrix} \quad (6.13)$$

Because the tensor (6.12) is isotropic, it corresponds to the normal force per unit area bound inward on each face of the volume element. This uniform compression changes the fluid element's volume with no its shape, which can be endured by the fluid element. The tensor (6.13) represents the departure of the stress tensor from an isotropic form. The diagonal components of this tensor have zero-sum in view of Eq. (6.11). It represents equal and opposite forces per unit area, acting on opposing faces of the volume element. The forces on at least one pair of opposing faces constitute a tension, and the forces on at least one pair constitute a compression. Such forces act to change the shape of the volume element: (1) a pure translation, (2) a pure strain along the principal axes and (3) a rotation (associated with the vorticity).

Moreover, this tendency cannot be offset by any volume force acting on the element, because such forces become arbitrarily small compared to surface forces ($V \rightarrow 0$). That is, in the limit that the element's volume tends to zero).

A fluid can be defined as a material that changes its shape for applied forces. It follows that if the diagonal components of the tensor (6.13) are non-zero anywhere in the fluid, the fluid at that point is moving. Hence, in a static fluid we conclude that the principal stresses, σ'_{11} , σ'_{22} , and σ'_{33} , must be equal to one another at all points. It means that the stress tensor has the isotropic form (6.12) in a stationary fluid. Irrespective of the orientation of the coordinate axes, the components of an isotropic tensor are rotationally invariant.

Because fluids at rest are in a state of compression without shear forces, the stress tensor must have only diagonal terms. The stress tensor of fluid can be expressed as:

$$\sigma_x = \sigma_y = \sigma_z = -p \quad (6.14)$$

According to Pascal's law, in a stationary fluid, the force per unit at a given point is the same in all directions. The pressure is normal to the surface on which it acts. Its magnitude is independent of the surface orientation. So this gives rise to the relatively simple form of the equation of motion for inviscid flow. The stress tensor is defined as,

$$\sigma_{ij} = -p\delta_{ij} \quad (6.15)$$

where $p = -\sigma_{ii}/3$ is the static pressure: that is, minus the normal stress acting in any direction.

When the fluid is moving the pressure, defined as the average normal force on a fluid element, the average normal stress is defined as $(\sigma_{11} + \sigma_{22} + \sigma_{33})/3 = \sigma_{ii}/3$. This is taken to be $-p$ in several otherwise fine texts but it is strictly true only for simple mono atomic gases. In general there is a discrepancy between the average normal stress and the pressure. It is convenient to define pressure in a moving fluid as minus the mean normal stress,

$$p = -\frac{1}{3}\sigma_{ii} \quad (6.16)$$

We can split the stress tensor in a moving fluid into two parts as the sum of an isotropic part, $p\delta_{ij}$ which tends to change the volume of the body in a static fluid, and a remaining non-isotropic part, τ_{ij} , which includes any shear stresses. Hence, the deviator tensor may be expressed as:

$$\sigma_{ij} = -p\delta_{ij} + \tau_{ij} \quad (6.17)$$

Since σ_{ij} and δ_{ij} are symmetric tensors, we know that τ_{ij} is symmetric,

$$\tau_{ji} = \tau_{ij} \quad (6.18)$$

The deviatoric stress tensor τ_{ij} is a consequence of fluid motion. It can be defined as the difference between the pressure and the total stress tensor. If a static fluid is at rest, the fluid appears stationary and the deviatoric stress tensor will be zero. If fluid is constant moving, it has a spatially uniform velocity field and the deviatoric stress tensor is also zero. Therefore, we know the deviatoric stress tensor is driven by velocity gradients within the fluid.

For Newtonian fluids, the relation between stress τ_{ij} and rate of strain $\partial v_i / \partial x_j$ are linear. That is,

$$\tau_{ij} = C_{ijkl} \frac{\partial v_k}{\partial x_l} \quad (6.19)$$

where C_{ijkl} is a coefficient tensor of rank 4.

In principle there are $3^4 = 81$ coefficients. Because there is independent of orientation in space, the fourth-order tensor C_{ijkl} is isotropic, i.e., the same in all rotated coordinate frames. The problem is how to find its fourth order equivalent. The most general expression for an isotropic fourth-order tensor is

$$C_{ijkl} = \alpha\delta_{ij}\delta_{kl} + \beta\delta_{ik}\delta_{jl} + \gamma\delta_{il}\delta_{jk} \quad (6.20)$$

where α , β , and γ are arbitrary scalars. From Eqs. (6.19) and (6.20) we know that it follows,

$$\tau_{ij} = \alpha \frac{\partial v_k}{\partial x_k} \delta_{ij} + \beta \frac{\partial v_i}{\partial x_j} + \gamma \frac{\partial v_j}{\partial x_i} \quad (6.21)$$

From Eq. (6.18), τ_{ij} is a symmetric tensor that $\beta = \gamma$,

$$\tau_{ij} = \alpha e_{kk}\delta_{ij} + 2\beta e_{ij} \quad (6.22)$$

where $e_{ij} = \frac{1}{2} \left(\frac{\partial v_i}{\partial x_j} + \frac{\partial v_j}{\partial x_i} \right)$ is called the *rate of strain tensor*.

Because τ_{ij} is a traceless tensor, we yields $3\alpha = -2\beta$.

$$\tau_{ij} = 2\mu \left(e_{ij} - \frac{1}{3} e_{kk} \delta_{ij} \right) \quad (6.23)$$

where $\mu = \beta$.

From Eq. (6.17) the stress tensor in an isotropic Newtonian fluid is expressed as:

$$\sigma_{ij} = -p\delta_{ij} + 2\mu \left(e_{ij} - \frac{1}{3} e_{kk} \delta_{ij} \right) \quad (6.24)$$

where p and μ are arbitrary scalars.

For simple shearing motion the viscosity coefficient μ can be obtained from Eq. (6.23). With $\frac{\partial v_1}{\partial x_2}$ as the only non-zero velocity derivative, all of the components of τ_{ij} are zero apart from the shear stresses

$$\tau_{12} = \tau_{21} = \mu \frac{\partial v_1}{\partial x_2} \quad (6.25)$$

When parallel plane layers of fluid slide over one another, the coefficient μ is the constant of proportionality between the rate of shear and the tangential force per unit area. The force acting between layers of fluid undergoing slide motion tends to oppose the motion, which implies that $\mu > 0$.

6.2.2 Conservation Laws for Mass and Momentum

Suppose that some bulk fluid property θ in mass or momentum is a non-negative density. The total amount of the property contained in the fixed volume V is

$$\Theta = \int_V \theta dV \quad (6.26)$$

where the integral is taken over all elements of control volume V .

Let dS be an outward directed element of the bounding surface of V . The volume of fluid that flows per second across the element is $v \cdot dS$. Thus, the amount of the fluid property that is convected across the element per second is $\theta v \cdot dS$. Finally, convected out of volume V by fluid flow across its bounding surface S , the net amount of the property is

$$\Phi_\Theta = \oint_S \theta v \cdot dS \quad (6.27)$$

where the integral is taken over all outward elements of S .

Suppose that the property in question is created within the volume V at the rate S_θ per second. The conservation equation for the fluid property takes the form

$$\frac{d\Theta}{dt} = S_\Theta - \Phi_\Theta \quad (6.28)$$

where Φ_Θ is termed the flux of the property out of V , S_Θ is called the net generation rate of the property within V .

That is, the increasing rate in the property amount contained in V is the difference between the generation rate of the property in V , and the rate at which the property is convected out of V by fluid flow.

6.2.2.1 Mass Conservation

Supposed that there is a fixed volume V , surrounded by a surface S , the mass m of a fluid with density ρ in a volume V is expressed as:

$$m = \iiint_V \rho dV \quad (6.29)$$

where dV is an element of V . The mass is flowing across S and out of V is

$$\Phi_m = \iint_S \rho v \cdot dS \quad (6.30)$$

where dS is an outward directed element of S .

Suppose that mass is being added or subtracted from space in a given time. Mass conservation requires that the increasing rate of the mass contained in V , adding the net mass flux out of V , should equal zero,

$$\frac{dm}{dt} + \Phi_m = 0 \quad (6.31)$$

Supposed that there is no mass generation in V , mass conservation simply can be described as:

$$\iiint_V \frac{\partial \rho}{\partial t} dV + \iint_S \rho v \cdot dS = 0 \quad (6.32)$$

If the divergence theorem is used, Eq. (6.32) becomes

$$\iiint_V \left[\frac{\partial \rho}{\partial t} + \nabla \cdot (\rho v) \right] dV = 0 \quad (6.33)$$

So Eq. (6.33) will hold for any control volume, That is,

$$\frac{\partial \rho}{\partial t} + \nabla \cdot (\rho v) = 0 \quad (6.34)$$

The quantity $\partial \rho / \partial t$ represents the time derivative of the fluid mass density at the fixed point r . If we steady flow is assumed, the time derivative of the density will be zero. Equation (6.34) is called the equation of continuity.

6.2.2.2 Navier-Stokes Equation

Consider a property γ (e.g. temperature, density, velocity component) of the fluid element in space. In general, this will depend on the time, t , and on the position (x, y, z) of the fluid element at that time. In a small time δt , suppose that the element moves from (x, y, z) to $(x + \delta x, y + \delta y, z + \delta z)$. It contains exactly the same material at the two times. But there will be a corresponding small change in γ , denoted by $\delta \gamma$. For example, the rate of change of the density $\rho = \rho(x, t)$ of a particle instantaneously at x is

$$\frac{D\rho}{Dt} = \left(\frac{\partial \rho}{\partial t} \right) + \left(\frac{\partial \rho}{\partial x} \right) \left(\frac{\partial x}{\partial t} \right) + \left(\frac{\partial \rho}{\partial y} \right) \left(\frac{\partial y}{\partial t} \right) + \left(\frac{\partial \rho}{\partial z} \right) \left(\frac{\partial z}{\partial t} \right) = \frac{\partial \rho}{\partial t} + \nu \cdot \nabla \rho \quad (6.35)$$

If the continuity Eq. (6.34) is combined, it can be rewritten as:

$$\frac{1}{\rho} \frac{D\rho}{Dt} = \frac{D \ln \rho}{Dt} = -\nabla \cdot \nu \quad (6.36)$$

Supposed that there is a volume element V that is moving with the fluid. As the fluid element in volume is convected, we can use the divergence theorem. That is,

$$\frac{DV}{Dt} = \oint_S v \cdot dS = \oint_S v_i dS_i = \iiint_V \frac{\partial v_i}{\partial x_i} dV = \iiint_V \nabla \cdot v dV \quad (6.37)$$

where S is the bounding surface of the fluid element.

As we take the limit where $V \rightarrow 0$, $\nabla \nu$ will be approximately constant across the element. Then we obtain,

$$\frac{1}{V} \frac{DV}{Dt} = \frac{D \ln V}{Dt} = \nabla \cdot \nu \quad (6.38)$$

Hence, we conclude that the divergence of the fluid velocity at a given point in space specifies the fractional rate of increase in the volume of an infinitesimal co-moving fluid element at that point. Supposed that a surface S surrounds a fixed volume V , the i -component of total linear momentum contained in V is

$$P_i = \iiint_V \rho v_i dV \quad (6.39)$$

The flux of i -momentum across S is

$$\Phi_i = \oint_S \rho v_i v_j dS_j \quad (6.40)$$

Momentum conservation holds that the increasing rate of the net i -momentum of the fluid contained in V , adding the flux of i -momentum out of V , is equal to the rate of i -momentum generation in V . From Newton's second law of motion, the latter quantity is equal to the i -component of the net force acting on the fluid bounded in V . Thus, we obtain

$$\frac{dP_i}{dt} + \Phi_i = f_i \quad (6.41)$$

Finally, the i-component of the net force acting on the fluid in V is redefined as:

$$\iiint_V \frac{\partial(\rho v_i)}{\partial t} dV + \iint_S \rho v_i v_j dS_j = \iiint_V F_i dV + \iint_S \sigma_{ij} dS_j \quad (6.42)$$

Because the volume V is non-time-varying and the divergent theorem is used, Eq. (6.42) becomes

$$\iiint_V \left[\frac{\partial(\rho v_i)}{\partial t} + \frac{\partial(\rho v_i v_j)}{\partial x_j} \right] dV = \iiint_V \left[F_i + \frac{\partial \sigma_{ij}}{\partial x_j} \right] dV \quad (6.43)$$

Rearranging Eq. (6.43), we obtain

$$\left(\frac{\partial \rho}{\partial t} + v_j \frac{\partial \rho}{\partial x_j} + \rho \frac{\partial v_j}{\partial x_j} \right) v_i + \rho \left(\frac{\partial v_i}{\partial t} + v_j \frac{\partial v_i}{\partial x_j} \right) = F_i + \frac{\partial \sigma_{ij}}{\partial x_j} \quad (6.44)$$

From the continuity Eq. (6.34), the first term in tensor notation is

$$\frac{\partial \rho}{\partial t} + v_j \frac{\partial \rho}{\partial x_j} + \rho \frac{\partial v_j}{\partial x_j} = 0 \quad (6.45)$$

So we obtain the following fluid equation of motion,

$$\rho \left(\frac{\partial v_i}{\partial t} + v_j \frac{\partial v_i}{\partial x_j} \right) = F_i + \frac{\partial \sigma_{ij}}{\partial x_j} \quad (6.46)$$

If Eqs. (6.24) and (6.46) are combined, the equation of fluid motion for an isotropic and Newtonian fluid is expressed as:

$$\rho \frac{Dv_i}{Dt} = F_i - \frac{\partial p}{\partial x_i} + \frac{\partial}{\partial x_j} \left[\mu \left(\frac{\partial v_i}{\partial x_j} + \frac{\partial v_j}{\partial x_i} \right) \right] - \frac{\partial}{\partial x_i} \left(\frac{2}{3} \mu \frac{\partial v_j}{\partial x_j} \right) \quad (6.47)$$

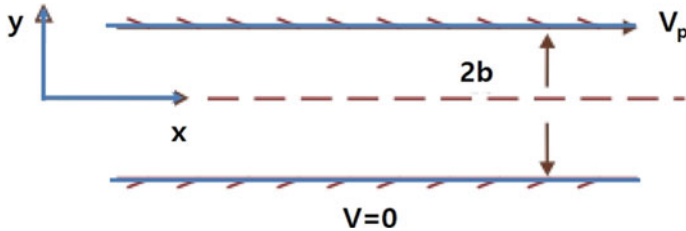
This equation is generally known as the Navier-Stokes equation. If there are no strong temperature gradients in the fluid, the Navier-Stokes equation can be simplified:

$$\rho \frac{Dv_i}{Dt} = F_i - \frac{\partial p}{\partial x_i} + \mu \left(\frac{\partial^2 v_i}{\partial x_j \partial x_j} + \frac{1}{3} \frac{\partial^2 v_j}{\partial x_i \partial x_j} \right) \quad (6.48)$$

And vector form for Eq. (6.48) becomes,

$$\rho \frac{Dv}{Dt} \equiv \rho \left[\frac{\partial v}{\partial t} + (v \cdot \nabla) v \right] = F - \nabla p + \mu \left[\nabla^2 v + \frac{1}{3} \nabla (\nabla \cdot v) \right] \quad (6.49)$$

Example 6.2 Consider the steady-state 2D-flow of an incompressible Newtonian fluid in a long horizontal rectangular channel. The bottom surface is stationary, whereas the top surface is moved horizontally at the constant velocity, V_p . Determine the velocity field in the channel. Assume fully developed flow.



Assumption: (1) Newtonian fluid and Navier-Stokes equation is applicable, (2) Two-dimensional flow, and (3) Fully developed flow.

$$\text{Apply continuity: } \frac{\partial \rho}{\partial t} + \nabla \cdot (\rho v) = 0 \Rightarrow \frac{\partial V_x}{\partial x} + \frac{\partial V_y}{\partial y} = 0$$

For fully developed flow, first term is zero. V_y is constant along y direction. But V_y at $y = \pm b$ (no-slip condition).

$$\rho \left[\frac{\partial V_x}{\partial t} + V_x \frac{\partial V_x}{\partial x} + V_y \frac{\partial V_x}{\partial y} \right] = - \frac{\partial p}{\partial x} + \mu \left[\frac{\partial^2 V_x}{\partial x^2} + \frac{\partial^2 V_x}{\partial y^2} \right]$$

1st term is zero for steady state; $\partial V_x / \partial x$ for fully developed flow; $V_y = 0$. Therefore,

$$0 = - \frac{\partial p}{\partial x} + \mu \frac{\partial^2 V_x}{\partial y^2}$$

If no external pressure was applied for a long plate, $\partial p / \partial x$ will be 0

$$\mu \frac{\partial^2 V_x}{\partial y^2} = 0$$

Integrate twice,

$$\mu V_x = C_1 y + C_2$$

From boundary conditions: (1) $y = -b$, $V_x = 0$ (no slip condition), (2) $y = b$, $V_x = V_p$

Solving for velocity profiles in a Couette flow

$$V_x = \frac{V_p}{2} \left(1 + \frac{y}{b} \right)$$

6.2.3 Bernoulli's Equation

The beginning part of the eighteenth century saw the golden age of theoretical fluid dynamics, studied by the work of Johann and Daniel Bernoulli and, in particular, by Leonhard Euler. At this time the relation between pressure and velocity in an inviscid and incompressible flow was first understood. The resulting equation is $p + \frac{1}{2}\rho V^2 = \text{const}$, which is called Bernoulli's equation. Though Euler first presented it, Bernoulli's equation is one of the most famous equation in fluid dynamics.

Consider the x component of the momentum from Navier-Stokes Eq. (6.49). For an inviscid flow with no body forces, this equation becomes

$$\rho \frac{Du}{Dt} = -\frac{\partial p}{\partial x} \quad (6.50)$$

For steady flow, Eq. (6.50) is then written as

$$u \frac{\partial u}{\partial x} + v \frac{\partial u}{\partial y} + w \frac{\partial u}{\partial z} = -\frac{1}{\rho} \frac{\partial p}{\partial x} \quad (6.51)$$

Multiply Eq. (6.51) by dx :

$$u \frac{\partial u}{\partial x} dx + v \frac{\partial u}{\partial y} dx + w \frac{\partial u}{\partial z} dx = -\frac{1}{\rho} \frac{\partial p}{\partial x} dx \quad (6.52)$$

Supposed that there is the flow along a streamline in three-dimensional space, we can substitute $udz - wdx = 0$, $vdx - udy = 0$ into Eq. (6.52). We have

$$u \left(\frac{\partial u}{\partial x} dx + \frac{\partial u}{\partial y} dy + \frac{\partial u}{\partial z} dz \right) = -\frac{1}{\rho} \frac{\partial p}{\partial x} dx \quad (6.53)$$

From calculus that given a function $u = u(x, y, z)$, Eq. (6.53) is written as

$$udu = \frac{1}{2} d(u^2) = -\frac{1}{\rho} \frac{\partial p}{\partial x} dx \quad (6.54)$$

In a similar fashion, from the y and z component of the momentum equation, we have

$$\frac{1}{2}d(v^2) = -\frac{1}{\rho}\frac{\partial p}{\partial y}dy \quad (6.55)$$

$$\frac{1}{2}d(w^2) = -\frac{1}{\rho}\frac{\partial p}{\partial z}dz \quad (6.56)$$

If adding Eqs. (6.54) through (6.56), we can yields

$$\frac{1}{2}d(u^2 + v^2 + w^2) = -\frac{1}{\rho}\left(\frac{\partial p}{\partial x}dx + \frac{\partial p}{\partial y}dy + \frac{\partial p}{\partial z}dz\right) \quad (6.57)$$

Here the following can be redefined as,

$$u^2 + v^2 + w^2 = V^2 \quad (6.58)$$

$$\frac{\partial p}{\partial x}dx + \frac{\partial p}{\partial y}dy + \frac{\partial p}{\partial z}dz = dp \quad (6.59)$$

If substituting Eqs. (6.58) and (6.59) into (6.57), we have

$$dp = -\rho V dV \quad (6.58)$$

Equation (6.58) is called Euler's equation for an inviscid flow with no body forces. It relates the velocity change along a streamline dV to the pressure change dp along the same streamline. If easily integrated between any two points 1 and 2 along a streamline with $p = \text{constant}$, we have

$$p_1 + \frac{1}{2}\rho V_1^2 = p_2 + \frac{1}{2}\rho V_2^2 \quad (6.59)$$

Equation (6.59) is Bernoulli's equation, which relates P_1 and V_1 at point 1 on a streamline to P_2 and V_2 at another point 2 on the same streamline. Equation (6.59) can also be written as

$$p + \frac{1}{2}\rho V^2 = \text{const} \quad (6.60)$$

6.3 Viscous Flow and Boundary Layers

6.3.1 Introduction

Viscous relates to the internal friction in a fluid. The effects of viscosity in aerodynamics are an inherent property of any real fluid, although it is necessary to study

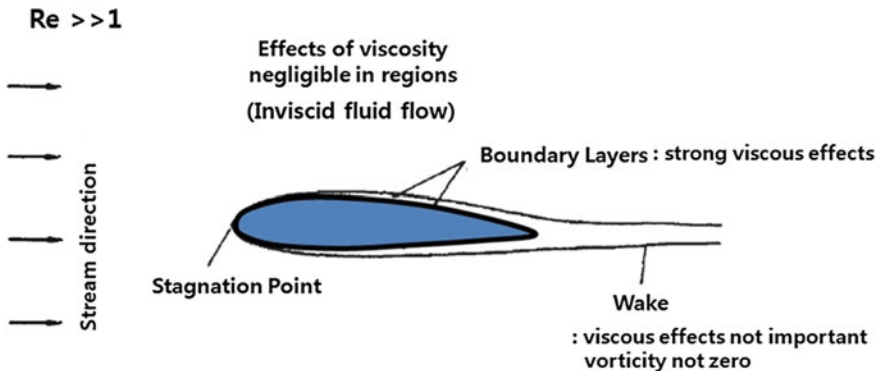


Fig. 6.4 Flow field around a body of reasonably slender form

inviscid fluid flow. In fluid mechanics, a boundary layer also is an important concept and refers to thin region adjacent to surface of a body where viscous forces dominate over inertia forces. The study of a boundary layer by engineers dates back to the beginning of the previous century (1904) when Prandtl contrived the idea of the boundary layer. To understand this concept, consider the flow of a fluid past a body of airfoil (Fig. 6.4).

In aerodynamics the fluid viscosity is relatively small because the Reynolds number is high. Unless the transverse velocity gradients are significant, the shearing stresses developed will be fairly small. Studies of flows past a body of airfoil show that the transverse velocity gradients are negligibly small throughout the flow field. In these boundary layers, however, large shearing velocities are generated with subsequent shearing stresses of significant magnitude.

The intermolecular forces between solids and fluids lead to the assumption that there is a condition of no slip that the relative velocity of the fluid tangential to the surface is everywhere zero. That is, the velocity of the first fluid layer close to the surface is moving with the same velocity as the surface one. Since the main stream velocity at a small distance from the surface in aerodynamics is significantly high, the shearing velocity gradients in this boundary region exist.

Since the entire lifting force is originated in normal pressures around the aerofoil surface, we can calculate the lift force from the inviscid flow that there is a flow field outside the boundary layers. The drag force is mainly due to the shearing stresses of the body surface in the boundary-layer. The equations of viscous motion can be simplified from Prandtl's boundary-layer concept. However, it is complex for engineer to understand the concepts of boundary layer and predict its behavior. To gain insight on the flow field, we have to study the boundary behavior based on the previous studies.

6.3.2 The Boundary-Layer Characteristics

Supposed that there is a flow around bluff body with a sharp leading edge, the boundary layer on any surface will grow from zero thickness at the leading edge of the body. For a typical aerofoil shape, boundary layers will develop from the front stagnation point. On proceeding downstream along a surface, large shearing gradients and stresses will develop adjacent to the surface because of the relatively large velocities in the main stream and no slip condition at the surface. As the fluid near the surface passes downstream, the boundary layer of retarded fluid grows in thickness.

Consider a small element of fluid, having a unit length δx in the direction of motion and a thickness δy normal to the flow direction. The shearing stress on the lower face AB is $\tau = \mu \frac{\partial u}{\partial y}$, while the shearing stress on the upper face CD is $\tau + \frac{\partial \tau}{\partial y} \delta y$, assuming u is increasing with y . Thus the resultant shearing force in the x-direction is $(\tau + \frac{\partial \tau}{\partial y} \delta y) - \tau = \frac{\partial \tau}{\partial y} \delta y$ where $\tau = \mu \frac{\partial u}{\partial y}$. The net shear force on the element $= (\mu \frac{\partial^2 u}{\partial y^2}) \delta y$. Unless μ be zero, it follows that $\frac{\partial^2 u}{\partial y^2}$ is finite and therefore the rate of change of the velocity gradient in the boundary layer must also be continuous.

For the stream-wise pressure forces acting on the fluid element, the net pressure force is $(\frac{\partial p}{\partial x}) \delta x$. Because total thickness of the boundary layer is very small, the pressure hardly varies a normal to the surface. Consequently, the net transverse pressure force is zero to a very good approximation. At this stage it is assumed that $\frac{\partial p}{\partial x} = 0$ (Fig. 6.5).

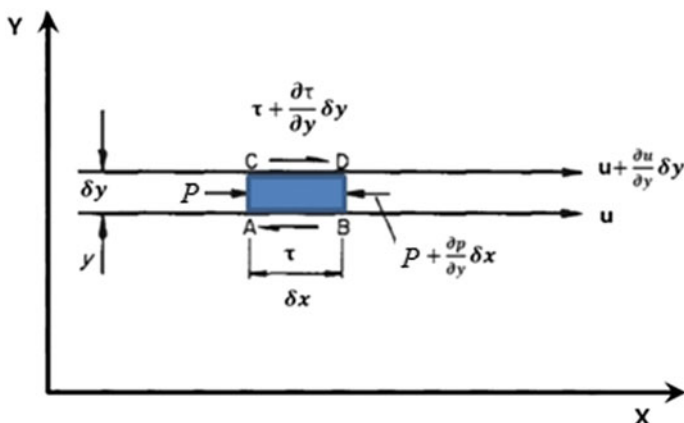


Fig. 6.5 The stream-wise pressure forces acting on the fluid element

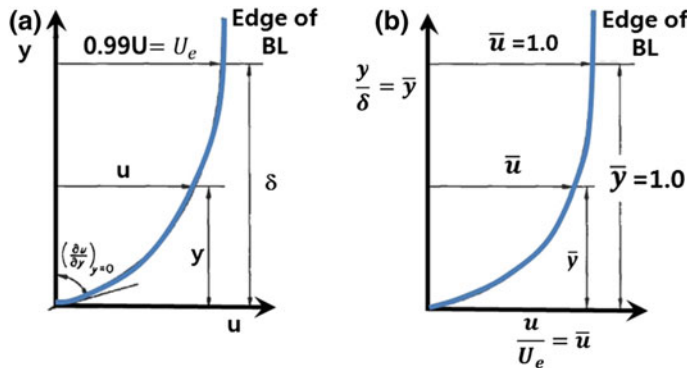


Fig. 6.6 A smooth curve of the general form $u(y)$

If the velocity u is plotted against the distance y , a smooth curve of the general form shown in Fig. 6.6a will develop. At the surface the curve is not tangential to the u axis because of an infinite gradient $\frac{\partial u}{\partial y}$. Therefore there is an infinite shearing stress at the surface. As the shearing gradient decreases at some distance from the surface, the retarding action decreases. When $\frac{\partial u}{\partial y}$ becomes very small, the shear stress becomes negligible, although theoretically a small gradient must exist out to $y = \infty$.

The thickness of boundary layer δ is a distance from the surface such that the velocity u is 99% of the local mainstream velocity U . To compare boundary-layer profiles of different thickness, the profile shape can be non-dimensionally expressed by writing $\bar{u} = \frac{u}{U_e}$, and $\bar{y} = \frac{y}{\delta}$. The profile shape is given by $\bar{u} = f(\bar{y})$. Over the range $y = 0$ to $y = \delta$, the velocity parameter \bar{u} varies from 0 to 0.99 (Fig. 6.6b).

In boundary-layer flows there are two different regimes (1) laminar flow, and (2) turbulent flow. In laminar flow the layers of fluid slide smoothly over one another and there is no interchange of fluid mass between adjacent layers. On the contrary, in turbulent flow there is a significant seemingly random motion, in the form of velocity fluctuations both along the mean direction of flow and perpendicular to it. As a result, there are considerable transports of mass between adjacent layers. Owing to these fluctuations the velocity profile frequently varies with time. A time-averaged, or mean, velocity profile might be defined. As there is a mean velocity gradient in the flow, there will be corresponding interchanges of stream-wise momentum between the adjacent layers that will result in shearing stresses. These shearing stresses are of much greater magnitude than those developed from the result of purely viscous action. The velocity profile in a turbulent boundary layer is significantly controlled by these Reynolds stresses.

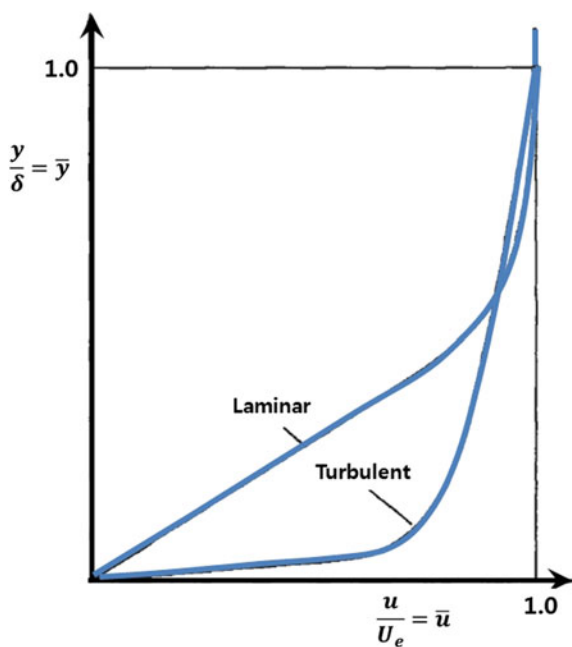
The velocity profiles between laminar and turbulent flow due to shearing stresses are different. They are those representatives of a flat plate where there is no streamwise pressure gradient. In the laminar boundary layer, energy of the main stream is conveyed to the low velocity fluid near the surface through the viscosity

and its small penetration. As the boundary-layer flow reduces considerably velocity, the shearing stress τ is given by $\tau = \mu \frac{\partial u}{\partial y}$ and the shearing stress at wall is $\tau_w = \mu \left(\frac{\partial u}{\partial y} \right)_{y=0}$.

In the turbulent boundary layer, Reynolds stresses are due to mass interchanges in a direction perpendicular to the surface so that energy from the main stream easily penetrates to fluid layers near the surface. Because of them, the turbulent boundary can get out of the direct influence of the wall having a velocity that is not much less than that of the mainstream. Because the velocity fluctuations perpendicular to the wall are evidently damped out, the flow is a viscous flow in a very limited region immediately adjacent to the surface—viscous sub-layer. As the shearing action becomes purely viscous, the velocity falls very sharply, almost linearly, within it, to zero at the surface. Since the wall shearing stress at the surface depends on viscosity only, i.e. $\tau_w = \mu \left(\frac{\partial u}{\partial y} \right)_w$, the surface friction stress in a turbulent layer will be much greater than that in a laminar layer (Fig. 6.7).

A laminar boundary layer starts to develop from the leading edge. It gradually grows in thickness from zero at the leading edge to constant on the surface where a transition to turbulence occurs rapidly. Under the influence of some destabilizing factors, the boundary layer becomes unstable and transits to a turbulent flow. This transition also is accompanied by a corresponding rapid thickening of the layer. Beyond this transition region, the turbulent boundary layer continues to thicken steadily. Because of the greater shear stresses in the turbulent boundary layer its

Fig. 6.7 Typical laminar-layer profile and a typical turbulent layer profile



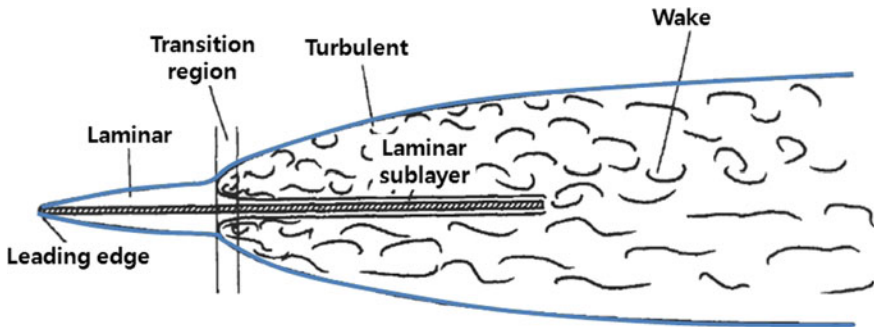


Fig. 6.8 The boundary layer developed on the surface of a flat plate

thickness is greater than that for a laminar one. At the trailing edge the boundary layer joins with the one from the other surface to form a wake of retarded velocity (Fig. 6.8).

On a flat plate, because the laminar profile has a constant shape at each point along the surface, one non-dimensional relationship for velocity profile can sufficiently be expressed as $\bar{u} = f(\bar{y})$. It also is applicable to that of the turbulent layer. Due to much work both theoretically and experimentally, profile shape on flat-plate boundary-layer studies can simplify. However, in most aerodynamic problems, the surface is of a streamline form such as a wing or fuselage. The major difference, affecting the boundary layer flow in these cases, is that the mainstream velocity and hence the pressure in a stream-wise direction is no longer constant.

The net stream-wise force acting on a small fluid element in the boundary layer is $\frac{\partial \tau}{\partial y} \delta y - \frac{\partial p}{\partial x} \delta x$. When the pressure decreases, the velocity along the edge of the boundary layer will increase. The external pressure gradient is said to be favorable. Because $\frac{\partial p}{\partial x} < 0$, noting that $\frac{\partial \tau}{\partial y} < 0$. The stream-wise pressure forces help to counter the effects of the shearing action and shear stress at the wall. Consequently, the flow is not decelerated so markedly at the wall, leading to a fuller velocity profile, and the boundary layer grows more slowly along the surface than for a flat plate.

On the other hands, when the pressure increases, mainstream velocity will decrease along the surface. The external pressure gradient is un-favorable. The pressure forces reinforce the effects of the shearing action and shear stress at the wall. Consequently, the flow decelerates significantly near the wall and the boundary layer grows more rapidly than in the case of the flat plate. Under these circumstances the velocity profile is much less full than for a flat plate and develops a point of inflexion. If the adverse pressure gradient is sufficiently strong or prolonged, the flow near the wall is much decelerated that it begins to reverse direction. Flow reversal indicates that the boundary layer has separated from the surface (Fig. 6.9).

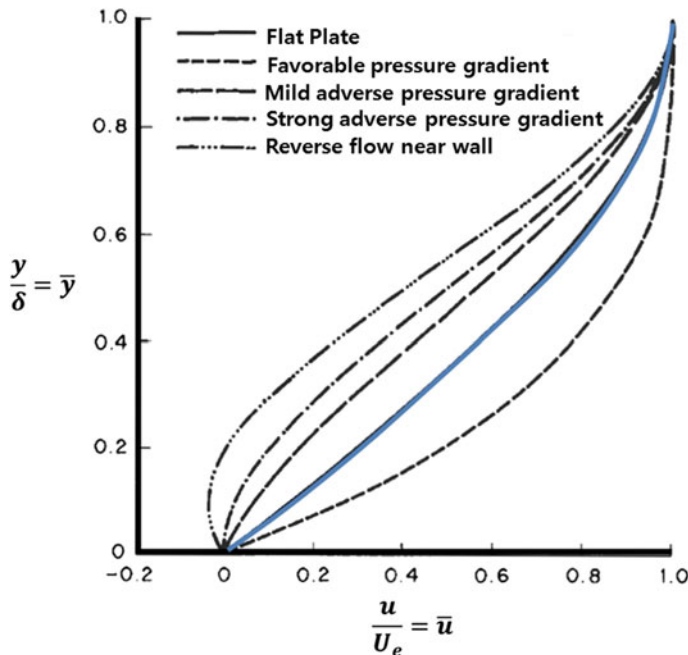


Fig. 6.9 Effect of external pressure gradient on the velocity profile in the boundary layer

6.3.3 The Boundary-Layer Equations

If Reynolds number over a flat plate is infinite, the flow becomes simple. The streamlines are everywhere parallel to the flat plate and equal to U_∞ , at the free stream infinitely far from the plate. There would be no drag since the shear stress at the wall is zero. From experiments on flat plates the potential flow solution at high Reynolds number is a good approximation. Even though the drag at high Reynolds number is very small in applications of aerodynamics, it is very important to estimate how much it is.

Prandtl explained how the Navier-Stokes equations may be simplified for application in the boundary layer. He assumed that the potential flow is a good approximation everywhere except in a thin boundary layer. Because the boundary layer is thin significantly, it does not affect the flow outside it. The flow velocity at the edge of the boundary layer is a good approximation for the flow velocity along the surface. For the flat plate, the velocity at the edge of the boundary layer is U_∞ . In the flow over a streamlined body, the velocity at the edge of boundary layer varies and is denoted by U_e .

At high Reynolds numbers the boundary-layer thickness, δ , is very small when compared with the length, L , of the plate (or streamlined body). Hypothetically, we can assume that $Re_L \rightarrow \infty$, $\delta \rightarrow 0$. Thus if the small parameter ε is introduced,

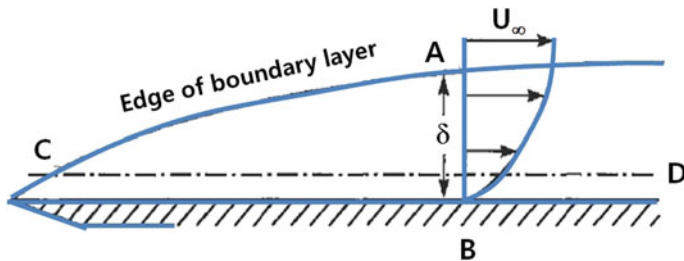


Fig. 6.10 The changes across the boundary layer along line AB

$$\varepsilon = \frac{1}{Re_L} \quad (6.61)$$

We would expect that $\delta \rightarrow 0$, so that

$$\frac{\delta}{L} \propto \varepsilon^n \quad (6.62)$$

where n is a positive exponent that is to be determined.

If the boundary layer along line AB in Fig. 6.10 changes, we can estimate the magnitude of velocity gradient within the laminar boundary layer. An approximation is roughly expressed as,

$$\frac{\partial u}{\partial y} \cong \frac{U_\infty}{\delta} = \frac{U_\infty}{L} \frac{1}{\varepsilon^n} \quad (6.63)$$

Although this is very rough, it is valid for the high Reynolds number. Using a special symbol for the approximation, this is recognized as:

$$\frac{\partial u}{\partial y} = O\left(\frac{U_\infty}{L} \frac{1}{\varepsilon^n}\right) \quad (6.64)$$

For a streamlined body, we use x to denote the distance along the surface from the leading edge (or stagnation point) and y to be the distance along the local normal to the surface. Since the boundary layer is very thin, its thickness is much smaller than the local radius of curvature of the surface. We can use the Cartesian form, Eq. (6.49), of the Navier-Stokes equations.

Because the velocity varies along the edge of the boundary layer, we can replace U_∞ with U_e .

$$\frac{\partial u}{\partial y} = O\left(\frac{U_e}{\delta}\right) = O\left(\frac{U_e}{L} \frac{1}{\varepsilon^n}\right) \quad (6.65)$$

Equation (6.65) can apply to a boundary layer around a streamlined body. Engineers think of $O(U_e/\delta)$ as meaning order of magnitude of U_e/δ . We can estimate $\frac{\partial u}{\partial y}$ directly.

To estimate this quantity $\frac{\partial u}{\partial x}$, we should consider the changes along the line CD in Fig. 6.10. Evidently, we know that $u = U_\infty$, at C. But as D approach from the leading edge of the plate, $u \rightarrow 0$. The total change of u along the line CD is $U_\infty - 0$. Because total distance is $\Delta x \cong L$, this quantity $\frac{\partial u}{\partial x}$ can be expressed as

$$\frac{\partial u}{\partial x} = O\left(\frac{U_e}{L}\right). \quad (6.66)$$

To estimate $\frac{\partial^2 u}{\partial y^2}$ along the vertical line AB, At B the estimate for $\frac{\partial u}{\partial y}$ holds Eq. (6.66) whereas at A, $\frac{\partial u}{\partial y} \cong 0$. Therefore, the total change of $\frac{\partial u}{\partial y}$ over a distance δ is approximately $\frac{U_\infty}{\delta} - 0$. In the general case we obtain,

$$\frac{\partial^2 u}{\partial y^2} = O\left(\frac{U_e}{\delta^2}\right) = O\left(\frac{U_e}{L^2} \varepsilon^{2n}\right) \quad (6.67)$$

In a similar way we deduce that

$$\frac{\partial^2 u}{\partial x^2} = O\left(\frac{U_e}{L^2}\right) \quad (6.68)$$

We begin with two dimensional continuity Eq. (6.34),

$$\underbrace{\frac{\partial u}{\partial x}}_{O(U_e/L)} + \underbrace{\frac{\partial v}{\partial y}}_{O(v/(L \varepsilon^n))} = 0 \quad (6.69)$$

To have the same order of magnitude for both terms, we can deduce from Eq. (6.69) that

$$v = O\left(U_e \frac{\delta}{L}\right) = O(U_e \varepsilon^n) \quad (6.70)$$

Because the slope of the streamlines in the boundary layer is equal to $\frac{v}{u}$, it will be given $\frac{\delta}{L}$. We know that Eq. (6.70) is correct. Assume steady flow, no body-force, and divide throughout by ρ (noting that the kinematic viscosity $v = \frac{\mu}{\rho}$), we will now use Eqs. (6.65)–(6.68) and (6.70) to estimate the orders of magnitude of the terms in two dimensional Navier-Stokes Eqs. (6.49). That is,

$$\underbrace{u \frac{\partial u}{\partial x}}_{O(U_e^2/L)} + \underbrace{v \frac{\partial u}{\partial y}}_{O(U_e^2/L)} = - \underbrace{\frac{1}{\rho} \frac{\partial p}{\partial x}}_{O(\text{unknown})} + \underbrace{v \left(\frac{\partial^2 u}{\partial x^2} \right)}_{O(vU_e/L^2) = O(\varepsilon U_e^2/L)} + \underbrace{v \left(\frac{\partial^2 u}{\partial y^2} \right)}_{O(vU_e/(L^2\varepsilon^{2n})) = O(\varepsilon^{1-2n}U_e^2/L)} \quad (6.71)$$

$$\underbrace{u \frac{\partial v}{\partial x}}_{O(\varepsilon^n U_e^2/L)} + \underbrace{v \frac{\partial v}{\partial y}}_{O(\varepsilon^n U_e^2/L)} = - \underbrace{\frac{1}{\rho} \frac{\partial p}{\partial y}}_{O(\text{unknown})} + \underbrace{v \left(\frac{\partial^2 v}{\partial x^2} \right)}_{O(vU_e\varepsilon^n/L^2) = O(\varepsilon^{1+n}U_e^2/L)} + \underbrace{v \left(\frac{\partial^2 v}{\partial y^2} \right)}_{O(vU_e/(L^2\varepsilon^n)) = O(\varepsilon^{1-n}U_e^2/L)} \quad (6.72)$$

Now $\varepsilon = 1/Re_L$ is a very small quantity so that a quantity of $O(\varepsilon U_e^2/L)$ is negligible compared with one of $O(U_e^2/L)$. It therefore follows that the second term on the right-hand side of Eq. (6.71) can be dropped in comparison with the terms on the left-hand side. What about the third term on the right-hand side of Eq. (6.71)? If $2n = 1$, it will be the same order of magnitude as those on the left-hand side. If $2n < 1$, this remaining viscous term will be negligible compared with the left-hand side. This cannot be so, because we know that the viscous effects are not negligible within the boundary layer. On the other hand, if $2n > 1$, the terms on the left-hand side of Eq. (6.71) will be negligible in comparison with the remaining viscous term.

For the flat plate for which $\frac{\partial p}{\partial x} \equiv 0$, Eq. (6.71) reduces to $\frac{\partial^2 u}{\partial y^2} = 0$. This can be readily integrated to give $u = f(x)y + g(x)$.

Note that, as it is a partial derivative, arbitrary functions of x , $f(x)$ and $g(x)$, take the place of constants of integration. In order to satisfy the no-slip condition ($u = 0$) at the surface, $y = 0$, $g(x) = 0$, so that $u \propto y$. This does not conform to the required smooth velocity profile depicted in Fig. 6.6.

We therefore conclude that the only possibility that fits the physical requirements is

$$2n = 1 \quad \text{implying} \quad \delta \propto \varepsilon^{1/2} \left(= \frac{1}{\sqrt{Re_L}} \right) \quad (6.73)$$

And Eq. (6.71) simplifies to

$$u \frac{\partial u}{\partial x} + v \frac{\partial u}{\partial y} = - \frac{1}{\rho} \frac{\partial p}{\partial x} + v \left(\frac{\partial^2 u}{\partial x^2} \right) \quad (6.74)$$

It is now plain that all the terms in Eq. (6.72) must be $O(\varepsilon^{0.5}U_e^2/L)$ or even smaller and are therefore negligibly small compared to the terms retained in Eq. (6.74). We therefore conclude that Eq. (6.72) simplifies to

$$\frac{\partial p}{\partial y} \cong 0 \quad (6.75)$$

This implies that p can be determined in advance from the potential-flow solution and depends only on x . Equation (6.74) can be expressed as:

$$u \frac{\partial u}{\partial x} + v \frac{\partial u}{\partial y} = - \underbrace{\frac{1}{\rho} \frac{\partial p}{\partial x}}_{\text{a known function of } x} + v \left(\frac{\partial^2 u}{\partial x^2} \right) \quad (6.76)$$

Equations (6.69) plus (6.76) are usually known as the Prandtl boundary-layer equations. To sum up, the velocity profiles within the boundary layer can be obtained as follows: (i) Determine the potential flow around the body; (ii) From this potential-flow solution determine the pressure and the velocity along the surface; (iii) Solve Eqs. (6.69) and (6.76) subjected to the following boundary conditions:

$$u = v = 0 \quad \text{at} \quad y = 0 \quad (6.77)$$

$$u = U_e \quad \text{at} \quad y = \delta(\text{or} \quad \infty) \quad (6.78)$$

The boundary condition, $u = 0$, is usually referred to the no-slip condition. The second boundary condition, $v = 0$, is referred to the no-penetration condition because fluid cannot pass into the wall. The third boundary condition is applied at the boundary-layer edge where the flow velocity is required to the potential-flow solution.

6.3.4 Blasius Solution for Laminar Boundary Layer

If we can solve the continuity equation and momentum equation, we can derive the drag friction coefficient and boundary layer thickness. To obtain these results, the boundary layer partial differential equations need to be reduced to a single ordinary differential equation.

Let us first introduce the stream function in order to satisfy the continuity equation.

$$u(x, y) = \frac{\partial \psi}{\partial y} \quad (6.79)$$

$$v(x, y) = - \frac{\partial \psi}{\partial x} \quad (6.80)$$

We can observe that the stream solution will satisfy the continuity Eq. (6.69). Substituting u and v expressed in terms of the stream function into the x-momentum Eq. (6.76) for flat plate, one finds

$$\frac{\partial \psi}{\partial y} \frac{\partial^2 \psi}{\partial x \partial y} - \frac{\partial \psi}{\partial x} \frac{\partial^2 \psi}{\partial y^2} = v \frac{\partial^3 \psi}{\partial y^3} \quad (6.81)$$

The question here would be how the stream function is to be determined in order to satisfy the momentum equation. Because there is no length scale at flat plate, the non-dimensional velocity profile u/U_∞ should remain unchanged when plotted against the non-dimensional coordinate normal to the wall y/δ . These assumptions would suggest that there is a similarity solution because the flow looks similar in any direction at any time. This is,

$$\frac{u}{U_\infty} = f(\eta) \quad (6.82)$$

where η is a dimensionless parameter related to $y/g(x)$ and $g(x)$ is related to the boundary layer thickness $\delta(x)$. This suggests that $g(x)$ is some function of the coordinate x along the plate and some constant B . That is,

$$\eta = Bx^q y \quad (6.83)$$

For similarity, the stream function is a function of some variable x , a constant A and $f(\eta)$

$$\psi = Ax^p f(\eta) \quad (6.84)$$

To find the unknown parameters, we substitute the derivatives of the stream function in Eq. (6.81) by using the boundary conditions and rewrite results,

$$(p+q)f'^2 - pff'' = v \frac{B}{A} x^{-p+q+1} f''' \quad (6.85)$$

Because of similarity reasons, the equation should be independent of x . That is,

$$-p + q + 1 = 0 \quad (6.86)$$

With the boundary conditions we are able to solve the set of equations.

$$u(x, 0) = 0 \quad (6.87a)$$

$$\frac{\partial \psi}{\partial y}(x, 0) = 0 \quad (6.87b)$$

$$ABx^{p+q}f'(0) = 0 \quad (6.87c)$$

We know that Eq. (6.87c) has non-trivial solution. That is,

$$f'(0) = 0 \quad (6.88)$$

The second boundary condition

$$v(x, 0) = 0 \quad (6.89a)$$

$$-\frac{\partial \psi}{\partial x}(x, 0) = 0 \quad (6.89b)$$

$$-Apx^{p-1}f(0) - ABqyx^{p+q+1}f'(0) = 0 \quad (6.89c)$$

Because $f'(0) = 0$, the non-trivial solution would be

$$f(0) = 0 \quad (6.90)$$

And the final boundary condition

$$u(x, \infty) = U_\infty \quad (6.91a)$$

$$\frac{\partial \psi}{\partial y}(x, \infty) = U_\infty \quad (6.91b)$$

$$ABx^{p+q}f'(\infty) = U_\infty \quad (6.91c)$$

For this equation to be satisfied we need to set

$$p + q = 0 \quad (6.92)$$

With Eqs. (6.86) and (6.92) we can solve for p and q .

$$p = \frac{1}{2} \quad (6.93a)$$

$$q = \frac{1}{2} \quad (6.93a)$$

From Eq. (6.91c) we know that,

$$f'(\infty) = 1 \quad (6.94a)$$

$$AB = U_\infty \quad (6.94b)$$

With Eqs. (6.85) and (6.94) we can derive

$$\frac{\mu B}{\rho A} = 1 \quad (6.95)$$

From Eqs. (6.94b) and (6.95) we know that

$$B = \sqrt{\frac{U_\infty \rho}{\mu}} \quad (6.96a)$$

$$A = \sqrt{\frac{U_\infty \mu}{\rho}} \quad (6.96b)$$

As all the unknown parameters are obtained, we can summarize as:

$$\frac{1}{2} f \cdot f'' + f''' = 0 \quad (6.97a)$$

$$f = f' = 0 \text{ at } \eta = 0 \quad (6.97b)$$

$$f' \rightarrow 1 \text{ as } \eta \rightarrow \infty \quad (6.97c)$$

Non-dimensional variable η (the so-called similarity variable) and the stream function

$$\eta = \sqrt{\frac{U_\infty}{vx}} y \quad (6.98a)$$

$$\psi = \sqrt{vx} f(\eta) \quad (6.98b)$$

In terms of the new variables velocity components become

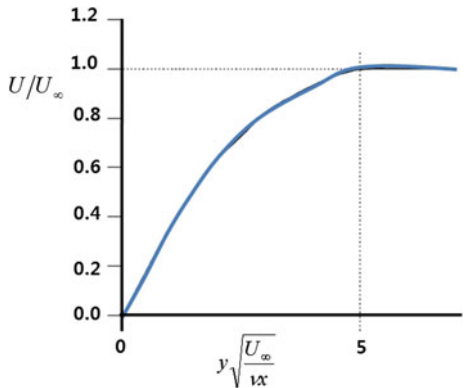
$$u = U_\infty \cdot f' \quad (6.99a)$$

$$v = \frac{1}{2} \left(\frac{vU_\infty}{x} \right)^{1/2} (\eta f' - f) \quad (6.99b)$$

Equation (6.97) may only be solved using a numerical approach. If f, f' , and f'' are all known at a certain dimensionless height η , numerical method may be utilized to find the solution at $(\eta + h)$. The results of numerical calculations.

From the Blasius curve (Fig. 6.11), we can derive the expression for the approximated boundary layer thickness. Because the approximation is congruent, the calculation is,

Fig. 6.11 The Blasius laminar boundary layer solution for X components of the velocity profile



$$y\sqrt{\frac{U_\infty}{vx}} = 5 \text{ for } \frac{U_x}{U_\infty} = 0.99 \quad (6.100a)$$

Boundary layer thickness is

$$\delta(x) = 5\sqrt{\frac{vx}{U_\infty}} = \frac{5x}{Re_x^{1/2}} \quad (6.101)$$

Shear stress on the surface

$$\tau_0 = \mu \left(\frac{\partial U_x}{\partial y} \right)_{y=0} = \mu U_\infty \sqrt{\frac{U_\infty}{vx}} f''(0) \quad (6.102)$$

Because $f''(0) = 0.332$ from the numerical solution of Blasius problem, frictional drag force is

$$F = b \int_0^L \tau_0 dx = 0.664 b U_\infty \sqrt{U_\infty \mu \rho L} \quad (6.103)$$

We know that coefficient of friction is

$$C_f = \frac{F}{\frac{1}{2} \rho U_\infty^2 (bL)} = \frac{1.328}{\sqrt{Re}} \quad (6.104)$$

6.3.5 Velocity Boundary Layer for Turbulent Flow

Turbulence is still an unsolved problem in fluid dynamics. The formulas used to describe turbulence are based on data from experiments combined with theory. The velocity boundary layer thickness for incompressible turbulent flow over flat plate is given as

$$\delta(x) \cong \frac{0.37x}{\text{Re}_x^{1/5}} \quad (6.105)$$

The total skin friction drag coefficient for incompressible turbulent flow over an infinitesimally at plate are given as

$$C_f \cong \frac{0.074}{\text{Re}_x^{1/5}} \quad (6.106)$$

6.4 Parametric Accelerated Life Testing of Fluid Systems

For solid-state diffusion of impurities in silicon, the junction equation J might be expressed as:

$$J = A \sinh(a\xi) \exp\left(-\frac{Q}{kT}\right) \quad (6.107)$$

On the other hands, the reaction process that is dependent on speed might be expressed as:

$$K = a \frac{kT}{h} e^{-\frac{\Delta E}{kT}} \sinh\left(\frac{aS}{kT}\right) \quad (6.108)$$

So the reaction rate K from Eqs. (6.107) and (6.108) can be summarized as:

$$K = B \sinh(aS) \exp\left(-\frac{E_a}{kT}\right) \quad (6.109)$$

If the reaction rate in Eq. (6.109) takes an inverse function, the generalized stress model can be obtained as,

$$TF = A[\sinh(aS)]^{-1} \exp\left(\frac{E_a}{kT}\right) \quad (6.110)$$

The range of the hyperbolic sine stress term $[\sinh(aS)]^{-1}$ in Eq. (6.110) increases the stress as following: (1) initially $(S)^{-1}$ in a small effect, (2) $(S)^{-n}$ is

considered a medium effect, and (3) $(e^{aS})^{-n}$ has a high effect. Accelerated testing usually is usually conducted in the medium stress range. The hyperbolic sine stress term of Eq. (6.110) in medium range can be redefined as following:

$$TF = A(S)^{-n} \exp\left(\frac{E_a}{kT}\right) \quad (6.111)$$

The internal (or external) stress in a product is difficult to quantify and use in accelerated testing. Thus, stresses in mechanical systems may come from the loads like four aerodynamic forces; thrust, weight, lift and drag force in boundary layer. For a mechanical system, when replacing stress with effort, the time-to-failure can be modified as:

$$TF = A(S)^{-n} \exp\left(\frac{E_a}{kT}\right) = A(F)^{-\lambda} \exp\left(\frac{E_a}{kT}\right) \quad (6.112)$$

From the time-to-failure in Eq. (6.112), the acceleration factor can be defined as the ratio between the proper accelerated stress levels and typical operating conditions. The acceleration factor (AF) can be modified to include the effort concepts:

$$AF = \left(\frac{S_1}{S_0}\right)^n \left[\frac{E_a}{k} \left(\frac{1}{T_0} - \frac{1}{T_1} \right) \right] = \left(\frac{F_1}{F_0}\right)^\lambda \left[\frac{E_a}{k} \left(\frac{1}{T_0} - \frac{1}{T_1} \right) \right] \quad (6.113)$$

To carry out parametric ALTs, the sample size equation with the acceleration factors in Eq. (8.35) might be expressed as:

$$n \geq (r+1) \cdot \frac{1}{x} \cdot \left(\frac{L_{BX}^*}{AF \cdot h_a} \right)^\beta + r \quad (6.114)$$

If the reliability of the mechanical system was targeted, number of required test cycles (or mission cycles) can be obtained for given sample size. Through parametric ALTs, the faulty designs of fluid system can be identified to achieve the reliability target.

6.5 Mechanical Vibrations

6.5.1 Introduction

We will introduce the subject of vibrations in reliability design of mechanical system because most product including human activities involve vibration in one form or other. We hear by our eardrums if something like the design problems in the mechanical system happens. Most of vibration study in the early of last century

motivated by understanding the natural phenomena and developing mathematical theories to describe the vibration of physical systems. On the other hands, many modern investigations have been concentrated on the product design such as automobile and airplane.

To analyze the vibration of the mechanical systems, product can be typically modeled as mass in the form of the body, spring in the form of suspension and damper in the form of shock absorbers when the induced forces like the skin drag of airplane wing are applied. For example, an airplane wing has the distributed mass of the wing. Due to a variety of loads in field, the wing deforms so that it can be modeled as a spring. Because of that, the deflection of the wing arise damping due to relative motion between components such as joints, connections and support as well as internal friction due to micro-structural defects in the material. After mechanical products are modeled, they are classified and analyzed like single-degree-of-freedom systems. After engineer see the results, they judge whether the action plans such as vibration isolation are required. If necessary, engineer will redesign the system. In general whenever the natural frequency of a product coincides with the frequency of the external excitation like wind, there occurs a resonance, which leads to excessive deflections and finally failure.

Mechanical system often arise vibration problems due to faulty design of mechanical system. For example, Blade and disk vibrations in turbines cause the rapid wear and excessive noise of machine parts such as bearings and gears. Though vibrations in turbines cause mechanical failures like fatigue, there is no alternative for engineers to prevent the failures. The transmission of vibration in mechanical products also results in human discomfort and product failures. Thus the vibration study in the reliability design of mechanical system is to (1) figure out the vibration phenomena by modeling and testing of mechanical system, and (2) reduce vibration through proper design of machines and their mountings. Finally, when mechanical system is subjected to loads like random vibration, the final design of the mechanical system confirms if its reliability target is achieved by parametric ALT.

6.5.2 Mechanical Systems and Their Modeling

As a first step of vibration study, mechanical system is modeled as single-degree-of-freedom systems or the others. Vibration is a motion that repeats itself in a given time interval. Typical example of vibration is pendulum swinging. Regardless of lumped systems or distributed systems, the modeling of Mechanical system includes a means for storing potential energy (spring or elasticity), a means for storing kinetic energy (mass or inertia), and a means by which energy is gradually lost (damper) (Fig. 6.12).

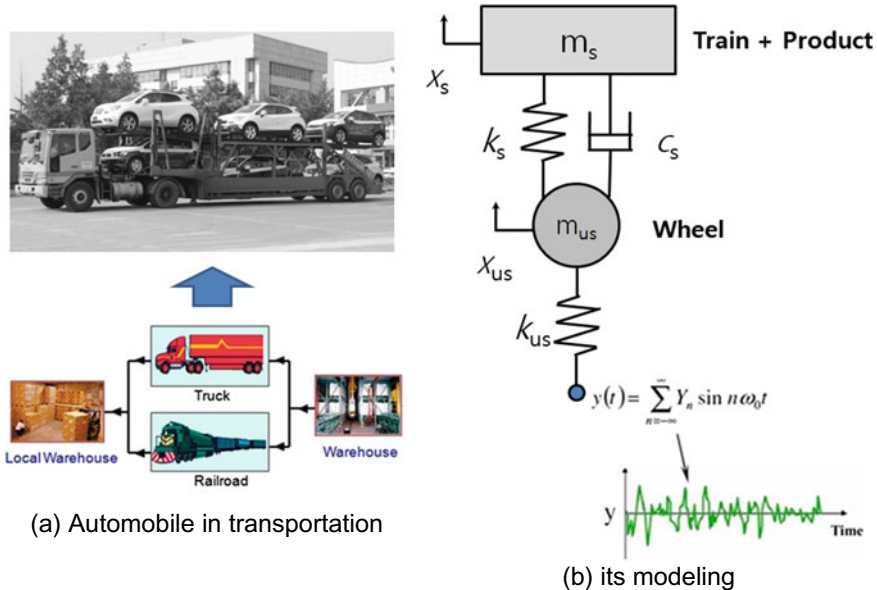


Fig. 6.12 Automobile subjected to random vibrations in transportation

Only the most important features considered in the vibration analysis predicts the behavior of the product under specified input conditions. Thus the analysis of a vibrating system usually involves mathematical modeling, derivation of the governing equations, solution of the equations, and interpretation of the results.

Step 1: Mathematical Modeling and its Governing Equations. The purpose of mathematical modeling is to represent all the important features—mass, spring and damping—of the mechanical system. To illustrate the procedure of refinement used in mathematical modeling, consider the automobile subjected to random vibrations in transportation shown in Fig. 5.30. The most useful mathematical model of a vehicle suspension system is the quarter car model and can evaluate the ride quality of product mounted on vehicle like train or automobile [4].

Though it is two DOF and four state variables, it serves the purpose of figuring out the vehicle motion in transportation. The assumed model of the vehicle consists of the sprung mass and the un-sprung mass, respectively. The sprung mass m_s represents 1/4 of the body of the vehicle, and the un-sprung mass m_{us} represents one wheel of the vehicle. The main suspension is modeled as a spring k_s and a damper c_s in parallel, which connects the un-sprung to the sprung mass. The tire (or rail) is modeled as a spring k_{us} and represents the transfer of the road force to the un-sprung mass (Fig. 6.13)

The governing differential equations of motion for the quarter car model can be represented as:

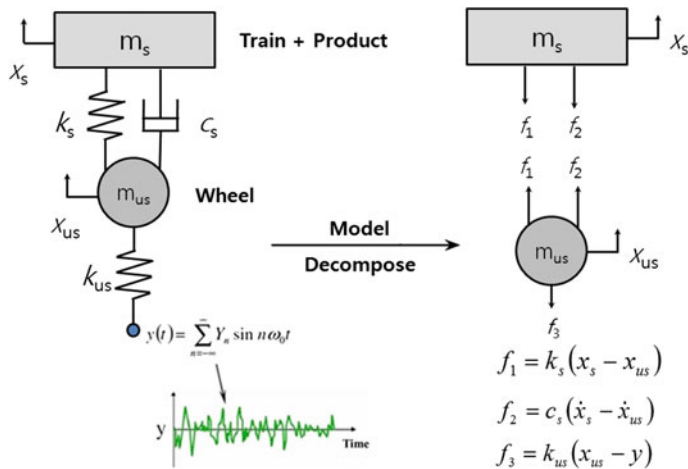


Fig. 6.13 A quarter car model and its decomposition

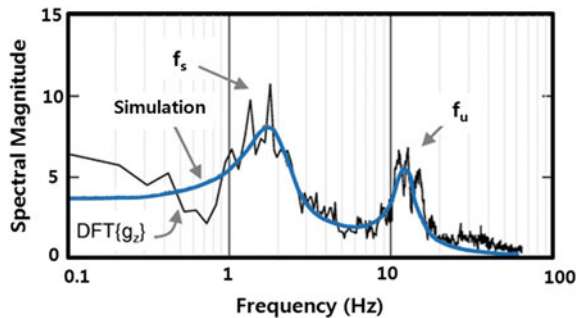
$$\begin{bmatrix} m_s & 0 \\ 0 & m_{us} \end{bmatrix} \begin{bmatrix} \ddot{x}_s \\ \ddot{x}_{us} \end{bmatrix} + \begin{bmatrix} c_s & -c_s \\ -c_s & c_s \end{bmatrix} \begin{bmatrix} \dot{x}_s \\ \dot{x}_{us} \end{bmatrix} + \begin{bmatrix} k_s & -k_s \\ -k_s & k_{us} + k_s \end{bmatrix} \begin{bmatrix} x_s \\ x_{us} \end{bmatrix} = \begin{bmatrix} 0 \\ k_{us}y \end{bmatrix} \quad (6.117)$$

As a result, Eq. (6.109) can be expressed in a matrix form

$$[M]\ddot{X} + [C]\dot{X} + [K]X = F \quad (6.118)$$

Step 2: Solution of the Governing Equations and its Interpretation. By analysis of mechanical system, the governing equations of motion in Eq. (6.93) can be solved to find the response of the mechanical system and the results are verified by testing. Depending on the nature of the problem, we can use one of the following analysis techniques for finding the solution: (1) standard methods of solving differential equations, (2) Laplace transform methods, (3) matrix methods, and (4) numerical methods. Finally, when Eq. (6.93) is numerically integrated, we can obtain the frequency (or time) response of the state variables (Fig. 6.14).

Fig. 6.14 Typical frequency response for a quarter car model



6.5.3 Reduction of the Vibratory Motion Due to the Mass

We will discuss with the response of mechanical systems subjected to excitations. First, it presents the derivation of the equation of motion and its solution when a single degree of freedom system is subjected to excitation. Consider a reciprocating compressor as shown in Fig. 6.15.

Because compressor operates a constant speed, the equation of motion of this system subjected to a harmonic force $F(t) = F_0 \cos \omega t$ can be given by

$$m\ddot{x} + c\dot{x} + kx = F_0 \cos \omega t \quad (6.119)$$

The particular solution of Eq. (6.119) is also expected to be harmonic; we assume it in the form

$$x_p(t) = X \cos(\omega t - \phi) \quad (6.120)$$

where X and ϕ are constants to be determined. X and denote the amplitude and phase angle of the response, respectively. By substituting Eq. (6.120) into Eq. (6.119), we arrive at

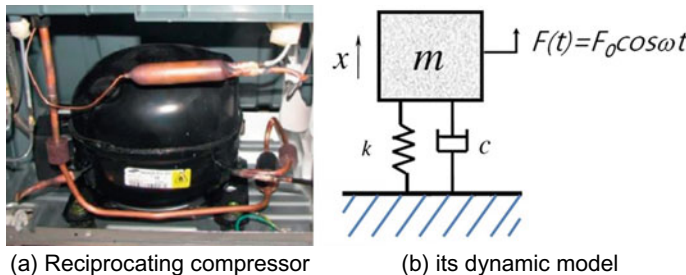


Fig. 6.15 A reciprocating compressor model

$$X[(k - m\omega^2) \cos(\omega t - \phi) - c\omega \sin(\omega t - \phi)] = F_0 \cos \omega t \quad (6.121)$$

Using the trigonometric relations in Eq. (6.121) and equating the coefficients of $\cos \omega t$ and $\sin \omega t$ on both sides of the resulting equation, we obtain

$$\begin{aligned} X[(k - m\omega^2) \cos \phi + c\omega \sin \phi] &= F_0 \\ X[(k - m\omega^2) \sin \phi - c\omega \cos \phi] &= 0 \end{aligned} \quad (6.122)$$

Solution of Eq. (6.122) gives

$$X = \frac{F_0}{\left[(k - m\omega^2)^2 + \omega^2 c^2 \right]^{1/2}} \quad (6.123)$$

And

$$\phi = \tan^{-1} \left(\frac{c\omega}{k - m\omega^2} \right) \quad (6.124)$$

By inserting the expressions of X and ϕ from Eqs. (6.123) and (6.124) into Eq. (6.120), we obtain the particular solution of Eq. (6.119). Dividing both the numerator and denominator of Eq. (6.123) by spring k and making the following substitutions we obtain

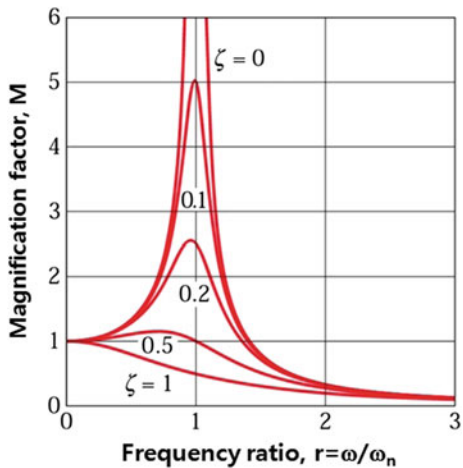
$$M = \frac{X}{\delta_{st}} = \frac{1}{\left[\left\{ \left[1 - \left(\frac{\omega}{\omega_n} \right)^2 \right]^2 + \left[2\zeta \frac{\omega}{\omega_n} \right]^2 \right\} \right]^{1/2}} = \frac{1}{\sqrt{(1 - r^2)^2 + (2\zeta r)^2}} \quad (6.125)$$

The quantity M is called the magnification factor. In a lightly damped system when the forcing frequency nears the natural frequency ($r \approx 1$) the amplitude of the vibration can get extremely high. This phenomenon is called resonance. In rotor bearing systems any rotational speed that excites a resonant frequency is referred to as a critical speed. If resonance occurs in a mechanical system, it can be very harmful—leading to eventual failure of the system. Consequently, one of the major reasons for vibration analysis is to predict when this type of resonance may occur and then to determine what steps to take to prevent it from occurring. Adding damping can significantly reduce the magnitude of the vibration. Also, the magnitude can be reduced if the natural frequency can be shifted away from the forcing frequency by changing the stiffness or mass of the system.

The magnification factor depends on the frequency ratio and the damping factor and is illustrated as:

In many applications, the isolation is required to reduce the motion of the mass (machine) under the applied force. The displacement amplitude of the mass m due to the force $F(t)$ can also be expressed as:

Fig. 6.16 Magnification factor (or displacement transmissibility) in accordance with frequency ratio r and the damping factor ζ



$$T_d = \frac{X}{\delta_{st}} = \frac{1}{\sqrt{(1 - r^2)^2 + (2\zeta r)^2}} \quad (6.126)$$

It is the displacement transmissibility or amplitude ratio and indicates the ratio of the amplitude of the mass, X , to the static deflection under the constant force, δ_{st} . The variation of the displacement transmissibility with the frequency ratio r for several values of the damping ratio is shown in Fig. 6.16. The following observations can be described:

1. The displacement transmissibility increases to a maximum value at

$$r = \sqrt{1 - 2\zeta^2} \quad (6.127)$$

Equation (6.102) shows that, for small values of damping ratio the displacement transmissibility (or the amplitude of the mass) will have maximum at $r \approx 1$. Thus the value of $r \approx 1$ is to be avoided in practice. In most cases, the excitation frequency is fixed and hence we can avoid by altering the value of the natural frequency which can be accomplished by changing the value of either or both of m and k .

2. The amplitude of the mass, X , approaches zero as r increases to a large value. The reason is that at large values of r , the applied force $F(t)$ varies very rapidly and the inertia of the mass prevents it from following the fluctuating force.

6.5.4 Vibration Design of Mechanical Product

Vibration design of mechanical product is related to the vibration isolation which reduces the undesirable effects of vibration. So action plans for mechanical design involve the insertion of a mounting rubber between the mechanical product and the source of vibration so that a reduction in the dynamic response of the system is achieved under specified conditions of vibration excitation.

Vibration isolation can be used in (1) the base of a vibrating machine is protected against large unbalanced forces of mechanical system such as compressor and (2) the product is protected from environmental conditions like transportation. The first type of isolation is used when mechanical system is subjected to an excitation force. For example, in a commercial refrigerator, reciprocated compressor acts on the product, which are transmitted to the refrigerator basement. Vibration (or noise) can cause discomfort to customer.

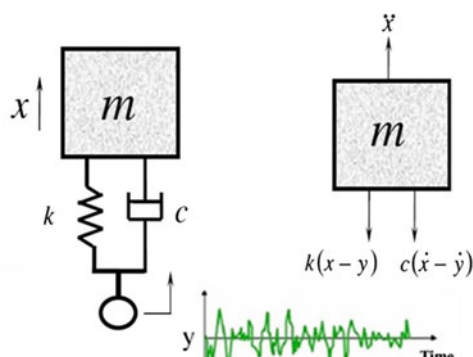
In these applications, vibration isolation is to reduce the vibratory motion of the system under the applied force. Thus transmissibility becomes important for this of isolators. When product is mounted in a train, it will be subjected to a random vibration in transportation from the base. Hence a mounting rubber between the product and the base is placed to reduce the transmitted force. The mounted rubber is assumed to have both elasticity and damping and is modeled as a spring k and a dashpot c . Refrigerator compressor can then be modeled as a single-degree-of-freedom system (Fig. 6.17).

To derive the transmitted force, first of all, without base excitation, it is assumed that the operation of the product gives rise to a harmonically varying force $F = F_0 \cos \omega t$. The equation of motion of the product is given by

$$m\ddot{x} + c\dot{x} + kx = F_0 \cos \omega t \quad (6.128)$$



(a) Refrigerator compressor



(b) single-degree-of-freedom model

Fig. 6.17 A simplified refrigerator model subjected to random vibrations

Since the transient solution dies out after some time, only the steady-state solution will be left. The steady-state solution of Eq. (6.120) is given by

$$x(t) = X \cos(\omega t - \phi) \quad (6.129)$$

where

$$X = \frac{F_0}{\left[(k - m\omega^2)^2 + \omega^2 c^2 \right]^{1/2}} \quad (6.130)$$

and

$$\phi = \tan^{-1} \left(\frac{\omega c}{k - m\omega^2} \right) \quad (6.131)$$

The force transmitted to the base through the spring and the dashpot, F_T is given by

$$F_T(t) = kx(t) + c\dot{x}(t) = kX \cos(\omega t - \phi) - c\omega X \sin(\omega t - \phi) \quad (6.132)$$

The magnitude of the total transmitted force (F_T) is given by

$$\begin{aligned} F_T(t) &= \left[(kx)^2 + (c\dot{x})^2 \right]^{1/2} = X \sqrt{k^2 + \omega^2 c^2} \\ &= \frac{F_0(k^2 + \omega^2 c^2)^{1/2}}{\left[(k - m\omega^2)^2 + \omega^2 c^2 \right]^{1/2}} \end{aligned} \quad (6.133)$$

The transmissibility or transmission ratio of the isolator (T_f) is defined as the ratio of the magnitude of the force transmitted to that of the exciting force:

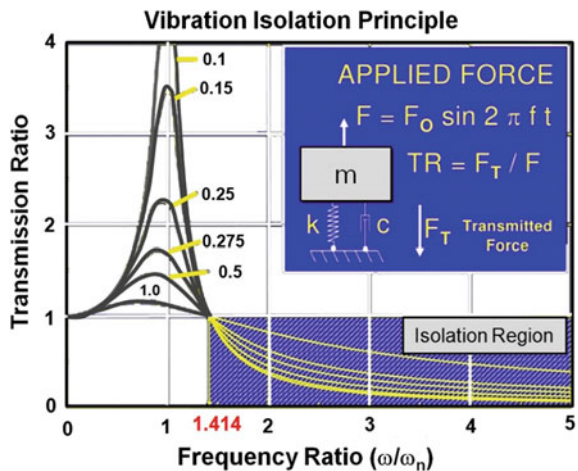
$$\begin{aligned} T_f &= \frac{F_T}{F_0} = \left\{ \frac{k^2 + \omega^2 c^2}{(k - m\omega^2)^2 + \omega^2 c^2} \right\}^{1/2} \\ &= \left\{ \frac{1 + (2\zeta r)^2}{(1 - r^2)^2 + (2\zeta r)} \right\}^{1/2} \end{aligned} \quad (6.134)$$

where $r = \omega/\omega_n$ is the frequency ratio.

The variation of T_f with the frequency ratio $r = \omega/\omega_n$ is shown in Fig. 6.18. In order to achieve isolation, the force transmitted to the foundation needs to be less than the excitation force. It can be seen that the forcing frequency has to be greater than times the natural frequency of the system in order to achieve isolation of vibration.

For small values of damping ratio and for frequency ratio the force transmissibility, given by Eq. (6.110), can be approximated as

Fig. 6.18 A simplified refrigerator model subjected to random vibrations



$$T_f = \frac{F_T}{F_0} \approx \frac{1}{r^2 - 1} \quad (6.135)$$

The following observations can be made from Fig. 6.18:

1. The magnitude of the force transmitted to the foundation can be reduced by decreasing the natural frequency of the system (ω_n)
2. The force transmitted to the foundation can also be reduced by decreasing the damping ratio. However, since vibration isolation requires $r > \sqrt{2}$, the machine should pass through resonance during start-up and stopping. Hence, some damping is essential to avoid infinitely large amplitudes at resonance.
3. Although damping reduces the amplitude of the mass (X) for all frequencies, it reduces the maximum force transmitted to the foundation only if $r < \sqrt{2}$. Above that value, the addition of damping increases the force transmitted.
4. If the speed of the machine (forcing frequency) varies, we must compromise in choosing the amount of damping to minimize the force transmitted. The amount of damping should be sufficient to limit the amplitude X and the force transmitted while passing through the resonance, but not so much to increase unnecessarily the force transmitted at the operating speed.

Example 6.3 An exhaust fan, rotating at 1000 RPM, is to be supported by four springs, each having a stiffness of K . If only 10% of the unbalanced force of the fan is to be transmitted to the base, what should be the value of K ? Assume the mass of the exhaust fan to be 40 kg.

Since the transmissibility has to be 0.1, the forcing frequency is given by $\omega = (1000 \times 2\pi)/60 = 104.72$ rad/s and the natural frequency of the system by

$$\omega_n = \left(\frac{k}{m}\right)^{1/2} = \left(\frac{4K}{40}\right)^{1/2} = \frac{\sqrt{K}}{3.1623}.$$

By assuming the damping ratio to be $\zeta = 0$, we obtain from Eq. (5.75),

$$T_f = 0.1 = \frac{1}{r^2 - 1} = \frac{1}{\left(\frac{104.72 \times 3.1623}{\sqrt{K}}\right)^2 - 1}$$

This leads to

$$\frac{331.1561}{\sqrt{K}} = 3.3166 \quad K = 9.97 \text{ N/m}$$

Chapter 7

Mechanical System Failures



Abstract This chapter will discuss the effect of structural material that is subjected to (random) loads. Fatigue fracture catastrophically occurs in product lifetime when there are stress raisers such as holes, notches, or fillets in design. To understand the structural damage, engineer might understand the basic concepts of mechanics of materials—stress, mechanics of material, deformation, slip, fracture, and fatigue. To withstand their own loads, mechanical structures are designed to have proper stiffness and strength. Requirements on stiffness, being the resistance against reversible deformation, may depend on their applications. Strength, the resistance against irreversible deformation, is always required to be high. If improperly designed, small portions of product will suddenly fracture in its lifetime. To understand the design of product—automobile, bridge, skyscrapers, and the others, engineer should figure out why the mechanical system failures will happen. Through the current reliability methodology engineer still doesn't know whether product design overcomes (random) loads in its lifetime. For example, the failure of mechanical system like aircraft wing during a long flight can occur in short time or tens of thousands of vibration load cycles. To assess the product damage, we need new reliability methodology like parametric accelerated life testing in the design process. And we also will deal with the mechanical corrosion in the later section.

Keywords Mechanical system failures • Fracture • Fatigue • Design • Failure analysis

7.1 Introduction

Failure of mechanical system is fatigue and fracture due to repetitive loads. Fatigue was coined by France engineer Jean-Victor Poncelet in the middle of the nineteenth century. Fatigue meant to represent that the material got tired due to repeated loading, and eventually disintegrated [1]. The National Bureau of Standards and Battelle Memorial Institute estimated the costs for failure due to fracture to be \$119 billion per year in 1982 [2]. The required costs are important, but the safety of many failures in human life and injury is infinitely more so.

Fracture mechanics is the study field concerned with the study how cracks in materials propagate. It uses methods of analytical solid mechanics to calculate the driving force on a crack and those of experimental solid mechanics to characterize the material's resistance to fracture. When subjected to a variety of loading, fractures have occurred in improper design. Design against fracture still has area of current research and its final goal.

As seen in Fig. 7.1, stress is a physical quantity that expresses the response of the material on the unit area (A) acted in the external (or internal) forces (F). And strain is physical deformation response of a material to stress. A result of stresses in the vertical axis has the corresponding strains along the horizontal axis. Mild steel passes proportional limit, yield point, ultimate stress point into fracture.

$$\sigma = \frac{F}{A} \quad (7.1)$$

The linear portion of the stress-strain curve is the elastic region and the slope is Young's Modulus. The elastic range ends when the material reaches its yield strength. After the yield point, the curve typically decreases slightly and deformation continues. Strain hardening and plastic deformation begins until it reaches the ultimate tensile stress.

Deformation refers to any changes in the shape of an object due to an applied force. Elastic deformation is that once the forces are no longer applied, the object returns to its original shape. This type of deformation involves stretching of the atoms bonds. Linear elastic deformation is governed by Hooke's law, which states:

$$\sigma = E\varepsilon \quad (7.2)$$

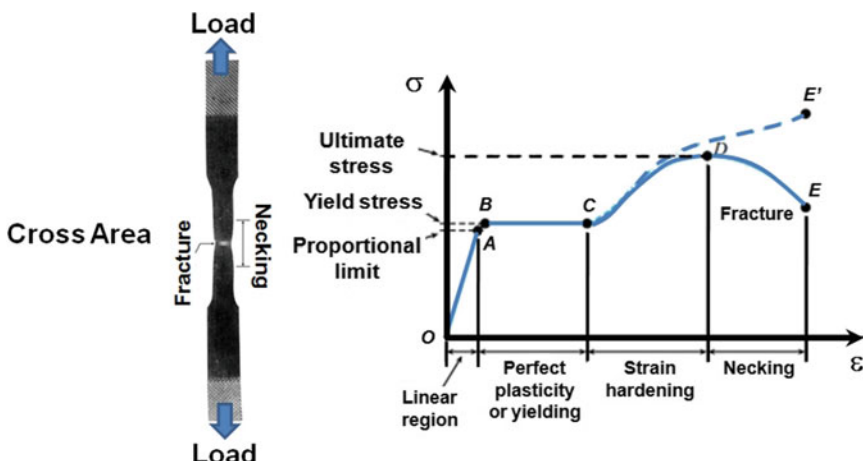


Fig. 7.1 Definition of stress and stress-strain curve

where σ is the applied stress, E is Young's modulus, and ϵ is the strain.

Applied force consists of tension, compression, shear, and torsion (Fig. 7.2). Tensile means the material is under tension. The forces acting on it are trying to stretch the material. Compression is when the forces acting on an object are trying to squash it.

- Axial loading (tension/compression/bending)—The applied forces are collinear with the longitudinal axis of the member. The forces cause the member to either stretch or shorten.
- Transverse loading (shear)—Forces applied perpendicular to the longitudinal axis of a member. Transverse loading causes the member to bend and deflect from its original position, with internal tensile and compressive strains accompanying the change in curvature of the member. Transverse loading also induces shear forces that cause shear deformation of the material and increase the transverse deflection of the member.
- Torsional loading—twisting action caused by a pair of externally applied equal and oppositely directed force couples acting on parallel planes or by a single external couple applied to a member that has one end fixed against rotation.

If a single crystal of a metal is stressed in tension beyond its elastic limit, it elongates slightly that it is called plastic deformation (Fig. 7.3). Plastic deformation involves the breaking and remaking of atomic bonds. Plastic deformation may take place by slip, twinning or a combination of both methods. Plastic deformation cannot be restored to its initial state by changes, i.e. irreversible process. Under

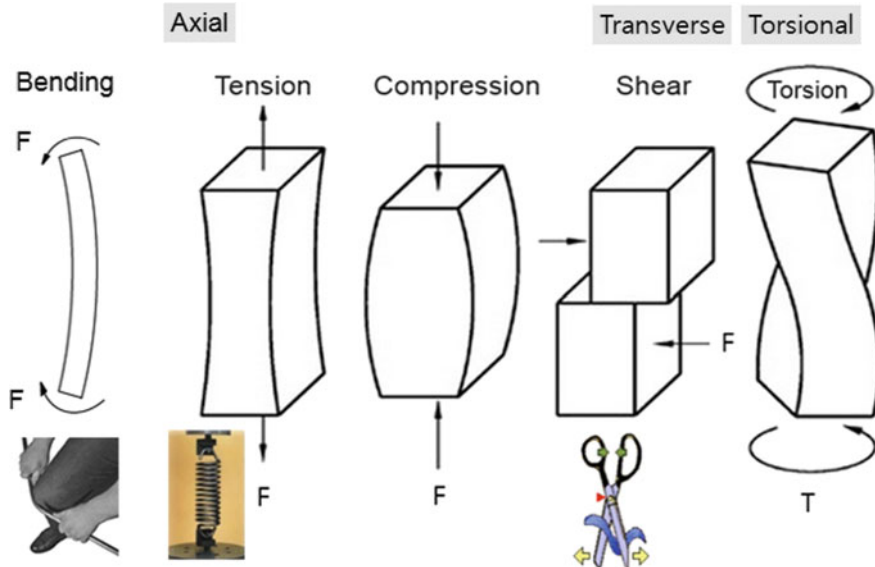


Fig. 7.2 A variety of stresses due to five kinds of static loads

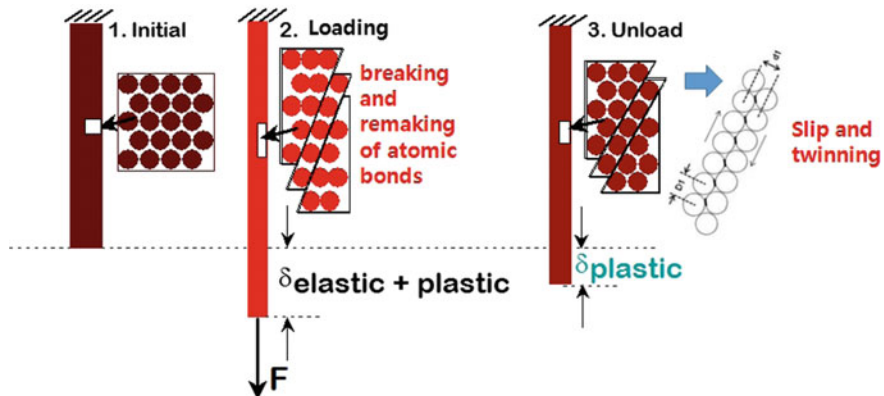


Fig. 7.3 Plastic deformation (metals) for axial force

tensile stress, plastic deformation is characterized by a strain hardening region, necking region and finally, fracture (also called rupture).

Many materials are made up of many grains which may have second phase particles and grain boundaries. It is therefore easier to study plastic deformation in a single crystal to eliminate the effects of grain boundaries and second phase particles. The way a crack propagates through the material is indicative for the following fracture mechanisms—(1) ductile (shear) fracture, (2) brittle (cleavage) fracture, (3) fatigue, (4) crazing, and (5) de-adhesion.

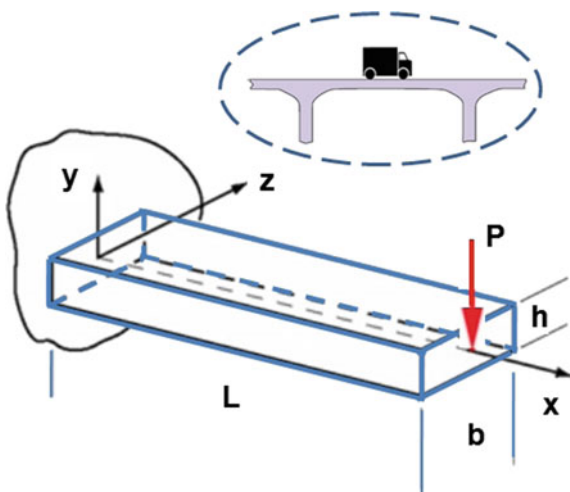
During strain hardening the material becomes stronger through the movement of atomic dislocations. The necking phase is indicated by a reduction in cross-sectional area of the specimen. Necking begins after the ultimate strength is reached. During necking, the material can no longer withstand the maximum stress and the strain in the specimen rapidly increases. Plastic deformation ends with the fracture of the material. Fracture is the separation of a single body into pieces by an applied stress.

7.2 Strength of Mechanical Product

7.2.1 Introduction

Strength of product, called as mechanics of materials, deal with the strength and physical performance of mechanical/civil structures subjected to various types of loading (Fig. 7.4). Engineer should understand these fundamental concepts—stresses and strains, deformations and displacements, elasticity and inelasticity, strain energy, and load-carrying capacity. These concepts underlie the design and analysis of a huge variety of mechanical and structural systems.

Fig. 7.4 Tip-loaded cantilever beam



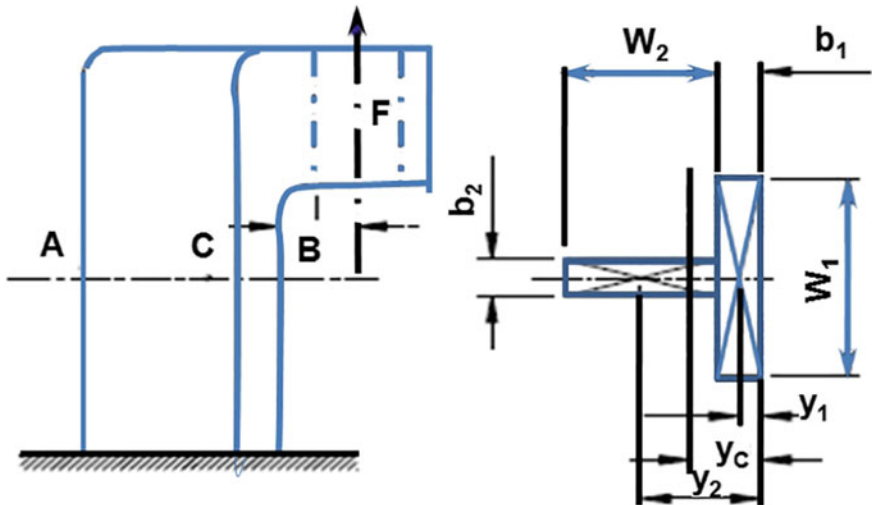
The solid bodies include bars with axial loads, shafts in torsion, beams in bending, and columns in compression. The principal objective of mechanics of materials is to determine the stresses, strains, and displacements in structures and their components due to the loads. If engineer can find all values of the loads cause failure, a complete shape of the mechanical structures can be drawn to withstand the deformation.

An understanding of mechanical behavior also is essential for the safe design of all types of structures, whether airplanes and antennas, buildings and bridges, machines and motors, or ships and spacecraft. Because those subjects deal primarily with the forces and motions associated with particles and rigid bodies, statics and dynamics are essential. To design the mechanical system on the basis of the stresses and strains, engineers use the physical properties of the materials as well as numerous theoretical laws and concepts.

Leonardo da Vinci (1452–1519) and Galileo Galilei (1564–1642) made the first attempts at developing a theory of beams. Though Leonardo da Vinci made the crucial observations, he lacked Hooke's law and calculus to complete the theory. On the other hands, Galileo was held back by an incorrect assumption he made. They performed experiments to determine the strength of wires, bars, and beams, though they did not develop adequate theories to explain their test results.

The famous mathematician Leonhard Euler (1707–1783) developed the mathematical theory of columns and calculated the critical load of a column in 1744. Without appropriate tests to back up his theories, Euler–Bernoulli beam theory remained unused for over a hundred years. Bridges and buildings continued to be designed by precedent until the late 19th century, when the Eiffel Tower and Ferris wheel demonstrated the validity of the theory on large scales. Now they are the basis for the design and analysis of most columns—tip-loaded cantilever beam. Therefore, I will focus on the Euler–Bernoulli beam theory to understand the strength of mechanical product.

Example 7.1 As seen in below Figure, the structure has the cross-section of an upright (points A, B, and C; locate point C). Data: $F = 50 \text{ kN}$; $L = 35 \text{ mm}$; $b_1 = 30 \text{ mm}$; $b_2 = 20 \text{ mm}$; $W_1 = 85 \text{ mm}$; $W_2 = 70 \text{ mm}$. Material: cast iron, grade 200. Find the value of the factor of safety (FS).



(a) Centroid of the cross-section:

$$y_C = \frac{A_1 y_1 + A_2 y_2}{A_1 + A_2} = \frac{b_1 w_1 y_1 + b_2 w_2 y_2}{b_1 w_1 + b_2 w_2} = \frac{30 \cdot 85 \cdot 15 + 20 \cdot 70 \cdot 65}{30 \cdot 85 + 20 \cdot 70} = 32.75 \text{ mm}$$

(b) Equivalent bending load:

$$M = F(L + y_C) = 50 \times 10^3 (35 + 32.75) = 3,387,500 \text{ Nm}$$

(c) Component stresses. The direct stress (bending stress):

$$\sigma_r = \frac{F}{A} = \frac{50 \times 10^3}{3950} = 12.65 \frac{\text{N}}{\text{mm}^2}$$

- moment of inertia of the cross-section:

$$\begin{aligned}
 I_{xx} &= \frac{w_1 b_1^3}{12} + w_1 b_1 \left(y_C - \frac{b_1}{2} \right)^2 + \frac{b_2 w_2^3}{12} + b_2 w_2 (b_1 + 0.5w_2 - y_C)^2 \\
 &= \frac{85 \times 30^3}{12} + 85 \cdot 30(32.75 - 0.5 \cdot 30) + \frac{20 \times 70^3}{12} + 20 \cdot 70(30 + 0.5 \cdot 70 - 32.75)^2 \\
 &= 3,022,413.5 \text{ mm}^4
 \end{aligned}$$

- Section modulus of the cross-section (point A; CA = 67.25 mm):

$$W_{xx}^A = \frac{I_{xx}}{CA} = \frac{3,022,413.6}{67.25} = 44,942.9 \text{ mm}^3$$

- Section modulus of the cross-section (point B; CB = 32.75 mm):

$$W_{xx}^B = \frac{I_{xx}}{CB} = \frac{3,022,413.6}{32.75} = 92,287.4 \text{ mm}^3$$

- Bending stress (point A): $\sigma_g^A = \frac{M}{W_{xx}^A} = \frac{3,387,500}{44,942.9} = 75.4 \frac{N}{\text{mm}^2}$
- Bending stress (point B): $\sigma_g^B = \frac{M}{W_{xx}^B} = \frac{3,387,500}{92,287.4} = 36.7 \frac{N}{\text{mm}^2}$

- (d) Maximum stress (points A & B):

$$\begin{aligned}
 \sigma_{\max}^A &= \sigma_r - \sigma_g^A = 12.6 - 75.4 = -62.8 \frac{N}{\text{mm}^2}; \\
 \sigma_{\max}^B &= \sigma_r + \sigma_g^B = 12.6 + 36.7 = 49.3 \frac{N}{\text{mm}^2}
 \end{aligned}$$

- (e) Factor of safety: $FS = \frac{R_u}{\sigma_{\max}^B} = \frac{200}{49.3} = 4.06$

(Ultimate strength is 200 MPa for cast iron grade 200).

7.2.2 Classical Beam Theory—Euler–Bernoulli Beam Theory

Euler–Bernoulli beam theory plays an important role in structural analysis because it provides the mechanical engineer with a simple means of calculating the load-carrying and deflection characteristics of beams. Beams are the most common type of structural component in mechanical/civil engineering. A beam is a bar-like structural member whose primary function is to support transverse loading and

carry it to the supports. By “bar-like” it is meant that one of the dimensions is considerably larger than the other two.

A variety of beam model can be used at a pre-design stage because they provide valuable insight into the behavior of mechanical structures. A beam is defined as a structure having one of its dimensions much larger than the other two. The axis of the beam is defined along that longer dimension, and a cross-section normal to this axis is assumed to smoothly vary along the span or length of the beam. A number of mechanical parts are beam-like structures—lever arms, shafts, wings, and fuselages.

To understand the deflection of beam subjected to static force, we should understand a fundamental assumption—no deformations occur in the plane of the cross-section. Consequently, the in-plane displacement field can be represented simply by two rigid body translations and one rigid body rotation.

As seen in Fig. 7.5, the beam under consideration extends from $x = 0$ to $x = L$ and has a bending rigidity EI , which may be a function of x . If the transverse load $w(x)$ is given in units of force per length, the unknown fields are the transverse displacement $w(x)$, rotation $\theta(x)$, curvature $\kappa(x)$, bending moment $M(x)$ and transverse shear $V(x)$. The Euler–Bernoulli beam equation can be derived from a combination of four distinct equations. That is,

(1) Kinematics:

$$\chi = -\theta = -\frac{dw}{dx} = -w' \quad \kappa = \frac{d^2w}{dx^2} = w'' = \theta' \quad (7.3)$$

where θ is the rotation of a cross section and κ the curvature of the deflected longitudinal axis.

(2) Constitutive:

$$M = EI \frac{d^2w}{dx^2} = EI\kappa \quad (7.4)$$

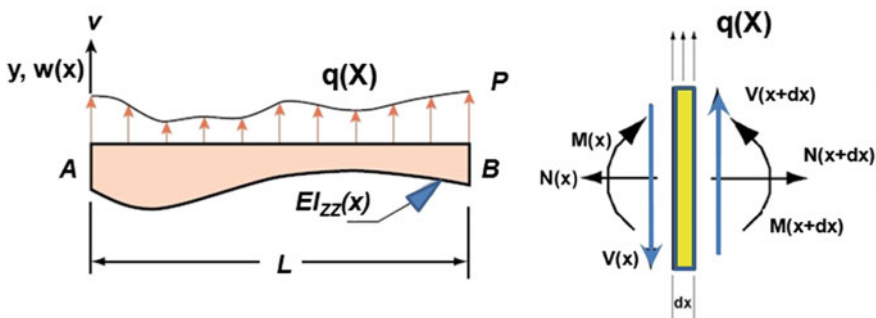


Fig. 7.5 Elastic-beam theory and slice equilibrium relations

(3) Resultants:

$$M(x) = \iint y \cdot \sigma(x, y) dy dz \quad V(x) = \iint \sigma(x, y) dy dz \quad (7.5)$$

(4) Equilibrium

Axial force balance:

$$0 = N(x + dx) - N(x) \Rightarrow N(x) = \text{constant} \quad (7.7)$$

Transverse force balance:

$$\begin{aligned} 0 &= q(x)dx + V(x + dx) - V(x) \\ &= q(x)dx + (V(x) + V'(x)dx + o(dx)) - V(x) \Rightarrow 0 = V'(x) + q(x) \\ &= dx[V'(x) + q(x)] \end{aligned} \quad (7.8)$$

Momentum balance about ‘ $x + dx$ ’

$$\begin{aligned} 0 &= V(x)dx - M(x + dx) + M(x) + (q(x)dx)dx \\ &= V(x)dx - (M(x) + M'(x)dx) + M(x) + (q(x)dx)dx/2 \Rightarrow 0 = -M'(x) + V(x) \\ &= dx[-M'(x) + V(x) + q(x)dx/2] \end{aligned} \quad (7.9)$$

If summarizing, balance equations are expressed as:

$$V = \frac{dM}{dx} = M'(x), \quad \frac{dV}{dx} + q = V' + q = M'' + q = 0 \quad (7.10)$$

To relate the beam’s out-of-plane displacement w to its loading q , the results of the four beam sub-categories should be combined as Kinematics → Constitutive → Resultants → Equilibrium. To eliminate V , we first combine the two equilibrium equations

$$\frac{d^2M}{dx^2} = -q(x) \quad (7.11)$$

Next replace the moment resultant M with its definition in terms of the direct stress σ ,

$$\frac{d^2}{dx^2} \left(\iint y \cdot \sigma \cdot dy \cdot dz \right) = -q(x) \quad (7.12)$$

Use the constitutive relation to eliminate stress σ in favor of the strain ϵ , and then use kinematics to replace ϵ in favor of the normal displacement w ,

$$\frac{d^2}{dx^2} \left(E \iint y \cdot \varepsilon \cdot dy \cdot dz \right) = -q(x) \quad (7.13)$$

$$\frac{d^2}{dx^2} \left(E \frac{d\chi}{dx} \iint y^2 \cdot dy \cdot dz \right) = -q(x) \quad (7.14)$$

$$\frac{d^2}{dx^2} \left(E \frac{d^2 w}{dx^2} \iint y^2 \cdot dy \cdot dz \right) = q(x) \quad (7.15)$$

As a final step, if recognizing that the integral over y^2 is the definition of the beam's area moment of inertia $I = \iint y^2 \cdot dy \cdot dz$, finally, the Euler-Bernoulli beam equation can be obtained as following:

$$\frac{d^2}{dx^2} \left(EI \frac{d^2 w}{dx^2} \right) = q(x) \quad (7.16a)$$

$$\frac{d}{dx} \left(EI \frac{d^2 w}{dx^2} \right) = V(x) \quad (7.16b)$$

$$EI \frac{d^2 w}{dx^2} = M(x) \quad (7.16c)$$

Example 7.2 (Cantilever Load under Tip Point Load)

As is defined in Fig. 7.6a, the problem is cantilever load under tip point load. Using the FBD pictured in Fig. 7.6b, and stating moment equilibrium with respect to X (to eliminate the effect of the transverse shear force V_y at that section) gives

$$M_z(x) = -Px$$

For convenience we scale $y(x)$ by EI_{zz} so that the ODE linking bending moment to deflection is $EI_{zz}y''(x) = M_z(x) = -Px$. Integrating twice:

Constant EI_{zz}

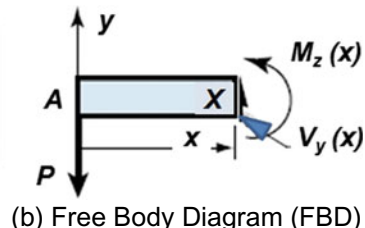
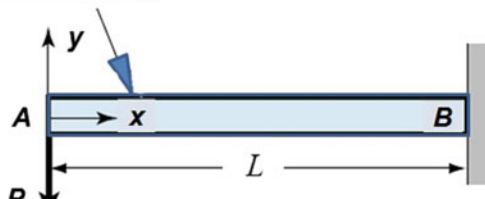


Fig. 7.6 Beam problem for Example 7.1

$$EI_{zz}y'(x) = -\frac{Px^2}{2} + C_1$$

$$EI_{zz}y(x) = -\frac{Px^3}{6} + C_1x + C_2$$

The kinematic boundary conditions for the cantilever are $y'(L) = 0$ and $y(L) = 0$ at the fixed end B. The first one gives $E I_{zz} y'(L) = -PL^2/2 + C_1 = 0$, whence $C_1 = PL^2/2$. The second one gives $E I_{zz} y(L) = -PL^3/6 + C_1L + C_2 = -PL^3/6 + PL^3/2 + C_2 = 0$ whence $C_2 = -PL^3/3$.

Substituting into the expression for $y(x)$ gives

$$y(x) = -\frac{P}{6EI_{zz}}(x^3 - 3L^2x + 2L^3) = (L-x)^2(2L+x)$$

Of particular interest is the tip deflection at free end A, which is the largest one. Setting $x = 0$ yields

$$y(0) = y_A = -\frac{PL^3}{6EI_{zz}}$$

The negative sign indicates that the beam deflects downward if $P > 0$.

Example 7.3 (Cantilever Beam under Triangular Distributed Load)

The problem is defined in Fig. 7.7a. Using the FBD pictured in Fig. 7.7b, again doing moment equilibrium with respect to X gives

$$M_z(x) = -\frac{1}{2}w(x) \cdot x \cdot \left(\frac{1}{2}x\right) = -\frac{wx^3}{6L}$$

Integrating $EI_{zz}y''(x) = M_z(x)$ twice yields

$$EI_{zz}y'(x) = -\frac{wx^2}{24L} + C_1$$

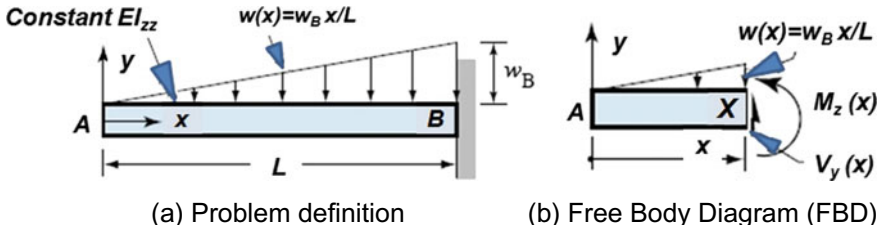


Fig. 7.7 Beam problem for Example 7.2

$$EI_{zz}y(x) = -\frac{wx^5}{120L} + C_1x + C_2$$

As in Example 7.1, the kinematic BCs for the cantilever are $y'(L) = 0$ and $y(L) = 0$ at the fixed end B. The first one gives $EI_{zz}y'(L) = -w_B L^3/24 + C_1 = 0$, whence $C_1 = w_B L^3/24$. The second one gives $EI_{zz}y(L) = -w_B L^4/120 + C_1 L + C_2 = 0$ into the expression for $y(x)$ we obtain the deflection curve as

$$y(x) = -\frac{1}{EI_{zz}L} \left(-\frac{w_B}{120}x^5 + \frac{w_B L^4}{24}x - \frac{w_B L^5}{30} \right) = -\frac{w_B}{120EI_{zz}L} (x^5 - 5L^4x + 4L^5)$$

Of particular interest is the tip deflection at free end A, which is the largest one. Setting $x = 0$ yields

$$y(0) = y_A = -\frac{w_B L^4}{30EI_{zz}}$$

The negative sign indicates that the beam deflects downward if $w_B > 0$.

Example 7.4 (Simply Supported Beam Under Uniform Load)

The problem is defined in Fig. 7.8a. Using the FBD pictured in Fig. 7.8b, writing down moment equilibrium with respect to X gives the bending moment

$$M_z(x) = R_A x - \frac{1}{2}wx^2 = \frac{1}{2}wLx - \frac{1}{2}wx^2 = \frac{1}{2}wx(L-x)$$

Integrating $EI_{zz}y''(x) = M_z(x)$ twice yields

$$EI_{zz}y'(x) = \frac{wLx^2}{4} - \frac{wx^3}{6} + C_1 = \frac{wLx^2}{12}(3L-2x) + C_1$$

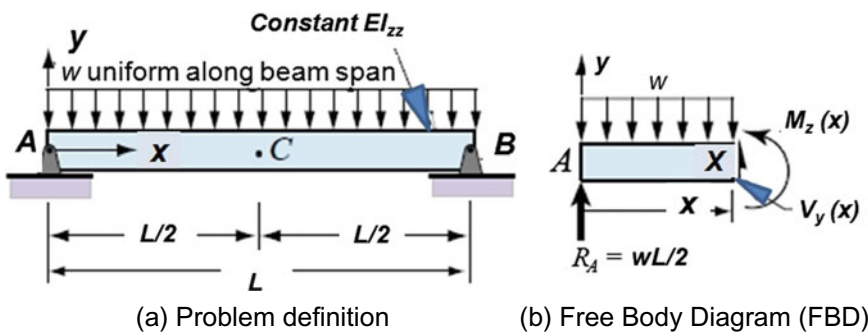


Fig. 7.8 Beam problem for Example 7.3

$$EI_{zz}y(x) = \frac{wLx^3}{12} - \frac{wx^4}{6} + C_1x + C_2 = \frac{wx^3}{12}(2L - x) + C_1x + C_2$$

The kinematic BCs for a SS beam are $y_A = y(0) = 0$ and $y_B = y(L) = 0$. The first one gives $C_2 = 0$ and the second one $C_1 = -wL^3/24$. Substituting into the expression for $y(x)$ gives, after some algebraic simplifications,

$$y(x) = -\frac{w}{24EI_{zz}}x(L-x)(L^2+Lx-x^2)$$

Note that since $y(x) = y(L-x)$ the deflection curve is symmetric about the mid-span C. The mid-span deflection is the largest one:

$$y_C = y(L/2) = -\frac{5wL^4}{384EI_{zz}}$$

The negative sign indicates that the beam deflects downward if $w_B > 0$.

7.3 Mechanism of Slip

If mechanical product (or parts) is subjected to the repetitive stress (or loads), permanent deformation occur at initial stage. Slip occurs on planes that have highest planer density of atoms and in the direction with highest linear density of atoms (Fig. 7.9). That is, slip occurs in directions in which the atoms are most closely packed since this requires the least amount of energy. Therefore they can slip past

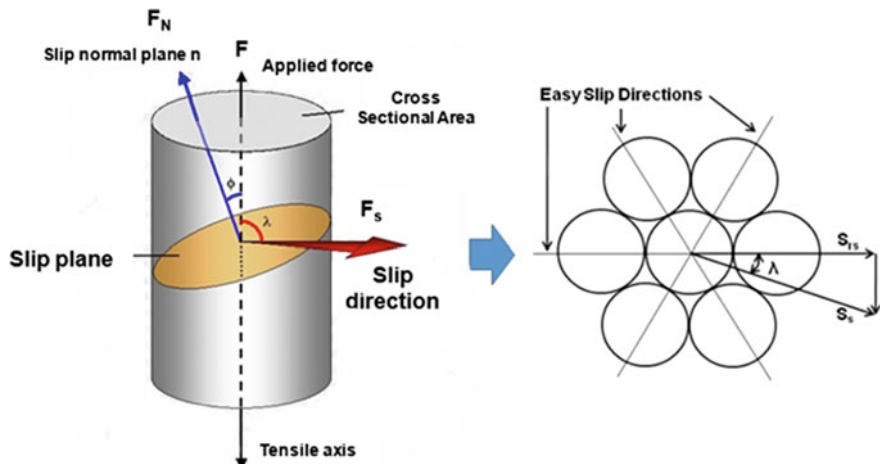


Fig. 7.9 Components of force on a slip plane

each other with force. Slip flow depends upon the repetitive structure of the crystal which allows the atoms to shear away from their original neighbors. It therefore slides along the face and join up with the atom of new crystals.

Slip takes place as a result of simple shearing stress. Resolution of axial tensile load F gives two loads. One F_s is shear load along the slip plane and the other F_N a normal tensile load perpendicular to the plane. By analysis and experiment maximum shear stress happen sat 45° . Above Fig. 7.4 right shows the packing of atoms on a slip plane. We know that there are three directions in which the atoms are close-packed, and these would be the easy slip directions.

Portions of the crystal on either side of a specific slip plane move in opposite directions and come to rest with the atoms in nearly equilibrium positions, so that there is very little change in the lattice orientation. Thus the external shape of the crystal is changed without destroying it. Schematically, slip can be explained in a face centered cubic (FCC) lattice. The (111) plane is the slip plane having maximum number of atoms (densest plane). It intersects the (001) plane in the line AC, (110) direction having maximum number of atoms on it. Slip is seen as a movement along the (111) planes in the close packed (110) direction (Fig. 7.10a).

From the schematic diagram of slip in a FCC crystal, one may assume that the atoms slip consecutively, starting at one place or at a few places in the slip plane, and then move outward over the rest of the plane. For instance, if one tries to slide the entire rug as one piece, the resistance is too much. What one can do is to make a wrinkle in the rug and then slide the whole rug a little at a time by pushing the wrinkle along. A similar analogy to the wrinkle in the rug is the movement of an earthworm. It advances in a direction by advancing a part of its body at a time.

By application of the shear force, first an extra plane of atoms (called a dislocation) forms above the slip plane. On application of force, bond between atoms breaks and creates a new bond between atoms and a dislocation. On continued application of force, this dislocation advances by breaking old bonds and making new bonds. In the next move, bond between atoms is broken and a new bond is made between atoms, resulting in a dislocation. Thus, this dislocation moves across the slip plane and leaves a step when it comes out at the surface of the crystal. Each time the dislocation moves across the slip plane, the crystal moves one atom spacing (Fig. 7.10b).

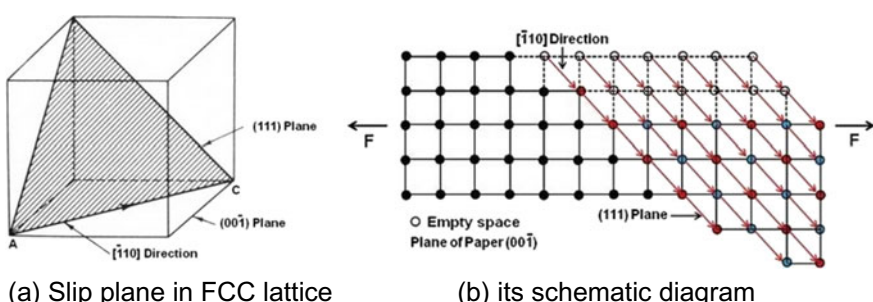


Fig. 7.10 Schematic diagram of slip plane in FCC lattice

7.4 Fatigue Failure

7.4.1 Introduction

About 95% of all structural failures occur through a fatigue mechanism. When a crack is subjected to cyclic loading, the crack tip will travel a very short distance in each loading cycle, provided that the stress is high enough, but not too high to cause sudden global fracture. It is nearly impossible to detect any progressive changes in material behavior during the fatigue process, so failures often occur without warning. Periods of rest, with the fatigue stress removed, do not lead to any measurable healing or recovery. With the naked eye we can see a ‘clam shell’ structure in the crack surface. Under a microscope ‘striations’ can be seen, which mark the locations of the crack tip after each individual loading cycle. This mechanism is referred to as fatigue. Because crack propagation is very small in each individual load cycle, a large number of cycles are required before total failure occurs.

Fatigue may occur when a member is subjected to repeated cyclic loadings. The fatigue phenomenon shows itself in the form of cracks developing at particular locations in the structure. Cracks can appear in diverse types of structures such as: planes, boats, bridges, frames, cranes, overhead cranes, machines parts, turbines, reactors vessels, canal lock doors, offshore platforms, transmission towers, pylons, masts and chimneys.

Design faults such as stress raisers are deformed. After repetitive deformations, cracks will begin to appear. Depending on the material, shape, and how close to the elastic limit it deforms, failure may require a lot of deformation cycles. Structures subjected to repeated cyclic loadings can undergo progressive damage, which is called fatigue. The phenomenon was first discovered still in the 19th century by observing poor service life of railroad axles designed based upon static design limits (Fig. 7.11).

The fatigue life of a structural detail subjected to repeated cyclic loadings is defined as the number of stress cycles it can stand before failure. The physical effect of a repeated load on a material is different from the static load. Failure always may be brittle fracture regardless of whether the material is brittle or ductile. Mostly fatigue failure occurs at stress well below the static elastic strength of the material.

Depending upon the member or structural detail geometry, its fabrication or the material used, four main parameters can influence the fatigue strength—(1) the stress difference, or as most often called stress range, (2) the structural geometry, (3) the material, (4) the environment.

7.4.2 Fluctuating Load

Most of the machine elements are subjected to variable, fluctuating loading. This type of loading is very dangerous not only because limiting stresses are



Fig. 7.11 Facture of train wreck due to metal fatigue failure of rail from Wikipedia

considerably lower than those established for static loading, but because of the nature of material failure, it happen abruptly without any traces of yielding.

Three different fluctuating stress-time modes are symmetrical about zero stress, asymmetrical about zero stress, and random stress cycle. For reversed stress cycle, amplitude is symmetric about a mean zero stress level. It alternates from σ_{max} to σ_{min} of equal magnitude. Repeated stress cycle is asymmetrical about σ_{max} and σ_{min} relative to zero stress level. Random stress cycle is that stress level fluctuates very randomly in amplitude and frequency.

For asymmetrical about zero stress, A fluctuating load (stress) that arise fatigue are characterized by mean stress σ_m , the range of stress $\Delta\sigma$, the amplitude stress σ_a , ratio of the mean stress over the amplitude stress χ , and the stress ratio R (see Fig. 7.12), They are represented as the following Eqs. (7.22)–(7.26).

$$\sigma_m = \frac{(\sigma_{max} + \sigma_{min})}{2} \quad (7.17)$$

$$\Delta\sigma = (\sigma_{max} - \sigma_{min}) \quad (7.18)$$

$$\sigma_a = \frac{(\sigma_{max} - \sigma_{min})}{2} \quad (7.19)$$

$$\chi = \frac{\sigma_m}{\sigma_a} \quad (7.20)$$

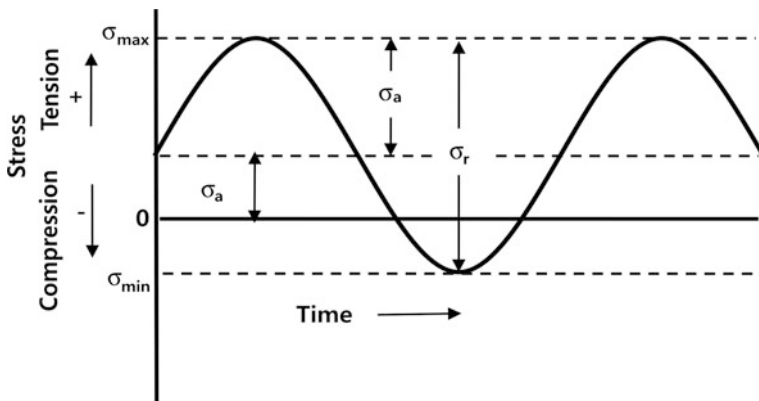


Fig. 7.12 Fatigue: failure under fluctuating and cyclic stresses asymmetrical about zero stress

$$R = \sigma_{\min}/\sigma_{\max} \quad (7.21)$$

There are two characteristic load patterns: one with $\chi = 1$, the load is pulsating; and one with $\chi = 0$, the load is reversed. The latter one is the most dangerous form of load variation.

The stress limit for fluctuating loading (the endurance limit) is defined as a value of stress that is safe for a given specimen irrespective of the number of load repetitions. It stays usually in a close relationship to the ultimate stress limit.

As seen in Fig. 7.13, another cyclic stresses that arise fatigue are (1) periodic and symmetrical about zero stress, (2) random stress fluctuations. In mechanical/civil system such as bridges, aircraft, machine components, and automobiles, fatigue failure under fluctuating/cyclic stresses are required:

- A maximum tensile stress of sufficiently high value
- A large enough variation or fluctuation in the applied stress, and
- A sufficiently large number of applied stress cycles.

There are two ways to determine when component is in danger of metal fatigue; either predicts when failure will occur due to the material/force/shape/iteration combination, and replace the vulnerable materials before this occurs, or perform inspections to detect the microscopic cracks and perform replacement once they occur. Selection of materials not likely to suffer from metal fatigue during the life of the product is the best solution, but not always possible. Avoiding shapes with sharp corners limits metal fatigue by reducing stress concentrations, but does not eliminate it.

Fatigue is a critical failure mechanism to be considered in product designs. It is a process in which damage accumulates due to the repetitive loads below the yield point, which is brittle-like even in normally ductile materials. Fatigue cracks begin very small and initially grow very slowly until the crack length approaches the

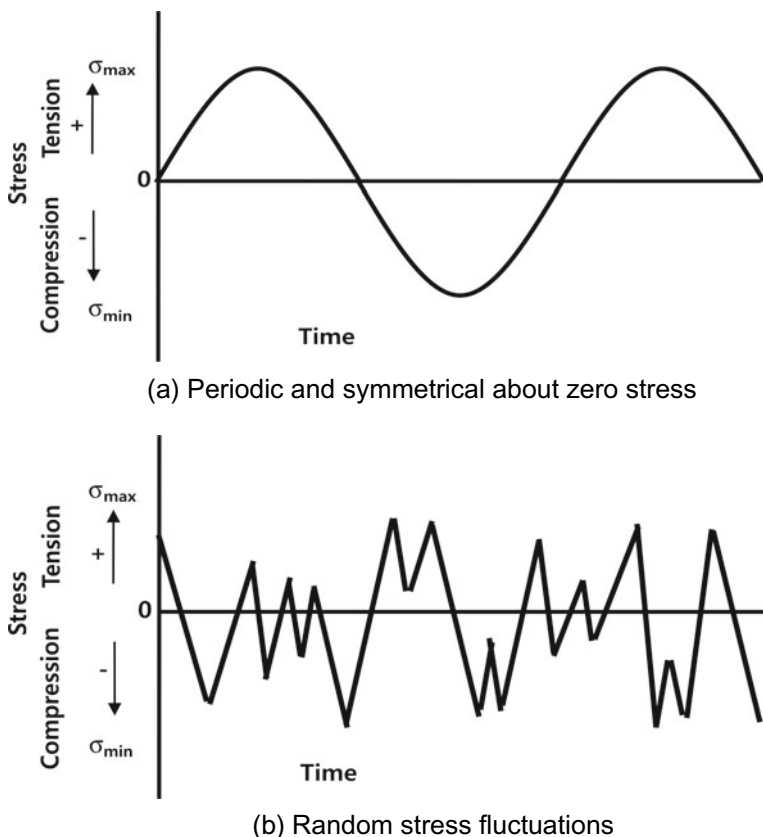


Fig. 7.13 Fatigue: failure under fluctuating and cyclic stresses

critical length. So it is dangerous because it is difficult to initially detect cumulative fatigue damage with the naked eye until the crack has grown to near critical length. Typical fracture surface is perpendicular to direction of applied stress. Fatigue failure has three distinct stages: (1) crack initiation in the areas of stress concentration (near stress raisers), (2) incremental crack propagation, and (3) final catastrophic failure.

The examples of “fatigue” for a multitude of reasons has been studied as the disaster of Comet aircraft and Versailles rail accident occurred when they became large enough to propagate catastrophically (see Chap. 2). Fatigue failure occur in both metallic and non-metallic materials, and are responsible for about estimated 80–90% of all structural failures—automobile crank-shaft, motor shaft, bridges, aircraft landing gear machine components, and the others. Thus, designing for maximum stress will not ensure adequate product lifetime. Most fracture induced belongs to this category.

Engineering stress is irregular around stress raisers such as holes, notches, or fillets that concentrate on the stress. For complex drawings, engineer frequently neglects these design flaws that might cause the product recalls. For instance the vibration of aircraft wing during a long flight can result in tens of thousands of load cycles. If designed improperly, these structures will fracture. It is important to find the design faults. In Chap. 8 we will discuss how to find the faulty designs by using the parametric ALT.

The central difficulty in designing against fracture in high-strength materials is that the presence of cracks can modify the local stresses to such an extent that the elastic stress analyses done so carefully by the designers are insufficient. When a crack reaches a certain critical length, it can propagate catastrophically through the structure, even though the gross stress is much less than would normally cause yield or failure in a tensile specimen. The term “fracture mechanics” refers to a vital specialization within solid mechanics in which the presence of a crack is assumed, and we wish to find quantitative relations between the crack length, the material’s inherent resistance to crack growth, and the stress at which the crack propagates at high speed to cause structural failure.

Fast fracture can occur within a few loading cycles. For example, fatigue failures in 1200 rpm motor shafts took less than 12 h from installation to final fracture, about 830,000 cycles. On the other hand, crack growth in slowly rotating process equipment shafts has taken many months and more than 10,000,000 cycles to fail.

7.4.3 Stress Concentration at Crack Tip

Although most engineering structures and machine components are designed such that the nominal stress remains elastic ($S_n < \sigma_{ys}$), stress concentrations due to faulty design in mechanical system often cause plastic strains to develop in the vicinity of notches where the stress is elevated due to the stress concentration effect.

Fracture strength of a material is related to the cohesive forces between atoms. One can estimate that the theoretical cohesive strength of a material should be one-tenth of the elastic modulus (E). However, the experimental fracture strength for brittle material is normally E/100—E/10,000 below this theoretical value. This much lower fracture strength is caused from the stress concentration due to the presence of microscopic flaws or cracks found either on the surface or within the material. As seen in Fig. 7.14, stress profile along X axis is concentrated at an internal, elliptically-shaped crack.

Stress has a maximum at the crack tip and decreased to the nominal applied stress with increasing distance away from the crack. Flaws such stress concentrators or stress raisers have the ability to amplify the stress at a given point. The magnitude of amplification depends on crack geometry and orientation.

Inglis's solution (1913) not only utilized elliptical coordinates to solve the elliptical hole problem, but he also used complex numbers. He derived the results

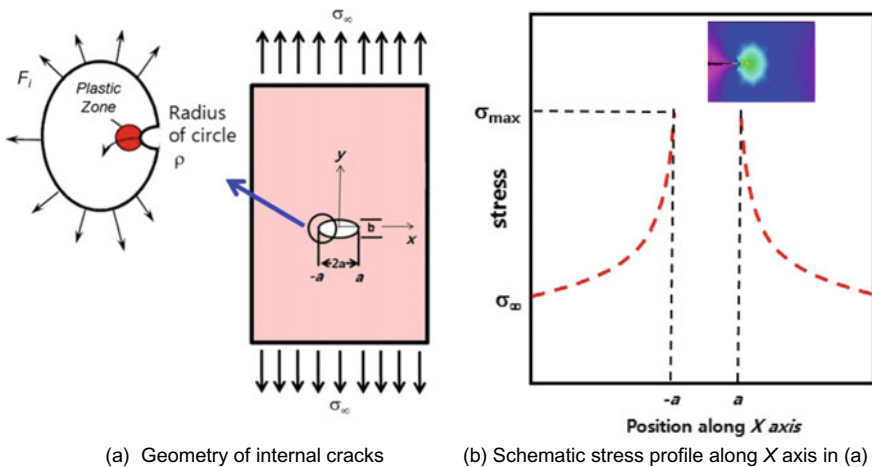


Fig. 7.14 Stress concentration at crack tip positions

with endlessly efforts. The maximum stress at the tip of the ellipse is related to its size and shape by

$$\sigma_{\max} = \sigma_{\infty} \left[1 + 2 \frac{a}{b} \right] \quad (7.22)$$

It is clear that Inglis's elliptical result reduces to the familiar $\sigma_{\max} = 3\sigma_{\infty}$ for the special case of a hole when $a = b$. On the other hand, the max stress is predicted to go to infinity as the ellipse flattens to form a crack ($b \rightarrow 0$).

The radius of curvature, ρ , at the tip of an ellipse is related to its length and width by

$$\rho = \frac{b^2}{a} \quad (7.23)$$

Solving this for b and substituting into the a/b ratio in $\sigma_{\max} = \sigma_{\infty} (1 + 2a/b)$ gives.

If the crack is similar to an elliptical hole through plate and is oriented perpendicular to applied stress, the maximum stress σ_{\max} occurs at a crack tip and approximated by Eq. (7.24)

$$\sigma_{\max} = \sigma_{\infty} \left[1 + 2 \sqrt{\frac{a}{\rho}} \right] \quad (7.24)$$

where ρ = radius of curvature, σ_{∞} = applied stress, σ_{\max} = stress at crack tip, a = half-length of internal crack or the full length for a surface flaw.

The magnitude of the nominal applied tensile stress is σ_∞ ; the radius of the curvature of the crack tip is ρ ; and a represents the length of a surface crack, or half the length of an internal crack. For a relatively long micro-crack, the factor $(a/\rho)^{1/2}$ may be very large. So Eq. (7.24) can be modified as:

$$\sigma_{\max} \cong 2\sigma_\infty \left(\frac{a}{\rho}\right)^{1/2} \quad (7.25)$$

The ratio of the maximum stress and the nominal applied tensile stress is denoted as the stress concentration factor K_t . The stress concentration factor is a simple measure of the degree to which an external stress is amplified at the tip of a small crack and described as:

$$K_t = \frac{\sigma_{\max}}{\sigma_\infty} \approx 2 \left(\frac{a}{\rho}\right)^{1/2} \quad (7.26)$$

Because an external stress is amplified at the tip of a crack, Eq. (7.26) can be rearranged as:

$$\sigma_{\max} = 2\sigma_\infty \left(\frac{a}{\rho}\right)^{1/2} = K_t \sigma_\infty \quad (7.27)$$

Stress amplification not only occurs at small flaws or cracks on a microscopic level of material but can also occur in sharp corners, holes, fillets, and notches on the macroscopic level. Cracks with sharp tips propagate easier than cracks having blunt tips. Because of amplifying an applied stress, stress concentration may occur at microscopic defects, internal discontinuities (voids/inclusions), sharp corners, scratches and notches that are often called stress raisers. Stress raisers are typically more destructive in brittle materials. Ductile materials have the ability to plastically deform in the region surrounding the stress raisers which in turn evenly distributes the stress load around the flaw. The maximum stress concentration factor results in a value less than that found for the theoretical value. Since brittle materials cannot plastically deform, the stress raisers will create the theoretical stress concentration situation.

The magnitude of this amplification depends on micro-crack orientations, geometry and dimensions. For example, stress concentration at sharp corners depends on fillet radius (Fig. 7.15).

7.4.4 Crack Propagation and Fracture Toughness

Cracks with sharp tips propagate easier than cracks having blunt tips. In ductile materials, plastic deformation at a crack tip “blunts” develops to the crack. Elastic

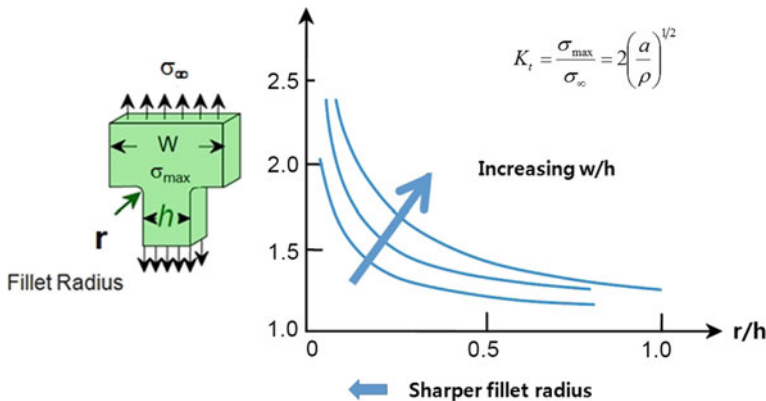


Fig. 7.15 Stress concentration at sharp corners in accordance with fillet radius [3]

strain energy is stored in material as it is elastically deformed. This energy is released when the crack propagates. And creation of new surfaces requires energy.

When a crack has grown into a solid to a depth a , a region of material adjacent to the free surfaces is unloaded, and its strain energy released. A simple way of visualizing this energy release is to regard two triangular regions near the crack flanks, of width a and height πa , as being completely unloaded, while the remaining material continues to feel the full stress σ . The total strain energy U released is then the strain energy per unit volume times the volume in both triangular regions:

$$U^* = -\frac{\sigma^2}{2E} \cdot \pi a^2 \quad (7.28)$$

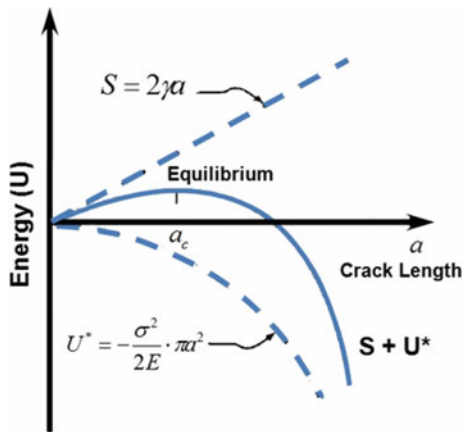
Here the dimension normal to the x-y plane is taken to be unity, so U is the strain energy released per unit thickness of specimen. This strain energy is liberated by crack growth. But in forming the crack, bonds must be broken, and the requisite bond energy is in effect absorbed by the material. The surface energy S associated with a crack of length a (and unit depth) is:

$$S = 2\gamma a \quad (7.29)$$

where γ is the surface energy and the factor 2 is needed since two free surfaces have been formed.

As shown in Fig. 7.16, the total energy associated with the crack is then the sum of the (positive) energy absorbed to create the new surfaces, plus the (negative) strain energy liberated by allowing the regions near the crack flanks to become unloaded.

Fig. 7.16 Total energy associated with the crack



As the crack grows longer, the quadratic dependence of strain energy on a eventually dominates the surface energy, and beyond a critical crack length a_c the system can lower its energy by letting the crack grow still longer. Up to the point where $a = a_c$, the crack will grow only if the stress is increased. Beyond that point, crack growth is spontaneous and catastrophic.

The value of the critical crack length can be found by setting the derivative of the total energy $S + U$ to zero:

$$\frac{\partial(S + U)}{\partial a} = 2\gamma - \frac{\sigma_f^2}{E} \cdot \pi a = 0 \quad (7.30)$$

Since fast fracture is imminent when this condition is satisfied, we can solve Eq. (7.30). Critical stress that is required for crack propagation is described as:

$$\sigma_c = \left(\frac{2E\gamma_s}{\pi a} \right)^{1/2} \quad (7.31)$$

where γ_s = specific surface energy.

When the tensile stress at the tip of crack exceeds the critical stress value, the crack propagates and results in fracture. Most metals and polymers have plastic deformation. For ductile materials specific surface energy γ_s should be replaced with $\gamma_s + \gamma_p$ where γ_p is plastic deformation energy. So Eq. (7.31) can be described as:

$$\sigma_c = \left(\frac{2E(\gamma_s + \gamma_p)}{\pi a} \right)^{1/2} \quad (7.32)$$

For highly ductile materials, $\gamma_p \gg \gamma_s$ is valid. So Eq. (7.32) can be modified as:

$$\sigma_c = \left(\frac{2E\gamma_p}{\pi a} \right)^{1/2} \quad (7.33)$$

All brittle materials contain a population of small flaws that have variety of sizes. When the magnitude of the tensile stress at the tip of crack exceeds the critical stress value, the crack propagates and results in fracture. Very small and virtually defect-free metallic and ceramic materials have been produced with fracture strength that approaches their theoretical values.

Example 7.5 There is a long plate of glass subjected to a tensile stress of 30 MPa. If the modulus of elasticity and specific surface energy for this glass are 70 GPa and 0.4 J/m², find out the critical length of a surface flaw that can have no fracture.

From Eq. (7.32), $E = 70$ GPa, $\gamma_s = 0.4$ J/m², $\sigma = 30$ MPa. So the critical length can be obtained as

$$a_c = \left(\frac{2E\gamma_s}{\pi\sigma^2} \right) = \left(\frac{2 \cdot 70 \text{ GPa} \cdot 0.4 \text{ J/m}^2}{\pi \cdot (30 \text{ MPa})^2} \right) = 2.0 \times 10^{-6} \text{ m}$$

Fracture toughness K_c is a material's resistance to fracture when a crack is present. It therefore means the amount of stress required to propagate a flaw. It can be described as:

$$K_c = \sigma_c \sqrt{\pi a} \quad (7.34)$$

Fracture toughness depends on temperature, strain rate and microstructure. Its magnitude diminishes with increasing strain rate and decreasing temperature. If yield strength due to alloying and strain hardening improve, fracture toughness will increase with reduction in grain size.

7.4.5 Crack Growth Rates

The metal fatigue begins at an internal (or surface) flaw by the concentrated stresses, and progress initially of shear flow along slip planes. As previously mentioned in Sect. 7.2, slip can happen (111) plane in a FCC lattice because the atoms are most closely packed. Over a number of random loading cycles in field, this slip generates intrusions and extrusions that begin to resemble a crack. A true crack running inward from an intrusion region may propagate initially along one of the original slip planes, but eventually turns to propagate transversely to the principal normal stress.

After repeated loadings, the slip bands can grow into tiny shear-driven micro-cracks. These Stage I cracks can be described as a back and forth slip on a

series of contiguous crystallographic plane to form a band. It is within this slip bands that the process of pores nucleation and coalescence. The process eventually leads to micro cracks formation. Often, extrusion and intrusions may also appear which, being a very localized discontinuity, results in a much faster micro crack formation.

Micro cracks join to form a macro crack in Stage II of fatigue. Now the crack is already long enough to escape shearing stress control and be driven by normal stress which produces a continuous growth, cycle by cycle, on a plane that is no longer crystallographic, but rather normal to external loads. Ahead of this macro crack two plastic lobes are generated by stress concentration. The cracks grow perpendicular to the dominant stress and increases dramatically by plastic stresses at the crack tip as seen in Fig. 7.17.

It is vital that engineers be able to predict the rate of crack growth during load cycling in aircraft as well as in other engineering structures, so that the problematic parts be replaced or repaired before the crack reaches a critical length. A great deal of experimental evidence supports the view that the crack growth rate can be corrected with the cycle variation in the stress intensity factor [4]:

$$\frac{da}{dN} = A \Delta K^m \quad (7.35)$$

where da/dN is the fatigue crack rate per cycle, $\Delta K = K_{min} - K_{max}$ is the stress intensity factor range during the cycle, and A and m are parameters that depend the material, environment, frequency, temperature and stress ratio.

Fatigue crack propagation rate during Stage II depends on stress level, crack size, and materials. This is sometimes known as the “Paris Law,” and leads to plots similar to that shown in Fig. 7.18.

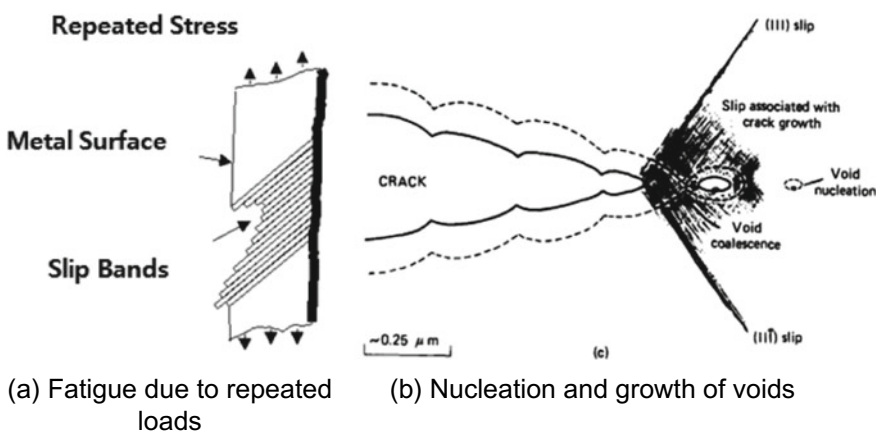
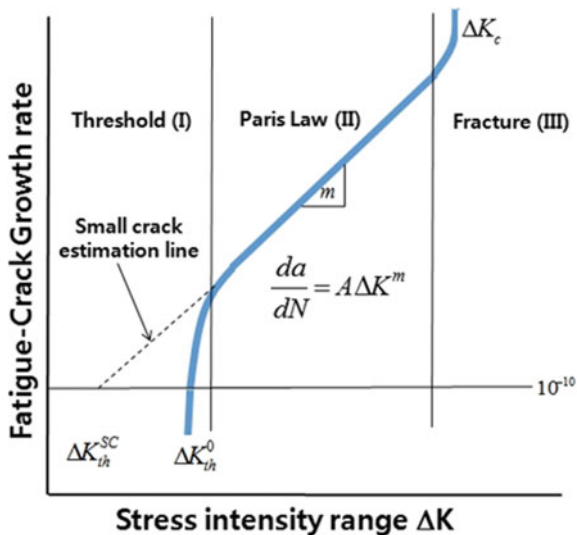


Fig. 7.17 A schematic diagram of general slip producing nucleation and growth of voids

Fig. 7.18 Paris law for fatigue crack growth rates



Some specific values of the constants m and A for various alloys are given in Table 7.1. The exponent m is often near 4 for metallic systems, which might be rationalized as the damage accumulation being related to the volume V_p of the plastic zone: since the volume V_p of the zone scales with r_p^2 and $r_p \propto K_I^2$, then $da/dn \propto \Delta K^4$.

7.4.6 Fatigue Analysis

7.4.6.1 Introduction

The majority of component designs involve parts subjected to fluctuating or cyclic loads. Such loading induces fluctuating or cyclic stresses that often result in failure by fatigue. About 95% of all structural failures occur through a fatigue mechanism. The concept of fatigue that describes structural system subjected to repeated loadings was originated in the mid-eighteenth century in the railroad industry.

Table 7.1 Numerical parameters in the Paris equation

Alloy	m	A
Steel	3	10^{-11}
Aluminum	3	10^{-12}
Nickel	3.3	4×10^{-12}
Titanium	5	10^{-11}

When fatigue failures of railway axles became a widespread problem in the middle of the nineteenth century, this drew attention to cyclic loading effects. This was the first time that many similar components had been subjected to millions of cycles at stress levels well below the monotonic tensile yield stress.

The modern study of fatigue is generally dated from the work of A. Wöhler, a German engineer in the railroad system in the mid-nineteenth century. Wöhler was chief superintendent of rolling stock on the Lower Silesia-Brandenberg Railroad. Wöhler was concerned by the causes of fracture in rail car axles after prolonged use. A railcar axle is essentially a round beam in four-point bending, which produces a compressive stress along the top surface and a tensile stress along the bottom. After the axle has rotated a half turn, the bottom becomes the top and vice versa, so the stresses on a particular region of material at the surface vary repeatedly from tension to compression. Though the metal became tired, fatigue was named to describe this type of damage. This is now known as fully reversed fatigue loading. Some of Wöhler's data are for Krupp axle steel and are plotted, in terms of nominal stress (S) versus number of cycles to failure (N), on what has become known as the S-N diagram. Each curve on such a diagram is still referred to as a Wöhler line (see Fig. 7.19).

Since 1830, it has been recognized that metal under a repetitive or fluctuating load will fail at a stress level lower than required to cause failure under a single application of the same load. Figure 7.20 shows a bar-shaped component subjected to a uniform sinusoidal varying force. After a period of time, a crack can be seen to initiate on the circumference of the hole. This crack will then propagate through the component until the remaining intact section is incapable of sustaining the imposed stresses and the component fails.

Fig. 7.19 Some of Wöhler's data for rail car axles steel on the S-N diagram [5]

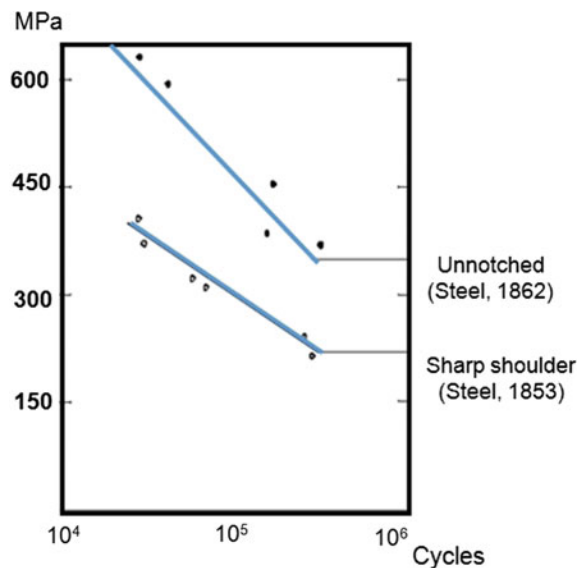
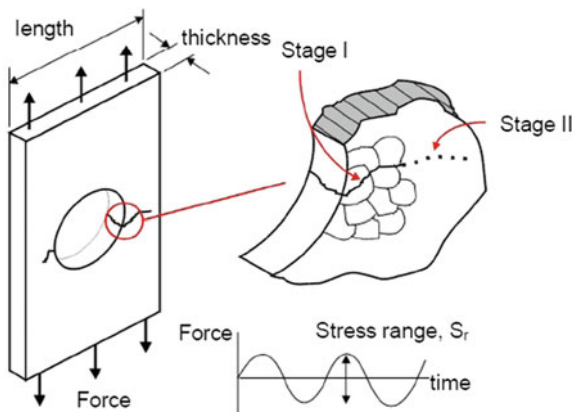


Fig. 7.20 Bar-shaped component subjected to a uniform sinusoidal varying force



The physical development of a crack is generally divided into 2 separate stages. These relate to the crack initiation phase (Stage I) and the crack growth phase (Stage II). Fatigue cracks initiate through the release of shear strain energy. The following diagram shows how the shear stresses result in local plastic deformation along slip planes. As the sinusoidal loading is cycled, the slip planes move back and forth like a pack of cards, resulting in small extrusions and intrusions on the crystal surface. These surface disturbances are approximately $1\text{--}10 \mu$ in height and constitute embryonic cracks.

A crack initiates in this way until it reaches the grain boundary. The mechanism at this point is gradually transferred to the adjacent grain. When the crack has grown through approximately 3 grains, it is seen to change its direction of propagation. Stage I growth follows the direction of the maximum shear plane, or 45° to the direction of loading. The physical mechanism for fatigue changes during Stage II. The crack is now sufficiently large to form a geometrical stress concentration. A tensile plastic zone is created at the crack tip as shown in the following diagram. After this stage, the crack propagates perpendicular to the direction of the applied load.

7.4.6.2 Fatigue Design Methods

Fatigue design deals with the study of cracks how they form and how they grow due to cyclic stress. As described in previous section, total fatigue life consists of (1) cycles to form a crack and (2) cycles to grow a crack to failure. Figure 7.21 indicates the iterative nature of design fatigue and the need for significant input items such as geometry, load history, environment, design criteria, material properties, and processing effects. With these inputs, fatigue is performed through synthesis, analysis, and testing. This requires selecting the configuration, material, and processes, performing stress analysis, choosing a design life and cumulative damage model, and making a computational life prediction/estimation. This is

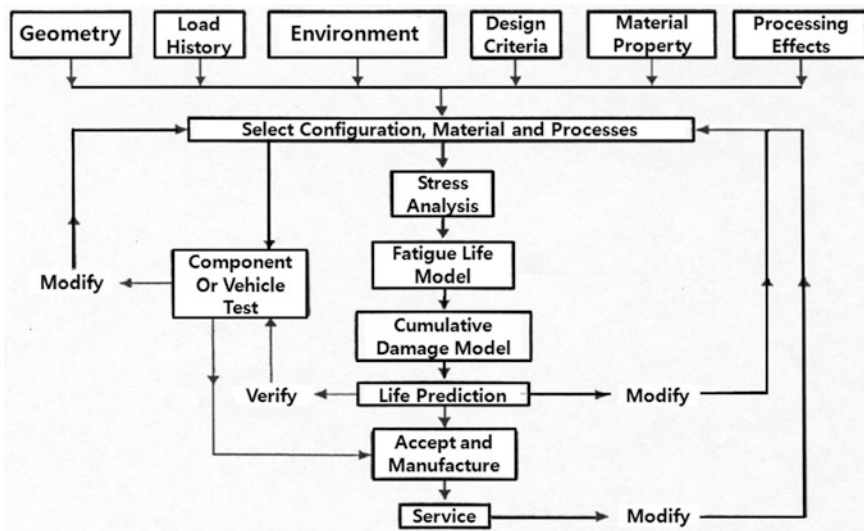


Fig. 7.21 Fatigue design flow chart

followed by durability testing, which can suggest modification or the decision to accept and manufacture the product and put it into service. Evaluation of service usage and success is part of the fatigue method.

Choosing the fatigue life model is a significant decision. Currently four such models exist for fatigue engineers. These are:

1. The nominal stress-life (S-N) model, first formulated between the 1850s and 1870s.
2. The local strain-life (ϵ -N) model, first formulated in the 1960s.
3. The fatigue crack growth ($da/dN-\Delta K$) model, first formulated in the 1960s.
4. The two-stage model, which consists of combining models 2 and 3 to incorporate both macroscopic fatigue crack formation (nucleation) and fatigue crack growth.

As noted, the S-N model has been available for about 150 years, while the other models have been available only since the 1960s. The nominal S-N model uses nominal stresses and relates these to local fatigue strengths for notched and un-notched stresses members. The local ϵ -N model deals directly with local strain at a notch, and this is related to smooth specimen strain-controlled fatigue behavior. Several analytical models can be used to determine local strains from global or nominal stresses or strains. The fatigue crack growth $da/dN-\Delta K$ model requires the use of fracture mechanics and integration of the fatigue crack growth rate equation to obtain the number of cycles required to grow a crack from a given length to another length and/or to fracture. This model can be considered a total fatigue life model when it is used in conjunction with information on the existing initial crack

size following manufacture. The two-stage method incorporates the local ε -N model to obtain the life to the formation of a small macro-crack, following manufacture. The two-stage method incorporates the local ε -N model to obtain the life to the formation rate equation for the remaining life.

Neuber's rule is used to convert an elastically computed stress or strain into the real stress or strain when plastic deformation occurs. For example, we may compute a stress with elastic assumptions at a notch to be $K_t S$ and this stress exceeds the strength of the material. The real stress will be somewhere on the materials stress-strain curve at some point σ .

7.4.6.3 Basic Concepts of the ε -N Method

The strain life method had its major development during the 1960s. It is based on the premise that the local stresses and strains around a stress concentration control the fatigue life. Although most structures and machine components have nominal stresses that remain elastic, occasional high loads and stress concentrations cause plastic deformation around notches. Fatigue damage is dependent on the local plastic strains around stress concentrators.

The materials deformation during a fatigue test (or in field) is measured in the form of a hysteresis loop. After the initial transient behavior the material stabilizes and the same hysteresis loop is obtained for every loading cycle. Each strain range tested will have a corresponding stress range that is measured. The cyclic stress strain curve is a plot of all of this data (Fig. 7.22).

The local plastic strains are controlled by the elastic deformation of the surrounding elastic material. Even though external loads are applied, the local region is strain or deformation controlled. The strain resistance of the material is a better measure of the fatigue performance than the stress resistance. Strain controlled tests are always conducted in axial loading. Deflections are controlled and converted into strain. The resulting forces are measured to compute the applied stress. Metals undergo transient behavior when they are first cycled.

As seen in Fig. 7.23, the material becomes stronger with each loading cycle into the plastic range. Other materials loose strength when they are repeatedly plastically deformed. After the initial transient behavior most materials have steady state behavior described by the hysteresis loop. During the fatigue test the strain range, $\Delta\varepsilon$, is controlled and the resulting stabilized stress range, $\Delta\sigma$, is recorded along with the cycles to failure. In strain life testing cycles to failure is converted to reversals to failure. One cycle has two reversals and a symbol $2N_f$ is used.

Before plotting the strain vs. fatigue life, the total strain that was controlled during the test is divided into the elastic and plastic part. The elastic strain is computed as the stress range divided by the elastic modulus. Plastic strain is obtained by subtracting the elastic strain from the total strain.

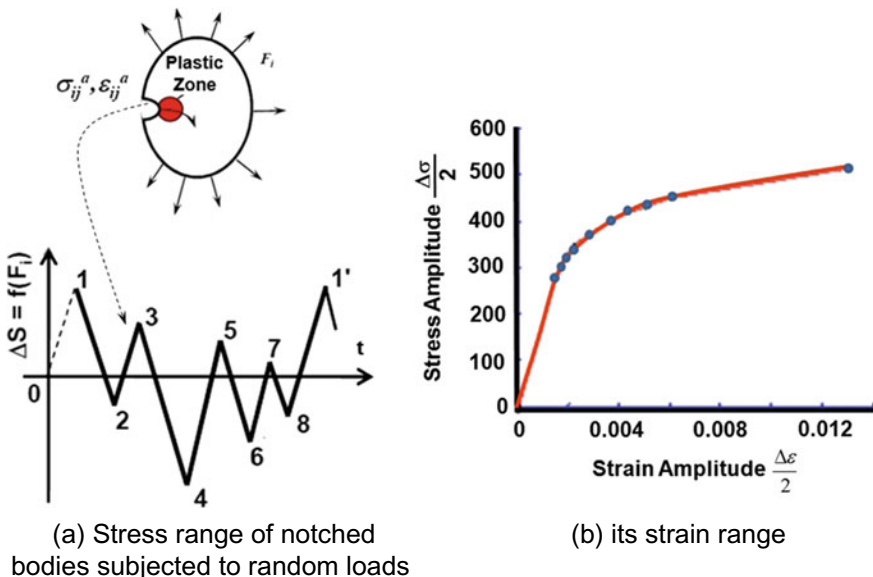
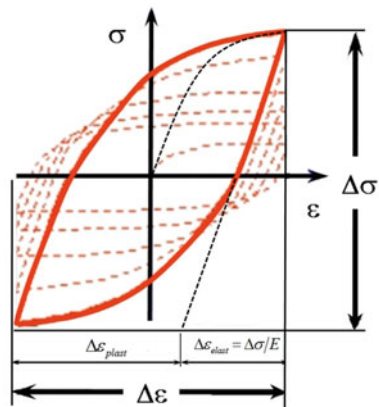


Fig. 7.22 Strain range tested versus a corresponding stress range

Fig. 7.23 Steady state behavior of $\Delta\epsilon$ and $\Delta\sigma$ described by the hysteresis loop



In cases where lifetime is dominated by fatigue crack initiation, common to use stress-life (S-N) curves and empirical fits to the data:

$$\sigma_a = \sigma'_f (2N_f)^b \quad (\text{Basquin's Law}) \quad (7.36)$$

$$\sigma_a = \frac{\Delta\sigma}{2} = \frac{\Delta\epsilon_e E}{2} \quad (7.37)$$

Thus, for high cycle Fatigue we can described as,

$$\Delta\epsilon_e/2 = \sigma_a/E = \left(\sigma'_f/E\right) (2N_f)^b \quad (7.38)$$

According to Coffin and Manson, the number N_R of cycles to fracture in the low-fatigue regime is related to the amplitude of the applied cyclic plastic deformation $\Delta\epsilon_p$. That is,

$$\Delta\epsilon_p/2 = \sigma_a/E = \epsilon'_f (2N_f)^c \quad (7.39)$$

Test data is then fit to a simple power function to obtain the material constants; fatigue ductility coefficient, ϵ'_f , fatigue ductility exponent, c , fatigue strength coefficient, σ'_f , and fatigue strength exponent, b . The total strain is then obtained by adding the elastic and plastic portions of the strain to obtain a relationship between the applied strain and the fatigue life (Fig. 7.24).

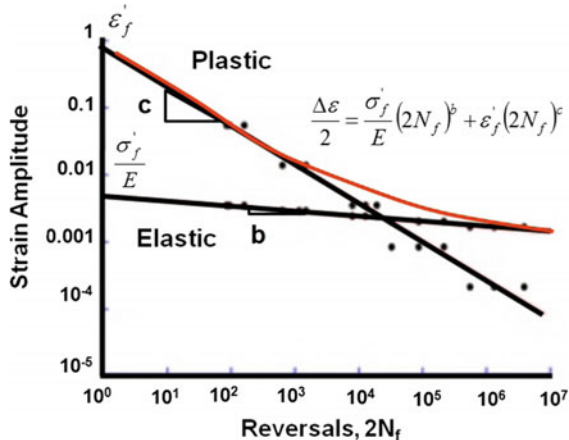
If Eqs. (7.38) and (7.39) combine, we can obtain,

$$\frac{\Delta\epsilon}{2} = \frac{\sigma'_f}{E} (2N_f)^b + \epsilon'_f (2N_f)^c \quad (7.40)$$

7.4.6.4 Local Strain-Life (ϵ -N) Model (Neuber Method)

One of the objectives of fatigue analysis is to predict the magnitudes of the local cyclic stresses and strains experienced at the stress raisers of many components subjected to repetitive loading. Most estimates of component stress, however, have been calculated elastically by means of either traditional manual calculations or elastic FEA methods. It is then necessary to translate the elastic calculated stress at

Fig. 7.24 Total strain obtained by adding the elastic and plastic portions of the strain



the critical locations into estimates of elastic-plastic stress and strain behavior. Of the several methods of accomplishing this translation, the one most popularly adopted by most software methods is the Neuber plasticity correction.

The Neuber method allows a conversion of fictitious wholly elastic stress values obtained from a FEM to “real” elastic-plastic values. This is the basic condition for any computation done through the local elastic-plastic strain analysis. Neuber’s rule states, with some mathematical proof, that the product of the elastic solution is equal to the product of the real elastic plastic solution (Fig. 7.25).

The basic assumption of the method looks like this:

$$\frac{1}{2} \sigma_{plast} \cdot \varepsilon_{plast} = \frac{1}{2} \sigma \cdot \varepsilon \quad (7.41)$$

The fictitious state of the left hand side is purely elastic and allows a use of Hooke’s law. The right hand side respects the real elastic-plastic work diagram. Fatigue analysis requires stress data from several loadings. There are methods to scale the stresses, since they are linearly related to the amount of force, double the force and stress will double as well if the system still has linear behavior. For example, if you load a pencil with 10 kg there will be stresses and some deformation. If you load a pencil with 20 kg, the pencil will break instead of having double the stress and deformation. There are two ways to solve this problem, the

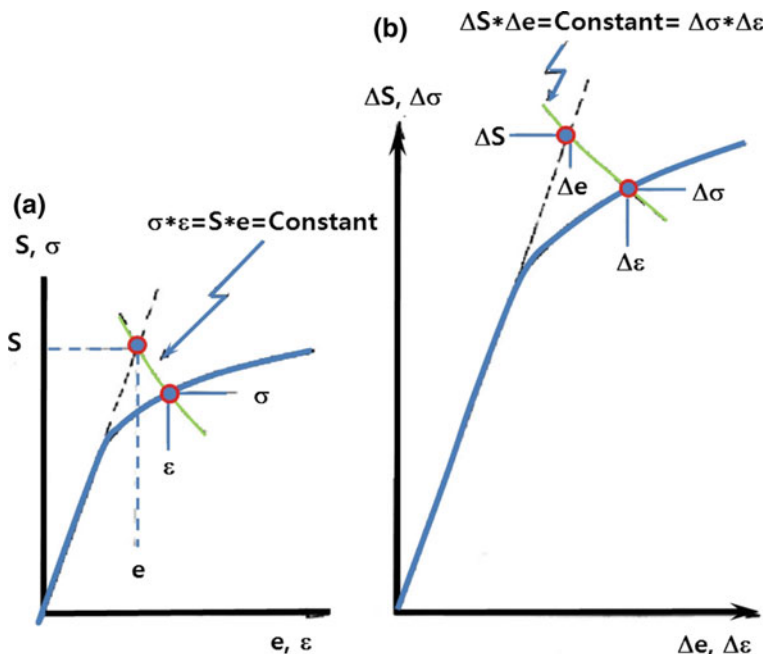


Fig. 7.25 a Initial stress-strain curve, b Hysteresis loop stress-strain curve

first is to do a nonlinear stress analysis with a complex material model (wood surrounding some graphite) which would take a lot of analysis time. Or, you can stick with the simple linear analysis then do a Neuber correction [6–8] and judge the new stress. Exceeding the yield might cause permanent deformation, whereas exceeding the ultimate tensile strength would cause the system to fail.

For durability analysis, the Neuber approximation is a well-known method to estimate the local elastic-plastic stresses σ_{plast} in notches based on linear-elastic FEM stress results σ_{elast} .

With the Young's Modulus E and the non-linear strain ε_{plast} , it can be expressed as

$$\sigma_{plast} \cdot \varepsilon_{plast} = const. = \frac{\sigma^2}{E} \quad (7.42)$$

The cyclic stress strain curve describes the behavior of the material after it has been plastically deformed in service a few times. A simple power function is fit to this curve to obtain three material properties. Using the Ramberg-Osgood equation [9] for the description of the cyclic stress strain curve,

$$\varepsilon_{plast} = \frac{\sigma_{plast}}{E} + \left(\frac{\sigma_{plast}}{K'} \right)^{1/n'} \quad (7.43)$$

where the cyclic hardening coefficient K' and cyclic hardening exponent n' are introduced.

We should be notified that the plastic part of strain is in all cases described by parameters of Basquin-Manson-Coffin curve, since it can be proved that:

$$n' = \frac{b}{c}; \quad K' = \frac{\sigma'_f}{\left(\varepsilon'_f\right)^n} \quad (7.44)$$

Thus the final non-linear equation for determination of elastic-plastic stress state is:

$$\sigma_{plastic}^2 = \sigma \cdot \left[\sigma + E \cdot \varepsilon'_f \cdot \left(\frac{\sigma}{\sigma'_f} \right)^{\frac{c}{b}} \right] \quad (7.45)$$

Pospíšil later stated that the equation should be rewritten and equipped with a further parameter m in order to include all possible types of component shapes and loading:

$$\sigma_{plastic}^2 = \sigma^m \cdot \left[\sigma + E \cdot \varepsilon'_f \cdot \left(\frac{\sigma}{\sigma'_f} \right)^{\frac{c}{b}} \right]^{(1-m)} \quad (7.46)$$

7.5 Facture Failure

7.5.1 Introduction

Fracture is the separation of a body into pieces subjected to stress. Fracture takes place whenever the applied loads (or stresses) are more than the resisting strength of the body. It starts with a crack that breaks without making fully apart. Fracture due to overstress is probably the most prevalent failure mechanism in mechanical/civil system and might be classified as ductile (shear) fracture, brittle (cleavage) fracture, fatigue fracture, crazing, and de-adhesion.

When a crack propagates, new free surface is generated, having a specific surface energy γ . This energy is provided by the external load and is also available as stored elastic energy. Not all available energy, however, is used for the generation of new crack surfaces. It is also transformed into other energies, like kinetic energy or dissipative heat. When a lot of available energy is used for crack growth, the fracture is said to be brittle. When a lot of energy is transformed into other energies, mainly due to dissipative mechanisms, the fracture is indicated to be ductile.

As seen in Fig. 7.26, brittle fracture is the failure of a material with minimum of plastic deformation. Brittle fracture propagates rapidly on a crack with minimum energy absorption and plastic deformation. Brittle fracture occurs along characteristics crystallographic planes called as cleavage planes. The mechanism of Brittle fracture was initially explained by Griffith theory [10]. Griffith postulated that in a brittle material there are micro cracks which act to the concentrated stress at their tips. The crack could come from a number of sources as flow occurred during solidification or a surface scratch. When plastic deformation at the crack tip is prohibited, the crack can travel through grains by splitting atom bonds in lattice planes. This cleavage fracture will prevail in materials with little or no closed-packed planes, having HCP or BCC crystal structure.

Brittle materials are glasses, ceramics, some polymers, metals. They have the following characteristics:

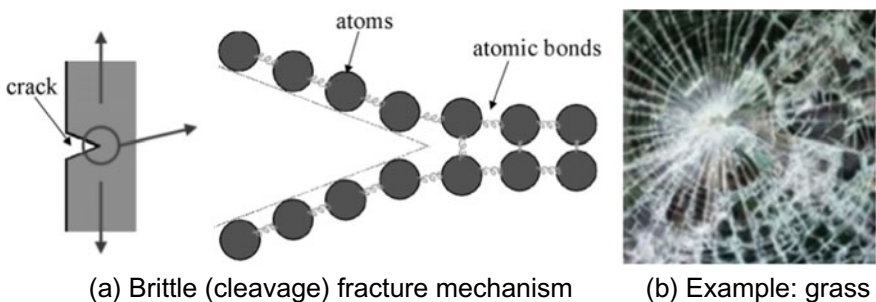


Fig. 7.26 Brittle (cleavage) fracture mechanism

- No appreciable plastic deformation
- Crack propagation is very fast
- Crack propagates nearly perpendicular to the direction of the applied stress
- Crack often propagates by cleavage—breaking of atomic bonds along specific crystallographic planes (cleavage planes).

For ductile fracture, when a crystalline material is loaded, dislocations will start to move through the lattice due to local shear stresses. Also the number of dislocations will increase. Because the internal structure is changed irreversibly, the macroscopic deformation is permanent (plastic). The dislocations will coalesce at grain boundaries and accumulate to make a void. These voids will grow and one or more of them will transfer in a macroscopic crack.

Because the origin and growth of cracks is provoked by shear stresses, this mechanism is referred to as shearing. Plastic deformation is essential, so this mechanism will generally be observed in FCC crystals, which have many closed-packed planes. The fracture surface has a 'dough-like' structure with dimples, the shape of which indicate the loading of the crack (see Figs. 7.27 and 7.28).

- Brittle Fracture: Separation along crystallographic planes due to breaking of atomic bonds (V-shaped Chevron, Cleavage, Inter-granular)

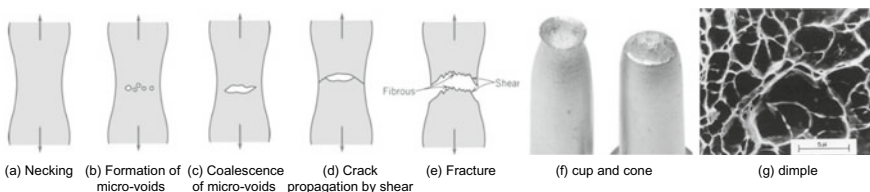
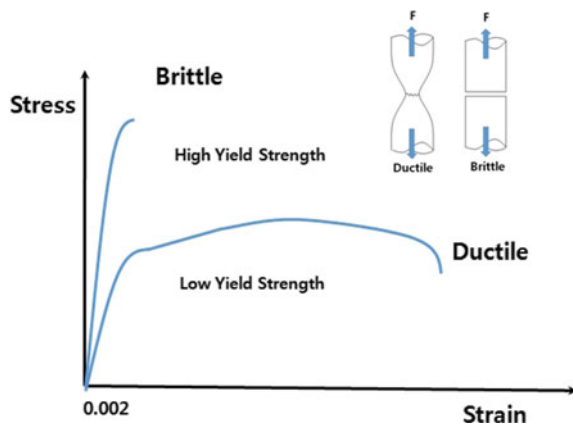


Fig. 7.27 Ductile fracture failure mechanism

Fig. 7.28 Brittle versus ductile fracture in material



- Ductile Fracture: Initiation, growth and coalescence of micro-voids (Cup-and-cone, Dimple)

However, commercial material is made up of polycrystalline, whose crystal axes are oriented at random. When polycrystalline material is subjected to stress, slip starts first in those grains in which the slip system is most favorably situated with respect to the applied stress. Since contact at the grain boundaries is maintained, it may be necessary for more than one slip system to operate. The rotation into the axis of tension brings other grains, originally less favorably oriented, into a position where they can now deform. As deformation and rotation proceed, the individual grains tend to elongate in the direction of flow.

When a crystal deforms, there is some distortion of the lattice structure. This deformation is greatest on the slip planes and grain boundaries and increases with deformation. This is evident by an increase in resistance to further deformation. The material is undergoing strain hardening or work hardening. Since dislocations pile up at grain boundaries, metals can be hardened by reducing the size of the grains.

7.5.2 **Ductile-Brittle Transition Temperature (DBTT)**

The Ductile-to-Brittle Transition Temperature (DBTT) is widely observed in metals that are dependent on the composition of the metal. For some steels the transition temperature can be around 0 °C, and in winter the temperature in some parts of the world can be below this. As a result, some steel structures are very likely to fail in winter. The controlling mechanism of this transition still remains unclear despite of large efforts made in experimental and theoretical investigation. All ferrous materials (except the austenitic grades) exhibit a transition from ductile to brittle when tested above and below a certain temperature, called as ductile-to-brittle transition temperature (DBTT). FCC metals such as Cu, Ni remain ductile down to very low temperatures. For ceramics, this type of transition occurs at much higher temperatures than for metals (Fig. 7.29).

Steels were used having DBTT's just below room temperature. Low temperatures can severely become brittle steels. At higher temperature, the impact energy is large, corresponding to a ductile mode of fracture. As the temperature is lowered, the impact energy drops suddenly over a relatively narrow temperature range which corresponds to the mode of brittle fracture. Fatigue cracks nucleated at the corners of square hatches and propagated rapidly by brittle fracture.

Since the famous weld fractures in some US army ships (Liberty Ships, tankers) during World War II are investigated, the ductile-to-brittle transition can be measured by impact testing such as Charpy V-notch testing (Fig. 7.30). Although the tensile stress-strain curve already provides an indication for brittle/ductile failure, the standard experiment to investigate this is the Charpy V-notch test. The main advantage of this test is that it provides a simple measure for the dissipated energy during fast crack propagation.

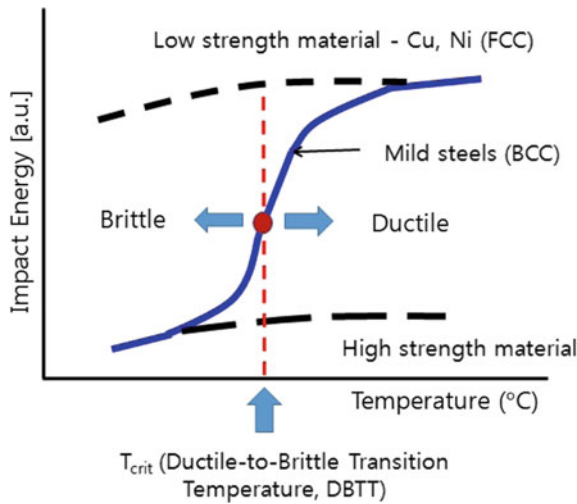


Fig. 7.29 Ductile-to-brittle transition temperature

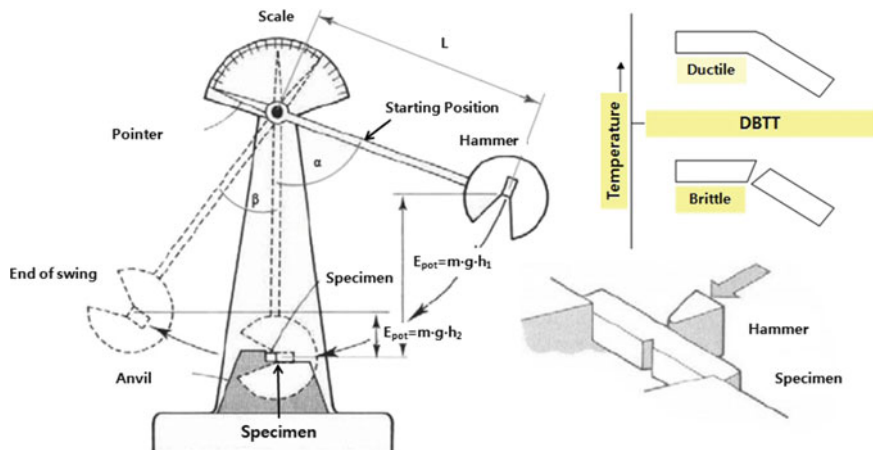


Fig. 7.30 Schematic of a conventional Charpy V-notch testing

The specimen is a beam with a 2 mm deep V-shaped notch, which has a 90° angle and a 0.25 mm root radius. It is supported and loaded as in a three-point bending test. The load is provided by the impact of a weight at the end of a pendulum. A crack will start at the tip of the V-notch and runs through the specimen. The material deforms at a strain rate of typically 103 s^{-1} . The energy which is dissipated during fracture can be calculated easily from the height of the pendulum weight, before and after impact. The dissipated energy is the Impact Toughness C_v .

The impact toughness can be determined for various specimen temperatures T . For intrinsic brittle materials like high strength steel, the dissipated energy will be low for all T . For intrinsic ductile materials like FCC-metals, C_v will be high for all T . A large number of materials show a transition from brittle to ductile fracture with increasing temperature.

7.6 Stress–Strength Analysis

Stress–strength interference analysis in reliability engineering is the analysis of the strength of the materials and the interference of the stresses placed on the materials [11]. It also is useful to understand the design of mechanical components in automobile, refrigerator, and the other. A mechanical product's probability of failure is equal to the probability that the stress experienced by that product will exceed its strength. If given one probability distribution function for a product's stress and its strength, the probability of failure can be estimated by calculating the area of the overlap between the two distributions. This overlapping region may be also referred to as stress-strength interference (Fig. 7.31).

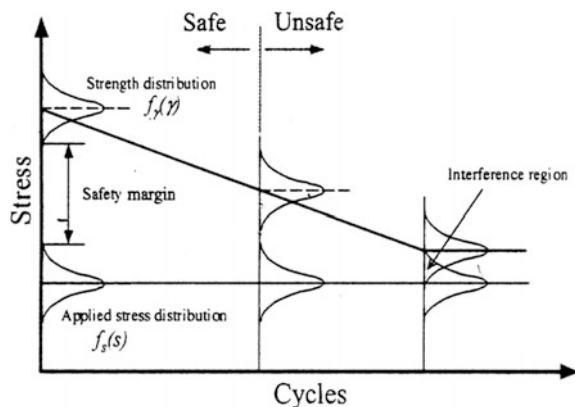
If the distributions for both the stress and the strength both follow a normal distribution, the expected probability of failure, F , can be calculated as:

$$F = P[\text{stress} \geq \text{strength}] = \int_0^{\infty} f_{\text{strength}}(x) \cdot R_{\text{stress}}(x) dx \quad (7.47)$$

The expected reliability, R , is calculated as:

$$R = P[\text{stress} \leq \text{strength}] = \int_0^{\infty} f_{\text{stress}}(x) \cdot R_{\text{strength}}(x) dx \quad (7.48)$$

Fig. 7.31 Applied fatigue stress-strength interference model



There are two ways to increase reliability: (1) increase the difference (or safety margin) between the mean stress and strength values, (2) decrease the standard deviations of the distributions of stress and strength. The estimates of stresses and strengths for all component of a product would be perfectly accurate, but this is too costly to accomplish. And the stress conditions depend on the way the product is used— the customer profiles and environmental conditions.

However, if there are the design failures like stress raiser in product structure, stress–strength interference analysis is not a good expression that can express the root cause of product recalls. So the weakest part first will fracture before the product reaches to the lifetime that will be equivalent to safety margin. The strength distribution mainly depends on the material used in the product, its dimensions and the manufacturing process. To improve the product reliability, the product in the design phase should increase its strength by using the optimal design and reliability testing. The best way to explain the product failure is the parametric accelerated life testing that will be explained in Chaps. 8 and 9.

Environmental stresses have a distribution with a mean μ_x and a standard deviation S_x and component strengths have a distribution with a mean μ_y and a standard deviation S_y . The overlap of these distributions is the probability of failure Z . This overlap is also referred to stress-strength interference.

If stress and strength are normally distributed random variables and are independent of each other, the standard normal distribution and Z tables can be used to quantitatively determine the probability of failure. First, the Z-statistic is calculated as follows:

$$Z = -\frac{\mu_x - \mu_y}{\sqrt{S_x^2 + S_y^2}} \quad (7.49)$$

Using the Z value table for a standard normal distribution, the area above the calculated Z-statistic is the probability of failure. $P(Z)$ can be determined from a Z table or a statistical software package.

Example 7.6 If μ_x is 2500 kPa, μ_y is 4500 kPa, S_x is 500 kPa, and S_y is 400 kPa, the probability of failure can be calculated:

$$Z = -\frac{\mu_x - \mu_y}{\sqrt{S_x^2 + S_y^2}} = -\frac{2500 - 4500}{\sqrt{500^2 + 400^2}} = 2.34$$

Using the Z-value table for a standard Normal distribution, the area above a Z value of 2.34 (2.34 standard deviations) is 0.0096. Therefore, the probability of failure is 0.96%. Likewise, reliability is $1 - 0.0096 = 0.9904$ or 99.04%.

7.7 Failure Analysis

7.7.1 Introduction

Using microscopy and spectroscopy, failure analysis is to search out the root cause of failed components in field and to improve product reliability. Failure analysis is designed to identify the failure modes, the failure site, and the failure mechanism. It determines the root causes of the design and recommend failure prevention methods for the problematic mechanical product in field.

The process begins with the most non-destructive techniques and then proceeds to the more destructive techniques, allowing the gathering of unique data from each technique throughout the process. The sequence of procedures is visual inspection, electrical testing, non-destructive evaluation, and destructive evaluation.

As seen in Fig. 7.32, failure mechanism of product might be classified as overstress mechanisms and wearout mechanisms. Some modes of failure mechanisms are excessive deflection, buckling, ductile fracture, brittle fracture, impact, creep, relaxation, thermal shock, wear, corrosion, stress corrosion cracking, and various types of fatigue. Over time, as more is understood about a failure, the root cause evolves from a description of symptoms and outcomes. The more complex the product or situation, the more necessary a good understanding of its failure cause is to ensuring its proper action plans.

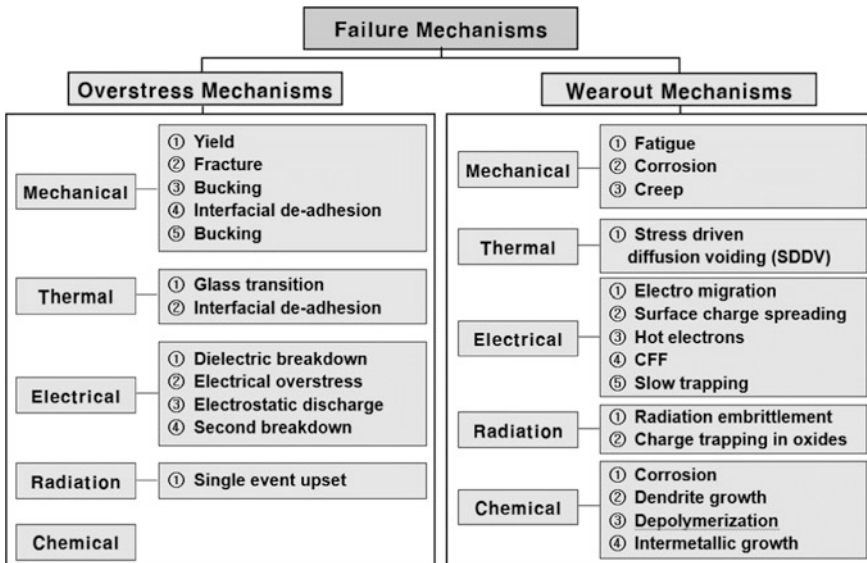


Fig. 7.32 Typical failure mechanisms in product

Under user environment conditions, product materials may be degraded by loads or corrosion processes, such as rusting in the case of iron and steel. Such processes can also be affected by load in the mechanisms of stress corrosion cracking and environmental stress cracking.

7.7.2 *Procedure of Failure Analysis*

To improve reliability of product or modules, the design of a part structure requires the engineer to minimize the possibility of failure. It therefore is a critical process to understand the failure mechanics—fracture and fatigue. Reliability engineer is familiar with appropriate design principles that can be employed to prevent the failures. By design feedback, reliability engineer can modify the design by correcting the missing design parameters. Manufacturers also need to know “why things fail” as much as they know “how things work.”

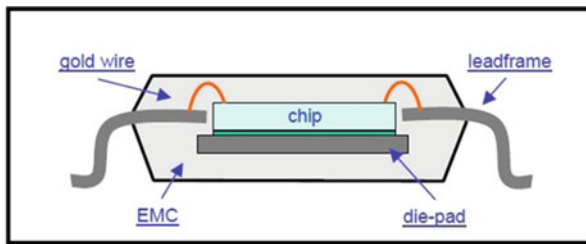
Failure analysis is a systematic examination of failed products to determine the root cause of failure and to use such information to eventually improve product reliability (see Fig. 7.33). Failure analysis is designed to (1) identify the failure modes (the way the product failed), (2) find the failure site (where the product failure occurred), (3) confirm the failure mechanism (the physical phenomena involved in the failure), (4) determine the root cause (the design, defect, or loads which led to failure), and (5) recommend failure prevention methods.

It will inspect whether the load applied cyclically or was overload, the direction of the critical load, and the influence of outside forces such as residual stresses. Then, accurately knowing the physical roots of the failure leads to pursue the human errors or the latent causes of these physical roots. Failure analysis might be classified as non-destructive analysis and destructive analysis.

The process begins with the most non-destructive techniques and then proceeds to the more destructive techniques, allowing the gathering of unique data from each technique throughout the process. When properly analyzed, this data leads to a viable failure mechanism. The use of destructive techniques in the early process leads to lose the valuable information that might be required later. The sequence of procedures is:

- Visual Inspection
- Mechanical or Electrical Testing
- Non-Destructive Evaluation
- Destructive Evaluation (using relevant techniques)

To increase the product reliability, the results of failure mechanism must be modeled by the physics-of-failure (PoF). It allows designers to properly select materials, which minimize the susceptibility of future designs to failure by degrading it. In addition, it allows the user to select environmental and operational loads that minimize the susceptibility of the current design to failure during product lifetime.



Failure Classification

Physical Failure (Structure)

- Popcorn
- Delamination
- Crack (Package/Die)

Electrical Failure (Connection)

- Open
- Short
- Leakage
- Function

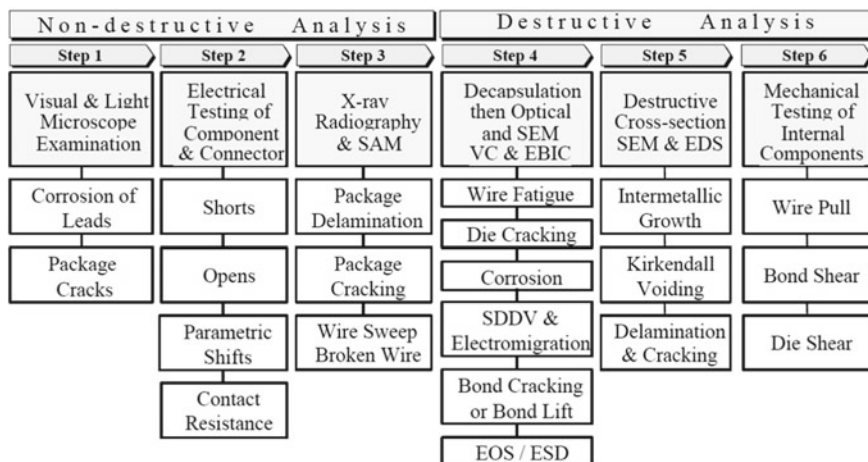
In-Process Failure (Production)

- Front-end (before molding)
- Back-end (After molding)
- Testing (FT/Burn-in)

Reliability Failure (Qualification)

- Temperature
- Humidity
- Pressure
- Voltage

(a) Structure of conventional package in semi-conduct



(b) Procedure of failure analysis in electrical system (example)

Fig. 7.33 Failure analysis in electrical system

The identification of the critical failure mechanisms and failure sites of assemblies in field also permits the development of a focused accelerated test program. The benefits of accelerated testing enable the proper test stresses (e.g., temperature,

tension, compression, shear) to reach failure in the shortest time without changing the failure mechanism or mode.

The failure distribution in the accelerated tests can be converted to a failure distribution in the user environment using the acceleration factors calculated by the PoF models like generalized stress model that will be discussed in Chap. 8. Typical equipments of failure analysis in product might be used as optical microscope, X-ray, SEM, SAM, FTIR and the others (Fig. 7.34).

Non-Destructive Evaluation (NDE) is designed to provide as much information on the failure site, failure mechanism, and root cause of failure without causing any damage to the product or removing valuable information. A significant amount of failure information is available through visual inspection and the more traditional NDE methods—X ray or SAM.

For mechanical or electronic device, X-ray microscopy assesses the internal damage, defects, and degradation in micro-electronic devices. Illuminating a sample with X-ray energy provides images based on material density that allow characterization of solder voiding, wire-bond sweep, and wire-bond breakage in components. Consequently, X-ray microscopy is a powerful non-destructive tool for pinpointing failure sites in product (Fig. 7.35).

As destructive evaluation, Scanning Electron Microscopy (SEM) is a natural extension of optical microscopy. The use of electrons instead of a light source provides much higher magnification (up to 100,000 times) and much better depth of field, unique imaging, and the opportunity to perform elemental analysis and phase identification.

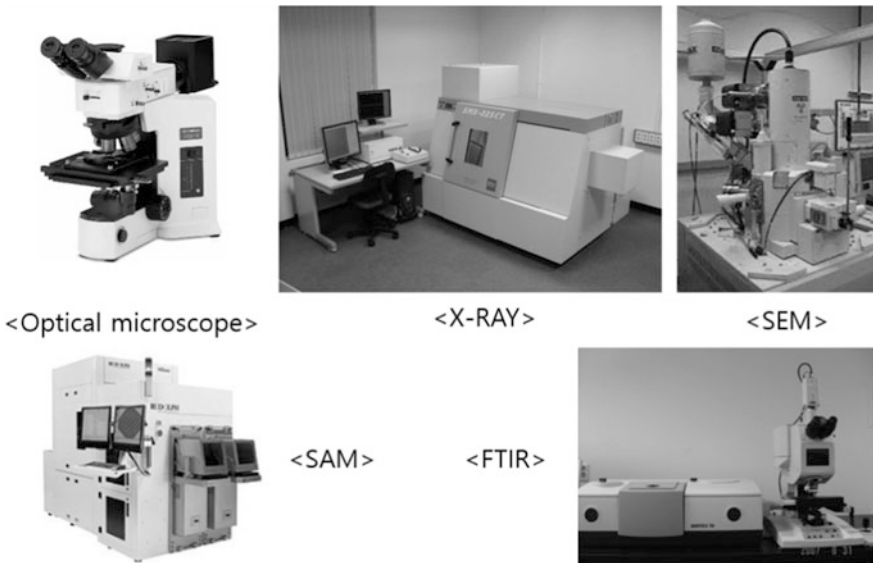
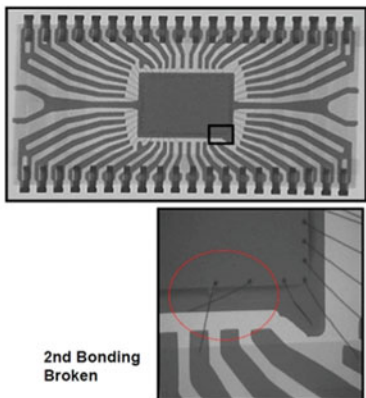
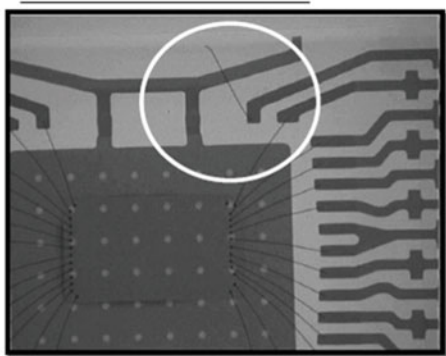


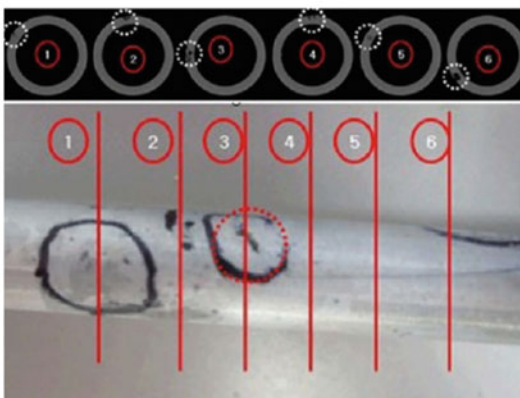
Fig. 7.34 Typical equipments of failure analysis



Inner wire neck broken

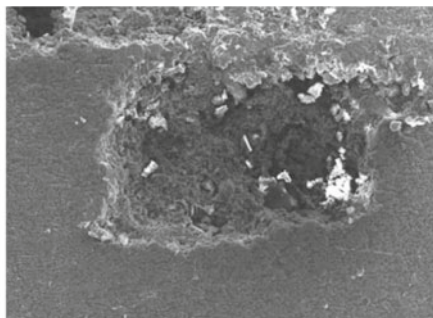
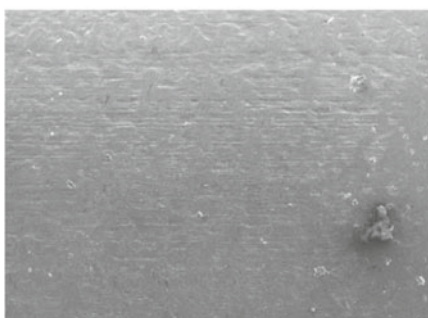


(a) X-ray analysis of 2nd Bonding Broken and Inner wire neck broken (example)



(b) X-Ray Microscopy showing a pitting corrosion on the evaporator tube (example)

Fig. 7.35 Failure analysis using X-ray microscopy in product



SEM Fractography showing a pitting corrosion on the evaporator tube

7.7.2.1 Case Study: PAS (Photo Angle Sensor) in Automobile

- Summary: No ignition of automobile due to the frequent failures of the PAS application IC in field (Fig. 7.36a)
- Electrical test (by curve tracer): Electrical open of Pin #4 (Fig. 7.36b)
- Non-Destructive Inspection by Scanning Acoustic Microscope, X-Ray radiography
 - SAM: Die paddle (top, bottom), lead-frame de-lamination (Fig. 7.36c)
 - X-ray radiography: Package crack (Fig. 7.36d)
- Microscopy analysis (by SEM): Wedge bond open of Pin #4 (Fig. 7.36e)

For de-lamination in semi-conductor, when surface mount device is mounted, because the whole package is exposed to high temperature and humidity, there are problems such as de-lamination of resin from frame materials or absorbed moisture inside package vapor blasts, and resulting in package deformation or pop-corning crack (Fig. 7.37).

7.7.3 Case Study: Fracture Faces of Product Subjected to Loads

Fatigue failure can be recognized from the specimen fracture surface with the different growth zones and the major physical features: (1) region of slow crack growth is usually evident in the form of a “clamshell” concentric around the location of the initial flaw—void, (2) clamshell region often contains concentric “beach marks” at which the crack may become large enough to satisfy the energy or stress intensity criteria for rapid propagation, (3) final phase produces the granular rough surface before final brittle fracture.

For example, the suction reed valves open and close to allow refrigerant to flow into the compressor during the intake cycle of the piston. Due to repetitive stresses, the suction reed valves of domestic refrigerator compressors used in the field were cracking and fracturing, leading to failure of the valve. From SEM microscopy, the fracture started in the void of the suction reed valve, propagated, and fractured to the end (Fig. 7.38).

The fracture face of a fatigue failure shows both the load types (bending, tension, torsion or a combination) and the magnitude of the load. To understand the type of load, look at the direction of crack propagation. It is always going to be perpendicular to the plane of maximum stress. The following examples reflect the fracture paths on accordance with a variety of loads.

Figure 7.39 describes the reversed torsional fatigue failure of splined shaft from a differential drive gear. The mating halves of the fracture reveal how two separate cracks initiated in a circumferential recess adjacent to the end of the splines and began to propagate into the cross section following helical paths. Because the

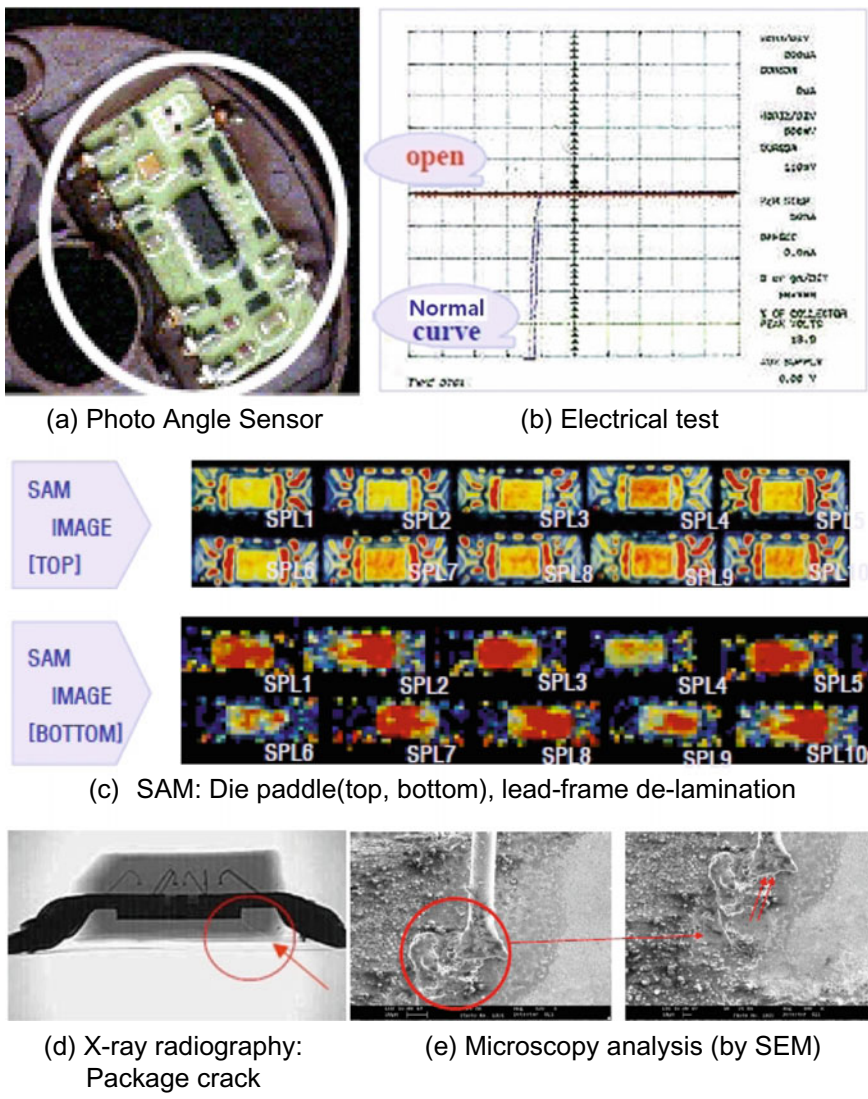


Fig. 7.36 Failure analysis: PAS application IC in automobile

cycles of twisting forces acted in opposite directions, each crack follows opposing helices which progressively reduced the effective cross sectional area and, consequently, increased the levels of cyclic stresses from the same applied loads. Shortly before the shaft finally broke bending forces initiated a third crack at the opposite side of the shaft and this had begun to propagate as a plane fracture at 90° to the shaft axis until the splined end finally broke away.

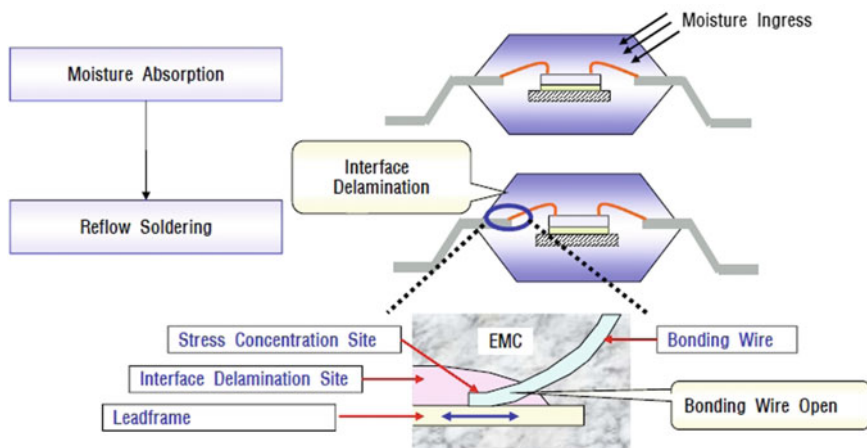


Fig. 7.37 Failure mechanism: de-lamination in semi-conductor

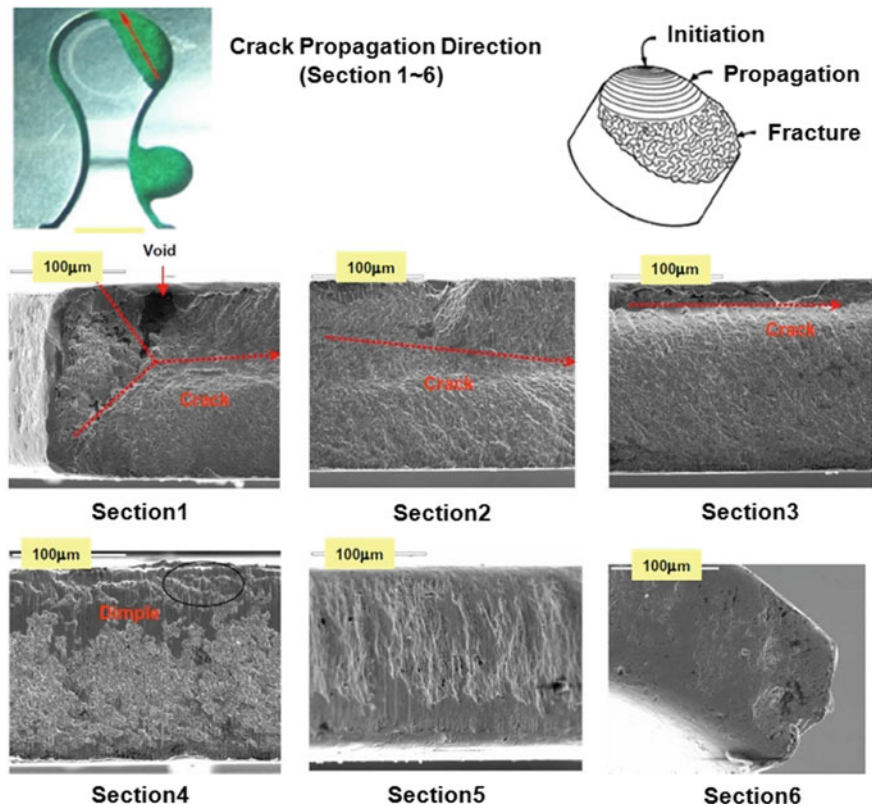


Fig. 7.38 Fatigue fracture surface of compressor suction reed valve due to impact

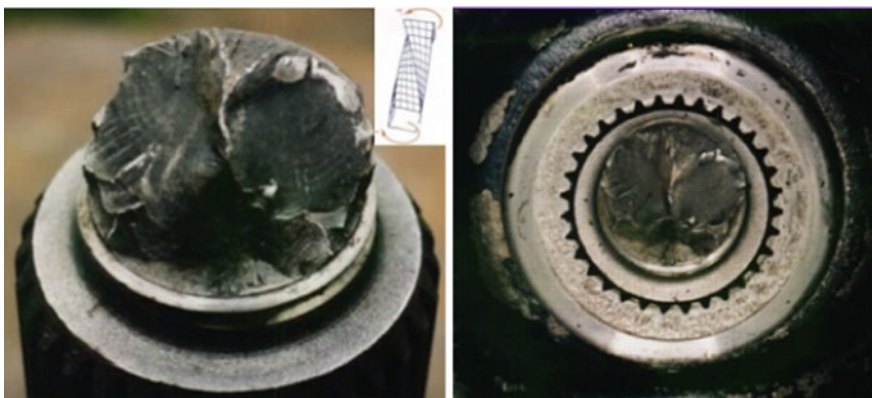


Fig. 7.39 Fatigue failure of splined shaft due to reversed torsional loads (example)

Torsional fatigue is involved in 10–25% of rotating equipment failures. Torsion fatigue failures can identify them as the fracture oriented 45° to the shaft centerline. The fracture face typically has one or more origins, a fatigue zone with progression lines and an instantaneous zone. A large fatigue zone and small instantaneous zone mean the fatigue load was small. A small fatigue zone and large instantaneous zone mean the fatigue load was high.

Torsional fatigue fractures frequently occur in a shaft that is inside a hub or coupling. These fractures usually start at the bottom of a keyway and progress around the shaft's circumference. In Fig. 7.27, the fracture travels around the shaft, climbing toward the surface so the outer part of the shaft looks like it was peeled away. The fracture surface has characteristics of a fatigue fracture: one or more origins, ratchet marks and a fatigue zone with progression lines. The shaft fragment is usually held in place by the coupling or hub, so there is typically a very small or no instantaneous zone.

A shaft fracture may have both torsion and bending fatigue forces. When this occurs, the orientation of the fracture face may vary from 45° to 90° with respect to the shaft centerline. As the fracture is closer to 90°, the shaft combines dominant bending with torsion. The fracture angle therefore offers key evidence as following:

- Closer to 90°, it is a dominant bending force.
- Midway between 45° and 90°, it is a combination of torsion and bending forces.
- Closer to 45°, it is a dominant torsion force.

Evidence of torsional fatigue also may be found on gear and coupling teeth. Most equipment runs in one direction, so wear is expected on one side of a gear or coupling teeth. Wear on both sides of a gear or coupling teeth that rotate in one direction is an indication of varying torsional force. When coupling alignment is good and wear occurs uniformly on both sides of all coupling teeth, it usually indicates torsional vibration. Alignment quality can be verified from vibration

spectra and phase readings. An absence of 2X running speed spectral peaks and uniform phase across the coupling occurs when the alignment is good.

7.8 Corrosion Materials

7.8.1 Introduction

Corrosion is defined as “the degradation of materials by chemical reaction with the environment in which the material resides.” This is because of metal oxidation. As metals have a tendency to return to their natural state, it is a natural process which produces either salt or oxides. It requires four elements—anode, cathode, an electrolyte, and a metallic path (Fig. 7.40).

The electrochemical reactions that lead to corrosion or loss of metal are chief among the mechanisms of degradation in metals. The potential for metallic corrosion exists whenever two metals, one acting as a cathode, the other as an anode, are surrounded by an aqueous electrolyte and connected electronically so as to complete an electrical short circuit. As the metal dissolves or corrodes, two reaction zones can be identified. The anodic reaction can be written as:



For oxidation of iron, first the iron gets oxidized into ferrous ions [Fe (II)] with the loss of two electrons.

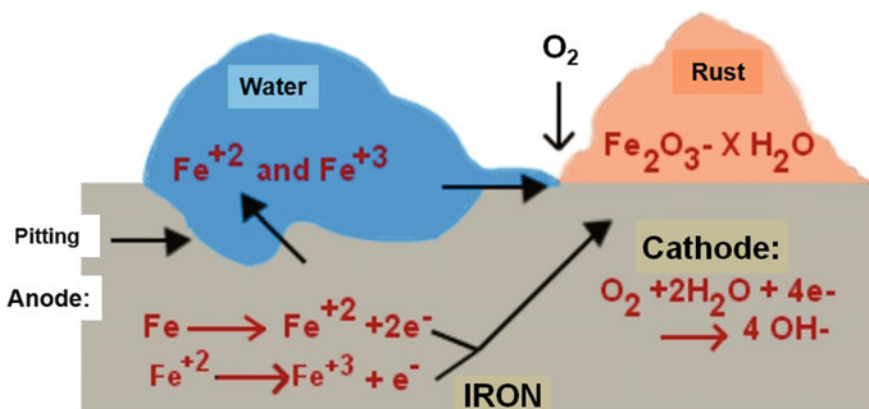
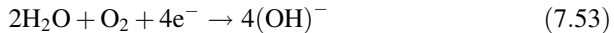


Fig. 7.40 Corrosion mechanism in iron (example)

The ferrous ions again get oxidized into ferric ions [Fe(III)] in the presence of water and oxygen.



The electrons are consumed in cathodic regions where ions are reduced or discharged. In acidic environments the cathodic reduction reaction



The ferric ions combine with oxygen and form ferric oxide [iron (III) oxide]. This ferric oxide gets hydrated with water. The mechanism for the rusting process is similar to the electrochemical cell. The electrons formed during the oxidation of iron are conducted through the metal. Thus, the iron ions diffuse from the water layer to the metal surface where oxygen is present. This is an electrochemical cell where iron acts as the anode and oxygen gas as the cathode. The aqueous solution of ions behaves like a “salt bridge”.

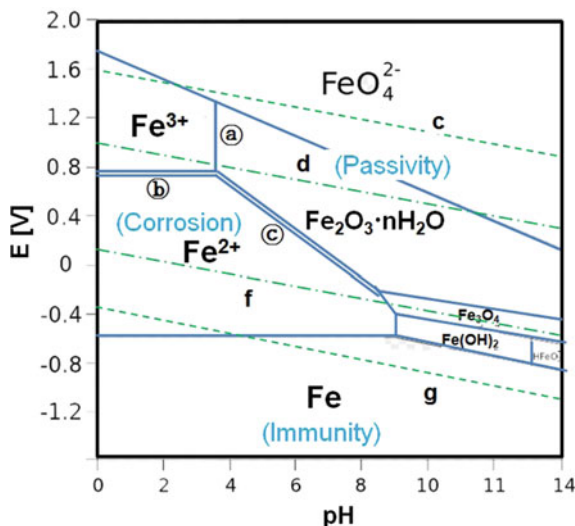
7.8.2 Pourbaix Diagrams

A useful way to graphically depict thermodynamic aspects of aqueous metallic corrosion is through Pourbaix diagrams. These diagrams map the oxidizing power, or potential, (E) of electrolyte solutions versus their acidity or alkalinity (pH). The result is a kind of metal-water phase diagram with boundaries defining regions of stable phases (e.g., ions, oxides, compounds) that either promote the tendency of metals to corrode or remain passive. Construction of Pourbaix diagrams is straightforward in principle, but involved in practice.

A potential-pH diagram for iron (Pourbaix diagram) shown in Fig. 7.41 indicates the areas of immunity, passivity and corrosion of iron in the function of potential and pH. Several separate areas-regions can be seen on the diagram. The region at the bottom of the diagram indicates the condition where iron is immune and thermodynamically stable. This region includes the reduction conditions (low value of potential) across the entire range of pH from acidic to basic environment. In both areas (the large one on the left side of the diagram (oxidizing and acidic environment) and the small one at the far right (reduction and alkaline), iron reacts and forms the soluble corrosion products and corrosion takes place. The central area in this Pourbaix diagram shows the region of the passive state of iron.

Low E values represent a reducing environment. High E values represent an oxidizing environment. The pE scale is intended to represent the concentration of the standard reducing agent (the e^-) analogously to the pH scale representing the concentration of standard acid (H^+). The pE values are obtained from reduction potentials by dividing E° by 0.059.

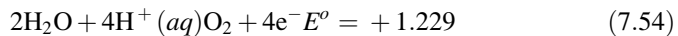
Fig. 7.41 Pourbaix diagram of iron (example)



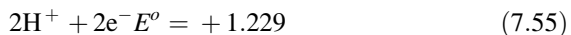
Key to features on the Pourbaix diagram of iron:

- (1) Solid lines separate species related by acid-base equilibria (line ④)
 - It shows the pH at which half of the 1 M iron is Fe^{3+} and half is precipitated as Fe(OH)_2
 - Pourbaix diagrams incorporate Z^1/r calculations and acid-base equilibria
 - The position of an acid-base equilibrium is dependent on the total concentration of iron: (i) reducing the total concentration of Fe^{3+} will drop the driving force of the precipitation. (ii) reducing the total iron concentration from 1 M to 10^{-6} M (more realistic concentrations for geochemists and corrosion engineers) shifts the boundary from pH 1.7 to pH 4.2. (iii) in more dilute solutions, the soluble species have larger predominance areas.
- (2) Solid double lines separate species related by redox equilibria
 - redox equilibria of species not involving hydrogen or hydroxide ions appear as horizontal boundaries (line ⑤)
 - redox species of species involving hydrogen or hydroxide appear as diagonal boundaries because they are in part acid-base equilibria (line ⑥)
 - diagonal boundaries slope from upper left to lower right because basic solutions tend to favor the more oxidized species
- (3) Longer dashed lines enclose the theoretical region of stability of the water to oxidation or reduction (lines d & f) while shorter dashed lines enclose the practical region of stability of the water (lines e & g)
 - Dashed line d represents the potential of water saturated with dissolved O_2 at 1 atm (very well aerated water).

- Above this potential water is oxidized to oxygen:



- (i) theoretically water should be oxidized by any dissolved oxidizing agent $E^\circ > 1.229$
 - (ii) in practice, about 0.5 V of additional potential is required to overcome the overvoltage of oxygen formation (dashed line e)
- (4) Dashed line f represents the potential of water saturated with dissolved H_2 at 1 atm pressure (high level or reducing agents in solution).
- (5) Below this potential water is reduced to hydrogen:



- (i) in practice, an overvoltage effect prevents significant release of hydrogen until the lower dashed line g is reached

Example 7.6 Any point on the diagram will give the thermodynamically most stable (theoretically the most abundant) form of the element for that E and pH. $E = +0.8$ V and pH = 14 predominant form is FeO_4^{2-} .

7.8.3 Major Modes of Corrosion

7.8.3.1 Uniform Corrosion

This is a uniform and general attack, in which the entire metal surface area exposed to the corrosive environment is converted into its oxide form. In this case corrosion damage occurs uniformly over large areas of metal or alloy surfaces without any localized attack. Low-carbon steels and copper alloys are subject to such attack. In the passive state the rate of corrosion is essentially negligible. Protection is typically provided by a thin oxide film. However, if passivity is destroyed by puncturing the oxide, the metal becomes active, with effective anodic and cathodic sites constantly shifting, so that metal loss is uniform. Because it is the uniform thinning of a metal and corrosion does not penetrate very deep inside, it is relatively easy to protect against uniform corrosion. The most familiar example is the rusting of steel in air.

Uniform corrosion is assumed to be most common form of corrosion and particularly responsible for most the materials loss. Traditionally, however it is not recognized as dangerous form of corrosion, because thickness reduction rate can predict by simple tests and available protection methods are efficient. Actual methods are application of coatings, cathodic protection or possibly change of environment or material.

Aqueous corrosion of iron (Fe) in H_2SO_4 solution is examples of uniform attack since Fe can dissolved (oxidize) at a uniform rate according to the following anodic and cathodic reactions, respectively.



As seen in Fig. 7.42, atmospheric corrosion of a steel structure is also a common example of uniform corrosion, which is manifested as a brown-color corrosion layer on the exposed steel surface. This layer is a ferric hydroxide compound known as Rust. The formation of Brown Rust is as follows:

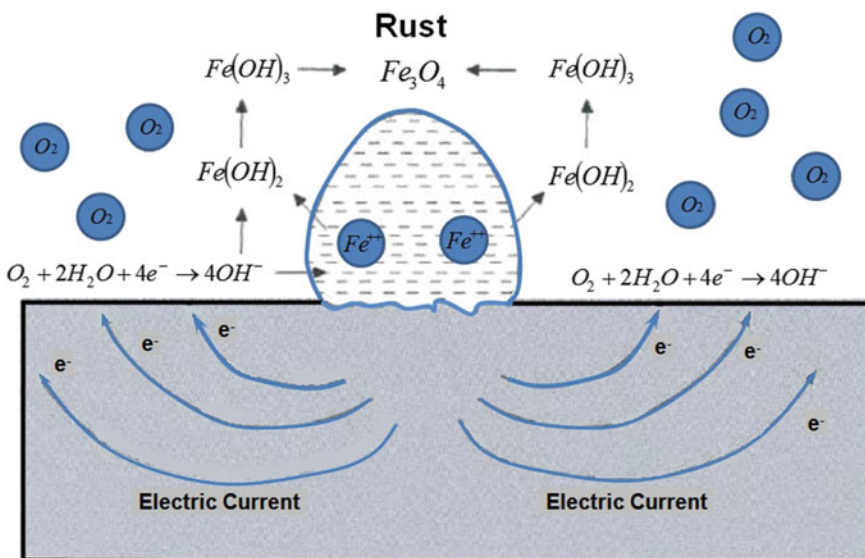
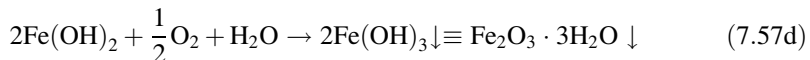
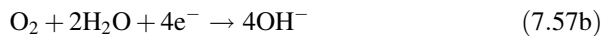
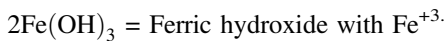
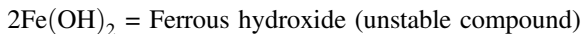


Fig. 7.42 Mechanism of uniform corrosion: atmospheric corrosion of a steel structure

where ($\times 2$) = Multiplying factor for balancing the number of electron



7.8.3.2 Galvanic Corrosion

Two different metals (alloys) are required for galvanic action. Galvanic corrosion is magnified when the anode is small and the cathode large. When dissimilar metals in electrical contact are immersed in an electrolyte, an electrochemical cell (i.e., a battery) is produced. The more active metal becomes the negatively charged electrode, or anode, while the more noble metal becomes the positively charged electrode, or cathode. Examples of such a size effect occur commonly in electronics when electrodeposited noble metal coatings are used to protect less noble substrates, e.g., Au on Ni.

Galvanic corrosion occurs when two metals with different electrochemical potentials or with different tendencies to corrode are in metal-to-metal contact in a corrosive electrolyte. When two metals with different potentials are joined, such as copper (+0.334 V) and iron (-0.440 V), a galvanic cell is formed. A cell in which the chemical change is the source of energy, is called a galvanic cell. The corrosion which is caused due to the formation of the galvanic cell is, therefore, called galvanic corrosion. The driving force for corrosion is a potential difference between different materials. This force was described by Luigi Galvani, late in the eighteenth century. Between the two different materials connected through an electrolyte, the less noble will become the anode and tend to corrode (Fig. 7.43).

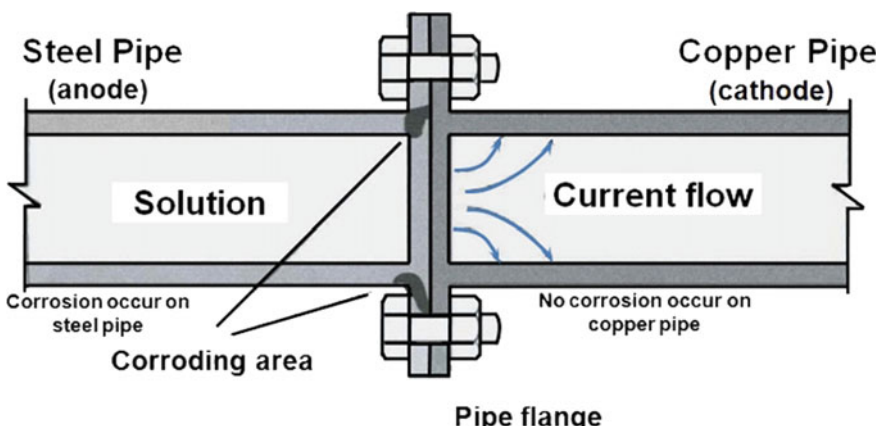


Fig. 7.43 Galvanic corrosion between copper (+0.334 V) and iron (-0.440 V)

For the formation of a galvanic cell, the following components are required: (1) A cathode, (2) An anode, (3) An electrolyte, and (4) A metallic path for the electron current. In the case of copper and steel, copper has a more positive potential according to the e.m.f. series (+0.334 V), hence, it acts as a cathode. On the other hand, iron has a negative potential in the e.m.f series (-0.440 V), hence, it is the anode. As a matter of principle, in a galvanic cell, the more noble metal always becomes the cathode and the less noble always the anode. Moisture acts as an electrolyte and the metal surface provides a metallic path for the electron current to travel.

The following factors significantly affect the magnitude of galvanic corrosion: (1) position of metals in the galvanic series, (2) the nature of the environment. For instance, water containing copper ions, like seawater, are likely to form galvanic cells on a steel surface of the tank. If the water in contact with steel is either acidic or contains salt, the galvanic reaction is accelerated because of the increased ionization of the electrolyte. In marine environments, galvanic corrosion may be accelerated due to increased conductivity of the electrolyte. In cold climates, galvanic corrosion of buried material is reduced because of the increased resistivity of soil. In warm climates, on the other hand, it is the reverse because of the decreased resistivity of the soil. (3) Area, distance and geometric effects.

The anode to cathode area ratio is extremely important as the magnitude of galvanic corrosion is seriously affected by it. The area ratio can be unfavorable as well as favorable. The area ratio of the anode to cathode plays a dominant role in galvanic corrosion. As a given amount of current flows in a galvanic couple, the current density at the anode or cathode controls the rate of corrosion. For a given amount of current, the metal with the smallest area has the largest current density and, hence, is more damaged if corrosion occurs at it.

It is a known principle that the solution conductivity varies inversely with the length of the conduction path. Most corrosion damage is caused by current which cover short paths. Hence, the greatest galvanic damage is likely to be encountered near the junction of the two metals and the severity would be decreased with increased length. If two different metals are far away from each other, there would be no risk of galvanic corrosion, because of very little current flow.

7.8.3.3 Pitting Corrosion

As the description implies, pit or hole formation is the form of attack during pitting corrosion. Localized pitting attack generally occurs while the bulk of surface is passive. Chloride and other halogen ions to a lesser extent are notorious for initiating pitting attack in otherwise passive metals and alloys. For the pitting of stainless steel in the presence of Cl^- ions, a suggested mechanism is shown in Fig. 7.44.

Corrosion begins with the loss of passivity caused by the local destruction of the thin chromium oxide passive film. A copious production of Al^{3+} ions attracts Cl^- , where hydrolysis occurs by the reaction

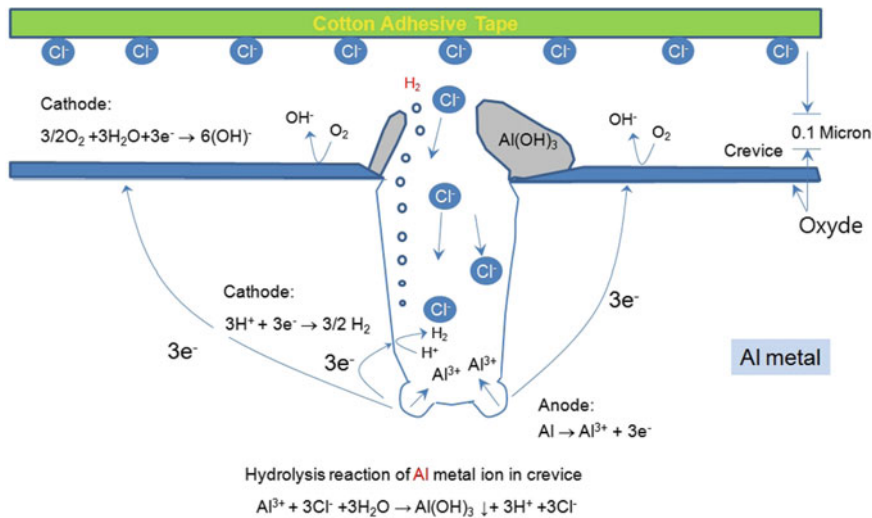


Fig. 7.44 Model for the pitting of aluminum in the presence of chloride ions



The crevice corrosion mechanism on the evaporator tubing that was made of aluminum might be briefly explained as: (1) As chlorine Cl^- attacks, the oxide passive film breaks down and melts in the condensing water; (2) rapid aluminum oxidation: $\text{Al} \rightarrow \text{Al}^{3+} + 3\text{e}^-$ then occurs and dissolves in the water (3) with a large surface cathode, a small anode pitting area forms; (4) electro-migration then moves chlorine Cl^- into the pits on evaporator tube; (5), As the voltage drop (or IR drop) between the external surface and the pit, the driving force for pitting increases and pitting propagates faster; (6) repetitive hydrolysis reactions of aluminum metal in crevice is created by the reaction: $\text{Al}^{3+} + 3\text{H}_2\text{O} \rightarrow \text{Al}(\text{OH})_3 + 3\text{H}^+$.

In the process, $\text{Al}(\text{OH})_2$ forms, and the pH is lowered at the pit initiation site. The acid chloride solution further accelerates anodic dissolution, which in turn concentrates more chloride at the pit, etc., in this so-called self-propagating.

7.8.3.4 Fretting Corrosion

Tin, plated solder, and other electrical contact materials often suffer corrosion-accelerated wear when the contacting metals undergo small-amplitude, cyclic rubbing or fretting. Particles chemically dissolve and mechanically detach, leaving a surface geometry behind that generally increases the contact resistance.

7.8.3.5 Stress Corrosion Cradling (SCC)

Corrosion in the presence of tensile stress accelerates the damage to the metal surface. The mechanisms are not well understood, but it is thought that applied or internal stress causes atoms to leave the anodic tips of incipient cracks, thereby sharpening them. Usually, particular environment-metal combinations are associated with SCC, e.g., chlorides for stainless steel, ammonia for copper, and H₂S for low-carbon steel. Residual thermal stresses, or those induced by bending electrical lead wires, in combination with moisture serve to promote such cracking. When the loading is cyclic rather than static, the stress-corrosion damage is known as corrosion fatigue.

7.8.3.6 Atmospheric Corrosion

This form of corrosion attack stems from the environment, but without the presence of a bulk electrolyte. Instead, the electrolyte is usually a thin film of moisture that condenses from the atmosphere when the relative humidity is sufficiently high. The electrolytic process of metal migration on nominally insulating substrates occurs in this manner.

References

1. Timoshenko SP (1953) History of strength of materials. McGraw-Hill Book Co., New York
2. Anderson TL (1991) Fracture mechanics: fundamentals and applications. CRCPress, BocaRaton
3. Neugebauer GH (1943) Stress concentration factors and their effect in design. Prod Eng: NY A 14:82–87
4. Paris PC, Gomez MP, Anderson WE (1961) A rational analytic theory of fatigue. Trend Eng 13:9–14
5. Wöhler A (1870) Über die Festigkeitsversuche mit Eisen und Stahl. Zeitschrift für Bauwesen. 20:73–106
6. Neuber H (1961) Theory of stress concentration for shear strained prismatical bodies with arbitrary non linear stress strain law. J Appl Mech 544–550
7. Topper TH, Wetzel RM, Morrow J (1969) Neuber's rule applied to fatigue of notched specimens ASTM. J Mater 4(1):200–209
8. Tipton S (1991) A review of the development and use of Neuber's rule for fatigue analysis. SAE Paper 910165
9. Ramberg W, Osgood WR (1943) Description of stress-strain curves by three parameters. Technical note no. 902 Washington, DC National Advisory Committee for Aeronautics
10. Griffith AA (1921) The phenomena of rupture and flow in solids. Philos Trans R Soc London, A 221:163–198
11. ASME (1965) Mechanical reliability concepts. In: ASME design engineering conference. ASME, New York

Chapter 8

Parametric Accelerated Life Testing in Mechanical/Civil System



Abstract As a new methodology for reliability design of mechanical system, parametric Accelerated Life Testing (ALT) for different modules will be introduced in this chapter. It consists of parametric ALT plan, generalized life-stress failure model with a new effort concept, acceleration factor, and sample size equation. As applying the accelerated loads to the mechanical structure, the weakest parts in product will reveal. Mechanical engineer can modify the product design to have enough strength and stiffness. Engineer therefore is to confirm whether the final design of mechanical system meets the reliability target. However, there are pending questions—actual testing time and sample size—how to carry out reliability testing. If a few of samples are selected, the statistical data accuracy for reliability testing will decrease. If a sufficient quantity of parts is tested, the test cost will demand considerably. Therefore, the best solution that can decrease the testing time and the sample size is the accelerated life testing that is based on the load analysis. If so, the weakest parts in product (or module) will be exposed. Engineer can solve the problematic designs by correcting them. To save the testing time and decrease sample size, parametric ALT is a kind of solution. The accelerated factors could be found in analyzing the load conditions of real dynamics system. It also requires deriving the sample size equation with accelerated factors. Therefore, if reliability target is assigned, we can carry out reliability testing.

Keywords Reliability · Parametric accelerated life testing (ALT) · Sample size equation · Accelerated factor (AF)

8.1 Introduction

Reliability describes the ability of a system or module to function under stated conditions for a specified period of time [1]. Reliability is often illustrated in a diagram called “the bathtub curve” shown as the top curve in Fig. 8.1. The first part of the curve, called the “infant mortality period”, represents the introduction of the product in the market. In this period, there is a decreasing rate of failure. It is then

followed by what is usually called the “normal” life period with a low but consistent failure rate. It then ends with a sharp increase in failures as the product reaches the end of its useful life. If product in the mechanical/civil systems were to exhibit the failure profile in the bathtub curve with a large number of failures in the early life of product, it would be difficult for the system to be successful in the marketplace. Improving the reliability of a system through reliability testing—parametric ALT should reduce its failure rate from the traditional failure rate typified by the bathtub curve to the failure rate represented by a flat, straight line with the shape parameter β in Fig. 8.1. With the second curve, there are low failure rates throughout the lifetime of the system or component until reaching the end of its useful life that the failure rate begins to increase.

The product reliability function can be quantified from the expected product lifetime L_B and failure rate λ in Fig. 8.1 as follows:

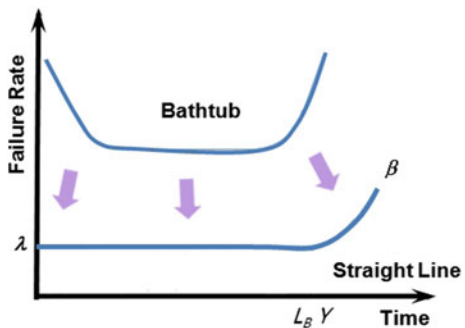
$$R(L_B) = 1 - F(L_B) = e^{-\lambda L_B} \cong 1 - \lambda L_B \quad (8.1)$$

In a practical sense, this proportionality is applicable below about 20% of cumulative failure rate [2]. Improving the design of a mechanical system to increase its reliability can be achieved by quantifying the targeted product lifetime L_B and failure rate λ by finding the appropriate control parameters affecting reliability and then modifying the design with the results from parametric accelerated life testing.

Generally, modules in mechanical products are connected independently in serial. $R_i(t)$ will be called the reliability of module i at time t , and $F_i(t) = 1 - R_i(t)$ will be called the unreliability of module i at time t , for $i = 1, 2, \dots, n$. In the same way, $R(t)$ will be called the system reliability, and $F(t) = 1 - R(t)$ will be called the system unreliability at time t .

Example 8.1 Consider a serially connected mechanical product of three independent modules. At a specified point of time t the module reliabilities are $R_1 = 0.95$, $R_2 = 0.97$, and $R_3 = 0.94$. The system reliability at time t is $R = R_1 \cdot R_2 \cdot R_3 = 0.95 \cdot 0.97 \cdot 0.94 \approx 0.866$.

Fig. 8.1 Bathtub curve and straight line with slope β toward the end of the life of the product



8.2 Mechanical Product Breakdown

8.2.1 Introduction

Typical modern products involved in mechanical system can be outlined as automobile, airplane, domestic appliance, machine tools, agricultural machinery, and heavy construction equipment. They are a collection of module arranged in a specific design in order to achieve desired functions with acceptable performance and reliability. The types of modules, their quantities, their qualities and the manner in which they are arranged within the system have a direct effect on the product's reliability. Therefore, in addition to the reliability of the modules, the relationship between these modules is also considered and decisions as to the choice of module can be made to improve or optimize the overall system reliability, maintainability and/or availability. This reliability relationship is usually expressed using logic diagrams, such as reliability block diagrams (RBDs) and/or fault trees.

They can break down several modules to the individual parts. Based on the market data, the reliability target could be assigned to the product modules like Table 8.1. The targeted reliability of each module can be quantified as the expected product lifetime L_B and failure rate λ in Eq. (8.1). The reliability Testing will be centered on the module of product. For example, if the targeted reliability of refrigerator is allocated as B20 life 5 year, the reliability for compressor will be B4 life 5 year.

And it is reasonable to carry out the reliability testing per module because test cost for system or component is higher than that of module.

8.2.2 Reliability Block Diagram

The reliability block diagram is a graphical method that describes how system and main module connected in product. The configurations of complicated system such as automobile can be generated from the series or parallel connections between modules that consist of mechanical mechanism and their structure. In a reliability block diagram, components are symbolized by rectangular blocks, which are connected by straight lines according to their logic relationships. Depending on the purpose of system analysis, a block may represent a lowest-level component, module, subsystem, and system. It is treated as a block box for which the physical

Table 8.1 Reliability target for mechanical system (part count method)

Level	Quantity	Target	Remark
System	1 System	B20 life 10 year	Refrigerator
Module	5 Units	B4 life 10 year	Compressor
Component	500 Components	B0.04 life 10 year	–

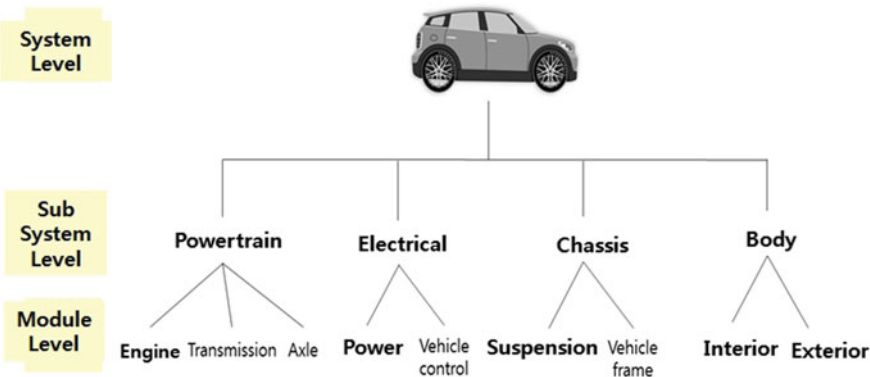


Fig. 8.2 Automobile that consists of multi-modules connected serially

details may not need to be known. The reliability of the object that a block represents is the only input that connects system reliability evaluation. RBDs facilitate the computation of system reliability from module reliabilities (Fig. 8.2).

8.2.3 Product Configurations in RBD—Serial or Parallel

A system is said to be a series system if the failure of one or more modules within the system results in failure of the entire system. In the serial configuration, failure of either components (A_1 or A_2) causes system failure. The mechanical product that consists of multiple modules is the serial system at two hierarchical levels. For example, automobile is serially connected in power-train, electrical and control system, chassis, and body. In the same manner an automobile engine with six cylinders is in series because the engine is said to have failed if one or more cylinders connected in parallel mechanically are failed. On the other hands, in the parallel configuration—redundancy, if most of components do not work, the system will fail. In constructing a reliability block diagram, physical configurations in series or parallel do not indicate the same logic relations from a standpoint of reliability.

Suppose that a mechanical series system like automobile consists of n mutually independent modules. Here mutual independence implies that the failure of one module does not affect the life of other modules. By definition, successful operation of a system requires all components to be functional. From probability theory, the system reliability is

$$R = \Pr(E) = \Pr(E_1 \cdot E_2 \cdots E_n) \quad (8.2)$$

where E_i is the event that module i is operational, E the event that the system is operational, and R the system reliability.

Because of the independence assumption, this becomes

$$R = \Pr(E) = \Pr(E_1) \cdot \Pr(E_2) \cdots \Pr(E_n) = \prod_{i=1}^n R_i \quad (8.3)$$

where R_i the reliability of module i .

Let's consider a simple case where the times to failure of n modules in a system are modeled with the exponential distribution. The exponents reliability function for module i is $R_i(t) = \exp(-\lambda_i t)$. The exponential reliability function for component i is $R_i(t) = \exp(-\lambda_i t)$, where λ_i is the failure rate of component i . Then from (8.3), the system reliability can be written as

$$R(t) = \exp\left(-t \sum_{i=1}^n \lambda_i\right) = \exp(-\lambda t) \quad (8.4)$$

where λ is the failure rate of the system $\lambda = \sum_{i=1}^n \lambda_i$ and t is product lifetime.

Product lifetime determine the shortest module. To increase it, the shortest module should modify its design by using the parametric ALT.

8.2.4 Automobile

Figure 8.3 shows the hierarchical configuration of an automobile connected serially from system to main modules. An automobile is a wheeled motor vehicle used for transportation. It consists of engine, body and main parts, electrical and electronics, interior, power-train and chassis, miscellaneous auto parts—air conditioning system (A/C), bearings, hose and other miscellaneous parts. An automobile is a four-wheeled, self-powered motor designed to run on roads for transport of one to eight people. Automobile is broken down further into multiple lower-level subsystems that have each own mechanism and their structure. From a reliability perspective, the automobile is a series system which fails if one or more subsystems in automobile break. The blocks of the automobile in the reliability block diagram represent the first-level subsystems, the second-level modules, and the others which their reliabilities are known. The reliability block diagram of a typical automobile contains over 20,000 blocks which is including the parts. However, reliability design of automobile might focus on the modules. They can easily calculate the module reliability because of the connection of serial system.

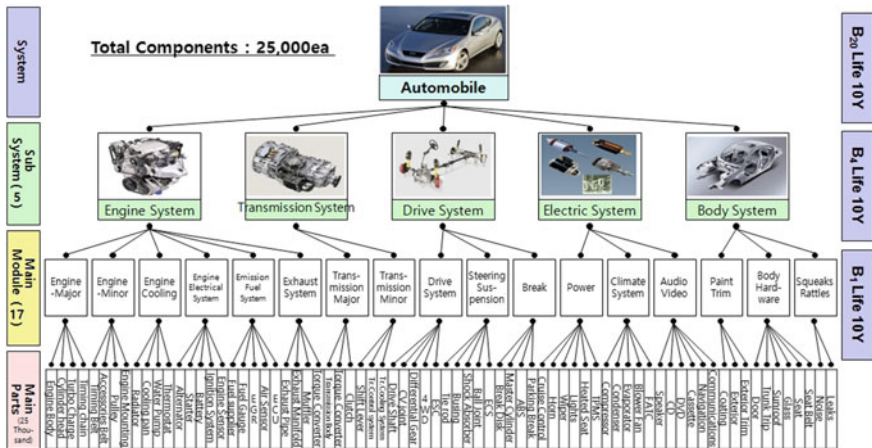


Fig. 8.3 Breakdown of automobile with multi-modules

8.2.4.1 Automobile Reliability Block Diagram

Block diagrams are widely used in engineering and science and exist in many different forms. For the purposes of product reliability analysis, they can be used to describe the interrelation between the system and the modules. When used in this fashion, the block diagram is referred to as a reliability block diagram (RBD). A reliability block diagram is a graphical representation of the modules of the system and how they are reliability-wise related (connected). It should be noted that this may differ from how the modules are physically connected. For example, consider the drivetrain in a two-wheel drive car. The configuration in which the

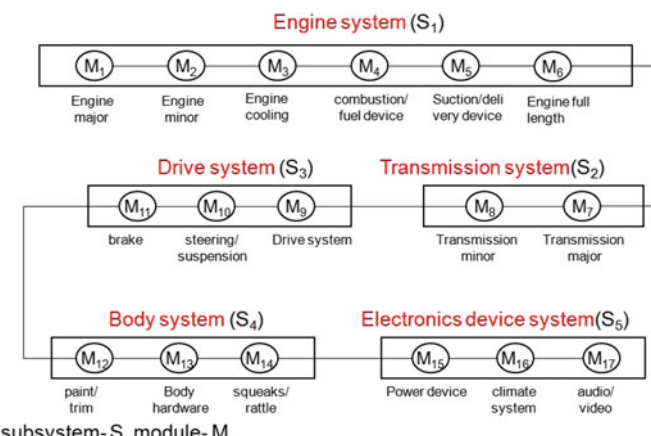


Fig. 8.4 Typical block diagram of automobile (example)

transmission, driveshaft, differential, axles and wheels are physically connected is quite different from their reliability-wise configuration.

Each block in RBD represents the automobile module of interest—engine, drive, transmission, body, and electronics device. A reliability block must include information as to how this module fails. Once the blocks' properties have been defined, the blocks can then be connected in a reliability-wise manner to create a reliability block diagram for the system. This diagram demonstrates the effect of the success or failure of a module on the success or failure of the automobile (Fig. 8.4).

8.2.5 *Airplane*

Airplanes for their intended purpose are constructed with multiple modules that have their own mechanism and structures. For instance, commercial airliners are designed for carrying a passenger or cargo payload, long range and greater fuel efficiency amphibious airplanes. On the other hands, fighter jets are designed to perform high speed maneuvers and provide close support to ground troops. Some aircraft have specific missions: (1) amphibious airplanes have a unique design that allows them to operate from both land and water, (2) helicopters also have the ability to hover over an area for a period of time. The design and planning process, including safety tests, can last up to four years. The design specifications of the aircraft during the design process often are established. When the design has passed through these processes, the company constructs a limited number of prototypes for testing on the ground.

Figure 8.5 shows the hierarchical configuration of a passenger airplane that consists of airframe parts, wings, fuselage, propulsion (engine), aviation controls and instruments, air conditioning system (A/C), bearings, hose and other miscellaneous airplane parts. From a reliability perspective, the airplane is a series system which fails if one or more subsystems (or module) in airplane break. The blocks of the airplane in the reliability block diagram represent the first-level subsystems, the second-level modules, which their reliabilities are known. The reliability block diagram of a typical airplane contains over 1,000,000 blocks which is including the parts. Reliability design of airplane will focus on the modules that are serially connected like other mechanical system.

8.2.6 *Domestic Appliance*

Domestic appliance is a large machine used for routine housekeeping tasks such as cooking, washing laundry, or food preservation. Multiple modules in product consist of its own mechanism and structure. Examples include refrigerator, air conditioner, washing machine, and cleaner. Major appliances that use electricity or

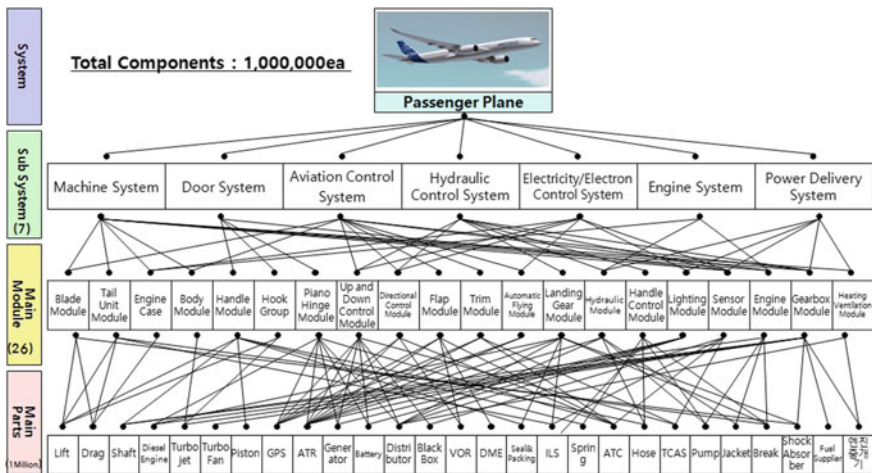


Fig. 8.5 Breakdown of airplane with multi-modules

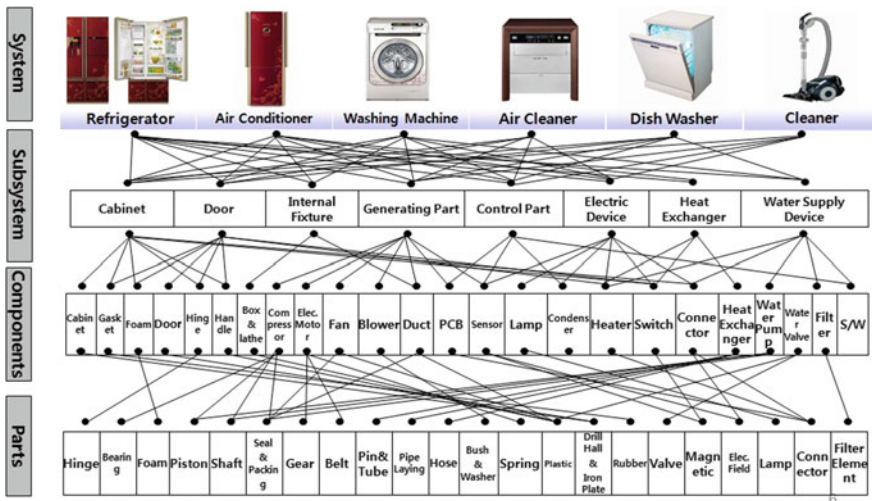


Fig. 8.6 Breakdown of an appliance including refrigerator with multi-modules

fuel are bigger and not portable. They may have special electrical connections, connections to gas supplies, or special plumbing and ventilation arrangements that may be permanently connected to the appliance (Fig. 8.6).

The hierarchical configuration of an appliance consists of cabinet, door, internal fixture (selves, draws), controls and instruments, generating parts (motor or compressor), heat exchanger, water supply device, and other miscellaneous parts. The reliability block diagram of a typical appliance contains over 1000 blocks which is

including the parts. Reliability design of domestic appliance will focus on the modules. They can easily calculate the module reliability because of the connection of serial system.

8.2.7 Machine Tools

A machine tool is a machine for shaping or machining metal or other rigid materials, usually by cutting, boring, grinding, shearing, or other forms of deformation. Multiple modules in product consist of its own mechanism and structure. Machine tools employ some sort of tool that does the cutting or shaping. All machine tools have some means of constraining the work piece and provide a guided movement of the parts of the machine. Thus the relative movement between the work piece and the cutting tool is controlled or constrained by the machine (Fig. 8.7).

The hierarchical configuration of machine tools consists of automatic tool or pallet changing device, spindle unit, drive unit, hydro-power unit, tilting index table, turret head, cooler unit, CNC controller and other miscellaneous parts. The reliability block diagram of typical machine tools contains over 1000 blocks which is including the parts. Reliability design of machine tools will focus on the modules. They can easily calculate the module reliability because of the connection of serial system.

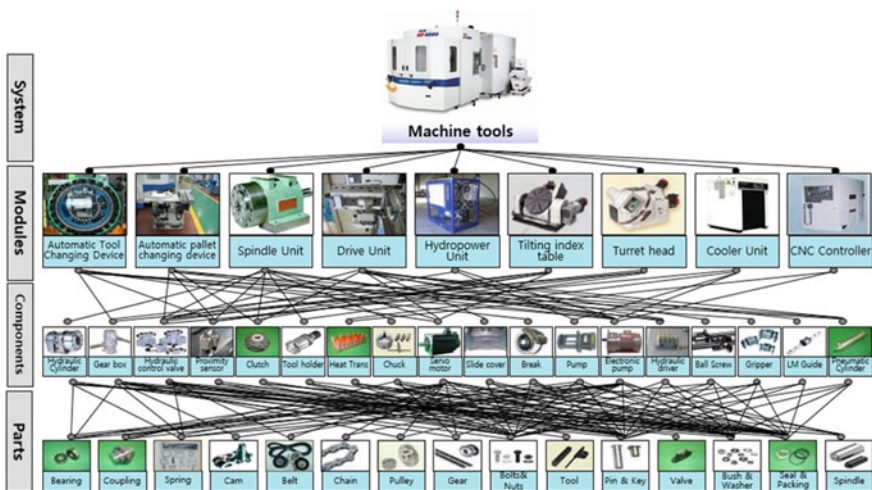


Fig. 8.7 Breakdown of Machine tools with multi-modules

8.2.8 Agricultural Machinery and Heavy Construction Equipment

Agricultural machinery such as tractor is used in the operation of an agricultural area or farm. Multiple modules in product consist of its own mechanism and structure. The hierarchical configuration of agricultural machinery such as automobile consists of engine device, power supply unit, hydraulic unit, electric device, linkage, PTO driving unit, and other miscellaneous parts. The reliability block diagram of a typical appliance contains over 4000 blocks which is including the parts (Fig. 8.8).

The hierarchical configuration of a construction machine such as excavator consists of engine device, electric device, track system, upper appearance system, driving system, main control valve unit, hydraulic operation machine system, cooling system, and other miscellaneous parts. Multiple modules in product consist of its own mechanism and structure. The reliability block diagram of a typical appliance contains over 5000 blocks which is including the parts (Fig. 8.9).

Heavy equipment refers to heavy-duty vehicles, specially designed for carrying out construction tasks, most frequently ones operating earthwork. They are also known as heavy machines, heavy trucks, construction equipment, heavy vehicles, or heavy hydraulics. They usually comprise five equipment systems: engine, traction, structure, power train, control and information. Some equipment frequently uses hydraulic drives as a primary source of motion. Reliability design of agricultural machinery and heavy construction equipment will focus on the modules. They can easily calculate the module reliability because of the connection of serial system.

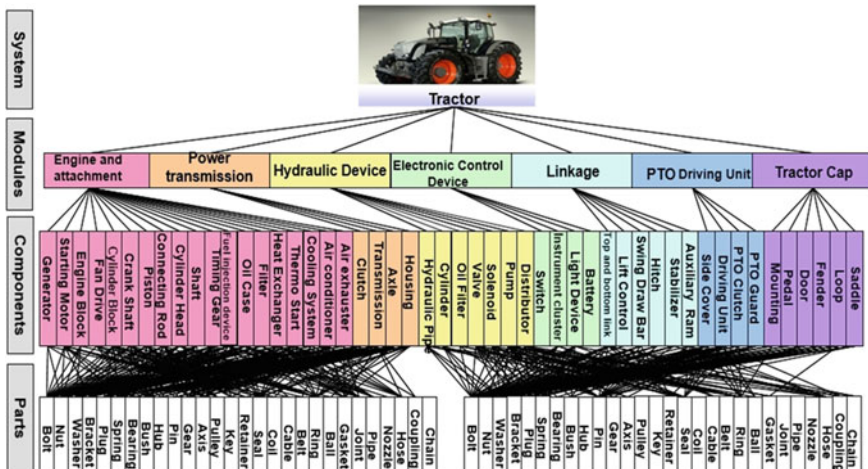


Fig. 8.8 Breakdown of tractor with multi-modules

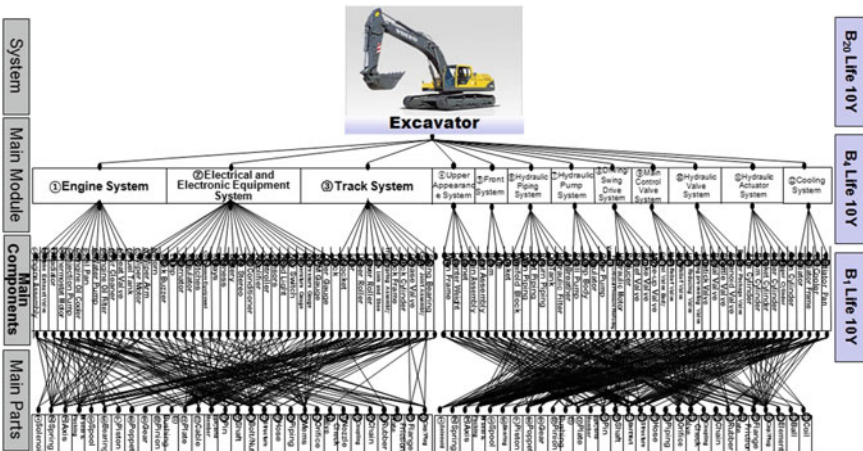


Fig. 8.9 Breakdown of excavator with multi-modules

8.3 Reliability Design in Mechanical System

8.3.1 Introduction

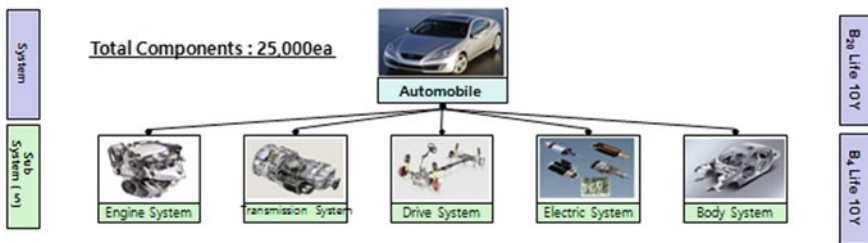
Reliability can be achieved by getting the targeted reliability of product—lifetime L_B and failure rate λ . After searching out the defective configuration of structures and modifying them, it has a good quality—enough strength and stiffness. Reliability design for new product starts in the early stage of design process. It can be summarized the following process—(1) reliability targeting, (2) reliability testing and Weibull analysis, (3) finding the design problem of the suspected parts and modifying it, and (4) proving the effectiveness through the analysis of the field failure data.

Mechanical product consists of multiple modules. Based on the market data, modules might meet the assigned reliability target. If targeted module carries out reliability testing for significantly longer time under accelerated conditions, the parametric ALTs might decrease the testing time and sample size. If probably well, engineer obtains the faulty designs that are missed in the design phase of the mechanical system. These new reliability methodologies in the reliability embedded design process will provide the reliability quantitative (RQ) test specifications—mission cycles—that conforms to the reliability target. Therefore, we need the reliability methodology: (1) parametric ALT plan, (2) accelerated factor, and (3) sample size equation.

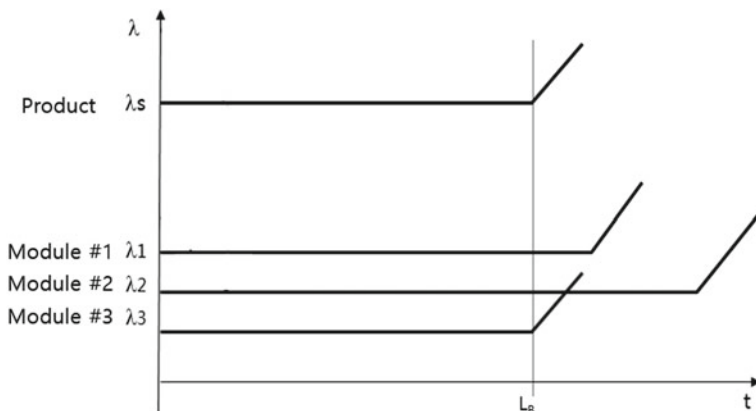
8.3.2 Parametric ALT Plan for Mechanical System

As you can see in Fig. 8.10, a product like automobile can consist of several different modules. For example, automobiles consists of modules, such as the engine, transmission, drive, electrical, and body parts. Suppose that there were no initial failures in a product, one core module #3 will seriously damage the reliability of the whole product. the product lifetime could be represented by the product lifetime for module #3 in Fig. 8.10. The cumulative failure rate of the product over its lifetime would be the sum of the failure rate of each module as seen in Fig. 8.10b. Therefore, engineer needs the reliability growth plans to increase the module lifetime and decrease the failure rate. And product lifetime can be extended by modifying its design.

If the product lifetime was given by Y and the accumulated failure was X , the yearly failure rate can be calculated by dividing the accumulated failure X by product lifetime Y . The product reliability may be expressed as L_{BX} life Y years with a yearly failure rate of X/Y .



(a). Breakdown of Automobile with multi-modules



(b). Product lifetime L_B and failure rate λ with multi-modules

Fig. 8.10 Product lifetime L_B and failure rate λ_s with multi-modules

Table 8.2 Overall parametric ALT plan of product

No	Reliability	Market data		Expected design				Targeted design	
		Modules	Yearly failure rate, %/year	B_x Life, year	Yearly failure rate, %/year			B_x Life, year	Yearly failure rate, %/year
1	Module A	0.34	5.3	New	×5	1.70	1.1	0.15	12 (x = 1.8)
2	Module B	0.35	5.1	Given	×1	0.35	5.1	0.15	12 (x = 1.8)
3	Module C	0.25	4.8	Modified Motor	×2	0.50	2.4	0.10	12 (x = 1.2)
4	Module D	0.20	6.0	Modified	×2	0.40	3.0	0.10	12 (x = 1.2)
5	Module E	0.15	8.0	Given	×1	0.15	8.0	0.1	12 (x = 1.2)
6	Others	0.50	12.0	Given	×1	0.50	12.0	0.5	12 (x = 6.0)
Total	R-Set	1.79	7.4	–	–	3.60	3.7	1.10	12 (x = 13.2)

Based on failure data from the field, the parametric accelerated life testing plan of the product can be classified as a newly designed module, modified module, and similar module. For example, Table 8.2 shows the parametric ALT for mechanical product with several modules. For module D, a modified module, the yearly failure rate was 0.2%/year and L_{Bx} life was 6 years from the field data. Because this was a modified design, the expected failure rate was 0.4%/year and the expected L_{Bx} life was 3.0. To increase the targeted product life, the lifetime of the new design was targeted to be $L_{Bx}(x = 1.2)$ 12 years with a yearly failure rate of 0.1%. The product reliability might be determined by summing the failure rates of each module and lifetimes of each module. The product reliability is targeted to be over a yearly failure rate of 1.1% and $L_{Bx}(x = 13.2)$ 12 years (Table 8.1).

In targeting the reliability of new module where there was no reliability data in market, the data for similar modules are often used as a reference. If there has been major redesign of the module, the failure rate in the field may be expected to be higher. Thus, the predicted failure rates will depend on the following factors:

1. How well the new design maintains a similar structure to the prior design,
2. For each new module, new manufacturers are assumed to supply parts for the product,
3. Magnitude of the loads compared to the prior design, and
4. How much technological change and additional functions are incorporated into the new design.

So for Module A, the expected failure rate was 1.7%/year and its expected lifetime was 1.1 years because there was no field data on the reliability of the new

design. The reliability of the new design was targeted to be over L_{Bx} ($x = 1.8$) 12 years with a yearly failure rate of 0.15%. To meet the expected product lifetime, the parametric ALT should help identify design parameters that could affect the product reliability.

8.4 Reliability Targeting of Mechanical Product

8.4.1 *Introduction*

If the system reliability target is setting in the product planning, it will sequentially be allocated to individual subsystem, module, and components at the stage of the product design. When each module achieves the allocated reliability, the overall system reliability target can be attained. Reliability allocation is an important step in the reliability-embedded design process. The benefits of reliability allocation can be summarized as follows.

- Reliability allocation defines a reliability target for each module. The product has a number of module or subsystem, which are manufactured by suppliers or internal departments. It is important that company share all related parties with the reliability target before delivering the end product to customer.
- Quantitative reliability targets for modules encourage responsible parties to improve the current status of product reliability through use of reliability techniques—reliability testing.
- Mandatory reliability requirements for product (or module) are closely connected with engineering activities aimed at meeting other customer expectations in the reliability-embedded design process.
- Reliability allocation requires a deep understanding of product hierarchical structure in the reliability block diagram. The process leads to identify the part of design weakness and subsequently improve it.
- As a result, reliability allocation can work on input of other reliability tasks. For example, reliability assigned to a module will be used to design verification through reliability testing like parametric ALT.

Reliability allocation is fundamentally a repetitive process to achieve the product reliability. It is conducted in the early design stage to support concept design when available information is restricted. As the design process proceeds, the overall reliability target might be reallocated to reduce the cost of achieving the reliability goal. The allocation process may be invoked by the failure of one or more modules to attain the assigned reliability due to technological limitations. The process is also repeated whenever a major design change takes place.

8.4.2 Criteria and Method of Reliability Allocation

Because some parts are assigned to extremely high reliability goals, it may be unachievable at all. On the other hands, though there are critical components whose failure causes safety, environmental or legal consequences, it will be allocated to low-reliability targets. It is important to establish some criteria that should be considered in reliability allocation.

The task of reliability allocation is to select part reliability targets, $R_1^*, R_2^*, \dots, R_n^*$ which satisfy the following equality equation:

$$R_S^* \leq g(R_1^*, R_2^*, \dots, R_n^*) \quad (8.5)$$

Mathematically, there are an infinite number of such sets. Clearly, these sets are not equally good, and even some of them are unfeasible. The common criteria are described:

1. Failure possibility. Parts that have a high likelihood of failure previously should be given a low-reliability target because of the intensive effort required to improve the reliability. Conversely, for reliable parts, it is reasonable to assign a high-reliability goal.
2. Complexity. The number of constituent parts (or modules) within a subsystem reflects the complexity of the subsystem. A higher complexity leads to a lower reliability. It is similar to the purpose of failure possibility.
3. Criticality. The failure of some parts may cause severe effects, including, for example, loss of life and permanent environmental damage. The situation will be severe when such parts have a high likelihood of failure. Apparently, criticality is a product of severity and failure probability, as defined in the FMEA technique described in Chap. 4. If a design cannot eliminate severe failure modes, the parts should have the lowest likelihood of failure. Consequently, high-reliability goals should be assigned to them.
4. Cost. Cost is an essential criterion that is a target subject to minimization in the commercial industry. The cost effects for achieving reliability depend on parts. Some parts induce a high cost to improve reliability a little because of the difficulty in design, verification, and production. So it may be beneficial to allocate a higher-reliability target to the parts that have less cost effect to enhance reliability.

Though several methods for reliability allocation have been developed, the simplest method suggested here is the equal allocation method. This method can only be applied when the system reliability configuration is in series. The system reliability is calculated by:

$$R_S^* = \prod_{i=1}^n R_i \quad (8.6)$$

The allocated reliability for each subsystem is:

$$R_i = (R_S^*)^{1/k} \quad (8.7)$$

8.5 Failure Mechanics and Design

As seen in Fig. 8.11, if mechanical structure is subject to (random) repetitive stress, it will fracture in lifetime. The typical failure mechanisms of mechanical system are fracture and fatigue. The design of mechanical product can be described as two factors: (1) the load (or stress) on the structure, (2) the structure (shape and materials). If there is void (faulty design) in the structure subjected to loads, the structure will collapse like Fig. 8.11. On the other hands, if structure has a good quality—enough strength and stiffness, it will endure loads and fracture near targeted product lifetime. For example, if the repeated load is applied at the stress raisers such as shoulder fillet, the structure that damage is accumulated will crack. And then the system will fracture suddenly after repetitive stresses in its lifetime. The product engineer would want to reshape the faulty design or move away where the stress is applied. This is a design concept.

To withstand the loads, a product engineer would seek to find design solutions: (1) modify design shape, and (2) change the material type. The failure site of the product structure could be found when the failed products are taken apart in the field or after the failed samples of a parametric ALT. The engineer should identify the failure by the reliability testing—parametric ALT before launching new product. This failure mechanics, design, and reliability testing might be applicable to both mechanical and electronic products because the electric products are typically housed in mechanical systems. So it is a critical process to search out the faulty design by FEA or experimentally using the reliability testing (or parametric ALT).

With the advent of Finite Element Analysis (FEA) tools, design failure such fatigue can now be assessed in a virtual environment. Though FEA fatigue

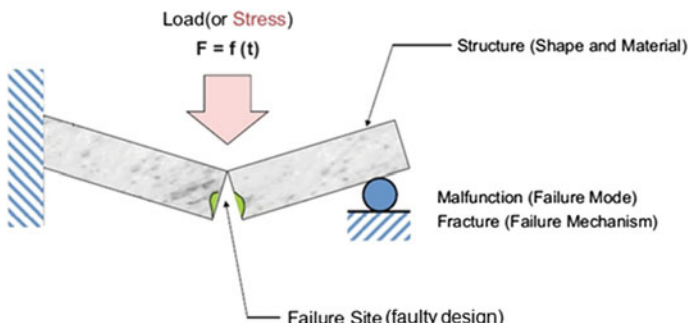


Fig. 8.11 Failure mechanics and mechanical system design

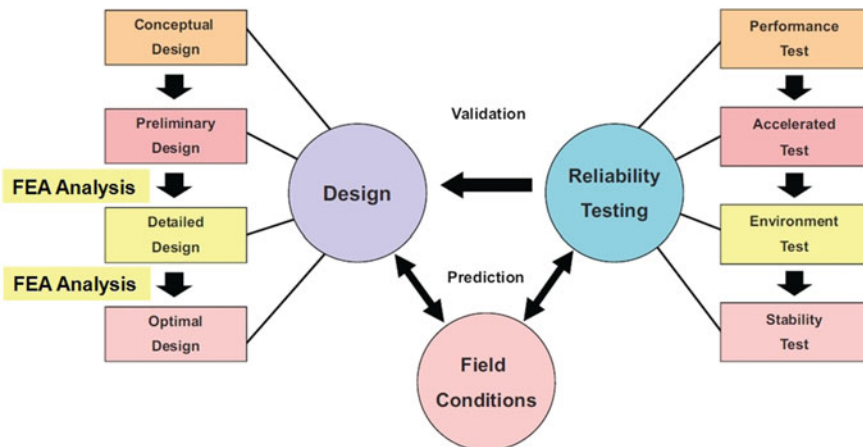


Fig. 8.12 Optimal design and reliability assessment

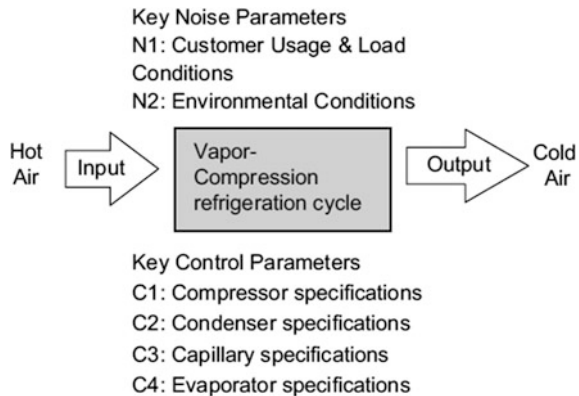
assessments do not completely replace fatigue testing, they will find the detailed or optimal design in the structure of new product. However, though the system goes from preliminary design to an optimized design, product might have design defects. If modules have a problem due to an improper design, engineer will confirm if new design withstand loads in the product lifetime (Fig. 8.12).

As described in the previous Sect. 8.2, the mechanical product such as appliance, car, and aircraft consists of a multiple of modules. These modules can be put together in a system and have an input and output similar. They also have their own (intended) functions just as refrigerator (a vapor compressor cycle) that generates the cold air to what is shown in Fig. 8.13. In the field, if a mechanical/civil module functions improperly, consumers would request the module replaced. If the field usage conditions are fully understood, reliability engineers could be reproduced in the laboratory testing to be identical to those of the failure in field.

Under a variety of environmental and operational conditions, reliability engineers search for potential failure modes by testing in the laboratory. They will determine the failure mechanisms from the failed samples. They can create an action plan to reduce the chance of failure. However, it may not be easy to identify all failure modes attributable to the improper design because, in mechanical/civil systems, the failure modes come from repetitive stresses which may not be captured in initial testing.

Consequently, modules with specific intended functions need to be robustly designed to withstand a variety of loads. In determining product lifetime, the robust design in module determines the control factor (or design parameters) to endure the noise factor (or stress) and properly work the system, which has the reliability target —part failure rate λ and lifetime L_B . Such reliability targeting is known to be conventionally achieved through the Taguchi methods (SDE) and the statistical design of experiment [3–8].

Fig. 8.13 Typical robust design schematic (example: refrigerator)



Taguchi methods, known to robust designs, use the loss function which quantifies the amount of loss based on deviation from the target performance. It puts a design factor in an optimal location where using cost function random “noise” factors are less likely to hurt the design and it helps determine the best control factors (or design parameters). However, for an uncomplicated mechanical/civil structure, such as a beam, Taguchi methods should take into account a considerable number of design parameters. In the design process it is not possible to consider the whole range of the physical, chemical and the mathematical conditions that could affect the design.

Another experimental methodology, new parametric ALT methods with reliability quantitative test specifications (RQ), should be introduced so that the product can withstand a variety of repetitive loads and determine the critical design parameters affecting reliability. Parametric ALT can also be used to predict product reliability—lifetime, L_B and failure rate, λ . The new parametric ALT discussed in the next section has a sample size formulation that enables an engineer to determine the design parameters and achieve the targeted product reliability—lifetime L_B and failure rate λ [9–21].

8.6 Parametric Accelerated Life Testing

8.6.1 Introduction

Parametric accelerated life testing uses the sample size equation with Acceleration Factor (AF). It is a process that helps engineers to experimentally find the faulty designs. If the reliability target of module in mechanical product is allocated, engineer for module with final design will carry out the reliability testing until Reliability Quantitative (RQ) test specifications. At each ALT stage it can help

them better estimate expected lifetime L_B , failure rate of module λ . It finally determines whether overall product reliability is achieved.

If reliability target for mechanical module is targeted, actual testing time h_a is determined by the sample size equation. Based on the testing data, the shape parameter β is calculated from a Weibull distribution chart. So it is important to derive the proper sample size equation with the whole parameters—targeted lifetime L_B , acceleration factor AF , reliability target x , and the allowed number of failures r .

As mechanical system is subjected to repetitive loads, it will fail in lifetime. So the failure mechanism is fracture or fatigue. After the dominant failure mechanism for product is determined, it is essential to derive the life-stress model under the expected physical and chemical conditions. A grasp of physical of failure (PoF) also is required to understand the failure mechanism. If product is subjected to loads and there is design failure, it will collapse. So we know that the sole factor is stress (or loads).

Reliability engineers must determine how the stresses (or loads) act on the system structure, which help to categorize the potential failure mechanisms under the range in environmental and operational conditions. Engineers need to develop a testing plan with appropriate accelerated load conditions to determine the dominant failure mechanisms affecting product lifetime. In the accelerated life testing the failure mechanisms of test samples should be identical to that under normal conditions experienced in the field. When we carry out reliability testing, the shape parameter for accelerated conditions in Weibull chart should match those under normal field conditions.

A parametric ALT for reliability testing involves three key steps:

- (1) By creating a life-stress model, engineer might determine the acceleration factor under severe conditions.
- (2) Assuming an initial shape parameter that is implied by the load intensity of wear failure in the Weibull distribution, we derive the necessary sample size to carry out reliability testing until the mission cycles (or Reliability Quantitative test specifications) equivalent to the allocated reliability target.
- (3) With sample size equation, carry out testing for extended test periods. In each ALTs as quantifying the reliability from the multiplication of the estimated L_{Bx} life and failure rate λ , we can ensure the reliability of final design for mechanical system.

Degradation by loads is a fundamental phenomenon to all mechanical products. For instance, the critical parameters such as strength will degrade with time. In order to understand the useful lifetime of the part, it is important to be able to model how critically important product parameters degrade with time.

8.6.2 Acceleration Factor (AF)

Reliability concerns arise when some critically important mechanical/civil strength due to stress degrades with time. Let S represent a critically important part parameter like strength and let us assume that S change monotonically and relatively slowly over the lifetime of the part, mentioned in Chap. 6 (stress-strength interference model). A Taylor expansion about $t = 0$ produces the Maclaurin series like Eq. 8.8:

$$S(t) = S_{t=0} + \left(\frac{\partial S}{\partial t} \right)_{t=0} t + \frac{1}{2} \left(\frac{\partial^2 S}{\partial t^2} \right)_{t=0} t^2 + \dots \quad (8.8)$$

It will be assumed that the higher order terms in the expansion can be approximated by simply introducing a power-law exponent m and writing the above expansion in a shortened form:

$$S = S_0 [1 \pm A_0(t)^m] \quad (8.9)$$

where A_0 is a part-dependent constant.

The power-law model is one of the most widely used forms for time-dependent degradation. For convenience of illustration, let us assume that the critical parameter S is decreasing with time and $A_0 = 1$. Equation (8.9) reduces to:

$$1 - \frac{S}{S_0} = (t)^m \quad (8.10)$$

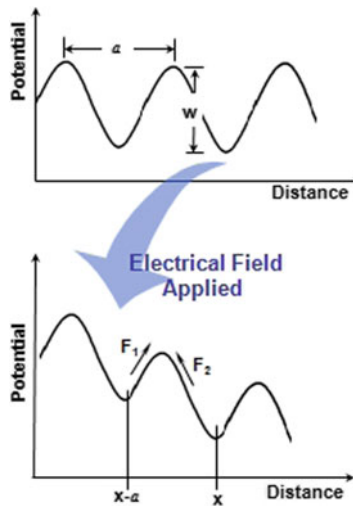
For $m = 1$, one will expect the linear degradation. On the other hand, for $m > 1$, the degradation will increase strongly with time and eventually lead to a catastrophic condition.

In reliability engineering, the development of the acceleration factor is fundamental importance to the theory of accelerated life testing. The acceleration factor speeds up the degradation of product and permits one to take time-to-failure data very rapidly under accelerated stress conditions. And it can extrapolate the accelerated time-to-failure results into the future for a given set of operational conditions. The acceleration factor must be modeled using the time-to-failure (*TF*) models. The acceleration factor is defined as the ratio of the expected time-to-failure under normal operating conditions to the time-to-failure under some set of accelerated stress conditions.

$$AF = \frac{(TF)_{operation}}{(TF)_{stress}} \quad (8.11)$$

Since the *TF* under normal operation may take many years to occur, experimental determination of the acceleration factor is impractical. However, if one has proper time-to-failure models, one can develop the acceleration factor from the *TF* models.

For solid-state diffusion of impurities in silicon, there are some following processes: (1) electro-migration-induced voiding; (2) build-up of chloride ions; (3) trapping of electrons or holes. The junction equation J might be expressed as:



$$\begin{aligned}
 J &= [aC(x - a)] \cdot \exp\left[-\frac{q}{kT}\left(w - \frac{1}{2}a\xi\right)\right] \cdot v \\
 &\quad [\text{Density/Area}] \cdot [\text{Jump Probability}] \cdot [\text{Jump Frequency}] \\
 &= -\left[a^2 ve^{-qw/kT}\right] \cdot \cosh\frac{qa\xi}{2kT} \frac{\partial C}{\partial x} + \left[2ave^{-qw/kT}\right] C \sinh\frac{qa\xi}{2kT} \\
 &= \Phi(x, t, T) \sinh(a\xi) \exp\left(-\frac{Q}{kT}\right) \\
 &= A \sinh(a\xi) \exp\left(-\frac{Q}{kT}\right)
 \end{aligned} \tag{8.12}$$

where Q is energy, a is coefficients, and A is constants.

Reaction process that is dependent to speed might be expressed as:

$$\begin{aligned}
 K &= K^+ - K^- = a \frac{kT}{h} e^{-\frac{\Delta E - aS}{kT}} - a \frac{kT}{h} e^{-\frac{\Delta E + aS}{kT}} \\
 &= a \frac{kT}{h} e^{-\frac{\Delta E}{kT}} \sinh\left(\frac{aS}{kT}\right)
 \end{aligned} \tag{8.13}$$

where k is Boltzmann's Constant, T is absolute temperature, S is stress, and A constants.

So the reaction rate K can be summarized as:

$$K = B \sinh(aS) \exp\left(-\frac{E_a}{kT}\right) \quad (8.14)$$

where E_a is the activation energy, and B constants.

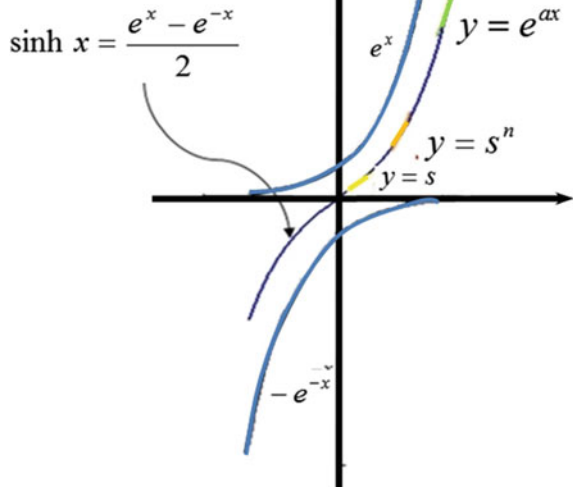
If the reaction rate in Eq. (8.14) takes an inverse number, the generalized stress model can be obtained like McPherson's derivation [22],

$$TF = A[\sinh(aS)]^{-1} \exp\left(\frac{E_a}{kT}\right) \quad (8.15)$$

Because this life-stress model equation was derived from a model of micro-depletion (void) in the failure domain, it should be relevant to general failure prediction regardless of whether it is a mechanical, civil or electronic system. Thus, the fatigue in a mechanical/civil system, coil degradation in a motor, bond-pad corrosion in an IC, etc., can be captured by Eq. (8.15).

The range of the hyperbolic sine stress term $[\sinh(aS)]$ in Eq. (8.15) is increasing the stress as following: (1) initially (S) in low effect, (2) $(S)^n$ in medium effect, and (3) $(e^{aS})^n$ in high effect initially linearly increasing. Accelerated testing usually happens in the medium stress range (see Fig. 8.14).

Fig. 8.14 Properties of the hyperbolic sine stress term $[\sinh(aS)]$



Thus, time to failure in the level of medium stress can then be described as

$$TF = A(S)^{-n} \exp\left(\frac{E_a}{kT}\right) \quad (8.16)$$

The internal (or external) stress in a product is difficult to quantify and use in accelerated testing because stress can be obtained by analytic method. It is necessary to modify Eq. (8.16) into a more applicable form. The power (or energy flow) in a physical system can generally be expressed as efforts and flows (Table 8.3). Thus, stresses in mechanical/civil or electrical systems may come from the efforts (or loads) like force, torque, pressure, or voltage [23].

For a mechanical/civil system, when replacing stress with effort, the time-to-failure can be modified as

$$TF = A(S)^{-n} \exp\left(\frac{E_a}{kT}\right) = A(e)^{-\lambda} \exp\left(\frac{E_a}{kT}\right) \quad (8.17)$$

where λ = power index or damage coefficient.

Because the material strength degrades slowly, it may require long times to test a module until failure occurs. The main hurdles to finding wear induced failures and overstressed failures are the testing time and cost. To solve these issues, the reliability engineer often prefers testing under severe conditions. Due to overstress the module failures can be easily found with parametric ALT.

The more the accelerated conditions, the shorter the testing time will be. Consequently, sample size will decrease in the accelerated regions that will be discussed with the reduction factor in the latter section. This concept is critical to performing accelerated life tests, but the range of the accelerated life tests will be determined by whether the results in the accelerated tests are the same to that in normally found in the field.

The stress-strain curve is a way to visualize behavior of material when it is subjected to load (see Fig. 8.15). A result of stresses in the vertical axis has the corresponding strains along the horizontal axis. Mild steel subjected to loads passes specification limits (proportional limit), operating limits (elastic limit), yield point, ultimate stress point into fracture (destruct limit). In accelerated testing, the appropriate accelerated stress levels (S_1 or e_1) will typically fall outside the specification limits but inside the operating limits.

When a module has been tested for a number of hours under the accelerated stressed condition, one wants to know the equivalent operation time at the normal

Table 8.3 Energy flow in the multi-port physical system

Modules	Effort, $e(t)$	Flow, $f(t)$
Mechanical translation	Force, $F(t)$	Velocity, $V(t)$
Mechanical rotation	Torque, $\tau(t)$	Angular velocity, $\omega(t)$
Compressor, Pump	Pressure difference, $\Delta P(t)$	Volume flow rate, $Q(t)$
Electric	Voltage, $V(t)$	Current, $i(t)$

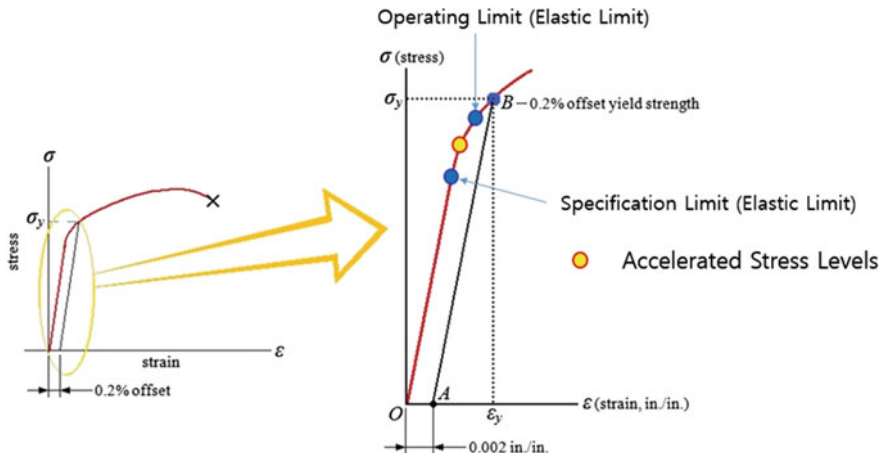


Fig. 8.15 Strain-Stress curve in mild steel

stress condition. After the multiple accelerated testing under diverse conditions, the equivalent operation time at normal (or actual) operation time can be obtained.

From the time-to-failure in Eq. (8.17), the acceleration factor can be defined as the ratio between the proper accelerated stress levels and normal stress levels. The acceleration factor (*AF*) also can be modified to include the effort concepts:

$$AF = \left(\frac{S_1}{S_0} \right)^n \left[\frac{E_a}{k} \left(\frac{1}{T_0} - \frac{1}{T_1} \right) \right] = \left(\frac{e_1}{e_0} \right)^\lambda \left[\frac{E_a}{k} \left(\frac{1}{T_0} - \frac{1}{T_1} \right) \right] \quad (8.18)$$

where *n* is stress dependence and λ is cumulative damage exponent that depends on materials.

It is important to note that the acceleration factor is very special because the acceleration factor is the independent coefficient *A*. This means that even though the time-to-failure *TF* must be expressed as a distribution of time-to-failure, the acceleration factor is unique and depends on the kinetic value (λ , E_a), not on part-to-part variation.

The first term is the outside effort (or load) and the second is the internal energy in Eq. (8.18). Under severe conditions, the outside higher load drops the energy barrier and the accelerated (or high) temperature activates the material elements. In the end, the material degrades and fails. The equation has two parameters which are temperature and effort. Using a three-level test under accelerated conditions, these parameters can be obtained. And the quantified value, *activation energy* E_a , is called the reaction rate due to temperature rises.

Under severe conditions, the duty effect with repetitive stress (or load) involves the on/off cycles, which shortens module lifetime [24]. The equation needed to determine the sample size for the parametric ALT is discussed in the next section.

8.6.3 *Derivation of General Sample Size Equation*

As mentioned previously, due to the cost and time limit, it is difficult to test large samples for reliability testing of product. If fewer components are tested and the confidence interval is greater, the results of reliability testing in a statistical analysis will become more uncertain. For a more precise result it is necessary that enough samples are tested. This, however, can increase the time and cost in testing. Thus, it is important to develop method for the accelerated testing, using the sample size equation with acceleration factor in Eq. (8.18). It allows the core testing methods for securing reliability information as inexpensively as possible in the reliability-embedded product developing process.

For the lifetime assessment, the confidence levels are necessary because it is not possible to gather the lifetimes of limited several sample size. In statistics, the failure behavior of the limited sample may strongly deviate from the actual failure behavior of the population itself. The core concept offers a further help through the confidence levels, which can specify the confidence of the test results and estimate the failure behavior of the population.

In statistical test planning the first step involves determining how the sample size should be extracted of the inspection lots or population. The test samples are chosen randomly for a representative test sample. The sample size is connected with the confidence levels and the statistical range of the measured failure values. Another important point establishes a suitable test strategy—complete tests, incomplete (censored) test, and accelerated testing for shortening times.

The best statistical case is a complete test that all test samples of the population are subjected to a lifetime test. This means that the test is run until the last parts has failed. Thus, failure times for all parts are useful for further product lifetime assessment. However, engineer should remember why the lifetime testing in company is carried out. That is, for new product, the missing design parameters is found and corrected before market launching.

In order to reduce the time and effort involved in a lifetime testing, it is reasonable to carry out censored tests and (or) the accelerated testing. The tests are carried out until a certain predetermined lifetime (Type I censoring) or until a certain number of failed components have been reached with accelerated condition (Type II censoring). If fewer or limited parts are censored, the statistical assessment becomes more uncertain. Thus, to save the testing time and decrease the sample size, parametric accelerated life testing in mechanical/civil system has to be developed.

From various developed methods to estimate the shape parameter (or characteristic life) sample size in Weibull distribution, the Weibayes analysis is well known and widely accepted method. However, its mathematical complexity makes it difficult to apply it directly to determined sample size. Failures ($r \geq 1$) need to be distinguished from no failure ($r = 0$) cases. Hence, it is necessary to develop a simplified sample size equation from the Weibayes analysis.

The Cumulative Distribution Function (CDF) in Weibull can be expressed as:

$$F(t) = 1 - e^{-\left(\frac{t}{\eta}\right)^\beta} \quad (8.19)$$

The Weibull reliability function, $R(t)$, is expressed as:

$$R(t) = e^{-\left(\frac{t}{\eta}\right)^\beta} \quad (8.20)$$

In statistics, maximum-likelihood estimation (MLE) is a method of estimating the parameters of a statistical model—some unknown mean and variance that are given to a data set. Maximum likelihood selects the set of values of the model parameters that maximizes the likelihood function. The characteristic life η_{MLE} from the Maximum Likelihood Estimation can be derived as:

$$\eta_{MLE}^\beta = \sum_{i=1}^n \frac{t_i^\beta}{r} \quad (8.21)$$

If the confidence level is $100(1 - \alpha)$ and the number of failure is $r \geq 1$, the characteristic life, η_α , would be estimated,

$$\eta_\alpha^\beta = \frac{2r}{\chi_\alpha^2(2r+2)} \cdot \eta_{MLE}^\beta = \frac{2}{\chi_\alpha^2(2r+2)} \cdot \sum_{i=1}^n t_i^\beta \quad \text{for } r \geq 1 \quad (8.22)$$

Presuming there is no failures, p -value is α and $\ln(1/\alpha)$ is mathematically equivalent to Chi-Squared value, $\frac{\chi_\alpha^2(2)}{2}$. The characteristic life η_α , would be represented as:

$$\eta_\alpha^\beta = \frac{2}{\chi_\alpha^2(2)} \cdot \sum_{i=1}^n t_i^\beta = \frac{1}{\ln \frac{1}{\alpha}} \cdot \sum_{i=1}^n t_i^\beta, \quad \text{for } r = 0 \quad (8.23)$$

Thus, Eq. (8.22) is established for all cases $r \geq 0$ and can be redefined as follows:

$$\eta_\alpha^\beta = \frac{2}{\chi_\alpha^2(2r+2)} \cdot \sum_{i=1}^n t_i^\beta \quad \text{for } r \geq 0 \quad (8.24)$$

To evaluate the Weibull reliability function in Eq. (8.24), the characteristic life can be converted into L_B life as follows:

$$R(t) = e^{-\left(\frac{L_B}{\eta}\right)^\beta} = 1 - x \quad (8.25)$$

After logarithmic transformation, Eq. (8.25) can be expressed as:

$$L_{BX}^\beta = \left(\ln \frac{1}{1-x} \right) \cdot \eta^\beta \quad (8.26)$$

If the estimated characteristic life of p -value α , η_α , in Eq. (8.24), is substituted into Eq. (8.26), we obtain the B_X life equation:

$$L_{BX}^\beta = \frac{2}{\chi_\alpha^2(2r+2)} \cdot \left(\ln \frac{1}{1-x} \right) \cdot \sum_{i=1}^n t_i^\beta \quad (8.27)$$

If the sample size is large enough, the planned testing time will proceed as:

$$\sum_{i=1}^n t_i^\beta \cong n \cdot h^\beta \quad (8.28)$$

The estimated lifetime (L_{BX}) in test should be longer than the targeted lifetime (L_{BX}^*)

$$L_{BX}^\beta \cong \frac{2}{\chi_\alpha^2(2r+2)} \cdot \left(\ln \frac{1}{1-x} \right) \cdot n \cdot h^\beta \geq L_{BX}^{*\beta} \quad (8.29)$$

Then, sample size equation is expressed as follows:

$$n \geq \frac{\chi_\alpha^2(2r+2)}{2} \cdot \frac{1}{\left(\ln \frac{1}{1-x} \right)} \cdot \left(\frac{L_{BX}^*}{h} \right)^\beta \quad (8.30)$$

However, most lifetime testing has insufficient samples. The allowed number of failures would not have as much as that of the sample size.

$$\sum_{i=1}^n t_i^\beta = \sum_{i=1}^r t_i^\beta + (n-r)h^\beta \geq (n-r)h^\beta \quad (8.31)$$

If Eq. (8.31) is substituted into Eq. (8.27), B_X life equation can be modified as follows:

$$L_{BX}^\beta \geq \frac{2}{\chi_\alpha^2(2r+2)} \cdot \left(\ln \frac{1}{1-x} \right) \cdot (n-r)h^\beta \geq L_{BX}^{*\beta} \quad (8.32)$$

Then, sample size equation with the number of failure can also be modified as:

$$n \geq \frac{\chi_\alpha^2(2r+2)}{2} \cdot \frac{1}{\left(\ln \frac{1}{1-x} \right)} \cdot \left(\frac{L_{BX}^*}{h} \right)^\beta + r \quad (8.33)$$

From the generalized sample size Eq. (8.33), we can proceed reliability testing (or parametric ALT testing) under any failure conditions ($r \geq 0$). Consequently it also confirms whether the failure mechanism and the test method are proper.

8.6.4 Derivation of Approximate Sample Size Equation

As seen in Table 8.4, for a 60% confidence level, the first term $\frac{\chi^2_{\alpha}(2r+2)}{2}$ in Eq. (8.33) can be approximated to $(r + 1)$ [25]. And if the cumulative failure rate, x , is below about 20%, the denominator of the second term $\ln \frac{1}{1-x}$ approximates to x by Taylor expansion.

Then the general sample size Eq. (8.33) can be approximated as follows:

$$n \geq (r + 1) \cdot \frac{1}{x} \cdot \left(\frac{L_{BX}^*}{h} \right)^{\beta} + r \quad (8.34)$$

If the acceleration factors in Eq. (8.19) are added into the planned testing time h , Eq. (8.35) will be modified as:

$$n \geq (r + 1) \cdot \frac{1}{x} \cdot \left(\frac{L_{BX}^*}{AF \cdot h_a} \right)^{\beta} + r \quad (8.35)$$

The normal operating cycles of the product in its lifetime are calculated under the expected customer usage conditions. If failed number, targeted lifetime, accelerated factor, and cumulative failure rate are determined, the required actual testing cycles under the accelerated conditions can be obtained from Eq. (8.35). ALT equipment in mechanical/civil system will be designed based on the load analysis and the operating mechanism of the product. Using parametric ALT with approximated sample size of an acceleration factor, the failed samples in the design phase can be found. From the required cycles (or Reliability Quantitative (RQ) test specifications), h_a , it determines whether the reliability target is achieved. For example, without considering the acceleration factor, the calculation results of two sample size equations are presented in Table 8.5.

Table 8.4 Characteristics of $\frac{\chi^2_{\alpha}(2r+2)}{2}$ at $\alpha = 60\%$ confidence level

r	$1 - \alpha$	$\frac{\chi^2_{0.4}(2r+2)}{2}$	$\frac{\chi^2_{\alpha}(2r+2)}{2} \approx r + 1$	$1 - \alpha$
0	0.4	0.92	1	0.63
1	0.4	2.02	2	0.59
2	0.4	3.11	3	0.58
3	0.4	4.18	4	0.57

Table 8.5 The calculated sample size with $h = 1080$ h testing time

β	Failure number	Sample size	
		Equation (8.33) by Minitab	Equation (8.34)
2	0	3	3
2	1	7	7
3	0	1	1
3	1	3	3

If the estimated failure rate from the reliability testing is not bigger than the targeted failure rate (λ^*), the number of sample size (n) might also be obtained. The estimated failure rate with a commonsense level of confidence (λ) can be described as:

$$\lambda^* \geq \lambda \cong \frac{r + 1}{n \cdot (AF \cdot h_a)} \quad (8.36)$$

By solving Eq. (8.37), we can also obtain the sample size

$$n \geq (r + 1) \cdot \frac{1}{\lambda^*} \cdot \frac{1}{AF \cdot h_a} \quad (8.37)$$

Multiplying the targeted lifetime (L_{Bx}^*) into the numerator and denominator of Eq. (8.38), we can yield another sample size equation.

$$n \geq (r + 1) \cdot \frac{1}{\lambda^* \cdot L_{Bx}^*} \cdot \frac{L_{Bx}^*}{AF \cdot h_a} = (r + 1) \cdot \frac{1}{x} \cdot \left(\frac{L_{Bx}^*}{AF \cdot h_a} \right)^1 \quad (8.38)$$

Here, we know that $\lambda^* \cdot L_{Bx}^*$ is transformed into the cumulative failure rate x .

We can see two equations for sample size that have a similar form Eq. (8.35) to (8.38). It is interesting that the exponent of the third term for two equations is 1 or β , which is greater than 1 for wear-out failure. Because the sample size equation for the failure rate is included and the allowed failed numbers r is 0, the sample size equation Eq. (8.35) for the lifetime might be a generalized equation to achieve the reliability target.

If the testing time of an item (h) is more than the targeted lifetime (L_{Bx}^*), the reduction factor R is close to 1. The generalized equation for sample size in Eq. (8.35) might be rewritten as follows:

$$n \geq (r + 1) \cdot \frac{1}{x} \quad (8.39)$$

And if the targeted reliability for module is allocated to B_1 life 10 years, the targeted lifetime (L_{Bx}^*) is easily obtained from the calculation by hand. For refrigerator, the number of operating cycles for one day was 5; the worst case was 9. So the targeted lifetime for ten years might be 32,850 cycles.

And the other type of sample size equation that is derived by Wasserman [26] can be expressed as:

$$\begin{aligned} n &= -\frac{\chi_{\alpha}^2(2r+2)}{2m^{\beta} \ln R_L} = \frac{\chi_{\alpha}^2(2r+2)}{2m^{\beta} \ln R_L^{-1}} = \frac{\chi_{\alpha}^2(2r+2)}{2m^{\beta} \ln(1 - F_L^{-1})} \\ &= \frac{\chi_{\alpha}^2(2r+2)}{2} \cdot \frac{1}{\ln(1 - F_L^{-1})} \cdot \left(\frac{L_{BX}}{h}\right)^{\beta} \end{aligned} \quad (8.40)$$

where $m \cong h/L_{BX}$, $n \gg r$.

When $r = 0$, sample size equation can be obtained as:

$$\begin{aligned} n &= \frac{\ln(1 - C)}{m^{\beta} \ln R_L} = \frac{-\ln(1 - C)}{-m^{\beta} \ln R_L} = \frac{\ln(1 - C)^{-1}}{m^{\beta} \ln R_L^{-1}} = \frac{\ln \alpha^{-1}}{m^{\beta} \ln R_L^{-1}} \\ &= \frac{\chi_{\alpha}^2(2)}{2} \cdot \frac{1}{\ln(1 - F_L^{-1})} \cdot \left(\frac{L_{BX}}{h}\right)^{\beta} \end{aligned} \quad (8.41)$$

So Wasserman's sample size equation Eq. (8.41) is similar to Eq. (8.35).

Especially, the ratio between product lifetime versus the testing time in Eq. (8.34) can be defined as reduction factor. It can be used to determine if accelerated life testing is proper. That is,

$$R = \left(\frac{L_{BX}^*}{h}\right)^{\beta} = \left(\frac{L_{BX}^*}{AF \cdot h_a}\right)^{\beta} \quad (8.42)$$

To effectively proceed the parametric accelerated life testing, we have to find the severe conditions that will increase the accelerated factor (AF) and the shape factor β . At that time the location and shape of the failed product in both market and parameter ALT results are similar. If the actual testing time h_a is longer than the testing time that is specified in the reliability target, the reduction factor will be less than one. So we can obtain the accelerated conditions that can decrease the testing time and sample size number.

Example 8.1 Specification design for reliability testing.

If there is driver module that consists of motor and gear speed reducer in refrigerator, design the testing specification for parametric ALT.

Reliability target of module is set up as B4 Life 5 Year.

System Usage for 5 years: $(2 \text{ h/day}) \cdot (360 \text{ day/Year}) \cdot (5 \text{ Year}) = 3600 \text{ h}$.

If testing time is carried out till system usage $R = 1$ (reduction factor is 1), the sample size will be calculated as:

$$n \cong \frac{1}{x} = \frac{1}{0.04} = 25$$

Initially, the parametric ALT will proceed as the following conditions:

$r = 0$, 3600 h (150 day testing), $n = 25$, (Common sense Level of Confidence)

To save the testing time, if applied torque is 1.6 times under the toughest conditions, accelerated factor in Eq. 8.18 is obtained as:

$$\begin{aligned} AF &= \left(\frac{S}{S_o}\right)^n \cdot \exp\left[\frac{Ea}{k} \left(\frac{1}{T_o} - \frac{1}{T}\right)\right] \\ &= \left(\frac{e}{e_o}\right)^\lambda \cdot \exp\left[\frac{Ea}{k} \left(\frac{1}{T_o} - \frac{1}{T}\right)\right] \\ &= \left(\frac{0.16 \text{ kg cm}}{0.1 \text{ kg cm}}\right)^2 \cdot \exp\left[\frac{0.56 \text{ eV} \cdot 1.6 \times 10^{-19}}{1.38 \times 10^{-23}} \left(\frac{1}{293} - \frac{1}{313}\right)\right] = 10 \end{aligned}$$

Under accelerated testing conditions, the testing is $AF = 10$, $r = 0$, 360 h (15 day testing), $n = 25$.

To save the sample size, if the testing time will increase three times, reduction factor in Eq. (8.42) is obtained as:

$$\left(\frac{L_{BX}}{AF \cdot h}\right)^\beta = \left(\frac{3600}{10 \times 360 \times 3}\right)^3 = \frac{1}{27}$$

The final schedule of drive lifetime testing can be designed as
 $AF = 10$, $r = 0$, 1080 h (45 day testing), $n = 1$, (Shape Parameter = 3).

8.7 The Reliability Design of Mechanical System and Its Verification

8.7.1 Introduction

Completing the design of a new product requires two kinds of activities—managerial and technical skills. Managerial skill includes adopting a process improvement approach, such as Capability Maturity Model Integration (CMMI), and controlling quality, which Japan has pursued for over sixty years (starting with training by Dr. W. Edwards Deming at the Japanese Union of Scientists and Engineers) [27]. Technical skill involves using a product-specific validation and verification approach.

CMMI has been developed by the Software Engineering Institute at Carnegie Mellon University [28]. It outlines five organizational levels; from lowest to highest, these are initial, managed, defined, quantitatively managed, and optimizing. The purpose of assessing the level of organization is to raise it to the highest level, at which developing engineer and manager including CEO expect to produce perfect products. This is not an exact approach, but a technique to back up and assess the principal manufacturing process.

Quality control is mainly related to manufacturing. Its focus is how to assure that item variations are within the tolerances of already determined specifications. Therefore, quality control methods are dimensionally different than the verification of new product designs, since the product developer should establish the necessary specifications for new products as well as their tolerances. Quality control is not generally an activity in the design area, but a necessary activity in the manufacturing field in Fig. 8.16.

Let's consider product-specific verification as a technical skill. Generally, engineers check numerous design items when developing new products. In the NASA Systems Engineering Handbook [29], there are sixteen activities under the heading "Verification Procedures," almost all of which involve testing. The keywords include identification of test configuration, test objective, test criteria, test equipment, and location of test activity. Similarly, verification of software includes test strategy, test plan, test procedure, test scenario sorting deficiencies, and so on. But these are general comments or recommendations that may vary according to the activity and the test article, and therefore are not mandatory. Of course the test is required if applicable specifications exist, but that is not sufficient.

From a verification viewpoint, NASA Handbook addresses tasks used to test products, but does not establish the detailed specification standards as the frame of reference in which these tasks might be carried out. It is not acceptable for verifiers to use their discretion when verifying product performance. Carefully established specifications prevent verification activities to deviate from the determined process. Thus, when failure occurs, it is possible to determine whether the specifications are

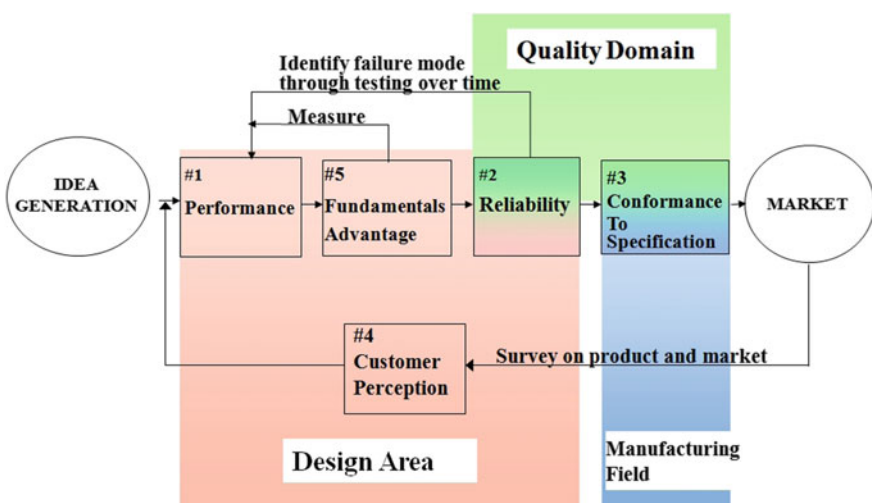


Fig. 8.16 Confusing quality control: (1) R&D, (2) QA (Performance/Reliability), (3) Manufacture QC

inappropriate or whether verifiers are incorrectly conforming to the specifications. Sometimes we can also identify omissions in the verification specifications.

Verification specifications should be established over the full range of functions fitted to each product. A thorough use of available technology and related measures to address issues might be applied at an early stage of product development. Why don't developing engineer and manager require verification specifications for each product? The reason lies in the engineers' answers. Product-assurance specialists may insist that all related verification activities are included in a "thick document." And they may add that the activities performed are completely reviewed and revised by related specialists. Furthermore, if developing engineer and manager figure out the technical details, he would understand all he wanted to know the design details like differences between quality defects and failures. However, there is gap between design engineer and manager including CEO. Especially, manager can't understand the complex situations when engineers are in design. This is a kind of trap. If the technical details become specification, the situation will change.

8.7.2 Reliability Quantitative (RQ) Specifications

Technology concepts related product could be explained with common sense, although some concepts of new technology take time to be understood. Everyone understands new product design concepts if the related staff explains them in everyday communication. Fortunately, the technology concepts related to design verification is not difficult to grasp because we, as consumers, use product. For example, the technology concepts to reduce the noise level of a car engine would be difficult to understand but assessing the performance improvement would be easy since we can hear it. The concepts of design verification related specification are less complex than that of design itself, and should be easily grasped by developing engineer and manager. If developing engineer and manager have difficulty understanding the verification document, there are illogical sections not to be explained with common sense when the engineers write it. The necessary logic of "thick document" is clarified for any layman to be understood and controversial as seen in Table 8.6.

Three kinds of simple logic might be addressed in the verification document. Firstly, the information is divided into two activities: verification-specifications establishment and related execution. Secondly, procedures for how to extract anticipated issues in a new product need to be addressed in the verification specifications, avoiding omissions of necessary specifications and adding some details pertaining to the product for a complete set of specs. Thirdly, verification specifications should be classified into categories according to technological fields in order for related specialists to review their accuracy. Verification specifications might be clearly presented, providing brief summaries to clarify the entire specification concepts.

Additionally, there are two other issues involved in establishing verification specifications. First of all, we think that new products can check the combinations

Table 8.6 Double ambiguity of product quality

Product Value = Function of Product Quality and Price			
	Reliability	Durability	Conformance-Quality
Meaning of basic quality			
Concept	Product life	Failure rate	Conformance to specifications
Unit	Year	Percent/Year Percent/Hour	Percent ppm
Probability	Weibull distribution	Exponential distribution	Normal distribution
Activities	Design change or establishing specification		Inspection, Screening

of specifications used for similar products. This is a misunderstanding. Potential problems inherent in new products cannot be identified using old specifications. The new product incorporates innovative structures, new materials, and different software for upgrading performance and decreasing cost. These cannot be adequately tested using existing specifications.

By using the previous specifications, new failure mechanisms is not easy to be identified for products that have the design modifications. In addition to updating the specifications, we should also consider what new testing might be effective. For example, is it possible to apply the test specifications for the Boeing 777 fuselage made of aluminum alloys to the Boeing 787 Dreamliner fuselage, which incorporates new materials, like CFRP? Obviously, we know that the previous test specs would be improper.

The other issue is that reliability quantitative specifications that can use the parametric ALT as one of methodology mentioned in previous sections include estimating item lifetime. Product recalls caused by the design missing during customer use could tarnish the company's reputation. But most people consider this task beyond the scope of possibility. Generally obtaining quantitative results in reliability analysis is very difficult. Reliability specialist Patrick O'Connor wrote in Practical Reliability Engineering that there are basically three kinds of situations—small, moderately large, and very large numbers of factors and interactions [30]. A small number of factors can be predicted with the physical model. A large number can be predicted with statistical models. Predictive power diminishes, however, in the case of a moderately large number of factors pertaining to reliability.

Reliability prediction is a necessary task to be undertaken. Let's look at a product in the standpoint of reliability problems. We know that there are a few sites in product that are weaker than other sites. Reliability specialists can presume the location of the weakest site and/or its failure mechanisms, though they don't know whether the failure will actually happen in the targeted lifetime, or how high the failure rate would be. So if we extract one or two failure sites in the product, mostly in a given module or unit, and classify their failure mechanisms into two categories of reliability—lifetime L_B and failure rate λ within lifetime—the factors related to reliability estimation are decreased, and the cases pertaining to moderately large factors become small-factor-number cases. Thus we can make quantitative estimations about reliability issues—mainly lifetime under normal conditions. This is the simple explanation to understand developing engineer and manager.

Let's describe in common sense terms the basic concepts of the required statistics and methods pertaining to establish the quantitative lifetime specification, which developing engineer and manager can easily understand the B_X Life as reliability quantitative specifications in Fig. 8.17. For instance, take automobiles. Assume that we test one hundred cars in Germany for ten years and find no trouble (10 years, 160,000 km). We can conclude that the car's failure rate is below 1% per ten years, which is called "B₁ life 10 years." When we conclude that the car's failure rate is below 1% per ten years, its confidence level reaches around 60%, called the common sense level of confidence. Of course, we cannot test products for

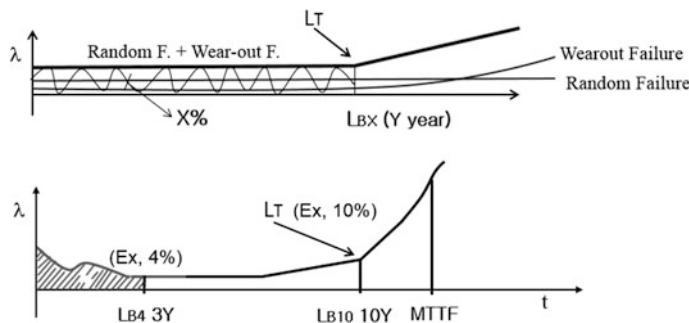


Fig. 8.17 Reliability Index; B_X Life (L_{Bx})

ten years before market release. So we make the accelerated vehicle testing by imposing heavy loads and high temperature until we reach an acceleration factor of ten. This will reduce the test period by one-tenth, or one year. Thus we test one hundred items for one year (16,000 km), or one week without stoppage (7 days \times 24 h \times 100 km/h = 16,800 km). The next step is to reduce the sample size.

Then, if you increase the testing time, the items would achieve a sufficiently degraded state and many would fail after the test; therefore, we can greatly reduce the sample size, because one or two failed samples would yield enough data to identify the problem area and make corrective action plans. Increasing the test time by four times, or to one month, reduces the necessary sample size by the square of the inverse of the test-time multiplier, to one-sixteenth (square of one quarter), or six engines. The final test specification, then, is that six engines should be tested for one month under elevated load and temperature conditions with the criterion that no failure is found. This concept, called Parametric Accelerated Life Testing, is the key to reliability quantitative specifications.

We also cannot guarantee the behavior of a product over ten years under the extreme environments. These test conditions would be appropriate to mechanical/civil system (or components), like power engines, but the test conditions are not fit to assess the degradation of paint on the automobile body. In addition to testing the new engine, we should devise quantitative test methods for other components—new electrical components (including batteries), electronic control units, lighting systems, or coating materials. According to the identified failure mechanisms, testing must be conducted by subassembly to heighten acceleration.

Without such quantitative lifetime testing, we can't identify all the failures influencing the product's lifetime because there would be unanticipated failures. For example, at prototype testing, the lifetime of a tub in a washing machine was lengthened at first parametric ALT by the missing structural design changes—a corner radius increase, rib insertion, and so on. The final parametric ALT, however, showed a weakening of strength in the plastic due to a chemical reaction; the problem was solved by changing the release agent of the injection molding process—something no one could have been predicted as the solution. Note that this

method reveals exact failure modes, including totally unexpected ones, that other methods, like FMEA (failure mode and effects analysis), cannot identify.

For the CFRP of the 787 Dreamliner, the failure mechanism is a kind of delamination, which can be found in pressure/humidity/temperature cycling and ultraviolet irradiation testing. If the acceleration factor for testing this is calculated using an adequate life-stress model (time-to-failure model) and the sample size is determined according to the B_X life target, then quantitative results can be derived. Note that we should check the possibility of failure due to various overstresses, such as bird strikes, with sufficiently degraded samples. For the electrical systems in the 787 engineers should incorporate the same components used in other commercial airplanes (and different combinations of them), assessing the possibilities of over-stress failures under reliability marginal stresses, since they can assure lifetime reliability. But for new components like the lithium-ion battery, the failure mechanics as well as the stresses produced in the aircraft environment have been changed. Thus, we cannot presume what kind of failure mechanisms would occur due to chemical reaction until the projected lifetime reaches. Generally, chemical failure mechanisms are delicate and thus difficult to identify and reproduce, which means that the acceleration conditions and related factors can be hard to determine. Thus they should test until lifetime under almost normal conditions, and the behavior of sufficiently degraded components should be checked under the rated stresses and overstresses. The media have reported various accidents or disasters due to unanticipated failure mechanisms in chemical items, such as the fires occurring in the Sony lithium-ion battery in notebook computers in 2005, Firestone tires causing Ford Explorer rollovers in the 1970s, wire bundles incorporating silver-plated copper wire leading to fire in the Apollo 1 cabin in 1967, and so on.

8.7.3 Conceptual Framework of Specifications for Quality Assurance

Returning to the subject of establishing verification specifications, there are plenty of specifications that have few explanations technically. It is difficult to find articles that explain to establish specifications; there have been a few research studies about it. So let's consider how to anticipate issues in a new product and to configure a series of verification specifications responding to them, and how to develop specifications that will identify these issues accurately.

Here is one such methodology. First, select an existing product to be compared with the new one. All its relevant specifications are listed except the unnecessary specifications. Secondly, because inevitably the similar but older product has the intractable problems to be listed, we must devise new specifications to address these issues. Ongoing problems indicate that any counter-measures have not resolved the real cause because of the inadequate analysis. Nonetheless, the original design idea may be faulty. The existing product would be solved by using precise problem

analysis, and the new product would be handled by identifying and fixing the problem before releasing the next model. To correct the existing problems in similar products, it is important to add the verification specifications. Sometimes the potential problems of the subassemblies manufactured by a new supplier also might be considered.

Thirdly, the newly designed portions—those that differ from the current comparable product—should be listed and the potential issues related to them should be predicted. Verification specifications need to be devised to address these problems. Especially note that all items incorporating new chemical materials should be tested to item lifetime under new quantitative specifications because a new kind of wear-out failure could occur near the item lifetime. Moreover, it is very difficult to computer-simulate and clarify diverse chemical reactions over an item's life cycle.

Finally, the new product will also have performance fundamentals unique to it, which sometimes provide a competitive edge over competitors. Such comparative advantages in performance fundamentals might be checked with the newly established specifications.

A complete set of verification specifications in Fig. 8.18 might be summarized as four types of data: (1) all the verification specifications for the comparable product(s); (2) specifications to fix existing problems in the comparable product; (3) specifications that deal with the potential issues in the newly designed portions; and (4) specifications checking newly incorporated performance features. The specifications responding to the latter three categories are all established anew. The purpose of sectioning potential issues in a new product is to check whether necessary issues have been omitted.

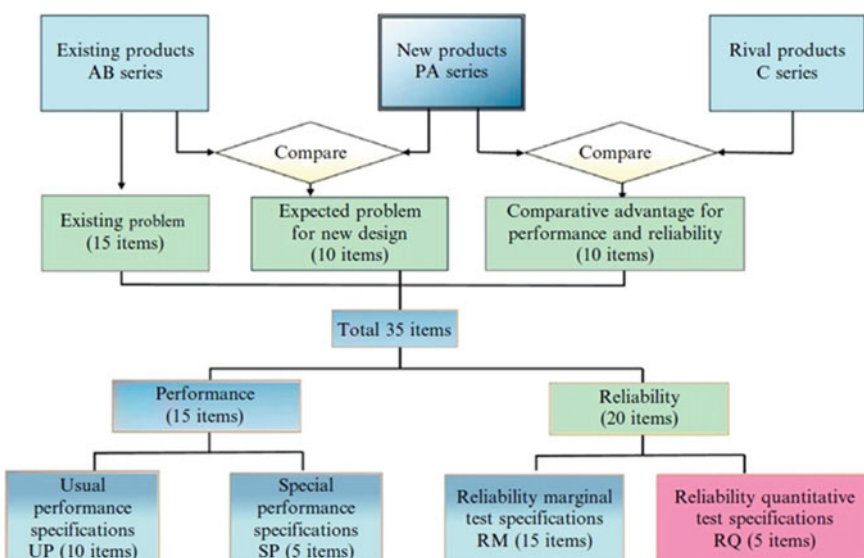


Fig. 8.18 Complete testing sets of verification specifications for Quality Assurance

All specifications enumerated according to this model would be classified, initially, into two groups: performance specifications and reliability specifications. If an issue to be identified is related to material rupture or degradation over time, it is a reliability issue; if not, it is a performance issue. The specifications are further divided into four categories: Usual Performance specifications (UP), Special Performance specifications (SP), Reliability Marginal test specifications (RM), and Reliability Quantitative test specifications (RQ).

UPs check the expected performance by the usual operator or consumer. SPs check performance under extraordinary environments, such as tropical heat or elevated electromagnetic fields. RMs are used for identifying physical changes under severe or peculiar conditions, including unusual usage environments like electrostatic overstress or lightning surges. Finally, RQs are for reviewing the product state under normal conditions and for estimating the product lifetime, the B_X life (lifetime of the cumulative failure rate X%), and the annual failure rate within lifetime. Note that the lifetime index MTTF refers to the time-point at which about 60% of the production lot fails, which is an unacceptable rate.

Parametric accelerated life testing mentioned in the previous sections uses the sample size equation with acceleration factor. It also is a process that helps designers find the optimal design parameters, which can help them better estimate expected lifetime L_B , failure rate of module λ , and determine the overall product reliability. Reliability quantitative (RQ) test specifications are used to estimate the required lifetime (or cycle) if reliability target of product— B_x life Y years is given. Parametric accelerated life testing (ALT) might be related to the RQ test specifications. And the examples of parametric ALT will be discussed with the Chap. 8.

8.8 Testing Equipments for Quality and Reliability

8.8.1 *Introduction*

In today's competitive market, more companies are looking to application specific automatic testing equipment versus functional testing methods. That's because the traditional testing process did not apply for complex systems such as aero and automotive engines. High product performance and reliability are a basic requirement and sometimes the only difference between products of various manufacturers. Test equipment verifies the performance and reliability of mechanical, electrical, hydraulic and pneumatic products. These include tool testers, hi-pot testers, power cord and power supply cord testers, automatic test equipments for a variety of purpose, and leakage current testers.

Product quality is a critical aspect for companies who are struggling to retain customers in these days of fast eroding brand loyalty. Testing equipment companies designs and builds production test equipment. They specialize in R&D test equipment, authentication test equipment and quality control test equipment for

mass production. Test equipment is categorized as overall performance test, durability (life) test, accelerated test, safety test and environmental test, etc. (Fig. 8.19).

Test equipment has multi-disciplinary systems that are incorporating machine design, material science, industrial engineering, statistics, electrical & electronics, and computing system. As product development requires substantially high level of performance and reliability in the limited developing time of product, equipment for testing the performance and reliability of product is growing at a significant scale.

In the stage of the detail design, testing equipment companies are to develop the test equipment that is applicable to be gratified at the specifications of end users. They provide the latest state-of-the-art test equipment to rental centers, electrical service facilities, manufacturers and OEMs. In over half century they have learned what end users want. Their experiences are reflected in a number of important concepts in hardware and software designs of test equipment. When a request for a test equipment development is received, testing equipment companies promises to provide customized support by analyzing the necessary requirements for installation and trial runs of the developed equipment.

The Quality, Safety, and Life of product could be increased by reliability testing. Product reliability testing is a specialized field that requires deep understanding of the product and a state of the art infrastructure to deliver the goods. Product reliability testing equipment is to help companies to test reliability of their products. Thus, reliability testing equipment should have a user requirement—purpose, required power, testing items, control precision, data processing speed, automation

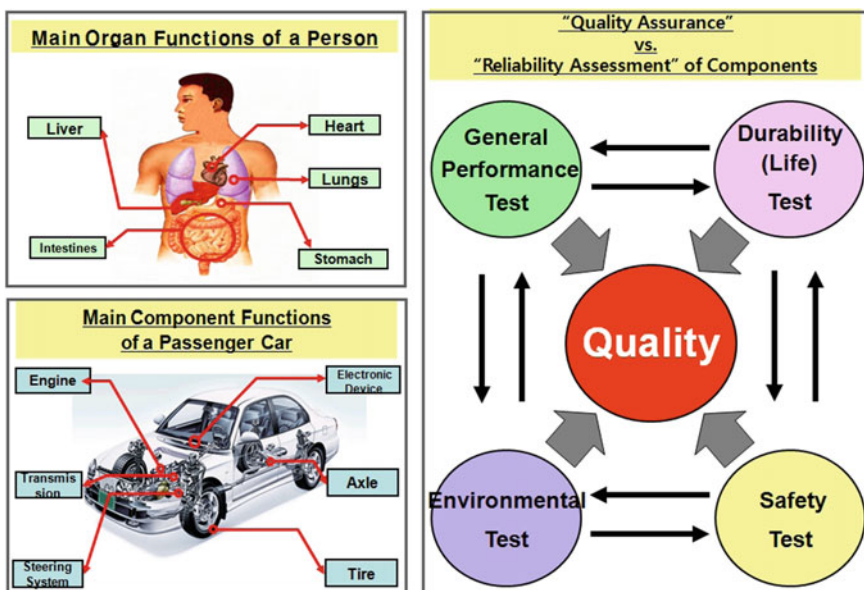


Fig. 8.19 Reliability assessment concept for developing testing equipment

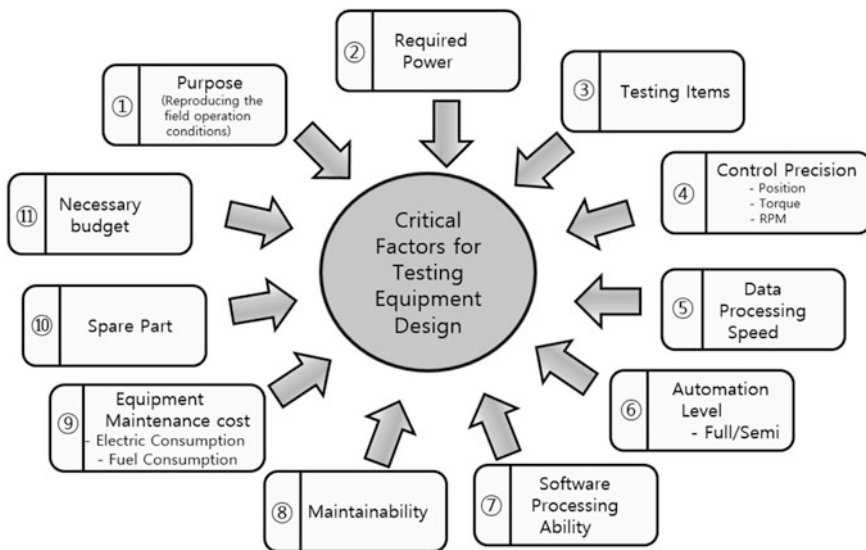


Fig. 8.20 Considerations for developing testing equipment

level, software processing ability, maintainability, equipment maintenance cost, spare part, and necessary budget (Fig. 8.20).

Testing equipment insures the reliability, safety and performance of products they manufacture, use, service or rent. As product technology advances, testing equipment are required to (1) make products reliable, (2) meet the international standards, and (3) offer the Product/Parts Reliability, Failure Analysis, Test Structure (Design, Verification and Test), Technology Qualification Support for product, and environmental Measurement Services (humidity, temperature, etc.).

Consequently, testing equipment type for product R&D development can be classified as: (1) Testing Equipment for General Performance, (2) Testing Equipment for Durability (Life), (3) Testing Equipment for Accelerated Testing, (4) Testing Equipment for (Combined) Environment, (5) Testing Equipment for Quality Control of Mass Production, (5) Testing Equipment for Maintenance and Repair. As seen in Fig. 8.21, there are a variety type of testing equipment and their company in global that cannot be quantified.

Today testing equipment companies also look to custom designed and manufactured automatic testing equipment that can functionally test new units that employ advanced technologies. By going beyond simple parametric testing that limits the use of commercial off the shelf testers, specialty-built functional automatic testing equipment helps guarantee high intrinsic availability and long-lived performance “to spec” in the field, thereby facilitating the acceptance and success of new technologies in the marketplace.

They often specialize in selling test equipment and offering a variety of services to survive the marketplace. They buy, sell, lease sell all kind of new, refurbished,



Fig. 8.21 Type of quality testing equipment

and used equipments. They also buy networking equipment, used test equipment and used measurement equipment from leading manufacturers. Whether end users are any reseller, they offer a cost effective solution that will save time and money.

8.8.2 Procedure of Testing Equipment Development (Example: Solenoid Valve Tester)

Development procedure of testing equipment can be briefly summarized in Fig. 8.22. For example, the test equipment of solenoid valve tester in nuclear power plant will be suggested. The testing equipment would test the intended functionality of product and its reliability.

Step 1 Characteristic Study of Product to be tested

A solenoid valve is operated by an electric current through a solenoid. For more than 440 nuclear power plants in the world, a solenoid valve has equipped nearly every plant. As seen in Fig. 8.23, nuclear-qualified and critical solenoid valves have the following applications:

- Emergency core cooling systems
- Emergency generator systems
- Steam generator feed-water systems
- Containment sampling systems
- Auxiliary feed-water systems
- Liquid radiation waste systems
- Turbine bypass systems.

Nuclear-qualified solenoid valves are indispensable parts of any nuclear plant safety application. Each has passed the most rigorous testing for nuclear equipment and environmental qualification (EQ). These solenoid valves are produced with a high degree of designed-in quality and proven performance.

Additionally, solenoid valves offers desirable product advantages such as diodes that provide simple surge protection for control, quick-disconnect connectors for increased safety and reduced maintenance, and radiation-resistant elastomers for long life.

In the 1950s solenoid valves were onboard the first nuclear powered submarine, the USS Nautilus. Later, solenoid valves protected the earliest commercial nuclear power plants. In 1978 solenoid valves were among the first and only to be nuclear-qualified to IEEE and RCC-E specifications. Solenoid valves from specialized nuclear line are specifically designed for environments with high radiation, temperature, and seismic requirements.

Consequently, test equipment for a solenoid valve should satisfy the following specifications:

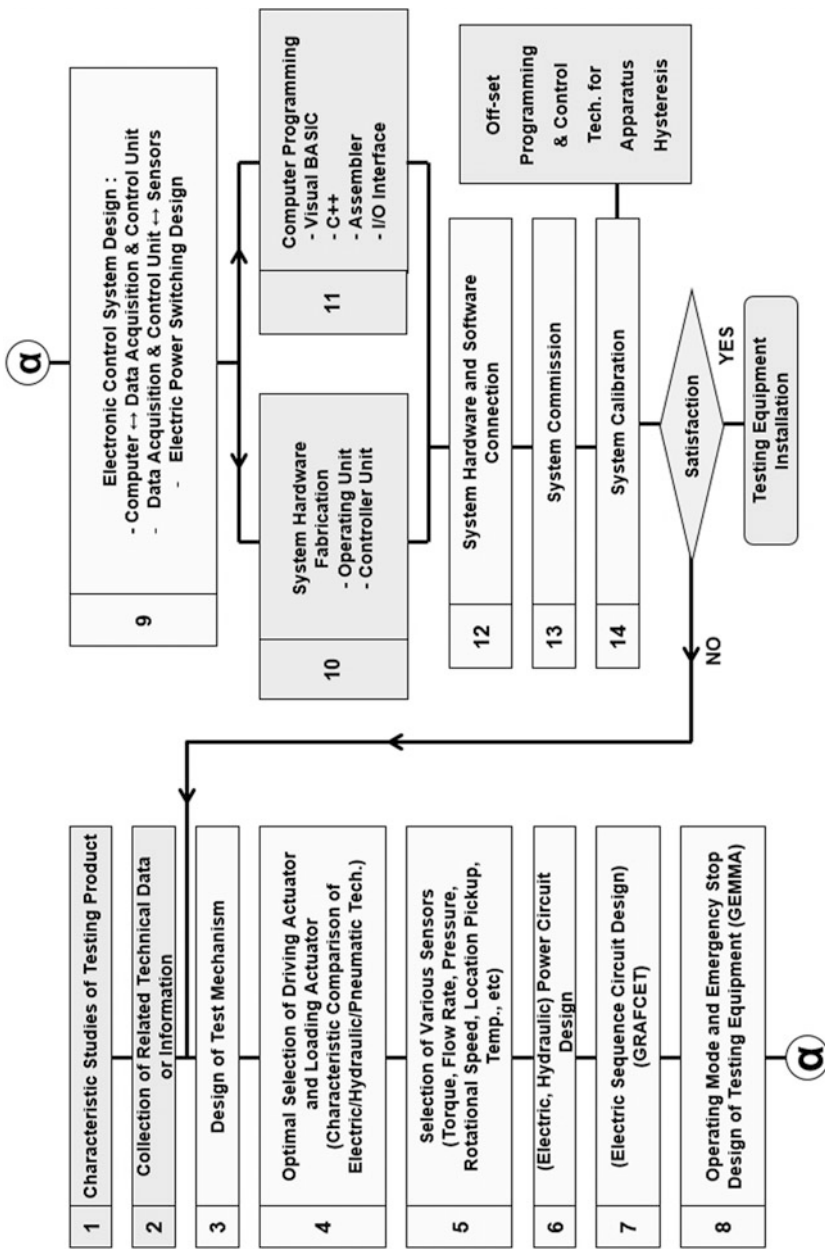


Fig. 8.22 Procedure of testing equipment development

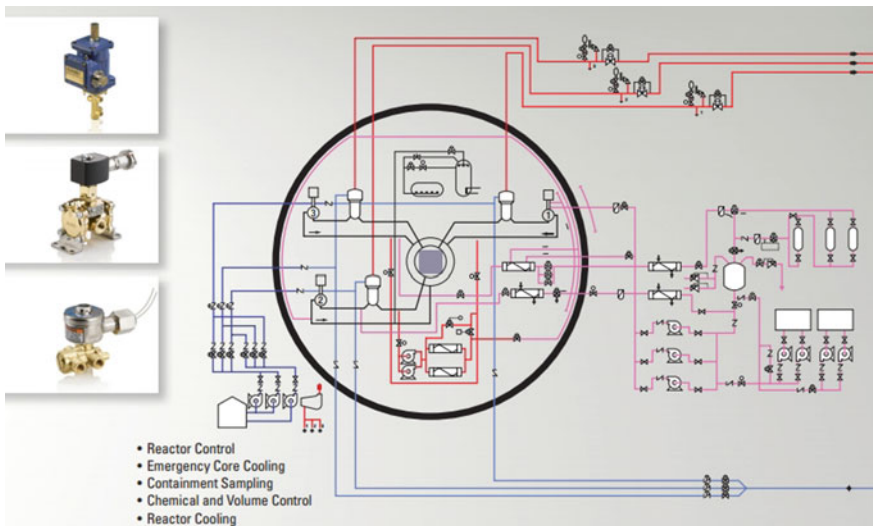


Fig. 8.23 Usage of solenoid valve in nuclear power plant

- ISO 6358: 1989 (E) Pneumatic fluid power—Components using compressible fluids—Determination of flow-rate characteristics
- IEEE-323: 2003—Standard for Qualifying Class 1E Equipment for Nuclear Power Generating Stations

Step 2 Collect Related Technical Information/Data

As seen in Figs. 8.24 and 8.25, nuclear solenoid valves meet the rigorous demands and high expectations of the nuclear industry. They have applications for nuclear qualified 2, 3, and 4-way solenoid valves. Especially, nuclear 2-way valves are qualified for mild environmental applications as defined in IEEE-323-2003. The qualification program consisted of a series of four sequential aging simulation phases (thermal, wear, radiation, and vibration).

- IEEE-323: 2003—Standard for Qualifying Class 1E Equipment for Nuclear Power Generating Stations.

Qualification consists of subjecting solenoid valve to the following tests as required by the previously noted IEEE-323 specifications.

- A. Thermal aging
- B. Wear aging
- C. Pressurization aging
- D. Radiation aging
- E. Vibration aging



Fig. 8.24 Type of solenoid valve for nuclear power plant

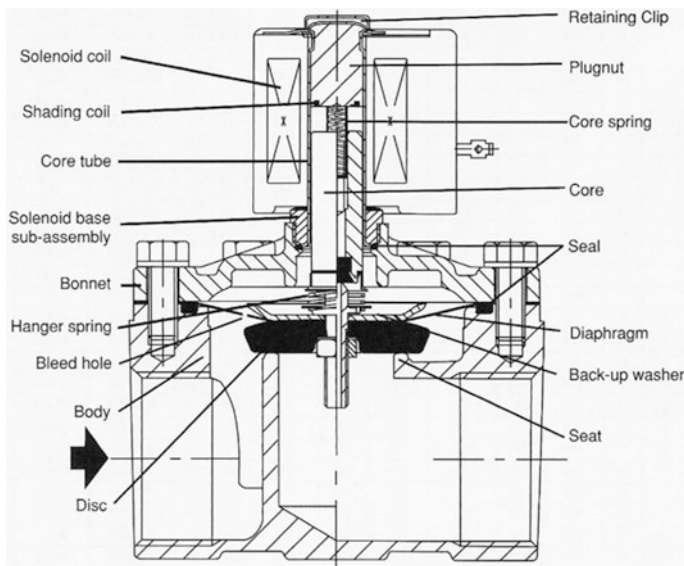


Fig. 8.25 Structure of solenoid valve for nuclear power plant

- F. Seismic event simulation
- G. Radiation event simulation
- H. LOCA/MSLB/HELB environmental simulation

All solenoid valves are designed with the following special features:

1. Type N Construction (NS Series), Class H (NP Series) coil insulation.
2. Elastomers (gaskets, O-rings, discs): all materials designed to meet high radiation and high temperature degradation effects.
3. Specially designed solenoid enclosures to withstand Loss-of-Coolant-Accident (LOCA) environment.
4. Designed to meet seismic loading.

2-way Nuclear Power (NP) solenoid valves are widely used for pilot control of diaphragm and cylinder actuated valves (and other applications) used in nuclear power plants. Selection of the proper valve for a specific application is of paramount importance. This engineering information section describes principles of operation, types of solenoid valves, and types of solenoid enclosures, and materials to assist you in the proper selection of a valve.

A nuclear solenoid valve is a combination of two basic functional units: (1) a solenoid, consisting of a coil and a magnetic plunger (or core); and (2) a valve body containing an orifice in which a disc is positioned to stop or allow flow. The valve is opened or closed by movement of the magnetic plunger (or core), which is drawn into the solenoid when the coil is energized. Solenoid valves feature a pack less construction. The solenoid is mounted directly on the valve and the core assembly is enclosed in a sealed tube inside the solenoid coil. This construction provides a compact, leak-tight assembly, without the need of a stuffing box or sliding stem seal.

Direct-acting solenoid valves operate from zero kPa (no minimum pressure is required for the valve to operate), to the individual valve's maximum rated pressure. Because of the wide range of sizes, construction materials, and pressures, direct-acting qualified valves in brass or stainless steel are found to the many applications found in nuclear power plants. Two 2-way direct acting types are available as follows: normally Closed: closed when de-energized and open when energized. Normally Open: open when de-energized and closed when energized.

Step 3 Design of Test Mechanism

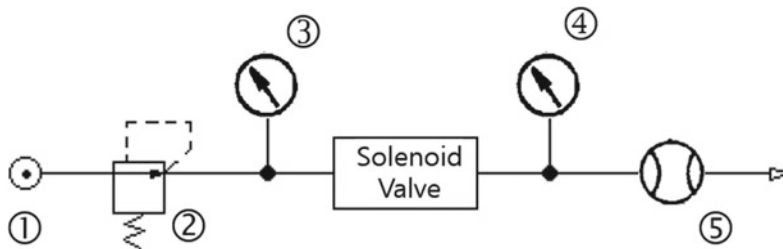
Method to determinate flow rate characteristic of the solenoid valve is based on increasing upstream pressure while the pressurized air goes through a mass flow sensor. The method of standard ISO 6358 is explained to two equations which describe the flow rate through the orifices.

$$q_m = C p_1 \rho_0 \sqrt{\frac{T_0}{T_1}} \quad \text{for} \quad \frac{p_2}{p_1} \leq b \quad \text{choked flow} \quad (8.43)$$

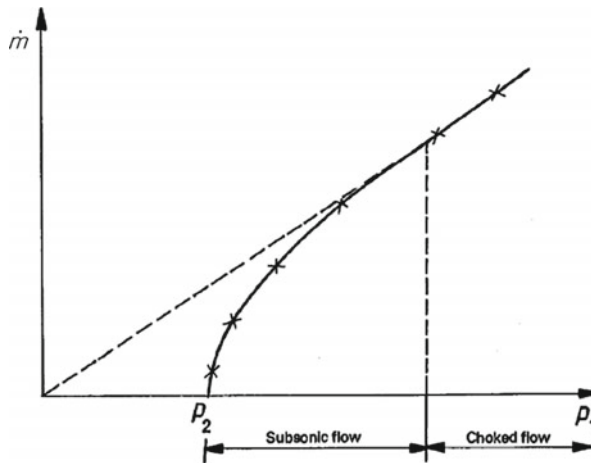
$$q_m = Cp_1 \rho_0 \sqrt{\frac{T_0}{T_1}} \sqrt{1 - \left(\frac{p_2 - b}{1 - b} \right)^2} \quad \text{for } \frac{p_2}{p_1} > b \quad \text{subsonic flow} \quad (8.44)$$

Custom equipment was manufactured for measuring the flow rate characteristics based on “increasing the upstream pressure”. Part of the valve holding the valve nozzle was replaced with the special equipment. With this setup it was possible to set the nozzle to a required fixed position. Without modifications this could not be done.

Figure 8.26a shows the measuring station which was used for measurement and Fig. 8.26b shows the curvature of dependence flow rate on the upstream pressure. This method has been applied only on solenoid valve because preparing special



(a) Schematic of measuring the flow characteristics of solenoid valve
(1-pressurized air source, 2 - pressure regulator, 3/4 - pressure sensor,
5 - flow meter)



(b) Dependence flow rate on the upstream pressure.

Fig. 8.26 Measuring flow rate characteristic by increasing upstream pressure

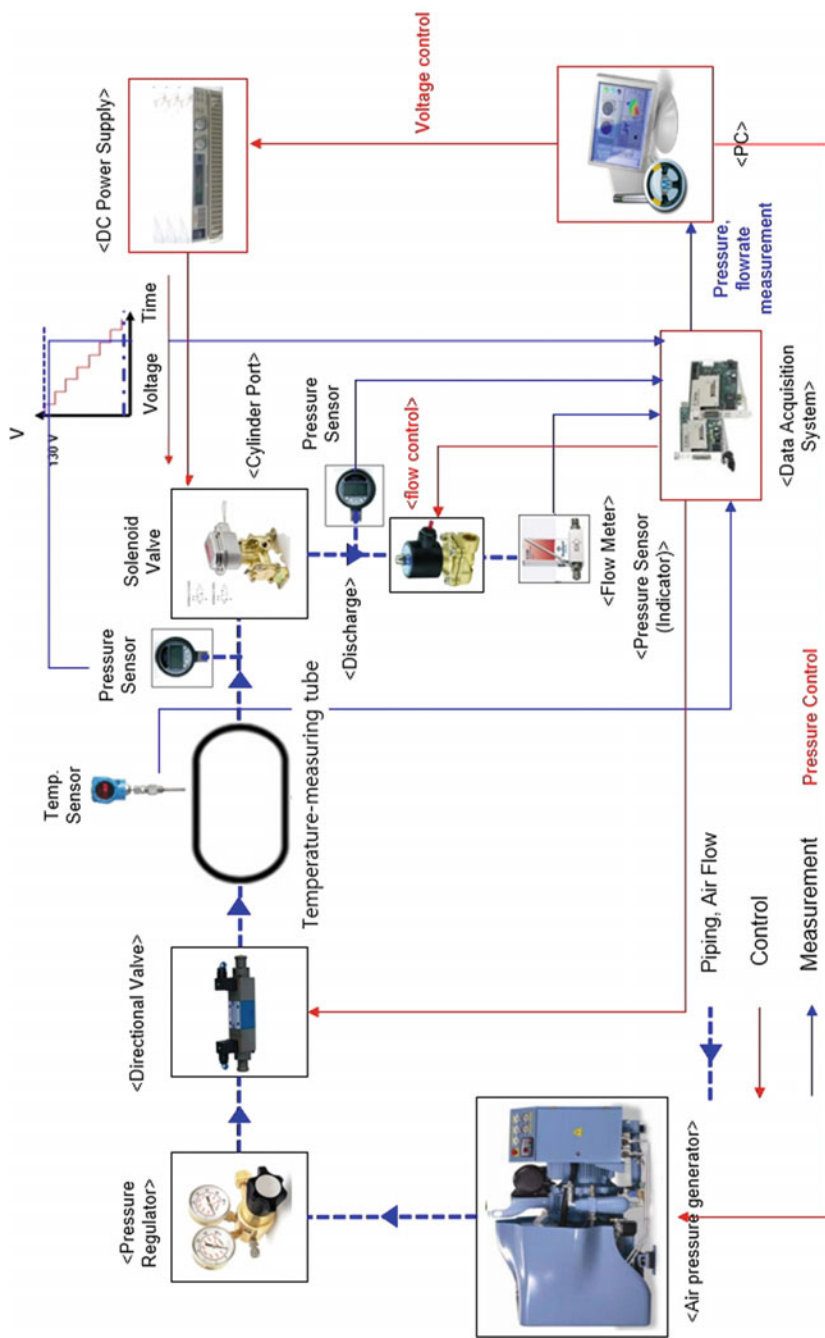


Fig. 8.27 Schematic control diagram of measuring flow rate characteristics of solenoid valve

equipment for holding the nozzle in a constant position is very expensive and work intensive.

Step 4–13 Making the solenoid testing equipment

These steps consist of optimal setting of driving actuator and loading actuator, selection of various sensors, design power (electric/hydraulic) circuit, design sequence circuit, design operating mode, design automatic stop mode, electronic control system design, computer \leftrightarrow DAQ & control unit, DAQ & control unit \leftrightarrow sensor, electric power switching circuit design, fabrication of system hardware, fabrication of operating unit, fabrication of controller, computer programming by LabVIEW and MATLAB, and combine system hardware and software (see Figs. 8.27, 8.28 and 8.29).

For creating a simulation of pneumatic fluid power—determination of flow-rate characteristics of solenoid valve using compressible fluids, MATLAB® Simulink may be used. It makes possible to compare a lot of measured data with mathematical models, which was a great contribution to the work. Measurements made with the two valves were compared to theoretical values.

Figure 8.30 shows two Simulink models created to determine sonic conductance C and the critical pressure ratio b from the measured data. The flow rate characteristic was measured by increasing upstream pressure as depicted in Fig. 8.31.

Step 14–15 System simulation, test run and calibration

The result is shown in Fig. 8.32 Measured data are represented as circles. Line curvature represents theoretical approximation obtained as a numerical solution searching sonic conductance C and the critical pressure ratio b. The results are $C = 6.329 \times 10^{-9} \text{ m}^3/(\text{s*Pa})$, $b = -0.1527$, which can be obtained from MATLAB® and indicates the solenoid valve characteristics. And this method might

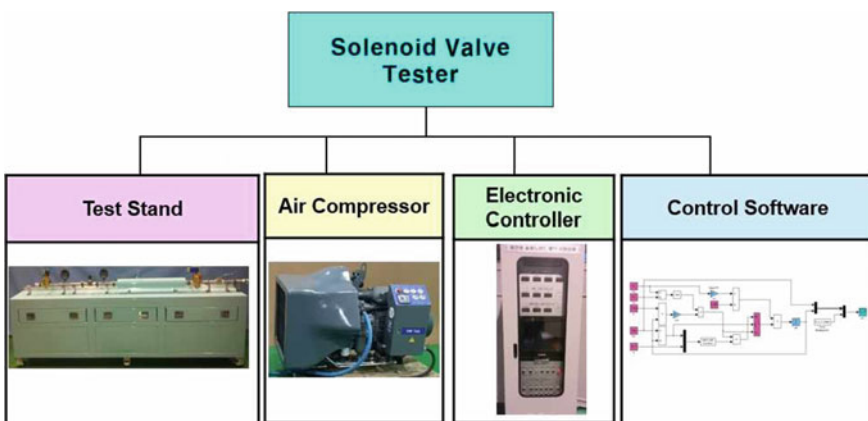


Fig. 8.28 Solenoid valve tester

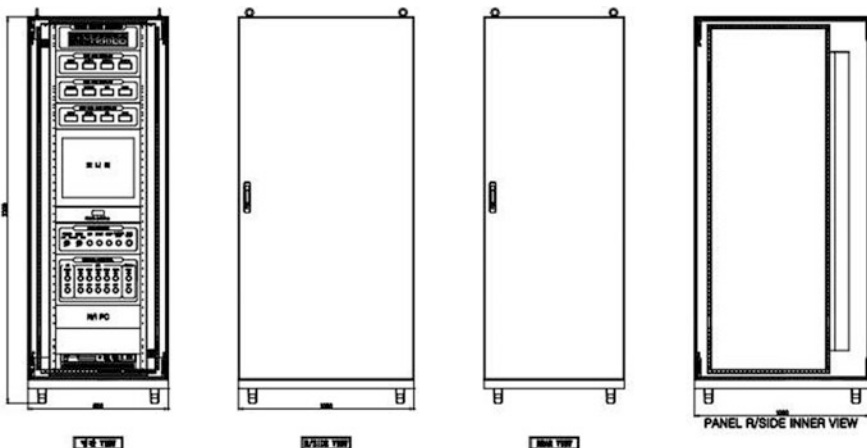


Fig. 8.29 Appearance of electronic controller

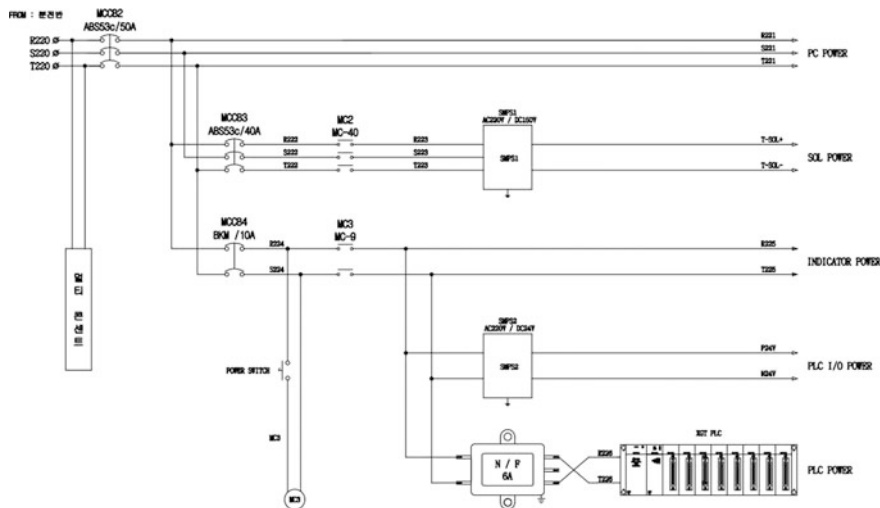


Fig. 8.30 Electrical power connection (example)

be applied only on solenoid valve because preparation of the special equipment for holding the nozzle in constant position is very expensive and work intensive.

Values of critical pressure ratio b for each final pressure in the tank were determined based on knowledge that the linear part of the curvature of the charge is described by Eq. (8.1) and the behaviors of flow rate in the second part of the curvature is described by Eq. (8.2). Of note is that the critical pressure ratio b

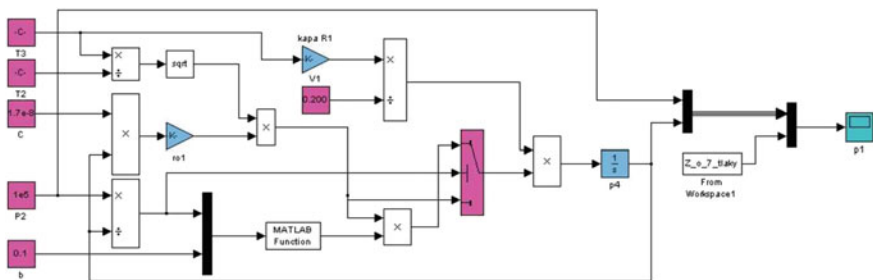


Fig. 8.31 Simulation schematic of a tank charge in MATLAB[®] Simulink

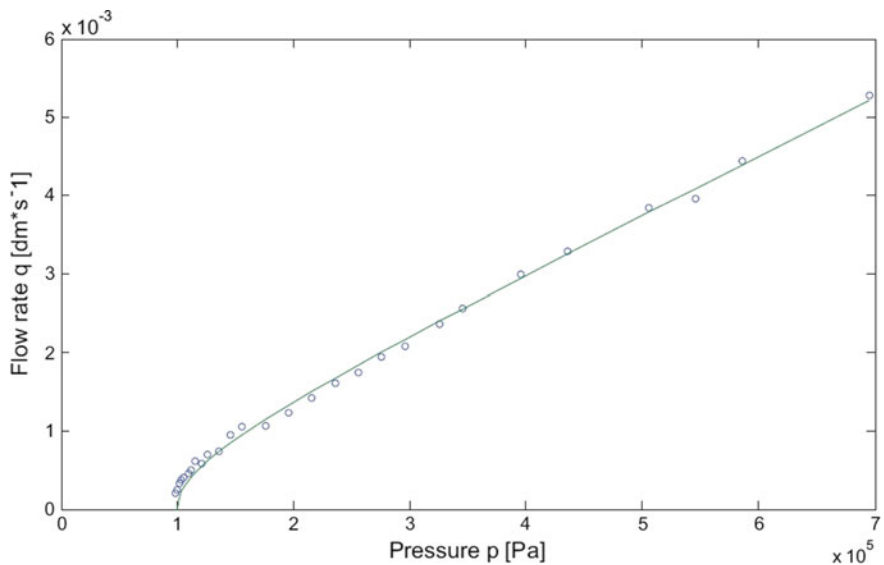


Fig. 8.32 Dependence of flow rate to the upstream pressure—data from the ISO 6358 method measurement

expresses the divide of the downstream and the upstream pressure which flow becomes choked.

For determination of the critical pressure ratio a derivative of smoothed measured data was made, and the point where the derivative exchanges determines the mentioned critical pressure ratio. The values of sonic conductance C were determined from the equation which describes the flow rate through the orifices for subsonic flow.

References

1. 1990 IEEE Standard Glossary of Software Engineering Terminology. IEEE STD 610.12-1990. Standards Coordinating Committee of the Computer Society of IEEE, New York
2. Kreyszig E (2006) Advanced engineering mathematics, 9th edn. John Wiley and Son, NJ, p 683
3. Taguchi G (1978) Off-line and on-line quality control systems. In: Proceedings of the international conference on quality control Tokyo, Japan
4. Taguchi G, Shih-Chung T (1992) Introduction to quality engineering: bringing quality engineering upstream. ASME, New York
5. Ashley S (1992) Applying Taguchi's quality engineering to technology development. Mechanical Engineering
6. Wilkins J (2000) Putting Taguchi methods to work to solve design flaws. Qual Prog 33(5):55–59
7. Phadke MS (1989) Quality engineering using robust design. Prentice Hall, NJ
8. Byrne D, Taguchi S (1987) Taguchi approach to parameter design. Qual Prog 20(12):19–26
9. Woo S, Pecht M (2008) Failure analysis and redesign of a helix upper dispenser. Eng Fail Anal 15(4):642–653
10. Woo S, O'Neal D, Pecht M (2009) Improving the reliability of a water dispenser lever in a refrigerator subjected to repetitive stresses. Eng Fail Anal 16(5):1597–1606
11. Woo S, O'Neal D, Pecht M (2009) Design of a hinge kit system in a kimchi refrigerator receiving repetitive stresses. Eng Fail Anal 16(5):1655–1665
12. Woo S, Ryu D, Pecht M (2009) Design evaluation of a French refrigerator drawer system subjected to repeated food storage loads. Eng Fail Anal 16(7):2224–2234
13. Woo S, O'Neal D, Pecht M (2010) failure analysis and redesign of the evaporator tubing in a Kimchi refrigerator. Eng Fail Anal 17(2):369–379
14. Woo S, O'Neal D, Pecht M (2010) Reliability design of a reciprocating compressor suction reed valve in a common refrigerator subjected to repetitive pressure loads. Eng Fail Anal 7 (4):979–991
15. Woo S, Pecht M, O'Neal D (2009) Reliability design and case study of a refrigerator compressor subjected to repetitive loads. Int J Refrig 32(3):478–486
16. Woo S, O'Neal D, Pecht M (2011) Reliability design of residential sized refrigerators subjected to repetitive random vibration loads during rail transport. Eng Fail Anal 18 (5):1322–1332
17. Woo S, Park J, Pecht M (2011) Reliability design and case study of refrigerator parts subjected to repetitive loads under consumer usage conditions. Eng Fail Anal 18(7):1818–1830
18. Woo S, Park J, Yoon J, Jeon H (2012) The reliability design and its direct effect on the energy efficiency. energy efficiency—the innovative ways for smart energy, the future towards modern utilities. InTech: Chapter 11
19. Woo S (2015) The reliability design of mechanical system and its Parametric ALT. In: Handbook of materials failure analysis with case studies from the chemicals, concrete and power industries. Elsevier: Chapter 11, pp 259–276
20. Woo S, O'Neal D (2016) Improving the Reliability of a domestic refrigerator compressor subjected to repetitive loading. Engineering 8:99–115
21. Woo S, O'Neal D (2016) Reliability design of the hinge kit system subjected to repetitive loading in a commercial refrigerator. Challenge J Struct Mech 2(2):75–84
22. McPherson J (1989) Accelerated testing. packaging, vol 1. Electronic Materials Handbook ASM International, pp 887–894
23. Karnopp DC, Margolis DL, Rosenberg RC (2012) System dynamics: modeling, simulation, and control of mechatronic systems, 5th edn. John Wiley & Sons, New York
24. Ajiki T, Sugimoto M, Higuchi H (1979) A new cyclic biased THB power dissipating ICs. In: Proceedings of the 17th International Reliability Physics Symposium, San Diego, CA

25. Ryu D, Chang S (2005) Novel concept for reliability technology. *Microelectron Reliab* 45 (3):611–622
26. Wasserman G (2003) Reliability verification, testing, and analysis in engineering design. Marcel Dekker, p 228
27. Deming WE (1950) Elementary principles of the statistical control of quality. Japan: JUSE
28. CMMI Product Team (2002) Capability maturity model integration (CMMI) Version 1.1, continuous representation. Report CMU/SEI-2002-TR-011, Software Engineering Institute Pittsburgh PA: Software Engineering
29. NASA (2007) System engineering handbook. NASA Headquarters, Washington, p 92. (NASA/SP-2007-6105 Rev 1)
30. O'Connor P (2002) Practical reliability engineering. Wiley, New York, p 159

Chapter 9

Parametric ALT and Its Case Studies



Abstract Final mechanical products through design process are designed to have no enough strength and stiffness in product lifetime. Even though properly designed, mechanical products have faulty designs. By parametric ALT, engineer might find and correct them. At that time it is important to have deep insights how to apply the reliability testing. In this chapter, parametric ALT and its case studies will be applicable to a variety of mechanical product—automobile, construction equipment, appliance, airplane, and the others. Parametric ALT is a kind of methodology to confirm if mechanical products in the reliability-embedded design process satisfy the reliability target. The parametric ALT has the following procedure: (1) setting reliability target, (2) determining the accelerated factor, (3) if sample size is given, the parametric ALT will be carried out to the testing time required to meet the reliability target (or its specification). By identifying the faulty designs and modify them, new product will confirm if the reliability target achieves.

Keywords Parametric ALT · Case studies · Mechanical engineering system

9.1 Failure Analysis and Redesign of Ice-Maker

The basic function of a refrigerator is to store fresh and/or frozen foods. Now refrigerators become to provide other functions—dispensing ice and water. As the functions of refrigerator and its parts increase, market pressure for product cost reduction leads to the use of cheaper parts. Refrigerator functions are consistently reliable during customer usage. The refrigerator can be designed for reliability by determining proper parameters and their levels of its parts.

However, minor design parameters may be neglected in the design review, resulting in product failure in use. Products with minor design flaws may result in recalls and loss of brand name value. Furthermore, product liability law requires manufacturers to design products more safely in the European Union and the United States. Preventing such outcomes is a major objective of the product development process—design, production, shipping, and field testing.

Conventional methods, such as product inspection, rarely identify the reliability problems occurring in market use. Instead, optimally designing for reliability requires the extensive testing at each development step. As a result, the cost of quality assurance and appraisal can increase significantly. As a solution, most global companies focus on accelerating life testing (ALT). ALT can help shorten the product development cycles and identify diverse design flaws. ALT should be performed with sufficient samples and testing time, with equipment designed to match expected product loads.

Figure 9.1 shows the SBS refrigerator with ice dispenser and the mechanical parts of the ice bucket assembly. The assembly consists of the bucket case, helix support, helix dispenser clamp, blade dispenser, helix upper dispenser, and blade, as shown in Fig. 9.1b. The helix upper dispenser in the ice bucket of refrigerators with ice dispenser systems has been fracturing in field, causing loss of the dispensing function (see Figs. 9.2 and 9.3). Thus reproducing the failure mode to assess how to prevent the fracture of the helix upper dispenser was critical. The data on failed products in the market place are important to understand the use environment of customer of the product and helping to pinpoint root causes.

Field data indicated that the damaged products may have two structural design flaws: (1) a 2 mm gap between the blade dispenser and the helix upper dispenser, and (2) a weld line around the impact area of the helix upper dispenser. Due to the

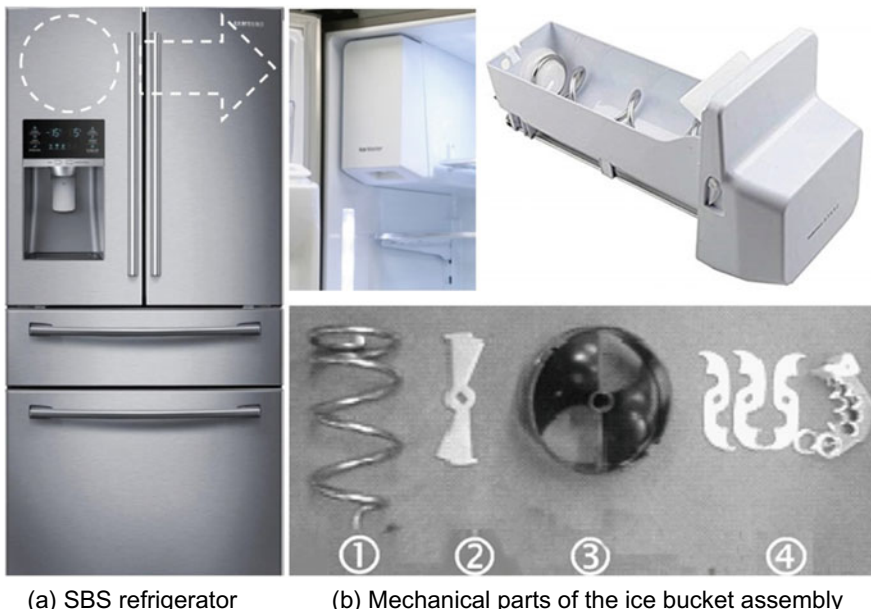


Fig. 9.1 SBS refrigerator and ice bucket assembly

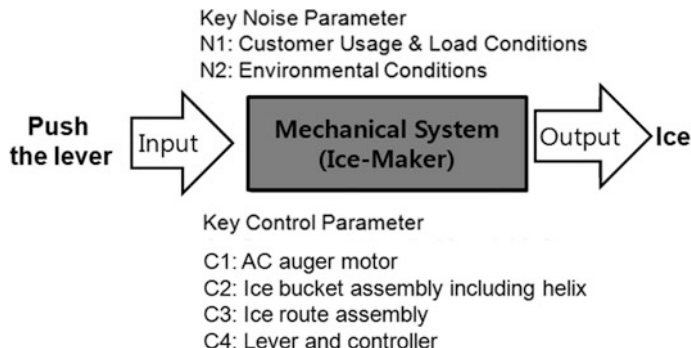


Fig. 9.2 Robust design schematic of ice-maker

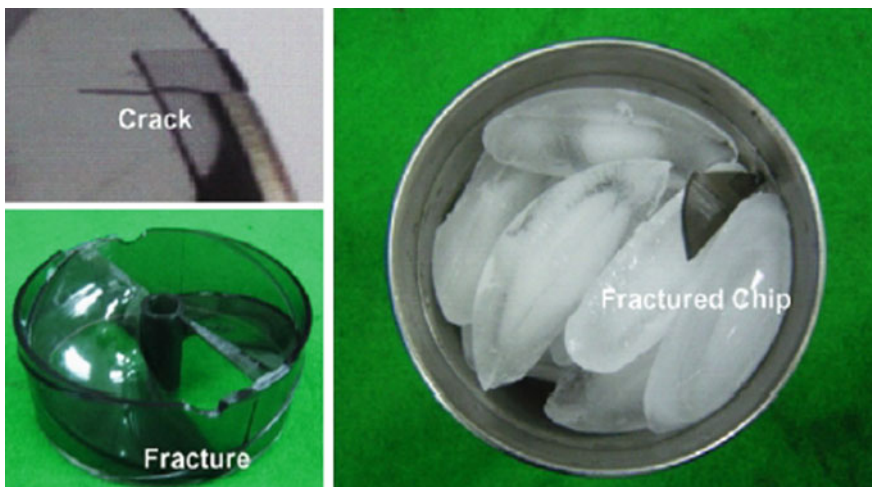


Fig. 9.3 A damaged product after use

gap, the rotating blade dispenser impacts the fixed helix upper dispenser. Because of the weld line, a crack may occur. The temperature of the product was below -20°C .

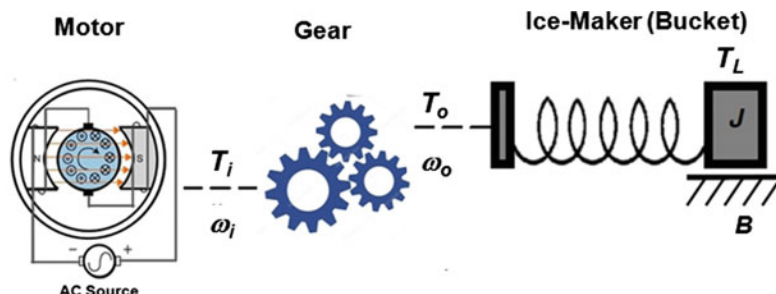
If repetitive loads are applied to the product structure and there are the design faults, the structure will fail before its desired lifetime. Therefore, an ice-maker's actual lifetime depended on faulty parts like the helix upper dispenser. To reproduce and correct the part(s), an engineer was required to conduct reliability testing like parametric ALT for a new design. The process consisted of (1) a load analysis for returned product, (2) utilizing parametric ALTs with action plans, and (3) verifying if reliability target of final designs are achieving.

Ice-making involves several repetitive mechanical processes: (1) the filtered water supplies the tray; (2) water freezes into ice by the cold air in the heat exchanger; (3) the ice is harvested until the bucket is full. When the customer

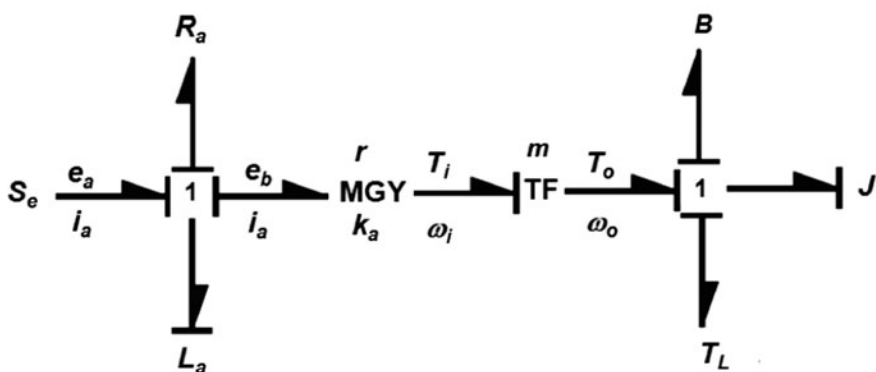
pushes the lever by force, cubed or crushed ice is then dispensed. In this ice-making process the ice-maker parts receive a variety of mechanical loads.

In the United States, refrigerators are designed to produce 10 cubes per use and up to 200 cubes a day. Because the ice-maker system is repetitively used in both cubed and crushed ice modes, it is continuously subjected to mechanical loads. Ice production also may be influenced by customer usage conditions such as water pressure, ice consumption, refrigerator notch settings, and the number of times the door is opened.

Figure 9.4 provides an overview of the schematic of an ice-maker (or its mechanism). It represents the mechanical load transfer in the ice bucket assembly using a bond graph model. To generate enough torque to crush the ice, an AC motor provides power through the gear system which is then transferred to the ice bucket assembly. Through the helix blade dispenser and the upper dispenser in the bucket, the ice is distributed by the blade. If subjected to different loads, the ice can also be crushed.



(a) Schematic diagram of auger motor and ice bucket assembly.



(b) Bond graph modeling of auger motor and ice bucket assembly

Fig. 9.4 Design concept of ice-maker

As seen in Fig. 9.4, the bond graph can be conventional in state space representation to group terms by state variables. The modeling of ice bucket assembly can be expressed as

$$\begin{bmatrix} di_a/dt \\ d\omega/dt \end{bmatrix} = \begin{bmatrix} -R_a/L_a & 0 \\ mk_a & -B/J \end{bmatrix} + \begin{bmatrix} i_a \\ \omega \end{bmatrix} + \begin{bmatrix} 1/L_a \\ 0 \end{bmatrix} e_a + \begin{bmatrix} 1 \\ -1/J \end{bmatrix} T_L \quad (9.1)$$

The mechanical stress (or life) of the ice bucket assembly depends on the disturbance load T_L in Eq. (9.1). The accelerated life testing applies the breakdown stress between low and high level to the helix upper dispenser. Because the stress depends on applied stress, the life-stress model (LS model) can be modified as

$$TF = A(S)^{-n} = A(T_L)^{-\lambda} \quad (9.2)$$

The acceleration factor (AF) can be derived as

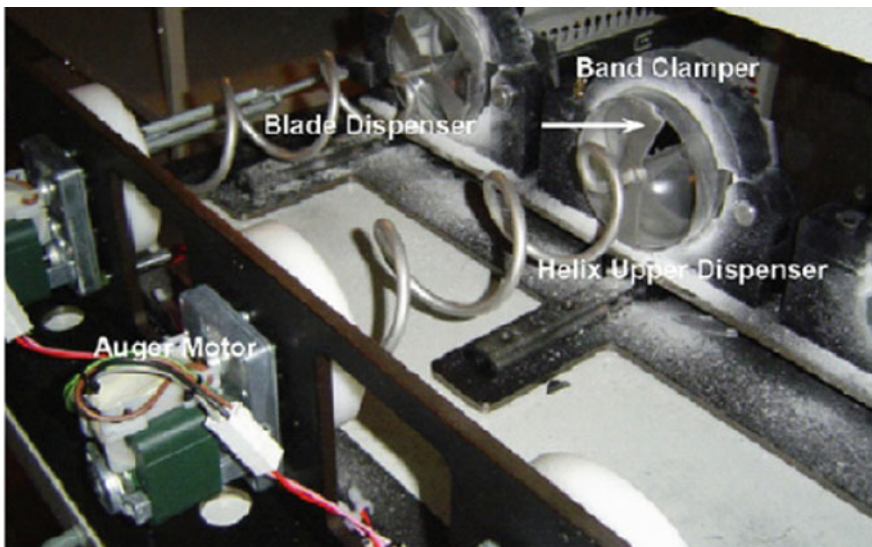
$$AF = \left(\frac{S_1}{S_0}\right)^n = \left(\frac{T_1}{T_0}\right)^{\lambda} \quad (9.3)$$

The ice dispenser of customer is used an average of approximately 3–18 times per day. Under maximum use for 10 years, the dispenser incurs about 65,700 usage cycles. Data from the motor company specifies that normal torque is 0.69 kN cm and maximum torque is 1.47 kN cm. Assuming the quotient $\lambda = 2$, the acceleration factor is approximately 5 in Eq. (9.3).

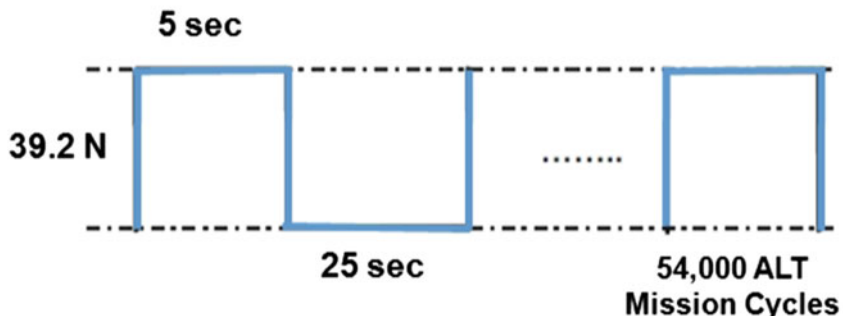
Supposed test sample numbers are 10 pieces and shape parameter β is 2, the test cycles calculated in Eq. (8.35) were 42,000 cycles, respectively. The parametric ALT was designed to ensure a B1 of 10 years life with about a 60% level of confidence that it would fail less than once during 42,000 cycles.

Figure 9.5 shows the ALT equipment for the reproduction of the failed structural parts in the field and the duty cycles for the disturbance load T_D . The equipment in the chamber was designed to operate to about -30°C of temperature. The controller outside can start or stop the equipment and indicate the completed test cycles, and the test periods, such as sample on/off time. To apply the maximum disturbance torque T_{Pulse} , two parts—the helix upper dispenser and the band clamer—were bolted together. When the controller outside the chamber gives the start signal, the auger motor rotates the clamp helix dispenser, the helix upper dispenser and the blade dispenser. At this point, the rotating blade dispenser will impact the fixed helix upper dispenser to the maximum mechanical disturbance torque (1.47 kN cm).

Figure 9.6 shows the failed product in the field and a sample after accelerated life testing. In the photo, the shape and location of the broken pieces in the failed market product are identical to those in the ALT results. Figure 9.7 represents the graphical analysis of the ALT results and field data on a Weibull plot. For the shape parameter, the estimated value in the first ALT is 2.0. However, the final value obtained on the Weibull plot was 4.8.



(a) Equipment used in accelerated life testing



(b) Duty cycles

Fig. 9.5 Equipment used in accelerated life testing and duty cycles of disturbance load T_{Pulse}

These methodologies are valid to reproduce the field failures because (1) the location and shape of the fractures in both market and ALT results are similar; and (2) on the Weibull, the shape parameters of the ALT results, β_1 and market data, β_2 , are very similar. The calculated reduction factor R also is 0.001 from the experiment data—product lifetime, acceleration factor, actual mission cycles, and shape parameter. Consequently, we know that this parameter ALT is effective to save the testing time and sample size.

The fracturing and cracking of both the fielded products and the ALT results occur in the contact area of the blade dispenser. These structural flaws generate the concentrated mechanical stress when the blade dispenser, made of stainless steel, hits the polycarbonate helix upper dispenser at a right angle. Due to the 2 mm gap

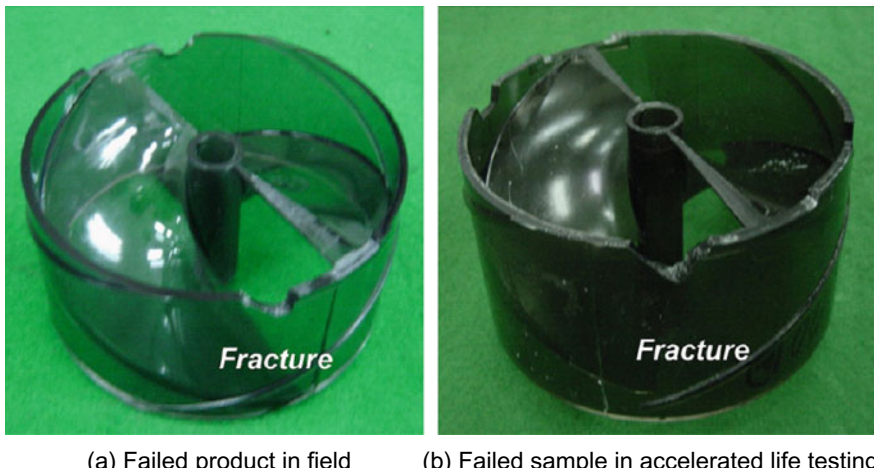


Fig. 9.6 Failed product in field and ALT

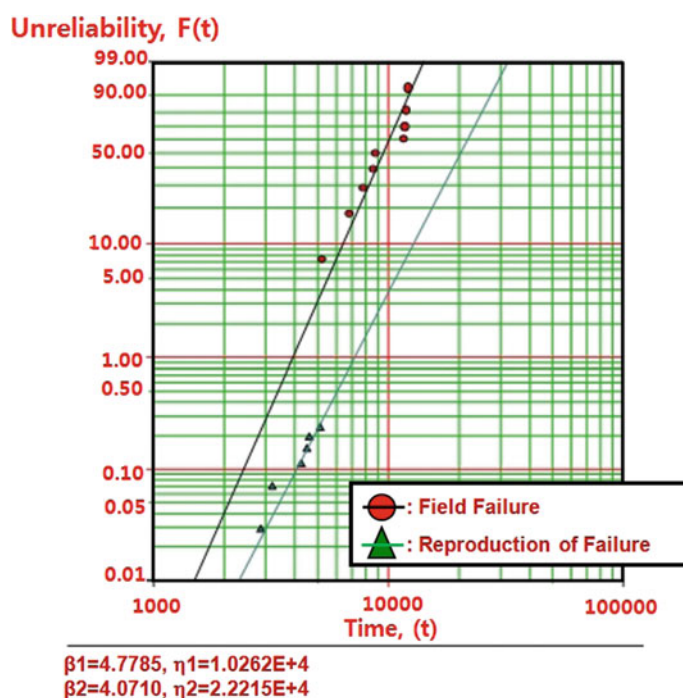


Fig. 9.7 Field data and results of ALT on Weibull chart

between the blade dispenser and helix upper dispenser and the impact (1.47 kN cm) of the blade dispenser, it is particularly fragile due to the weld line near the impact area of the helix upper dispenser under -20°C (Fig. 9.8).

Failure analysis identified the root cause of the failed product as the 2 mm gap between the blade dispenser and the helix upper dispenser, and the weld line. To improve the reliability of the newly designed helix upper dispenser, a second ALT was implemented with a key controllable design improvement—no gap in the samples. Based on the first ALT, the AF and β values in the second ALT were 2.2 and 4.8. The test cycles and test sample number calculated in Eq. (8.35) were 54,000 cycles and 6 pieces respectively. For the second ALT, all samples were failed at 17,000, 25,000, 28,200, and 38,000 cycles. In the second ALT results the failed test samples were still found in mission test cycles.

For the failed samples, the design improvement in the third ALT was to add ribs on the side and front of the impact area. These redesigned samples were implemented for the third ALT. Supposed test sample numbers are 6 pieces and shape parameter β is 4.8, the test cycles and test sample calculated in Eq. (8.35) were 54,000 cycles, respectively. The ALT was designed to ensure a B1 of 10 years life with about a 60% level of confidence that it would fail less than once during 54,000 cycles. In the third ALT results, the samples did not crack and fracture until 75,000 cycles of testing. Consequently, the improved helix upper dispenser will meet the reliability target—B1 life 10 years.

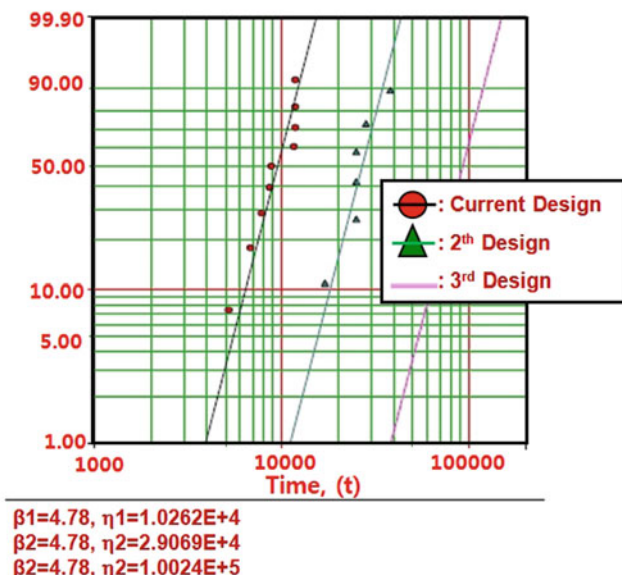
Table 9.1 shows the results obtained from the third ALT. The B1 life of the redesigned samples was 14 years. When the design of the current product was compared with that of the newly designed one, the B1 life expanded about fourteen times, from 1.4 to 14 years. The design improvements of eliminating the gap and reinforcing the ribs were very effective in enhancing the reliability of the samples (see Fig. 9.9).



Fig. 9.8 Structure of helix upper dispenser

Table 9.1 Results of ALT

	1st ALT	2nd ALT	3rd ALT
	Initial design	Second design	Final design
In 54,000 cycles, no crack and fracture of helix	170 cycles: 1/10 (10%) 5200 cycles: 1/10 (20%) 7880 cycles: 2/10 (40%) 8800 cycles: 2/10 (60%) 11,600 cycles: 4/10 (100%)	17,000 cycles: 1/6 (17%) 25,000 cycles: 3/6 (67%) 28,200 cycles: 1/6 (83%) 38,000 cycles: 1/6 (100%)	54,000 cycles: OK Max 75,000 cycles: OK
Helix upper dispenser structure			
Material and specification	PC + SUS ($t = 1.2$) Gap C1: 2 mm → 0 mm	Roundness corner of torsional shaft C2: R0.5 mm → R2.0 mm	PC + SUS ($t = 1.2$) Gap: 0 mm Added rib on side and front of helix

Unreliability, $F(t)$ **Fig. 9.9** Result of ALT plotted in Weibull chart

9.2 Residential Sized Refrigerators During Transportation

Figure 9.10 shows a typical residential sized French door refrigerator and the mechanical compartment at the bottom rear of the refrigerator. As refrigerators were transported to the final destinations by rail, they were subjected to random vibrations from the bottom. These vibrations were continually transmitted to the refrigerator (or machine compartment) while train was moving. The compressor rubber mounts were tearing and the connecting tubes in the mechanical compartments of refrigerators were fracturing. Because the tubes were fracturing, refrigerant was leaking out of the tubes, which resulted in the refrigerator losing its ability to either cool or freeze products. Field data indicated that the damaged products might have had design flaws. The design flaws combined with the repetitive random loads in transportation could cause failure.

Based on the field data, the rail transportation was expected to move a refrigerator 7200 km from Los Angeles to Boston in 7 days (L_B^*). For its machine compartment (or module), B_1 life should be kept for the transported distance (see Fig. 9.11).

A random vibration in refrigeration system is motion which is non-deterministic. The random vibrations in field are that the higher amplitude is the smaller frequency. On the other hands, the lower amplitude is the larger frequency. It follows the normal distribution. Refrigerator is subjected to ride on a rough road or rail, wave height on the water. A measurement of the acceleration spectral density is the usual way to specify random vibration. As seen in Fig. 9.12, a refrigerator subjected to base is random vibrations and their power spectral density.

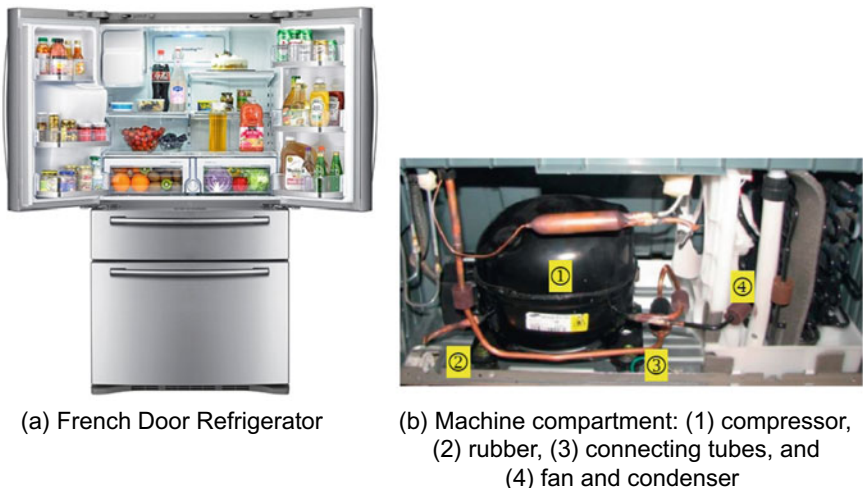
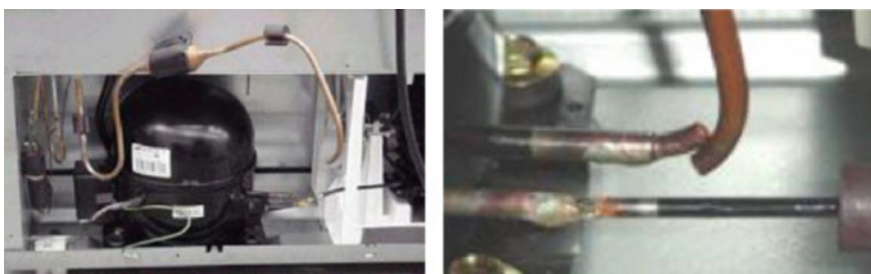
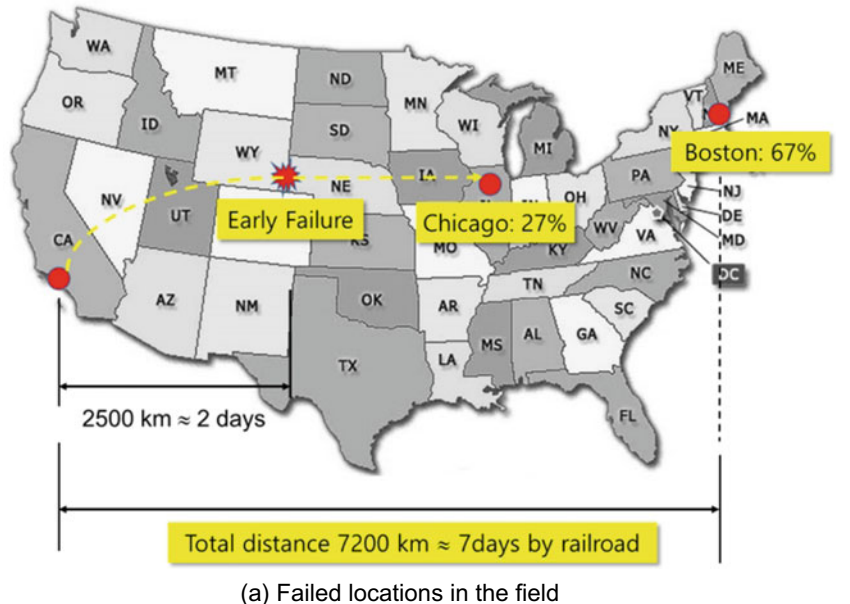


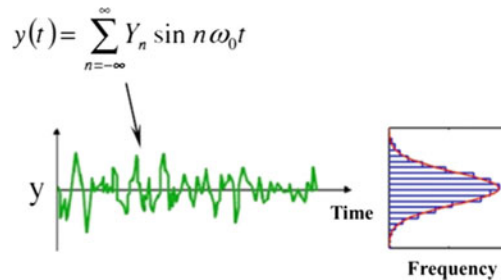
Fig. 9.10 French door refrigerator and machine compartment (or module)



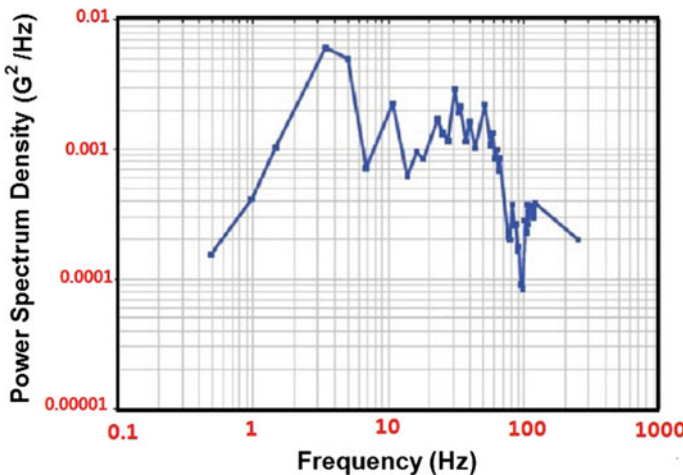
(b) Failed connecting tubes in the mechanical compartment

Fig. 9.11 Fracture of the refrigerator connecting tubes in the field

To evaluate the ride quality of product and its mechanism mounted on vehicle like train or automobile, the most useful mathematical model of a vehicle suspension system is the quarter car model. Though it is two DOF and four state variables, it serves the purpose of figuring out the vehicle motion in transportation. The assumed model of the vehicle consists of the sprung mass and the unsprung mass, respectively. The sprung mass m_s represents 1/4 of the body of the vehicle, and the unsprung mass m_{us} represents one wheel of the vehicle. The main suspension is modeled as a spring k_s and a damper c_s in parallel, which connects the unsprung to the sprung mass. The tire (or rail) is modeled as a spring k_{us} and represents the transfer of the road force to the unsprung mass (see Fig. 9.13).



(a) A refrigerator subjected to base random vibrations



(b) Typical intermodal random vibration in the United States

Fig. 9.12 Refrigerators subjected to base random vibrations and their power spectral density

The governing differential equations of motion for the quarter car model can be represented as:

$$m_s \ddot{x}_s + c_s (\dot{x}_s - \dot{x}_{us}) + k_s (x_s - x_{us}) = 0 \quad (9.4)$$

$$m_{us} \ddot{x}_{us} + c_s (\dot{x}_{us} - \dot{x}_s) + (k_{us} + k_s)x_{us} - k_s x_s = k_{us}y \quad (9.5)$$

So the above equations of motion can be concisely represented as:

$$\begin{bmatrix} m_s & 0 \\ 0 & m_{us} \end{bmatrix} \begin{bmatrix} \ddot{x}_s \\ \ddot{x}_{us} \end{bmatrix} + \begin{bmatrix} c_s & -c_s \\ -c_s & c_s \end{bmatrix} \begin{bmatrix} \dot{x}_s \\ \dot{x}_{us} \end{bmatrix} + \begin{bmatrix} k_s & -k_s \\ -k_s & k_{us} + k_s \end{bmatrix} \begin{bmatrix} x_s \\ x_{us} \end{bmatrix} = \begin{bmatrix} 0 \\ k_{us}y \end{bmatrix} \quad (9.6)$$

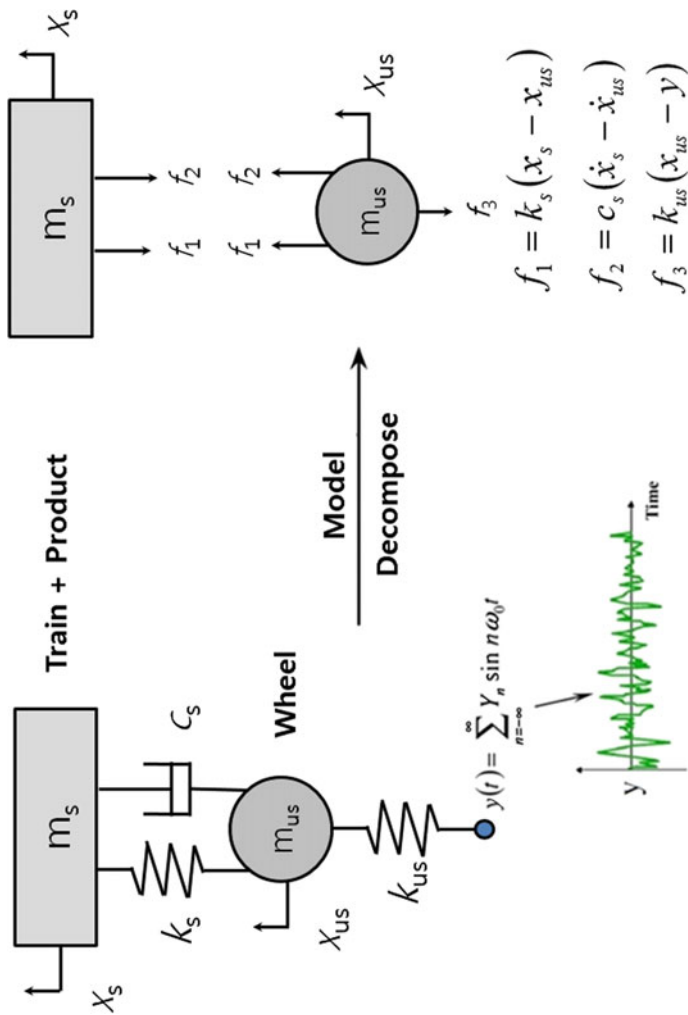


Fig. 9.13 A simplified model of the refrigerator subjected to repetitive random vibrations

As a result, Eq. (9.6) can be expressed in a matrix form

$$[M]\ddot{X} + [C]\dot{X} + [K]X = F \quad (9.7)$$

Because stress depends on the transmitted force, the acceleration factor (AF) can be expressed as the product of the amplitude ratio of acceleration R and force transmissibility Q . That is,

$$AF = \left(\frac{S_1}{S_0}\right)^n = \left(\frac{F_1}{F_0}\right)^\lambda = \left(\frac{a_1 F_T}{a_0 kY}\right)^\lambda = (R \times Q)^\lambda \quad (9.8)$$

Here the force transmitted to the refrigerator can be expressed as force transmissibility Q . That is,

$$Q = \frac{F_T}{kY} = r^2 \left[\frac{1 + (2\zeta r)^2}{(1 - r^2)^2 + (2\zeta r)^2} \right] \quad (9.9)$$

For natural frequency ($r = 1.0$) and small damping ratio ($\zeta = 0.1$), the force transmissibility Q had a value of approximately 5.1 and the amplitude ratio of acceleration R was 4.17. Using a stress dependence of 2.0, the acceleration factor in Eq. (9.9) was found to be approximately 452.0 (Table 9.2).

Suppose that the shape parameter was 6.41 based on field data and the allowed failed numbers r was 0, the test time and the number of samples from Eq. (8.35) would be 40 min and 3 pieces for the first ALT. To meet the reliability target B_1 , there needs to be no fractured sample at the connecting tube of the refrigerator in 40 min that might be the Reliability quantitative (RQ) test specifications (Fig. 9.14).

For the first ALT, the connecting tubes in the mechanical compartments of three samples at 20 min were fracturing and the compressor rubber mounts were tearing during x-axis vibration tests. The estimated lifetime L_{B1} was approximately 3 days and estimated failure rate of the design samples λ was 2.9%/day. The shape and location of the failure in the ALT were similar to those seen in the field. The reduction factor R also is 0.013 from the acceleration factor = 452 and shape parameter = 6.13. Consequently, we know that this parameter ALT is effective to save the testing time and sample size (Fig. 9.15).

Table 9.2 ALT conditions in refrigerator

System conditions	Worst case	ALT	AF
Transmissibility, Q ($r = 1.0, \zeta = 0.1$)	—	5.1 (from Eq. 9.5)	5.1①
Amplitude ratio of acceleration, R (a_1/a_0)	0.24g	1g	4.17②
Total AF (= ① × ②) ²			452

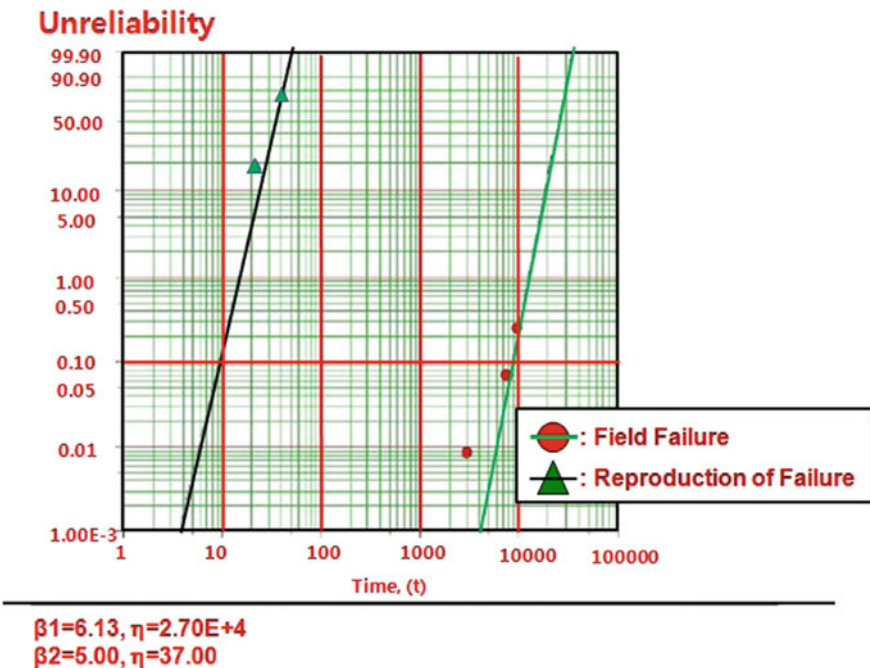


Fig. 9.14 Field data and results of accelerated life test on Weibull chart

The modified design parameters for the compressor compartment (or module) was modified as follows: (1) the shape of compressor rubber mount (C_1 : gap reduction, $1.2 \rightarrow 0.5$ mm), (2) the shape of the connecting tube design (C_2) (Fig. 9.16).

With these modified parameters, a second ALT was carried out and there were no problem at 40 and 60 min. The estimated lifetime L_{B1} was more than 7 days and the estimated failure rate of the design samples λ was less than 0.14%/day. Over the course of the two ALTs, refrigerators with the targeted B_1 life were expected to survive without failure during cross country rail transport in the US. Table 9.3 shows a summary of the results of the ALTs, respectively.

9.3 Water Dispenser Lever in a Refrigerator

Figure 9.17 shows the Bottom Mounted Freezer (BMF) refrigerator with the newly designed water dispenser that consists of the dispenser cover (1), spring (2), and dispenser lever (3). The mechanism is operated: as the consumer presses the lever, the dispenser system will operate and supply water through its line. To properly work this function in product lifetime, the dispenser system needs to robustly be designed to handle the operating conditions subjected to it by the consumers who purchase and use the BMF refrigerator (Figs. 9.17 and 9.18).

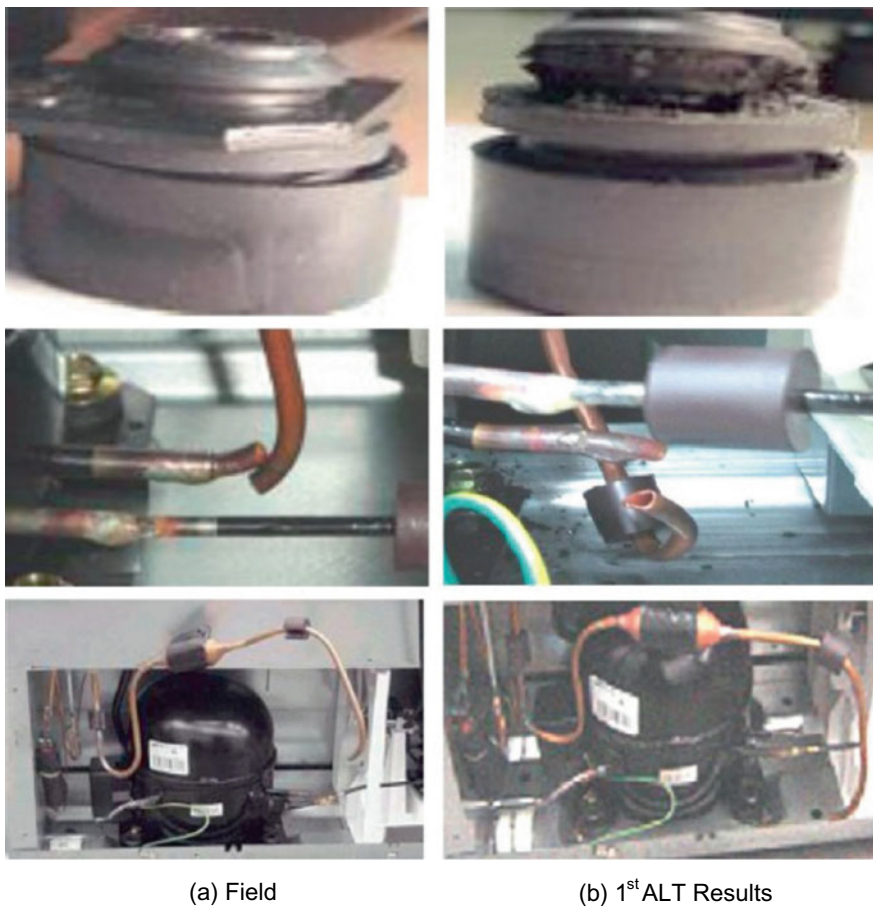


Fig. 9.15 Failure of refrigerator tubes in the field and 1st ALT result

In the field, the dispenser lever in the refrigerators had been fracturing, causing loss of the dispensing function. The field data on the failed products were important for understanding the use environment of consumers and helping to pinpoint design changes that needed to be made in the product. The dispenser system of a bottom-mounted refrigerator in field were cracking and fracturing under unknown consumer usage conditions. The damaged products might have had structural design flaws, including sharp corner angles resulting in stress risers in high stress areas. The design flaws combined with the repetitive loads on the dispenser lever could cause a crack to occur (Fig. 9.19).

The mechanical lever assembly of the water dispensing system consisted of many mechanical structural parts—the dispenser cover, spring, and dispenser lever. Depending on the consumer usage conditions, the lever assembly experienced repetitive mechanical loads in the water dispensing process. Figure 9.20 shows the

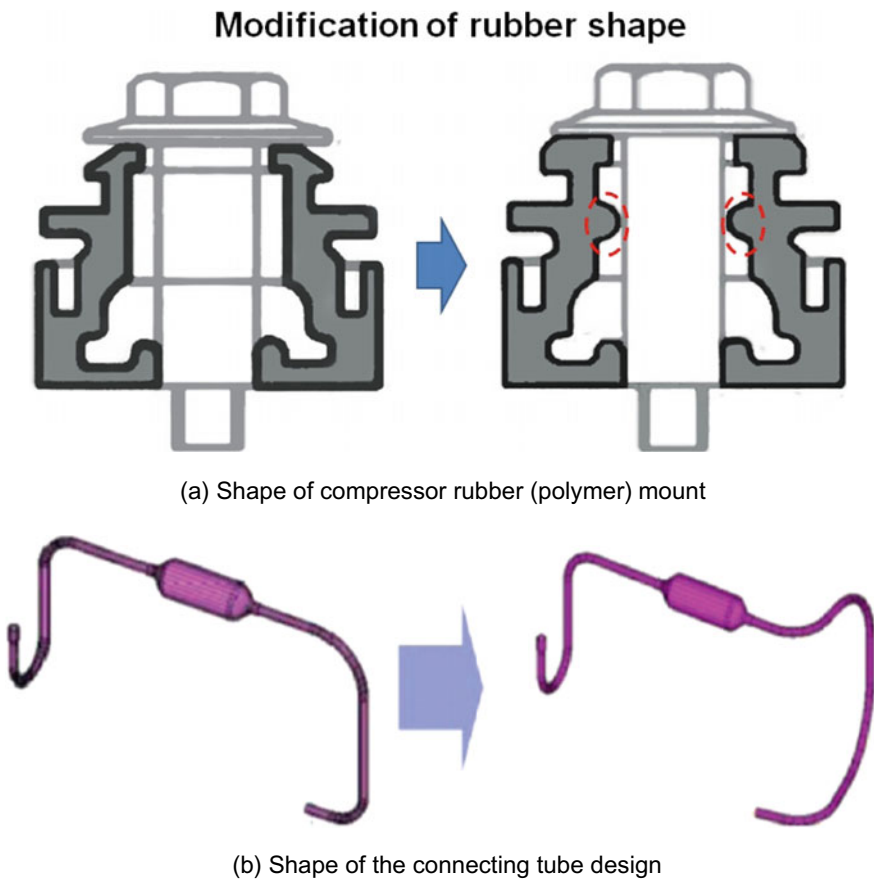


Fig. 9.16 Modified design parameters of machine department (or module)

functional design concept of the mechanical dispensing system. As a cup presses on the lever to dispense water, water will dispense. The number of water dispensing cycles will be influenced by consumer usage conditions. In the United States, the typical consumer requires a BMF refrigerator to dispense water from four up to 20 times a day.

Because the stress of the lever hinge depends on the applied pressure force of the consumer, the life-stress model (LS model) can be modified as

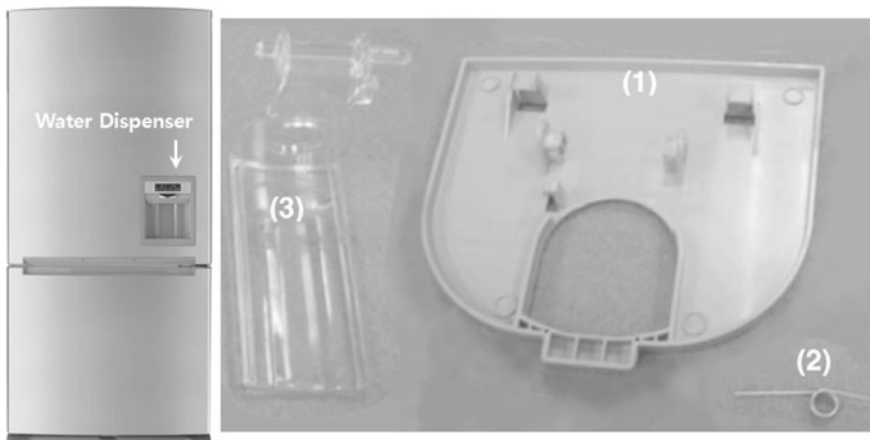
$$TF = A(S)^{-n} = A(F)^{-\lambda} \quad (9.10)$$

The acceleration factor (AF) can be derived as

$$AF = \left(\frac{S_1}{S_0}\right)^n = \left(\frac{F_1}{F_0}\right)^{\lambda} \quad (9.11)$$

Table 9.3 Results of ALT

	1st ALT	2nd ALT
	Initial design	Second design
In 40 min fracture of the connecting tube in refrigerator is less than 1	20 min: 1/3 fracture 40 min: 2/3 fracture	40 min: 3/3 OK 60 min: 3/3 OK
Machine room in refrigerator		
Material and specification	C1 Shape of the compressor rubber C2 Connecting tube design	



(a) BMF refrigerator

(b) Mechanical parts of the dispenser lever assembly:
Dispenser cover (1), Spring (2) and Dispenser lever (3)**Fig. 9.17** BMF refrigerator and dispenser assembly

Key Noise Parameters
N1: Customer usage & load conditions
N2: Environmental conditions

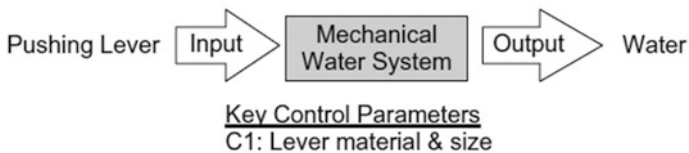


Fig. 9.18 Robust design schematic of water dispensing

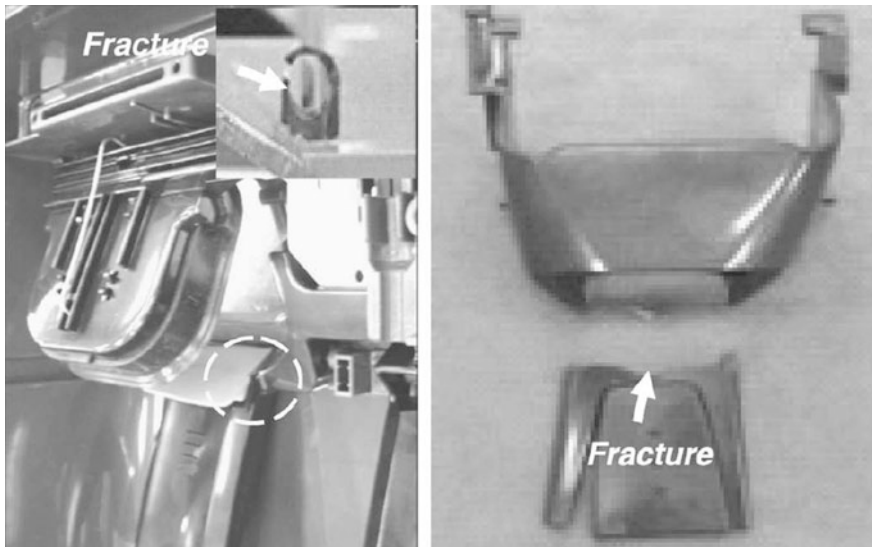


Fig. 9.19 A damaged product after use

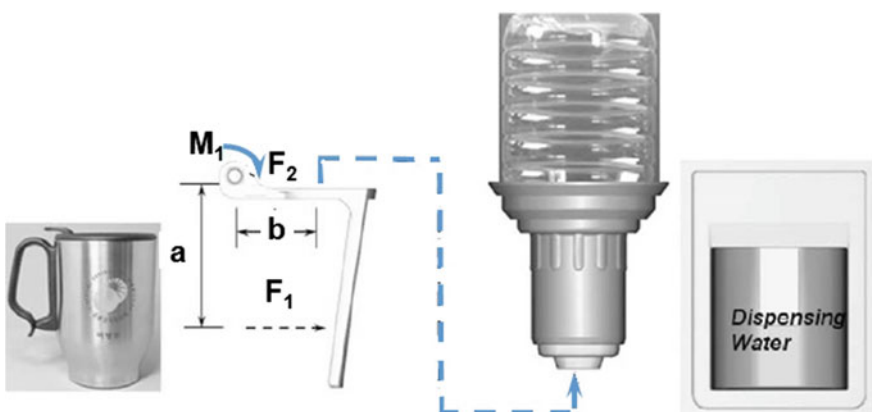
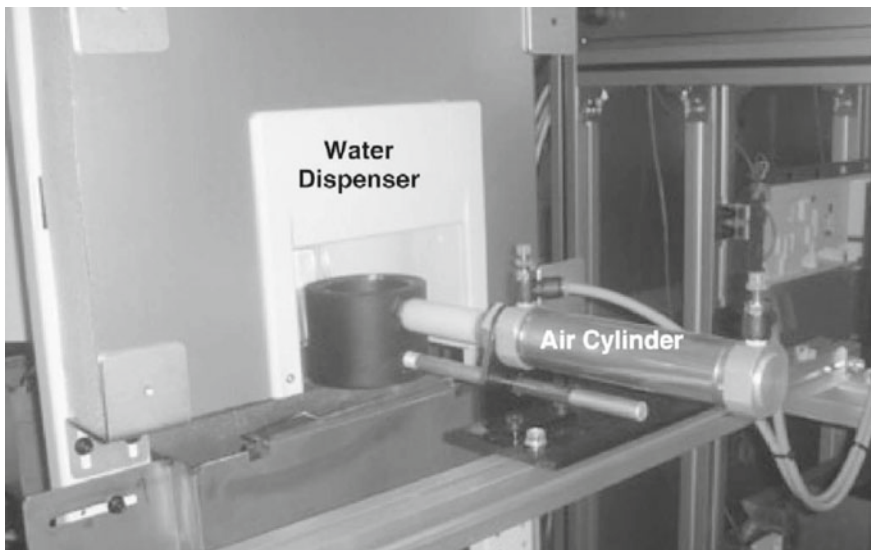


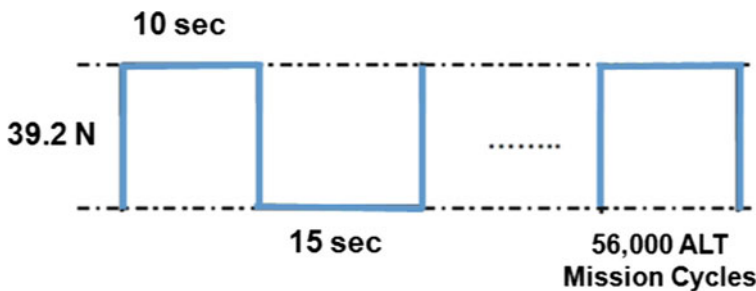
Fig. 9.20 Design concept of mechanical dispensing system

The dispenser is used on average 4–20 times per day. With a life cycle design point of 10 years, the dispenser incurs about 73,000 usage cycles. The applied force is supposed to have 19.6 N which is the maximum force applied by the typical consumer. Doubling the applied force for the ALT to 39.2 N and using a stress dependence of 2.0, the acceleration factor is found to be approximately four in Eq. (9.11).

The test cycles and test sample calculated in Eq. (8.35) were 56,000 cycles and 8 pieces, respectively. The ALT was designed to ensure a B1 of 10 years life with about a 60% level of confidence that it would fail less than once during 56,000 cycles. Figure 9.21a shows the experimental setup of the ALT with labeled equipment for the robust design of the dispenser. Figure 9.21b shows the duty cycles for the pushing force F.



(a) Test equipment of water dispenser used in accelerated life testing



(b) Duty cycles of repetitive load F

Fig. 9.21 Equipment used in accelerated life testing and duty cycles of repetitive load F

An air cylinder controlled the pushing force, F of the cup. When the start button in the controller panel gave the start signal, the air cylinder with the mug-shape cup pressed the dispenser lever. At this point, the cup impacted the dispenser lever at the maximum mechanical force of 39.2 N.

Figure 9.22 shows the failed product from the field and from the accelerated life testing. In the photos, the shape and location of the failure in the ALT were similar to those seen in the field because of the stress raiser such as lever corner with no rounding. The reduction factor R also is 0.009 from the acceleration factor (AF) = 5 and shape parameter (β) = 3.5. Consequently, we know that this parameter ALT is effective to save the testing time and sample size. These stress raisers in lever like no rounding should be improved to meet the reliability target of lever in the design phase.

Figure 9.23 also shows the photograph of the ALT results and field data on Weibull plot. The shape parameter in the first ALT was estimated at 2.0. For the final design, the shape parameter was obtained from the Weibull plot and was determined to be 3.5. These methodologies were valid in pinpointing the weak designs responsible for failures in the field and supported by two findings in the data. The location and shape also, from the Weibull plot, the shape parameters of the ALT, β_1 , and market data, β_2 , were found to be similar.

The fracture of the dispenser lever in both the field products and the ALT test specimens occurred in both the front corner of the lever and the hinge (Fig. 9.24). The repetitive applied force in combination with the structural flaws may have caused cracking and fracture of the dispenser lever. The design flaw of sharp corners/angles resulting in stress risers in high stress areas can be corrected by implementing fillets on the hinge rib and front corner as well as increasing the hinge rib thickness. Through a finite element analysis, it was determined that the concentrated stresses resulting in fracture at the shaft hinge and the front corner were 9.37 and 5.66 MPa, respectively.

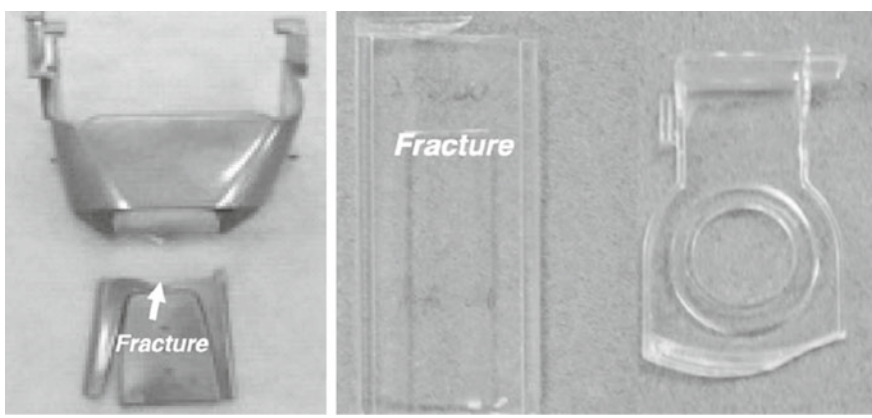


Fig. 9.22 Failed products in field and ALT

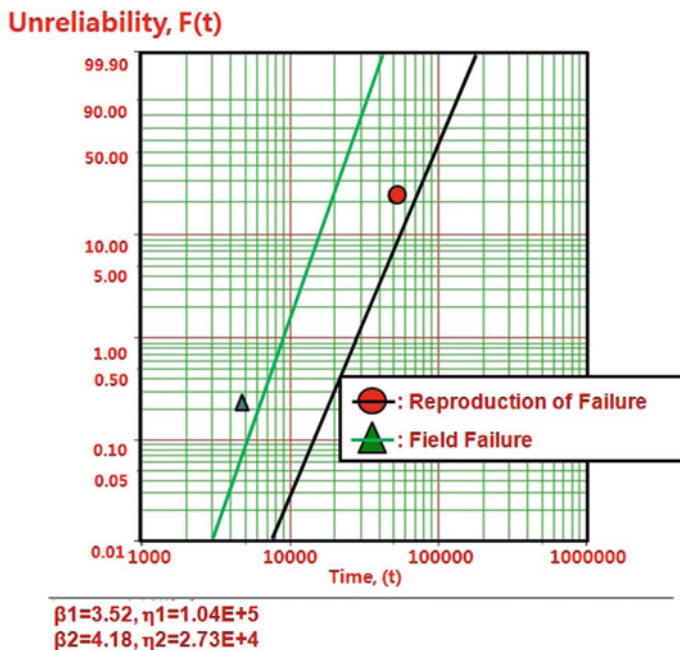


Fig. 9.23 Photograph of the ALT results and field data and Weibull plot

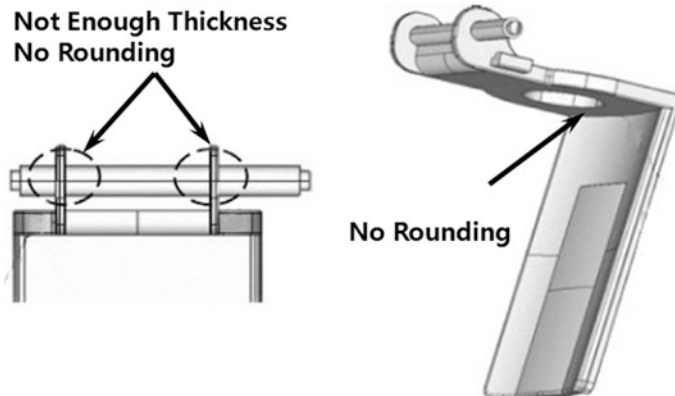


Fig. 9.24 Structure of failing dispenser lever in field

The confirmed values of AF and β in Fig. 9.23 were 4.0 and 3.5, respectively. The recalculated test cycles and sample size calculated in Eq. (8.35) were 56,000 and 8 EA, respectively. To meet the reliability target—B1 life 10 years, ALTs were performed to determine the design parameters and their proper levels. In the ALTs

the dispenser lever fractured at the front corner of the lever and at the hinge in the 1st ALT, at the front corner of the lever in the 2nd ALT, and at the front of the lever in the 3rd ALT.

Tables 9.4 shows the results of the design parameters confirmed from a tailored set of ALTs and a dispenser lever with high fatigue strength was redesigned by parametric ALTs (see Table 9.5). With these modified parameters, the BMF refrigerator can repetitively dispense water for a longer period without failure. Based on the modified design parameters, corrective measures taken to increase the life cycle of the dispenser system included: (1) increase the hinge rib rounding, C1, from 0.0 to 2.0 mm; (2) increase the front corner rounding, C2, from 0.0 to 1.5 mm; (3) increase the front side rounding, C3, from 0.0 to 11.0 mm; (4) increase the hinge rib thickness, C4, from 1.0 to 1.8 mm; and (5) increase the front lever thickness, C5, from 3.0 to 4.0 mm.

Figure 9.25 shows the graphical results of ALT plotted in a Weibull chart. Applying the new design parameters to the finite element analysis the stress concentrations in the shaft hinge decreased from 8.37 to 6.82 MPa and decreased in the front corner from 5.66 to 3.31 MPa. Over the course of the three ALTs the B1 life of the samples increased from 8.3 years to over 10.0 years. We know that reliability target of new dispenser lever is satisfied by using parametric ALTs.

Table 9.4 Redesigned dispenser lever

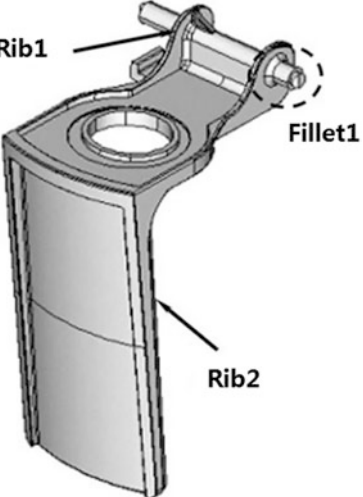
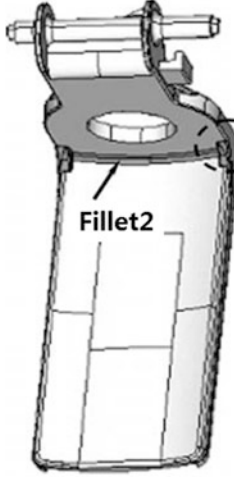
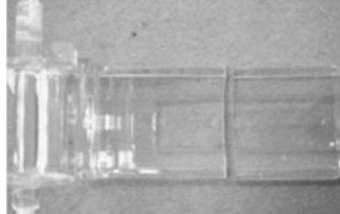
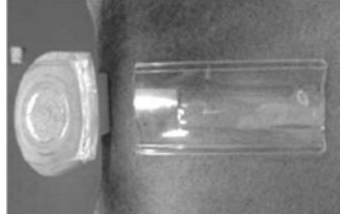
 Rib1 Rib2 Fillet1	 Fillet2 Fillet3
Rib1C1: T1 mm → T1.8 mm (first ALT) Rib2 C2: T3 mm → T4 mm (third ALT) Fillet1 C3: R0 mm → R1.5 mm (first ALT) → R2.0 mm (second ALT)	Fillet2 C4: R0 mm → R1.5 mm (first ALT) Fillet3 C5: R0 mm → R8 mm (first ALT)

Table 9.5 Results of ALT

	1st ALT		2nd ALT		3rd ALT	
	Initial design	Second design	Final design			
In 56,000 cycles, fracture of dispenser is less than 1	52,000 cycles: 2/8 fracture 74,000 cycles: 6/8 OK	56,000 cycles: 8/8 OK 67,500 cycles: 1/8 fracture 92,000 cycles: 7/8 OK	56,000 cycles: 8/8 OK 68,000 cycles: 8 fracture 92,000 cycles: 7/8 OK			
Dispenser lever structure						
Material and specification	Rib1: T1.0 mm → T1.8 mm Fillet 1: R0.0 mm → R1.5 mm Fillet 2: R0.0 mm → R1.5 mm	Fillet 1: R1.5 mm → R2.0 mm Fillet 2: R8.0 mm → R11.0 mm	Rib2: T3.0 mm → T4.0 mm			

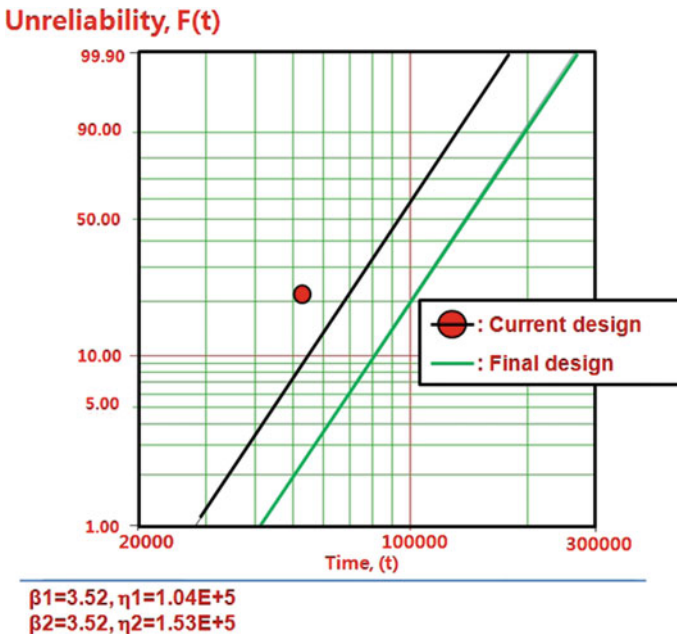


Fig. 9.25 Results of ALT plotted in Weibull chart

9.4 Refrigerator Compressor Subjected to Repetitive Loads

A reciprocating compressor is a positive-displacement machine that uses a piston to compress a gas and deliver it at high pressure through slider-crank mechanism. A crankshaft in compressors of inside-by-side (SBS) refrigerators is redesigned to reduce noise and improve energy efficiency. For these applications, the compressor in lifetime needs to be designed robustly to operate under a wide range of customer usage conditions (Fig. 9.26).

A refrigerator consists of a compressor, a condenser, a capillary tube and an evaporator. The refrigerant enters the compressor at a low pressure. It then leaves the compressor and enters the condenser at some elevated pressure; the refrigerant is condensed as heat is transferred to the surroundings. The refrigerant then leaves the condenser as a high-pressure liquid. The pressure of the liquid is decreased as it flows through the expansion valves, and as a result, some of the liquid flashes into cold vapor. The remaining liquid at a low pressure and temperature is vaporized in the evaporator as heat is transferred from the fresh/freezer compartment. This vapor then reenters the compressor. The main function of the refrigerator is to provide cold air from the evaporator to the freezer and refrigerator compartments and preserve the foods (Fig. 9.27).

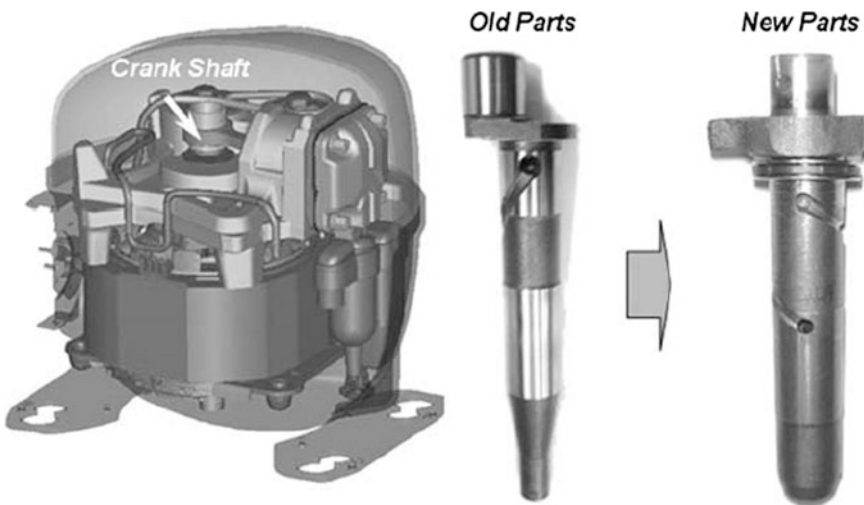


Fig. 9.26 Redesigned compressor and crankshaft

A capillary tube controls the flow in the refrigeration system and drops the high pressure of the refrigerant in the condenser to the low pressure in the evaporator. In a refrigeration cycle design, it is necessary to determine both the condensing pressure, P_c and the evaporating pressure, P_e . These pressures depend on ambient conditions, customer usage conditions, and heat exchanger capacity in the initial design stage.

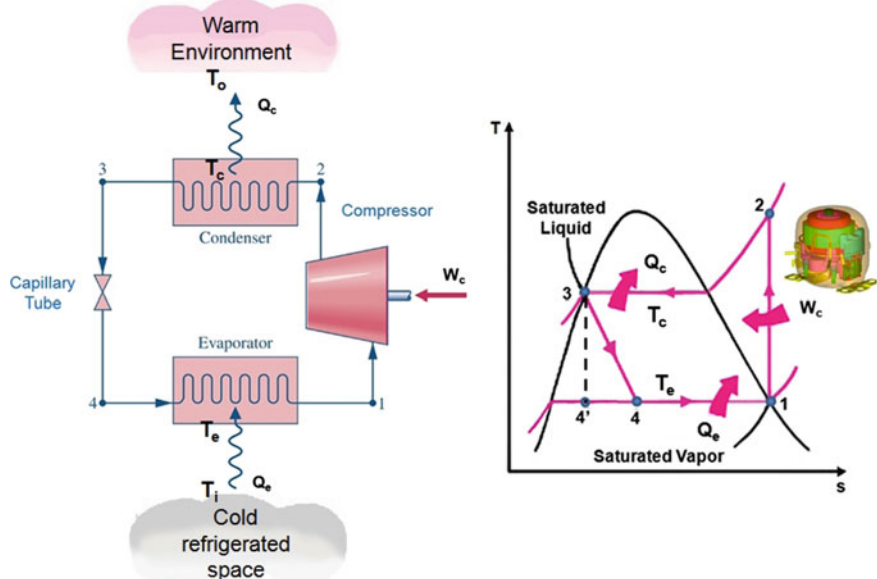
To derive the life-stress model and acceleration factor, the time to failure (TF) can be estimated from the McPherson's derivation:

$$TF = A(S)^{-n} \exp\left(\frac{E_a}{kT}\right) \quad (9.13)$$

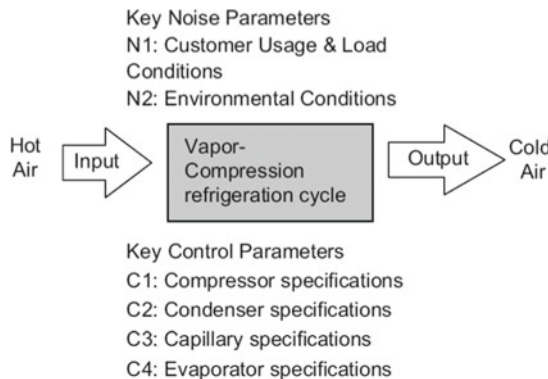
To use Eq. (9.13) for accelerated testing, it needs to be modified and put into a more applicable form, not using stress term. A refrigeration system operates on the basic vapor-compression refrigeration cycle. The compressor receives refrigerant from the low-side (evaporator) and then compresses and transfers the refrigerant to the high-side (condenser) of the system. The capillary tube controls the flow in a refrigeration system and drops the high pressure of the refrigerant in the condenser to the low pressure in the evaporator. In a refrigeration cycle design, it is necessary to determine the condensing pressure, P_c and evaporating pressure, P_e (Fig. 9.26a).

The mass flow rate of refrigerant in a compressor can be modeled as

$$\dot{m} = PD \times \frac{\eta_v}{v_{suc}} \quad (9.14)$$



(a) A vapor-compression refrigeration cycle and T-s diagram



(b) Parameter diagram of refrigeration cycle

Fig. 9.27 A vapor-compression refrigeration cycle and its parameter diagram

The mass flow rate of refrigerant in a capillary tube can be modeled as

$$\dot{m}_{\text{cap}} = A \left[\frac{- \int_{P_3}^{P_4} \rho dP}{\frac{2}{D} f_m \Delta L + \ln \left(\frac{\rho_3}{\rho_4} \right)} \right]^{0.5} \quad (9.15)$$

By conservation of mass, the mass flow rate can be determined as:

$$\dot{m} = \dot{m}_{\text{cap}} \quad (9.16)$$

The energy balance in the condenser can be described as

$$Q_c = \dot{m}(h_2 - h_3) = (T_c - T_o)/R_c \quad (9.17)$$

The energy balance in the evaporator can be described as

$$Q_e = \dot{m}(h_1 - h_4) = (T_i - T_e)/R_e \quad (9.18)$$

When nonlinear Eq. (9.16) through (9.18) are solved, the mass flow rate, \dot{m} , evaporator temperature, T_e , and condenser temperature, T_c can be obtained. Because the saturation pressure, P_{sat} , is a function of temperature, the evaporator pressure, P_e (or condenser pressure P_c), can be obtained as:

$$P_e = f(T_e) \text{ or } P_c = f(T_c) \quad (9.19)$$

One source of stress in a refrigeration system may come from the pressure difference between suction pressure, P_{suc} , and discharge pressure, P_{dis} .

For the theoretical single-stage cycle, the stress of the compressor depends on the pressure difference suction pressure, P_{suc} , and discharge pressure, P_{dis} . That is,

$$\Delta P = P_{\text{dis}} - P_{\text{suc}} \cong P_c - P_e \quad (9.20)$$

By repeating the on and off cycles, the life of compressor shortens. The oil lubrication then relieves the stressful wear and extends the compressor life. Because the stress of the compressor depends on the pressure difference of the refrigerator cycle, the life-stress model in Eq. (9.13) can be modified as

$$TF = A(S)^{-n} \exp\left(\frac{E_a}{kT}\right) = A(\Delta P)^{-n} \exp\left(\frac{E_a}{kT}\right) \quad (9.21)$$

The acceleration factor (AF) from Eq. (9.21) can be derived as

$$AF = \left(\frac{S_1}{S_0}\right)^n \left[\frac{E_a}{k} \left(\frac{1}{T_0} - \frac{1}{T_1} \right) \right] = \left(\frac{\Delta P_1}{\Delta P_0} \right)^\lambda \left[\frac{E_a}{k} \left(\frac{1}{T_0} - \frac{1}{T_1} \right) \right] \quad (9.22)$$

The normal number of operating cycles for one day was approximately ten; the worst case was twenty-four. Under the worst case, the objective compressor cycles for ten years would be 87,600 cycles.

The normal pressure was 1.07 MPa at 42 °C and the compressor dome temperature was 90 °C. It was measured after T type thermocouple pierced into the top compressor. For the accelerated testing, the acceleration factor (AF) for pressure at 1.96 MPa was 3.37 and for the compressor with a 120 °C dome temperature was 3.92 with a quotient, λ , of 2. The total AF was approximately 13.2 (Table 9.6).

Table 9.6 ALT conditions in a vapor compression cycles

System conditions		Worst case	ALT	AF
Pressure, MPa	High side	1.07	1.96	3.36③ (= (①/②) ²)
	Low side	0.0	0.0	
	ΔP	1.07①	1.96②	
Temp., °C	Dome temp.	90	120	3.92④
Total AF (= ③ × ④)		—		13.2

The parameter design criterion of the newly designed compressor can be more than the reliability target life—B1 life ten years. Assuming the shape parameter β was 1.9, the test cycles and test sample numbers calculated in Eq. (8.35) were 18,000 cycles and 30 pieces, respectively. The ALT was designed to ensure a B1 of ten years life with about a sixty-percent level of confidence that it would fail less than once during 18,000 cycles.

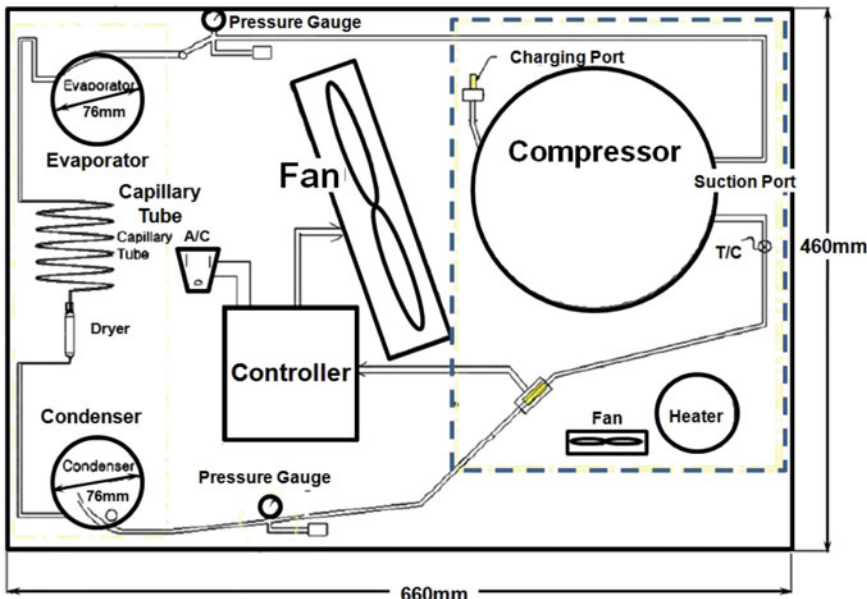
Figure 9.28 shows the ALT equipment used for the life testing in the laboratory. Figure 9.29 shows the duty cycles for the repetitive pressure difference, ΔP . For the ALT experiments, a simplified vapor-compression refrigeration system was fabricated. It consisted of an evaporator, compressor, condenser, and capillary tube. The inlet to the condenser section was at the top and the condenser outlet was at the bottom.

The condenser inlet was constructed with quick coupling and had a high-side pressure gauge. A ten gram refrigerator dryer was installed vertically at the condenser inlet. A thermal switch was attached to the condenser tubing at the top of the condenser coil to control the condenser fan. The evaporator inlet was at the bottom. At a location near the evaporator outlet, pressure gauges were installed to enable access to the low side for evacuation and refrigerant charging.

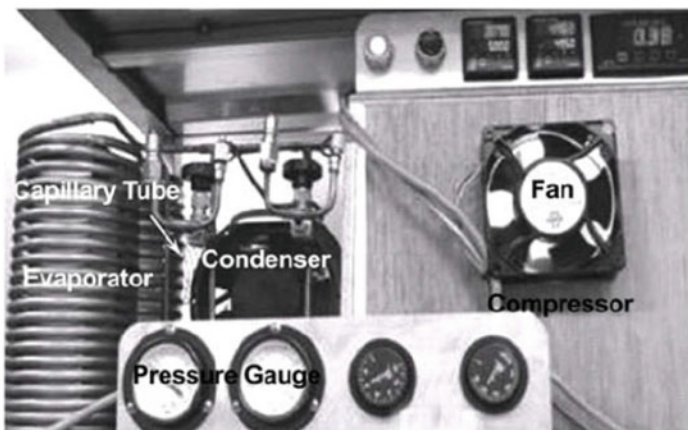
The condenser outlet was connected to the evaporator outlet with a capillary tube. The compressor was mounted on rubber pads and was connected to the condenser inlet and evaporator outlet. A fan and two 60 W lamps maintained the room temperature within an insulated (fiberglass) box. A thermal switch attached on the compressor top controlled a 51 m³/h axial fan compressor, condenser, and capillary tube.

In SBS units sold it was found that the crankshafts of some compressors were locking. Locking refers to the inability of the electric stator to rotate the crankshaft, due to a failure of one or more components within the compressor under a range of unknown customer usage conditions. Field data indicated that the damaged products may have had a design flaw—oil lubrication problems. Due to this design flaw, the repetitive loads could create undue wear on the crankshaft and cause the compressor to lock.

Figure 9.30 shows the crankshaft of a locked-up compressor from the field and two samples from the accelerated life testing at 10,504 cycles. In the photo, the shape and location of the parts in the failed product from the field were similar to those in the ALT results. Figure 9.31 represents the graphical analysis of the ALT results and



(a) A drawing of the test system



(b) Photograph

Fig. 9.28 Equipment used in accelerated life testing

field data on a Weibull plot. For the shape parameter, the estimated value in the previous ALT was 1.9. It was concluded that the methodologies used were valid in pinpointing the weaknesses in the original design of the units sold in the market because (1) the location and shape of the locking crankshaft from both the field and ALT were similar; and (2) on the Weibull, the shape parameters of the ALT results, β_1 and market data, β_2 , are very similar. The reduction factor R also is 0.15 from the

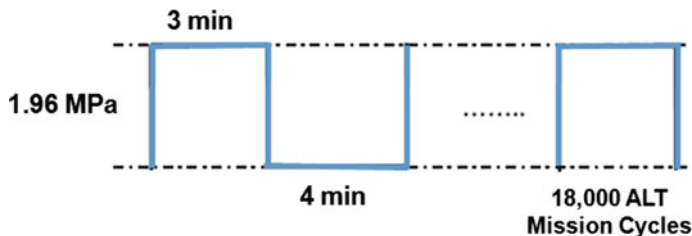


Fig. 9.29 Duty cycles of repetitive pressure difference on the compressor

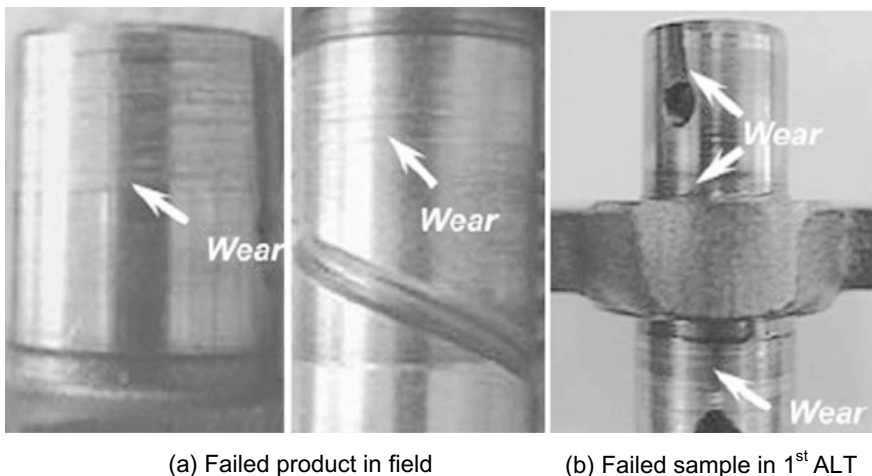


Fig. 9.30 Failed product in field and 1st ALT

acceleration factor (AF) = 13.2 and shape parameter (β) = 1.9. Consequently, we know that this parameter ALT is effective to save the sample size.

When both the locked compressors from the field and the ALT compressor were cut apart, severe wear was found in regions of the crankshaft where there was no lubrication—the friction area between shaft and connecting rod, and also the friction area between crankshaft and block. The locking of the compressor resulted from several design problems when compressor rotated and oil did not lubricate evenly. There was (1) no oil lubrication in some regions of the crankshaft (Fig. 9.32); (2) a low starting RPM (1650 RPM) (Fig. 9.32); and, (3) a crankshaft made from material with a wide range of hardness (FCD450) (Fig. 9.33).

The missing design parameters in 1st ALT were the lack of an oil lubrication region, low starting RPM, and weak crankshaft material. These compressor design flaws may cause the compressor to lock up suddenly when subjected to repetitive loads under customer's operation conditions. To improve it, the parameter design criterion of the newly designed samples was more than the target life, B1, of ten years. The confirmed values β on Weibull chart was 1.9. When the second ALT and third ALT proceeded, the recalculated test cycles and sample size calculated in

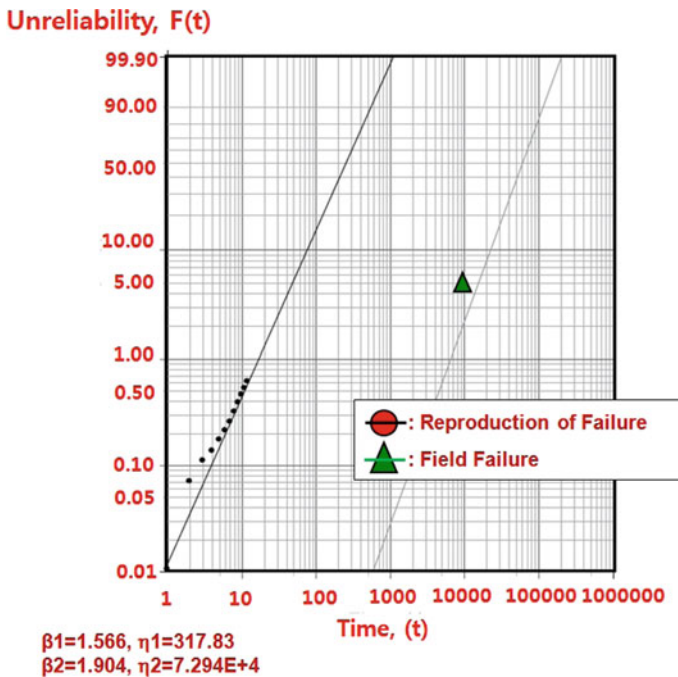


Fig. 9.31 Field data and results of ALT on Weibull chart

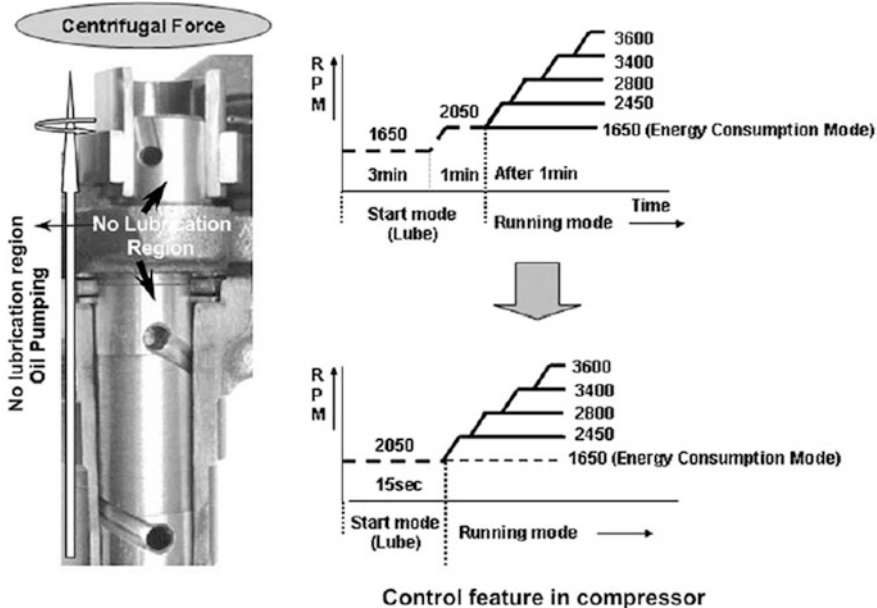


Fig. 9.32 No lubrication region in crankshaft and low starting RPM (1650 RPM)

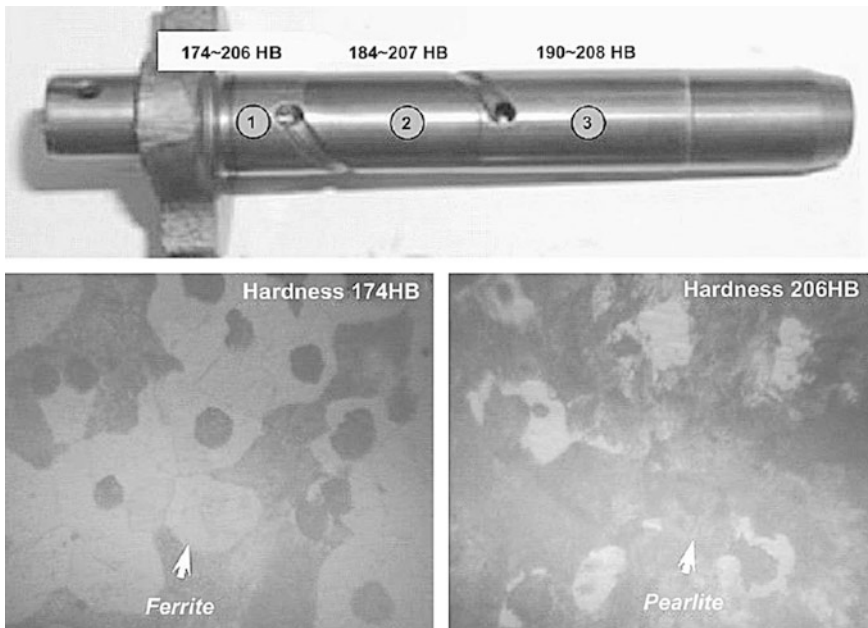


Fig. 9.33 A large variation of hardness (FCD450) in crankshaft

Eq. (8.35) were 18,000 and 30 pieces, respectively. Based on the B1 life of ten years, the first, second, and third ALTs were performed to obtain the design parameters and their proper levels. We found the interference wear on crankshaft at 18,000 cycles. The compressor failure in the first ALT was due the compressor locking. In the second ALT, it was due to interference between the crankshaft and a thrust washer.

To improve the lubrication problems in the crankshaft, it was redesigned as the relocated lubrication holes, new groove and new shaft material FCD500 (Fig. 9.34). To avoid the wear between crankshaft and washer, the minimum clearance was increased from 0.141 to 0.480 mm (Fig. 9.35). With these modified design parameters, newly designed compressor in the SBS refrigerators can operate in the duty cycles of on and off repetitively with reliability target—B1 life ten years.

The modified design parameters, with the corrective action plans, included (1) the modification of the oil lubrication region, C1; (2) increasing the starting RPM, C2, from 1650 to 2050; (3) changing the crankshaft material, C3, from FCD450 to FCD500; and (4) modifying the thrust washer dimension, C4 (see Table 9.7).

Table 9.7 provides a summary of the ALT results. Figure 9.36 show the results of ALT plotted in a Weibull chart. With the improved design parameters, the B1 life of the samples in the first, second and third ALTs lengthen from 3.8 years to over 10.0 years. During the third ALT, no problems were found with the compressor.

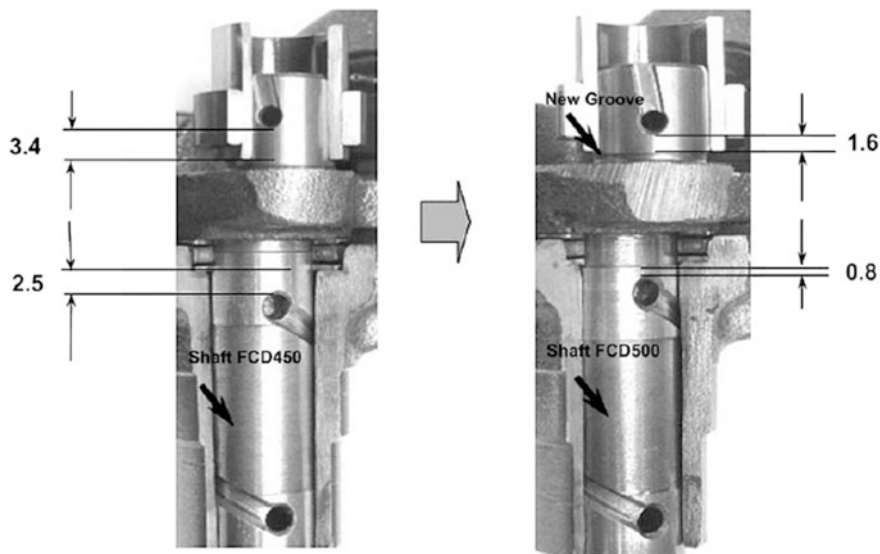


Fig. 9.34 Redesigned crankshaft in first ALT

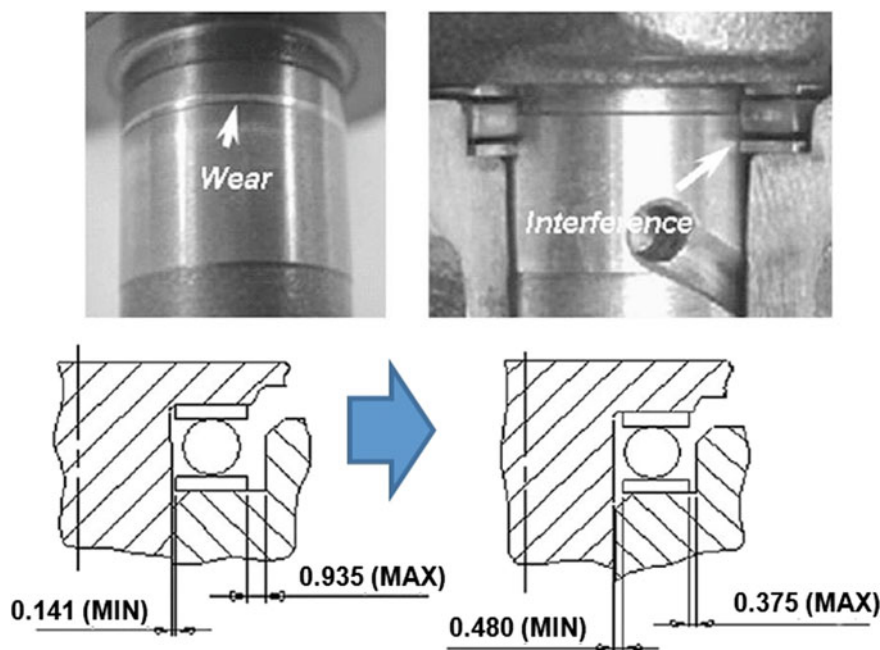
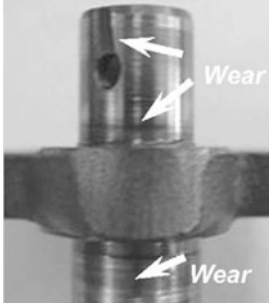


Fig. 9.35 Redesigned crankshaft in second ALT

Table 9.7 Results of ALT

	1st ALT	2nd ALT	3rd ALT
	Initial design	Second design	Final design
In 18,000 cycles, locking is less than 1	10,504 cycles: 2/30 locking 18,000 cycles: 28/30 OK	18,000 cycles: 2/30 wear 18,000 cycles: 28/30 OK	18,000 cycles: 30/30 OK 20,000 cycles: 30/30 OK
Crank shaft structure			
Material and specification	FCD450/FCD450 One new groove Location modification of oil supply holes	Modification of washer dimension	

9.5 Hinge Kit System (HKS) in a Kimchi Refrigerator

Figure 9.37 shows the Kimchi refrigerator with the newly designed hinge kit system through spring-damper mechanism. When a consumer closes the refrigerator door, they want to close it conveniently and comfortable. For this function, the hinge kit system needs to robustly be designed to handle the operating conditions subjected to it by the consumers who purchase and use the Kimchi refrigerator (Fig. 9.38). Originally HKS was the spring mechanism that could decrease the speed of door closing due to door weight. Because its damping effects at 0°–10° (door angle) were not up to much, the spring-damper mechanism in HKS was changed to improve this. Before launching newly designed HKS, we had to find the design faults and verify its reliability. The hinge kit assembly consists of the kit cover, shaft, spring, oil damper, and kit housing, as shown in Fig. 9.37b. In the field, the hinge kit assembly in the refrigerators had been fracturing, causing the door not to close easily. Thus, the data on the failed products in the field were important for understanding the usage environment of consumers and helping to pinpoint design changes that needed to be made in the product.

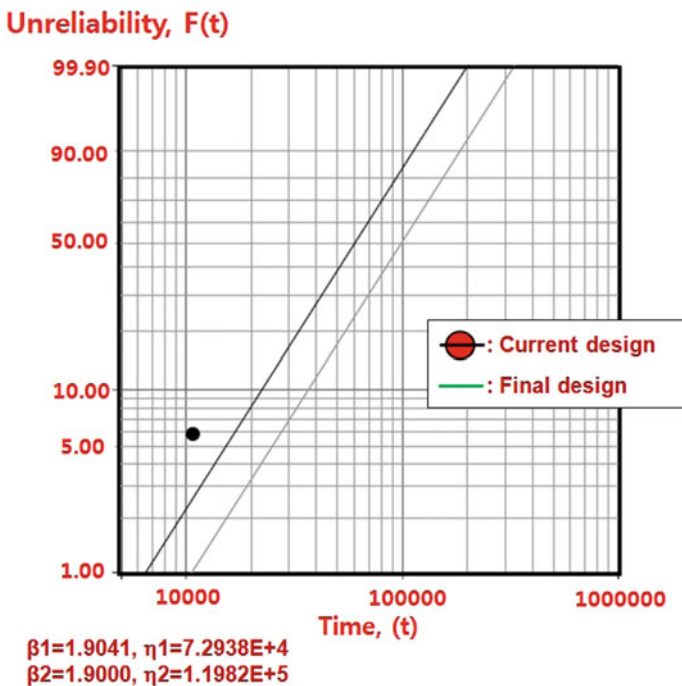


Fig. 9.36 Results of ALT plotted in Weibull chart

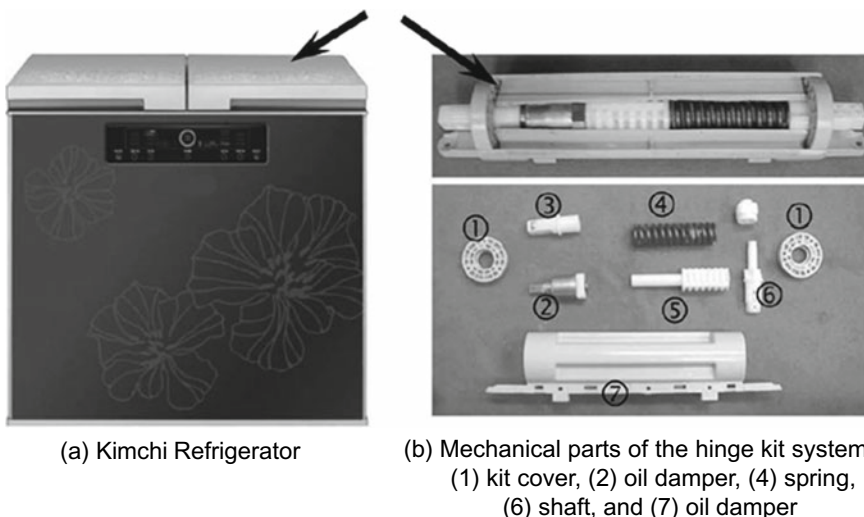


Fig. 9.37 Kimchi refrigerator and hinge kit assembly

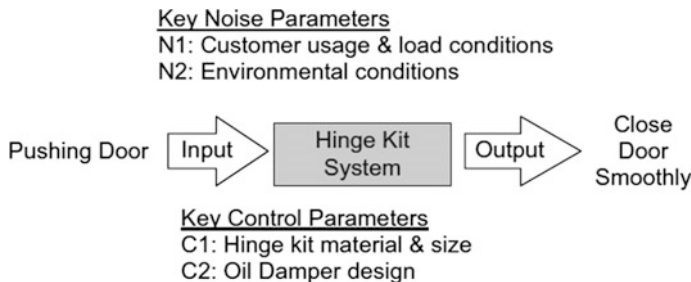


Fig. 9.38 Robust design schematic of hinge kit system

In the field, parts of the hinge kit system of a Kimchi refrigerator were failing due to cracking and fracturing under unknown consumer usage conditions (Fig. 9.39). Field data indicated that the damaged products might have had structural design flaws, including sharp corner angles and not enough enforced ribs resulting in stress risers in high stress areas. These design flaws combined with the repetitive loads on the hinge kit system could cause a crack to occur, and thus cause failure.

The mechanical hinge kit assembly of the door closing function consisted of many mechanical structural parts. Depending on the consumer usage conditions, the hinge kit assembly receives repetitive mechanical loads when the door is closed. Door closing involves two mechanical processes: (1) the consumer opens the door to take out the stored food and (2) they then close the door by force.

Figure 9.40 shows the functional design concept of the mechanical hinge kit system in the accelerated testing. As the consumer presses the refrigerator door, the hinge kit system helps to close the door smoothly. If analyzed as free body diagram, the stress due to the weight momentum of the door is concentrated on the hinge kit system. The number of door closing cycles will be influenced by consumer usage conditions. In the Korean domestic market, the typical consumer requires a Kimchi refrigerator the door system to open and close between three and ten times a day. The moment balance around the door system with an accelerated weight and the hinge kit system can be represented as

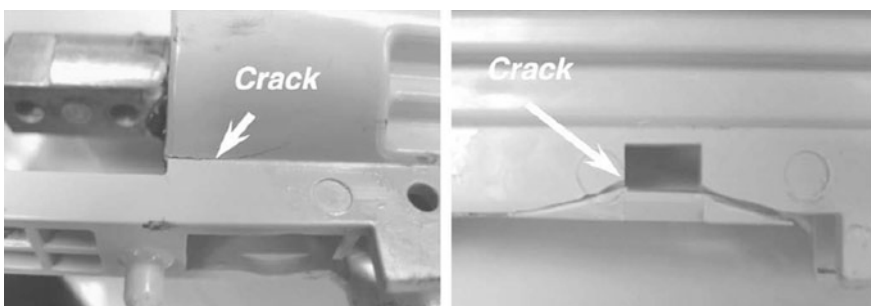


Fig. 9.39 Damaged products after use

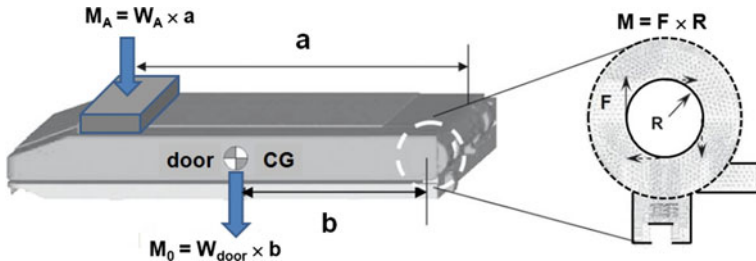


Fig. 9.40 Design concept of mechanical hinge kit system in the accelerated testing

The moment balance around the HKS without accelerated weight in Fig. 9.40 can be represented as

$$M_0 = W_{door} \times b = T_0 = F_0 \times R \quad (9.23)$$

The moment balance around the HKS with an accelerated weight can be represented as

$$M_1 = M_0 + M_A = W_{door} \times b + W_A \times a = T_1 = F_1 \times R \quad (9.24)$$

Because F_0 is impact force in normal conditions and F_1 is impact force in accelerated weight, the stress on the HKS depends on the applied impact. Under the same temperature and impact concept, the life-stress model (LS model) can be modified as

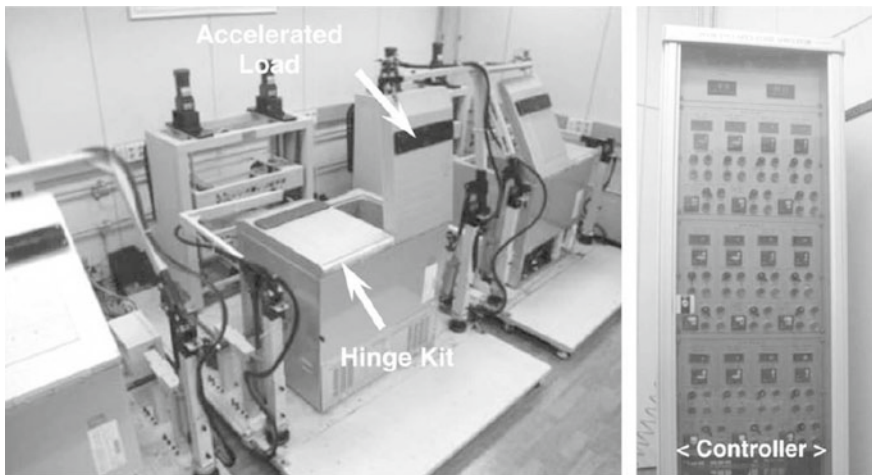
$$TF = A(S)^{-n} = AT^{-\lambda} = A(F \times R)^{-\lambda} \quad (9.25)$$

The acceleration factor (AF) can be derived as

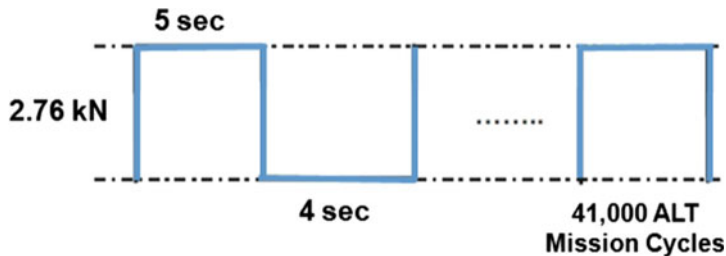
$$AF = \left(\frac{S_1}{S_0}\right)^n = \left(\frac{T_1}{T_0}\right)^\lambda = \left(\frac{F_1 \times R}{F_0 \times R}\right)^\lambda = \left(\frac{F_1}{F_0}\right)^\lambda \quad (9.26)$$

The closing of the door occurs an estimated average 3–10 times per day. With a life cycle design point of 10 years, the hinge kit incurs about 36,500 usage cycles. For the worst case, the applied force around the hinge kit is 1.10 kN which is the maximum force applied by the typical consumer. The applied force for the ALT with accelerated weight is 2.76 kN. Using a stress dependence of 2.0, the acceleration factor is found to be approximately 6.3 in Eq. (9.26).

For the reliability target B1 of 10 years, the test cycles and test sample numbers calculated in Eq. (8.35) were 34,000 cycles and six pieces, respectively. The ALT was designed to ensure a B1 life ten years with about a sixty-percent level of confidence that it would fail less than once during 34,000 cycles. Figure 9.41a



(a) Equipment used in accelerated life testing



(b) Duty cycles of repetitive load F

Fig. 9.41 Equipment used in accelerated life testing and duty cycles of repetitive load F

shows the experimental setup of the ALT with labeled equipment for the robust design of the hinge kit system. Figure 9.41b shows the duty cycles for the impact force F .

The control panel on the top started or stopped the equipment, and indicated the completed test cycles and the test periods such as sample on/off time. The door closing force F was controlled by the accelerated load applied to the door. When the start button in the controller panel gave the start signal, the simple hand-shaped arms held and lifted the Kimchi refrigerator door. At this point it impacted the hinge kit with the maximum mechanical impact force due to the accelerated weight (2.76 kN).

Figure 9.42 shows the failed product from the field and from the accelerated life testing, respectively. In the photos the shape and location of the failure in the ALT were similar to those seen in the field.

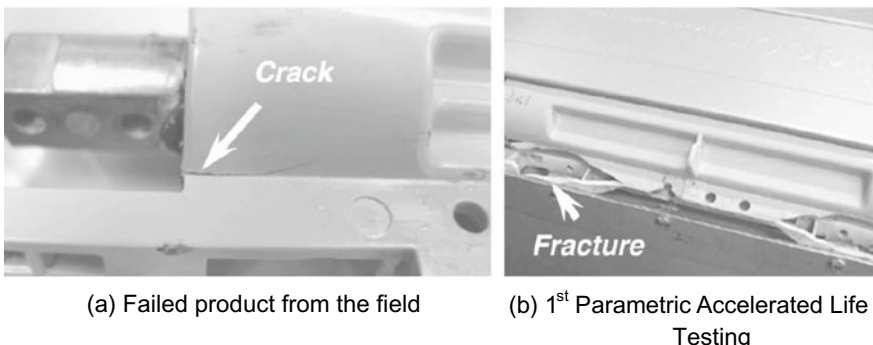


Fig. 9.42 Failed products in field and 1st ALT

Figure 9.43 represents the graphical analysis of the ALT results and field data on a Weibull plot. The shape parameter in the first ALT was estimated at 2.0. For the final design, the shape parameter obtained from the Weibull plot was determined to be 2.1.

Unreliability

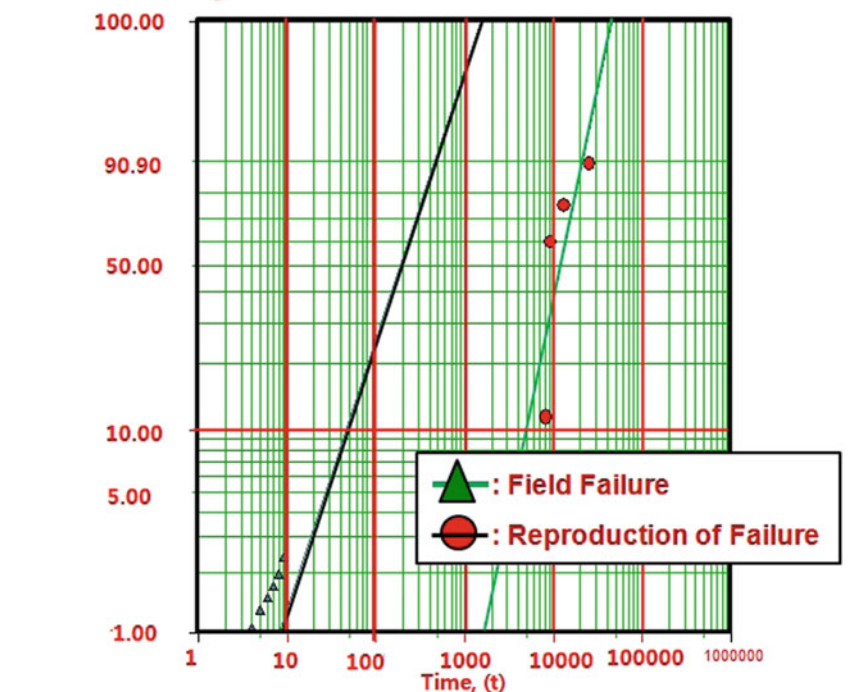


Fig. 9.43 Field data and results of ALT on Weibull chart

These methodologies were valid in pinpointing the weak designs responsible for failures in the field and supported by two findings in the data. The location and shape from the Weibull plot, the shape parameters of the ALT (β_1) and market data (β_2) were found to be similar. The reduction factor R also is 0.016 from the experiment data—product lifetime, acceleration factor, actual mission cycles, and shape parameter. Consequently, we know that this parameter ALT is effective to decrease the sample size.

The fracture of the hinge kit in both the field products and the ALT test specimens occurred in the housing of the kit (Fig. 9.44a). The oil damper leaked oil in the hinge kit assembly (Fig. 9.44b). The repetitive applied force in combination with the structural flaws may have caused the fracturing of the hinge kit housing and the leak of the oil damper. The concentrated stresses of the housing hinge kit were approximately 21.2 MPa, based on finite element analysis. The stress risers in high stress areas resulted from the design flaws of sharp corners/angles, housing notches, and poorly enforced ribs.

The corrective action plans was to implement fillets, add the enforced ribs, and remove the notching on the housing of the hinge kit (Fig. 9.45). Applying the new design parameters to the finite element analysis, the stress concentrations in the housing of hinge kit decreased from 21.2 to 18.9 MPa.

The sealing structure of the oil damper had a 0.5 mm gap in the O-ring/Teflon/O-ring assembly. Due to the wear and impact, this sealing with the gap leaked easily. The sealing structure of the redesigned oil damper has no gap with Teflon/O-ring/Teflon (Fig. 9.46). The parameter design criterion of the newly designed samples was more than the target life—B1 life 10 years. The confirmed values of AF and β in Fig. 9.43 were 6.3 and 2.1, respectively. The test cycles and sample size recalculated in Eq. (8.35) were 41,000 and six pieces, respectively. Based on the targeted BX and sample size, three ALTs were performed to obtain the design parameters and their proper levels. In the second ALTs the fracture of hinge kit

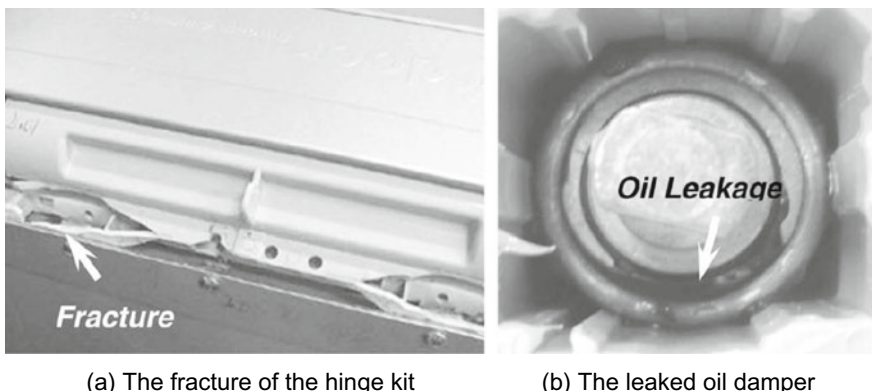


Fig. 9.44 Structure of failing hinge kit system in accelerated testing

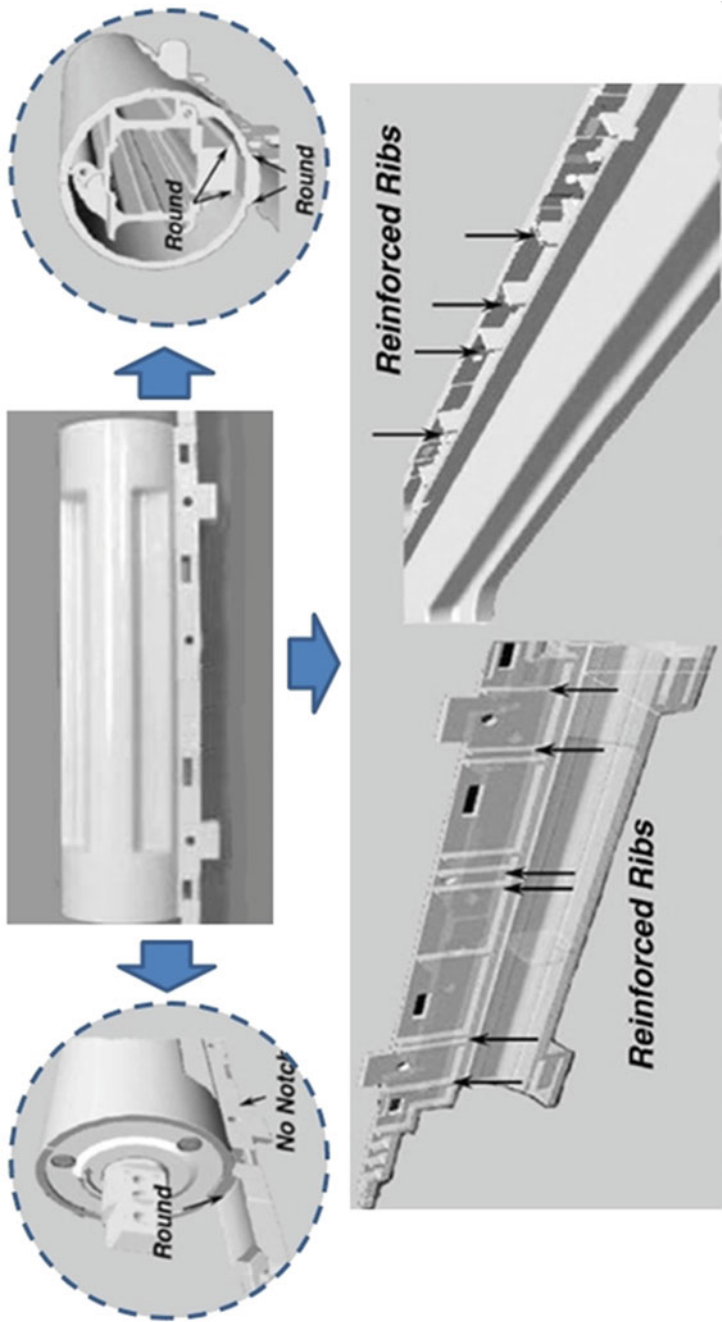


Fig. 9.45 Structure of newly designed hinge kit system

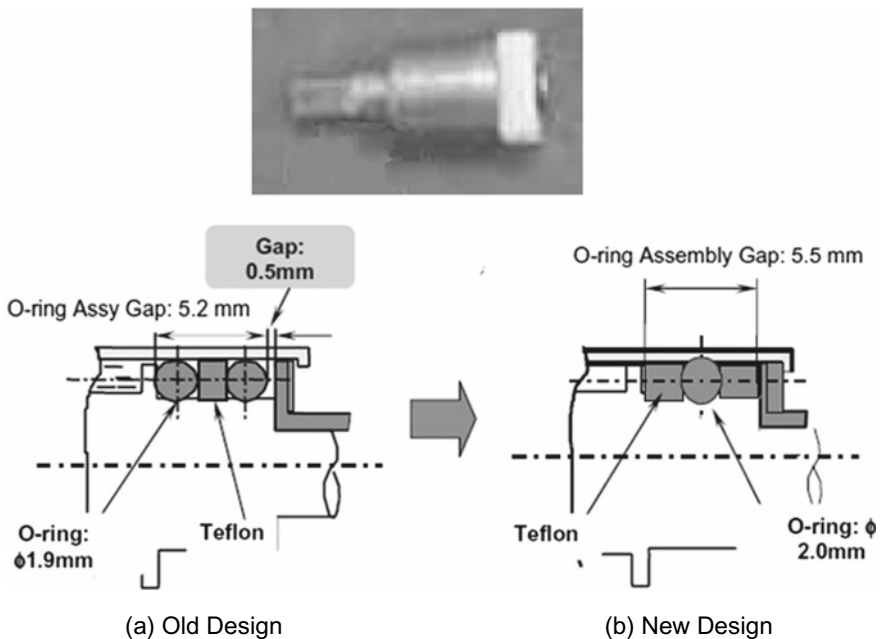


Fig. 9.46 Sealing structure of redesigned oil damper

cover occurs due to the repetitive impact stresses and its weak material. The cover housing of hinge kit assembly was modified by the material change from the plastics to the Al die-casting (Fig. 9.47).

The modified design parameters with corrective action plans were (1) the modification of the housing hinge kit (Fig. 9.45); (2) the modification of the oil sealing structure (see Fig. 9.46); (3) the material change of the cover housing (see Fig. 9.47).

Table 9.8 shows the summary of the results of the ALTs, respectively. With these modified parameters, the Kimchi refrigerator can smoothly close the doors for a longer period without failure. Figure 9.48 shows the graphical results of the ALT plotted in a Weibull chart. Over the course of three ALTs the B1 life of the samples increased from 8.3 years to over 10.0 years.

9.6 Refrigerator Drawer System

Figure 9.49 shows a French refrigerator with the newly Freezer drawer designed handle and drawer mechanism. In the field, the refrigerator drawer and handle system had been failing, causing consumers to replace their refrigerators (Fig. 9.50). The specific causes of failures of the refrigerator drawers during

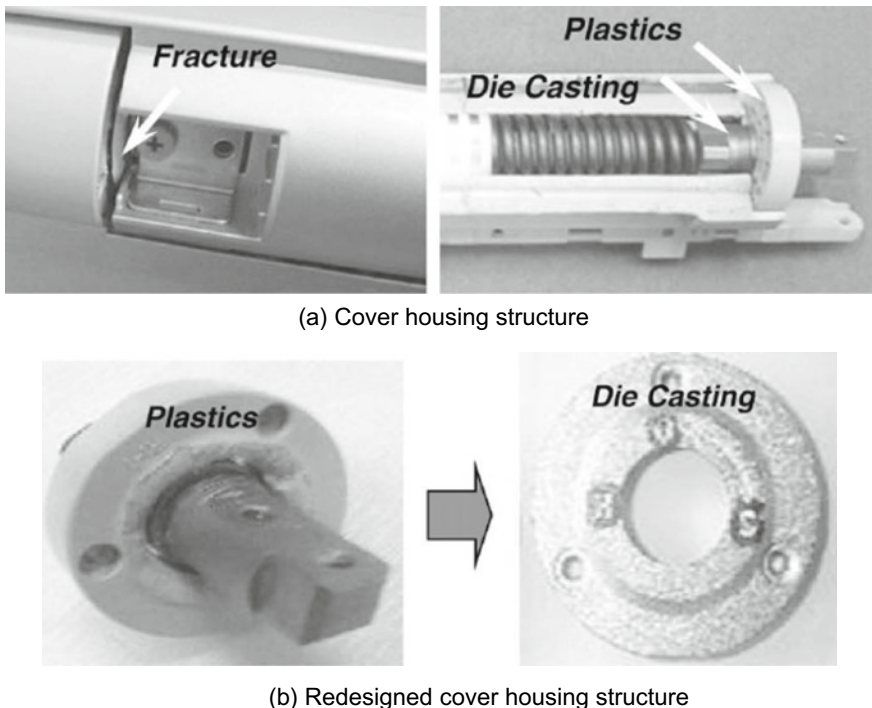


Fig. 9.47 Redesigned cover housing structure

operation were repetitive stress and/or the consumer improper usage. Field data indicated that the damaged products had structural design flaws, including sharp corner angles and weak ribs that resulted in stress risers in high stress areas.

To have convenient access to fresh food, a consumer stores food in a refrigerator. Putting food in the refrigerator drawer involves opening the drawer to store or takeout food, closing the drawer by force. Depending on the consumer usage conditions, the drawer and handle parts receive repetitive mechanical loads when the consumer opens and closes the drawer.

Figure 9.51 shows the functional design concept of the drawer and handle system. The stress due to the weight load of the food is concentrated on the handle and support slide rail of the drawer. Thus, the drawer must be designed to endure these repetitive stresses. The force balance around the drawer and handle system can be expressed as:

$$F_{draw} = \mu W_{load} \quad (9.27a)$$

Because the stress of the drawer and handle system depends on the food weight in Eq. (9.27a), the life stress model (LS model) can be modified as follows:

Table 9.8 Results of ALT

	1st ALT Initial design	2nd ALT Second design	3rd ALT Final design
In 41,000 cycles, fracture is less than one.	3340 cycles: 2/6 crack 15,000 cycles: 4/6 crack	7900 cycles: 1/6 crack 9200 cycles: 3/6 crack 14,000 cycles: 1/6 crack 26,200 cycles: 1/6 crack	41,000 cycles: 6/6 OK 74,000 cycles: 6/6 OK
Hinge kit structure			
Material and specification	C1: Redesigned housing hinge kit C2: Oil damper	C3: Plastic → Al die casting	

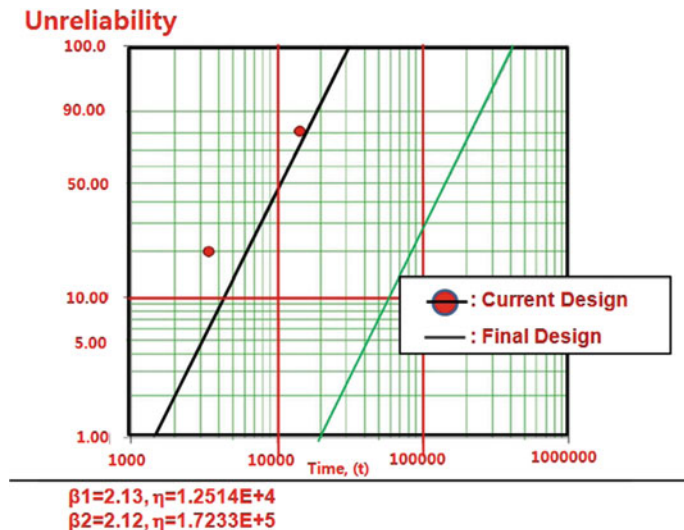


Fig. 9.48 Results of ALT plotted in Weibull chart



Fig. 9.49 Refrigerator and drawer assembly

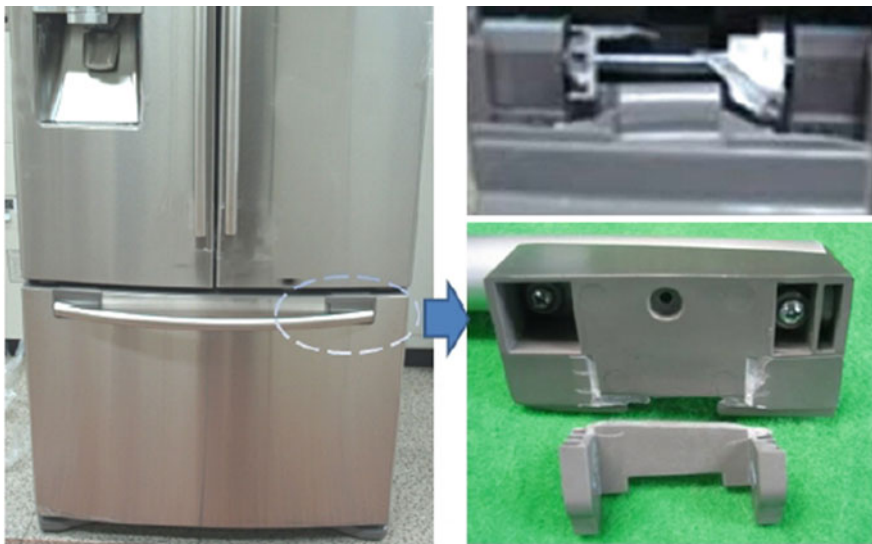


Fig. 9.50 A damaged product after use

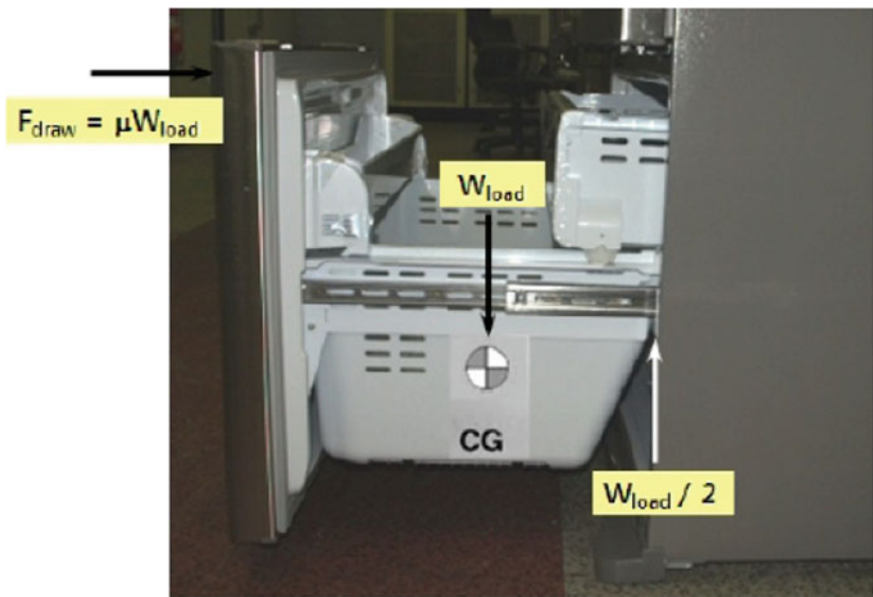
$$TF = A(S)^{-n} = A(F_{draw})^{-\lambda} = A(\mu W_{load})^{-\lambda} \quad (9.27b)$$

The acceleration factor (AF) can be derived as

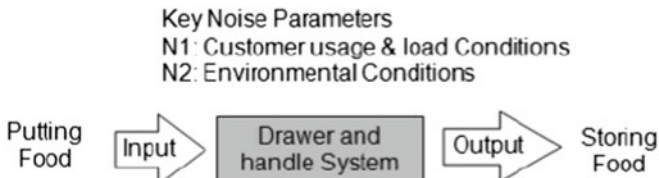
$$AF = \left(\frac{S_1}{S_0} \right)^n = \left(\frac{F_1}{F_0} \right)^\lambda = \left(\frac{\mu W_1}{\mu W_0} \right)^\lambda = \left(\frac{W_1}{W_0} \right)^\lambda \quad (9.28)$$

The normal number of operating cycles for one day was approximately 5; the worst case was 9. Under the worst case, the objective drawer open/close cycles for ten years would be 32,850 cycles. For the worst case, the food weight force on the handle of the drawer was 0.34 kN. The applied food weight force for the ALT was 0.68 kN. With a quotient, λ , of 2, the total AF was approximately 4.0 using Eq. (9.28). The parameter design criterion of the newly designed drawer can be more than the reliability target life—B1 life 10 years. Assuming the shape parameter β was 2.0, the test cycles and test sample numbers calculated in Eq. (8.35) were 67,000 cycles and 3 pieces, respectively. The ALT was designed to ensure a B1 life of 10 years with about a 60% level of confidence that it would fail less than once during 67,000 cycles.

Figure 9.52 shows ALT equipment and duty cycles for the repetitive food weight force, F_{draw} . For the ALT experiments, the control panel on top of the testing equipment started and stopped the drawer during the mission cycles. The food load, F , was controlled by the accelerated weight load in the drawer storage. When a button on the control panel was pushed, mechanical arms and hands pushed and pulled the drawer repetitively.



(a) Design concept of mechanical handle and drawer mechanism



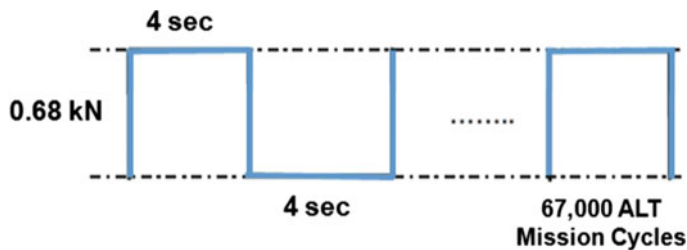
(b) Parameter diagram of handle and drawer system

Fig. 9.51 Functional design concept of the handle and drawer system

The fracture of the drawer in the first occurred in the handle (Fig. 9.53b). On the other hands, in second ALTs slide rails were fractured (Fig. 9.54). These design flaws in the handle and slide rails can result in a fracture when the repetitive food load is applied. To prevent the fracture problem and release the repetitive stresses, the handle and slide rails were redesigned. For first ALT the corrective action plan for the design parameters included: (1) increasing the width of the reinforced handle, C1, from 90 to 122 mm. For second ALT the corrective action plan for the design parameters included: (1) increasing the handle hooker size, C2, from 8 to 19 mm; (2) increasing the rail fastening screw number, C3, from 1 to 2; (3) adding an inner chamber and plastic material, C4, from HIPS to ABS; (4) thickening the boss, C5, from 2.0 to 3.0 mm; (5) adding a new support rib, C6 (Table 9.9).



(a) ALT equipment and controller



(b) Duty cycles of repetitive food weight force on the drawer

Fig. 9.52 ALT equipment and duty cycles

The parameter design criterion of the newly designed samples was more than the reliability target life—B1 life ten years. The confirmed value, β , on the Weibull chart in Fig. 9.55 was 3.1. The reduction factor R also is 0.0014 from the acceleration factor (AF) = 4 and shape parameter (β) = 3.13. Consequently, we know that this parameter ALT is effective to save the testing time and sample size.

For the second ALT, the test cycles and sample size recalculated in Eq. (8.35) were 32,000 and 3 pieces, respectively. In the third ALT, no problems were found with the drawer after 32,000 cycles and 65,000 cycles. We therefore concluded that the modified design parameters were effective. Figure 9.56 shows the results of the 1st ALT and 3rd ALT plotted in a Weibull chart. Table 9.10 provides a summary of the ALT results. With the improved design parameters, B1 life of the samples in the third ALT was lengthened to more than 10.0 years.

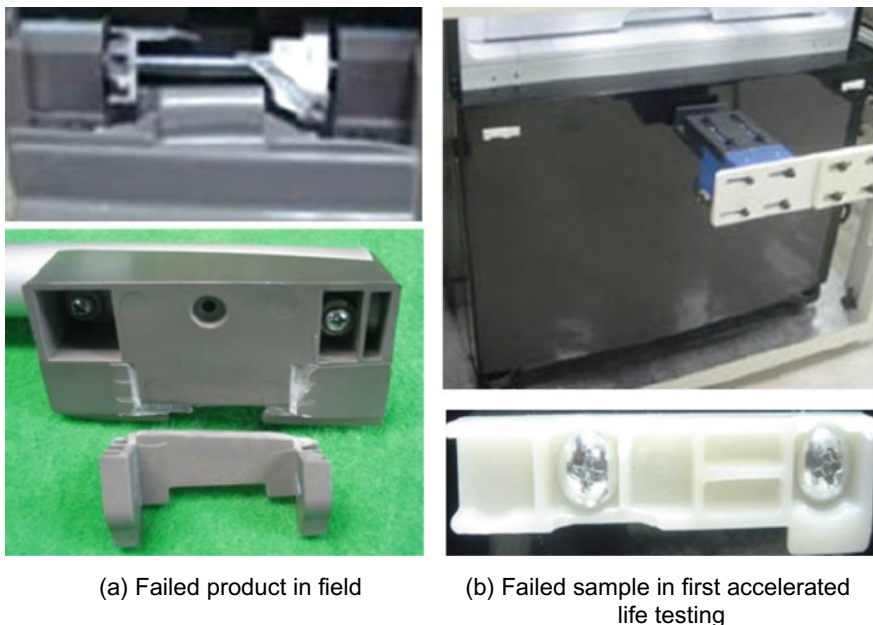
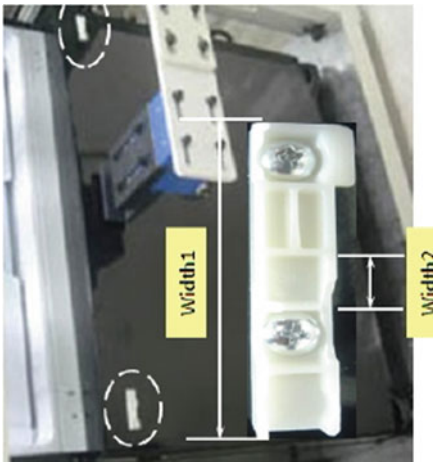


Fig. 9.53 Failed products in field and first ALT



Fig. 9.54 Failed slide rails in second ALT

Table 9.9 Redesigned handle and right/left slide rail

Handle	Right/left slide rail
	 <p>The photograph shows the handle and slide rail assembly. Two dimensions are labeled: Width1 (the distance from the left edge of the rail to the center of the handle) and Width2 (the distance between the two handles).</p> <p>C1: Width L90 mm → L122 mm (1st ALT) C2: Width L8 mm → L19 mm (1st ALT)</p> <p>C3: Rail fastening screw number 1 → 2 (2nd ALT) C4: Chamfer: Corner chamfer C5: Plastic material HIPS → ABS (2nd ALT) C6: Boss thickness 2.0 → 3.0 mm (2nd ALT) C7: New support rib (2nd ALT)</p>

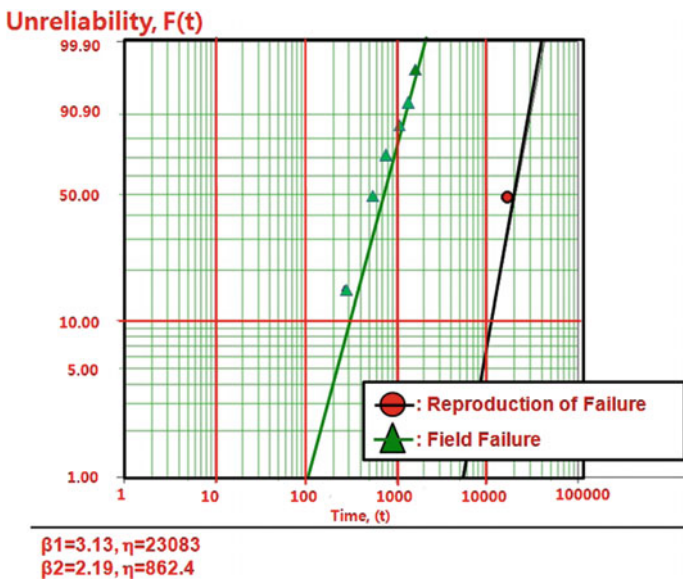


Fig. 9.55 Field data and results of 1st ALT on Weibull chart

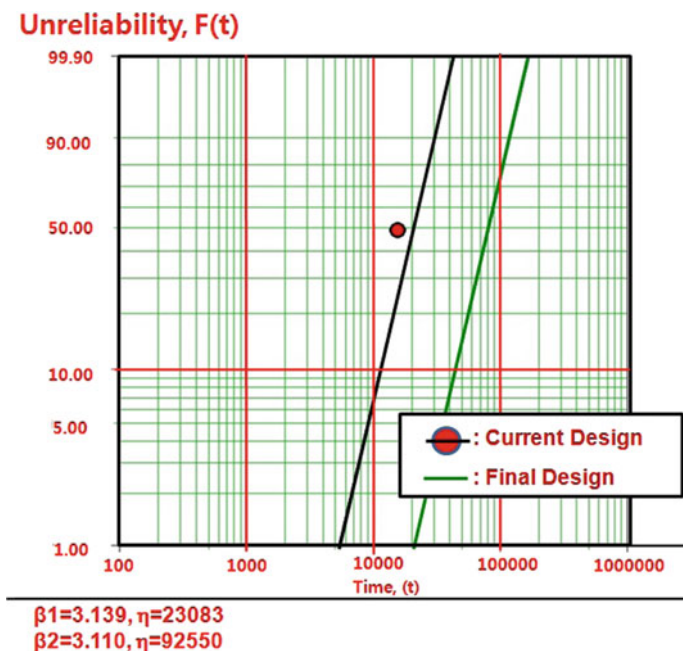
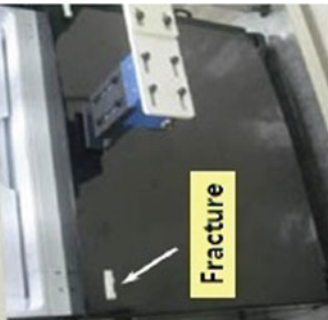


Fig. 9.56 Results of 1st ALT and 3rd ALT plotted in Weibull chart

Table 9.10 Results of ALTs

	1st ALT Initial design	2nd ALT Second design	3rd ALT Final design
In 32,000 cycles, fracture is less than one	7,500 cycles: 2/3 crack 12,000 cycles: 12,000 No problem	16,000 cycles: 2/3 crack	32,000 cycles: 3/3 OK 65,000 cycles: 3/3 OK
Hinge kit structure			
Material and specification	Width1: L90 → L122 Width2: L8 → L19.0	Rib1: new support rib boss: 2.0 → 3.0 mm Chamfer1: Corner Material: HIPS → ABS	

9.7 Compressor Suction Reed Valve

In the field, the suction reed valve in the compressor of the commercial refrigerator had been fracturing, causing loss of the cooling function (Fig. 9.57). The data on the failed products in the field were important for understanding how consumers used the refrigerators and pinpointing design changes that needed to be made to the product. The suction reed valves open and close to allow refrigerant to flow into the compressor during the intake cycle of the piston. Due to design flaws and repetitive stresses, the suction reed valves of domestic refrigerator compressors used in the field were cracking and fracturing, finally leading to failure of the compressor.

The fracture started in the void of the suction reed valve and propagated to the end (Fig. 9.58). Specific customer usage conditions and load patterns leading to the failures were unknown. Because the compressor would lock up when the suction reed valve fractured, the function of refrigerator was lost and customers would ask to have the refrigerator replaced. To solve this problem, it was very important to reproduce the field failure mode of the suction reed valve in the laboratory and correct it.

A refrigerator compressor assembly is a simple mechanical system that operates according to the basic principles of thermodynamics. The compressor receives refrigerant from the low-side (evaporator) and then compresses and transfers it to the high-side (condenser) of the system. Most compressor manufacturers are making every effort to develop more efficient, high-volumetric compressors. For

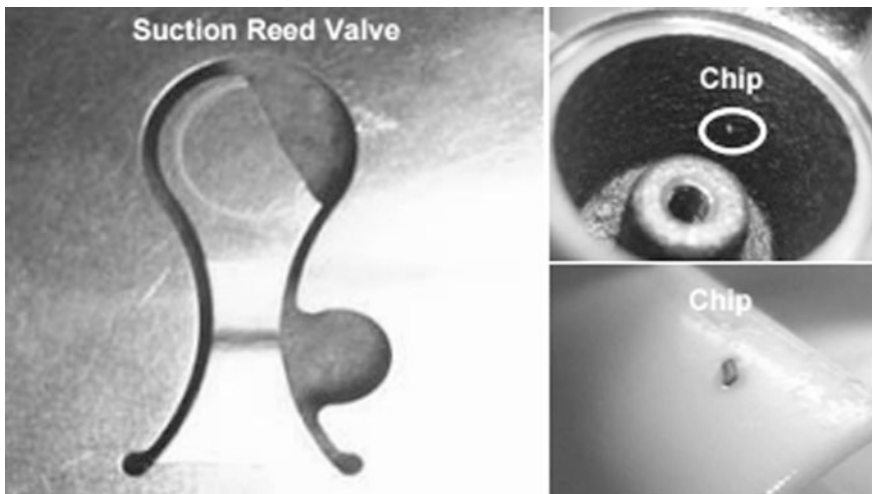


Fig. 9.57 Fracture of the compressor suction reed valve in the field

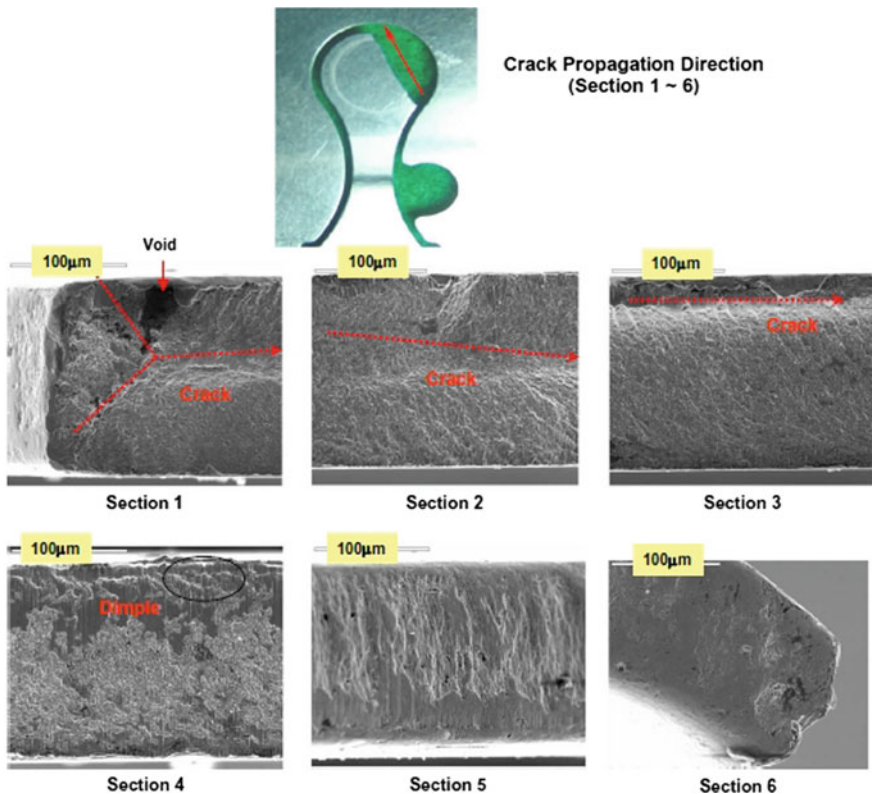


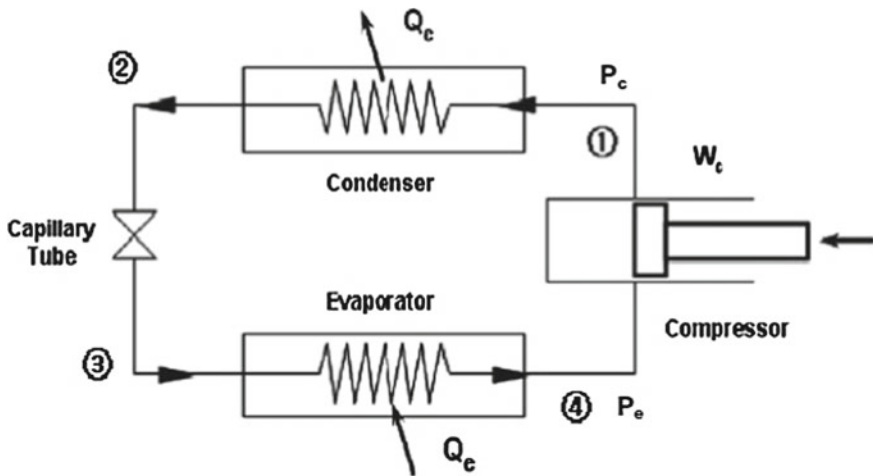
Fig. 9.58 Fractography of the compressor suction reed valve on SEM

these applications, the compressor needs to robustly be designed to operate under a wide range of customer usage conditions. The compressor assembly in the refrigerator in question consists of many mechanical parts, including the crankshaft, piston, valve plate (1), and suction reed valve (2) (see Figs. 9.59 and 9.60).

Analysis of the failed compressors from the field led to the postulate that there were two structural design flaws: (1) the suction reed valve had an overlap with the valve plate; and (2) the valve plate had a sharp edge (Fig. 9.61). When the suction reed valve impacted the valve plate over a long enough period of time, it would fracture.

As previously analyzed in Sect. 9.4, the stress of the compressor depends on the pressure difference suction pressure, P_{suc} , and discharge pressure, P_{dis} . That is,

$$\Delta P = P_{dis} - P_{suc} \cong P_c - P_e \quad (9.29)$$

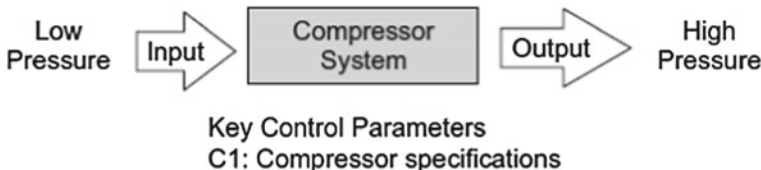


(a) Compressor system in a vapor-compression refrigeration cycle

Key Noise Parameters

N1: Customer Usage & Load Conditions

N2: Environmental Conditions



(b) Parameter diagram of compressor system

Fig. 9.59 Schematic diagram for a compressor system

For a refrigeration system, the time-to-failure, TF , can be modified as

$$TF = A(S)^{-n} \exp\left(\frac{E_a}{kT}\right) = A(\Delta P)^{-\lambda} \exp\left(\frac{E_a}{kT}\right) \quad (9.30)$$

The acceleration factor (AF) can be modified to include the load from Eq. (9.30):

$$AF = \left(\frac{S_1}{S_0}\right)^n \left[\frac{E_a}{k} \left(\frac{1}{T_0} - \frac{1}{T_1} \right) \right] = \left(\frac{\Delta P_1}{\Delta P_0} \right)^\lambda \left[\frac{E_a}{k} \left(\frac{1}{T_0} - \frac{1}{T_1} \right) \right] \quad (9.31)$$

The system was subjected to 22 on-off cycles per day under normal operating conditions. A worst case scenario was also simulated with 98 on-off cycles per day. Under the worst case conditions, the compressor operation for 10 years would be 357,700 cycles.

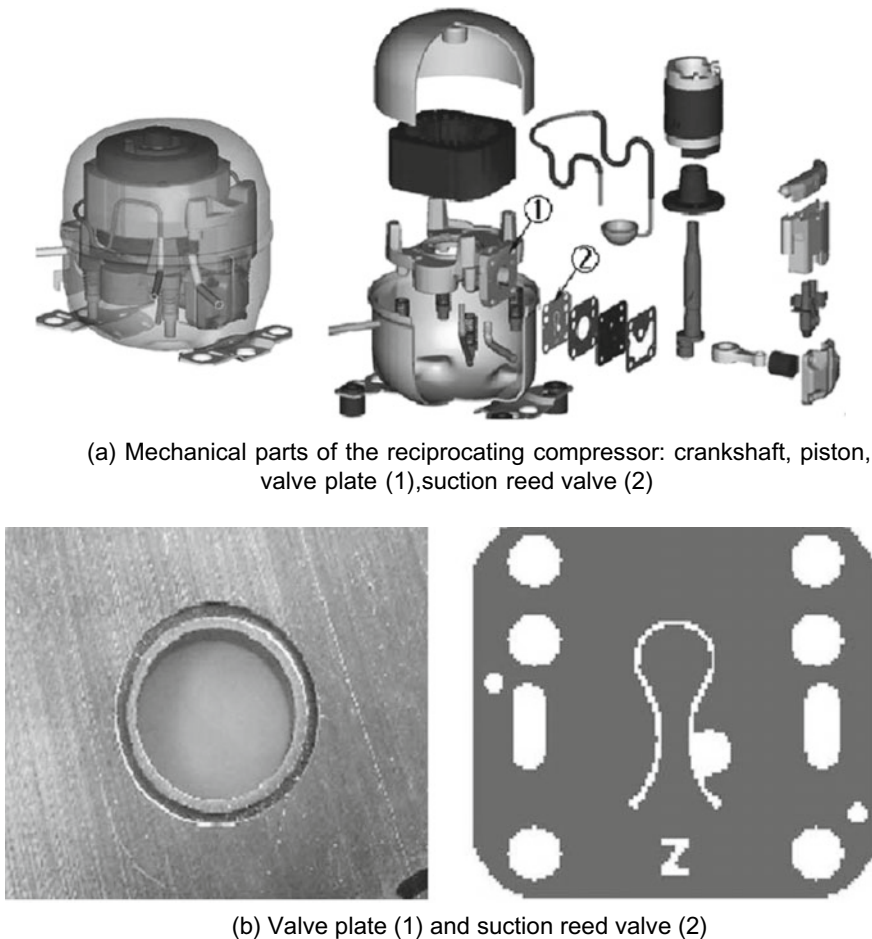


Fig. 9.60 Reciprocating compressor and mechanical parts

From the test data of the worst case, normal pressure was 1.27 MPa and the compressor dome temperature was 90 °C. For accelerated life testing, the acceleration factor (AF) for pressure was 2.94 MPa and the compressor dome temperature was 120 °C. With a quotient, λ , of 2, the total AF was calculated using Eq. (9.26) to be 20.9 (see Table 9.11).

With a shape parameter, β , of 1.9, the test cycles and test sample numbers calculated in Eq. (8.35) were 40,000 cycles and 20 pieces, respectively. The ALT was designed to assure a B1 life 10 years with about a 60% level of confidence that no unit would fail during 40,000 cycles.

For the ALT experiments, a simplified vapor compression refrigeration cycle was fabricated. It consisted of an evaporator, compressor, condenser, and capillary tube. A fan and two 60-W lamps maintained the temperature within the insulated

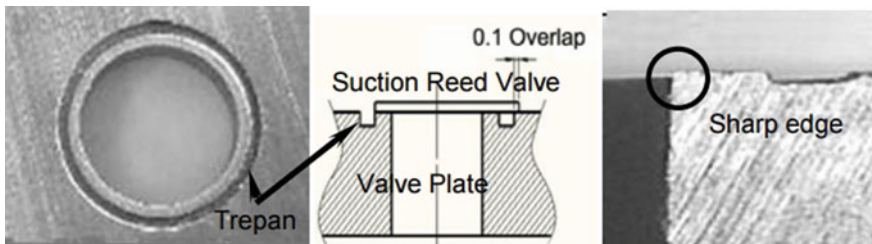


Fig. 9.61 Structure of suction reed and valve plate

Table 9.11 ALT conditions in a vapor-compression cycles

System conditions		Worst case, gauge	ALT, gauge	AF
Pressure, kg/ cm ²	High side	13.0	30.0	5.3③ (= (①/②) ²)
	Low side	0.0	0.0	
	ΔP	13①	30②	
Temp., °C	Dome Temp.	90	120	3.92④
Total AF (= ③ × ④)		—		20.9

(fiberglass) box. A thermal switch attached on the compressor top controlled a 51 m³/h axial fan. The test conditions and test limits were set up on the control board. As the test began, the high-side and low-side pressures could be observed on the pressure gauge (see Fig. 9.62).

One sample in the first ALT ($n = 20$) failed after 8687 cycles. The confirmed value, β , based on field data was 1.9. The shapes and locations of the failures in samples from the first ALT and the field were similar (Fig. 9.63). The reduction

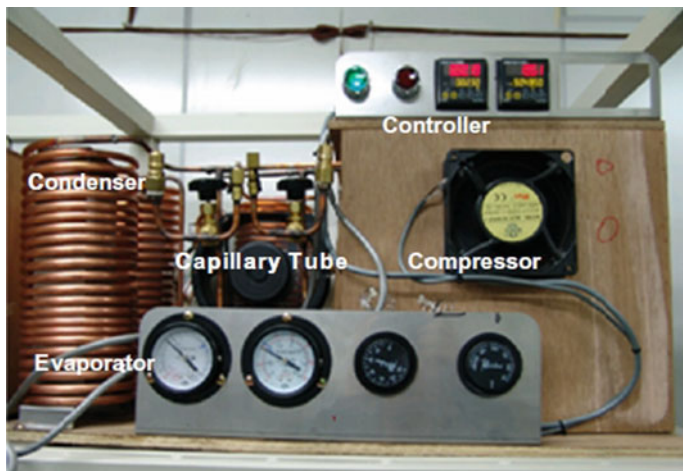


Fig. 9.62 Equipment for the compressor accelerated life tests

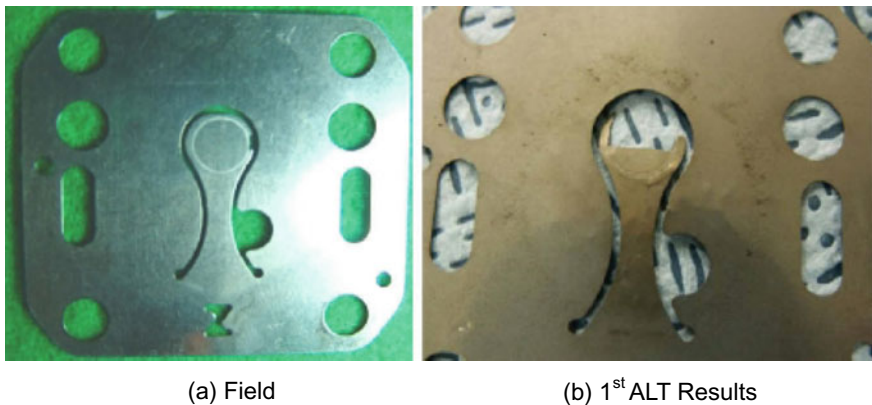


Fig. 9.63 Failure of suction reed valve in marketplace and first ALT result

factor R also is 0.2 from the acceleration factor, $AF = 20.9$ and shape parameter, $\beta = 1.89$. Consequently, we know that this parameter ALT is effective to save the testing time and sample size.

The fracture of the suction reed valve came from its weak structure. It had the following characteristics: (1) an overlap with the valve plate; (2) weak material (0.178t); and (3) a sharp edge on the valve plate, previously mentioned in Fig. 9.61.

When the suction reed valve impacted the valve plate continually, it will suddenly fracture. The dominant failure mode of the compressor was leakage and locking due to the cracking and fracturing of the suction reed valve.

Figure 9.64 shows the redesigned suction reed valve and the valve plate. The valve controls the refrigerant gas during the process of suction and compression in

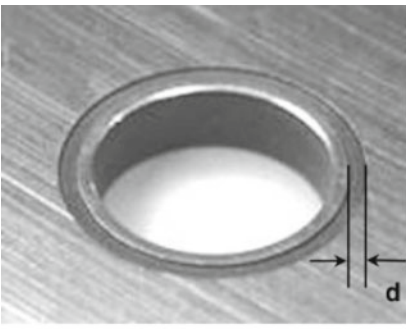
 $d = 0.73 \text{ mm} \rightarrow 1.25\text{mm}$ Adding Ball Peening && Brush Process	 SANDVIK 20C 0.178t (Carbon Steel) \rightarrow SANDVIK 7C 0.178t (Stainless Steel) Adding tumbling process
(a) Valve plate	(b) Suction reed valve

Fig. 9.64 Redesigned suction reed and valve plate

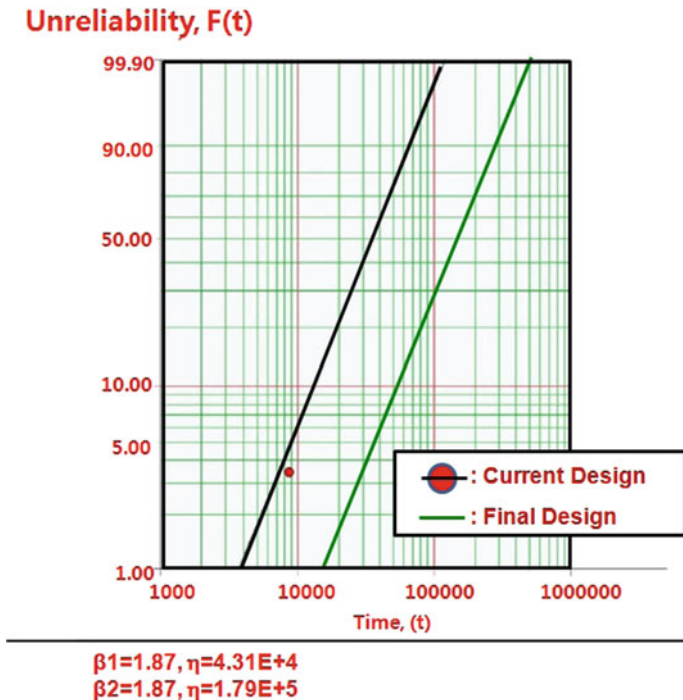


Fig. 9.65 Result of ALTs plotted in Weibull chart

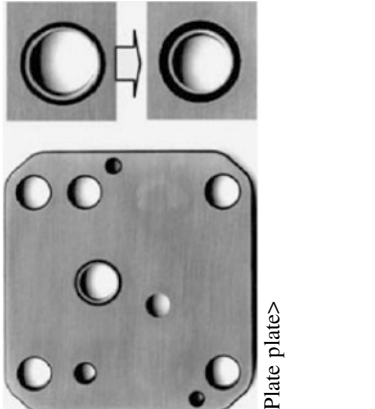
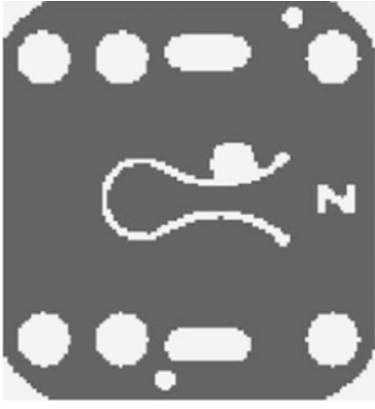
the compressor. The suction reed valve required high bending/impact fatigue properties. The modified design parameters were: (1) increasing the trespan size of the valve plate from 0.73 to 1.25 mm, C1; (2) changing the material property from carbon steel (20C) to stainless steel (7C), C2; (3) adding a ball peening and tumbling process during the treating of suction reed valve, C3.

It would appear that the ALT methodology was valid for reproducing the failure found in the field. First, the location and shape of the fractured suction reed valves from the field and those in the ALT results were similar. Figure 9.65 and Table 9.12 show the graphical results of an ALT plotted in a Weibull chart and the summary of the results of the ALTs, respectively.

9.8 Failure Analysis and Redesign of the Evaporator Tubing

Figure 9.66 shows the Kimchi refrigerator with the aluminum cooling evaporator tubing suggested for cost saving. When a consumer stores the food in the refrigerator, the refrigerant flows through the evaporator tubing in the cooling enclosure

Table 9.12 Results of the ALTs

	1st ALT Initial design	2nd ALT Second design
In 23,000 cycles, crack of suction reed valve is less than 1	8687 cycles: 1/20 8687 cycles: 19/20 stop	23,000 cycles: 60/60 OK 29,000 cycles: 60/60 OK
Suction reed valve and plate structure		
Material and specification		<p><Suction reed valve></p> <p>C1: Trespan size d: 0.73 mm → 1.25 mm C2: Adding ball peening and rush process C3: SANDVIK 20C: 0.178t → 0.203t C4: Extending tumbling 4 h → 14 h</p>



(a) Kimchi Refrigerator



(b) Mechanical parts of the hinge kit system: Inner Case (1), Evaporator tubing (2), Lokring (3), and Cotton adhesive tape (4)

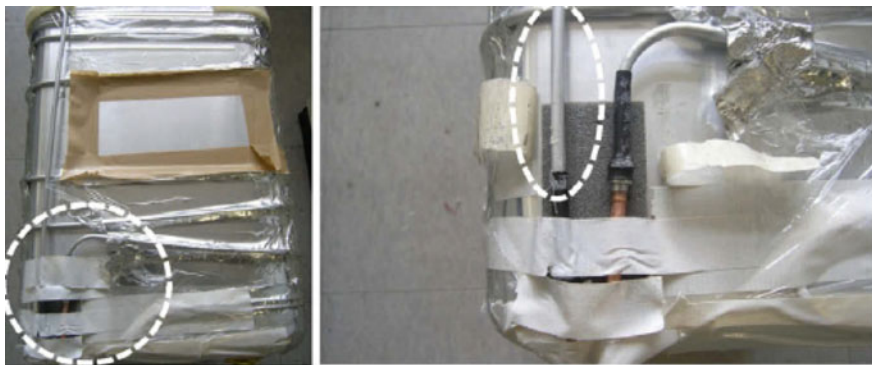
Fig. 9.66 Kimchi refrigerator (a) and the cooling evaporator assembly (b)

to maintain a constant temperature and preserve the freshness of the food. To perform this function, the tube in the evaporator need to be designed to reliably work under the operating conditions it is subjected to by the consumers who purchase and use the Kimchi refrigerator. The evaporator tube assembly in the cooling enclosure consists of an inner case (1), evaporator tubing (2), Lokring (3), and adhesive tape (4), as shown in Fig. 9.66b.

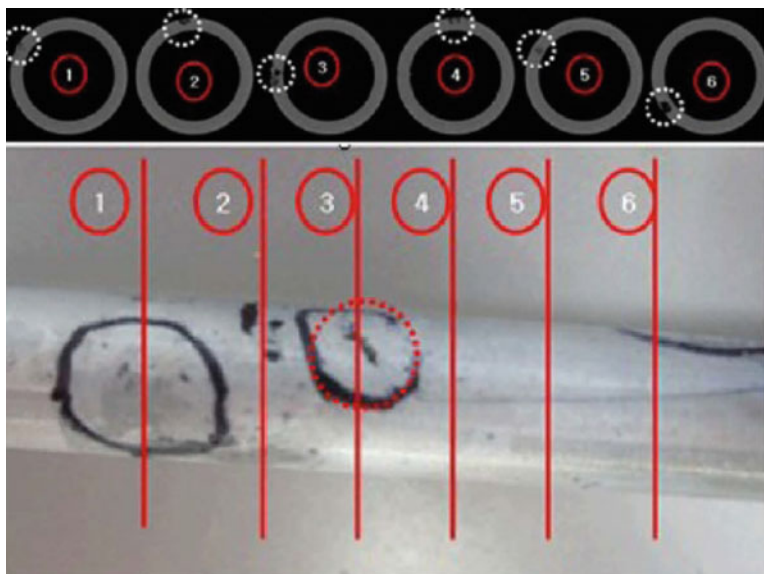
In the field, the evaporator tubing in the refrigerators had been pitting, causing loss of the refrigerant in the system and resulting in the loss of cooling in the refrigerator. The data on the failed products in the field were important for understanding the usage environment of consumers and pinpointing design changes that needed to be made to the product (Fig. 9.67).

Field data indicated that the damaged products might have had design flaws. The design flaws combined with the repetitive loads could cause failure. The pitted surfaces of a failed specimen from the field were characterized by a scanning electron microscopy (SEM) and EDX spectrum (Fig. 9.68). We found a concentration of the chlorine in the pitted surface (Table 9.13). When Ion Liquid Chromatography (ILC) was used to measure the chlorine concentration, the result for the tubing having had the cotton adhesive tape was 14 PPM. In contrast, the chlorine concentration for tubing having had the generic transparent tape was 1.33 PPM. It was theorized that the high chlorine concentration found on the surface must have come from the cotton adhesive tape.

As mentioned in Fig. 9.66, the evaporator tubing assembly in the cooling enclosure of the Kimchi refrigerator consists of many mechanical parts. Depending on the consumer usage conditions, the evaporator tubing experienced repetitive thermal duty loads due to the normal on/off cycling of the compressor to satisfy the



(a) Pitted evaporator tube in field



(b) X-Ray Photography showing a pitting corrosion on the evaporator tube

Fig. 9.67 A damaged product after use

thermal load in the refrigerator. Because the refrigerant temperatures are often below the dew point temperature of the air, condensation can form on the external surface of the tubing.

Figure 9.69 shows a robust design schematic overview of the cooling evaporator system. Figure 9.70 shows the failure mechanism of the crevice (or pitting) corrosion that occurs because of the reaction between the cotton adhesive tape and the aluminum evaporator tubing. As a Kimchi refrigerator operates, water acts as an electrolyte and will condense between the cotton adhesive tape and the aluminum tubing. The crevice (or pitting) corrosion will begin.

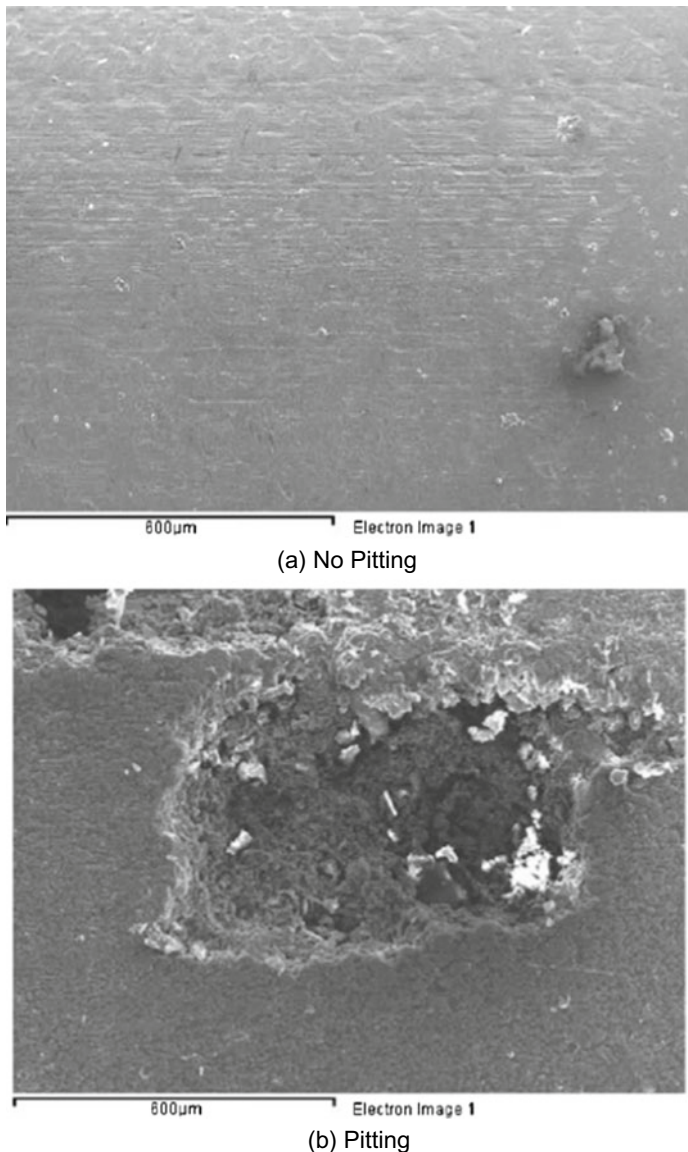


Fig. 9.68 SEM fractography showing a pitting corrosion on the evaporator tube

Table 9.13 Chemical composition of the no pitting and pitting surfaces

	No pitting	Pitting		
	Weight	Atomic	Weight	Atomic
O	11.95	19.65	25.92	37.39
Al	97.29	90.74	69.29	59.61
Cl	0.33	0.23	3.69	2.41
Si	0.42	0.39	0.66	0.55
Ca			0.70	0.40
K			0.50	0.30
Na			0.34	0.34
Totals	100.00		100.00	

Key Noise Parameters

N1: Customer usage & load conditions

N2: Environmental conditions

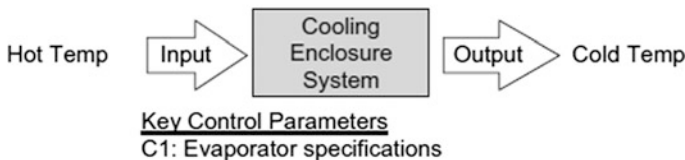


Fig. 9.69 Robust design schematic of a cooling enclosure system

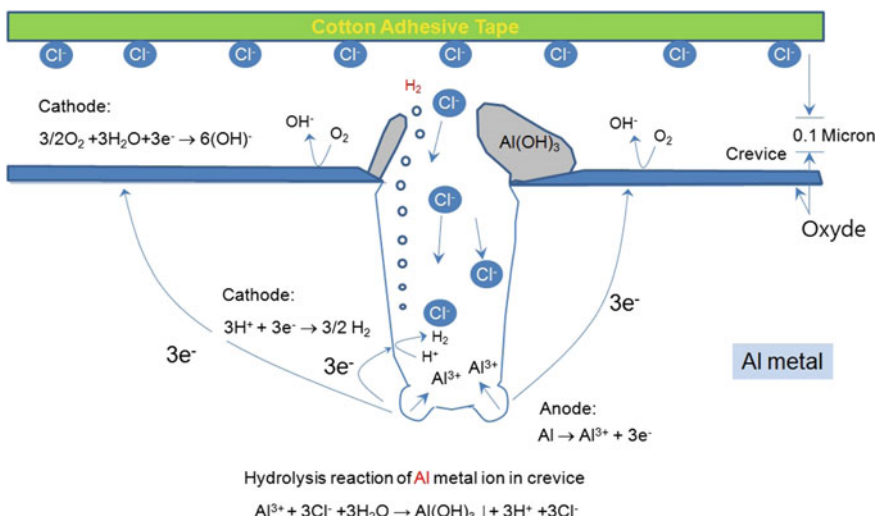


Fig. 9.70 An accelerating corrosion in the crevice due to low PH, high Cl^- concentration, de-passivation and IR drop

The crevice (or pitting) corrosion mechanism on the aluminum evaporator tubing can be summarized as: (1) passive film breakdown by Cl^- attack; (2) rapid metal dissolution: $\text{Al} \rightarrow \text{Al}^{+3} + 3\text{e}^-$; (3) electro-migration of Cl into pit; (4) acidification by hydrolysis reaction: $\text{Al}^{+3} + 3\text{H}_2\text{O} \rightarrow \text{Al}(\text{OH})_3 \downarrow + 3\text{H}^+$; (5) large cathode: external surface, small anode area: pit; (6) the large voltage drop (i.e., “IR” drop, according to Ohm’s Law $V = I \times R$, where R is the equivalent path resistance and I is the average current) between the pit and the external surface is the driving force for propagation of pitting.

The number of Kimchi refrigerator operation cycles is influenced by specific consumer usage conditions. In the Korean domestic market, the compressor can be expected to cycle on and off 22–99 times a day to maintain the proper temperature inside the refrigerator.

Because the corrosion stress of the evaporator tubing depends on the corrosive load (F) that can be expressed as the concentration of the chlorine, the life-stress model (LS model) can be modified as

$$TF = A(S)^{-n} = A(F)^{-\lambda} = A(\text{Cl}\%)^{-\lambda} \quad (9.32)$$

The acceleration factor (AF) can be derived as

$$AF = \left(\frac{S_1}{S_0}\right)^n = \left(\frac{F_1}{F_0}\right)^\lambda = \left(\frac{\text{Cl}_1\%}{\text{Cl}_0\%}\right)^\lambda \quad (9.33)$$

The compressor in a Kimchi refrigerator is expected to cycle on average 22–99 times per day. With a life cycle design point of 10 years, the Kimchi refrigerator incurs 359,000 cycles. The chlorine concentration of the cotton adhesive tape was 14 PPM. To accelerate the pitting of the evaporator tubing, the chlorine concentration of the cotton tape was adjusted to approximately 140 PPM by adding some salt. Using a stress dependence of 2.0, the acceleration factor was found to be approximately 100 in Eq. (9.33).

For B1 life of 10 years, the test cycles and test sample numbers with the shape parameter $\beta = 6.41$ calculated in Eq. (8.35) were 4700 cycles and 19 pieces, respectively. The ALT was designed to ensure a B1 of 10 years life with about a sixty percent level of confidence that it would fail less than once during 4700 cycles. Figure 9.71a shows the Kimchi refrigerators in accelerated life testing and an evaporator tubing in the enclosure contained a 0.2 M NaCl water solution. Figure 9.71b shows the duty cycles for the corrosive force (F) due to the chlorine concentration.

Figure 9.72 shows the failed product from the field and from the accelerated life testing respectively. In the photos, the shape and location of the failure in the ALT were similar to those seen in the field. Figure 9.73 shows a graphical analysis of the ALT results and field data on a Weibull plot. These methodologies were valid in



Fig. 9.71 Kimchi refrigerators in accelerated life testing and duty cycles of repetitive corrosive load F

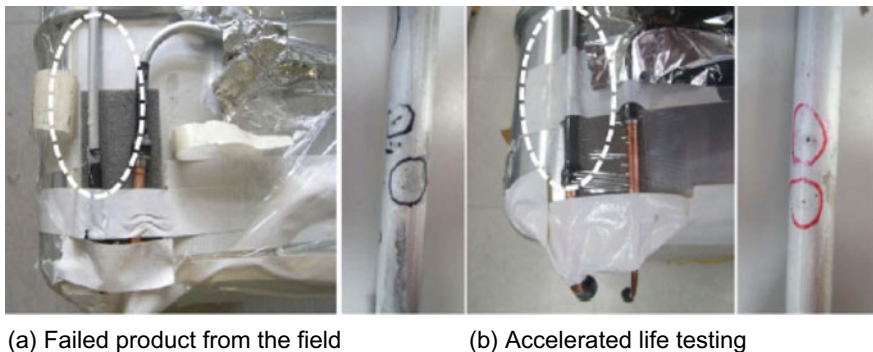


Fig. 9.72 Failed products in field and ALT

pinpointing the weak designs responsible for failures in the field and were supported by two findings in the data. The location and shape also, from the Weibull plot, the shape parameters of the ALT, (β_1), and market data, (β_2), were found to be similar.

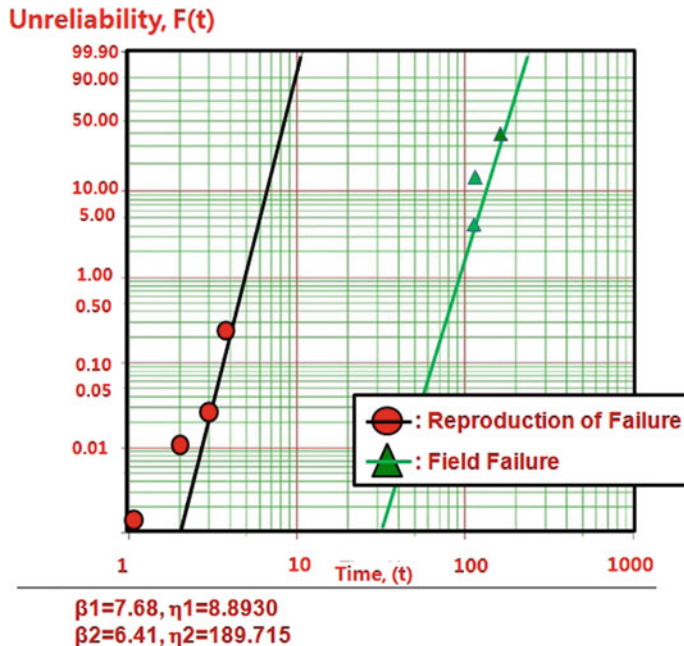


Fig. 9.73 Field data and results of ALT on Weibull chart

The pitting of the evaporator tubing in both the field products and the ALT test specimens occurred in the inlet/outlet of the evaporator tubing (Fig. 9.74). Based on the modified design parameters, corrective measures taken to increase the life cycle of the evaporator tubing system included: (1) extending the length of the contraction tube (C1) from 50.0 to 200.0 mm; (2) replacing the cotton adhesive tape (C2) with the generic transparent tape.

Figure 9.75 shows a redesigned evaporator tubing with high corrosive fatigue strength. The confirmed values of AF and β in Fig. 9.73 were 100.0 and 6.41, respectively. The test cycles and sample size recalculated in Eq. (8.35) were 5300 and 9 EA, respectively. Based on the target BX life, two ALTs were performed to obtain the design parameters and their proper levels. In the two ALTs the outlet of the evaporator tubing was pitted in the first test and was not pitted in the second test.

The repetitive corrosive force in combination with the high chlorine concentration of the cotton tape and the crevice between the cotton adhesive tape and the evaporator tubing contained the condensed water as an electrolyte may have been pitting.

With these modified parameters, the Kimchi refrigerator can reserve the food for a longer period without failure. Figure 9.76 and Table 9.14 show the graphical results of ALT plotted in a Weibull chart and the summary of the results of the ALTs, respectively. Over the course of the two ALTs the B1 life of the samples increased by over 10.0 years.

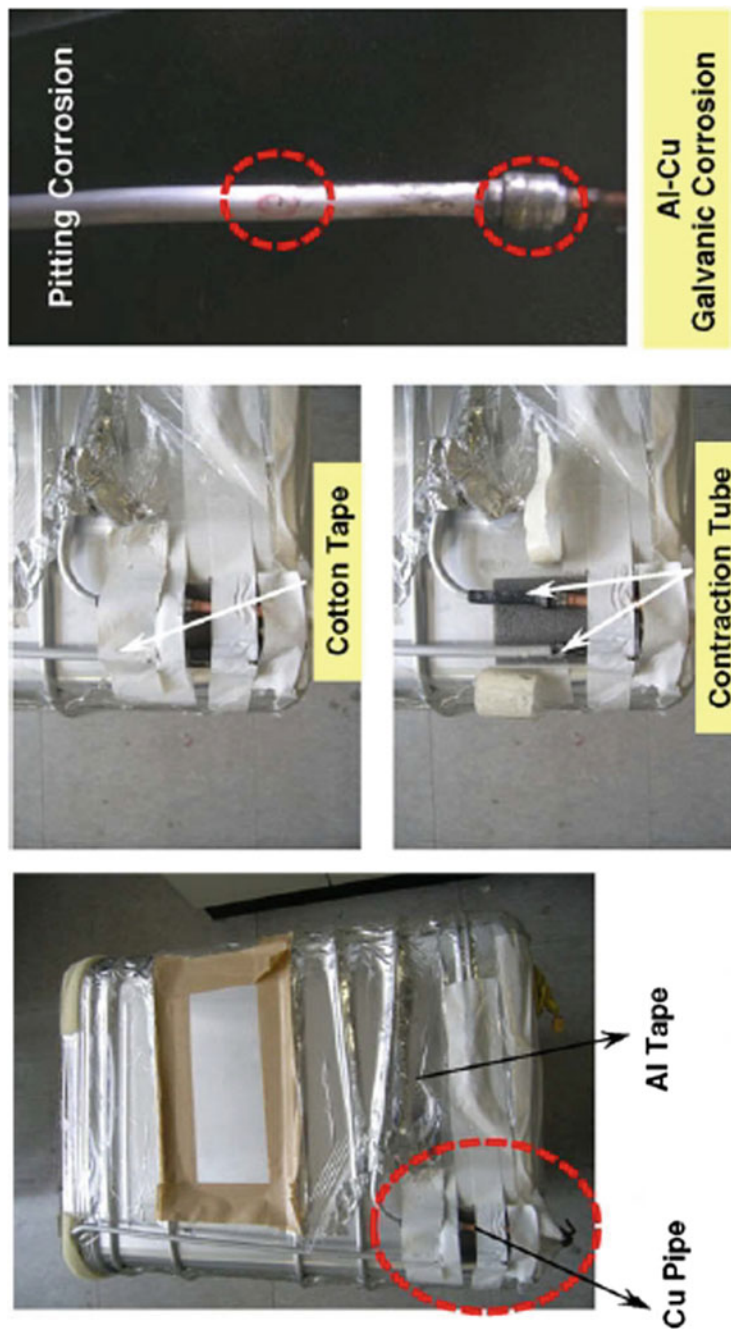


Fig. 9.74 Structure of pitting the corrosion tubing in field and the ALT test specimens

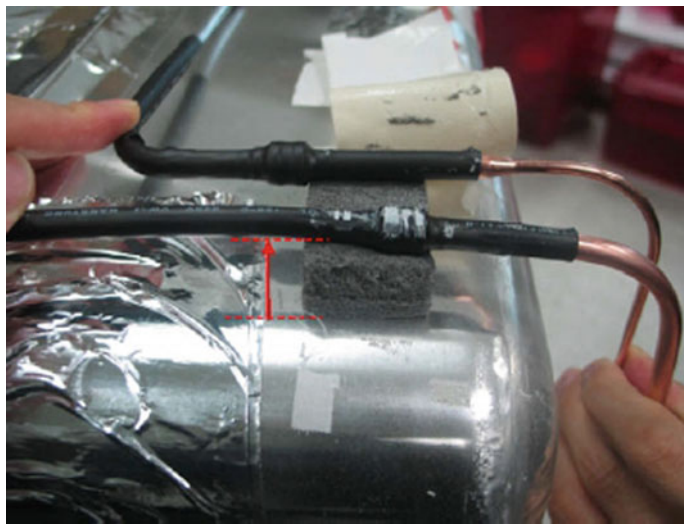


Fig. 9.75 A redesigned evaporator tubing

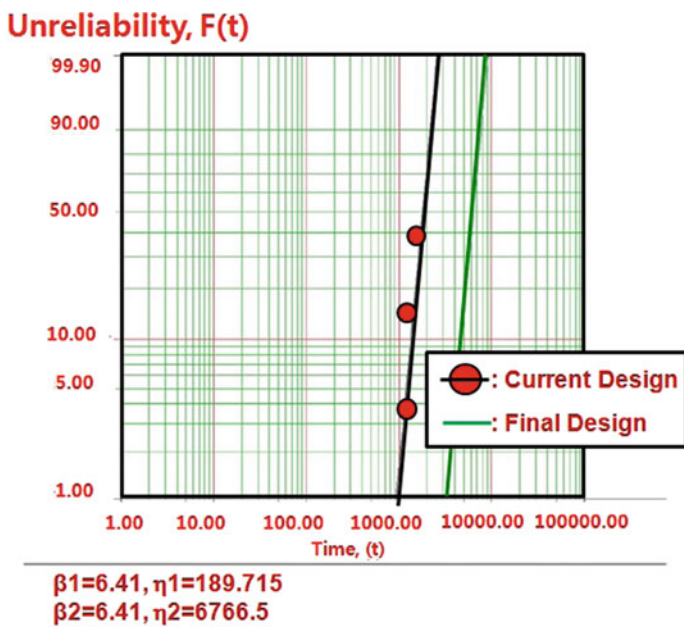


Fig. 9.76 Results of ALT plotted in Weibull chart

Table 9.14 Results of ALT

	1st ALT Initial design	2nd ALT Second design
In 5300 cycles, corrosion of evaporator pipe is less than 1	1130 cycles: 1/19 pitting 1160 cycles: 2/19 pitting 1690 cycles: 4/19 pitting 1690 cycles: 11/19 OK	5300 cycles: 9/9 OK
Evaporator pipe structure		
Material and specification	Length of the contraction tube, C1: 50.0 mm → 200.0 mm Adhesive tape type, C2: cotton type → generic transparent tape	

9.9 Improving the Noise of Mechanical Compressor

A reciprocating compressor is a positive-displacement machine that uses a piston to compress a gas and deliver it at high pressure through slider-crank mechanism. A refrigerator system, which operates using the basic principles of thermodynamics, consists of a compressor, a condenser, a capillary tube, and an evaporator. The vapor compression refrigeration cycle receives work from the compressor and transfers heat from the evaporator to the condenser. The main function of the refrigerator is to provide cold air from the evaporator to the freezer and refrigerator compartments. Consequently, it keeps the stored food fresh.

To improve its energy efficiency, designer would choose the good performance of compressor. Figure 9.77 shows a reciprocating compressor with redesigned rotor and stator. The redesign was developed to improve the energy efficiency and reduce the noise from the compressors in a side-by-side (SBS) refrigerator. For these applications, the compressor needed to be designed robustly to operate under a wide range of consumer usage conditions (Fig. 9.78).

As seen in Fig. 9.79, the reciprocating compressor in the refrigerators had been making noise in the field, causing the consumer to request replacement of their refrigerator. One of the specific causes of compressor failure during operation was the compressor suspension spring. When the sound level during compressor shutdown of problematic refrigerators in the field was recorded, the result was approximately 46 dB (6.2 sones). The design flaws of the suspension spring in the problematic compressor were the number of turns and the mounting spring diameter. When the compressor would stop suddenly, the spring sometimes would not grab the stator frame tightly and would cause the noise.

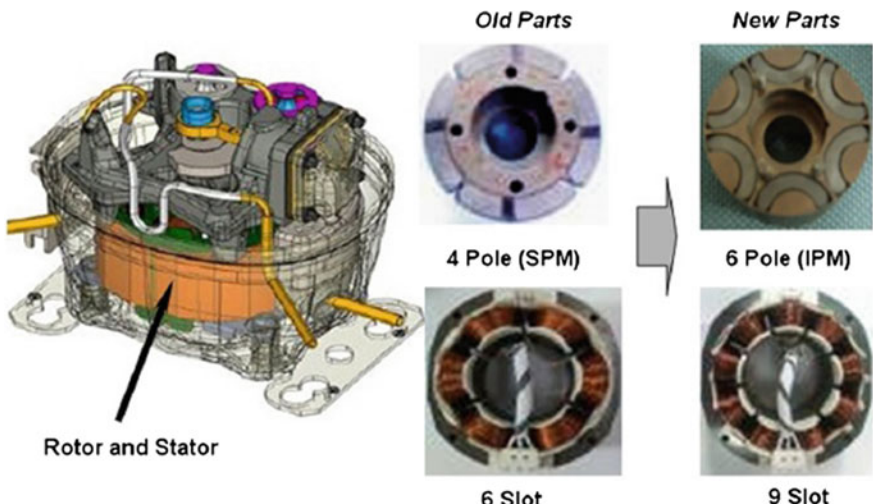
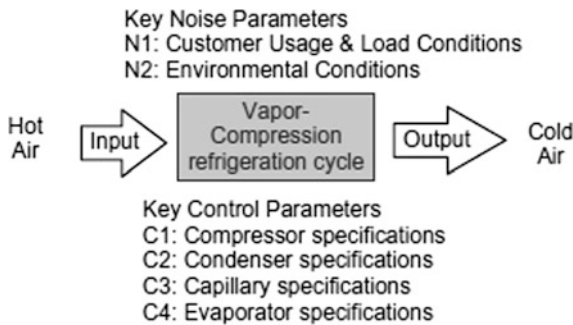
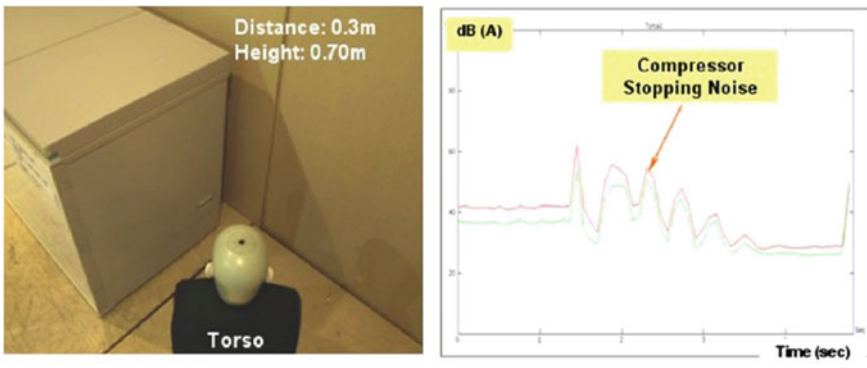
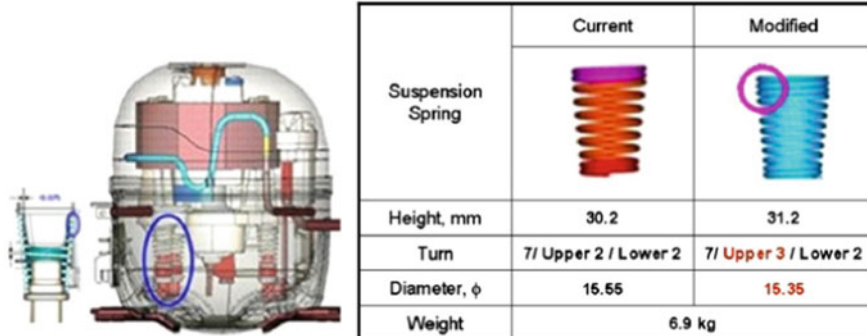


Fig. 9.77 Reciprocating compressors with redesigned rotor and stator

**Fig. 9.78** Parameter diagram of refrigeration cycle

(a) Compressor stopping noise recorded with torso



(b) Reciprocating compressor and the design flaws of suspension spring

Fig. 9.79 Stopping noise of the reciprocating compressor

After identifying the missing control parameters related to the newly designed compressor system, it was important to modify the defective compressor either through redesign of components or change the material used in the components. Failure analysis of marketplace data and accelerated life testing (ALT) can help to confirm the missing key control parameters and their levels in a newly designed compressor system.

To evaluate the ride quality of the new designed stator frame and piston-cylinder assembly mounted on compressor shell, compressor can be modeled as two degree of freedom (Fig. 9.80). Though it is simply four state variables in its model, it serves the purpose of figuring out the compressor motion in operation. The assumed model of the vehicle consists of the sprung mass and the unsprung mass, respectively. The sprung mass m_s represents the stator frame and piston-cylinder assembly, and the unsprung mass m_{us} represents the rotor-stator assembly. The main suspension is modeled as a spring k_s and a damper c_s in parallel, which connects the unsprung to the sprung mass. The compressor suspension spring on its shell is modeled as a spring k_{us} and represents the transfer of the road force to the unsprung mass.

$$m_s \ddot{x}_s + c_s (\dot{x}_s - \dot{x}_{us}) + k_s (x_s - x_{us}) = F \sin \omega t \quad (9.34)$$

$$m_{us} \ddot{x}_{us} + c_s (\dot{x}_{us} - \dot{x}_s) + (k_{us} + k_s)x_{us} - k_s x_s = 0 \quad (9.35)$$

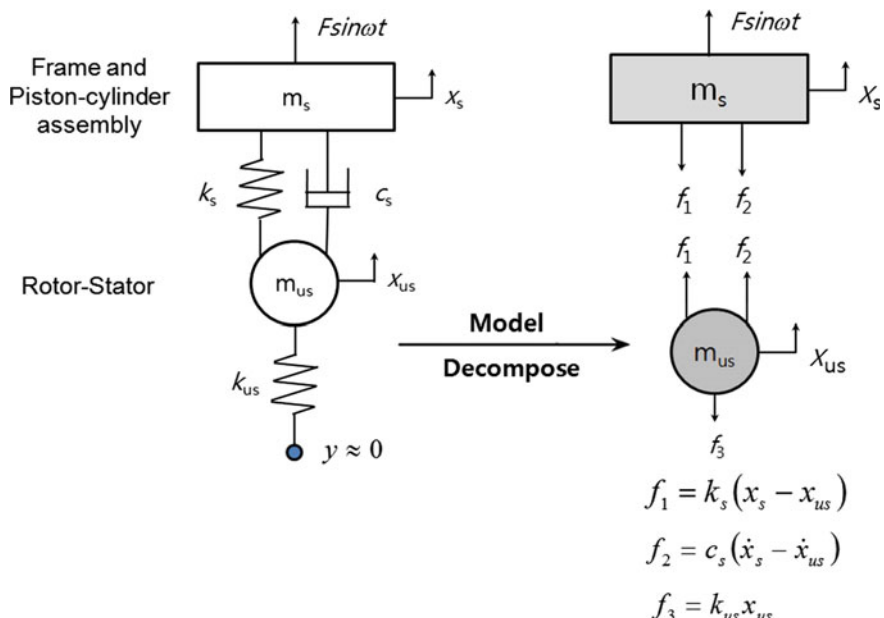


Fig. 9.80 A compressor assembly model and its decomposition

So the above equations of motion can be concisely represented as:

$$\begin{bmatrix} m_s & 0 \\ 0 & m_{us} \end{bmatrix} \begin{bmatrix} \ddot{x}_s \\ \ddot{x}_{us} \end{bmatrix} + \begin{bmatrix} c_s & -c_s \\ -c_s & c_s \end{bmatrix} \begin{bmatrix} \dot{x}_s \\ \dot{x}_{us} \end{bmatrix} + \begin{bmatrix} k_s & -k_s \\ -k_s & k_{us} + k_s \end{bmatrix} \begin{bmatrix} x_s \\ x_{us} \end{bmatrix} = \begin{bmatrix} F \sin \omega t \\ 0 \end{bmatrix} \quad (9.36)$$

As a result, Eq. (9.36) can be expressed in a matrix form

$$[M]\ddot{X} + [C]\dot{X} + [K]X = F \quad (9.37)$$

When Eq. (9.37) is numerically integrated, we can obtain the time response of the state variables. At this time we have to understand the excited force due to the compressor operation.

In a refrigeration cycle design, it is necessary to determine both the condensing pressure, P_c , and the evaporating pressure, P_e . One indicator of the internal stresses on components in a compressor depends on the pressure difference between suction pressure, P_{suc} , and discharge pressure, P_{dis} , previously mentioned in Sect. 9.4.

Because an excited force due to the reciprocating motion of piston comes from pressure difference between the condenser and evaporator, the general life-stress model (LS model) can be modified as:

$$TF = A(S)^{-n} = A(F)^{-\lambda} = A(\Delta P)^{-\lambda} \quad (9.39)$$

The acceleration factor (AF) can be derived as,

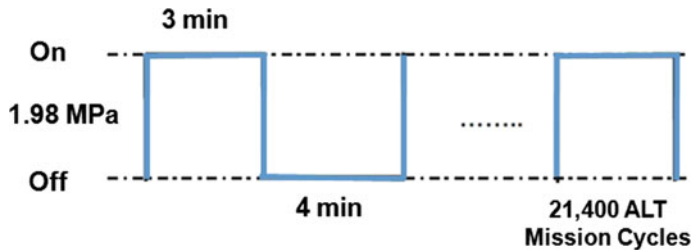
$$AF = \left(\frac{S_1}{S_0} \right)^n = \left(\frac{F_1}{F_0} \right)^\lambda = \left(\frac{\Delta P_1}{\Delta P_0} \right)^\lambda \quad (9.39)$$

The normal number of operating cycles for 1 day was approximately 24; the worst case was 74. Under the worst case, the objective compressor cycles for 10 years would be 270,100 cycles. From the ASHRAE Handbook test data for R600a, the normal pressure was 0.40 MPa at 42 °C and the compressor dome temperature was 64 °C. For the accelerated testing, the acceleration factor (AF) for pressure at 1.96 MPa was 12.6 with a quotient, λ , of 2. The total AF was approximately 29.2 (Table 9.15).

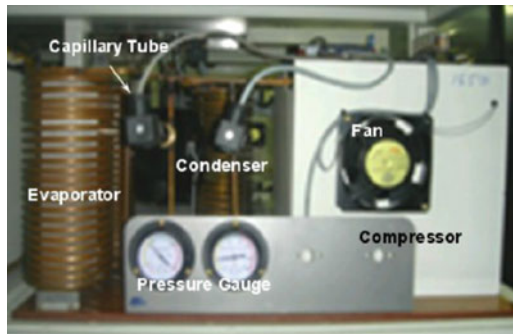
The parameter design criterion of the newly designed compressor can be more than the target life of B1 10 years. Assuming the shape parameter β was 2.0, the test cycles and test sample numbers calculated in Eq. (8.35) were 21,400 cycles and 100 pieces, respectively. The ALT was designed to ensure a B1 of 10 years life with about a 60% level of confidence that it would fail less than once during 21,400 cycles. Figure 9.81a shows the duty cycles for the repetitive pressure difference ΔP . For the ALT experiments, a simplified vapor compression refrigeration system was fabricated (see Fig. 9.81b).

Table 9.15 ALT conditions in a vapor compression cycles for R600a

System conditions		Worst case	ALT	AF
Pressure, MPa	High side	0.40	1.39	12.6
	Low side	0.02	0.4	
	ΔP	0.39	1.35	



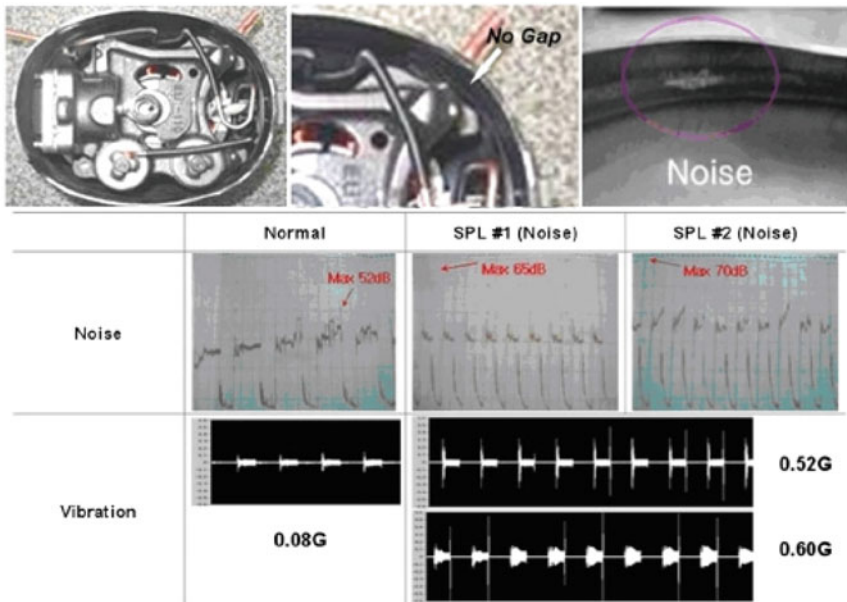
(a) Duty cycles of repetitive pressure difference on the compressor.



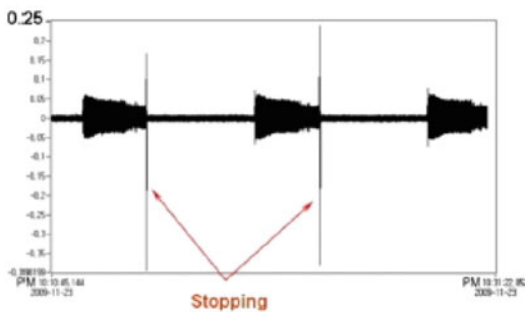
(b) Equipment used in Accelerated life testing.

Fig. 9.81 Duty cycles and equipment used in accelerated life testing

Figure 9.82 shows the stopping noise and vibration of a compressor from the accelerated life testing. In the chart, the peak noise level and vibration of a normal sample in the compressor were 52 dB and 0.09g when it stopped. On the other hand, for the failed sample #1, the peak noise levels and vibration were 65 dB and 0.52g. For the failed sample #2, the peak noise levels and vibration were 70 dB and 0.60g. Considering that the vibration specifications called for less than 0.2g, the failed sample vibrations violated the specification. When the problematic samples in ALT equipment were mounted on the test refrigerator, the vibration also was reproduced with 0.25g and violated the specification. In the field consumer would request the failed samples to be replaced. Figure 9.83 represents the graphical analysis of the ALT results and field data on a Weibull plot. For the shape parameter, the estimated value on the chart was 1.9.



(a) Results in ALT equipment



Unreliability, F(t)

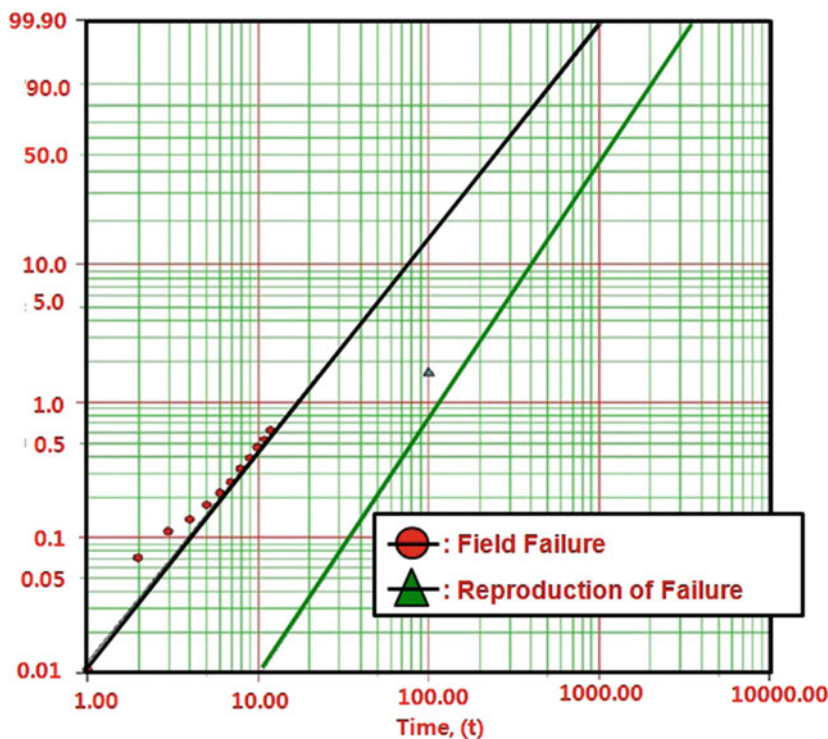
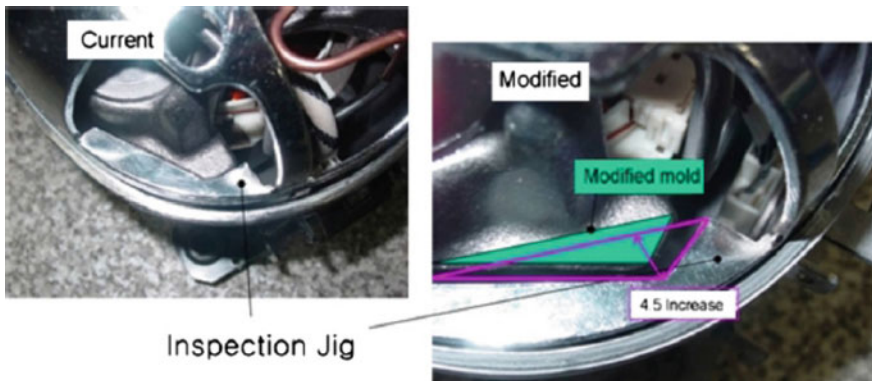
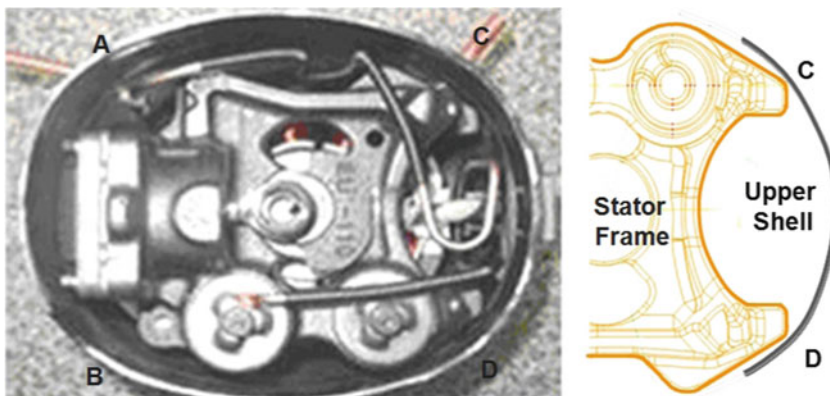


Fig. 9.83 Field data and results of ALT on Weibull chart

When the failed samples were cut apart, a scratch was found inside the upper shell of compressor where the stator frame had hit the shell. The gap between the frame and the shell was measured to be 2.9 mm. The design gap specification should have been more than 6 mm to avoid the compressor hitting the shell for the worst case. It was concluded that the stopping noise came from the hitting (or interference) between the stator frame and the upper shell. Thus, the tests pinpointed the design flaws in compressor (see Fig. 9.84a). For the shape parameter, the estimated value on the chart was 1.9 from the graphical analysis of the ALT results and field data on a Weibull plot. The vital missing parameter in the design phase of the ALT was a gap between the stator frame and the upper shell. These design flaws may make noise when the compressor stops suddenly. To reduce the noise problems in the frame, the shape of the stator frame were redesigned. As the test setup of the compressor assembly was modified to have more than a 6 mm gap, the gap size increased from 2.9 to 7.5 mm (Figs. 9.84b and 9.85).



(a) Modified inspection jig



Gap between frame and upper shell (Spec.: 6mm↑)

A	B	C	D
8.5	9.1	3.2	2.9

(b) Gap between the stator frame and the upper shell

Fig. 9.84 Modified inspection jig and gaps

The parameter design criterion of the newly designed samples was more than the target life, B1, of 10 years. The confirmed value, β , on the Weibull chart was 1.9. When the second ALT proceeded, the test cycles and sample size recalculated in Eq. (8.35) were 21,400 and 100 pieces, respectively. In the second ALT, no problems were found with the compressor in 21,400 cycles. We expect that the modified design parameters are effective.

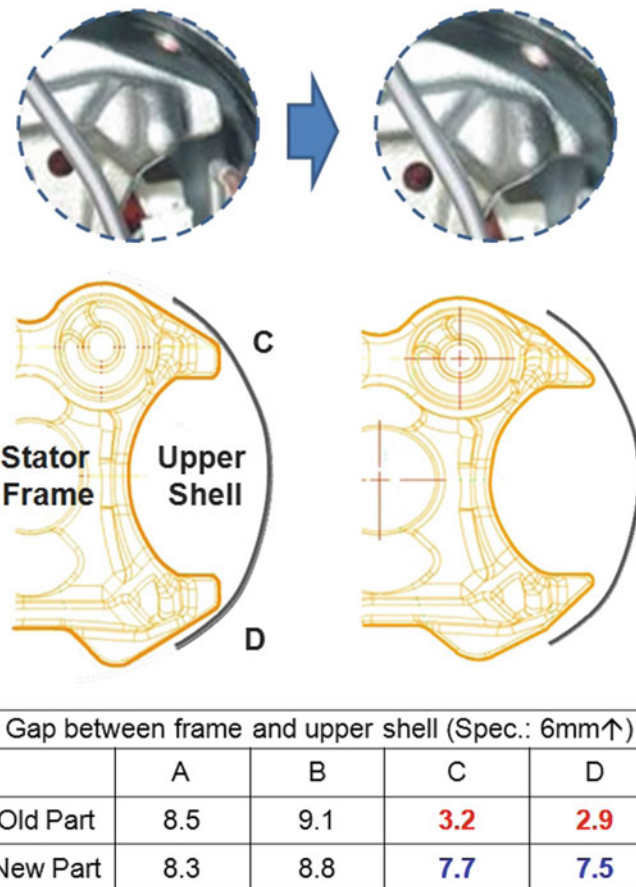


Fig. 9.85 Redesigned stator frame in second ALT

Figure 9.86 shows the results of ALT plotted in a Weibull chart. Table 9.16 provides a summary of the ALT results. With the improved design parameters, the B1 life of the samples in the second ALT lengthens more than 10.0 years.

9.10 French Refrigerator Drawer System

Figure 9.87 shows the French refrigerator with the newly designed drawer system that consists of box-rail mechanism. When a consumer put food inside the refrigerator, they want to have convenient access to it and have the food stay fresh. For this to occur, the draw system needs to be designed to withstand the operating conditions it is subjected to by users. The drawer assembly consists of a box, left/right of the guide rail, and a support center, as shown in Fig. 9.87b.

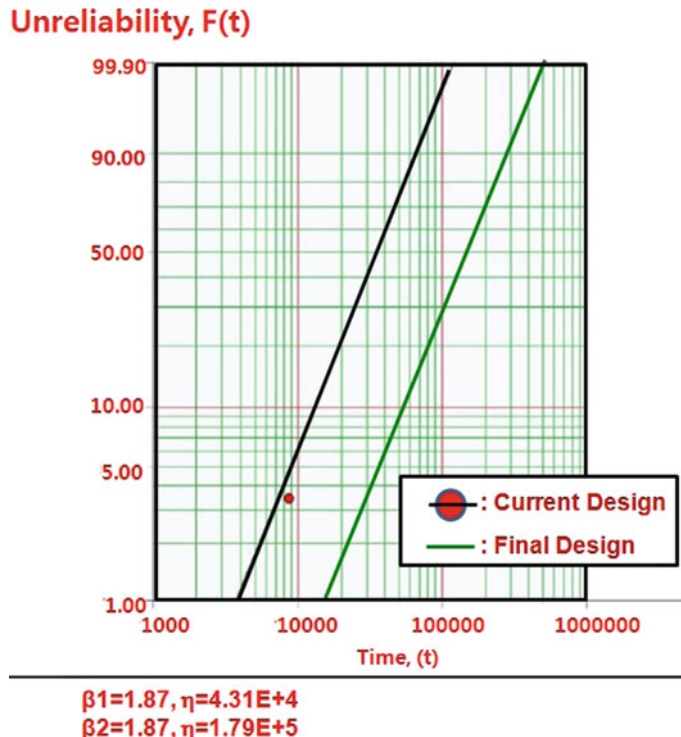


Fig. 9.86 Results of ALT plotted in Weibull chart

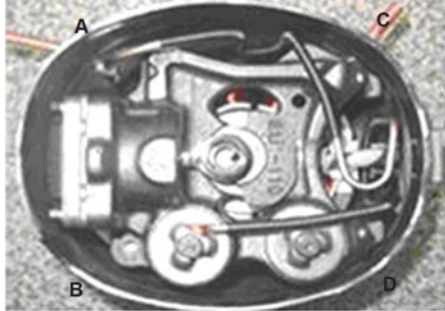
In the field, parts of the drawer system of a French refrigerator were failing due to cracking and fracturing under unknown consumer usage conditions. Thus, the data on the failed products in the field were important for understanding the usage environment of consumers and helping to pinpoint design changes that needed to be made in the product (Fig. 9.88).

Field data indicated that the damaged products might have had structural design flaws, including sharp corner angles and weak ribs that resulted in stress risers in high stress areas. These design flaws that were combined with the repetitive loads on the drawer system could cause a crack to occur, and thus cause failure.

The drawer assembly consists of many mechanical structural parts. Depending on the consumer usage conditions, the drawer assembly receives repetitive mechanical loads when the drawer is open and closed. Putting and storing food in the drawer involves two mechanical processes: (1) the consumer opens the drawer to store or take out the stored food and (2) they then close the drawer by force.

Figure 9.89 shows the functional design concept of the drawer system and its robust design schematic overview. As the consumer stores the food, the drawer system helps to keep the food fresh. The stress due to the weight load of the food is concentrated on the drawer box and its support rails. And thus it is important to overcome these repetitive stresses when designing the drawer.

Table 9.16 Results of ALT

	1st ALT	2nd ALT								
	Initial design	Second design								
In 21,400 cycles, locking is less than 1	100 cycles: 2/100 noise 100 cycles: 99/100 OK	21,400 cycles: 100/100 OK 20,000 cycles: 100/100 OK								
Compressor structure	 <p>Gap between frame and upper shell (Spec.: 6mm↑)</p> <table border="1"> <thead> <tr> <th>A</th> <th>B</th> <th>C</th> <th>D</th> </tr> </thead> <tbody> <tr> <td>8.5</td> <td>9.1</td> <td>3.2</td> <td>2.9</td> </tr> </tbody> </table>	A	B	C	D	8.5	9.1	3.2	2.9	
A	B	C	D							
8.5	9.1	3.2	2.9							
Material and specification	C1: Modification of the frame shape									



(a) French refrigerator (b) Mechanical parts of drawer: 1) a box, 2) left/right of the guide rail, and 3) a support center

Fig. 9.87 French refrigerator with the newly designed drawer system



Fig. 9.88 A damaged products after use

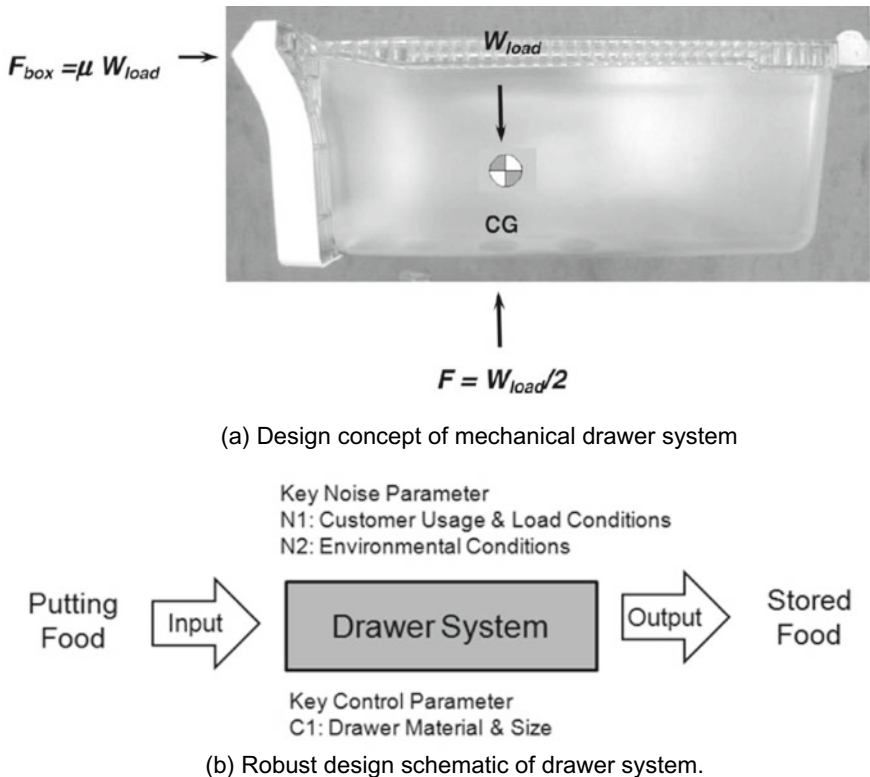


Fig. 9.89 Design concept and robust design schematic of mechanical drawer system

The number of drawer open and close cycles will be influenced by consumer usage conditions. In the United States, the typical consumer requires the drawer system of a French refrigerator to open and close between five and nine times a day.

The force balance around the drawer system can be represented as,

$$F_{\text{box}} = \mu W_{\text{load}} \quad (9.40)$$

Because the stress of the drawer system depends on the applied force from the foods weight, the life-stress model (LS model) can be expressed as

$$TF = A(S)^{-n} = A(F_{\text{box}})^{-\lambda} = A(\mu W_{\text{load}})^{-\lambda} \quad (9.41)$$

The acceleration factor (AF) can be derived as

$$AF = \left(\frac{S_1}{S_0}\right)^n = \left(\frac{F_1}{F_0}\right)^{\lambda} = \left(\frac{\mu W_1}{\mu W_0}\right)^{\lambda} = \left(\frac{W_1}{W_0}\right)^{\lambda} \quad (9.42)$$

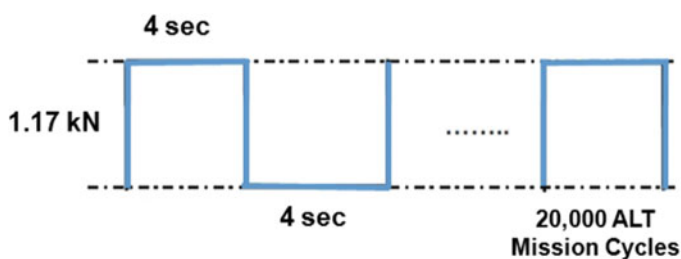
The open and closing of the drawer system occurs an estimated average five to nine times per day. With a life cycle design point of 10 years, the drawer would occur about 32,900 usage cycles. For the worst case, the weight force on the drawer is 0.59 kN which is the maximum force applied by the typical consumer. The applied weight force for the ALT was 1.17 kN. Using a stress dependence of 2.0, the acceleration factor was found to be approximately 4.0 using Eq. (9.42).

For B1 life, the test cycles and test sample numbers calculated in Eq. (8.35) were 39,000 cycles and six pieces, respectively. The ALT was designed to ensure a B1 life of 10 years life with about a 60% level of confidence that it would fail less than once during 39,000 cycles.

Figure 9.90 shows the experimental setup of the ALT with the test equipment and the duty cycles for the opening and closing force F . The control panel on the top of the testing equipment started and stopped the equipment, and indicated the completed test cycles and the test periods, such as sample on/off time. The drawer



(a) Equipment used in accelerated life testing.



(b) Duty cycles of repetitive load F on the drawer system

Fig. 9.90 Equipment used in accelerated life testing and duty cycles

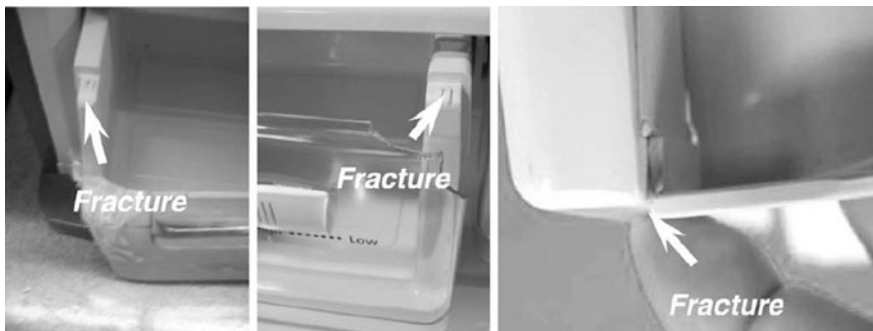


Fig. 9.91 Failed products in field (left) and 2nd ALT (right)

opening and closing force, F , was controlled by the accelerated weight load in the drawer system. When the start button in the controller panel gave the start signal, the simple hand-shaped arms held the drawer system. The arms then pushed and pulled the drawer with the accelerated weight force (1.17 kN).

Figure 9.91 shows the failed product from the field and from the accelerated life testing, respectively. In the photos, the shape and location of the failure in the ALT were similar to those seen in the field. Figure 9.92 represents the graphical analysis of the ALT results and field data on a Weibull plot.

The shape parameter in the first ALT was estimated at 2.0. For the final design, the shape parameter was obtained from the Weibull plot and was determined to be 3.6. These methodologies were valid in pinpointing the weak designs responsible for failures in the field and were supported by two findings in the data. In the photo, the shape and location of the broken pieces in the failed market product are identical to those in the ALT results. And the shape parameters of the ALT (β_1) and market data (β_2) were found to be similar from the Weibull plot. The reduction factor R also is 0.034 from the acceleration factor = 4.0 and shape parameter = 1.9. Consequently, we know that this parameter ALT is effective to save the testing time and sample size.

Initially when the accelerated load of 12 kg was put into drawer, the center support rail was bent and the rollers on the left and right rail were broken away (Fig. 9.93). The design flaws of the bent center rail and the breakaway roller resulted in drawers not sliding. The rail systems could be corrected by adding reinforced ribs on the center support rail as well as extruding the roller support to 7 mm (Table 9.17).

The fracture of the drawer in both the field products and the ALT test specimens occurred in the intersection areas of the box and its cover (Fig. 9.94). The repetitive food loading forces in combination with the structural design flaws may have caused the fracturing of the drawer. The design flaws of no corner rounding and poorly enforced ribs resulted in the high stress areas. These flaws can be corrected by implementing the fillets and thickening the enforced ribs (Table 9.17).

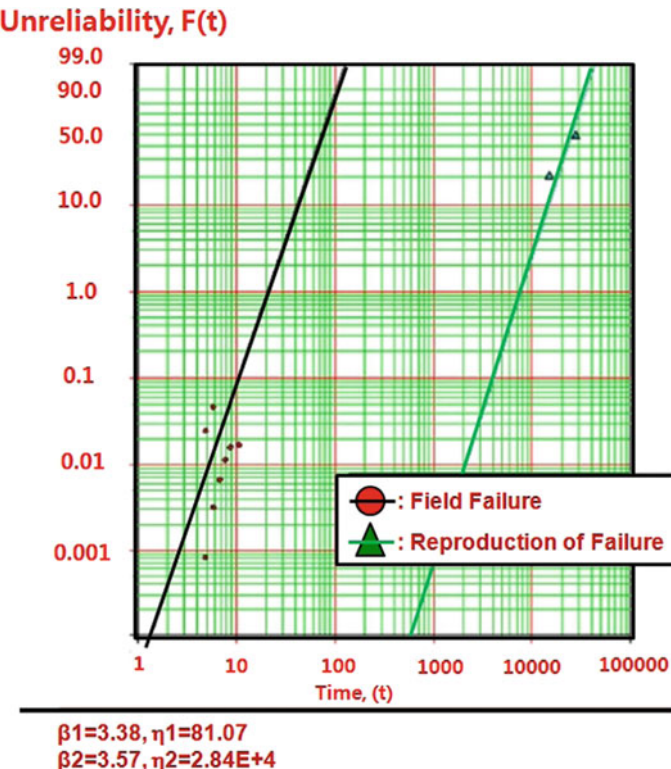


Fig. 9.92 Field data and results of ALT on Weibull chart

The confirmed values of AF and β in Fig. 9.92 were 4.0 and 3.6, respectively. The test cycles and sample size recalculated in Eq. (8.35) were 20,000 and six pieces, respectively. Based on the targeted B1 life of 10 years, third ALTs were performed to obtain the design parameters and their proper levels. Due to repetitive stresses, the left and right rails of the drawer system cracked (Fig. 9.95a) and the roller of the support center was sunken (Fig. 9.95b) in the first ALTs. Thus, a rib extruded 2 mm from the center support rail. And the left and light rail systems were corrected by design changes such as corner rounding and inserting ribs (Table 9.17).

Table 9.18 gives a summary of the results of the ALTs, respectively. Figure 9.96 shows the results of ALT plotted in a Weibull chart. With these modified parameters, the French refrigerator can smoothly open and close the drawers for a longer period without failure.

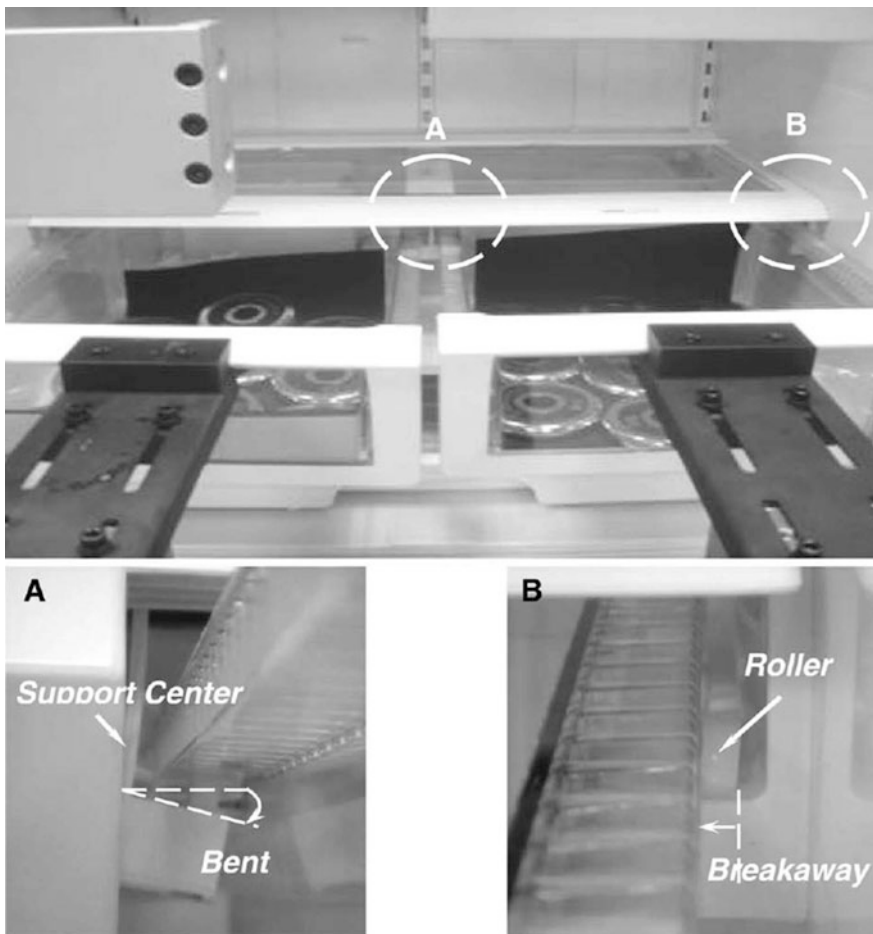
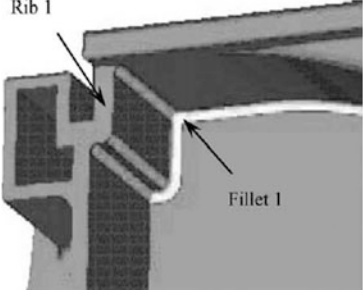
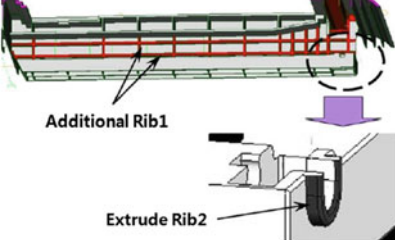


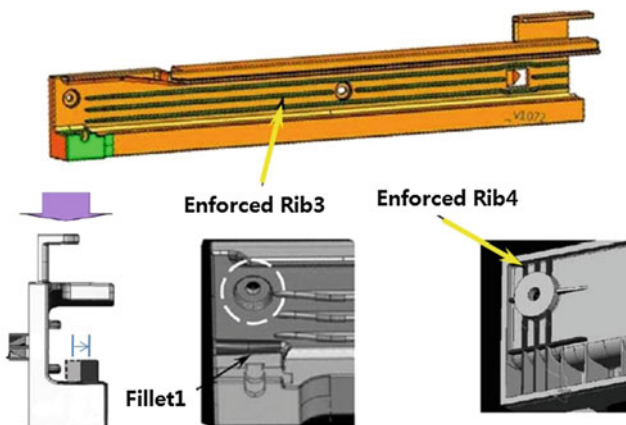
Fig. 9.93 Structural problems of the left, right, and center support rails in loading

9.11 Improving Reliability of the Hinge Kit System (HKS) in Refrigerator

When a consumer opens and closes a Kimchi refrigerator door, they should be able to accomplish this with minimal effort. Originally HKS was the spring mechanism that could decrease the speed of door closing due to door weight. Because its damping effects at 0° – 10° (door angle) were not up to much, the spring-damper mechanism in HKS was changed to improve this. Before launching newly designed HKS, we had to find the design faults and verify its reliability. The hinges of a door are a component of the door that is subjected to repetitive use over the life of the refrigerator. A new hinge kit system (HKS) was designed for the Kimchi

Table 9.17 Redesigned box and center support rail

Box	Center support rail
	
C1: Rib1 T2.0 mm → T3.0 mm C2: Fillet R0.0 mm → R1.0 mm <u>Guide rail (left/right)</u>	C3: Rib2 new added rib C4: Extending Rib1 L0.0 mm → L2.0 mm

**Extrude 1: Roller 7mm outside**

C5: Rib3 (new added rib, loading test)
C6: Extruder roller L0.0 mm → L7.0 mm
C7: Fillet R3 mm → R4 mm
C9: Rib4 new added back rib

refrigerator (see Fig. 9.97a) to improve the ease of opening and closing the door for the consumer. The HKS is shown in Fig. 9.97b consists of a kit cover, shaft, spring, and oil damper, etc.

The functional loss of the original HKS had been reported often by owners of the refrigerator. Thus, exact data analysis was required to find out the root cause of the defective HKS and what parameter in the HKS needed to be redesigned.



Fig. 9.94 Structure of failing drawer system in field

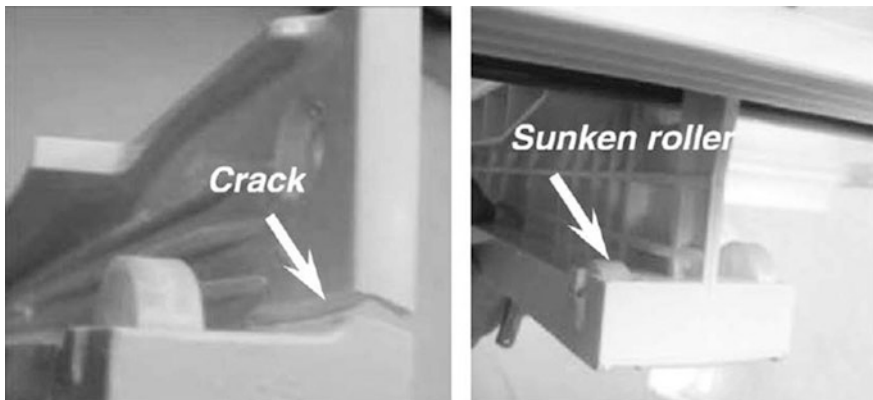


Fig. 9.95 Structural problems of the left/right rail (left) and center support rails (right) in 1st ALT

Figure 9.98 shows a damaged HKS which has two cracks that appeared after a period of use. It was not known under what usage conditions the failure occurred. When comprehensive data from the field were reviewed, it was concluded that the root cause of the HKS failure was a structural design flaw—no round of torsional shaft. Moreover, due to the repetitive loading of the opening and closing of the door, this design defect eventually led to creating the cracks of HKS.

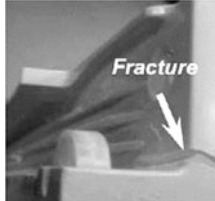
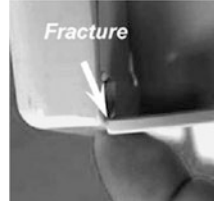
Figure 9.99 shows the robust design schematic overview of the HKS. Depending on the consumer usage conditions, HKS were subjected to different loads during the opening and closing of the refrigerator door.

Because the HKS is a relatively simple structure, it can be modeled with a simple force-moment equation (see Fig. 9.100). As the consumer opens or closes the refrigerator door, the stress due to the weight momentum of the door is concentrated on HKS.

The number of door closing cycles will be influenced by specific consumer usage conditions. The door system of the refrigerator is required to be opened and closed between three and ten times a day in the Korean domestic market.

The moment balance around the HKS can be represented as

Table 9.18 Results of ALT

	1st ALT Initial Design	2nd ALT Second Design	3rd ALT Final Design
In 20,000 cycles, fracturing is less than 1	3900 cycles: 3/6 fail 3900 cycles: 3/6 OK	15,000 cycles: 2/6 fail 29,000 cycles: 1/6 fail 29,000 cycles: 3/6 OK	20,000 cycles: 6/6 OK 45,000 cycles: 6/6 OK
Drawer structure			
Material and specification	Redesigned rail C1: Rib3 new added rib C2: Extrude1: L 0.0 mm → L 7.0 mm C3: Fillet2: R3 mm → R4 mm C4: Rib4: new added back	Redesigned box C5: Rib1 T2.0 mm → T3.0 mm C6: Fillet1 R0.0 mm → R1.0 mm	

$$M_0 = W_{door} \times b = T_0 = F_0 \times R \quad (9.43)$$

The moment balance around the HKS with an accelerated weight can be represented as

$$M_1 = M_0 + M_A = W_{door} \times b + W_A \times a = T_1 = F_1 \times R \quad (9.44)$$

Because F_0 is impact force in normal conditions and F_1 is impact force in accelerated weight, the stress on the HKS depends on the applied impact. Under the same temperature and load, the life-stress model (LS model) and can be modified as

$$TF = A(S)^{-n} = AT^{-n} = A(F \times R)^{-n} \quad (9.45)$$

The acceleration factor (AF) can be derived as

$$AF = \left(\frac{S_1}{S_0}\right)^n = \left(\frac{T_1}{T_0}\right)^n = \left(\frac{F_1 \times R}{F_0 \times R}\right)^n = \left(\frac{F_1}{F_0}\right)^n \quad (9.46)$$

Generally, the operating conditions for the HKS in a Kimchi refrigerator were approximately 0–43 °C with a relative humidity ranging from 0 to 95%, and 0.2–

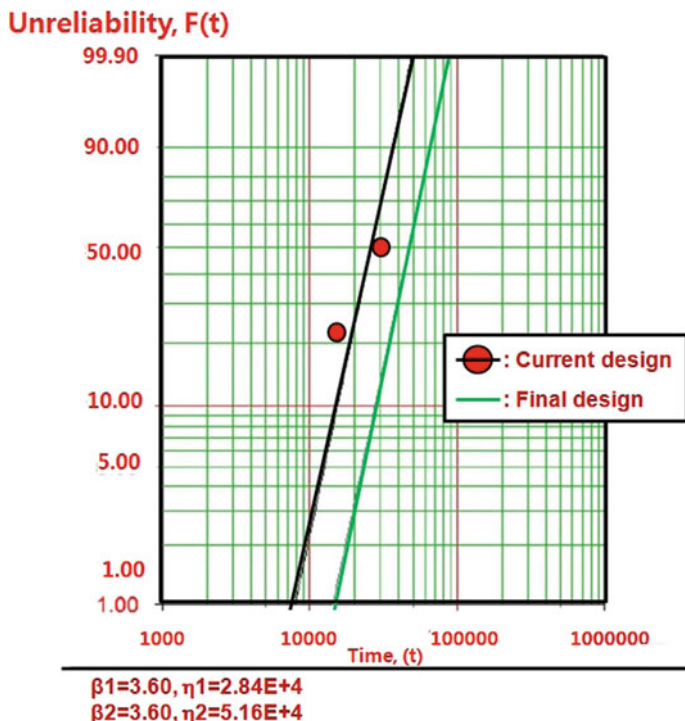


Fig. 9.96 Results of ALT plotted in Weibull chart

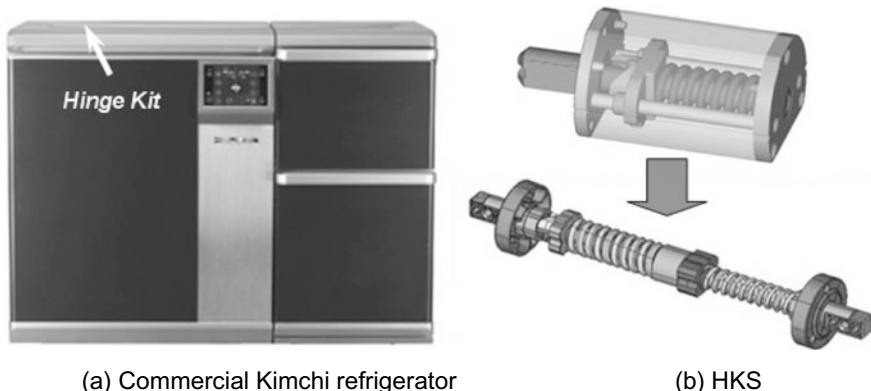


Fig. 9.97 Commercial Kimchi refrigerator and its HKS

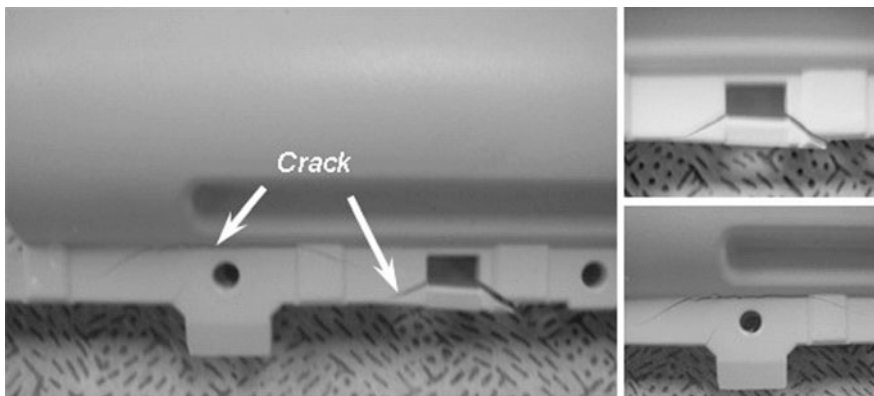


Fig. 9.98 A view of damaged hinge kit system after a period of use

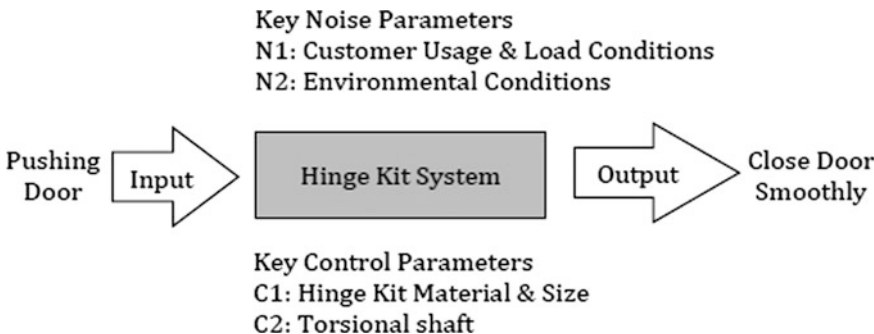


Fig. 9.99 Robust design schematic of HKS

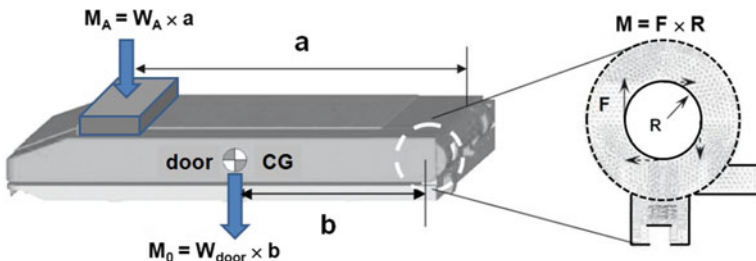


Fig. 9.100 Design concept of HKS

0.24g's of acceleration. The closing of the door occurred an estimated average of 3–10 times per day. With a life cycle design point for 10 years, HKS incurs about 36,500 usage cycles.

For the worst case, the impact force around the HKS was 1.10 kN which was the maximum force applied by the typical consumer. The impact force for the ALT with accelerated weight was 2.76 kN. Using a stress dependence of 2.0, the acceleration factor was found to be approximately 6.3 in Eq. (9.46). The test cycles and the numbers of samples used in the ALT were calculated from Eq. (8.35).

For the B1 life, the required target x was 0.01. The test cycles and test sample numbers calculated in Eq. (8.35) were 34,000 cycles and six units without failure, respectively. ALT was designed to ensure a B1 of 10 years life with about a 60% level of confidence that it would fail less than once during 34,000 cycles. Figure 9.101 shows the experimental setup of the ALT with labeled equipment for the robust design of HKS. Repetitive stress can be expressed as the duty effect that carries the on/off cycles and shortens part life [9]. Figure 9.102 shows the duty cycles for the impact force F.

The control panel was used to operate the testing equipment—the number of test time, starting or stopping the equipment, and the other. When the start button in the controller panel gave the start signal, the simple hand-shaped arms held and lifted

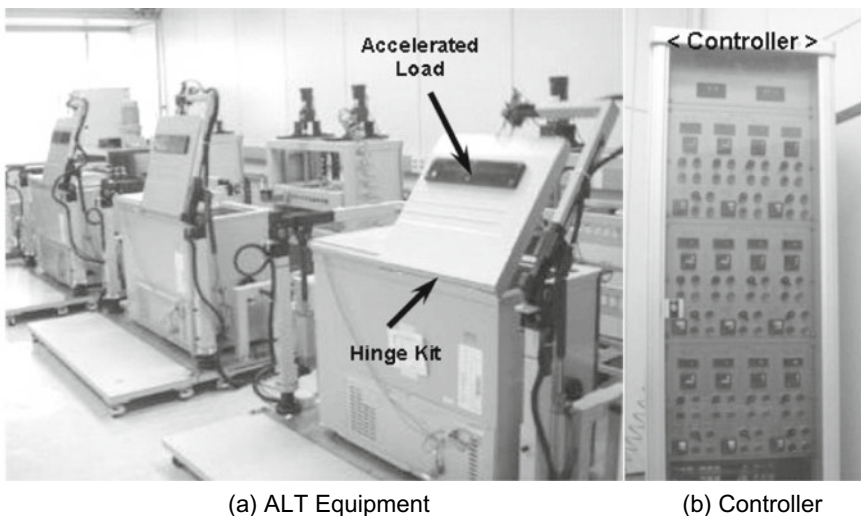


Fig. 9.101 Equipment used in accelerated life testing and controller

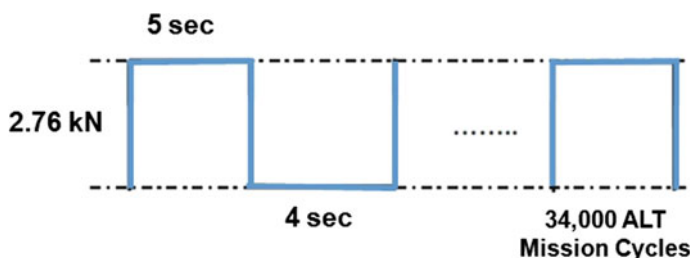


Fig. 9.102 Duty cycles of the repetitive impact load F on HKS

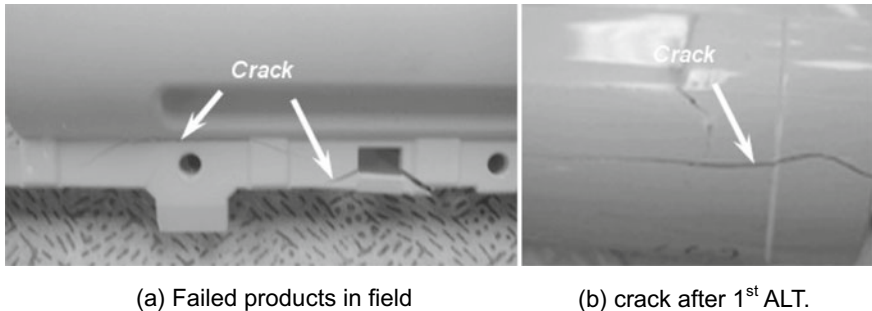


Fig. 9.103 Failed products in field and crack after 1st ALT

the Kimchi refrigerator door. As the door was closing, it was applied to the HKS with the maximum mechanical impact force due to the accelerated load (2.76 kN).

Figure 9.103 shows a photograph comparing the failed product from the field and from 1st accelerated life testing, respectively. As shown in the picture, the shape and location of the failure in the ALT were similar to those seen in the field. Figure 9.104 represented the graphical analysis of the ALT results and field data on a Weibull plot. The shape parameter in the first ALT was estimated at 2.0. From the Weibull plot, the shape parameter was confirmed to be 2.1.

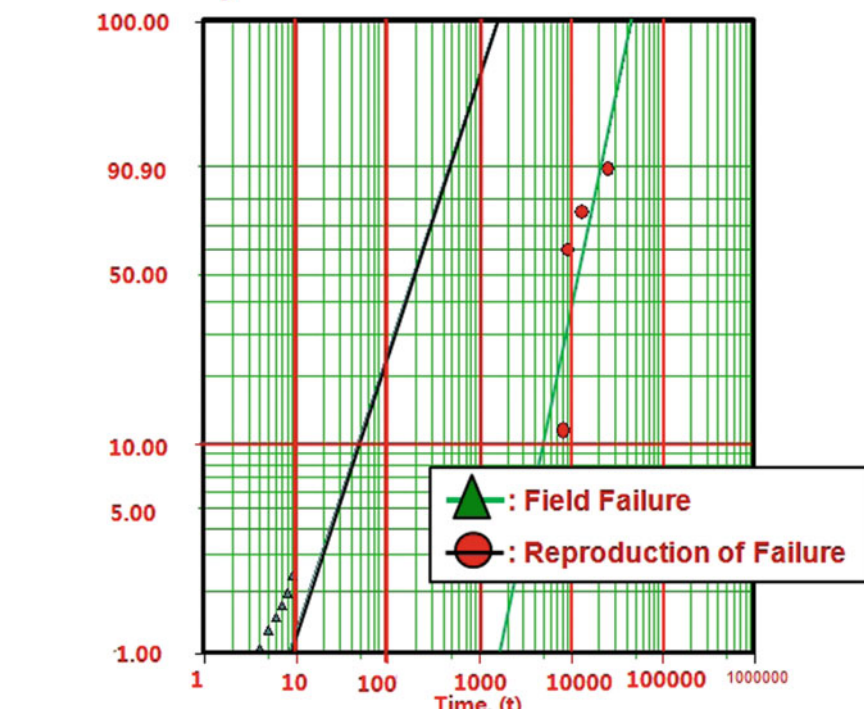
The defective shape of the ALT was very similar to that of the field. From the Weibull plot, the shape parameters of the ALT and market data were found to be similar. As supported by two findings in the data, these methodologies were valid in pinpointing the weak designs responsible for failures in the field, which determined the lifetime.

The fracture of the HKS in both the field products and the ALT test specimens occurred in the housing and support of the HKS (Fig. 9.105). The missing design variables of the HKS in the design phase came from no support structure. The repetitive applied force in combination with the structural flaws may have caused the fracturing of the HKS. The concentrated stresses of the HKS were approximately 21.2 MPa, based on finite element analysis. The stress risers in high stress areas resulted from the structural design flaws of not having any supporting ribs.

The corrective action plans was to add the support ribs (Fig. 9.106). Applying the new design parameters to the finite element analysis, the stress concentrations of the HKS decreased from 21.2 to 19.9 MPa. Therefore, the corrective action plan had to be made at the design stage before production.

The design target of the newly designed samples was more than the target life of a B1 of 10 years. The confirmed values of AF and β in Fig. 9.104 were 6.3 and 2.1, respectively. The recalculated test cycles and sample size in Eq. (7.35) for reliability target of B1 of 10 years were 41,000 and six units, respectively. Based on the BX and sample size, three ALTs were performed to obtain the design parameters and their proper levels. In the second ALTs the crack of torsional shaft occurred due to its sharp rounding and repetitive impact stresses (Fig. 9.107).

Unreliability



$$\beta_1 = 2.125, \eta = 1.43E+4$$

$$\beta_2 = 1.343, \eta = 245.70$$

Fig. 9.104 Field data and 1st ALT on Weibull chart

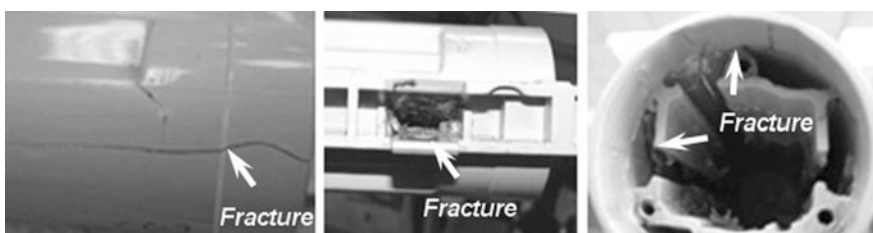


Fig. 9.105 Structure of failing HKS in 1st ALT

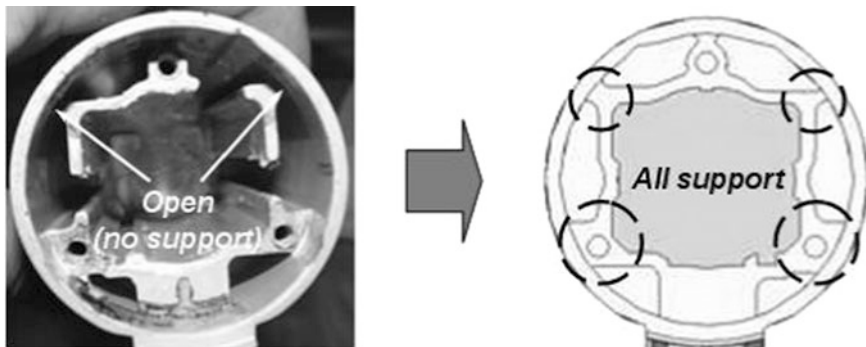


Fig. 9.106 Redesigned HKS structure



Fig. 9.107 Redesigned HKS structure

The torsional shaft of the HKS was modified by giving it more roundness from R0.5 mm to R2.0 mm at the corner of torsional shaft (see Fig. 9.108). Finally, the redesigned HKS could withstand the high impact force during closure of the door. With this design change, the refrigerator could also be opened and closed more comfortably.

Tables 9.19 and 9.20 show the design parameters confirmed from a tailored set of ALTs and the summary of the results of the ALTs, respectively. With these modified parameters, the Kimchi refrigerator door could be smoothly closed for a

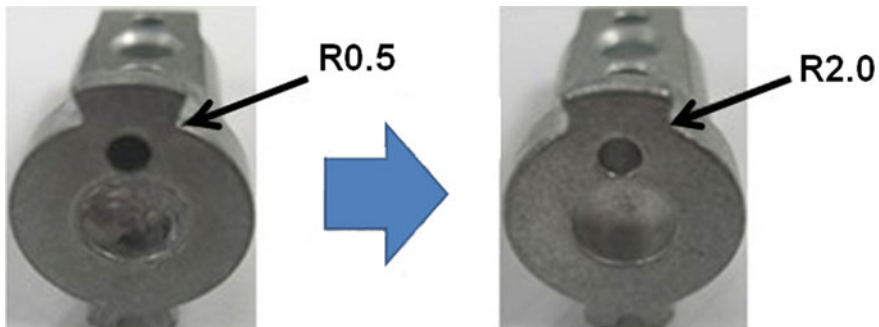


Fig. 9.108 Redesigned torsional shaft of HKS

Table 9.19 Vital parameters based on ALTs

CTQ	Parameters			Unit
Crack	KNP	N1	Impact force	MPa
	KCP	C1	Supporting structure	–
		C2	Corner roundness of torsional shaft	mm

Table 9.20 Results of ALT

	1st ALT	2nd ALT	3rd ALT
	Initial design	Second design	Final design
In 41,000 cycles, HKS has no crack	3000 cycles: 2/6 crack (HKS housing)	12,000 cycles: 4/6 crack (Torsional shaft)	41,000 cycles: 6/6 OK
HKS Structure			
Material and specification	Supporting rib C1: No → 2 supports	Roundness corner of torsional shaft C2: R0.5 mm → R2.0 mm	

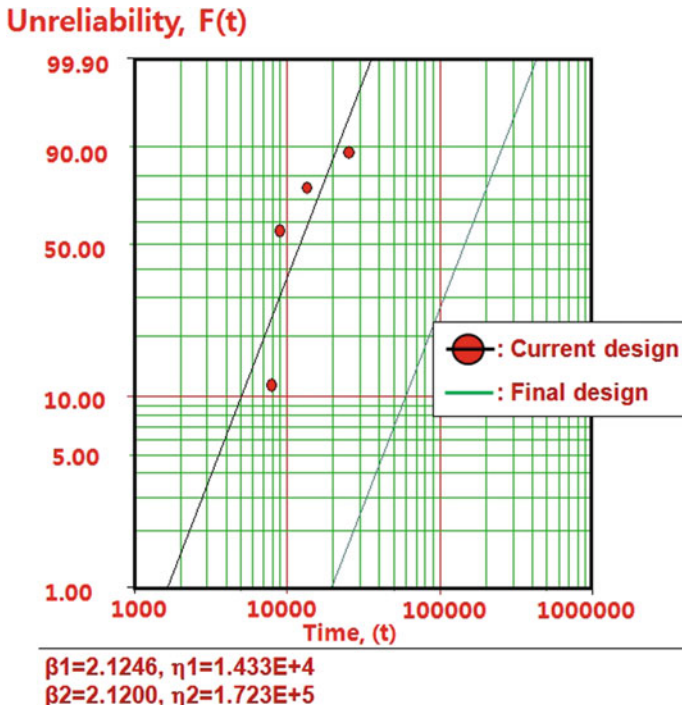


Fig. 9.109 Results of ALT plotted in Weibull chart

longer period without failure. Figure 9.109 shows the graphical results of the ALT plotted in a Weibull chart. Over the course of the three ALTs, the B1 life of the samples was guaranteed to be 10.0 years.

Chapter 10

Parametric ALT: A Powerful Tool for Future Engineering Development



Abstract This chapter will discuss the concept of system engineering that will be modern engineering. Mechanical product is developing under the principle of system engineering because it requires a lot of functions from customers. Product reliability becomes one of the product requirements in system engineering. So when mechanical system with the sophisticated technology put into plan, product reliability in the established design process should be implemented with reliability methodology like parameter ALT. If not, new product will be faced with quality problems. To settle down them, company will pay the quality costs.

Keyword System engineering (SE)

10.1 Introduction

Today new product such as automobiles, construction equipment, machine tools, airplane, domestic appliance, and bridges were designed under the principle of System Engineering (SE). SE is an interdisciplinary field of engineering on how complex engineering projects should be designed and managed over product life cycles. Issues such as design, manufacturing, reliability, logistics, coordination of different teams (requirement management), evaluation measurements and different disciplines become more difficult when dealing with large but complex projects. In system engineering all aspects of a system are considered, and integrated into a whole (Fig. 10.1).

Company also would like to survive the limitless competition through the new technology development. Because there are a lot of things in the design phase for short product developing time and costs, products often have inherent design problems. Due to their product recalls, engineers have become a critical factor to consider reliability in designing the product. The basic question is how to consider the reliability concept in the established design process. The company have new

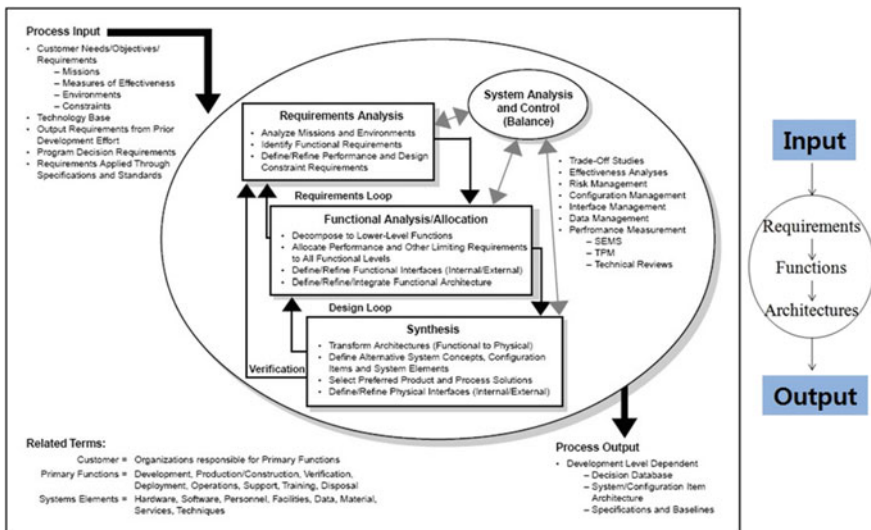


Fig. 10.1 The systems engineering process [1]

quantitative developing process that considers the reliability factor in parallel with the established design process. If not, company will confront numerous recalls in the market.

Product recalls might come from the faulty components that were missed in the process of R&D. When subjected to the wear out stress or overstress under the end user operating or environmental conditions, the problematic components mounted in product cause failure in their lifetime. New product should be developed in the quantitative developing process that is included in (1) reliability target, (2) reliability testing for developing products, (3) design feedback on testing results, and (4) the analysis of the field failure data.

A new methodology for reliability design therefore is required to prevent the product recalls in the mechanical/civil system. The traditional qualitative methods—Capability Maturity Model Integration (CMMI), FMEA and FTA is to look for the design problems on the documents. They only carry out to gather the design ideas or past experience by the representatives—planning, design, and production. Consequently, they often miss the chance to find a critical data in the design phase. The parametric ALT would be an alternative quantitative method to search out the missing design data because it uses the ALT plan, load analysis, and accelerated testing with actions plans.

All mechanical products are fabricated from a multiple of structure to carry out the customer—required functions, which will tend to degrade or break down abruptly by random loads in the field. When mechanical/civil products are subjected to random loads, they would start the void (design failures) in material (or structure), propagate, and rupture it. If failure such as fatigue or fracture occurs,

the product may no longer meet the required product functionality. To avoid failure, mechanical system should be designed to robustly withstand a variety of loads in a lifetime.

To accomplish the reliability design of modules in mechanical/civil product, the basic concepts of parametric ALT were discussed:—(1) Setting overall parametric ALT plan of product, (2) Failure mechanics, design and reliability testing, (3) Parametric accelerated life testing with an acceleration factor, and (4) Derivation of the sample size equation in Chap. 8. The failure modes and mechanisms of the mechanical system in the field and parametric ALT may come from the missing design parameters or design flaws not considered in the design process. In the design phase the mechanical products should reveal the design flaws and establish action plans. To do it, the detail case studies on the design flaws were suggested in Chap. 9.

With the study of faulty designs for the mechanical system, the parametric ALTs can be successful in proving a more reliable product or module with significantly longer life. The product or module with the modified design parameters will meet the reliability target. This reliability design methodologies will provide the reliability quantitative (RQ) test specifications of a mechanical structure that includes several assembly subjected to repetitive stresses under customer usage conditions. As a result, reliability-embedded design process will save the design modification cost because the problem number decreases (Fig. 10.2).

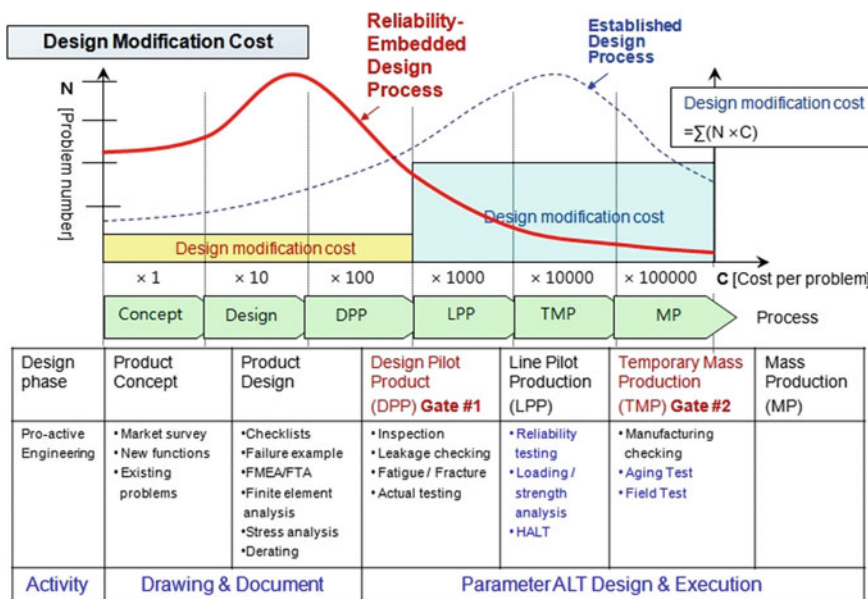


Fig. 10.2 Reliability-embedded design process

There are a variety of other mechanical systems—appliance, automobiles, airplane, machine tool, construction equipment, washing machines, and vacuum cleaners. For improving the reliability design of these systems, the faulty designs identified need to meet the targeted product (or module) reliability. And these principles of parametric ALT also are applicable to the area of civil engineering to design the construction structure. It is recommended that the faulty designs on these systems be further studied for reliability design of product in lifetime.

Reference

1. Defense of Department (2001) Systems engineering fundamentals. Defense Acquisition University Press, Fort Belvoir, Virginia, p 31